FUNDAMENTALS OF, AND APPLICATIONS BASED ON, QUORUM SENSING AND QUORUM SENSING INTERFERENCE

EDITED BY: Cristina García-Aljaro, Ana Otero and Tom Defoirdt
PUBLISHED IN: Frontiers in Microbiology

frontiers Research Topics

frontiers

ISSN 1664-8714
ISBN 978-2-88963-381-4
DOI 10.3389/978-2-88963-381-4

About Frontiers

Frontiers is more than just an open-access publisher of scholarly articles: it is a pioneering approach to the world of academia, radically improving the way scholarly research is managed. The grand vision of Frontiers is a world where all people have an equal opportunity to seek, share and generate knowledge. Frontiers provides immediate and permanent online open access to all its publications, but this alone is not enough to realize our grand goals.

Frontiers Journal Series

The Frontiers Journal Series is a multi-tier and interdisciplinary set of open-access, online journals, promising a paradigm shift from the current review, selection and dissemination processes in academic publishing. All Frontiers journals are driven by researchers for researchers; therefore, they constitute a service to the scholarly community. At the same time, the Frontiers Journal Series operates on a revolutionary invention, the tiered publishing system, initially addressing specific communities of scholars, and gradually climbing up to broader public understanding, thus serving the interests of the lay society, too.

Dedication to Quality

Each Frontiers article is a landmark of the highest quality, thanks to genuinely collaborative interactions between authors and review editors, who include some of the world's best academicians. Research must be certified by peers before entering a stream of knowledge that may eventually reach the public - and shape society; therefore, Frontiers only applies the most rigorous and unbiased reviews.
Frontiers revolutionizes research publishing by freely delivering the most outstanding research, evaluated with no bias from both the academic and social point of view. By applying the most advanced information technologies, Frontiers is catapulting scholarly publishing into a new generation.

What are Frontiers Research Topics?

Frontiers Research Topics are very popular trademarks of the Frontiers Journals Series: they are collections of at least ten articles, all centered on a particular subject. With their unique mix of varied contributions from Original Research to Review Articles, Frontiers Research Topics unify the most influential researchers, the latest key findings and historical advances in a hot research area! Find out more on how to host your own Frontiers Research Topic or contribute to one as an author by contacting the Frontiers Editorial Office: researchtopics@frontiersin.org

FUNDAMENTALS OF, AND APPLICATIONS BASED ON, QUORUM SENSING AND QUORUM SENSING INTERFERENCE

Topic Editors:
Cristina García-Aljaro, University of Barcelona, Spain
Ana Otero, University of Santiago de Compostela, Spain
Tom Defoirdt, Ghent University, Belgium

Background

Bacteria use quorum sensing (QS) circuits to coordinate various activities (among which biofilm formation and the expression of virulence factors) based on the presence of signaling molecules. Different families of signal molecules have been identified in Gram positive and Gram negative bacteria (e.g. autoinducer peptides and acyl homoserine lactones). Similarly, different quorum sensing antagonists interfering with these system have been found in nature, promoting a new and promising field of research, quorum sensing interference. One of the most intensively studied applications of quorum sensing interference is its use as an alternative or synergycally with antibiotics to fight (antibiotic-resistant) bacterial pathogens. Many studies have been published claiming quorum sensing inhibitory activity of natural and synthetic compounds. However, after decades of research, several questions regarding the suitability of this approach to fight bacterial pathogens remain unanswered, including the risk that pathogens will develop resistance against quorum quenching. Meanwhile, the interest in quorum sensing has increased considerably, and this has broadened the fields where it can find biotechnological, environmental and industrial applications, such as anti biofouling, steering fermentations, bioremediation and wastewater treatment.

Goal and scope

The goal of this Research Topic is to broaden the knowledge of the phenotypes regulated by quorum sensing and the advances in quorum sensing interference. Deciphering microorganism language and the different phenotypes regulated by microbial signalling systems is a frontier for the development of new tools for the management of microorganisms to fulfil human needs with a broad application in different areas such as medicine, environmental sciences and industry.

Citation: García-Aljaro, C., Otero, A., Defoirdt, T., eds. (2020). Fundamentals of, and Applications Based on, Quorum Sensing and Quorum Sensing Interference. Lausanne: Frontiers Media SA. doi: 10.3389/978-2-88963-381-4

Table of Contents

frontiers in Microbiology

ORIGINAL RESEARCH
published: 09 January 2019
doi: 10.3389/fmicb.2018.03324

Reducing Quorum Sensing-Mediated Virulence Factor Expression and Biofilm Formation in *Hafnia alvei* by Using the Potential Quorum Sensing Inhibitor L-Carvone

*Tingting Li[1], Yongchao Mei[2,3], Binbin He[2,3], Xiaojia Sun[2,3] and Jianrong Li[2,3]**

[1] Key Laboratory of Biotechnology and Bioresources Utilization (Dalian Minzu University), Ministry of Education, Dalian, China, [2] College of Food Science and Technology, Bohai University, Jinzhou, China, [3] National & Local Joint Engineering Research Center of Storage, Processing and Safety Control Technology for Fresh Agricultural and Aquatic Products, Jinzhou, China

Quorum sensing (QS), one of the most remarkable microbiological discoveries, is considered a global gene regulatory mechanism for various traits in bacteria, including virulence and spoilage. *Hafnia alvei*, an opportunistic pathogen and a dominant psychrophile, uses the *lux*-type QS system to regulate the production of virulence factors and biofilms, which are harmful to the food industry. Based on the QS interference approach, this study aimed to reveal the efficacy of L-carvone at sublethal concentrations on QS-regulated virulence factors and biofilm formation in *H. alvei.* QS inhibitory activity was demonstrated by the reduction in swinging motility (61.49%), swarming motility (74.94%), biofilm formation (52.41%) and acyl-homoserine lactone (AHL) production (0.5 μL/mL). Additionally, *in silico* analysis and RT-qPCR studies for AHL synthase HalI and QS transcriptional regulator HalR revealed a plausible molecular mechanism for QS inhibition by L-carvone. These findings suggest that L-carvone (a main component of spearmint essential oils) could be used as a novel quorum sensing inhibitor to control *H. alvei* in the food industry.

Keywords: *Hafnia alvei*, L-carvone, quorum sensing inhibitor, *in silico* analysis, RT-qPCR

OPEN ACCESS

Edited by:
Tom Defoirdt,
Ghent University, Belgium

Reviewed by:
Raphaël Lami,
Sorbonne Université, France
Vipin Chandra Kalia,
Konkuk University, South Korea

****Correspondence:***
Jianrong Li
lijianrong@bhu.edu.cn

Specialty section:
This article was submitted to Infectious Diseases, a section of the journal Frontiers in Microbiology

Received: *07 October 2018*
Accepted: *21 December 2018*
Published: *09 January 2019*

Citation:
Li T, Mei Y, He B, Sun X and Li J (2019) Reducing Quorum Sensing-Mediated Virulence Factor Expression and Biofilm Formation in Hafnia alvei by Using the Potential Quorum Sensing Inhibitor L-Carvone. Front. Microbiol. 9:3324. doi: 10.3389/fmicb.2018.03324

INTRODUCTION

Hafnia alvei is a Gram-negative, facultatively anaerobic, rod-shaped, motile bacterium of the family *Enterobacteriaceae*; it is an opportunistic pathogen and a dominant psychrophile found in putrid food (Vivas et al., 2008). It has been widely isolated from different food products, such as raw meat, dairy and aquatic products, and specially from various packed food products stored at low temperatures (Kennedy et al., 2010; Chen et al., 2011; Tan et al., 2014). Based on these characteristics, *H. alvei* is often considered a specific spoilage organism (SSO) that causes severe nutrition and safety problems in these food matrices by producing extracellular enzymes and siderophores, and forming biofilms. Recent studies have described the key roles of virulence factors

and biofilm production in *H. alvei*, which is regulated by quorum sensing (QS) systems (Viana et al., 2009; Hou et al., 2017b).

Quorum sensing is a process that allows single-cell organisms (like bacteria) cooperate, communicate, and act collectively. By this process, they can produce, release, detect, and establish connections with small chemical molecules called autoinducers, which in Gram-negative bacteria are acyl-homoserine lactones (AHLs). Thus, AHL-mediated QS systems are usually composed of the LuxI-type autoinducer synthetase, and cytoplasmic LuxR-type proteins, which are receptors activated by AHLs (Ng and Bassler, 2009). Among these two proteins, LuxR-type proteins have more complex functions. With the increase of bacterial density (achieving a certain threshold), the ligand-binding domain of the LuxR-type proteins will bind with AHLs, which will cause changes in the protein conformation and stimulate the formation of AI-LuxR compound proteins, and lead to the binding of the DNA-binding domain of these compound proteins to target genes, thereby regulating the expression of bacterial multiplex phenotypic features such as virulence factors and biofilms (Almeida et al., 2016). Therefore, interfering with AHL-mediated QS systems by using certain compounds, generally called QS inhibitors (QSIs), may be a better strategy to prevent bacterial food spoilage. Compared to antibiotics and antiseptics, QSIs aim to make the bacteria 'surrender' instead of killing them, which would weaken them from having resistance (Defoirdt, 2017).

Nowadays, many synthetic and natural products have been called QSIs; however, only a few of them have a therapeutic value, due to the instability or high toxicity of most other compounds (Defoirdt et al., 2013). Due to the property of low toxicity, some natural compounds from spice plants have been widely used as antimicrobial agents in the food industry, such as curcumin, vanillin, menthol, and cinnamaldehyde (Fitzgerald et al., 2003; Husain et al., 2015; Ding et al., 2017). Therefore, extracting natural compounds from spice plants to obtain effective QSIs has become a promising research hotspot. L-Carvone (or (*R*4)-(-)-carvone), a monoterpene, is the main component of spearmint essential oils from traditional spice plants and medical herbs. It is widely applied in the food field; it is used to enhance the fragrance and flavor in cooking, and in the beverage and the chewing gum industries (de Carvalho and da Fonseca, 2006). In many studies, L-carvone has been reported as an antimicrobial agent for foodborne pathogenic microorganisms (Friedman et al., 2002; Porfírio et al., 2017); however, there is still limited information about the relationship between spoilage bacteria and QSIs. Therefore, our study involves the characterization of the L-carvone-mediated inhibition of the QS activity of the biosensor strain *Chromobacterium violaceum* CV026, and subsequently, the determination of the effect of L-carvone on virulence factor and biofilm production in the spoilage bacterium *H. alvei*. Additionally, we further investigated the underlying mechanism of L-carvone as a potential QSI in *H. alvei*, by using the *in silico* analysis and RT-qPCR techniques. In this regard, the study has provided new information about the application of L-carvone as potential QSI and reference values for the effective control of spoilage bacteria.

MATERIALS AND METHODS

Reagents, Bacterial Strains, and Growth Conditions

L-Carvone (≥99% purity) and AHL standards including C_4-HSL, C_6-HSL, C_8-HSL, C_{10}-HSL, C_{12}-HSL, and C_{14}-HSL were obtained from Sigma-Aldrich (United States). The molecular biology reagents were purchased from Thermo Fisher Scientific (Shanghai, China). Other chemical reagents used in this study were of analytical grade, except for methanol (Chromatographic grade). The bacterial strains used in this study were *C. violaceum* CV026 and *H. alvei* Ha-01, as an AHL-reporter organism and a test strain, respectively. *C. violaceum* CV026 was provided by Dr. Yang (Xinjiang Shihezi University, Xinjiang, China) and *H. alvei* (ATCC 13337) Ha-01 was originally isolated and identified from putrid turbot by our group. *C. violaceum* CV026 was a mini-Tn5 mutant derived from *C. violaceum* ATCC 31532; it was kanamycin-resistant. It could respond only when exogenous AHLs were present, after which it produced the characteristic violet pigment, violacein. Both the strains were overnight cultured in Luria-Bertani (LB) broth (Qingdao Hopebio Co., Ltd., China), at 28°C and 160 rpm; however, the LB broth culture medium for CV026 required 20 μg/mL kanamycin.

Antibacterial Assay

Determination of the Minimum Inhibitory Concentration (MIC) of L-Carvone

The MIC of L-carvone against the selected bacteria was determined using the Oxford cup assay method, as described by Diao et al. (2014). Overnight-cultured (OD_{600} = 0.5, 250 μL) *C. violaceum* CV026 or *H. alvei* was inoculated in LB nutrient agar (25 mL) and poured into a plate that accommodated two autoclaved Oxford cups, which were removed when the agar solidified. Two hundred microliters of L-carvone (diluted to 2.0, 1.0, 0.5, 0.25, 0.125, and 0.0625 μL/mL using sterile water) were added to the wells, while sterile water served as the control. The plates were incubated at 28°C for 36 h and the bacterial growth states were observed. The minimum concentration at which there was no visible growth was defined as the MIC. Then, sub-MICs were selected for the further experiments using the above strains.

Determination of QSI Activity

Violacein Inhibitory Activity

The violacein inhibitory activity was determined by adopting the method described by Ia et al. (2012), with slight modifications. Overnight-cultured *C. violaceum* CV026 (250 μL) was inoculated in LB nutrient agar (25 mL) containing 10 μL of exogenous AHLs (C_6-HSL, 2 mg/mL). Afterwards, 200 μL of L-carvone at the sub-MICs was added to each well (diameter, 6 mm) on the plates, while 200 μL of sterilized water was used as the negative control. The plates were incubated at 28°C for 24 h, and the bacterial growth status was observed. Once no violet pigment was produced around the well, the violacein inhibitory activity was determined.

Quantitative Analysis of Violacein Production

Violacein produced by *C. violaceum* CV026 exposed to different concentrations (0.5, 0.25, 0.125, and 0.0625 μL/mL) of L-carvone was quantified as previously described by Choo et al. (2006). Different concentrations of L-carvone (described above) were mixed in 10 mL of LB broth containing 20 μg/mL C_6-HSL, along with *C. violaceum* CV026 overnight cultures, and incubated at 28°C for 48 h with shaking (160 rpm). At the same time, a similar experiment without C_6-HSL was performed, and the OD_{595} was measured to determine the effect of the above concentrations of L-carvone on the growth of the CV026.

The violacein pigment was extracted according to the method described by Kumar et al. (2015) with modifications. The cultures in each treatment group were vortexed, and 300 μL of these mixed cultures were taken in 1.5-mL tubes (Eppendorf). They were lysed (for 15 s) using 10% sodium dodecyl sulfate (SDS, 150 μL) at room temperature, and then, extracted (for 5 s) using butyl alcohol (600 μL). Finally, this solution was centrifuged (9,000 *g* for 5 min); violacein was contained in the organic layer. Then, the OD_{595} of each supernatant was measured in a 96-well microtiter plate.

Assay for Biofilm Formation

The 1.5-mL Eppendorf tubes (polypropylene material) were autoclaved, and the *H. alvei* overnight cultures (100 μL) were inoculated in 1 mL of LB broth containing various concentrations (0.5, 0.25, 0.125, and 0.0625 μL/mL) of L-carvone. Sterile water or 20 μg/mL C_6-HSL was used as the negative control or positive control (absence of L-carvone), respectively. The tubes were statically incubated at 28°C for 48 h. Then, the determination of biofilm was performed as described previously (Rode et al., 2007), with minor modifications. The cultures were discarded, and each tube was rinsed thrice with sterile water. The tubes were then naturally dried for 40 min and stained with 1 mL of 0.1% crystal violet (w/v) for 15 min at room temperature. After washing with sterile water, the biofilms were extracted using 33% acetic acid. The biofilm solutions were then transferred to a clean 96-well plate, and the OD_{595} values were measured using microplate photometers (Bio-Rad, United States).

Visualization of Biofilms by CLSM and SEM

To pre-form the biofilms, pieces of zinc (6 mm × 6 mm × 0.2 mm) were polished and immersed in LB broth containing sub-MICs of L-carvone or 20 μg/mL of C_6-HSL in 90-mm sterile plates (Thermo, United States). Overnight cultures of *H. alvei* (OD_{600} = 0.5, 100 μL) were inoculated in these plates and then statically incubated. After cultivation (at 28°C for 48 h), a piece of zinc (with an adhered biofilm) was transferred to a clean sterile plate and washed thrice with sterile phosphate buffer saline (PBS, pH 7.4) to remove the planktonic cells. For visualization by confocal laser scanning microscopy (CLSM), this zinc piece was stained with 0.01% (w/v) acridine orange (AO, dissolved in PBS) for 15 min in the dark. Then, the excessive AO was removed by washing with PBS, followed by fixing with antifade mounting medium Fluoromount-G™ (Yeasen, China) for 15 min under the same conditions. Finally, the samples were observed by CLSM (Leica SP5, German) (emission: 525 nm, excitation: 488 nm). For visualization analysis by scanning electron microscopy (SEM), the zinc piece was soaked in 2.5% glutaraldehyde (v/v) at 4°C for 5 h, dehydrated in graded ethanol (15 min for each grade). Subsequently, the SEM sample was obtained after drying with sterile air.

Swimming and Swarming Motility Assay

Motility experiments were performed on swimming (1% [w/v] tryptone, 0.5% [w/v] NaCl, and 0.3% [w/v] agar) or swarming (1% [w/v] peptone, 0.5% [w/v] NaCl, 0.5% [w/v] D-fructose, and 0.6% [w/v] agar) agar plates, as previously described (de la Fuente-Núñez et al., 2012), but with some modifications. These agar plates were supplemented with different concentrations (0.5, 0.25, 0.125, and 0.0625 μL/mL) of the L-carvone, before the agar solidified. Then, 5 μL of *H. alvei* overnight cultures (OD_{600} = 0.5) was inoculated at the center of the solidified plates, and the plate was incubated statically at 28°C for 48 h. The motility of *H. alvei* was evaluated by measuring the diameter of the swimming and swarming colonies. Plates supplemented with sterile water or 20 μg/mL C_6-HSL were used as a negative or positive control, respectively. At least three independent experiments for motility assays were performed.

AHL Analysis by GC-MS

AHLs Extraction

Dilutions (1/100) of *H. alvei* overnight cultures were incubated in LB broth (200 mL) in the presence of L-carvone (0.5, 0.25, 0.125, and 0.0625 μL/mL) for 24 h at 28°C in an Erlenmeyer flask. Bacterial cells were removed by centrifugation (9,000 *g* for 15 min). The supernatants were extracted using ethyl acetate supplemented with 0.1% acetic acid thrice, and then, the organic phases were evaporated using a rotary evaporator. The residues were re-dissolved in methanol (1 mL) and filtered through a 0.22-μm membrane (FilterBio, China) for GC-MS detection. For comparison, LB broth in the absence of L-carvone was used. C_{14}-HSL, as an internal standard, was added to each of the AHL samples at a concentration of 5 μg/mL.

GC-MS Detection

The AHL samples of *H. alvei* were further analyzed by GC-MS (7890N/5975, Agilent, United States), according to the method described by Zhu et al. (2016). A HP-5 MS capillary column (30 m length × 0.25 mm internal diameter × 0.25 μm film thickness) was used for the chromatographic separation of the AHLs. The injection volume was 1 μL, using a slit ratio of 50:1. The injector temperature was maintained at 200°C and the oven temperature was automated from 150 to 220°C at a rate of 10°C/min, followed by a 5°C/min increase to 250°C, and from 250 to 252.5°C at 0.5°C/min, with helium as the carrier gas, at a flow rate of 1 mL/min. The mass spectrometry conditions were as follows: the electron

ionization source was set to 70 eV, the MS Quad temperature was 150°C, the emission current was 500 μA, the MS Source temperature was 230°C. Data were acquired using the full-scan mode (m/z 35–800) and selected ion monitoring (SIM) mode (m/z 143).

RT-qPCR Analysis

Hafnia alvei was cultured in LB broth with sub-MICs of L-carvone at 28°C for growth until the logarithmic phase. *H. alvei* cultured without L-carvone was used as a negative control, while *H. alvei* cultured with C_6-HSL was used as a positive control. Total RNA was isolated from *H. alvei* using TRIzol Reagent (Thermo Scientific, United States), according to the manufacturer's guidelines. The quality of the isolated RNA was checked using standard agarose gel electrophoresis. The single-stranded cDNA was prepared in accordance with the protocol of RevertAid First Strand cDNA Synthesis Kit & DNase I (Thermo Scientific, United States), as stated by the manufacturer. The RT-qPCR experiment was performed by using BIO-RAD CFX Connect™ Real-Time PCR test system (BIO-RAD, United States) and Power SYBR® Green PCR Master Mix (Applied Biosystems, United States). The sequences of primers are listed in **Table 1**. The housekeeping gene *16S rRNA* was used as an internal reference. The conditions for RT-qPCR were as follows: initial denaturation at 95°C for 3 min, and 95°C for 10 s, 55°C for 20 s for annealing, 72°C for 20 s for extension, and 75°C for 5 s for collecting the fluorescence signal; 40 cycles were run. The melt curve was established in the range of 65–95°C. The relative expression of the objective genes was calculated by using the $2^{-\Delta\Delta CT}$ method, as previously described by Livak and Schmittgen (2001).

In silico Analysis

The lux-type protein sequences of *H. alvei* were HalI (acyl-homoserine-lactone synthase, AAP30849.1) and HalR (transcriptional regulators, AAP30848.1) and downloaded from the NCBI[1]. The models of these proteins were built and assessed the online tools SWISS-MODEL[2] (Bertoni et al., 2017; Bienert et al., 2017; Waterhouse et al., 2018) for docking studies. The water molecules associated with the protein model were removed and the missing hydrogen atoms were supplemented using Clean Protein module of Discovery Studio (DS). The 3D structures of the ligands including L-carvone, halogenated furanone C30 (a known QSI), and C_6-HSL were downloaded from the ZINC 12 database[3] and optimized in DS to obtain their possible lowest-energy conformations. The binding spheres that covered the active site residues were also obtained with DS, using the Define and Edit Binding Site module. Finally, docking of the ligands was subsequently performed using the Libdock algorithm.

[1]https://www.ncbi.nlm.nih.gov/

[2]https://www.swissmodel.expasy.org/

TABLE 1 | List of target genes and their respective primers used for RT-qPCR analysis.

Target gene	Primer type	Sequence (5′→3′)	Amplicon size (bp)
16S rRNA	Forward	GTCTGCAACTCGACTCCATGA	121
	Reverse	CTTTTGCAACCCACTCCCATG	
hall	Forward	CGGCTTGATTCCACTTCACC	132
	Reverse	GGGTCTGTATGAAGGGCAGT	
halR	Forward	CGGCTATACTTTCGTCCTGC	179
	Reverse	CTTCCGAAACTGACTGCACG	

The lux-type genes in H. alvei were hall and halR, respectively.

Statistical Analysis

Each experiment was performed in triplicate, and the data were presented as the mean values ± SD. The data were analyzed by one-way analysis of variance (ANOVA) along with Tukey test correction using the software SPSS Statistics 20.0. Graphs were constructed using Origin Pro 9.0. Differences with a p-value < 0.05 were considered significant.

RESULTS

Minimum Inhibitory Concentration (MIC) of L-Carvone

The MIC of L-carvone, with concentrations ranging from 0.0625 to 2 μL/mL, was estimated by the Oxford cup method. It was observed that the MIC of L-carvone for *C. violaceum* CV026 was 1.0 μL/mL; L-carvone did not influence the growth of *H. alvei* at the same concentration. Therefore, the sub-MICs (0.5, 0.25, 0.125, and 0.0625 μL/mL) were selected for further experiments in this study.

Effect of L-Carvone on Violacein Production in *C. violaceum* CV026

To determine whether L-carvone at the sub-MICs inhibited violacein production in CV026, two assays were performed. **Figure 1A** shows that a clear inhibitory zone was observed around the well on the purple pigment plate due to L-carvone; however, the control, sterile water, did not inhibit pigment production. Furthermore, the quantitative results of violacein production were obtained. L-Carvone showed a dose-dependent QSI activity and did not significantly inhibit bacterial growth at the sub-MICs (**Figure 1B**). The minimum violacein production rate (OD treatment group/OD control group) was only 48.25% at a 0.5 μL/mL concentration of L-carvone.

Effect of L-Carvone on Biofilm Formation in *H. alvei*

The results of biofilm formation after treatment with different concentrations of L-carvone are presented in **Table 2**. A minimum biofilm inhibition of 13.43% was observed when *H. alvei* was cultured with L-carvone at 0.0625 μL/mL;

[3]http://zinc.docking.org/

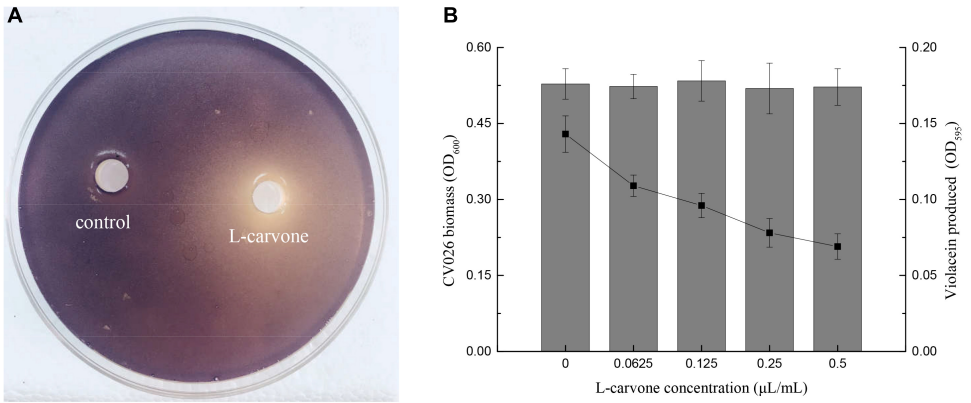

FIGURE 1 | Violacein inhibitory activity of L-carvone. **(A)** Inhibitory activity of L-carvone on the violacein production of CV026. **(B)** Quantitative analysis of CV026 biomass (columns) and violacein production (lines) at sub-inhibitory concentrations of L-carvone.

TABLE 2 | Inhibitory activity of L-carvone on biofilm formation by *H. alvei* (mean ± standard deviation).

Additive	Concentration	Biofilm formation[a]	Inhibitory rate (%)[b]
C_6-HSL	20 μg/mL	0.951 ± 0.004[c]	–
Control	0 μL/mL	0.685 ± 0.004[d]	–
L-carvone	0.0625 μL/mL	0.593 ± 0.007[e]	13.43
L-carvone	0.125 μL/mL	0.532 ± 0.010[e]	15.30
L-carvone	0.25 μL/mL	0.478 ± 0.003[f]	30.32
L-carvone	0.5 μL/mL	0.326 ± 0.005[g]	52.41

[a]Expressed as OD_{595} after incubation with crystal violet. [b]The inhibitory rate = (OD control group − OD treated group)/OD control group. [c−g]Significantly different means ($P < 0.05$).

a maximum biofilm inhibition of 52.41% was observed at am L-carvone concentration of 0.5 μL/mL. In contrast, biofilm formation in the C_6-HSL-treated group was visibly higher than that in the control group, which proves that the biofilm formation of *H. alvei* is positively regulated by the AHL-based QS system.

In this study, the biofilm states of the *H. alvei* strain in the presence of various concentrations of L-carvone were also observed by CLSM and SEM. The CLSM images showed thick and dense biofilms after C_6-HSL treatment, compared with the control group (**Figure 2A**), whereas L-carvone treatment significantly removed the microbes attached to the zinc surface (**Figure 2A**). The SEM images displayed similar results and showed a major disruption to the biofilm architecture as well as the reduction of the biofilm matrix (**Figure 2B**).

Effect of L-Carvone on Swimming and Swarming Motility of *H. alvei*

The migration distance of *H. alvei* grown on swimming and swarming agar plates at 28°C for 48 h is shown in **Figure 3**. The treatment of *H. alvei* with sub-MICs of L-carvone reduced the swimming motility significantly; the level of swimming motility inhibition due to L-carvone (0.0625–0.5 μL/mL) was 12.43–61.49%, as depicted in **Supplementary Table S1**. Similarly, swarming migration of *H. alvei* was also impaired considerably (23.29–74.94%) after treatment with L-carvone (**Supplementary Table S1**). However, the treatment of *H. alvei* with C_6-HSL promoted its motility.

Effect of L-Carvone on AHL Production in *H. alvei*

To investigate the effect of L-carvone on AHL production of test strain, the AHLs in the ethyl acetate crude extract of *H. alvei* were analyzed using GC-MS. After the AHL standards were separated individually, and their retention times were identified (**Supplementary Figure S1A**), we calculated the relative quantity of AHLs in the crude extracts based on the ratio of the peak area of the samples to that of the internal standard (C_{14}-HSL). The AHL types observed in the *H. alvei* crude extracts were C_6-HSL and C_8-HSL, at concentrations of 2.16 ± 0.06 and 2.27 ± 0.12 μg/mL, respectively. Treatment with L-carvone significantly reduced the AHL production (**Supplementary Figure S1C**); when treated with 0.5 μL/mL L-carvone, the minimal concentrations of C_6-HSL and C_8-HSL decreased to 0.16 ± 0.09 and 0.97 ± 0.04 μg/mL, respectively (**Supplementary Figure S1B**).

RT-qPCR

The RT-qPCR experiments were performed to understand the effect of L-carvone on the expression level of QS-regulated genes in *H. alvei*. The selected genes were lux-type genes, named *halI* and *halR*, respectively. Because in this QS system, the *halI* gene regulated AHL biosynthesis by encoding HalI (the AHL synthase), the *halR* gene responded to the corresponding AHL by encoding HalR (the transcriptional regulator), and further regulated the transcription of the downstream genes. The results obtained in this study show that L-carvone could selectively affect the QS system by significantly downregulating the relative expression levels of *halI* and *halR* (**Figure 4**). C_6-HSL, which was used as the positive control, could significantly upregulate the expression of the selected genes. Melt and amplification curves of the genes were established in **Supplementary Figure S3**.

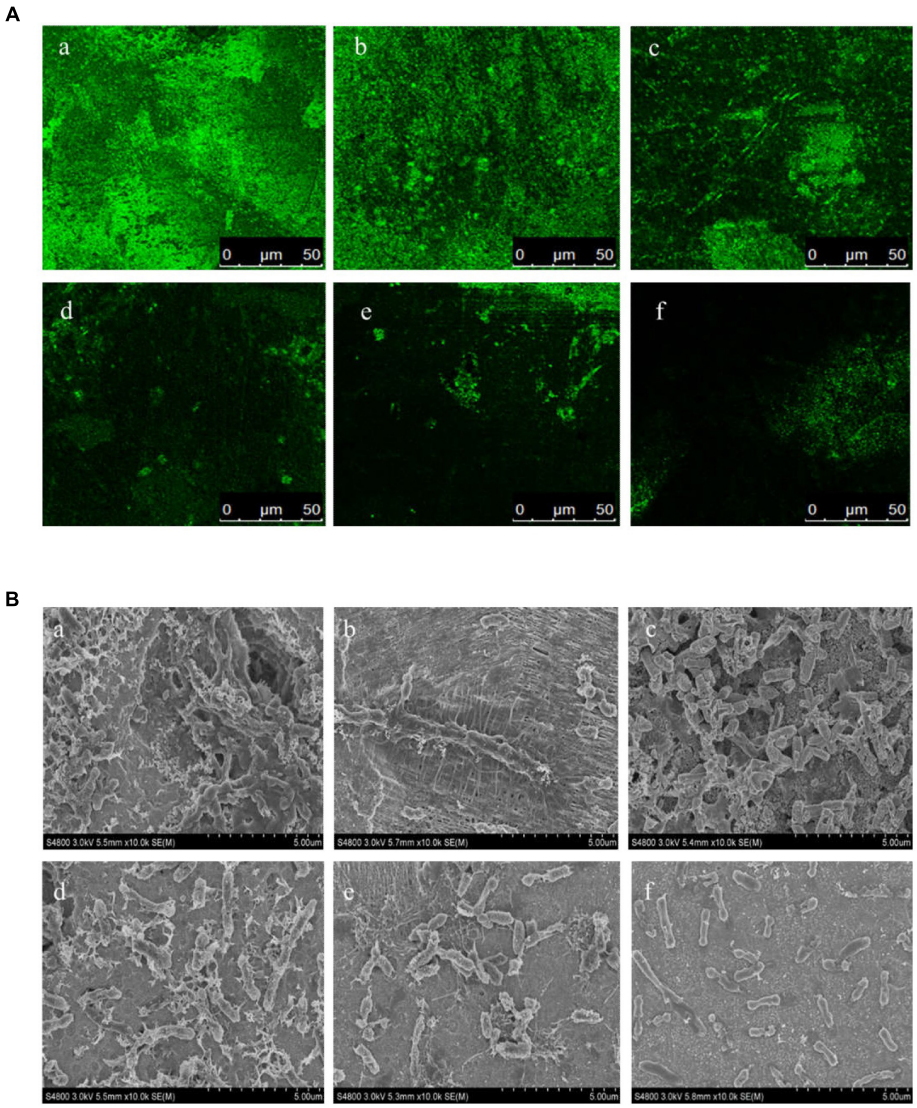

FIGURE 2 | Confocal laser scanning microscopy (CLSM) images **(A)** and SEM images **(B)** of the biofilm states of the *H. alvei* strain on zinc surfaces after different treatments. **(a)** 20 μg/mL C_6-HSL, **(b)** control, **(c–f)** L-carvone treatments at concentrations of 0.0625, 0.125, 0.25, and 0.5 μL/mL.

Homology Modeling and Model Assessment

At present, the three-dimensional (3D) structures of the HalI and HalR proteins have not yet been analyzed; therefore, homology modeling, based on the online tool SWISS-MODEL, was utilized to solve this problem. Modeling templates were matched using the amino acid sequences of HalI (acyl-homoserine-lactone synthase, AAP30849.1) and HalR (transcriptional regulators, AAP30848.1); the top 50 templates of each protein were obtained. The three best models of HalI and HalI proteins are listed in **Supplementary Table S2**, based on sequence similarities and the GMQE scores.

Model qualities were assessed by using QMEAN, which is a composite estimator and provides both global and local absolute quality estimates for models (Benkert et al., 2011). QMEAN *Z*-Scores of around zero are an indication of a high quality for a model; however, scores of −4.0 or lower indicated a low quality. Therefore, the results in **Supplementary Figures S2A–D** show that the best models for HalI and HalR proteins were the 1k4j.1.A (score of −1.85) and 5l07.1.B (score of −1.37) models, respectively; they were able to efficiently predict the 3D structures of Lux-type proteins in *H. alvei*.

In silico Analysis

In silico analysis studies of L-carvone provide an insight into the binding affinity of this potential QSI, with the model of HalI and HalR protein. For the QS transcriptional receptor HalR protein, the halogenated furanone C30 and C_6-HSL were docked as the control ligands. As shown in **Supplementary Table S3**, L-carvone docked with the active site of the HalI

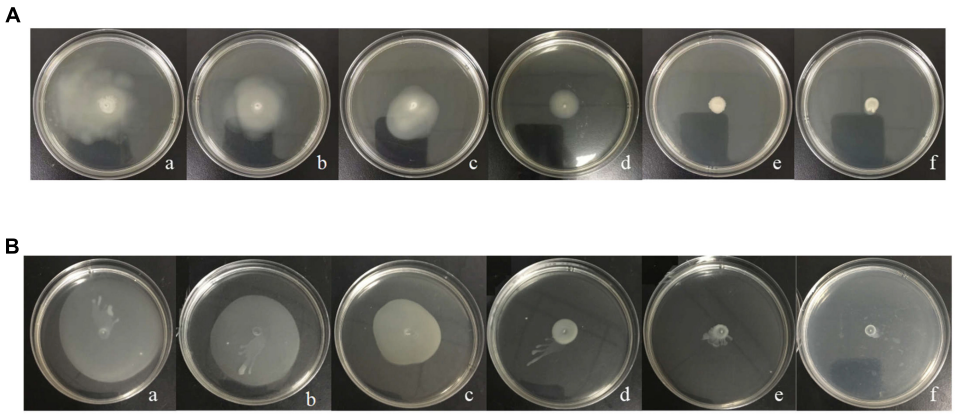

FIGURE 3 | Analysis of the inhibition of the motility of *H. alvei* by L-carvone. Swimming **(A)** and swarming **(B)** agar plates were incubated at 28°C and monitored after 48 h. **(a)** 20 μg/mL C6-HSL, **(b)** control, **(c–f)** 0.0625, 0.125, 0.25, and 0.50 μL/mL L-carvone.

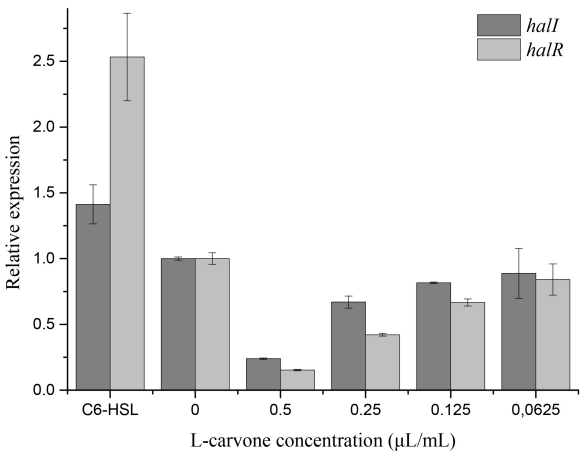

FIGURE 4 | Effect of L-carvone on the expression of QS-regulated genes of *H. alvei*. The lux-type genes of the QS system in *H. alvei* were *hall* and *halR*, respectively. The untreated group was used as a negative control, and the group treated with C_6-HSL was used as a positive control. The relative expression was considered as 1.

protein of *H. alvei*, with a LibDock score of 71.0676. Moreover, L-carvone (LibDock score of 66.7963) showed a better affinity toward HalR than the standard QSI, halogenated furanone C30 (LibDock score of 52.7221). However, both the ligands were observed to have a lower affinity toward HalR than the natural ligand C_6-HSL (LibDock score of 84.7765). **Figure 4** depicts the possible mechanism of the action of L-carvone in attenuating QS-regulated virulence factor and biofilm production in *H. alvei*.

DISCUSSION

There is increasing evidence that plant essential oils can act as potential QSIs, to reduce QS-mediated production of virulence factors and biofilms in microorganisms, and provide a new insight into controlling microbial communities (Zhang et al., 2018). Our data support this notion, revealing a potential QSI, L-carvone (the main component of spearmint essential oil), which interferes with violacein expression in *C. violaceum* CV026 and enters *H. alvei*, reducing its motility, biofilm formation, and expression of QS-related genes.

In this study, originally, sub-MICs of L-carvone were tested for their QSI activity using the CV026 strain (**Figure 1**). The biosensor strain CV026 can only respond to exogenous short-chain AHLs through the cytoplasmic transcription factor *CviR* (a LuxR homolog), which activates the expression of violacein in combination with the AHLs (McClean et al., 1997). Many studies have revealed that the reduction of violacein production without the growth of CV026 being affected is considered a direct evidence for the interference of the QS system (Venkadesaperumal et al., 2016; Liu et al., 2017). Based on the above evidences, this work further explored the QS interference activity of L-carvone on *H. alvei*, since the QS-mediated production of virulence factors and biofilms plays a key role in the growth of this spoilage organism (Hou et al., 2017b).

The bacterial cells in biofilms are more resistant to antiseptics and food processing conditions; this is likely to cause serious food safety issues (Bai and Rai, 2011). Consequently, studies on preventing biofilm formation are garnering special interest. Previous studies have indicated that the effects of L-carvone on biofilms of Gram-positive and Gram-negative bacteria are possibly different. Soumya et al. (2011) reported that the sub-MICs of L-carvone could reduce biofilm formation in *Pseudomonas aeruginosa* as a natural QS-inhibitory compound. However, in case of Gram-positive bacteria, the study by Leonard et al. (2010) indicated that carvone could increase biofilm production in *Listeria monocytogenes*, rather than inhibiting its production. Interestingly, Oliveroverbel et al. (2014) also showed that carvone could inhibit violacein and pyocyanin production in

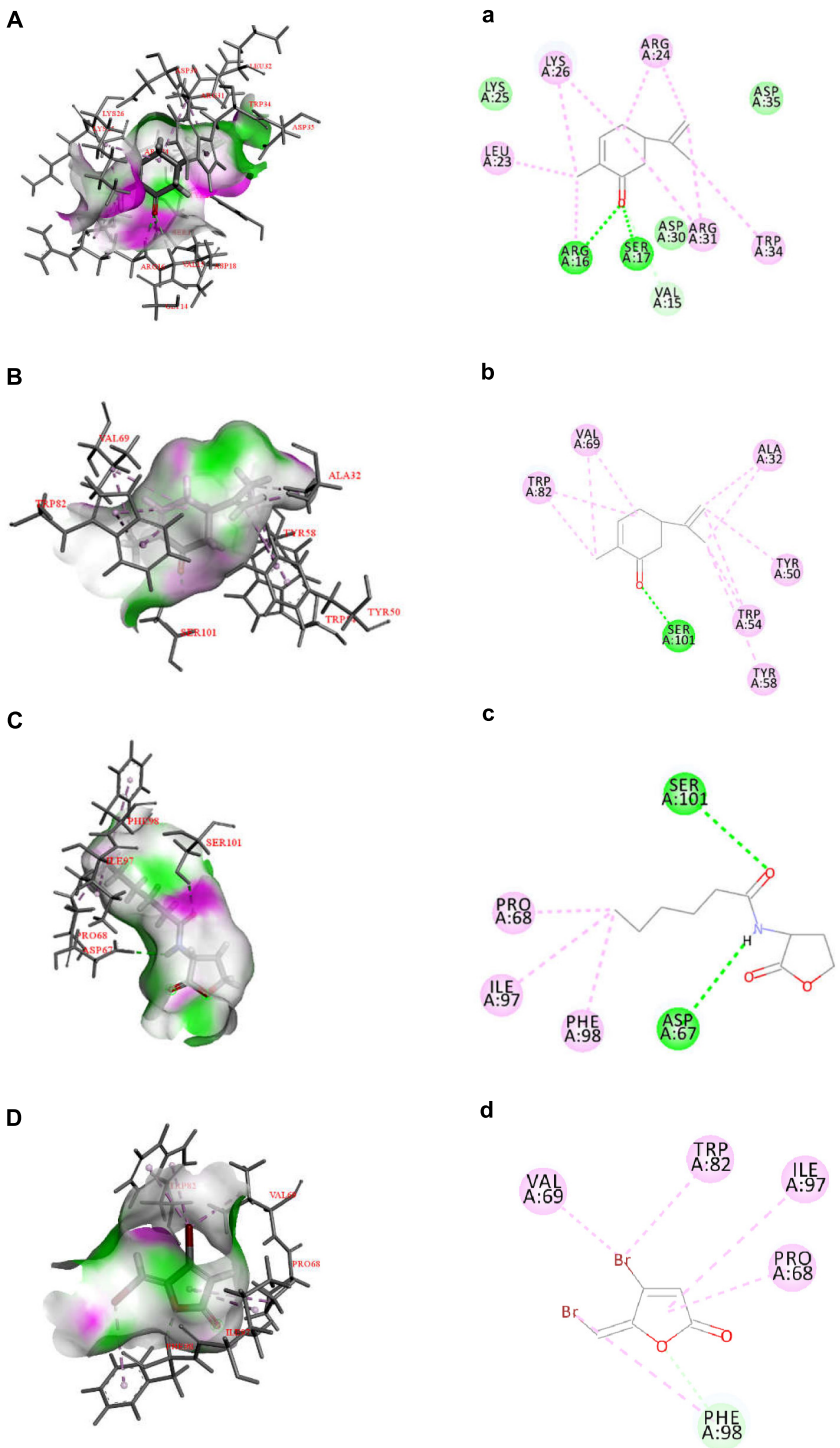

FIGURE 5 | Docked interactions of the native ligand C_6-HSL and compounds L-carvone as well as halogenated furanone C30 with the HalI and HalR protein model are shown as 2D diagrams **(A–D)** and 3D diagrams **(a–d)**. The key amino acids of the proteins are shown as thin sticks, ligands are shown as thick sticks, hydrogen bonds are shown as green lines, and hydrophobic forces are shown using a light violet color. Receptor surfaces were displayed as H bonds.

C. violaceum and *P. aeruginosa*, respectively, by interfering with their QS systems, and found that this inhibition was produced by its levorotary analog. Herein, for the first time, we have reported that at sub-MICs, L-carvone, a potential natural QSI, could significantly reduce biofilm formation by *H. alvei* at 28°C on polypropylene and zinc surfaces (**Table 2**

and **Figure 2**). This result was similar to those of the reports of Soumya and Oliveroverbel. A maximum inhibition of 52.41% was observed using a microplate photometer. Furthermore, *in situ* analysis of the biofilm matrix performed using SEM and LCSM was able to provide further information on the structure of the formed biofilms following different treatments (Azeredo et al., 2017). As reported by Gross (2017), biofilms were seen as 'Microbial cities' that included both infrastructure (generally embedded in polysaccharide matrixes) and social communication. CLSM and SEM images in our study clearly displayed a major disruption to this infrastructure and the reduction to the biofilm matrix (**Figure 2**). These results were similar to those of the study by Zhou et al. (2018), who found the Hordenine (a sprouting barley extract) could act as a novel QSI and inhibit biofilm formation in *P. aeruginosa*.

Quorum sensing-regulated flagellar-dependent motility (like swimming and swarming) is closely associated with biofilm formation. In addition, this motility (QS-regulated flagellar-dependent motility) is considered as a virulence factor because of its fundamental role in adhesion, colonization, and virulence expression of pathogens (Atkinson et al., 2006; Bluskadosh et al., 2013). Therefore, a decrease in motility would likely control the biofilm formation of *H. alvei* and weaken its infection ability. In the present study, treatments with L-carvone dose dependently inhibited the migration capacity of *H. alvei*. An L-carvone concentration of 0.5 μL/mL showed that the maximum inhibition levels of swimming and swarming motility were 61.49 and 74.94%, respectively. These results are consistent with those from an earlier study by Hou et al. (2017a), who demonstrated a significant inhibition of motility in *H. alvei* by the food additive dihydrocoumarin.

Due to the essential role of AHLs on the QS system, the effects of L-carvone treatment were characterized using GC-MS, and major changes in the AHL production by the *H. alvei* strain were observed. GC-MS, with the electron ionization mode, is a powerful tool for the rapid, easy, and selective determination of the AHL levels (Cataldi et al., 2004). The results indicated that L-carvone was able to significantly inhibit the production of both the primary AHLs (C_6-HSL and C_8-HSL) in *H. alvei*, especially reducing the C_6-HSL production from 2.16 to 0.16 μg/mL. Similarly, Luciardi et al. (2016) found that volatiles from food and medicinal plants could interfere with QS-mediated virulence expression in *P. aeruginosa* by reducing the biosynthesis of AHLs.

Quorum sensing in Gram-negative bacteria is predominantly controlled by LuxI/R-type proteins, which regulate the production of AHLs, expression of virulence factors, and formation of biofilms (Fuqua et al., 1994). To investigate the inhibitory mechanism of L-carvone on the QS system of *H. alvei*, relevant protein-molecular interactions were firstly evaluated by *in silico* analysis. According to the *in silico* results, we noticed high LibDock scores of the docking of L-carvone with the HalI (LuxI-type protein) and HalR (the LuxR-type protein) of *H. alvei* (**Supplementary Table S3**). In HalI, L-carvone was well embedded into a cavity in the vicinity of the active site, the key residues of which included ARG16, SER17, VAL15, ARG31, TRP34, ARG24, LYS26, and LEU23. Simultaneously, L-carvone formed three hydrogen bonds with ARG16, SER17, and VAL15 and showed a hydrophobic behavior with the other residues, as shown in **Figures 5A,a**. In HalR, L-carvone formed one hydrogen bond with SER101 and interacted with other residues (TRP82, VAL69, ALA32, TYR50, TRP54, TYR58, and SER101) via the hydrophobic effect (**Figures 5B,b**). C_6-HSL, as a positive control, formed two hydrogen bonds with SER101 and ASP67 (**Figures 5C,c**). However, the standard QSI, halogenated furanone C30, as a negative control, did not form any hydrogen bonds with HalR (**Figures 5D,d**).

The hydrogen-bonding interactions are considered to play a major role in the process where ligands dock with the LuxR-type receptor (Gerdt et al., 2015). In our study, L-carvone showed a better *in silico* affinity toward HalR than the halogenated furanone C30, because of a higher LibDock score and additional hydrogen bonds. L-carvone and C_6-HSL can form hydrogen bonds with the HalR protein at a common site, SER101, indicating a possible competitive action between them. Combined with the GC-MS results, these data confirm that the inhibitory mechanism of L-carvone on the QS system of *H. alvei* might involve the interaction of L-carvone with the HalI protein and subsequent interference of AHL biosynthesis in *H. alvei*. In addition, we also characterized the effects of L-carvone treatment using transcriptomics, and observed that the *halI* and *halR* genes were significantly downregulated in *H. alvei,* similar to the results reported in a previous research study (Zhou et al., 2018). The RT-qPCR results were consistent with those of the *in silico* analysis, which enhanced the credibility of the QS inhibitory mechanism of L-carvone.

CONCLUSION

In summary, the present study demonstrates that L-carvone had a significant inhibitory activity on the QS system by reducing the AHL-mediated production of virulence factors and biofilm formation in *H. alvei*. More specifically, L-carvone combined with the AHL synthase HalI via hydrogen bonds, which led to the disruption of AHL biosynthesis. Understanding the roles and functions of QS in food ecosystems can help in preventing the colonization of food surfaces, toxin formation, and proliferation of food-related bacteria. Therefore, L-carvone, with a QS inhibitory activity, is a promising agent for controlling foodborne pathogens and improving food safety.

AUTHOR CONTRIBUTIONS

TL and YM contributed to the conception of the study. YM performed the data analyses and wrote the manuscript. BH and XS contributed significantly to analysis and manuscript

preparation. JL helped to perform the analysis with constructive discussions. All authors contributed to manuscript revision, read and approved the submitted version.

FUNDING

This study was supported by a grant from the National Natural Science Foundation of China (No. 31471639) and the National Key R&D Program of China (Nos. 2018YFD0400601 and 2017YFD0400106).

SUPPLEMENTARY MATERIAL

The Supplementary Material for this article can be found online at: https://www.frontiersin.org/articles/10.3389/fmicb.2018.03324/full#supplementary-material

REFERENCES

Almeida, F. A., Pinto, U. M., and Vanetti, M. C. (2016). Novel insights from molecular docking of SdiA from *Salmonella enteritidis* and *Escherichia coli* with quorum sensing and quorum quenching molecules. *Microb Pathog.* 99, 178–190. doi: 10.1016/j.micpath.2016.08.024

Atkinson, S., Chang, C. Y., Sockett, R. E., Cámara, M., and Williams, P. (2006). Quorum sensing in *Yersinia enterocolitica* controls swimming and swarming motility. *J. Bacteriol.* 188, 1451–1461. doi: 10.1128/JB.188.4.1451-1461.2006

Azeredo, J., Azevedo, N. F., Briandet, R., Cerca, N., Coenye, T., Costa, A. R., et al. (2017). Critical review on biofilm methods. *Crit. Rev. Microbiol.* 43, 313–351. doi: 10.1080/1040841X.2016.1208146

Bai, A. J., and Rai, V. R. (2011). Bacterial quorum sensing and food industry. *Compr. Rev. Food Sci. F* 10, 183–193. doi: 10.1111/j.1541-4337.2011.00150.x

Benkert, P., Biasini, M., and Schwede, T. (2011). Toward the estimation of the absolute quality of individual protein structure models. *Bioinformatics* 27, 343–350. doi: 10.1093/bioinformatics/btq662

Bertoni, M., Kiefer, F., Biasini, M., Bordoli, L., and Schwede, T. (2017). Modeling protein quaternary structure of homo- and hetero-oligomers beyond binary interactions by homology. *Sci. Rep.* 7:10480. doi: 10.1038/s41598-017-09654-8

Bienert, S., Waterhouse, A., de Beer, T. A. P., Tauriello, G., Studer, G., Bordoli, L., et al. (2017). The SWISS-MODEL Repository-new features and functionality. *Nucleic Acids Res.* 45, D313–D319. doi: 10.1093/nar/gkw1132

Bluskadosh, I., Zilka, A., Yerushalmi, G., and Banin, E. (2013). The effect of pstS and phoB on quorum sensing and swarming motility in *Pseudomonas aeruginosa*. *PLoS One* 8:e74444. doi: 10.1371/journal.pone.0074444

Cataldi, T. R. I., Bianco, G., Frommberger, M., and Schmitt-Kopplin, P. (2004). Direct analysis of selected N-acyl-l-homoserine lactones by gas chromatography/mass spectrometry. *Rapid Commun. Mass. Sp.* 18, 1341–1344. doi: 10.1002/rcm.1480

Chen, T. R., Wei, Q. K., and Chen, Y. J. (2011). *Pseudomonas* spp. and hafnia alvei growth in UHT milk at cold storage. *Food Control.* 22, 697–701. doi: 10.1016/j.foodcont.2010.10.004

Choo, J. H., Rukayadi, Y., and Hwang, J. K. (2006). Inhibition of bacterial quorum sensing by *Vanilla* extract. *Lett. Appl. Microbiol.* 42, 637–641. doi: 10.1111/j.1472-765X.2006.01928.x

de Carvalho, C. C. C. R., and da Fonseca, M. M. R. (2006). Carvone: why and how should one bother to produce this terpene. *Food Chem.* 95, 413–422. doi: 10.1016/j.foodchem.2005.01.003

de la Fuente-Núñez, C., Korolik, V., Bains, M., Nguyen, U., Breidenstein, E. B., Horsman, S., et al. (2012). Inhibition of bacterial biofilm formation and swarming motility by a small synthetic cationic peptide. *Antimicrob Agents Ch.* 56:2696. doi: 10.1128/AAC.00064-12

Defoirdt, T. (2017). Quorum-sensing systems as targets for antivirulence therapy. *Trends Microbiol.* 26, 313–328. doi: 10.1016/j.tim.2017.10.005

Defoirdt, T., Brackman, G., and Coenye, T. (2013). Quorum sensing inhibitors: how strong is the evidence? *Trends Microbiol.* 21, 619–624. doi: 10.1016/j.tim.2013.09.006

Diao, W. R., Zhang, L. L., Feng, S. S., and Xu, J. G. (2014). Chemical composition, antibacterial activity, and mechanism of action of the essential oil from *Amomum kravanh*. *J. Food Protect.* 77:1740. doi: 10.4315/0362-028X.JFP-14-014

Ding, T., Li, T. T., Wang, Z., and Li, J. (2017). Curcumin liposomes interfere with quorum sensing system of *Aeromonas sobria* and in silico analysis. *Sci. Rep.* 7:8612. doi: 10.1038/s41598-017-08986-9

Fitzgerald, D. J., Stratford, M., and Narbad, A. (2003). Analysis of the inhibition of food spoilage yeasts by vanillin. *Int. J. Food Microbiol.* 86, 113–122. doi: 10.1016/S0168-1605(03)00059-X

Friedman, M., Henika, P. R., and Mandrell, R. E. (2002). Bactericidal activities of plant essential oils and some of their isolated constituents against *Campylobacter jejuni*, *Escherichia coli*, *Listeria monocytogenes*, and *Salmonella enterica*. *J. Food Protect.* 65, 1545–1560. doi: 10.4315/0362-028X-65.10.1545

Fuqua, W. C., Winans, S. C., and Greenberg, E. P. (1994). Quorum sensing in bacteria: the luxR-luxI family of cell density-responsive transcriptional regulators. *J. Bacteriol.* 176, 269–275. doi: 10.1128/jb.176.2.269-275.1994

Gerdt, J. P., Mcinnis, C. E., Schell, T. L., and Blackwell, H. E. (2015). Unraveling the contributions of hydrogen-bonding interactions to the activity of native and non-native ligands in the quorum-sensing receptor LasR. *Org. Biomol. Chem.* 13, 1453–1462. doi: 10.1039/C4OB02252A

Gross, M. (2017). Shining new light on quorum sensing. *Curr. Biol.* 27, R1293–R1296. doi: 10.1016/j.cub.2017.11.068

Hou, H. M., Jiang, F., Zhang, G. L., Wang, J. Y., Zhu, Y. H., and Liu, X. Y. (2017a). Inhibition of *Hafnia alvei* H4 biofilm formation by the food additive dihydrocoumarin. *J. Food Protection.* 80:842. doi: 10.4315/0362-028X.JFP-16-460

Hou, H. M., Zhu, Y. L., Wang, J. Y., Jiang, F., Qu, W. Y., Zhang, G. L., et al. (2017b). Characteristics of *N*-acylhomoserine lactones produced by *Hafnia alvei* H4 isolated from spoiled instant sea cucumber. *Sensors* 17:772. doi: 10.3390/s17040772

Husain, F. M., Ahmad, I., Khan, M. S., Ahmad, E., Tahseen, Q., Khan, M. S., et al. (2015). Sub-MICs of *Mentha piperita* essential oil and menthol inhibits AHL mediated quorum sensing and biofilm of Gram-negative bacteria. *Front. Microbiol.* 6:420. doi: 10.3389/fmicb.2015.00420

Ia, S. V. P., Agilandeswari, P., Musthafa, K. S., Karutha, P. S., and Veera, R. A. (2012). Antibiofilm and quorum sensing inhibitory potential of *Cuminum cyminum* and its secondary metabolite methyl eugenol against gram negative bacterial pathogens. *Food Res. Int.* 45, 85–92. doi: 10.1016/j.foodres.2011.10.022

Kennedy, J. E., Oblinger, J. L., and West, R. L. (2010). Fate of *Salmonella infantis*, *Staphylococcus aureus*, and *Hafnia alvei* in vacuum packaged beef plate pieces during refrigerated storage. *J. Food Sci.* 45, 1273–1277. doi: 10.1111/j.1365-2621.1980.tb06536.x

Kumar, N. V., Murthy, P. S., Manjunatha, J. R., and Bettadaiah, B. K. (2015). Synthesis and quorum sensing inhibitory activity of key phenolic compounds of ginger and their derivatives. *Food Chem.* 159, 451–457. doi: 10.1016/j.foodchem.2014.03.039

Leonard, C. M., Virijevic, S., Regnier, T., Combrinck, S., Jürgens, A., and Viljoen, A. M. (2010). Bioactivity of selected essential oils and some components on *Listeria monocytogenes* biofilms. *S. Afr. J. Bot.* 76, 676–680. doi: 10.1016/j.sajb.2010.07.002

Liu, Z., Pan, Y., Li, X., Jie, J., and Zeng, M. (2017). Chemical composition, antimicrobial and anti-quorum sensing activities of pummelo peel flavonoid extract. *Ind. Crop Prod.* 109, 862–868. doi: 10.1016/j.indcrop.2017.09.054

Livak, K. J., and Schmittgen, T. D. (2001). Analysis of relative gene expression data using real-time quantitative PCR and the 2-ΔΔCTmethod. *Methods* 25, 402–408. doi: 10.1006/meth.2001.1262

Luciardi, M. C., Pérez, H. M. V., Nora, M., Alicia, B., Arena, M. E., and Elena, C. (2016). Volatiles from subtropical convolvulaceae that interfere with bacterial

cell-to-cell communication as potential antipathogenic drugs. *Evid. Based. Compl. Alt.* 121, 1–8. doi: 10.1155/2016/7890260

McClean, K. H., Winson, M. K., Fish, L., Taylor, A., Chhabra, S. R., Camara, M., et al. (1997). Quorum sensing and *Chromobacterium violaceum*: exploitation of violacein production and inhibition for the detection of *N*-acylhomoserine lactones. *Microbioloy* 143, 3703–3711. doi: 10.1099/00221287-143-12-3703

Ng, W. L., and Bassler, B. L. (2009). Bacterial quorum-sensing network architectures. *Annu. Rev. Genet.* 43:197. doi: 10.1146/annurev-genet-102108-134304

Oliveroverbel, J., Barretomaya, A., Bertelsevilla, A., and Stashenko, E. E. (2014). Composition, anti-quorum sensing and antimicrobial activity of essential oils from *Lippia alba*. *Braz. J. Microbiol.* 45, 759–767. doi: 10.1590/S1517-83822014000300001

Porfírio, E. M., Melo, H. M., Pereira, A. M. G., Cavalcante, T. T. A., Gomes, G. A., de Carvalho, M. G., et al. (2017). In vitro antibacterial and antibiofilm activity of *Lippia alba* essential oil, citral, and carvone against *Staphylococcus aureus*. *Sci. World J.* 2017, 1–7. doi: 10.1155/2017/4962707

Rode, T. M., Langsrud, S., Holck, A., and Møretrø, T. (2007). Different patterns of biofilm formation in *Staphylococcus aureus* under food-related stress conditions. *Int. J. Food Microbiol.* 116, 372–383. doi: 10.1016/j.ijfoodmicro.2007.02.017

Soumya, E. A., Abdellah, H., Remmal, A., Saad, I. K., Hassan, L., and Remmal, A. (2011). In vitro activity of four common essential oil components against biofilm-producing *Pseudomonas aeruginosa*. *Res. J. Microbiol.* 6, 394–401. doi: 10.3923/jm.2011.394.401

Tan, J.-Y., Yin, W.-F., and Chan, K.-G. (2014). Quorum sensing activity of *Hafnia alvei* isolated from packed food. *Sensors* 14, 6788–6796. doi: 10.3390/s140406788

Venkadesaperumal, G., Rucha, S., Sundar, K., and Shetty, P. H. (2016). Anti-quorum sensing activity of spice oil nanoemulsions against food borne pathogens. *LWT-Food Sci. Technol.* 66, 225–231. doi: 10.1016/j.lwt.2015.10.044

Viana, E. S., Campos, M. E., Ponce, A. R., Mantovani, H. C., and Vanetti, M. C. (2009). Biofilm formation and acyl homoserine lactone production in *Hafnia alvei* isolated from raw milk. *Biol. Res.* 42, 427–436.

Vivas, J., Padilla, D., Real, F., Bravo, J., Grasso, V., and Acosta, F. (2008). Influence of environmental conditions on biofilm formation by *Hafnia alve*i strains. *Vet. Microbiol.* 129, 150–155. doi: 10.1016/j.vetmic.2007.11.007

Waterhouse, A., Bertoni, M., Bienert, S., Studer, G., Tauriello, G., Gumienny, R., et al. (2018). Swiss-model: homology modelling of protein structures and complexes. *Nucleic Acids Res.* 46, W296–W303. doi: 10.1093/nar/gky427

Zhang, Y., Kong, J., Xie, Y., Guo, Y., Cheng, Y., Qian, H., et al. (2018). Essential oil components inhibit biofilm formation in *Erwinia carotovora* and *Pseudomonas fluorescens* via anti-quorum sensing activity. *LWT-Food Sci. Technol.* 92, 133–139. doi: 10.1016/j.lwt.2018.02.027

Zhou, J. W., Luo, H. Z., Jiang, H., Jian, T. K., Chen, Z. Q., and Jia, A. Q. (2018). Hordenine, a novel quorum sensing inhibitor and anti-biofilm agent against *Pseudomonas aeruginosa*. *J. Agric. Food Chem.* 66, 1620–1628. doi: 10.1021/acs.jafc.7b05035

Zhu, J., Zhao, A., Feng, L., and Gao, H. (2016). Quorum sensing signals affect spoilage of refrigerated large yellow croaker (*Pseudosciaena crocea*) by *Shewanella baltica*. *Int. J. Food Microbiol.* 217, 146–155. doi: 10.1016/j.ijfoodmicro.2015.10.020

Conflict of Interest Statement: The authors declare that the research was conducted in the absence of any commercial or financial relationships that could be construed as a potential conflict of interest.

frontiers in Microbiology

ORIGINAL RESEARCH
published: 06 February 2019
doi: 10.3389/fmicb.2019.00188

Salinity-Mediated Increment in Sulfate Reduction, Biofilm Formation, and Quorum Sensing: A Potential Connection Between Quorum Sensing and Sulfate Reduction?

*Krishnakumar Sivakumar[1], Giantommaso Scarascia[1], Noor Zaouri[1], Tiannyu Wang[1], Anna H. Kaksonen[2] and Pei-Ying Hong[1]**

[1] Water Desalination and Reuse Center, Biological and Environmental Sciences and Engineering Division, King Abdullah University of Science and Technology, Thuwal, Saudi Arabia, [2] Land and Water, Commonwealth Scientific and Industrial Research Organization, Floreat, WA, Australia

OPEN ACCESS

Edited by:
Ana Maria Otero, University of Santiago de Compostela, Spain

Reviewed by:
Aindrila Mukhopadhyay, Lawrence Berkeley National Laboratory (DOE), United States
Xiao-Hua Zhang, Ocean University of China, China

***Correspondence:**
Pei-Ying Hong
peiying.hong@kaust.edu.sa

Specialty section:
This article was submitted to Microbial Physiology and Metabolism, a section of the journal Frontiers in Microbiology

Received: *19 October 2018*
Accepted: *23 January 2019*
Published: *06 February 2019*

Citation:
Sivakumar K, Scarascia G, Zaouri N, Wang T, Kaksonen AH and Hong P-Y (2019) Salinity-Mediated Increment in Sulfate Reduction, Biofilm Formation, and Quorum Sensing: A Potential Connection Between Quorum Sensing and Sulfate Reduction? Front. Microbiol. 10:188. doi: 10.3389/fmicb.2019.00188

Biocorrosion in marine environment is often associated with biofilms of sulfate reducing bacteria (SRB). However, not much information is available on the mechanism underlying exacerbated rates of SRB-mediated biocorrosion under saline conditions. Using *Desulfovibrio* (*D.*) *vulgaris* and *Desulfobacterium* (*Db.*) *corrodens* as model SRBs, the enhancement effects of salinity on sulfate reduction, *N*-acyl homoserine lactone (AHL) production and biofilm formation by SRBs were demonstrated. Under saline conditions, *D. vulgaris* and *Db. corrodens* exhibited significantly higher specific sulfate reduction and specific AHL production rates as well as elevated rates of biofilm formation compared to freshwater medium. Salinity-induced enhancement traits were also confirmed at transcript level through reverse transcription quantitative polymerase chain reaction (RT-qPCR) approach, which showed salinity-influenced increase in the expression of genes associated with carbon metabolism, sulfate reduction, biofilm formation and histidine kinase signal transduction. In addition, by deploying quorum sensing (QS) inhibitors, a potential connection between sulfate reduction and AHL production under saline conditions was demonstrated, which is most significant during early stages of sulfate metabolism. The findings collectively revealed the interconnection between QS, sulfate reduction and biofilm formation among SRBs, and implied the potential of deploying quorum quenching approaches to control SRB-based biocorrosion in saline conditions.

Keywords: salinity, biological sulfate reduction, biocorrosion, *Desulfovibrio vulgaris*, *Desulfobacterium corrodens*, quorum sensing inhibitors

INTRODUCTION

Limited availability of freshwater has led to the use of seawater in several industrial applications. High chloride and sulfate content in seawater coupled with biochemical reactions mediated by microorganisms accelerates the rate of biocorrosion in marine environments. Among these microorganisms, sulfate reducing bacteria (SRB) play a crucial role in biocorrosion and biofouling

through biofilm formation, hydrogen sulfide production and extracellular electron transfer (Beech et al., 2005; Kuang et al., 2007; Zhang et al., 2011; Kato, 2016; Scarascia et al., 2016).

Biocorrosion in marine environment has often been associated with SRB biofilms (Beech and Sunner, 2004). In *Desulfovibrio vulgaris* (an SRB) biofilm-associated cells, upregulation of hydrogenases and cytochrome *c*533, both of which act as electron conduits, suggest the role of SRB biofilms in microbial-induced corrosion (Pereira et al., 2011; Clark et al., 2012; Scarascia et al., 2016). Recent genomic studies have shown that *D. vulgaris* biofilm-associated cells often exhibit high levels of gene expression heterogeneity related to exopolysaccharide synthesis, histidine kinases involved in biofilm formation as well as hydrogenases and cytochromes (Zhang et al., 2007; Caffrey et al., 2008; Krumholz et al., 2015; Qi et al., 2016). Earlier studies have also reported on induction of putative formate dehydrogenases and Ech hydrogenases under saline conditions (Mukhopadhyay et al., 2006; Clark et al., 2012). Another study found that high levels of salinity (35 g/L NaCl) did not compromise the metabolic activity of carbon steel-associated SRB biofilms, which in turn exacerbated the rate of biocorrosion (De França et al., 2000). Taken together, it is hypothesized that salinity accelerates biocorrosion by inducing SRB-mediated biofilm formation and sulfate reduction at the gene expression level.

Earlier studies have already established the correlation between biofilm formation and quorum sensing (QS) (Davies et al., 1998; Hammer and Bassler, 2003; Parsek and Greenberg, 2005). It is therefore hypothesized that the increase in SRB biofilm formation and sulfate reduction in the saline environment would be associated with QS mechanisms. Previous studies have reported on the production of QS signal molecules such as *N*-acyl homoserine lactones (AHLs) [*N*-hexanoyl-homoserine lactone (C6-HSL) to *N*-dodecanoyl-homoserine lactone (C12-HSL)] by SRB species (Decho et al., 2009, 2010). Compared to other bacterial species such as *Vibrio* sp. and *Pseudomonas* sp., relatively little information is available on QS in SRB.

Extensive genomic mining of *Desulfovibrio* species mainly revealed the presence of proteins homologous to putative QS receptor proteins such as LuxR. However, since synthases were not discovered from genomic mining of SRBs, SRB-based LuxR proteins may be simply orphan receptors and hence, may or may not be involved in QS (Scarascia et al., 2016). Comprehensive genomic analysis of *Desulfovibrio* species has also revealed the presence of several two-component signal transduction systems, whose exact function in SRB biofilm formation is relatively unknown (Kawaguchi et al., 2008; Decho et al., 2010; Scarascia et al., 2016). It has been speculated that sensor histidine kinases, which dominate these signal transduction systems might be linked with cell–cell communication within SRB biofilms (Zhang et al., 2007; Rajeev et al., 2011). Hence, the exact mechanism of QS in SRBs as well as its linkage to sulfate reduction is largely unknown and it would be interesting to investigate the connection between QS, sulfate reduction and biofilm formation by SRBs under saline conditions.

To explore the connection between QS, sulfate reduction and biofilm formation by SRBs under saline conditions, *Desulfovibrio* (*D.*) *vulgaris* Hildenborough and *Desulfobacterium* (*Db.*) *corrodens* were used as model SRBs in this study. *D. vulgaris* is a well-studied SRB with its entire genome sequenced and annotated, whereas *Db. corrodens* is a highly corrosive SRB well suited to iron-rich environments, whose genome has been annotated but with no evidence on the presence of QS-based gene homologs (Bryant et al., 1977; Dinh et al., 2004; Heidelberg et al., 2004; Clark et al., 2007; Gittel et al., 2010). Both species were propagated in either saline or freshwater media in the presence of lactate and Na_2SO_4 as electron donor and acceptor, respectively. Enhanced rates of sulfate reduction, AHL production and biofilm formation by *D. vulgaris* and *Db. corrodens* were observed under saline conditions. To further understand the influence of salinity on SRB at the gene expression level, we quantified transcript levels of genes related to sulfate reduction, carbon utilization, biofilm formation-based hydrogenases and cytochromes as well as histidine kinases involved in cell–cell communication. The results demonstrated that transcript levels of all selected genes were significantly upregulated under saline conditions. Hence, salinity has a pronounced effect on sulfate reduction, biofilm formation and AHL production at genetic level by both planktonic cells and biofilms of SRB. Further, by deploying QS inhibitors, it was demonstrated that the correlation between QS and sulfate reduction displayed by SRBs is most significant during early stages of sulfate metabolism. The findings suggest that QSI could be deployed as potential biocides to inhibit SRB biofilm-mediated biocorrosion during the early phases of biofilm formation but not on mature SRB biofilm.

MATERIALS AND METHODS

Bacterial Strains, Media, and Culture Conditions

Desulfovibrio vulgaris Hildenborough (Heidelberg et al., 2004) and *Desulfobacterium corrodens* (DSM 15630) were propagated in either saline or freshwater media recommended by Leibniz Institute DSMZ, German Collection of Microorganisms and Cell Cultures. *D. vulgaris* strain used in this study harbors its 200 kbp native plasmid pDV1, whose presence has been reported to be crucial in its biofilm formation and maintenance (Clark et al., 2007). Saline medium (modified DSMZ medium 141) had the following composition (concentration in g/L) (salinity = 25.9g/L): KCl, 0.34; $MgCl_2.6H_2O$, 4.00; NH_4Cl, 0.25; $CaCl_2.2H_2O$, 0.14; K_2HPO_4, 0.14; NaCl, 20; yeast extract, 1; tryptone, 1. Dissolved ingredients were initially autoclaved and then supplemented with 5 g/L $NaHCO_3$ and 10 mL/L of DSMZ-141 vitamin solution (10×) and DSMZ-141 trace element solution (10×) from their respective filter-sterilized stock solutions (Bajracharya et al., 2015, 2017). Freshwater medium (modified DSMZ 641) had the following composition (concentration in g/L) (salinity = 4.17 g/L): $MgCl_2$, 2; K_2HPO_4, 0.50; NH_4Cl, 1; $CaCl_2$, 0.75; yeast extract, 1; tryptone, 1. The freshwater medium was autoclaved and further supplemented with 5 g/L $NaHCO_3$, 10 mL/L of DSMZ-141 vitamin solution

(10×) and 1 mL/L of SL-10 trace element solution (10×) (from DSMZ medium 503) (Kádár et al., 2003; Ünal et al., 2012). Sodium lactate and Na_2SO_4 at final respective concentrations of 20 mM (2.24 g/L) and 10 mM (1.42 g/L) were added to both media to serve as electron donor and acceptor, respectively (Bryant et al., 1977; McInerney and Bryant, 1981; Krumholz et al., 2015). The pH of the saline and freshwater media was adjusted to 7.30, and both media were filtered through 0.25 μm syringe filter prior transferring to sterile autoclaved anaerobic tubes. All the tubes were sealed with butyl rubber stoppers and then maintained under anaerobic environment by purging the media with N_2 for 10 min. Further, 0.50 g/L $Na_2S.9H_2O$ was added to saline and freshwater media inside anaerobic chamber (Coy Laboratory Products Inc., Grass Lake, MI, United States). All cultures were incubated at 30°C on a rotary shaker.

Sulfate Analysis

Sulfate concentration in extracted samples (diluted 100×) were quantified using a Dionex ICS-1600 Ion Chromatography system (Dionex Corp., Sunnyvale, CA, United States) equipped with a high-pressure pump, a sample auto-injector, a guard and separator column, a chemical suppressor, a conductivity cell and a data collection system with KOH as the eluent. Data collection and processing were regulated by software Chromeleon 7.0 (Dionex Corp., Sunnyvale, CA, United States) (Altland and Locke, 2012; Uzhel et al., 2016).

Quantification of Cell Density

Cell density of *D. vulgaris* and *Db. corrodens* propagated in saline and freshwater media were measured using Accuri C6 Flow cytometry system (BD Bioscience, Franklin Lakes, NJ, United States) using protocols described earlier (Cheng et al., 2016). Cell pellets harvested through centrifugation (12,000 × *g*, 15 min) was washed (two times) with 0.9% NaCl. Prior to flow cytometry, diluted cell suspensions (10^5–10^6 cells/mL) were stained with SYBR green (Invitrogen AG, Bazel, Switzerland), diluted 10^4-times from stock concentration (10^4-fold concentrated in DMSO) (Marie et al., 1997; Noble and Fuhrman, 1998). After staining, cells were incubated at room temperature under dark conditions for 15 min. About 50 μL of stained cells were injected at a flow rate of 35 μL/min to Accuri C6 Flow cytometry system and then excited at 488 nm to enumerate the cell density. In order to evaluate differences in morphological changes between saline and freshwater media, black spots within the flow cytometry gating region were observed. No significant change was observed, which suggested no change in morphology between saline and freshwater media.

Extraction and Quantification of Total *N*-Acyl Homoserine Lactones

For extraction of total AHLs, cell-free extracts of both SRB grown in saline and freshwater media were collected by centrifugation (12,000 × *g*, 15 min). Cell-free extracts were re-concentrated initially through lyophilization and then by resuspending the lyophilized fraction to 1/10th of the initial extracted volume in autoclaved H_2O (pH 6.7). Total AHLs were quantitatively determined using a bioassay with beta-glo (Promega, United States) as luminescence substrate (Kawaguchi et al., 2008; Decho et al., 2009). Bioluminescence assay was conducted using a flat white 96-well plate (Greiner Bio-One, Sigma-Aldrich, MI, United States). Briefly, 20 μL of samples were mixed with 80 μL of *Agrobacterium* (*A.*) *tumefaciens* NT1 biosensor prepared in AT medium (Kawaguchi et al., 2008). After incubation for 90 min at 30°C, 100 μL of Beta-Glo reagent were added into each well of the 96-well plate. After incubation for 30 min at room temperature, bioluminescence intensity of each sample was recorded using a microplate reader (TECAN M200, M200, Männedorf, Switzerland) (Kawaguchi et al., 2008; Decho et al., 2009). Biosensor *A. tumefaciens* NT1 harbors ß-galactosidase enzyme, whose expression is regulated by the presence of AHLs. Beta-galactosidase cleaves beta-glo substrate to form luciferin in the presence of AHLs, which generates luminescence (Kawaguchi et al., 2008). Each bioassay was conducted in triplicate to assess reproducibility. Different AHLs such as *N*-butanoyl-homoserine lactone (C4-HSL), *N*-hexanoyl-homoserine lactone (C6-HSL), *N*-octanoyl-homoserine lactone (C8-HSL), *N*-decanoyl-homoserine lactone (C10-HSL), *N*-dodecanoyl-homoserine lactone (C12-HSL), *N*-tetradecanoyl homoserine lactone (C14-HSL), *N*-hexadecanoyl homoserine lactone (C16-HSL) and *N*-octadecanoyl homoserine lactone (C18-HSL) were used to prepare standard curves to optimize the bioluminescence assay (**Supplementary Figure S1A**). Dominant AHLs produced by SRBs were analyzed using liquid chromatography (LC) – mass spectrometry (MS)/MS (Agilent Technologies, Santa Clara, CA, United States) using protocols described elsewhere (Ortori et al., 2011) (**Supplementary Figure S1B**). For LC-MS/MS analysis, a part of cell-free extract was mixed with equal volumes of dichloromethane. AHL extraction procedure was repeated three times, and the organic solvent was evaporated to complete dryness using anhydrous Na_2SO_4. Dried samples were re-dissolved in methanol prior to analysis (McClean et al., 1997).

Effect of Salinity on Sulfate Reduction and AHL Production

To elucidate effects of salinity on planktonic cells, *D. vulgaris* and *Db. corrodens* were propagated in saline and freshwater media using lactate and Na_2SO_4 as electron donor and electron acceptor respectively. Test conditions and media composition were as described earlier. A working volume of 22 mL was maintained in each anaerobic tube. Three biological replicates were used for each test conditions. About 1 mL of culture was extracted from anaerobic tubes every 24 h, and then centrifuged at 12,000 × *g* for 15 min. Harvested cell pellets were used to enumerate cell density with flow cytometry (Cheng et al., 2016). Cell-free supernatant was used to quantify sulfate concentration (100× diluted) and total AHLs produced, corresponding to each time interval. The effects of salinity were quantified in terms of specific sulfate reduction rate and specific AHL production rate (Fründ and Cohen, 1992; Detmers et al., 2001; Flodgaard et al., 2003; Bruhn et al., 2004). Specific sulfate reduction rate was defined in terms of total amount (μmoles) of sulfate reduced per cell per unit time

(μmoles of sulfate/cell/h), whereas specific AHL production rate was expressed in terms of the total amount (nmoles) of AHLs synthesized per cells per unit time (nmoles of AHLs/cell/h).

Effect of Salinity on Biofilm Formation

To elucidate effects of salinity on SRB biofilm formation, a static biofilm assay was conducted on *D. vulgaris* and *Db. corrodens* biofilms cultivated on a polystyrene flat bottom 96-well plate (Costar, Corning Inc., Corning, NY, United States). A total of eight biological replicates, with three technical replicates per each biological replicate, were used for this study. The biofilms were propagated using both saline and freshwater media. Biofilms were incubated at 30°C for 144 h within anaerobic chamber (Coy Laboratory Products Inc., Grass Lake, MI, United States). After 8 days, planktonic cells were removed and cells attached to the bottom of wells were washed with sterile 0.9% NaCl. Attached cells were then stained with 100 μL of 1% crystal violet (CV) reagent. After staining, cells were incubated at room temperature for 15 min. Excess CV was removed from each well, which was then air dried. Attached cells were then resuspended in 100 μL of 96% ethanol. Biofilm biomass was quantified in terms of OD_{590} using a microplate reader (SpectraMax 340PC384, Molecular Devices, CA, United States).

Reverse Transcription Quantitative Polymerase Chain Reaction (RT-qPCR)

Reverse transcription quantitative polymerase chain reaction (RT-qPCR)-based approach was selected to quantify the expression of target genes associated with sulfate utilization, carbon and energy metabolism as well as biofilm formation in *D. vulgaris*. The complete list of selected genes with their annotated functions and primers are listed in **Supplementary Table S1**. A detailed explanation for the selection of these target genes are also provided for as **Supplementary Information 1**. *D. vulgaris* biofilms were propagated in anaerobic serum bottles (working volume of 120 mL) using both saline and freshwater media, with three biological replicates each. Submerged fed-batch biofilm reactors were used to propagate biofilms on cellulose acetate (CA) coupons (5 mm × 5 mm) fastened together on a sterile 4" 22G needle (Air-Tite, Virginia Beach, VA, United States) and each reactor had three of such networks (five coupons per network) of cellulose acetate coupons. Tests were conducted in three phases, with each phase lasting for 7 days. At the end of each phase, half of the spent medium was replaced with fresh medium. At the end of the final phase, planktonic cells and CA membrane coupon-bound biofilms in the reactor were harvested separately. Briefly, coupons from each reactor were placed in 10 mL 0.9% NaCl and then individually subjected to ultrasonication at 25% amplitude with 2 s pulsating intervals for 3 min using a water-bath sonicator (Q500, Qsonica, Newton, CT, United States) (Cheng et al., 2016). Dispersed biofilm cells as well as freely suspended planktonic cells in the reactor were harvested through centrifugation (8,000 × *g*, 10 min) and used for extracting RNA after treatment with RNA protect (Qiagen, Hilden, Germany). The cell-RNA protect mixture was incubated for 5 min at room temperature and then centrifuged at 8,000 × *g* for 15 min. RNA-protected treated cell pellets were then stored at −80°C until RNA extraction. RNA extraction was performed using RNeasy Mini kits (Qiagen, Hilden, Germany) according to the manufacturer's protocol and RNA concentration was quantified using the Qubit 2.0 fluorometer (Thermo Fisher Scientific, San Jose, CA, United States) (Jumat et al., 2018). 1 μg of RNA extracts from biofilms were used as template for the synthesis of complementary DNA (cDNA) for RT-qPCR based on previously described protocols (Jumat et al., 2018). Target genes were amplified from the *D. vulgaris* genome using polymerase chain reaction (PCR). PCR products were cloned to pCR2.1 cloning vectors (Thermo Fisher Scientific, San Jose, CA, United States) and then transformed to *E. coli* TOP10 cells (Thermo Fisher Scientific, San Jose, CA, United States). The plasmids encoding each respective target gene were extracted using Plasmid Miniprep protocol (Promega, Madison, WI, United States). Based on the empirical relationship between plasmid DNA concentration, insert and vector size, the plasmid copy number was calculated. Plasmid DNA were then subjected to successive 10-fold serial dilutions to prepare the standard curve between the threshold cycle (C_T) and plasmid DNA copy number. The amplification efficiency and regression coefficient (R^2) corresponding to standard curves for each target gene are provided in **Supplementary Table S1**. The volumes of reagents used for RT-qPCR were as follows: Fast SYBR Green Master Mix (Thermo Fisher Scientific, San Jose, CA, United States), 10 μL; forward and reverse primers, 0.4 μL each; cDNA template, 1 μL and PCR grade H_2O, 8.2 μL. RT-qPCR was conducted using Applied Biosystems® QuantStudio 3 Real-Time PCR system (Thermo Fisher Scientific, San Jose, CA, United States). RT-qPCR cycle also included a melting curve analysis through an increase in temperature from 60 to 95°C for 5 s at 0.5°C interval. The copy numbers of each target gene estimated from the RT-qPCR standard curve were normalized against the single copy housekeeping gene Recombinase A *recA* (DVU1090). *recA* has displayed lower levels of gene expression heterogeneity in *D. vulgaris* biofilm growth mode, compared to other internal reference gene such as 16S rRNA (DV16SA) and glyceraldehyde 3-phosphate dehydrogenase (DVU0565), in accordance with previous studies (Zhang et al., 2007; Clark et al., 2012; Qi et al., 2014, 2016). Threshold cycle data values of *recA* extracted from *D. vulgaris* planktonic cells and biofilms are shown in **Supplementary Table S2**, and further demonstrated a low level of gene expression heterogeneity in this study.

Quantification of Extracellular Polysaccharides and Proteins

Extracellular polysaccharides and proteins (EPS) from cellulose acetate membrane coupons-attached biofilms were detached through ultrasonication in 10 mL 0.9% NaCl, as mentioned in the previous section. After ultrasonication, the suspension harboring detached cells and EPS from CA membrane coupons was centrifuged (8,000 × *g*, 10 min). 0.25 μm syringe-filtered cell-free supernatant was used for quantification of EPS using liquid chromatography with organic carbon detector (LC-OCD) model-8 (DOC-Labor, Germany) equipped with a Toyopearl

size exclusion chromatography column TSK HW50S (Tosoh, Japan) (Dimension: 250 mm × 20 mm, particle size: 20–40 μm). Polysaccharides and proteins from total EPS were fractionated and resolved using organic carbon detector (OCD) and organic nitrogen detector (OND). ChromCALC uni software was used to determine the concentration of each fraction in organic matter below the curve based on the integration of the defined area (Huber et al., 2011; Stewart et al., 2013).

Evaluation of the Impacts of Quorum Sensing Inhibitors on SRB Planktonic Cells and Biofilms

To gain a better understanding of the role of QS in events leading to biocorrosion, three quorum sensing inhibitors (QSIs), (5Z)-4-bromo-5-(bromoethylene)-3-butyl-Z(5H)-furanone (bromofuranone), 3-oxo-D12-N-(2-oxocyclohexyl) dodecanamide (3-oxo-N) and γ-aminobutyric acid (GABA) (Sigma-Aldrich, MI, United States) were added to saline medium harboring *D. vulgaris* and *Db. corrodens* planktonic cells at different concentrations. Sub-inhibitory concentrations of QSI were selected from previous studies based on the effect of QSI on growth kinetics and biofilm formation (Hentzer et al., 2003; Smith et al., 2003; Ren and Wood, 2004; Chevrot et al., 2006). QSIs were deployed at sub-inhibitory concentrations (bromofuranone, 40 μM; 3-oxo-N, 20 μM; and GABA, 1 mM) and also at concentrations higher than sub-inhibitory concentrations, as follows: Bromofuranone (μM) – 80, 120, 160; 3-oxo-N (μM) – 40, 80, 120, 160; GABA (mM) – 1, 2, 5, 10, 20, 50. Planktonic SRB cells in saline medium without the addition of any QSI were used as a control in this study. Three biological replicates were maintained for each test condition, in a working volume of 22 mL. The effects of QSI on sulfate reduction, AHL production and specific growth rate were quantified. All concentrations of QSI described above were also used for biofilms to determine their effects on SRB biofilm formation.

Statistical Analysis

All statistical assays were performed using Data Analysis tool on Microsoft Excel 2017. The degree of correlation in kinetics involving sulfate reduction, AHL production and cell density for all test conditions was measured in terms of Spearman's rank correlation coefficient. The statistical significance tests were performed using two-tailed *t*-test on Microsoft Excel 2017.

RESULTS

Salinity Enhances Biofilm Formation by *D. vulgaris* and *Db. corrodens* but Does Not Promote Growth

D. vulgaris exhibited similar specific growth rates under saline and freshwater conditions, respectively (saline, 0.17 ± 0.02/d; freshwater, 0.14 ± 0.02/d; $p = 0.15$) (**Supplementary Figure S2A**). Similar trend was also observed for *Db. corrodens* (saline, 0.17 ± 0.03/d; freshwater, 0.16 ± 0.02/d; $p = 0.32$) (**Supplementary Figure S2B**). However, salinity significantly improved biofilm formation by *D. vulgaris* and *Db. corrodens*. Under saline conditions, *D. vulgaris* produced 1.5-times higher biofilm biomass than freshwater conditions (saline, OD_{590} = 1.80 ± 0.48; freshwater, OD_{590} = 1.17 ± 0.38; $p = 7.65 \times 10^{-6}$). Similarly, salinity also enhanced biofilm biomass of *Db. corrodens* by1.6-times (saline, OD_{590} = 1.64 ± 0.43; freshwater, OD_{590} = 1.03 ± 0.18; $p = 2.77 \times 10^{-6}$). In addition, higher polysaccharide to protein ratio for both *D. vulgaris* (2.05-folds) (saline, 0.76 ± 0.11 μg/μg; freshwater, 0.37 ± 0.05 μg/μg; $p = 0.02$) and *Db. corrodens* (2.0-folds) (saline, 0.56 ± 0.01 μg/μg; freshwater, 0.28 ± 0.06 μg/μg, $p = 0.03$) biofilms was observed under saline conditions.

Salinity Enhances Sulfate Reduction by *D. vulgaris* and *Db. corrodens*

Under saline conditions, *D. vulgaris* displayed significantly higher specific sulfate reduction rate (ca. 1.4- to 2.5-times, $p < 0.05$) during early (24 h), middle (48–72 h) and late exponential phases (96–120 h) as well as stationary phase (144–168 h) (**Figure 1A**) compared to that observed under freshwater conditions. Similarly, high specific sulfate reduction rates (ca. 1.3- to 2.3-times, $p < 0.05$) were observed for *Db. corrodens* under saline conditions during exponential phases (**Figure 1B**). However, *Db. corrodens* exhibited similar specific sulfate reduction rates during stationary phase (144–168 h, $p > 0.05$) under saline and freshwater conditions (**Figure 1B**).

Salinity Increases AHL Production by *D. vulgaris* and *Db. corrodens*

In saline medium, total AHLs for *D. vulgaris* ranged from 20 to 27 nM (**Supplementary Figure S2C**) and 6 to 10 nM for *Db. corrodens* during exponential and stationary phases. This amount is higher, when compared to freshwater conditions (*D. vulgaris*, 12–14 nM; *Db. corrodens*, 4–6 nM) (**Supplementary Figures S2C,D**). Under saline conditions, *D. vulgaris* exhibited ca. three to four times higher specific AHL production rate for all growth phases as compared to freshwater conditions ($p < 0.05$, **Figure 1C**). In the case of *Db. corrodens*, an increase in specific AHL production rate by ca. 1.5- to 2-times was observed between early to mid-exponential phases in saline medium ($p < 0.05$) but the significant difference was no longer apparent in the latter growth phases (**Figure 1D**).

High Correlation Between Sulfate Reduction and AHL Production Under Saline Conditions

A higher correlation between specific sulfate reduction rate and specific AHL production rate was observed for *D. vulgaris* ($R^2 = 0.87$; $p = 0.01$) under saline conditions compared to freshwater conditions ($R^2 = 0.75$; $p = 0.01$). Similarly, *Db. corrodens* exhibited higher correlation between specific sulfate reduction rate and specific AHL production rate in saline medium ($R^2 = 0.93$; $p = 0.03$) compared to freshwater medium ($R^2 = 0.73$; $p = 0.01$). In addition, both *D. vulgaris* and *Db. corrodens* displayed a higher correlation between

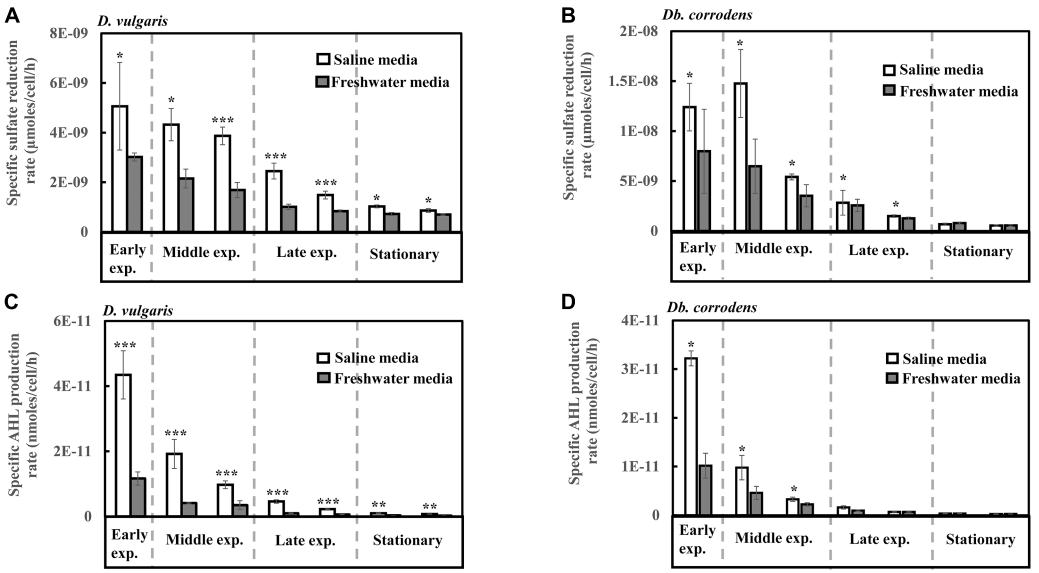

FIGURE 1 | Specific sulfate reduction and specific AHL production rates displayed by *D. vulgaris* and *Db. corrodens* in saline and freshwater media. **(A)** Specific sulfate reduction rate exhibited by *D. vulgaris* planktonic cells. **(B)** Specific sulfate reduction rate exhibited by *Db. corrodens* planktonic cells. **(C)** Specific AHL production rate exhibited by *D. vulgaris* planktonic cells. **(D)** Specific AHL production rate exhibited by *Db. corrodens* planktonic cells. Results are presented as mean ± standard deviation ($n = 3$). Significant difference: $*p < 0.05$; $**p < 0.01$; $***p < 0.001$. Early exp. corresponds to early exponential phase; Middle exp. corresponds to middle exponential phase; and Late exp. corresponds to late exponential phase.

sulfate reduction and AHL production during early and mid-exponential phase ($R^2 \geq 0.79$; $p < 0.05$) compared to late exponential and stationary phases ($R^2 \leq 0.63$; $p < 0.05$) in saline medium.

RT-qPCR Analysis Reveals an Increase in the Expression Levels of Targeted Genes Under Saline Conditions

RT-qPCR was conducted to quantify the abundance of specific genes related to sulfate reduction, carbon metabolism, hydrogenases and cytochromes, exopolysaccharide synthesis and signal response regulator in *D. vulgaris* biofilms propagated under saline and freshwater conditions. Key functions of all the respective genes are listed in **Supplementary Table S1**. Compared to freshwater conditions, expression levels of genes related to lactate metabolism like lactate dehydrogenase *ldh* (2.04-folds; $p = 0.03$) and pyruvate: ferredoxin oxidoreductase DVU3025 (2.19-folds; $p = 0.04$) were significantly upregulated under saline conditions (**Figure 2A**). High relative expression of genes involved in pyruvate and formate cycling such as pyruvate formate lyase DVU2272 (4.96-folds; $p = 0.02$) and formate dehydrogenases DVU0588 (7.71-folds; $p = 0.02$) was also detected under saline conditions (**Figure 2A**). The expression of all dissimilatory sulfite reductase subunits such as dissimilatory sulfite reductase alpha subunit *dsrA* (25-folds; $p = 0.02$), *dsrB* (1.92-folds; $p = 0.05$) and *dsrC* (2.49-folds; $p = 0.05$) was upregulated in saline conditions in *D. vulgaris* biofilms (**Figure 2B**). Although, no significant induction was detected for adenosine 5′-phosphosulfate reductase *aprA* and *aprB* ($p > 0.05$) (**Figure 2B**), sulfate adenyltransferase Sat, a key player in sulfate reduction was significantly upregulated (3.50-folds; $p = 0.03$) under saline conditions (**Figure 2B**). High abundance of periplasmic Fe hydrogenase alpha subunit *hydA* (2.73-folds; $p = 7.40 \times 10^{-5}$), NiFe hydrogenase alpha subunit *hynA*-1 (5.61-folds; $p = 2.20 \times 10^{-3}$) and NiFeSe hydrogenase *hysA*-1 (4.12-folds; $p = 0.02$) as well as Ech hydrogenases *echE* (14.88-folds; $p = 0.03$), echF (7.45-folds; $p = 0.03$) and cytochrome *c*553 DVU1817 (5.22-folds; $p = 6.30 \times 10^{-3}$) was also observed under saline conditions (**Figure 2C**). In addition, *c*3-type cytochromes harboring heme groups such as DVU3171 (5.14-folds; $p = 7.07 \times 10^{-3}$), DVU2524 (4.92-folds; $p = 8.03 \times 10^{-3}$) and DVU2809 (8.57-folds; $p = 0.04$) were also found to be significantly upregulated in the presence of salinity (**Figure 2C**). Lastly, salinity enhanced the expression of DVU0281 (3.58-folds; $p = 0.04$), which encodes for exopolysaccharide synthesis and DVU3062 (2.47-folds; $p = 9.60 \times 10^{-3}$), a histidine kinase involved in intracellular communication (**Figure 2D**). Apparently, expression of target genes was also found to be upregulated in case of *D. vulgaris* planktonic cells extracted from the biofilm reactor (**Supplementary Figure S3**).

Quorum Sensing Inhibitors Decrease Specific Growth Rates and Biofilm Formation of SRB in Saline Media

To further comprehend and establish the linkage between QS and sulfate reduction in SRB, *D. vulgaris* and *Db. corrodens* were propagated in saline media in the presence and absence of QSIs. **Figure 3** shows specific growth rate and biofilm biomass of *D. vulgaris* and *Db. corrodens* in saline medium in the presence and absence of QSI. Specific growth rate of *D. vulgaris* decreased

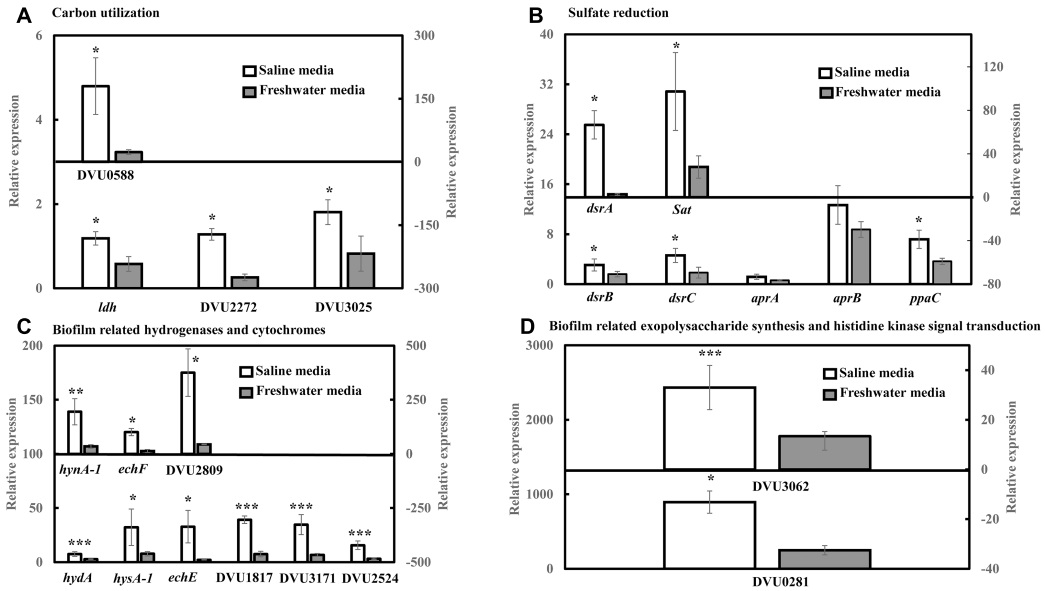

FIGURE 2 | RT-qPCR analysis of relative expression of selected genes related to carbon metabolism, sulfate reduction, electron transfer and biofilm formation in *D. vulgaris* biofilms under saline and freshwater conditions**. (A)** Relative expression of carbon metabolism enzymes lactate dehydrogenase *ldh*, pyruvate formate lyase DVU2272 and pyruvate dehydrogenase DVU3025 in the primary left *y*-axis, and formate dehydrogenase DUV0588 in the secondary right *y*-axis. **(B)** Relative expression of dissimilatory sulfite reductase *dsrB*, *dsrC*, adenosine 5′-phosphosulfate reductase *aprA*, *aprB* and pyrophosphatase *ppaC* in the primary left *y*-axis, and dissimilatory sulfite reductase alpha subunit *dsrA* and sulfate adenylytransferase *Sat* in the secondary right *y*-axis. **(C)** Relative expression of Fe hydrogenase *hydA*, NiFeSe hydrogenase *hysA*-1, Ech hydrogenases *echE*, formate dehydrogenase DVU1817and *c*3-type cytochromes DVU3171 and DVU2524 in the primary left *y*-axis, as well as NiFe hydrogenase *hynA*-1, Ech hydrogenase *echF*, and *c*3-type cytochrome DVU2809 in the secondary right *y*-axis. **(D)** Relative expression of exopolysaccharide synthesis protein DVU0281 in the primary left *y*-axis and sensor histidine kinase response regulator DVU3062 in the secondary right *y*-axis. Relative expression refers to the transcript level of a specific gene normalized with that of reference gene *recA*. Results are presented as mean ± standard deviation ($n = 3$). Significant difference: $*p < 0.05$; $**p < 0.01$; $***p < 0.001$.

significantly (ca. 1.41 to 2.65-times; $p < 0.05$) in the presence of bromofuranone ≥ 80 μM compared to the control (**Figure 3A**). The addition of 3-oxo-N ≥ 40 μM (ca. 1.72- to 2.71-times; $p < 0.05$) (**Figure 3B**) and GABA ≥ 5 mM (ca. 1.43- to 2.08-times; $p < 0.05$) (**Figure 3C**) resulted in similar decrease of specific growth rates of *D. vulgaris*. Likewise, at similar inhibitory concentrations, bromofuranone (ca. 2.35-times; $p < 0.05$), 3-oxo-N (ca. 1.33 to 2.32-times; $p < 0.05$) and GABA (ca. 1.84 to 2.70-times; $p < 0.05$) significantly decreased the specific growth rate of *Db. corrodens* (**Figure 3C**). Biofilm formation by *D. vulgaris* and *Db. corrodens* was compromised ($p < 0.05$) even at bromofuranone ≤ 40 μM, 3-oxo-N ≤ 20 μM and GABA ≤ 2 mM, as illustrated by the sharp decrease in biofilm biomass compared to control (**Figure 3**).

Quorum Sensing Inhibitors Inhibit Sulfate Reduction by SRBs in Saline Media

The effect of QSI with increasing concentrations on specific sulfate reduction rate during early, middle, late exponential and stationary phases is shown in **Figure 4**. Addition of bromofuranone ≥ 80 μM significantly decreased the specific sulfate reduction rate of *D. vulgaris* to ca. 0.52- to 0.71-times that of control ($p < 0.05$) (**Figure 4A** and **Supplementary Table S3**), while specific reduction rate of *Db. corrodens* decreased to ca. 0.72- to 0.84-times that of control ($p < 0.05$) during exponential phase (**Figure 4B** and **Supplementary Table S3**). In the presence of 3-oxo-N ≥ 40 μM, the specific sulfate reduction rate of *D. vulgaris* dropped to ca. 0.62 to 0.78-times of control ($p < 0.05$) (**Figure 4C** and **Supplementary Table S3**). The same is observed for *Db. corrodens* in the presence of 3-oxo-N during exponential phase (**Figure 4D** and **Supplementary Table S3**). Similarly, the specific sulfate reduction rate of *D. vulgaris* was ca. 0.58 to 0.83-times of control ($p < 0.05$) (**Figure 4E** and **Supplementary Table S3**) and that of *Db. corrodens* was ca. 0.60 to 0.84-times of control ($p < 0.05$) (**Figure 4F** and **Supplementary Table S3**) when exposed to GABA ≥ 5 mM. During stationary phase, decrease in specific sulfate reduction rate displayed by QSI-treated *D. vulgaris* and *Db. corrodens* was marginal (ca. 0.75- to 0.95-times of control; $p > 0.05$) compared to exponential phase (**Figure 4** and **Supplementary Table S3**).

Quorum Sensing Inhibitors Inhibit AHL Production by SRBs in Saline Media

Addition of bromofuranone (≥80 μM), 3-oxo-N (≥40 μM), and GABA (≥5 mM) to *D. vulgaris* reduced the specific AHL production rate to ca. 0.2- to 0.40-times of control during middle and late-exponential phases ($p < 0.05$) and to ca. <0.25-times of control during stationary phase ($p < 0.05$) (**Figures 5A,C,E** and **Supplementary Table S4**). Similarly, bromofuranone (≥80 μM), 3-oxo-N (≥40 μM) and GABA (>5 mM) considerably decreased

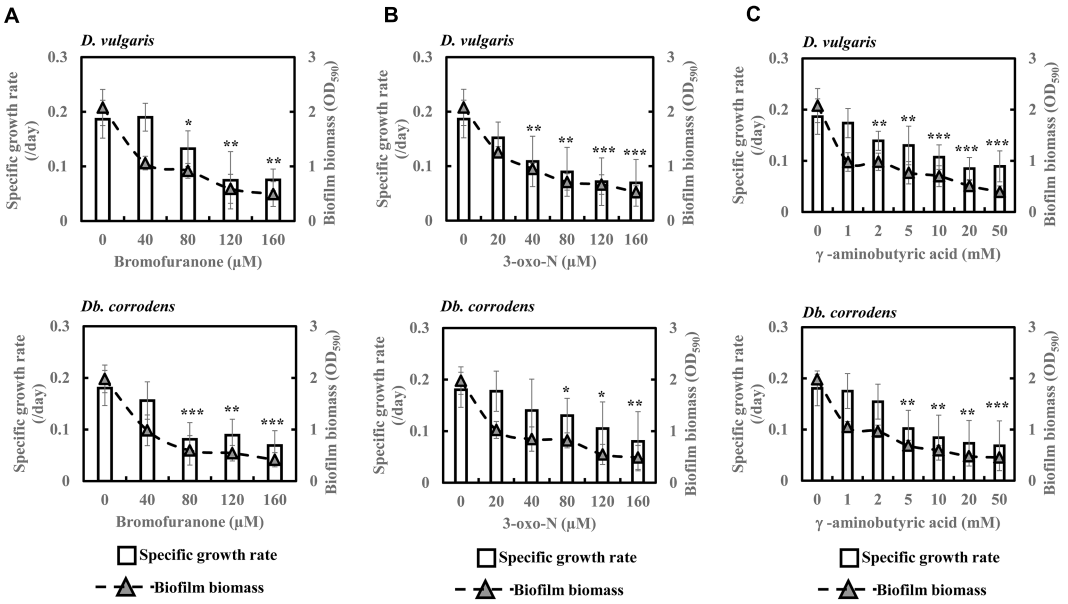

FIGURE 3 | Quorum sensing inhibitors (QSIs) and the effect on specific growth rate and biofilm formation of *D. vulgaris* and *Db. corrodens* in saline media. **(A)** Effect of bromofuranone on specific growth rate and biofilm formation of *D. vulgaris* (upper panel) and *Db. corrodens* (lower panel). **(B)** Effect of 3-oxo-N on specific growth rate and biofilm formation of *D. vulgaris* (upper panel) and *Db. corrodens* (lower panel). **(C)** Effect of γ-aminobutyric acid (GABA) on specific growth rate and biofilm formation of *D. vulgaris* (upper panel) and *Db. corrodens* (lower panel). Bar chart illustrates specific growth rate plot and dotted line scatter plot illustrates biofilm biomass plot. Results are presented as mean ± standard deviation ($n = 3$). Significant difference in specific growth rate: $^*p < 0.05$; $^{**}p < 0.01$; $^{***}p < 0.001$.

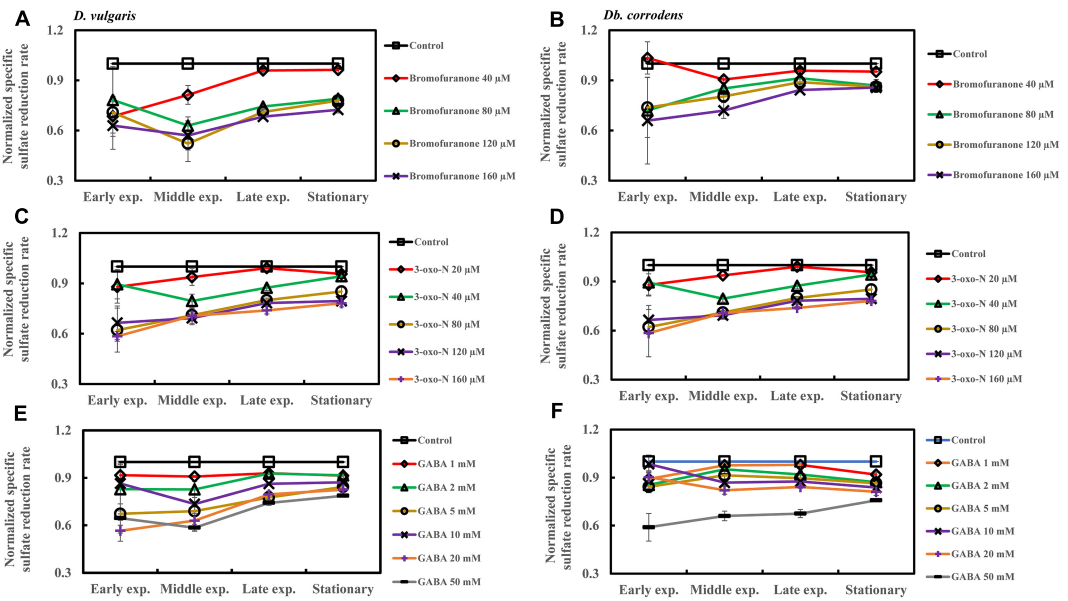

FIGURE 4 | Quorum sensing inhibitors (QSIs) and the effect on sulfate reduction by *D. vulgaris* and *Db. corrodens* in saline media. Specific sulfate reduction rate of QSI-treated *D. vulgaris* and *Db. corrodens* in saline medium was normalized with that of control (no QSI added) and plotted along *y*-axis. **(A)** Effect of bromofuranone on specific sulfate reduction rate exhibited by *D. vulgaris* planktonic cells in saline medium. **(B)** Effect of bromofuranone on specific sulfate reduction rate exhibited by *Db. corrodens* planktonic cells in saline medium. **(C)** Effect of 3-oxo-N on specific sulfate reduction rate exhibited by *D. vulgaris* planktonic cells in saline medium. **(D)** Effect of 3-oxo-N on specific sulfate reduction rate exhibited by *Db. corrodens* planktonic cells in saline medium. **(E)** Effect of γ-aminobutyric acid (GABA) on specific sulfate reduction rate exhibited by *D. vulgaris* planktonic cells in saline medium. **(F)** Effect of GABA on specific sulfate reduction rate exhibited by *Db. corrodens* planktonic cells in saline medium. Results are presented as mean ± standard deviation ($n = 3$). Early exp. corresponds to early exponential phase; Middle exp. corresponds to middle exponential phase; Late exp. corresponds to late exponential phase.

the specific AHL production rate of *Db. corrodens* during middle and late exponential phases (ca. <0.50-times of control; $p < 0.05$) and stationary phase (ca. <0.40-times of control; $p < 0.05$) (**Figures 5B,D,F** and **Supplementary Table S4**).

Increasing concentrations of QSIs (bromofuranone $\geq$ 80 μM; 3-oxo-N $\geq$ 40 μM and GABA $\geq$ 5 mM) decreased the overall correlation (R^2) between specific sulfate reduction rate and specific AHL production rate from 0.87 to 0.57–0.78 for *D. vulgaris* ($p < 0.05$) and to 0.54–0.73 for *Db. corrodens* ($p < 0.05$). Likewise, QSIs also decreased the correlation between specific sulfate reduction rate and specific AHL production rate during early and mid-exponential phases from 0.79 to a range of 0.27–0.56. This decrease in correlation was more apparent in the exponential phases compared to that observed during stationary phase.

DISCUSSION

Salinity is a key factor regulating the corrosion potential of a particular matrix. Increasing levels of salinity shifts corrosion potential in negative direction and hence, is often accompanied with increase in corrosion rates (Mansfeld et al., 2002). At the same time, saline environment favors the proliferation of SRBs such as *D. vulgaris* and *Db. corrodens* because of their ability to tolerate high salt stress (Lovley and Phillips, 1994; Blessing et al., 2001; Mukhopadhyay et al., 2006). An earlier study reported an increase in SRB cell numbers when salinity was increased from 13 g/L to 35 g/L, and a decline in SRB numbers as salinity increased further from 35 g/L to 80 g/L (hypersaline range). Coincidentally, biocorrosion rate was also highest when salinity was 35 g/L and when SRB were most abundant (De França et al., 2000). However, the earlier study only reported the overall sulfate reduction rates and did not normalize against cell numbers to obtain the specific sulfate reduction rates that would be more indicative of the sulfate reduction activity per cell.

In this study, it was first observed that the biofilm formation by *D. vulgaris* and *Db. corrodens* was higher in saline media than in freshwater media even though the specific growth rates of both SRB in both media were similar. It was then observed that the specific sulfate reduction rates were also higher in the saline media than in the freshwater media (**Figures 1A,B**), and that the higher specific sulfate reduction rate was accounted for by a higher expression of sulfate reduction genes in the saline media than in the freshwater media (**Figure 2**).

Although the mechanisms triggering the increased expression of sulfate reduction genes under saline conditions are not known, we infer that certain genes with possible dual roles in salinity tolerance and sulfate reduction were triggered by salinity. For example, oxidoreductases are often reported to be regulated by increasing saline content in media since oxidoreductases either serve as sensors or contribute to bacterial tolerance under saline environments (Bhatt and Weingart, 2008; Pumirat et al., 2010). Based on previous studies, the expression levels of NADH-dependent oxidoreductases such as lactate dehydrogenase, formate dehydrogenase, and succinate dehydrogenase were upregulated under saline conditions (Fu et al., 1989; Weerakoon et al., 2009; Pumirat et al., 2014). This corroborates with the finding of this study related to the upregulation of lactate dehydrogenase *ldh*, formate dehydrogenase DVU0588 and DVU1817 and pyruvate dehydrogenase DVU3025 by *D. vulgaris* biofilm cells under saline conditions. The increased expression of *ldh* and DVU3025 under saline conditions can subsequently lead to improved electron flow and overall metabolic activity (Heidelberg et al., 2004; Keller and Wall, 2011). Furthermore, sulfate reductive enzymes have been reported to be highly dependent on carbon metabolism genes (Pereira et al., 2008; Keller and Wall, 2011). This might explain the increase in specific sulfate reduction rates of *D. vulgaris* in saline media compared to freshwater media.

In addition, the upregulation of Ech hydrogenases as well as *c*3-type cytochromes likely suggest an improved electron flow within *D. vulgaris* under saline environment. The induction of formate dehydrogenases and Ech hydrogenases under saline conditions is consistent with that reported by earlier studies (Mukhopadhyay et al., 2006; Clark et al., 2012). It is therefore inferred that salinity elevates the expression of carbon metabolism enzymes and electron transfer machinery within SRB, which in turn leads to enhanced specific sulfate reduction rates as observed in this study and indirectly accelerating rates of SRB-mediated biocorrosion in seawater environments.

Coincidentally, the increase in both biofilm formation and specific sulfate reduction rates in both SRB species were observed along with an increase in the specific AHL production rates (**Figures 1C,D**), suggesting a potential connection between AHL and sulfate reduction. This is especially so during the early and mid-exponential phases, likely when carbon metabolism of SRBs is most active. Previous studies have demonstrated the production of AHLs by SRB (Decho et al., 2009) but their exact role within SRB was not elucidated. Signal molecules extracted from SRB within microbial mats have been implicated to be the driving force for metabolic activities and interspecies interactions within microbial mats (Decho et al., 2009, 2010) but no prior studies have demonstrated the inter-connection between AHL production, biofilm formation and sulfate reduction.

This study has demonstrated a potential link between AHL production, biofilm formation and sulfate reduction among SRBs under saline conditions. To an extent, enhanced expression of biofilm related genes and sulfate reductive enzymes under saline conditions allude toward interconnection between QS and sulfate reduction at transcriptomic level. However, the choice of biofilm related genes considered for this study might be limited to underpin the nature of this interconnection at molecular level. Based on our findings, it could be speculated that addition of AHLs extracted from SRBs might improve the overall specific sulfate reduction rate by *D. vulgaris* and *Db. corrodens*. Further studies that monitor the effects of exogenously added AHLs on sulfate reduction, possibly using transcriptomics approaches, could provide a more comprehensive means to establish the nature of interconnection between QS and sulfate reduction among SRBs.

Nevertheless, this study attempts to further verify the connection between AHL and sulfate reduction by applying QSI at varying concentrations. A decrease in specific sulfate reduction

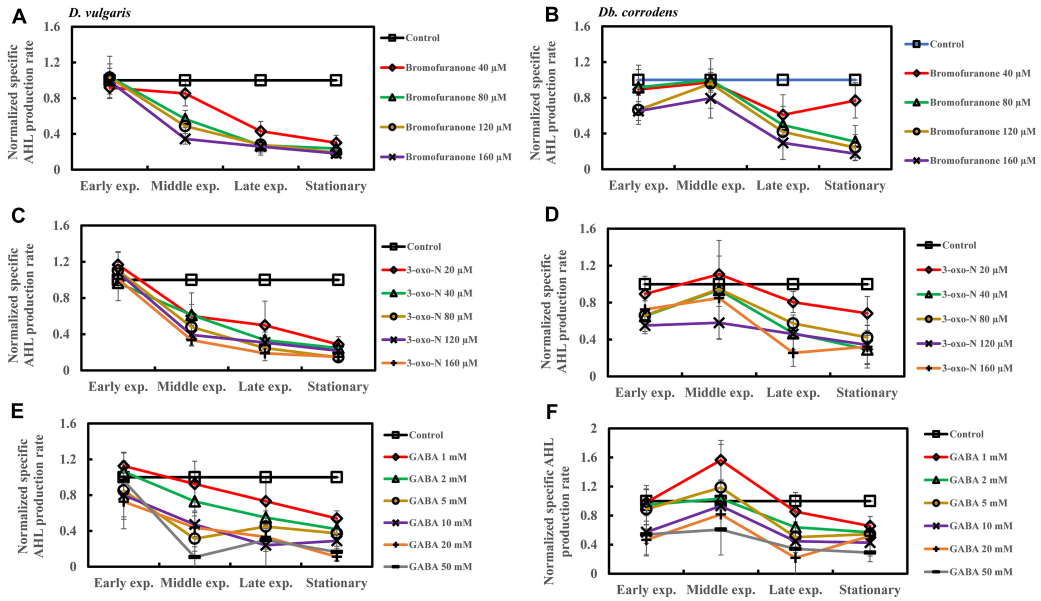

FIGURE 5 | Quorum sensing inhibitors (QSIs) and the effect on AHL production by *D. vulgaris* and *Db. corrodens* in saline media. Specific AHL production rate of QSI-treated *D. vulgaris* and *Db. corrodens* in saline medium was normalized with that of control (no QSI added) and plotted along *y*-axis. **(A)** Effect of bromofuranone on specific AHL production rate exhibited by *D. vulgaris* planktonic cells in saline medium. **(B)** Effect of bromofuranone on specific AHL production rate by *Db. corrodens* planktonic cells in saline medium. **(C)** Effect of 3-oxo-N on specific AHL production rate exhibited by *D. vulgaris* planktonic cells in saline medium. **(D)** Effect of 3-oxo-N on specific AHL production rate exhibited by *Db. corrodens* planktonic cells in saline medium. **(E)** Effect of γ-aminobutyric acid (GABA) on specific AHL production rate exhibited by *D. vulgaris* planktonic cells in saline medium. **(F)** Effect of GABA on specific AHL production rate exhibited by *Db. corrodens* planktonic cells in saline medium. Results are presented as mean ± standard deviation (n = 3). Early exp. corresponds to early exponential phase; Middle exp. corresponds to middle exponential phase; Late exp. corresponds to late exponential phase.

rates was observed during the exponential phase of SRB (**Figure 4** and **Supplementary Table S3**). This reduction in specific sulfate reduction rate was also accompanied by a considerable decline in both specific AHL production rate (**Figure 5** and **Supplementary Table S4**) and biofilm formation (**Figure 3**). The effect imposed by QSI was however not apparent during the late exponential or stationary phase. The findings collectively suggest that QS pathway could contribute in enhancing specific sulfate reduction rates of metabolically active SRB that propagate in saline environment. However, the exact pathways modulated by the QS mechanisms remain unknown.

Previous studies have reported the use of natural or synthetic compounds in saline conditions to quench QS in bacteria such as *Vibrio* (*V.*) *harveyi*, *V. vulnificus*, *Halomonas pacific* and complex microbial community attached to reverse osmosis membrane (Shen et al., 2006; Liaqat et al., 2014; Mai et al., 2015; Santhakumari et al., 2016). In those instances, the use of QSI demonstrated strong inhibition on biofilm formation. However, those studies did not evaluate if QSI approaches would be suitable to inhibit SRBs, and the associated sulfate reduction and biocorrosion rates. This is likely due to the lack of understanding on whether QS is indeed present among SRBs (Scarascia et al., 2016) and if present, whether there is a correlation with specific sulfate reduction rates. This study demonstrated that SRB biofilms are highly susceptible to QSI application, and a consequential decrease in specific sulfate reduction rates can indeed be achieved. Hence, QSI could be deployed as potential biocides to inhibit SRB biofilm-mediated biocorrosion during the early phases of biofilm formation. The efficacy of QSI however may be low on mature SRBs and biofilm.

CONCLUSION

In summary, by using *D. vulgaris* and *Db. corrodens* as model SRBs, we showed that saline conditions significantly increase the rates of specific sulfate reduction, AHL production and biofilm formation by *D. vulgaris* and *Db. corrodens*. By deploying QSIs, a potential connection between sulfate reduction and AHL production under saline conditions was demonstrated, which is most significant during early stages of sulfate metabolism. Insights from this study revealed the interconnection between QS, sulfate reduction and biofilm formation among SRBs. Furthermore, this study showed quorum quenching molecules could be deployed as an environmentally benign approach to control SRB at the early stages of growth and biofilm formation.

AUTHOR CONTRIBUTIONS

KS designed and performed the experiments, data analysis and wrote the manuscript. GS contributed to extraction and analysis of total AHLs and sulfate reduction. TW developed the protocol for quantification and analysis of total AHLs using

bioluminescence assay and LC-MS. NZ conducted quantification of extracellular polysaccharides and proteins. AK provided advice for cultivating sulfate reducing bacteria and comments on the manuscript. P-YH conceived and designed the experiments, analysis and interpretation of data, wrote the manuscript, supervised the research, and provided reagents and materials.

FUNDING

The research reported in this publication was supported by CRG funding URF/1/2982-01-01 from King Abdullah University of Science and Technology (KAUST) awarded to P-YH.

ACKNOWLEDGMENTS

AK thanks KAUST and CSIRO Land and Water for financial support. We would also like to thank Xiang Zhao in Bioscience Core Lab, King Abdullah University of Science and Technology for technical assistance in conducting RT-qPCR.

SUPPLEMENTARY MATERIAL

The Supplementary Material for this article can be found online at: https://www.frontiersin.org/articles/10.3389/fmicb.2019.00188/full#supplementary-material

REFERENCES

Altland, J. E., and Locke, J. C. (2012). Biochar affects macronutrient leaching from a soilless substrate. *HortScience* 47, 1136–1140.

Bajracharya, S., Ter Heijne, A., Benetton, X. D., Vanbroekhoven, K., Buisman, C. J., Strik, D. P., et al. (2015). Carbon dioxide reduction by mixed and pure cultures in microbial electrosynthesis using an assembly of graphite felt and stainless steel as a cathode. *Bioresour. Technol.* 195, 14–24. doi: 10.1016/j.biortech.2015.05.081

Bajracharya, S., Yuliasni, R., Vanbroekhoven, K., Buisman, C. J., Strik, D. P., and Pant, D. (2017). Long-term operation of microbial electrosynthesis cell reducing CO2 to multi-carbon chemicals with a mixed culture avoiding methanogenesis. *Bioelectrochemistry* 113, 26–34. doi: 10.1016/j.bioelechem.2016.09.001

Beech, I. B., and Sunner, J. (2004). Biocorrosion: towards understanding interactions between biofilms and metals. *Curr. Opin. Biotechnol.* 15, 181–186. doi: 10.1016/j.copbio.2004.05.001

Beech, I. B., Sunner, J. A., and Hiraoka, K. (2005). Microbe-surface interactions in biofouling and biocorrosion processes. *Int. Microbiol.* 8, 157–168.

Bhatt, S., and Weingart, C. L. (2008). Identification of sodium chloride-regulated genes in *Burkholderia cenocepacia*. *Curr. Microbiol.* 56, 418–422. doi: 10.1007/s00284-008-9114-z

Blessing, T. C., Wielinga, B. W., Morra, M. J., and Fendorf, S. (2001). CoIIIEDTA-reduction by *Desulfovibrio vulgaris* and propagation of reactions involving dissolved sulfide and polysulfides. *Envir. Sci. Technol.* 35, 1599–1603. doi: 10.1021/es001576r

Bruhn, J. B., Christensen, A. B., Flodgaard, L. R., Nielsen, K. F., Larsen, T. O., Givskov, M., et al. (2004). Presence of acylated homoserine lactones (AHLs) and AHL-producing bacteria in meat and potential role of AHL in spoilage of meat. *Appl. Environ. Microbiol.* 70, 4293–4302. doi: 10.1128/AEM.70.7.4293-4302.2004

Bryant, M., Campbell, L. L., Reddy, C., and Crabill, M. (1977). Growth of *Desulfovibrio* in lactate or ethanol media low in sulfate in association with H2-utilizing methanogenic bacteria. *Appl. Environ. Microbiol.* 33, 1162–1169.

Caffrey, S. M., Park, H. S., Been, J., Gordon, P., Sensen, C. W., and Voordouw, G. (2008). Gene expression by the sulfate-reducing bacterium *Desulfovibrio vulgaris* hildenborough grown on an iron electrode under cathodic protection conditions. *Appl. Environ. Microbiol.* 74, 2404–2413. doi: 10.1128/AEM.02469-07

Cheng, H., Xie, Y., Villalobos, L. F., Song, L., Peinemann, K.-V., Nunes, S., et al. (2016). Antibiofilm effect enhanced by modification of 1, 2, 3-triazole and palladium nanoparticles on polysulfone membranes. *Sci. Rep.* 6:24289. doi: 10.1038/srep24289

Chevrot, R., Rosen, R., Haudecoeur, E., Cirou, A., Shelp, B. J., Ron, E., et al. (2006). GABA controls the level of quorum-sensing signal in *Agrobacterium tumefaciens*. *Proc. Nati. Acad. Sci. U.S.A.* 103, 7460–7464. doi: 10.1073/pnas.0600313103

Clark, M. E., Edelmann, R. E., Duley, M. L., Wall, J. D., and Fields, M. W. (2007). Biofilm formation in *Desulfovibrio vulgaris* Hildenborough is dependent upon protein filaments. *Environ. Microbiol.* 9, 2844–2854. doi: 10.1111/j.1462-2920.2007.01398.x

Clark, M. E., He, Z., Redding, A. M., Joachimiak, M. P., Keasling, J. D., Zhou, J. Z., et al. (2012). Transcriptomic and proteomic analyses of *Desulfovibrio vulgaris* biofilms: carbon and energy flow contribute to the distinct biofilm growth state. *BMC Genomics* 13:138. doi: 10.1186/1471-2164-13-138

Davies, D. G., Parsek, M. R., Pearson, J. P., Iglewski, B. H., Costerton, J. W., and Greenberg, E. P. (1998). The involvement of cell-to-cell signals in the development of a bacterial biofilm. *Science* 280, 295–298. doi: 10.1126/science.280.5361.295

De França, F., Ferreira, C., and Lutterbach, M. (2000). Effect of different salinities of a dynamic water system on biofilm formation. *J. Ind. Microbiol. Biotechnol.* 25, 45–48. doi: 10.1038/sj.jim.7000020

Decho, A. W., Norman, R. S., and Visscher, P. T. (2010). Quorum sensing in natural environments: emerging views from microbial mats. *Trends Microbiol.* 18, 73–80. doi: 10.1016/j.tim.2009.12.008

Decho, A. W., Visscher, P. T., Ferry, J., Kawaguchi, T., He, L., Przekop, K. M., et al. (2009). Autoinducers extracted from microbial mats reveal a surprising diversity of N-acylhomoserine lactones (AHLs) and abundance changes that may relate to diel pH. *Environ. Microbiol.* 11, 409–420. doi: 10.1111/j.1462-2920.2008.01780.x

Detmers, J., Brüchert, V., Habicht, K. S., and Kuever, J. (2001). Diversity of sulfur isotope fractionations by sulfate-reducing prokaryotes. *Appl. Environ. Microbiol.* 67, 888–894. doi: 10.1128/AEM.67.2.888-894.2001

Dinh, H. T., Kuever, J., Mußmann, M., Hassel, A. W., Stratmann, M., and Widdel, F. (2004). Iron corrosion by novel anaerobic microorganisms. *Nature* 427:829. doi: 10.1038/nature02321

Flodgaard, L. R., Christensen, A. B., Molin, S., Givskov, M., and Gram, L. (2003). Influence of food preservation parameters and associated microbiota on production rate, profile and stability of acylated homoserine lactones from food-derived *Enterobacteriaceae*. *Int. J. Food Microbiol.* 84, 145–156. doi: 10.1016/S0168-1605(02)00405-1

Fründ, C., and Cohen, Y. (1992). Diurnal cycles of sulfate reduction under oxic conditions in cyanobacterial mats. *Appl. Environ. Microbiol.* 58, 70–77.

Fu, H., Hassett, D., and Cohen, M. (1989). Oxidant stress in *Neisseria gonorrhoeae*: adaptation and effects on L-(+)-lactate dehydrogenase activity. *Infect. Immun.* 57, 2173–2178.

Gittel, A., Seidel, M., Kuever, J., Galushko, A. S., Cypionka, H., and Könneke, M. (2010). Desulfopila inferna sp. nov., a sulfate-reducing bacterium isolated from the subsurface of a tidal sand-flat. *Int. J. Syst. Evol. Microbiol.* 60, 1626–1630. doi: 10.1099/ijs.0.015644-0

Hammer, B. K., and Bassler, B. L. (2003). Quorum sensing controls biofilm formation in *Vibrio cholerae*. *Mol. Microbiol.* 50, 101–104. doi: 10.1046/j.1365-2958.2003.03688.x

Heidelberg, J. F., Seshadri, R., Haveman, S. A., Hemme, C. L., Paulsen, I. T., Kolonay, J. F., et al. (2004). The genome sequence of the anaerobic, sulfate-reducing bacterium *Desulfovibrio vulgaris* Hildenborough. *Nat. Biotechnol.* 22:554. doi: 10.1038/nbt959

Hentzer, M., Wu, H., Andersen, J. B., Riedel, K., Rasmussen, T. B., Bagge, N., et al. (2003). Attenuation of *Pseudomonas aeruginosa* virulence by quorum sensing inhibitors. *EMBO J.* 22, 3803–3815. doi: 10.1093/emboj/cdg366

Huber, S. A., Balz, A., Abert, M., and Pronk, W. (2011). Characterisation of aquatic humic and non-humic matter with size-exclusion chromatography–organic carbon detection–organic nitrogen detection (LC-OCD-OND). *Water Res.* 45, 879–885. doi: 10.1016/j.watres.2010.09.023

Jumat, M. R., Haroon, M. F., Al-Jassim, N., Cheng, H., and Hong, P.-Y. (2018). An increase of abundance and transcriptional activity for acinetobacter Junii post wastewater treatment. *Water* 10:436. doi: 10.3390/w10040436

Kádár, Z., De Vrije, T., Budde, M. A., Szengyel, Z., Réczey, K., and Claassen, P. A. (2003). Hydrogen production from paper sludge hydrolysate. *Appl. Biochem. Biotechnol.* 107, 557–566. doi: 10.1385/ABAB:107:1-3:557

Kato, S. (2016). Microbial extracellular electron transfer and its relevance to iron corrosion. *Microb. Biotechnol.* 9, 141–148. doi: 10.1111/1751-7915.12340

Kawaguchi, T., Chen, Y. P., Norman, R. S., and Decho, A. W. (2008). Rapid screening of quorum-sensing signal N-acyl homoserine lactones by an in vitro cell-free assay. *Appl. Environ. Microbiol.* 74, 3667–3671. doi: 10.1128/AEM.02869-07

Keller, K., and Wall, J. (2011). Genetics and molecular biology of the electron flow for sulfate respiration in *Desulfovibrio*. *Front. Microbiol.* 2:135. doi: 10.3389/fmicb.2011.00135

Krumholz, L. R., Bradstock, P., Sheik, C. S., Diao, Y., Gazioglu, O., Gorby, Y., et al. (2015). Syntrophic growth of *Desulfovibrio alaskensis* requires genes for H2 and formate metabolism as well as those for flagellum and biofilm formation. *Appl. Environ. Microbiol.* 81, 2339–2348. doi: 10.1128/AEM.03358-14

Kuang, F., Wang, J., Yan, L., and Zhang, D. (2007). Effects of sulfate-reducing bacteria on the corrosion behavior of carbon steel. *Electrochim. Acta* 52, 6084–6088.

Liaqat, I., Bachmann, R. T., and Edyvean, R. G. (2014). Type 2 quorum sensing monitoring, inhibition and biofilm formation in marine microrganisms. *Cur. Microbiol.* 68, 342–351. doi: 10.1007/s00284-013-0484-5

Lovley, D. R., and Phillips, E. J. (1994). Reduction of chromate by *Desulfovibrio vulgaris* and its c3 cytochrome. *Appl. Environ. Microbiol.* 60, 726–728.

Mai, T., Tintillier, F., Lucasson, A., Moriou, C., Bonno, E., Petek, S., et al. (2015). Quorum sensing inhibitors from *Leucetta chagosensis* D endy, 1863. *Lett. Appl. Microbiol.* 61, 311–317. doi: 10.1111/lam.12461

Mansfeld, F., Hsu, C. H., Sun, Z., Örnek, D., and Wood, T. K. (2002). Technical note: ennoblement—a common phenomenon? *Corrosion* 58, 187–191. doi: 10.5006/1.3279868

Marie, D., Partensky, F., Jacquet, S., and Vaulot, D. (1997). Enumeration and cell cycle analysis of natural populations of marine picoplankton by flow cytometry using the nucleic acid stain SYBR Green I. *Appl. Environ. Microbiol.* 63, 186–193.

McClean, K. H., Winson, M. K., Fish, L., Taylor, A., Chhabra, S. R., Camara, M., et al. (1997). Quorum sensing and *Chromobacterium violaceum*: exploitation of violacein production and inhibition for the detection of N-acylhomoserine lactones. *Microbiology* 143, 3703–3711. doi: 10.1099/00221287-143-12-3703

McInerney, M. J., and Bryant, M. P. (1981). Anaerobic degradation of lactate by syntrophic associations of *Methanosarcina barkeri* and *Desulfovibrio species* and effect of H2 on acetate degradation. *Appl. Environ. Microbiol.* 41, 346–354.

Mukhopadhyay, A., He, Z., Alm, E. J., Arkin, A. P., Baidoo, E. E., Borglin, S. C., et al. (2006). Salt stress in *Desulfovibrio vulgaris* Hildenborough: an integrated genomics approach. *J. Bacteriol.* 188, 4068–4078. doi: 10.1128/JB.01921-05

Noble, R. T., and Fuhrman, J. A. (1998). Use of SYBR Green I for rapid epifluorescence counts of marine viruses and bacteria. *Aquat. Microb. Ecol.* 14, 113–118. doi: 10.3354/ame014113

Ortori, C. A., Dubern, J.-F., Chhabra, S. R., Cámara, M., Hardie, K., Williams, P., et al. (2011). Simultaneous quantitative profiling of N-acyl-L-homoserine lactone and 2-alkyl-4 (1H)-quinolone families of quorum-sensing signaling molecules using LC-MS/MS. *Anal. Bioanal. Chem.* 399, 839–850. doi: 10.1007/s00216-010-4341-0

Parsek, M. R., and Greenberg, E. (2005). Sociomicrobiology: the connections between quorum sensing and biofilms. *Trends Microbiol.* 13, 27–33. doi: 10.1016/j.tim.2004.11.007

Pereira, I. A., Ramos, A. R., Grein, F., Marques, M. C., Da Silva, S. M., and Venceslau, S. S. (2011). A comparative genomic analysis of energy metabolism in sulfate reducing bacteria and archaea. *Front. Microbiol.* 2:69. doi: 10.3389/fmicb.2011.00069

Pereira, P. M., He, Q., Valente, F. M., Xavier, A. V., Zhou, J., Pereira, I. A., et al. (2008). Energy metabolism in *Desulfovibrio vulgaris Hildenborough*: insights from transcriptome analysis. *Antonie Van Leeuwenhoek* 93, 347–362. doi: 10.1007/s10482-007-9212-0

Pumirat, P., Cuccui, J., Stabler, R. A., Stevens, J. M., Muangsombut, V., Singsuksawat, E., et al. (2010). Global transcriptional profiling of *Burkholderia pseudomallei* under salt stress reveals differential effects on the Bsa type III secretion system. *BMC Microbiol.* 10:171. doi: 10.1186/1471-2180-10-171

Pumirat, P., Vanaporn, M., Pinweha, P., Tandhavanant, S., Korbsrisate, S., and Chantratita, N. (2014). The role of short-chain dehydrogenase/oxidoreductase, induced by salt stress, on host interaction of *B. pseudomallei*. *BMC Microbiol.* 14:1. doi: 10.1186/1471-2180-14-1

Qi, Z., Chen, L., and Zhang, W. (2016). Comparison of transcriptional heterogeneity of eight genes between batch *Desulfovibrio vulgaris* biofilm and planktonic culture at a single-cell level. *Front. Microbiol.* 7:597. doi: 10.3389/fmicb.2016.00597

Qi, Z., Pei, G., Chen, L., and Zhang, W. (2014). Single-cell analysis reveals gene-expression heterogeneity in syntrophic dual-culture of *Desulfovibrio vulgaris* with *Methanosarcina barkeri*. *Sci. Rep.* 4:7478. doi: 10.1038/srep07478

Rajeev, L., Luning, E. G., Dehal, P. S., Price, M. N., Arkin, A. P., and Mukhopadhyay, A. (2011). Systematic mapping of two component response regulators to gene targets in a model sulfate reducing bacterium. *Genome Biol.* 12:R99. doi: 10.1186/gb-2011-12-10-r99

Ren, D., and Wood, T. K. (2004). (5Z)-4-bromo-5-(bromomethylene)-3-butyl-2 (5H)-furanone reduces corrosion from *Desulfotomaculum orientis*. *Environ. Microbiol.* 6, 535–540. doi: 10.1111/j.1462-2920.2004.00587.x

Santhakumari, S., Kannappan, A., Pandian, S. K., Thajuddin, N., Rajendran, R. B., and Ravi, A. V. (2016). Inhibitory effect of marine cyanobacterial extract on biofilm formation and virulence factor production of bacterial pathogens causing vibriosis in aquaculture. *J. Appl. Phycol.* 28, 313–324. doi: 10.1007/s10811-015-0554-0

Scarascia, G., Wang, T., and Hong, P.-Y. (2016). Quorum sensing and the use of quorum quenchers as natural biocides to inhibit sulfate-reducing bacteria. *Antibiotics* 5:39. doi: 10.3390/antibiotics5040039

Shen, G., Rajan, R., Zhu, J., Bell, C. E., and Pei, D. (2006). Design and synthesis of substrate and intermediate analogue inhibitors of S-ribosylhomocysteinase. *J. Med. Chem.* 49, 3003–3011. doi: 10.1021/jm060047g

Smith, K. M., Bu, Y., and Suga, H. (2003). Induction and inhibition of *Pseudomonas aeruginosa* quorum sensing by synthetic autoinducer analogs. *Chem. Biol.* 10, 81–89. doi: 10.1016/S1074-5521(03)00002-4

Stewart, T. J., Traber, J., Kroll, A., Behra, R., and Sigg, L. (2013). Characterization of extracellular polymeric substances (EPS) from periphyton using liquid chromatography-organic carbon detection–organic nitrogen detection (LC-OCD-OND). *Environ. Sci. Pollut. Res.* 20, 3214–3223. doi: 10.1007/s11356-012-1228-y

Ünal, B., Perry, V. R., Sheth, M., Gomez-Alvarez, V., Chin, K.-J., and Nüsslein, K. (2012). Trace elements affect methanogenic activity and diversity in enrichments from subsurface coal bed produced water. *Front. Microbiol.* 3:175. doi: 10.3389/fmicb.2012.00175

Uzhel, A., Zatirakha, A., Shchukina, O., Smolenkov, A., and Shpigun, O. (2016). Covalently-bonded hyperbranched poly (styrene-divinylbenzene)-based anion exchangers for ion chromatography. *J. Chromatogr. A* 1470, 97–103. doi: 10.1016/j.chroma.2016.10.009

Weerakoon, D. R., Borden, N. J., Goodson, C. M., Grimes, J., and Olson, J. W. (2009). The role of respiratory donor enzymes in *Campylobacter jejuni* host colonization and physiology. *Microb. Pathog.* 47, 8–15. doi: 10.1016/j.micpath.2009.04.009

Zhang, C., Wen, F., and Cao, Y. (2011). Progress in research of corrosion and protection by sulfate-reducing bacteria. *Procedia Environ. Sci.* 10, 1177–1182. doi: 10.1016/j.proenv.2011.09.188

Zhang, W., Culley, D. E., Nie, L., and Scholten, J. C. (2007). Comparative transcriptome analysis of *Desulfovibrio vulgaris* grown in planktonic culture and mature biofilm on a steel surface. *Appl. Microbiol. Biotechnol.* 76, 447–457. doi: 10.1007/s00253-007-1014-9

Conflict of Interest Statement: The authors declare that the research was conducted in the absence of any commercial or financial relationships that could be construed as a potential conflict of interest.

frontiers in Microbiology

ORIGINAL RESEARCH
published: 14 March 2019
doi: 10.3389/fmicb.2019.00455

Novel *N*-Acyl Homoserine Lactone-Degrading Bacteria Isolated From Penicillin-Contaminated Environments and Their Quorum-Quenching Activities

Hiroyuki Kusada[1†], Yu Zhang[1,2†], Hideyuki Tamaki[1,3], Nobutada Kimura[1] and Yoichi Kamagata[1*]*

[1] Bioproduction Research Institute, National Institute of Advanced Industrial Science and Technology, Tsukuba, Japan, [2] State Key Laboratory of Environmental Aquatic Chemistry, Research Center for Eco-Environmental Sciences, University of Chinese Academy of Sciences, Chinese Academy of Sciences, Beijing, China, [3] JST ERATO Nomura Microbial Community Control Project, University of Tsukuba, Tsukuba, Japan

OPEN ACCESS

Edited by:
Tom Defoirdt,
Ghent University, Belgium

Reviewed by:
Alan W. Decho,
University of South Carolina, United States
Mikael Elias,
University of Minnesota Twin Cities, United States

***Correspondence:**
Hideyuki Tamaki
tamaki-hideyuki@aist.go.jp
Yoichi Kamagata
y.kamagata@aist.go.jp

[†] These authors have contributed equally to this work

Specialty section:
This article was submitted to Antimicrobials, Resistance and Chemotherapy, a section of the journal Frontiers in Microbiology

Received: 23 October 2018
Accepted: 20 February 2019
Published: 14 March 2019

Citation:
Kusada H, Zhang Y, Tamaki H, Kimura N and Kamagata Y (2019) Novel N-Acyl Homoserine Lactone-Degrading Bacteria Isolated From Penicillin-Contaminated Environments and Their Quorum-Quenching Activities. Front. Microbiol. 10:455. doi: 10.3389/fmicb.2019.00455

N-Acyl homoserine lactones (AHLs) are signaling molecules used in the quorum sensing (QS) of Gram-negative bacteria. Some bacteria interfere with the QS system using AHL-inactivating enzymes, commonly known as quorum-quenching (QQ) enzymes. We have recently isolated a new QQ bacterium showing high resistance to multiple β-lactam antibiotics, and its QQ enzyme (MacQ) confers β-lactam antibiotic resistance and exhibits QQ activities. This observation suggests the possibility of isolating novel QQ bacteria from β-lactam antibiotic-resistant bacteria. In this direction, we attempted to isolate penicillin G (PENG)-resistant bacteria from penicillin-contaminated river sediments and activated sludge treating penicillin-containing wastewater and characterize their QQ activities. Of 19 PENG-resistant isolates, six isolates showed high QQ activity toward a broad range of AHLs, including AHLs with 3-oxo substituents. Five of the six AHL-degraders showed AHL-acylase activity and hydrolyzed the amide bond of AHLs, whereas the remaining one strain did not show AHL-acylase activity, suggesting that this isolate may likely possess alternative degradation mechanism such as AHL-lactonase activity hydrolyzing the lactone ring of AHLs. The 16S rRNA gene sequence analysis results categorized these six AHL-degrading isolates into at least five genera, namely, *Sphingomonas* (*Alphaproteobacteria*), *Diaphorobacter* (*Betaproteobacteria*), *Acidovorax* (*Betaproteobacteria*), *Stenotrophomonas* (*Gammaproteobacteria*), and *Mycobacterium* (*Actinobacteria*); of these, *Mycobacterium* sp. M1 has never been known as QQ bacteria. Moreover, multiple β-lactam antibiotics showed high minimum inhibitory concentrations (MICs) when tested against all of isolates. These results strongly demonstrate that a wide variety of β-lactam antibiotic-resistant bacteria possess QQ activities. Although the genetic and enzymatic elements are yet unclear, this study may infer the functional and evolutionary correlation between β-lactam antibiotic resistance and QQ activities.

Keywords: β-lactam antibiotic resistance, quorum sensing, quorum quenching, AHL-acylase, AHL-lactonase

INTRODUCTION

Bacteria communicate with one another using chemical signaling molecules. The sensing of auto-inducers allows bacteria to distinguish between low and high cell population densities as well as to adjust the gene expression in response to changes in cell number. This process, termed as quorum sensing (QS), allows bacterial cells to coordinately control the gene expression in the community. *N*-Acyl homoserine lactone (AHL)-dependent QS has been known to regulate many bacterial behaviors such as virulence (Givskov et al., 1998; Lindum et al., 1998; Burr et al., 2006; Xu et al., 2006) and biofilm formation (Hammer and Bassler, 2003; Labbate et al., 2004).

Over the past decade, several studies have been directed to understand the phenomenon of quorum quenching (QQ), a signal interference process that attenuates QS systems. QQ is a typical characteristic of a variety of organisms that degrade AHLs by enzymatic reactions (Dong and Zhang, 2005). Microbial communities harbor counter constituents and exhibit mechanisms as one of their survival strategies that hinder or compete with QS bacteria. Phylogenetically diverse AHL-inactivating bacteria that belong to the phyla *Proteobacteria* (genera *Acidovorax*, *Acinetobacter*, *Achromobacter*, *Alcaligenes*, *Alteromonas*, *Agrobacterium*, *Bosea*, *Brevundimonas*, *Comamonas*, *Delftia*, *Diaphorobacter*, *Klebsiella*, *Mesorhizobium*, *Ochrobactrum*, *Pseudomonas*, *Ralstonia, Roseomonas*, *Shewanella*, *Sphingomonas*, *Stenotrophomonas*, and *Variovorax*), *Bacteroidetes* (*Chryseobacterium*, *Flaviramulus*, and *Tenacibaculum*), and *Cyanobacteria* (*Nostoc*) have been isolated and characterized as QQ bacteria (Leadbetter and Greenberg, 2000; Flagan et al., 2003; Hu et al., 2003; Huang et al., 2003; Lin et al., 2003; Park et al., 2003; Uroz et al., 2003; Sio et al., 2006; Yoon et al., 2006; Romero et al., 2008, 2010; Chan et al., 2011; Christiaen et al., 2011; Mahmoudi et al., 2011; Chen et al., 2012; Wang et al., 2012; Zhang et al., 2013; Torres et al., 2016; Kusada et al., 2017). Furthermore, Gram-positive bacteria within the phyla, *Actinobacteria* (*Arthrobacter*, *Microbacterium*, *Nocardioides*, *Rhodococcus*, *Staphylococcus*, and *Streptomyces*), *Deinococcus-Thermus* (*Deinococcus*), and *Firmicutes* (*Bacillus* and *Solibacillus*) have been found to exhibit QQ activities, indicating that phylogenetically diverse bacteria may quench the AHL-based QS (Dong et al., 2000; Lee et al., 2002; Park et al., 2003; Uroz et al., 2003; d'Angelo-Picard et al., 2005; Wang et al., 2010; Morohoshi et al., 2012; Koch et al., 2014; Chan et al., 2015).

To date, two different types of QQ enzymes have been identified, namely, AHL-lactonase and AHL-acylase. In the earliest study, AHL-lactonase gene (*aiiA*) from *Bacillus* species strain 240B1 was cloned and shown to encode the lactonase enzyme that hydrolyzes the ester bond of the lactone ring to produce acyl homoserine (**Figure 1A**) (Dong et al., 2000). On the other hand, *Variovorax paradoxus* strain was found to degrade AHLs by an acylase, wherein the amide bond between the homoserine lactone (HSL) ring and the acyl chain was cleaved to release HSL and fatty acid (**Figure 1B**) (Leadbetter and Greenberg, 2000). Database retrieval by Kalia et al. (2011) for homologs of the characterized AHL-lactonases and -acylases in complete bacterial genomes have shown that the relatives of these enzymes are widespread in a diverse array of organisms, suggestive of the ubiquity of QQ systems in natural microbial communities (Kalia et al., 2011).

We have recently isolated a novel AHL-degrading bacterium, *Acidovorax* sp. MR-S7, that exhibits high resistance to multiple β-lactam antibiotics (Kusada et al., 2017). Our study revealed a novel AHL-acylase (MacQ) from MR-S7 that confers β-lactam antibiotic resistance and exhibits QQ activity (Kusada et al., 2017). Therefore, we hypothesize that functionally novel and hitherto-unidentified QQ bacteria may be present among multiple β-lactam antibiotic resistant bacteria. However, very little is known about organisms that exhibit both QQ activities and β-lactam antibiotic resistance. Such microorganisms are very rare, and only two strains, *Pseudomonas aeruginosa* PAO1 and *Acidovorax* sp. MR-S7, have been reported so far. Here, we report the characterization of the QQ activity and antibiotic resistance of multiple newly isolated β-lactam antibiotic-resistant bacteria and discuss their phylogenetic relevance with other known QQ bacteria.

MATERIALS AND METHODS

Sample Description

The environmental samples were obtained from the wastewater treatment plants in the penicillin G (PENG) production facility of the North China Pharmaceutical Group Corporation (NCPGC) and the receiving river, Wangyang River in Hebei Province, China. The wastewater from the PENG production factory is discharged into the Wangyang River after biological treatment (activated sludge treatment system), including anaerobic treatment, hydrolyzation and acidification, primary aerobic treatment, and secondary aerobic treatment. The average hydraulic residence time for each unit is about 30 h. The annual output of the excess sludge from the wastewater treatment plant (WWTP), which has been in operation since the 1990s, is 1,200 tons (dry weight). The wastewater in this plant contains 80% of wastewater from PENG production and 20% wastewater from the production of other antibiotics (cefalexin [CEFL], cefadroxil [CEFD], ampicillin [AMP], and amoxicillin [AMO]). The detected concentrations of PENG for activated sludge, river water, and sediment samples were 0.076 mg/kg, 0.000031 mg/L, and no detection, respectively. These low concentrations of PENG after the treatment clearly indicate the wastewater from PENG production could be properly treated by the activated sludge treatment system, suggesting that PENG-degrading bacteria would be present in the activated sludge sample.

The activated sludge and river sediment samples were obtained from the sludge concentration tanks that collect sludge samples from all of the biological treatment reactors and Wangyang River near the WWTP discharge outlet, respectively. The samples were collected in brown glass bottles that had been successively washed with tap water, ultra-pure water, and hexane and stored at 4°C in the dark.

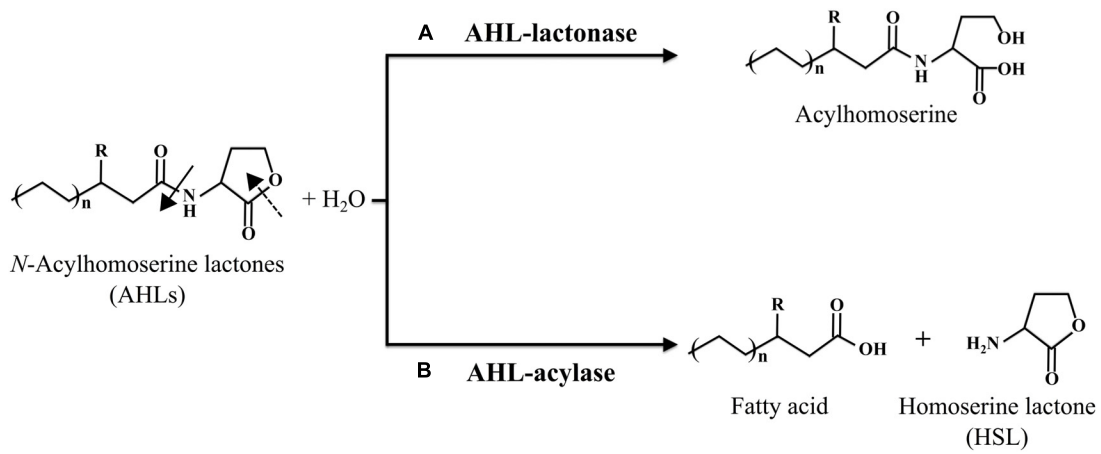

FIGURE 1 | The general structure of AHL signals and the corresponding degradation mechanisms of AHL-lactonase **(A)** and AHL-acylase **(B)**. Cleavage of the lactone ring by an AHL-lactonase enzyme (dashed arrow) yields the corresponding acyl homoserine. Cleavage of the amide bond by an AHL-acylase enzyme (filled arrow) yields the corresponding fatty acid and homoserine lactone (HSL) ring.

Isolation of Antibiotic-Resistant Bacteria Using Gellan Gum Medium

In this study, gellan gum-based media were used for the cultivation and isolation of antibiotic-resistant and AHL-degrading bacteria from the environmental samples, as gellan was found to be more effective than agar for the culturing of a diverse array of uncultured microorganisms (Tamaki et al., 2005, 2009). Activated sludge and sediment samples (500 μL) were suspended in sterile water and subjected to 10-fold serial dilutions. A series of medium plates (R2A-gellan gum) supplemented with 15, 30, 50, and 100 μg/mL of PENG were inoculated with 100-μL aliquots from different dilutions and incubated at 20°C for 4 weeks in the dark under aerobic conditions. Individual PENG-resistant colonies were purified thrice using fresh medium plates supplemented with 100 μg/mL of PENG and stored in 20% glycerol at −80°C.

The composition of R2A was as follows (per liter): 0.5 g each of yeast extract, peptone, acid hydrolysate of casein, glucose, and soluble starch; 0.3 g each of dipotassium phosphate and sodium pyruvate; and 0.05 g of magnesium sulfate. The pH values of these media were adjusted to 7.0 with 10 mM potassium phosphate buffer. The media were solidified with gellan gum (Wako, Tokyo, Japan) at a final concentration of 1.0%.

Identification and Phylogenic Analysis of Antibiotic-Resistant Isolates and AHL-Degrading Bacterial Strains

Phylogenetic identification of the antibiotic-resistant isolates was performed using the 16S rRNA gene sequencing analysis. DNA templates for polymerase chain reaction (PCR) amplification from isolates were extracted by FastDNA® Spin Kit (MP Biomedicals, Illkirch, France). The 16S rRNA genes of the isolates were PCR-amplified from the colonies using the primers 27F (5′-AGATTTGATCCTGGCTCAG-3′) and 1492R (5′-GGTTACCTTGTTACGACTT-3′). The PCR conditions included denaturation at 95°C for 9 min, followed by 40 cycles at 95°C for 1 min, 50°C for 1 min, and 72°C for 2 min. The final extension was performed at 72°C for 10 min. PCR products were purified with a MicroSpin S-400 HR column and used as templates for sequencing. Sequencing was performed with the primer 907R (5′-CCGTCAATTCMTTTGAGTTT-3′), a DTCS-Quick Start kit (Beckman Coulter, Fullerton, CA, United States), and a CEQ-2000 automated sequence analyzer (Beckman). The sequences of the resistant bacterial 16S rRNA gene clones with a range of about 500–600 bases were determined. All the 16S rRNA gene sequences of the antibiotic-resistant isolates were compared with those in the GenBank database[1] using the BLAST program (Altschul et al., 1990). For AHL-degrading bacteria, almost full 16S rRNA gene sequences (approximately 1,500 bp) were determined using primers 27F, 530F (5′-GTGCCAGCMGCCGCGG-3′), 907R, 1100F (5′-AAGTCCCGCAACGAGCGCA-3′), and 1492R. Multiple alignments of the 16S rRNA gene sequences of PENG-resistant isolates capable of degrading AHLs were performed with previously known QQ bacteria. The phylogenetic tree was constructed by neighbor-joining method using MEGA software (Tamura et al., 2011). Bootstrap values were estimated using neighbor-joining and maximum-likelihood methods (each 1,000 replications).

Bioassay of AHL-Degrading Activity

The tested AHL compounds included non-substituted C_6-HSL, C_8-HSL, C_{10}-HSL, C_{12}-HSL, and C_{14}-HSL as well as substituted 3-oxo-C_6-HSL, 3-oxo-C_8-HSL, 3-oxo-C_{10}-HSL, 3-oxo-C_{12}-HSL, and 3-oxo-C_{14}-HSL. AHL degradation assay was performed using AHL-detectable reporter (biosensor) strains, *Escherichia coli* JB525-MT102 (pJBA132) and *P. putida* F117 (pKR-C12) (Andersen et al., 2001; Steidle et al., 2001). Briefly, exogenous permeable AHL molecules bind to a LuxR-type response

[1]www.ncbi.nlm.nih.gov/BLAST

regulator protein and constitute AHL-LuxR complex within biosensor strains. The AHL-LuxR complex binds to the promoter region of a GFP reporter gene. Therefore, the degradation of AHLs by the sample could be characterized with a decrease or extinction in GFP fluorescence.

For the whole-cell assay to determine the AHL-degrading ability, 3-day cultures of the isolates were washed and re-suspended in 100 mM potassium phosphate buffer (pH 6.5). A total volume of 50 μL of the cell re-suspension and an equal volume of AHL (final concentration, 20 μM) were mixed and the mixture was incubated at 30°C in the dark with gentle agitation. The samples were treated with ultraviolet irradiation for 1 h to stop the reaction, and the reaction mixtures were diluted to an appropriate concentration and loaded into the wells of a 96-well microtiter plate. The biosensor strains were added into each well and the response of the biosensors after 4 h of incubation was analyzed with a SPECTRAmax® GEMINI XS Microplate Spectrofluorometer (Molecular Devices, Sunnyvale, CA, United States). Experiments were performed in triplicates.

Identification of AHL Degradation Metabolites

The activity of AHL-acylase was demonstrated with high-performance liquid chromatography (HPLC) analysis of the reaction mixtures containing chemically derivatized HSL rings using DANSYL chloride (5-dimethylamino-1-naphthalene sulfonyl chloride), as previously described (Lin et al., 2003). In brief, full-grown cultures of each isolate were mixed with 3 mM C_{10}-HSL and incubated at 30°C for 3 h. The digestion mixtures were extracted thrice with equal volumes of ethyl acetate, and the extracted organic phases were evaporated to dryness. The samples were re-dissolved in 200 μL of methanol, and the resulting 100 μL solutions were reacted with an equal volume of DANSYL chloride (Tokyo Chemical Industry Co., Ltd., Tokyo, Japan, 2.5 mg/mL in acetone) at 40°C for 4 h. After evaporation to dryness, 50 μL of 0.2 M HCl was added to the sample to hydrolyze any excess DANSYL chloride. For HPLC analysis, the samples were introduced onto a Develosil ODS-UG-3 column (4.6 × 150 mm, Nomura Chemicals, Aichi, Japan). Fractions were isocratically eluted with 50:50 methanol–water (v/v) at a flow rate of 0.5 mL/min (Shimadzu SPD-6AV UV-VIS spectrophotometric detector, Shimadzu C-R6A chromatopac and Shimadzu SCL-6B system controller). A control experiment was performed with phosphate-buffered saline (PBS) instead of the strain solution. Quorum-quenching bacterium *Acidovorax* sp. strain MR-S7 known to possess AHL-acylase activity (Kusada et al., 2017) and 2 mM HSL standard (Sigma) were used as positive controls.

Bioassay for AHL Production Activities

We performed the AHL production assay using GFP-based biosensor strain. In brief, the overnight culture fluids of isolates were extracted with equal volumes of ethyl acetate. The resulting liquid extractions were dispensed into the wells of a 96-well microtiter plate (Becton Dickinson, Franklin Lakes, NJ, United States) and treated with 50 μL of a fivefold-diluted overnight culture of the biosensor strain. The plate was statically incubated at 30°C for 4 h to induce detectable GFP expression from the reporter cell. *E. coli* strain (non-AHL producer) and C_{10}-HSL solution were used as the negative and positive control, respectively. Experiments were performed in triplicate for each strain.

Antibiotic Susceptibility Assay

Minimum inhibitory concentrations (MICs) of AHL-degrading bacteria were determined using microtiter plate dilution assays in R2A broth with about 1×10^5 cells/well, as previously described (Yajko et al., 1987; Riesenfeld et al., 2004). MICs were determined after 1, 2, and 3 days of incubation at 30°C in the dark. MICs were read using a Multiskan® Spectrum microplate spectrophotometer (Thermo Labsystems, Vantaa, Finland) and was defined as the lowest concentration of an antimicrobial agent at which the organism showed no visible growth (Yajko et al., 1987). *E. coli* strain EPI300™ (Epicentre, Madison, WI, United States) was used as a negative control. The criteria used for the interpretation of antimicrobial susceptibility were based upon the achievable levels of antimicrobial agents. The tested antibiotics were PENG, AMP, AMO, carbenicillin (CAR), piperacillin (PIP), CEFL, and CEFD. All these antibiotics are in common use, and the environmental samples used in the present study were polluted with wastewater from PENG, AMP, AMO, CEFL, and CEFD production. The antibiotics were tested at concentrations of 8, 16, 32, 64, 125, 250, and 500 μg/mL.

Chemicals

N-Hexanoyl-L-homoserine lactone (C_6-HSL), *N*-octanoyl-L-homoserine lactone (C_8-HSL), *N*-decanoyl-L-homoserine lactone (C_{10}-HSL), *N*-dodecanoyl-L-homoserine lactone (C_{12}-HSL), *N*-(3-oxo-hexanoyl)-L-homoserine lactone (3-oxo-C_6-HSL), *N*-(3-oxo-octanoyl)-L-homoserine lactone (3-oxo-C_8-HSL), and HSL standards were purchased from Sigma. *N*-(3-oxo-decanoyl)-L-homoserine lactone (3-oxo-C_{10}-HSL), *N*-(3-oxo-dodecanoyl)-L-homoserine lactone (3-oxo-C_{12}-HSL), and *N*-(3-oxo-tetradecanoyl)-L-homoserine lactone (3-oxo-C_{14}-HSL) were obtained from the Nottingham University in England.

Nucleotide Sequence Accession Numbers

The nucleotide sequences reported in this study were deposited in the GenBank database with accession numbers from AB646301 to AB646320.

RESULTS AND DISCUSSION

Isolation of Antibiotic-Resistant Bacteria From Penicillin-Contaminated Environmental Samples

To isolate phylogenetically diverse PENG-resistant bacteria from the environmental samples polluted with wastewater from PENG production, we used gellan gum-solidified media supplemented

TABLE 1 | Phylogenetic affiliations of microbes grown on PENG amended medium on the basis of 16S rRNA gene sequences by using the BLAST program in the GenBank database.

Taxonomic group and strains [a]	Closest species	Accession no.	Similarly (%)	Length (bp)
Alpha-proteobacteria				
S1	*Sphingomonas* sp. CC-MHH0539	KU248160	99	1240
S3	*Ochrobactrum pseudintermedium* ADV43	DQ365923	99	566
S20	*Bosea* sp. MF18	EF219051	99	556
Beta-proteobacteria				
S2	*Diaphorobacter* sp. GS-1	FJ158841	99	1489
S4	*Dechloromonas* sp. JDS6	AY084087	99	605
S5	*Dechloromonas agitata* A10	MG757543	92	568
S12	*Acidovorax temperans* Ls 4-1	KX622787	99	669
M8	*Dechloromonas* sp. Iso12-19	AB795533	99	611
M9	*Dechloromonas* sp. IsoEc.27	AB795517	96	569
M2	*Acidovorax* sp. Iso-33	KC768746	99	1488
M6	*Acidovorax* sp. Iso-33	KC768746	99	1465
M14	*Hydrogenophaga defluvii*	AM942546	98	577
Gamma-proteobacteria				
S15	*Pseudoxanthomonas kaohsiungensis* J36	AY650027	95	615
S17	*Stenotrophomonas* sp. LMG 19833	AJ300772	99	1476
M18	*Morganella morganii* FUA1245	HQ169126	98	665
M20	*Enterobacter cloacae* M380	HQ651838	97	611
M21	*Stenotrophomonas* sp. ICB209	FJ748674	98	660
Bacteroidetes				
S16	*Elizabethkingia* sp. ds13-11	HQ436416	99	598
Actinobacteria				
M1	*Mycobacterium chelonae* B14	JX010972	99	1481

[a] *S: Activated sludge; M: River sediment. As for AHL-degrading bacteria, the almost full 16S rRNA gene sequences (≈1,500 bp) were determined.*

with antibiotics (8, 16, 32, 64, 125, 250, and 500 μg/mL), as gellan was shown to be effective for cultivating phylogenetically novel and diverse bacteria (Tamaki et al., 2005, 2009). Ten and nine PENG-resistant individual colonies with characteristic morphologies and colors were isolated from the activated sludge and river sediment samples, respectively. The results of the 16S rRNA gene sequencing showed that these PENG-resistant isolates belong to at least 12 different genera across *Alphaproteobacteria*, *Betaproteobacteria*, *Gammaproteobacteria*, *Actinobacteria*, and *Bacteroidetes*. Of these, three isolates (S5, M9, and S15) showed low 16S rRNA gene sequence similarities (<97%) to any known bacterial species (**Table 1**).

Exploration of Novel AHL-Degrading Bacteria Among the PENG-Resistant Isolates

The PENG-resistant isolates were tested for QQ activity using GFP-based AHL biosensors. Based on the preliminary screening using biosensors toward 3-oxo-C_6-HSL and 3-oxo-C_{12}-HSL, six of the PENG-resistant strains exhibited AHL-degrading activity, as observed with biosensors toward 3-oxo-C_{12}-HSL after a 15 h incubation period (**Supplementary Table 1**). Thereafter, we selected the six resistant strains harboring high AHL-degrading ability (more than 50% degradation of the initial AHL) from the preliminary screening to further investigate QQ behaviors. Six isolates showed high capabilities of inactivating a broad range of AHLs, including AHLs with 3-oxo substituents. In particular, these strains exhibited higher QQ activities toward AHLs with long acyl chains than those with short acyl chains (**Table 2**).

Phylogenetic analysis based on almost full-length 16S rRNA gene sequences showed that the six QQ isolates were associated with three Gram-negative taxa, *Alphaproteobacteria* (*Sphingomonas* sp. S1), *Betaproteobacteria* (*Acidovorax* sp.

TABLE 2 | AHL-degrading behaviors of PENG resistant isolates[a].

Strain	AHL congeners								
	C_6	C_8	C_{10}	C_{12}	OC_6	OC_8	OC_{10}	OC_{12}	OC_{14}
S1	−	+++	+++	++	−	−	+	+	+
S2	−	+++	+++	++	−	++	+++	+++	+
S17	−	+++	+++	++	−	−	+++	+++	+
M1	−	+++	+++	++	−	−	+++	+++	+
M2	−	−	++	++	−	−	+++	+++	+
M6	+	−	+++	++	−	−	+++	+++	+

[a] *Biosensors for AHLs: E. coli JB525-MT102 (pJBA132) was used as s sensor strain for detecting C_6-HSL, C_8-HSL, C_{10}-HSL, C_{12}-HSL, 3-oxo-C_6-HSL (OC_6), 3-oxo-C_8-HSL (OC_8), 3-oxo-C_{10}-HSL (OC_{10}), 3-oxo-C_{12}-HSL (OC_{12}), and P. putida F117 (pKR-C12) was used for detecting 3-oxo-C_{14}-HSL (OC_{14}). The amount of remaining AHL was measured using bioassay after cultivation in a medium containing 20 μM AHL and biosensors for 4 h. The number of plus symbol relates to the amount of AHL degraded: +, 20–50% degradation of initial AHL; ++, 50–80%; +++, 80–100%.*

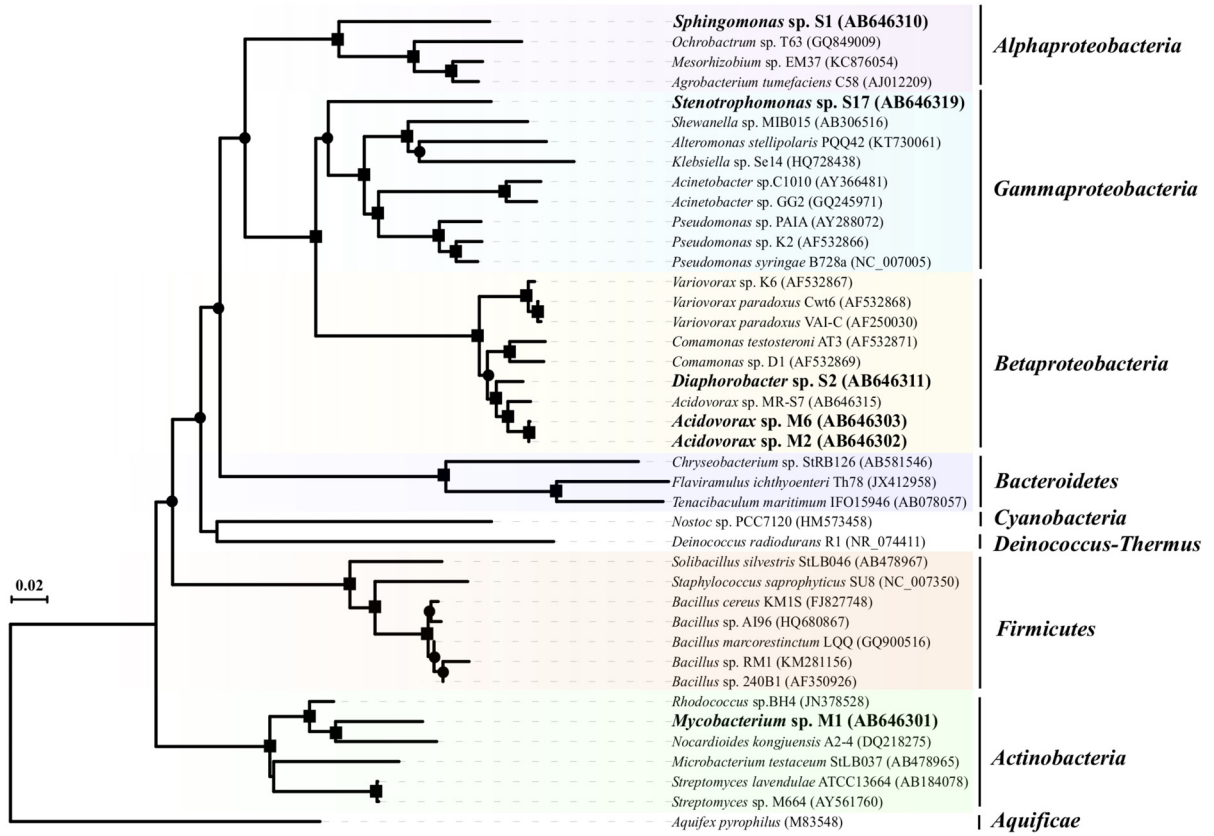

FIGURE 2 | Phylogenetic affiliations of the AHL-degrading isolates obtained in this study and the previously known AHL degraders based on their almost full length 16S rRNA gene sequences. The phylogenetic tree was constructed by neighbor-joining (NJ) method with Kimura's correction. The 16S rRNA gene sequence of *Aquifex pyrophilus* (M83548) was used as an outgroup. Bootstrap values of >50% and >80% estimated using neighbor-joining and maximum-likelihood methods (1,000 replications) are shown by circle and square at branching points, respectively. The six new AHL-degrading strains isolated in this study are shown in name with boldface.

M2, *Acidovorax* sp. M6 and *Diaphorobacter* sp. S2), and *Gammaproteobacteria* (*Stenotrophomonas* sp. S17) and one Gram-positive taxon, *Actinobacteria* (*Mycobacterium* sp. M1) (**Figure 2**). Although phylogenetically diverse QQ bacteria have been isolated so far, a Gram-positive bacterium within the genus *Mycobacterium* has never been shown to exhibit QQ activity.

To determine whether the six AHL degraders produce their own AHL isomers, a GFP-based biosensor strain was used (see method). The ethyl acetate extracts of six isolates as well as the negative control (non-AHL producer *E. coli*) showed low values of GFP fluorescence (**Supplementary Figure 1**). This result indicates that these six isolates lack the ability to produce biosensor-detectable AHL-like compounds. Although these six isolates were unable to produce AHLs, they might have the ability to sense exogenous AHLs produced by other bacteria, and the resulting QS system would enhance biofilm formation and antibiotic resistance. Indeed, our previous study demonstrated that a wide variety of exogenous AHLs induced biofilm formation of non-AHL producer, *Acidovorax* sp. strain MR-S7, and the MICs of AHL-supplemented (biofilm-forming) strain MR-S7 showed 5–10 folds higher resistance to various antibiotics (Kusada et al., 2014). Most human infections are localized within biofilms, where QS signaling is much more efficient due to localization of AHLs. The genetic information of these isolates (e.g., *luxR* gene encoding the AHL-responsive transcriptional regulator) and biochemical experiments provided in the future study would further verify the effect of QS on biofilm formation and antibiotic resistance.

Identification of AHL Degradation Products

To demonstrate the AHL degradation mechanism of these six isolates, HPLC analysis was performed to detect the presence of HSL ring generated by AHL-acylase activities. To determine whether HSL was released as an AHL degradation product, samples of the reaction mixture were treated with DANSYL chloride and analyzed by HPLC. The LC retention time of DANSYL chloride was 4.19 min, whereas that of the dansylated digestion mixtures from isolates (S1, S2, S17, M2, and M6) was around 6.0 min, identical to the retention time of the standard control of dansylated HSL and the dansylated digestion mixture from *Acidovorax* sp. MR-S7

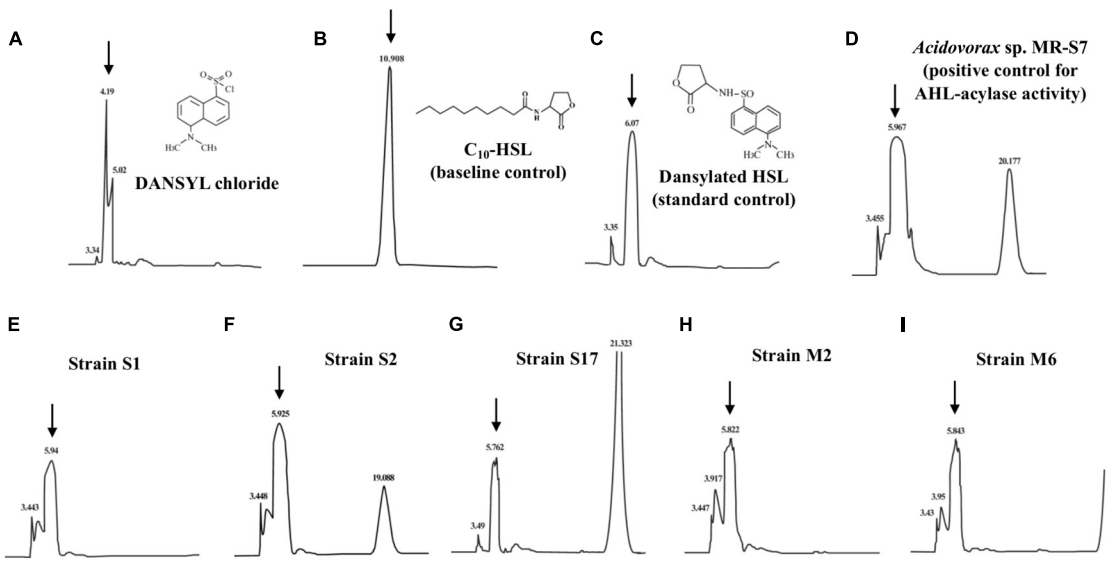

FIGURE 3 | Metabolite analysis of C_{10}-HSL degradation products by cell extract of the AHL degrading isolates. HPLC profiles of unreacted DANSYL chloride solution **(A)**, C_{10}-HSL **(B)**, dansylated HSL standard **(C)**, reaction product of C_{10}-HSL after incubation with cell extract of *Acidovorax* sp. MR-S7 **(D)**, strain S1 **(E)**, strain S2 **(F)**, strain S17 **(G)**, strain M2 **(H)**, and strain M6 **(I)**. Note that a dansylated digestion product and a dansylated HSL standard both eluted with retention time at 5.8–6.0 min.

known to degrade AHLs by AHL-acylase activity (**Figure 3** and **Supplementary Figure 2**). These results indicate that the five isolates were capable of degrading C_{10}-HSL with their AHL-acylase activities. Note that the remaining one isolate, strain M1, was able to degrade a wide range of AHLs but did not show AHL-acylase activity in the HPLC assay. This likely suggests that the strain M1 may possess the distinct degradation mechanism such as AHL-lactonase activity, though further investigation would be needed to reveal their QQ activities using purified enzymes.

β-Lactam antibiotics and AHLs are structurally similar as both compounds have ring structures and acyl side chains. In recent years, AHL-acylase enzymes were found to be also phylogenetically and structurally similar to β-lactam antibiotic resistance enzymes, β-lactam acylases. Besides, our group and other two research groups reported that AHL-acylases (MacQ, AhlM, and KcPGA) could function as β-lactam acylase, and indeed degrade PENG via hydrolysis of the amide bond (Park et al., 2005; Mukherji et al., 2014; Kusada et al., 2017). Furthermore, we recently solved the X-ray crystal structure of MacQ, and found that the degradation products of C_{10}-HSL and PENG by MacQ were commonly accommodated in the same hydrophobic active-site pocket, indicating that both compounds were hydrolyzed by MacQ in the same degradation mechanism (Yasutake et al., 2017). Perhaps, some AHL-acylases (β-lactam acylases) may have broad substrate specificity that appears to be structurally indistinguishable from both AHL-signals and β-lactam antibiotics. Further genetic and biochemical analyses of other AHL-acylases (β-lactam acylases) will be required to more fully assess the mechanism and relationships between QQ and antibiotic resistance.

β-Lactam Antibiotic Resistance Assay

We measured the MICs of seven different β-lactam antibiotics, including PENG, AMP, AMO, CAR, PIP, CEFL, and CEFD, toward the six AHL-degrading isolates (**Table 3**). In comparison with the control strain *E. coli* EPI300^{TM}, all of the AHL-degrading isolates displayed a high resistance profile to almost all β-lactam antibiotics examined. In addition, the comparison of the antibiotic resistance activities of the six isolates with those of the previously identified multiple β-lactam antibiotic resistant pathogens revealed that our isolates displayed comparable or even greater values of MICs to all of the seven β-lactam antibiotics tested (John and McNeill, 1980; Colom et al., 1995; Stapleton et al., 1995; Lauretti et al., 1999; Afzal-Shah et al., 2001; Dubois et al., 2002). In particular, strains S17 and M2 displayed high

TABLE 3 | Sensitivity of isolates to β-lactam antibiotics[a].

Strain	MIC (μg/ml)						
	PENG	AMP	AMO	CAR	PIP	CEFL	CEFD
S1	250	>500	250	>500	500	500	250
S2	>500	>500	500	>500	250	500	500
S17	>500	>500	>500	>500	>500	>500	>500
M1	125	>500	64	>500	>500	250	125
M2	>500	>500	>500	>500	>500	>500	>500
M6	500	>500	500	500	250	32	8
E. coli EPI300	32	16	8	16	8	16	16

[a] *Penicillin G (PENG); ampicillin (AMP); amoxicillin (AMO); carbenicillin (CAR); piperacillin (PIP); cefalexin (CEFL); cefadroxil (CEFD). The MIC (minimum inhibitory concentration) was defined as the lowest concentration of antibiotics at which the organism showed no visible growth.*

abilities to resist broad types of β-lactam antibiotics. The MICs for these strains were over 500 μg/mL of PENG, AMP, AMO, CAR, PIP, CEFL, and CEFD. These values were at least 31.3- to 62.5-fold higher than the values observed for the control strain *E. coli* EPI300^{TM} (<8–16 μg/mL) (**Table 3**). Furthermore, the MICs of AMP, PIP, and CAR were over 30-fold higher for the six AHL-degrading isolates than for the control strain *E. coli* EPI300^{TM}.

In total, six AHL-degrading isolates exhibited high antibiotic resistance and broad substrate specificities toward multiple β-lactams as well as AHL isomers. The knowledge relevant to such organisms possessing both multiple β-lactam antibiotic resistance and AHL degradation activities has been limited. Two multiple β-lactam antibiotic resistant bacteria, *P. aeruginosa* PAO1 and *Acidovorax* sp. MR-S7, have been reported to be able to degrade AHLs. In comparison to *P. aeruginosa* PAO1, our six isolates showed much higher resistance to β-lactams tested (MICs of AMP, CAR, and PIP toward strain PAO1 were 256, 64, and 4 μg/mL, respectively). Given that these six isolates degrading multiple β-lactams and AHLs were found across two phyla and four classes, our findings implicate a possibility that this versatile phenotypic bi-functionality may be more broadly present in bacteria dwelling in natural ecosystems and provide new insight into the diversity of organisms that simultaneously exhibit both multiple β-lactam antibiotic resistance and QQ activities. To further clarify the functional and evolutionary correlation between β-lactam antibiotic resistance and QQ activities, studies are warranted to identify the genetic elements responsible for conferring multiple β-lactam antibiotic resistance and QQ activities.

CONCLUSION

In this study, we successfully isolated six novel QQ bacteria from β-lactam antibiotic-resistant isolates obtained from PENG-polluted environmental samples and characterized their AHL- and β-lactam antibiotic-degrading properties. This study expands the diversity of organisms that possess two different and important physiological functions, QQ activity and β-lactam antibiotic resistance. In addition, our study provides a novel screening strategy for the identification of AHL-degrading and β-lactam antibiotic-resistant bacteria previously unidentified. Taken together with previous studies, our findings provide additional evidence that AHL-degrading bacteria may be the potential multiple β-lactam antibiotic resistant candidates that have long been overlooked.

AUTHOR CONTRIBUTIONS

YZ, HT, NK, and YK conceived the study and designed experiments. HK, YZ, NK, and HT performed experiments and analyzed the data. HK, HT, NK, and YK wrote the manuscript. All authors contributed to the discussion of the results obtained in this study, and reviewed and edited the manuscript.

FUNDING

This work was supported by the Ministry of Education, Culture, Sports, Science and Technology with a JSPS fellowship. This work was also partly supported by JST ERATO Grant Number JPMJER1502, Japan.

SUPPLEMENTARY MATERIAL

The Supplementary Material for this article can be found online at: https://www.frontiersin.org/articles/10.3389/fmicb.2019.00455/full#supplementary-material

REFERENCES

Afzal-Shah, M., Woodford, N., and Livermore, D. M. (2001). Characterization of OXA-25, OXA-26, and OXA-27, molecular class D beta-lactamases associated with carbapenem resistance in clinical isolates of *Acinetobacter baumannii*. *Antimicrob. Agents Chemother.* 45, 583–588. doi: 10.1128/AAC.45.2.583-588.2001

Altschul, S. F., Gish, W., Miller, W., Myers, E. W., and Lipman, D. J. (1990). Basic local alignment search tool. *J. Mol. Biol.* 215, 403–410. doi: 10.1016/S0022-2836(05)80360-2

Andersen, J. B., Heydorn, A., Hentzer, M., Eberl, L., Geisenberger, O., Christensen, B. B., et al. (2001). *gfp*-based *N*-acyl homoserine-lactone sensor systems for detection of bacterial communication. *Appl. Environ. Microbiol.* 67, 575–585. doi: 10.1128/AEM.67.2.575-585.2001

Burr, T., Barnard, A. M., Corbett, M. J., Pemberton, C. L., Simpson, N. J., and Salmond, G. P. (2006). Identification of the central quorum sensing regulator of virulence in the enteric phytopathogen, *Erwinia carotovora*: the VirR repressor. *Mol. Microbiol.* 59, 113–125. doi: 10.1111/j.1365-2958.2005.04939.x

Chan, K. G., Atkinson, S., Mathee, K., Sam, C. K., Chhabra, S. R., Camara, M., et al. (2011). Characterization of *N*-acylhomoserine lactone-degrading bacteria associated with the *Zingiber officinale* (ginger) rhizosphere: co-existence of quorum quenching and quorum sensing in *Acinetobacter* and *Burkholderia*. *BMC Microbiol.* 11:51. doi: 10.1186/1471-2180-11-51

Chan, K. G., Sulaiman, J., Yong, D. A., Tee, K. K., Yin, W. F., and Priya, K. (2015). Draft Genome Perspective of *Staphylococcus saprophyticus* Strain SU8, an *N*-Acyl Homoserine lactone-degrading bacterium. *Genome Announc.* 3:e01097-15. doi: 10.1128/genomeA.01097-15

Chen, J. W., Gan, H. M., Yin, W. F., and Chan, K. G. (2012). Genome sequence of *Roseomonas* sp. strain B5, a quorum-quenching *N*-acylhomoserine lactone-degrading bacterium isolated from Malaysian tropical soil. *J. Bacteriol.* 194, 6681–6682. doi: 10.1128/JB.01866-12

Christiaen, S. E., Brackman, G., Nelis, H. J., and Coenye, T. (2011). Isolation and identification of quorum quenching bacteria from environmental samples. *J. Microbiol. Methods* 87, 213–219. doi: 10.1016/j.mimet.2011.08.002

Colom, K., Fdz-Aranguiz, A., Suinaga, E., and Cisterna, R. (1995). Emergence of resistance to beta-lactam agents in *Pseudomonas aeruginosa* with group I beta-lactamases in Spain. *Eur. J. Clin. Microbiol. Infect. Dis.* 14, 964–971. doi: 10.1007/BF01691378

d'Angelo-Picard, C., Faure, D., Penot, I., and Dessaux, Y. (2005). Diversity of *N*-acyl homoserine lactone-producing and -degrading bacteria in soil and tobacco rhizosphere. *Environ. Microbiol.* 7, 1796–1808. doi: 10.1111/j.1462-2920.2005.00886.x

Dong, Y. H., Xu, J. L., Li, X. Z., and Zhang, L. H. (2000). AiiA, an enzyme that inactivates the acylhomoserine lactone quorum-sensing signal and attenuates the virulence of *Erwinia carotovora*. *Proc. Natl. Acad. Sci. U.S.A.* 97, 3526–3531. doi: 10.1073/pnas.97.7.3526

Dong, Y. H., and Zhang, L. H. (2005). Quorum sensing and quorum-quenching enzymes. *J. Microbiol.* 43, 101–109.

Dubois, V., Poirel, L., Marie, C., Arpin, C., Nordmann, P., and Quentin, C. (2002). Molecular characterization of a novel class 1 integron containing bla(GES-1) and a fused product of aac3-Ib/aac6'-Ib' gene cassettes in *Pseudomonas aeruginosa*. *Antimicrob. Agents Chemother.* 46, 638–645. doi: 10.1128/AAC.46.3.638-645.2002

Flagan, S., Ching, W. K., and Leadbetter, J. R. (2003). Arthrobacter strain VAI-A utilizes acyl-homoserine lactone inactivation products and stimulates quorum signal biodegradation by *Variovorax paradoxus*. *Appl. Environ. Microbiol.* 69, 909–916. doi: 10.1128/AEM.69.2.909-916.2003

Givskov, M., Ostling, J., Eberl, L., Lindum, P. W., Christensen, A. B., Christiansen, G., et al. (1998). Two separate regulatory systems participate in control of swarming motility of *Serratia liquefaciens* MG1. *J. Bacteriol.* 180, 742–745.

Hammer, B. K., and Bassler, B. L. (2003). Quorum sensing controls biofilm formation in *Vibrio cholerae*. *Mol. Microbiol.* 50, 101–104. doi: 10.1046/j.1365-2958.2003.03688.x

Hu, J. Y., Fan, Y., Lin, Y. H., Zhang, H. B., Ong, S. L., Dong, N., et al. (2003). Microbial diversity and prevalence of virulent pathogens in biofilms developed in a water reclamation system. *Res. Microbiol.* 154, 623–629. doi: 10.1016/j.resmic.2003.09.004

Huang, J. J., Han, J. I., Zhang, L. H., and Leadbetter, J. R. (2003). Utilization of acyl-homoserine lactone quorum signals for growth by a soil pseudomonad and *Pseudomonas aeruginosa* PAO1. *Appl. Environ. Microbiol.* 69, 5941–5949. doi: 10.1128/AEM.69.10.5941-5949.2003

John, J. F. Jr., and McNeill, W. F. (1980). Activity of cephalosporins against methicillin-susceptible and methicillin-resistant, coagulase-negative *staphylococci*: minimal effect of beta-lactamase. *Antimicrob. Agents Chemother.* 17, 179–183. doi: 10.1128/AAC.17.2.179

Kalia, V. C., Raju, S. C., and Purohit, H. J. (2011). Genomic analysis reveals versatile organisms for quorum quenching enzymes: acyl-homoserine lactone-acylase and -lactonase. *Open Microbiol. J.* 5, 1–13. doi: 10.2174/1874285801105010001

Koch, G., Nadal-Jimenez, P., Cool, R. H., and Quax, W. J. (2014). *Deinococcus radiodurans* can interfere with quorum sensing by producing an AHL-acylase and an AHL-lactonase. *FEMS Microbiol. Lett.* 356, 62–70. doi: 10.1111/1574-6968.12479

Kusada, H., Hanada, S., Kamagata, Y., and Kimura, N. (2014). The effects of *N*-acylhomoserine lactones, β-lactam antibiotics and adenosine on biofilm formation in the multi-β-lactam antibiotic-resistant bacterium *Acidovorax* sp. strain MR-S7. *J. Biosci. Bioeng.* 118, 14–19. doi: 10.1016/j.jbiosc.2013.12.012

Kusada, H., Tamaki, H., Kamagata, Y., Hanada, S., and Kimura, N. (2017). A novel quorum-quenching *N*-acylhomoserine lactone acylase from *Acidovorax* sp. strain MR-S7 mediates antibiotic resistance. *Appl. Environ. Microbiol.* 83:e00080-17doi: 10.1128/AEM.00080-17e00080-17

Labbate, M., Queck, S. Y., Koh, K. S., Rice, S. A., Givskov, M., and Kjelleberg, S. (2004). Quorum sensing-controlled biofilm development in *Serratia liquefaciens* MG1. *J. Bacteriol.* 186, 692–698. doi: 10.1128/JB.186.3.692-698.2004

Lauretti, L., Riccio, M. L., Mazzariol, A., Cornaglia, G., Amicosante, G., Fontana, R., et al. (1999). Cloning and characterization of blaVIM, a new integron-borne metallo-beta-lactamase gene from a *Pseudomonas aeruginosa* clinical isolate. *Antimicrob. Agents Chemother.* 43, 1584–1590. doi: 10.1128/AAC.43.7.1584

Leadbetter, J. R., and Greenberg, E. P. (2000). Metabolism of acyl-homoserine lactone quorum-sensing signals by *Variovorax paradoxus*. *J. Bacteriol.* 182, 6921–6926. doi: 10.1128/JB.182.24.6921-6926.2000

Lee, S. J., Park, S. Y., Lee, J. J., Yum, D. Y., Koo, B. T., and Lee, J. K. (2002). Genes encoding the *N*-acyl homoserine lactone-degrading enzyme are widespread in many subspecies of *Bacillus thuringiensis*. *Appl. Environ. Microbiol.* 68, 3919–3924. doi: 10.1128/AEM.68.8.3919-3924.2002

Lin, Y. H., Xu, J. L., Hu, J., Wang, L. H., Ong, S. L., Leadbetter, J. R., et al. (2003). Acyl-homoserine lactone acylase from *Ralstonia* strain XJ12B represents a novel and potent class of quorum-quenching enzymes. *Mol. Microbiol.* 47, 849–860. doi: 10.1046/j.1365-2958.2003.03351.x

Lindum, P. W., Anthoni, U., Christophersen, C., Eberl, L., Molin, S., and Givskov, M. (1998). *N*-Acyl-L-homoserine lactone autoinducers control production of an extracellular lipopeptide biosurfactant required for swarming motility of *Serratia liquefaciens* MG1. *J Bacteriol* 180, 6384–6388.

Mahmoudi, E., Hasanzadeh, N., Sayed-Tabatabaei, B. E., and Venturi, V. (2011). Isolation and identification of N-acylhomoserine lactone degrading bacteria from potato rhizosphere *Afr. J. Microbiol. Res.* 5, 1635–1642.

Morohoshi, T., Tominaga, Y., Someya, N., and Ikeda, T. (2012). Complete genome sequence and characterization of the *N*-acylhomoserine lactone-degrading gene of the potato leaf-associated *Solibacillus silvestris*. *J. Biosci. Bioeng.* 113, 20–25. doi: 10.1016/j.jbiosc.2011.09.006

Mukherji, R., Varshney, N. K., Panigrahi, P., Suresh, C. G., and Prabhune, A. (2014). A new role for penicillin acylases: degradation of acyl homoserine lactone quorum sensing signals by *Kluyvera citrophila* penicillin G acylase. *Enzyme Microb. Technol.* 56, 1–7. doi: 10.1016/j.enzmictec.2013.12.010

Park, S. Y., Kang, H. O., Jang, H. S., Lee, J. K., Koo, B. T., and Yum, D. Y. (2005). Identification of extracellular *N*-acylhomoserine lactone acylase from a *Streptomyces* sp. and its application to quorum quenching. *Appl. Environ. Microbiol.* 71, 2632–2641. doi: 10.1128/AEM.71.5.2632-2641.2005

Park, S. Y., Lee, S. J., Oh, T. K., Oh, J. W., Koo, B. T., Yum, D. Y., et al. (2003). AhlD, an *N*-acylhomoserine lactonase in *Arthrobacter* sp., and predicted homologues in other bacteria. *Microbiology* 149, 1541–1550. doi: 10.1099/mic.0.26269-0

Riesenfeld, C. S., Goodman, R. M., and Handelsman, J. (2004). Uncultured soil bacteria are a reservoir of new antibiotic resistance genes. *Environ. Microbiol.* 6, 981–989. doi: 10.1111/j.1462-2920.2004.00664.x

Romero, M., Avendano-Herrera, R., Magarinos, B., Camara, M., and Otero, A. (2010). Acylhomoserine lactone production and degradation by the fish pathogen *Tenacibaculum maritimum*, a member of the *Cytophaga-Flavobacterium-Bacteroides* (CFB) group. *FEMS Microbiol. Lett.* 304, 131–139. doi: 10.1111/j.1574-6968.2009.01889.x

Romero, M., Diggle, S. P., Heeb, S., Camara, M., and Otero, A. (2008). Quorum quenching activity in *Anabaena* sp. *PCC* 7120: identification of AiiC, a novel AHL-acylase. *FEMS Microbiol. Lett.* 280, 73–80. doi: 10.1111/j.1574-6968.2007.01046.x

Sio, C. F., Otten, L. G., Cool, R. H., Diggle, S. P., Braun, P. G., Bos, R., et al. (2006). Quorum quenching by an *N*-acyl-homoserine lactone acylase from *Pseudomonas aeruginosa* PAO1. *Infect. Immun.* 74, 1673–1682. doi: 10.1128/IAI.74.3.1673-1682.2006

Stapleton, P., Wu, P. J., King, A., Shannon, K., French, G., and Phillips, I. (1995). Incidence and mechanisms of resistance to the combination of amoxicillin and clavulanic acid in *Escherichia coli*. *Antimicrob. Agents Chemother.* 39, 2478–2483. doi: 10.1128/AAC.39.11.2478

Steidle, A., Sigl, K., Schuhegger, R., Ihring, A., Schmid, M., Gantner, S., et al. (2001). Visualization of *N*-acylhomoserine lactone-mediated cell-cell communication between bacteria colonizing the tomato rhizosphere. *Appl. Environ. Microbiol.* 67, 5761–5770. doi: 10.1128/AEM.67.12.5761-5770.2001

Tamaki, H., Hanada, S., Sekiguchi, Y., Tanaka, Y., and Kamagata, Y. (2009). Effect of gelling agent on colony formation in solid cultivation of microbial community in lake sediment. *Environ. Microbiol.* 11, 1827–1834. doi: 10.1111/j.1462-2920.2009.01907.x

Tamaki, H., Sekiguchi, Y., Hanada, S., Nakamura, K., Nomura, N., Matsumura, M., et al. (2005). Comparative analysis of bacterial diversity in freshwater sediment of a shallow eutrophic lake by molecular and improved cultivation-based techniques. *Appl. Environ. Microbiol.* 71, 2162–2169. doi: 10.1128/AEM.71.4.2162-2169.2005

Tamura, K., Peterson, D., Peterson, N., Stecher, G., Nei, M., and Kumar, S. (2011). MEGA5: molecular evolutionary genetics analysis using maximum likelihood, evolutionary distance, and maximum parsimony methods. *Mol. Biol. Evol.* 28, 2731–2739. doi: 10.1093/molbev/msr121

Torres, M., Rubio-Portillo, E., Anton, J., Ramos-Espla, A. A., Quesada, E., and Llamas, I. (2016). Selection of the *N*-acylhomoserine lactone-degrading bacterium *Alteromonas stellipolaris* PQQ-42 and of its potential for biocontrol in aquaculture. *Front. Microbiol.* 7:646. doi: 10.3389/fmicb.2016.00646

Uroz, S., D'Angelo-Picard, C., Carlier, A., Elasri, M., Sicot, C., Petit, A., et al. (2003). Novel bacteria degrading *N*-acylhomoserine lactones and their use as quenchers of quorum-sensing-regulated functions of plant-pathogenic bacteria. *Microbiology* 149, 1981–1989. doi: 10.1099/mic.0.26375-0

Wang, W. Z., Morohoshi, T., Ikenoya, M., Someya, N., and Ikeda, T. (2010). AiiM, a novel class of *N*-acylhomoserine lactonase from the leaf-associated bacterium *Microbacterium testaceum*. *Appl. Environ. Microbiol.* 76, 2524–2530. doi: 10.1128/AEM.02738-09

Wang, W. Z., Morohoshi, T., Someya, N., and Ikeda, T. (2012). AidC, a Novel *N*-acylhomoserine lactonase from the potato root-associated *Cytophaga-Flavobacteria-Bacteroides* (CFB) Group Bacterium *Chryseobacterium* sp. Strain StRB126. *Appl. Environ. Microbiol.* 78, 7985–7992. doi: 10.1128/AEM.02188-12

Xu, L., Li, H., Vuong, C., Vadyvaloo, V., Wang, J., Yao, Y., et al. (2006). Role of the luxS quorum-sensing system in biofilm formation and virulence of *Staphylococcus epidermidis*. *Infect. Immun.* 74, 488–496. doi: 10.1128/IAI.74.1.488-496.2006

Yajko, D. M., Nassos, P. S., and Hadley, W. K. (1987). Therapeutic implications of inhibition versus killing of *Mycobacterium avium* complex by antimicrobial agents. *Antimicrob. Agents Chemother.* 31, 117–120. doi: 10.1128/AAC.31.1.117

Yasutake, Y., Kusada, H., Ebuchi, T., Hanada, S., Kamagata, Y., Tamura, T., et al. (2017). Bifunctional quorum-quenching and antibiotic-acylase MacQ forms a 170-kDa capsule-shaped molecule containing spacer polypeptides. *Sci. Rep.* 7:8946. doi: 10.1038/s41598-017-09399-4

Yoon, J. H., Lee, J. K., Jung, S. Y., Kim, J. A., Kim, H. K., and Oh, T. K. (2006). *Nocardioides kongjuensis* sp. nov., an N-acylhomoserine lactone-degrading bacterium. *Int. J. Syst. Evol. Microbiol.* 56(Pt 8), 1783–1787. doi: 10.1099/ijs.0.64120-0

Zhang, Y., Tang, K., Shi, X., and Zhang, X. H. (2013). *Flaviramulus ichthyoenteri* sp. nov., an N-acylhomoserine lactone-degrading bacterium isolated from the intestine of a flounder (*Paralichthys olivaceus*), and emended descriptions of the genus Flaviramulus and *Flaviramulus basaltis*. *Int. J. Syst. Evol. Microbiol.* 63(Pt 12), 4477–4483. doi: 10.1099/ijs.0.053744-0

Conflict of Interest Statement: The authors declare that the research was conducted in the absence of any commercial or financial relationships that could be construed as a potential conflict of interest.

frontiers in Microbiology

ORIGINAL RESEARCH
published: 29 March 2019
doi: 10.3389/fmicb.2019.00611

Signal Disruption Leads to Changes in Bacterial Community Population

*Michael Schwab[1,2], Celine Bergonzi[1,2], Jonathan Sakkos[3], Christopher Staley[2,4], Qian Zhang[2,5], Michael J. Sadowsky[2,5,6], Alptekin Aksan[2,3] and Mikael Elias[1,2]**

[1] Department of Biochemistry, Molecular Biology and Biophysics, University of Minnesota, Twin Cities, St. Paul, MN, United States, [2] Biotechnology Institute, University of Minnesota, Twin Cities, St. Paul, MN, United States, [3] Department of Mechanical Engineering, University of Minnesota, Twin Cities, St. Paul, MN, United States, [4] Department of Surgery, University of Minnesota, Twin Cities, St. Paul, MN, United States, [5] Department of Soil, Water, and Climate, University of Minnesota, Twin Cities, St. Paul, MN, United States, [6] Department of Plant and Microbial Biology, University of Minnesota, Twin Cities, St. Paul, MN, United States

The disruption of bacterial signaling (quorum quenching) has been proven to be an innovative approach to influence the behavior of bacteria. In particular, lactonase enzymes that are capable of hydrolyzing the *N*-acyl homoserine lactone (AHL) molecules used by numerous bacteria, were reported to inhibit biofilm formation, including those of freshwater microbial communities. However, insights and tools are currently lacking to characterize, understand and explain the effects of signal disruption on complex microbial communities. Here, we produced silica capsules containing an engineered lactonase that exhibits quorum quenching activity. Capsules were used to design a filtration cartridge to selectively degrade AHLs from a recirculating bioreactor. The growth of a complex microbial community in the bioreactor, in the presence or absence of lactonase, was monitored over a 3-week period. Dynamic population analysis revealed that signal disruption using a quorum quenching lactonase can effectively reduce biofilm formation in the recirculating bioreactor system and that biofilm inhibition is concomitant to drastic changes in the composition, diversity and abundance of soil bacterial communities within these biofilms. Effects of the quorum quenching lactonase on the suspension community also affected the microbial composition, suggesting that effects of signal disruption are not limited to biofilm populations. This unexpected finding is evidence for the importance of signaling in the competition between bacteria within communities. This study provides foundational tools and data for the investigation of the importance of AHL-based signaling in the context of complex microbial communities.

Keywords: quorum sensing, lactonase, biofilm, microbial community, silica encapsulation

OPEN ACCESS

Edited by:
Tom Defoirdt,
Ghent University, Belgium

Reviewed by:
Chien-Yi Chang,
University of Bradford, United Kingdom
Qian Yang,
Yellow Sea Fisheries Research Institute (CAFS), China

****Correspondence:***
Mikael Elias
mhelias@umn.edu

Specialty section:
This article was submitted to Antimicrobials, Resistance and Chemotherapy, a section of the journal Frontiers in Microbiology

Received: *20 November 2018*
Accepted: *11 March 2019*
Published: *29 March 2019*

Citation:
Schwab M, Bergonzi C, Sakkos J, Staley C, Zhang Q, Sadowsky MJ, Aksan A and Elias M (2019) Signal Disruption Leads to Changes in Bacterial Community Population. Front. Microbiol. 10:611. doi: 10.3389/fmicb.2019.00611

INTRODUCTION

Bacterial quorum sensing (QS) is among the most prominent and studied communication systems used by bacteria (Bassler, 1999). Numerous bacteria produce and utilize chemical signal molecules to coordinate their behavior in a cell density-dependent manner (Miller and Bassler, 2001; LaSarre and Federle, 2013). Bacterial QS has been shown to also regulate virulence and biofilm formation (LaSarre and Federle, 2013). Biofilms are comprised of a hydrated matrix of polysaccharides, proteins and nucleic acids that ultimately allow bacteria to attach to surfaces and live in complex community structures (Costerton et al., 1999). These structured communities enable a multicellular-like existence that is distinct from the planktonic state (Stewart and Costerton, 2001).

Quorum quenching (QQ) relates to all processes that can interfere with QS (McClean et al., 1997). QQ is a strategy that is not aimed at killing bacteria or at limiting growth, but rather at controlling or changing the expression of different functions (Uroz et al., 2009). Consequently, QQ enzymes are naturally capable of interfering with this QS *via* the enzymatic degradation of autoinducer molecules (Zhang, 2003; LaSarre and Federle, 2013). This has been studied in the case of autoinducer-1, *N*-acyl homoserine lactones (AHLs) (Dong et al., 2000, 2001; Oh et al., 2012; Kim et al., 2013; Bzdrenga et al., 2016). Indeed, the disruption of bacterial signaling using QQ enzymes was previously shown to inhibit the production of virulence factors and biofilm production by numerous pathogens, both *in vitro* (Dong et al., 2000; Chow et al., 2014; Hraiech et al., 2014; Guendouze et al., 2017; Zhang et al., 2017) and *in vivo* (Dong et al., 2000; Hraiech et al., 2014). These properties have been instrumental in making QQ enzymes prime candidates for bacterial control in numerous fields of application. However, to achieve this goal, effort is required to overcome practical issues with use of QQ enzyme technology, such as low activity levels, activity at low or high temperatures, environmental stability, and production costs (Lee et al., 2016; Rémy et al., 2016).

A promising candidate to overcome the intrinsic limitations in current enzymes is the lactonase *Sso*Pox, isolated from the hyperthermophilic crenarcheon *Sulfolobus solfataricus* (Merone et al., 2005; Elias et al., 2007, 2008). This enzyme belongs to the Phosphotriesterase-Like Lactonase family (Afriat et al., 2006; Elias and Tawfik, 2012), and naturally hydrolyzes a broad range of AHLs, from C6 AHL to 3-oxo C12 AHL (Hiblot et al., 2013). The *Sso*Pox was shown to disrupt bacterial QS *in vitro* and *in vivo* (Hraiech et al., 2014; Guendouze et al., 2017). Additionally, this lactonase was reported to be catalytically active over a wide range of temperatures, from −19°C to 70°C (Merone et al., 2005; Rémy et al., 2016). Interestingly, this lactonase exhibits exceptional thermal stability (T_m = 106°C), resistance to denaturing agents, organic solvents, detergents, radiation, and proteases (Hiblot et al., 2012a; Rémy et al., 2016). A crystal structure of *Sso*Pox revealed the critical importance of residue W263, interacting with the bound lactone ring of the AHL molecule (Elias et al., 2007, 2008; Del Vecchio et al., 2009). Mutation of W263I allowed for generation of variants with even greater lactonase catalytic activity (Hiblot et al., 2013; Jacquet et al., 2017).

While the substrate specificity of several lactonases has been determined (Hiblot et al., 2012b, 2013, 2015; Bzdrenga et al., 2014; Mascarenhas et al., 2015; Tang et al., 2015; Bergonzi et al., 2016, 2017), the types of bacteria that can be controlled by these enzymes is unclear. Indeed, AHL-based QS and effects of QS interference were mostly described in Gram-negative bacteria (Chow et al., 2014; Hraiech et al., 2014; Ivanova et al., 2015a,b; Guendouze et al., 2017). Other studies report activity of lactonase of bacterial strains that are not known as using AHLs (Ivanova et al., 2015a; Mayer et al., 2015). The presence of bacteria expressing lactonases was shown to reduce biofouling in a membrane bioreactor (MBR) (Oh et al., 2012; Kim et al., 2013, 2015), as well as affect the community structure of microbes attached to the membrane (Jo et al., 2016). Despite this, tools and insights are missing to adequately decipher the mechanisms underlying these observations.

In order to determine the effects of AHL degradation in the context of a complex microbial community, we used a silica gel, bead-based, bioencapsulation technique. Silica is a cytocompatible material in which bacteria or their enzymes can be physically confined, retained within the matrix, and protected from the environment (Reátegui et al., 2012; Mutlu et al., 2013, 2015; Aukema et al., 2014; Sakkos et al., 2016, 2017). Here, we used encapsulated *Escherichia coli* cells overexpressing the lactonase *Sso*Pox W263I to produce enzymatically active beads. Because SsoPox is a hydrolase, and do not need any other recycling co-factor than water molecules, it does not need the cells to remain alive to maintain its catalytic activity. In fact, in this strategy, cells are used as "bags of enzymes." Encapsulation of bacteria overexpressing stable, engineered lactonases combines the intrinsic properties of the *Sso*Pox enzyme, the lower production costs associated with the use of cells instead of purified enzyme, and a robust, permeable silica structure facilitating the integration of this enzyme in water treatment systems.

Catalytically active capsules were used as an enzymatic filtration matrix to degrade AHL signaling molecules produced by a complex soil microbial community cultured in a recirculating system. We determined that the presence of the lactonase in the filtration beads leads to a very significant reduction of biofilm formation over the course of the experiment (21 days) and that this reduction is associated with a change of the microbial population forming the biofilm. This experimental system opens up a new way to study the importance of bacterial signaling in complex microbial communities, the effects of signal disruption using lactonases, and highlights the potential of these enzymes to serve in water treatment processes, including a recirculating system.

MATERIALS AND METHODS

Preparation of Silica Lactonase-Containing Beads

The QQ lactonase *Sso*Pox W263I and a negative control protein, an inactive mutant SsoPox 5A8 [carrying the mutations V27G/P67Q/L72C/Y97S/Y99A/T177D/R223L/L226Q/L228M/W263H, obtained previously (Hiblot et al., 2013; Bergonzi et al., 2018)] were overexpressed in *E. coli* BL21-pGro7 as previously described using the autoinducing media ZYP (Hiblot et al., 2012a, 2013; Jacquet et al., 2017). The use of the 5A8 mutant allows for the control of the used plasmids and protein expression, allowing us to link observations to the enzymatic activity of SsoPox W263I. Cultures were grown to $OD_{600\ nm}$ = 0.8 at 37°C, while shaking at 200 RPM, and after overnight induction of the lactonase (18°C, 0.2% L-arabinose, 200 RPM shaking), cells overexpressing proteins were centrifuged at 4,400 × *g* for 20 min at 4°C. Cells were re-suspended in 100 mM potassium phosphate buffer, pH 7, at a concentration of 0.4 g/mL wet weight to provide 0.2 g/mL for the 1× lactonase beads. Gel

beads (1 mm diameter) containing the lactonase/control bacteria cultures were made using a dripping method while gelation occurred, using a method similar to a previously used protocol (Mutlu et al., 2013). Polyethylene glycol (PEG, 400 mg) with an average molecular weight of 10,000 Da, was mixed with 4 mL acetic acid (0.01 M) until the PEG dissolved. A 2.5 mL aliquot of tetramethyl orthosilicate (TMOS) was added and allowed to stir for 30 min until the solution became clear. One milliliter of cell suspension (0.2 g/mL) was mixed with the PEG/TMOS/acetic acid solution and gelation occurred within a few minutes. The bacteria-encapsulated beads (8 mL) were added directly to empty 10 mL chromatography columns to create filtration cartridges. Encapsulated bacteria can remain variable for several weeks. A report on encapsulation using similar gels show a reduction of ∼93% of viable *E. coli* cells after 3 weeks (Reátegui et al., 2012). Cell leakage from the gel is possible, but was previously found to be non-significant in similar gels (Reátegui et al., 2012). A filter (GE Healthcare) at the outlet of the column ensured the amount of beads present in the column would be constant throughout the duration of the experiment. Two different types of bacteria-encapsulated silica beads were produced, (1) beads where *E. coli* cells overexpressing the lactonase *Sso*Pox W263I were entrapped (*lactonase beads)* and (2) beads where *E. coli* cells overexpressing the control protein (inactive mutant 5A8) were entrapped (*control beads*). These beads were used to produce three distinct filtration cartridges: (a) the 2× lactonase cartridge, containing only 8 mL of *lactonase beads*, (b) a control cartridge containing only 8 mL of *control beads,* and (c) a 1× lactonase cartridge containing a 1:1 ratio of *lactonase beads* and *control beads* (4 mL of each).

Kinetic Assays of Lactonase in Silica Gel

Lactonase-containing silica gel solution, and the control protein, were poured into individual wells of 96 well microplates and allowed to solidify. Enzyme activity was quantified over a ∼7 months period (28 weeks) in buffer. Each well contained 75 μL of gel and was stored at 4°C in the presence of the *pte buffer* (50 mM HEPES, pH 8, 150 mM NaCl, 0.2 mM $CoCl_2$) or the *lactonase buffer* (2.5 mM Bicine pH 8.3, 150 mM NaCl, 0.2 mM CoCl2, 0.2 mM cresol purple, and 0.5% DMSO). The gel plus the buffer volume was 200 μL providing a 6.2 mm path length. Enzyme kinetics were measured by using a microplate reader (Synergy HT, BioTek, United States; Gen5.1 software), facilitated by a high level of gel transparency. The kinetics of lactonase activity were determined as previously described (Hiblot et al., 2012b, 2015; Bergonzi et al., 2016, 2017). Lactonase activity was expressed in enzymatic units defined as μM of substrate hydrolyzed per min per mg of cells (wet weight). All kinetic measurements were performed as triplicates. The activities of lactonase and phosphotriesterase were corrected by subtracting activities control gels (containing *E. coli* cells overexpressing mutant 5A8). The chromogenic substrate paraoxon was used as a proxy for the enzyme activity in order to evaluate the durability of gels over time. Assays were done as previously described (Hiblot et al., 2012a; Gotthard et al., 2013; Jacquet et al., 2017) and were performed using 10 μL of 20 mM paraoxon (1 mM final concentration) and a 200 μL final reaction volume. The paraoxon degradation product (paranitrophenolate) was directly measured at 405 nm (ε = 17,000 M^{-1} cm^{-1} at pH 8.0). Activity over time was normalized to the measured activity at day 0.

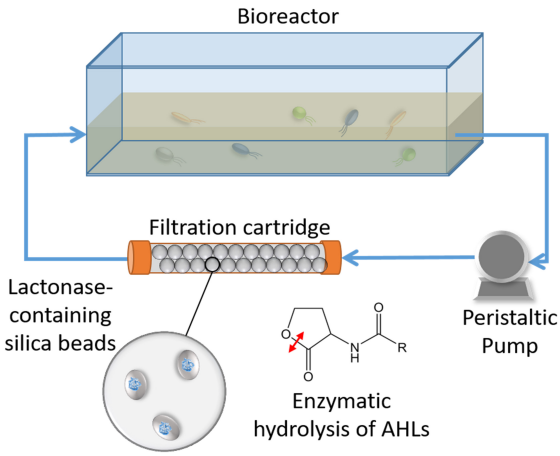

FIGURE 1 | Schematic representation of the experimental system. Bacterial communities are cultured in a tank vessel. A peristaltic pump is pumping the culture media through a filtration cartridge made of silica beads. The beads are entrapping *E. coli* cells that overproduced an engineered quorum quenching lactonase. As the system operates, the *N*-acyl homoserine lactone molecules (AHLs) produced by cultured bacteria are enzymatically degraded by the filtration cartridge.

Flow-Through Recirculating Bioreactor System

The flow-through system used in this study consisted of three 3 L tanks set up in parallel. The parallel circuit was achieved through the use of a multi-channel peristaltic pump (Masterflex L/S, Cole-Parmer, United States) (**Figure 1** and **Supplementary Figure S1**). A peristaltic pump provided an even flow rate of 18 mL/min to each tank. The flow-through filtration cassette consists of a 10 mL chromatography column filled with QQ gel beads or control beads. Each tank contained three liters of 15× diluted LB medium in water. A pre-separated 96-stripwell plate was submerged to the bottom so that individual wells could be harvested for biofilm quantification or DNA extraction. At the bottom of each bioreactor were 22 mm square microscope cover slips to be later used for biofilm imaging. For the inoculum, ∼5 g of soil (disturbed Waukegan Silt loam; sampled in march) was suspended in 40 mL of water. Soil community was chosen as a model system to this study. The suspension was centrifuged for 5 min at 500 × *g* and 200 μL of the cloudy supernatant was added to 30 mL of LB medium and allowed to grow for 16 h at 37°C, with shaking at 200 RPM. A 10 mL aliquot of this culture was inoculated into each tank and the system was allowed to run for 21 days at room temperature. During this time, measurements were taken every day to monitor $OD_{600\ nm}$ and pH of the water, and amount of biofilm present on multiple coverslip surfaces.

A second, independent experiment was performed similarly using soil samples from the same location (sampled in October)

using duplicate bioreactors. The system was allowed to run for 10 days, and samples were taken at days 3 and 10.

Attempts to measure the AHLs concentration in the culture media using the sensor *Chromobacterium violaceum* CV026 have failed, due to the apparent toxicity of the supernatants to the biosensor.

Effects of the Lactonase on a Complex Planktonic Community

The soil inoculum was used to inoculate 5 mL triplicate cultures (15× diluted LB medium) in 50 mL conical tubes. Tubes were incubated at 25°C and treated by adding to the culture media either inactive mutant SsoPox 5A8 enzyme or the improved mutant SsoPox W263I enzymes to a final concentration of 0.5 mg/mL. Samples were collected for DNA extraction after 3 and 7 days. In this experimental conditions, no biofilm could be visualized or quantified using crystal violet.

Biofilm Quantification

The submerged 96-stripwell plates were pre-broken so that individual wells could be extracted every day for measurements. Individual wells were extracted, in duplicate, for biofilm formation by using crystal violet biofilm quantification at 550 nm as previously described (Hraiech et al., 2014). To assess planktonic growth in the tanks, optical density of 200 μL samples were measured by using a 96 well plate spectrophotometer at 600 nm.

pH Measurements

pH values were measured with a meter (Orion Star A214, Thermo Fisher Scientific, United States). The pH of each bioreactor was monitored throughout the experiment (**Supplementary Figure S2**).

Sample Preparation for Imaging

Microscope cover glass samples were harvested for biofilm visualization analysis by using a Zeiss confocal microscope (West Germany, Cell Observer SD). The cover slips were fixed with 2% paraformaldehyde in 1× PBS for 1 h at room temperature, rinsed twice with 1× PBS, and fixed in a solution of 50% 1× PBS containing 50% EtOH. Samples were stored at −20°C for later processing. For imaging analyses, the stored samples were washed twice with 1× PBS and stained with 1× SYBR Gold nucleic acid stain (Thermo Fisher, United States) for 10 min, washed with 100% EtOH, and mounted onto microscope slides for fluorescence analysis. A 1:4 mixture of Citifluor:Vectashield was used as the mounting medium.

Microbial Community Analysis

Submerged wells from the stripwell plates were drained of excess cells/water and biofilm was scraped from the polypropylene well and into Powerbead® tubes for DNA extraction (DNeasy PowerSoil® DNA Extraction Kit, QIAGEN, Hilden, Germany). Purified DNA samples were submitted to the University of Minnesota's Genomics Center for 16S rRNA sequencing on the MiSeq platform at the University of Minnesota Genomics Center (Minneapolis, MN, United States). Each sample underwent amplification, dual-indexing, normalization, pooling, size selection, and a final QC prior to sequencing. The V4 region of the 16S rRNA gene was amplified by using primer set 515f (5′ – GTG CCA GCM GCC GCG GTA A – 3′) and 806R (5′ – GGA CTA CHV GGG TWT CTA AT – 3′). Negative (sterile water) controls were included throughout amplification and sequencing. Sequencing data were deposited to the Sequence Read Archive (SRA) under the accession number SRP156219.

Sequencing Data Analysis

All samples were processed using Mothur v1.35.1 (Schloss et al., 2009). Forward and reverse reads were paired-end joined using fastq-join software (Aronesty, 2013), and subjected to quality trimming using parameters previously described (Staley et al., 2015). High quality sequences were aligned against the SILVA database v.119.v4 (Pruesse et al., 2007), subjected to a 2% pre-cluster to remove sequence errors (Huse et al., 2010), and chimeras were removed using UCHIME v. 4.2.40 (Edgar et al., 2011). Operational taxonomic units (OTUs) were classified at 97% similarity using the furthest-neighbor algorithm and classified against the Ribosomal Database Project v.11.5 (Cole et al., 2008). For each sample, 1,250 sequences were used for final analyses. Alpha diversity indices were analyzed through the Mothur v1.35.1 program. Genus-level identification was achieved for the composition of the bacterial community. Analysis of similarity (ANOSIM) and analysis of molecular variances (AMOVA) were used to evaluate the beta diversity (community composition) among samples using Bray–Curtis dissimilarity matrices (BC) (Bray and Curtis, 1957; Excoffier et al., 1992; Clarke, 1993). Ordination of Bray–Curtis matrices was performed using principal coordinate analysis (PCoA) to further analyze diversity of sample days throughout the tank (Anderson and Willis, 2003). Pearson correlation was performed using Mothur v1.35.1 program to evaluate the correlation between the genera abundance under temporal change in different treatments. To visualize the distribution of taxonomies and diversities in microbial communities among the samples, "ggplot2" package in R v3.3.1 was used with rarefied relative abundance and OTUs at genus level (Aislabie et al., 2013). All of statistical analyses were done using $\alpha = 0.05$. Graphpad prism software was used to calculate student unpaired, two-tailed *t*-test values.

RESULTS AND DISCUSSION

Engineered Lactonase-Expressing Cells Entrapped *in silica* Capsules

Silica encapsulation is a method of choice for entrapping enzymes or cells due to their compatibility with biological molecules, mechanical properties, durability, stability, cost, and easy synthesis. Silica gels have been previously used to encapsulate bioreactive bacteria for bioremediation (Reátegui et al., 2012; Aukema et al., 2014; Sakkos et al., 2016, 2017). While most encapsulated bacteria may remain viable through the process of making the gels (Benson et al., 2018), it is likely to be unnecessary in this study, since the lactonase *Sso*Pox

is a metalloenzyme that only requires a water molecule as the nucleophile for the hydrolytic reaction (Elias et al., 2008). Therefore, cells can be viewed as "bags of enzymes" that disrupt the AHL signaling molecules produced by bacteria.

The engineered silica gels showed catalytic activity against lactones including lactones with short aliphatic chains (i.e., C6-AHL and γ-heptanoic lactone) and lactones with long acyl chains (i.e., C8-AHL and γ-undecanoic lactone). This observation is consistent with the enzyme activity in solution (**Figure 2A**), that is reported to degraded AHLs ranging from C6 to 3-oxo C12 AHL, and oxonolactone of numerous chain lengths with similar catalytic efficiencies (Hiblot et al., 2013). The measured activity demonstrates that the lactonase overproduced in *E. coli* cells is active inside the beads, and that different types of lactones can access its active site. The lactonase assay used in this study was pH-based and was previously described by us (Hiblot et al., 2012b; Bergonzi et al., 2016, 2017). While this assay allows for the monitoring of the lactone ring opening (generating a proton), it requires significant optimization of the activity buffer for each measurement due to the buffering capacity of the gel.

In order to better and more conveniently evaluate the durability of the silica gels over time, we used the chromogenic substrate paraoxon as a proxy for *Sso*Pox activity, as previously reported (Elias et al., 2008; Hiblot et al., 2012a, 2013).

Results in **Figure 2B** show that the lactonase-containing gel remains active for at least 39 weeks (∼9 months) in solution. This is 5 months longer than previous studies on atrazine degradation that were performed with a different enzyme but in similar conditions (Reátegui et al., 2012). The observed durability is consistent with the extreme stability of *Sso*Pox W263I, that remains stable for >300 days (∼10 months) at 25°C as a purified protein sample (Rémy et al., 2016). Interestingly, the activity of the enzymatic gel at T_0 increases over the course of the first 5 weeks of the experiment (approximately threefold). This may be caused by a change in the structure or porosity of the silica gel that could lead to an increased diffusion of the substrate into the enzyme active sites and may suggest that our current gel formulation could be optimized in future studies. Our success in obtaining silica gels containing engineered, overexpressed lactonases opens up a lot of new possibilities to study signal disruption in microbial communities.

Control of expression level, and the ability to engineer the lactonase, will be useful to optimize QQ in complex contexts. Additionally, because this technology in practice does not require purified enzyme, it may allow for the production of highly potent, specific beads to inhibit biofilms and biofouling in water filtration systems, at a low cost.

Silica Beads Containing Lactonase Enzyme Inhibit Biofilm Formation of Complex Microbial Communities in a Water Recirculating System

In this study, a water recirculating system was used to examine the influence of lactonase on soil bacterial community structure in planktonic cells. The water within the tank was pumped through a filtration cartridge (**Figure 1** and **Supplementary Figure S1**) containing different porous, lactonase-containing silica capsules (see section "Materials and Methods"). This experimental design was based on the hypothesis that water soluble AHLs produced by the microbial community growing in the tank would be filtered through the cartridge, and degraded by the lactonase enzyme.

The effects of the lactonase enzyme in the filtration cartridge on the microbial community was monitored at different levels by examining the pH of the tank medium and the optical density at 600 nm. The pH of the tank media increased from a starting value of ∼6.2 to a final value of ∼8.0 in all three experimental setups (**Supplementary Figure S2A**). Similarly, the $OD_{600\ nm}$, used as a proxy for cell density, slightly increased over the course

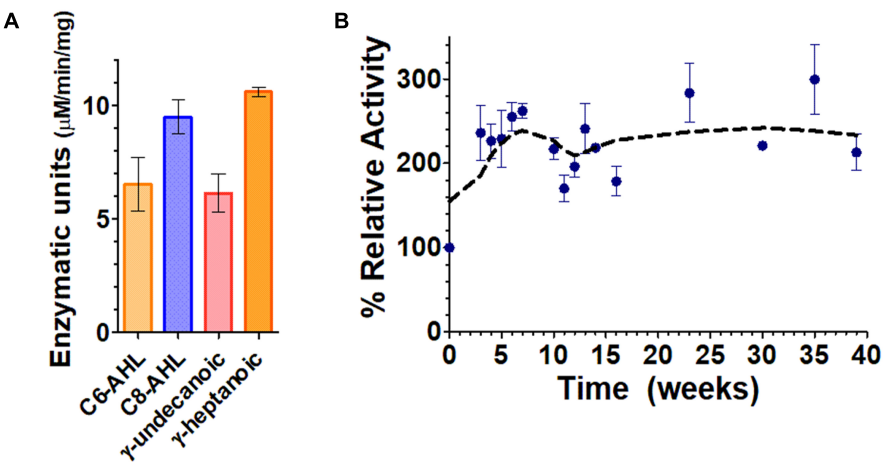

FIGURE 2 | Functionalized silica gel enzymatic activities and durability. **(A)** Lactone hydrolysis activity of the engineered silica gels containing the lactonase *Sso*Pox W263I using lactones with short aliphatic chains, i.e., γ-heptanoic lactone (γ-heptanolactone) and C6-AHL, as well as with lactones with longer aliphatic chains, i.e., C8-AHL and γ-undecanoic lactone as substrates. Lactonase activity is expressed in enzymatic units defined as μM of substrate hydrolyzed per min per mg of cells. **(B)** Activity of the enzymatic silica gels over time, using the chromogenic substrate paraoxon as a proxy for enzyme activity.

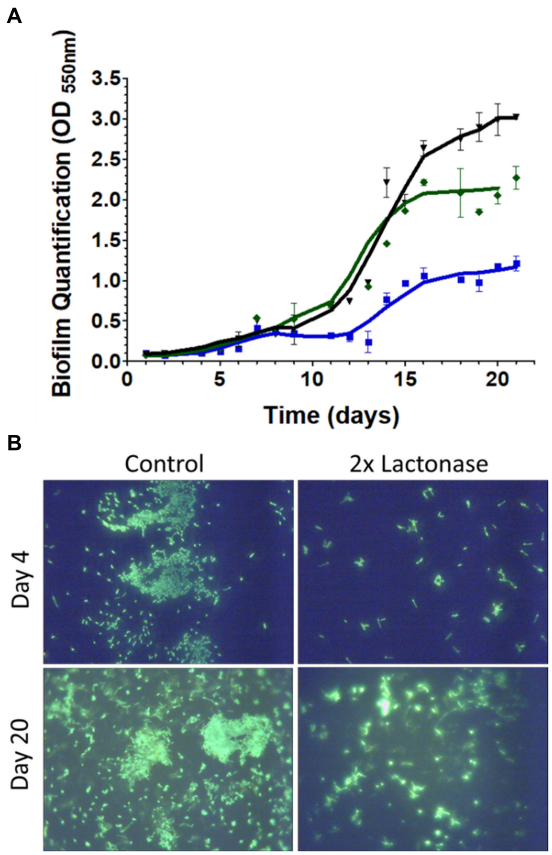

FIGURE 3 | Presence of lactonase reduces biofilm formation of the microbial community in the bioreactors. **(A)** Bioreactor parameters over the time course of the experiment (21 days). Measurements (duplicates) were performed on the three distinct bioreactors equipped with different filtration cartridges: the 2× lactonase cartridge, containing only *lactonase beads* (blue line), the control cartridge containing only *control beads* (dark line), and the 1× lactonase cartridge containing a 1:1 ratio of *lactonase beads* and *control beads* (green line). Biofilm quantification in submerged wells as quantified by crystal violet binding measured at 550 nm. **(B)** Glass slips submerged in the bioreactors were stained using SYBR gold DNA stain and visualized using a 60× magnification.

of the experiment in a similar fashion in the three bioreactors (**Supplementary Figure S2B**).

Biofilm formed and was quantified over the time course of the experiment in the bioreactors (**Figure 3A** and **Supplementary Figure S3**). Submerged plastic wells were sampled and assayed using crystal violet dye (**Supplementary Figure S4**). Measurements indicated that biofilms were slowly forming during the first 11 days of the experiments, and then accelerated in all bioreactors. Interestingly, there were no significant differences in biofilm quantification during the first 11 days of the experiment between filtration systems using lactonase or control beads. However, after 23 days in the presence of the lactonase beads, biofilm was reduced to ∼50% of that formed in the control. Biofilm reduction might even be greater since $OD_{600\ nm}$ measurements reached saturation in the control experiment. The degree of biofilm reduction is consistent with the observed reduction in biofilm dry weight in tubing [49–44% when comparing control and 2× lactonases after 21 days for pre-column and post column tubing, respectively (**Supplementary Figure S5**)]. Remarkably, inhibition of biofilm was observed as a function of lactonase concentration in the cartridge: inhibition was larger in the 2× concentration compared to the 1× concentration (∼50% and ∼30%, respectively) (**Figure 3A**). The reasons accounting for this enzyme dose dependence are unclear at this stage, and will be the subject of subsequent investigations in greater details.

Biofilm formation in the bioreactors was imaged in both the early and late stages of the experiment [days 4 and 20, respectively (**Figure 3B**)]. DNA staining of the submerged microscope slips revealed that the presence of lactonase in the filtration cartridge led to a reduction in the adhesion of cells to the coverslip surfaces. While we were unable to visualize the matrix in this experiment, it was apparent that the biofilms in the control tanks had more structure and maturity than did those formed in the lactonase treated tank. Interestingly, the reduction of cell attachment was also observed in the early stage of biofilm formation (by day 4) and may indicate the importance of signaling in both the biofilm attachment and maturation steps (Parsek and Greenberg, 2005). The presence of bacteria in our tested community, such as *Pseudomonas* and *Aeromonas* that are known to form biofilms, to utilize AHL-based QS and to be inhibited by lactonases (Cao et al., 2012; Guendouze et al., 2017), may partly explain the observed biofilm inhibition.

The ability of lactonase to inhibit complex biofilms was first evidenced using encapsulated microbes naturally expressing lactonases in MBR systems (Kim et al., 2013). Here, our study provides a comprehensive analysis of the dynamics of the effect of lactonase on a soil community, and with two different doses of the enzymatic quencher. Additionally, the demonstration in this study of the ability of entrapped, overexpressed and improved lactonases to inhibit biofilm formation in a recirculating system opens new perspectives for enzyme technology use in water treatment. It also raises questions about the specific mechanism of action of entrapped lactonases on the microbial community signaling. Because lactonase enzymes degrade the secreted signaling molecules (AHLs), no physical contact between the enzyme molecules and bacteria might be needed for its action. This hypothesis is consistent with our bioreactor design and our observed inhibition of biofilm formation. Questions concerning the diffusion ability of AHLs in various media will need to be investigated, as it may modulate the "action range" of the various AHLs, and consequently, of lactonases.

The Presence of a Lactonase Induces Changes in the Biofilm Microbial Composition

DNA from biofilm samples obtained from the three different bioreactors were isolated and submitted for amplicon sequencing of 16S rRNA (**Figure 4**). Samples were collected over the time course of the experiment to evaluate the population dynamics. Given the samples had relatively low diversity, we analyzed 1,250 sequences from each sample. This low diversity may be due

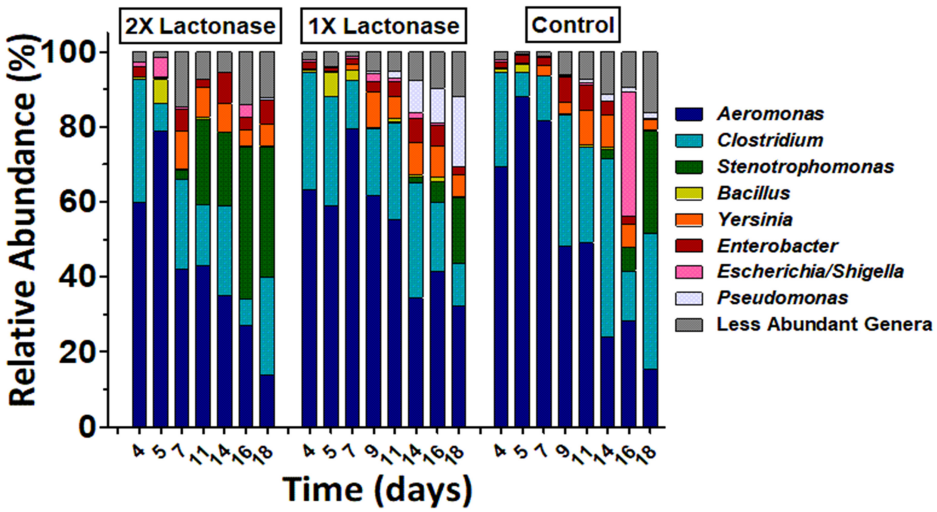

FIGURE 4 | Biofilm bacterial community changes as a function of lactonase concentration and time. Relative abundance of bacteria at the genus level in the three different bioreactors (2× lactonase; 1× lactonase and control) over time (from day 4 to day 18).

to the pre-culture step of soil samples that reduced microbial diversity, as described in other examples (Tabacchioni et al., 2000; Gorski, 2012). Taxonomic community composition, classified to genus, (**Figure 4**) and principle coordinate analysis (**Figure 5** and **Supplementary Figure S6**) indicated that microbial communities in all three replicate systems were very similar in the early stages of the experiment (ANOSIM, $p > 0.05$). For example, at day 4, *Aeromonas* represents 59.76, 63.20 and 69.52% of 2×, 1×, and control treatments, respectively. This was expected because all three bioreactors were inoculated with the same starting culture. However, notable differences in biofilm microbial communities were seen from day 7. By day 7, 42.2% of the microbial communities in biofilms from bioreactors treated with the highest concentration of lactonase (2×) were comprised by *Aeromonas*. In contrast, this bacterium comprised 79.7% and 81.7% of the community in the lactonase (1×) and control treatments, respectively (**Figure 4**). Principle coordinate analysis also highlighted that community composition starts to separate from control by day 7 (ANOSIM, $R = 0.625$, $p = 0.036$) (**Figure 5**).

Other notable differences include the relative populations of *Stenotrophomonas* (Gram-negative), *Pseudomonas* (Gram-negative), and *Clostridium* XIVa (Gram-positive) (**Figure 4**). For instance, the 2× lactonase bioreactor showed that *Stenotrophomonas* appeared much earlier than that seen in the 1× lactonase and control bioreactors (on day 14). In the 1× lactonase bioreactor, however, we observed an increase in the *Pseudomonas* population by day 11 and a gradual increase in its abundance within the community throughout the rest of the experiment. Lastly, in the later part of the experiment (days 9–18), the control bioreactor hosted a larger *Clostridium* population than did the two other bioreactors.

These experiments were repeated as an independent experiment performed in duplicates with a community from the same soil location but sampled at a different time of the year. We used the 1× lactonase concentration, and sampled two time points (day 3 and day 10) (**Supplementary Figure S7**). Interestingly, despite the different starting community composition, we can observe similar features. Notable differences are seen by day 10, including an increase of the *Stenotrophomonas* population in the presence of the enzyme (8% *versus* 1.5% in control). The *Pseudomonas*, specifically observed in the presence of lactonase as described above, are also favored in this independent run (15.7% *versus* 1.4%, $p < 0.05$). Lastly, the *Clostridium* group also varies (4.5% *versus* 14.2%; $p < 0.05$) and is less abundant in presence of lactonase than in the control bioreactor. These three groups are similarly affected by signal disruption using the lactonase in both independent experiments.

These data reveal that the presence of the lactonase enzyme of the filtration cassette lead to changes in the composition of the communities that occurred rapidly and were persistent throughout the experiment. Data show that these alterations of microbial communities occur in a lactonase dose-dependent fashion, and can be observed in biofilm communities.

The Presence of a Lactonase Induces Changes in the Microbial Composition in Suspension Culture

Experiments performed with the same starting community in smaller volumes (5 mL) of suspension cultures and in presence of the inactive 5A8 mutant or the lactonase *Sso*Pox W263I reveal similar alteration of the composition of the microbial community. Whereas in this experimental setup, no biofilm formation would be detected within the time frame (7 days), the analysis of sequencing data of culture supernatant samples to the genus-level (**Supplementary Figure S8**), PCoA (**Figure 5C**) and statistics (**Supplementary Tables S1**, **S2**) reveal that these suspension microbial communities are significantly different between treatments (ANOSIM, $R = 0.94$, $p < 0.001$). In fact, the compositions of the microbial population in presence or in

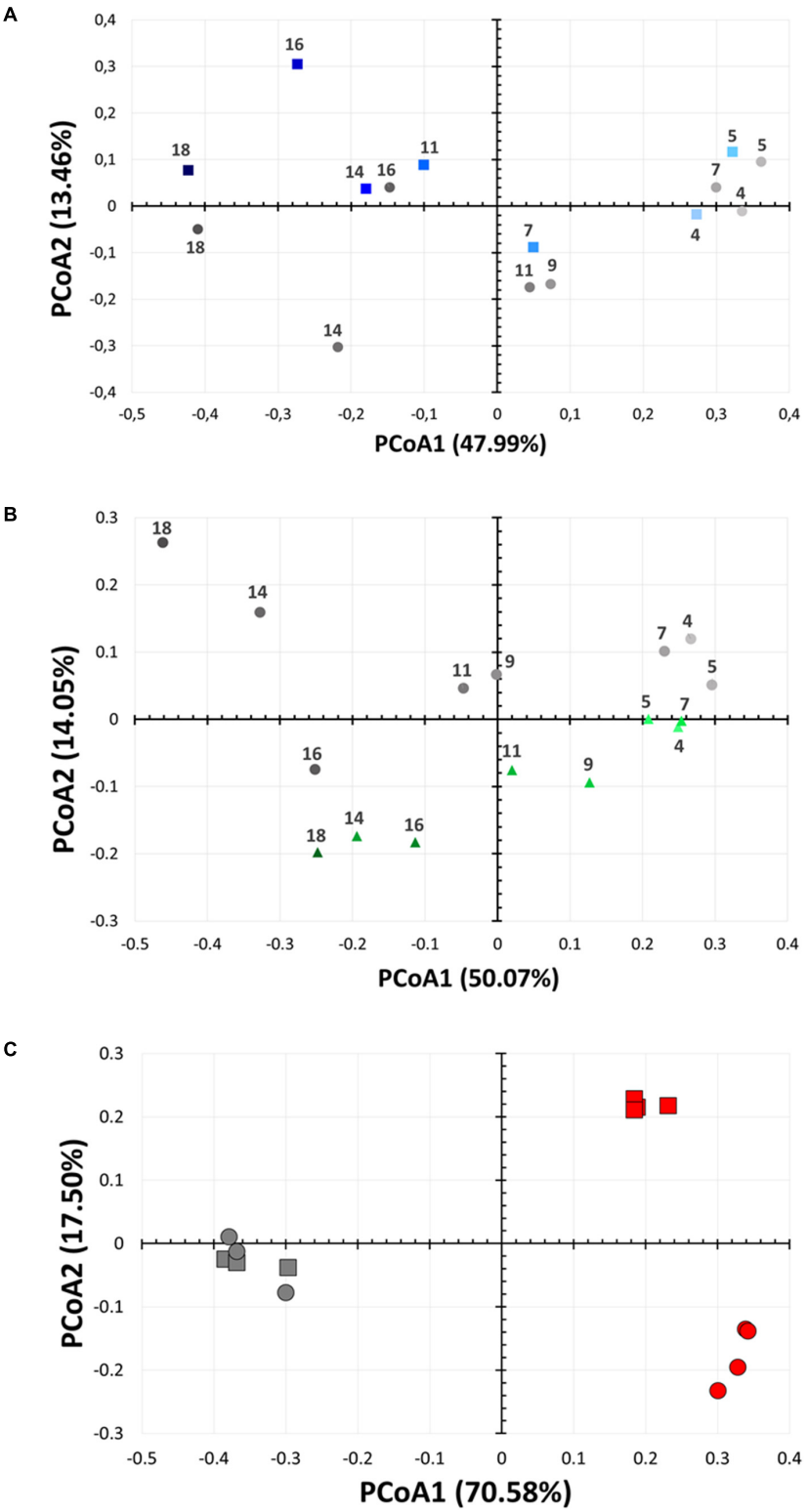

FIGURE 5 | Bacterial community changes as a function of lactonase concentration and time. Principal coordinate analysis of microbial biofilm communities from the bioreactors over time (from day 4 to day 18). Analysis are performed for **(A)** the 2× lactonase (blue squares) and control communities (gray circles) and **(B)** the 1× lactonase (green triangles) and control communities (gray circles). **(C)** Principal coordinate analysis of suspension microbial communities from a small scale suspension culture in presence (red) or absence (gray) of active lactonase. Data (n = 4 replicates) for days 3 and 7 are shown as squares and circles, respectively. Control group (n = 3 replicates) was treated with the inactive mutant SsoPox 5A8.

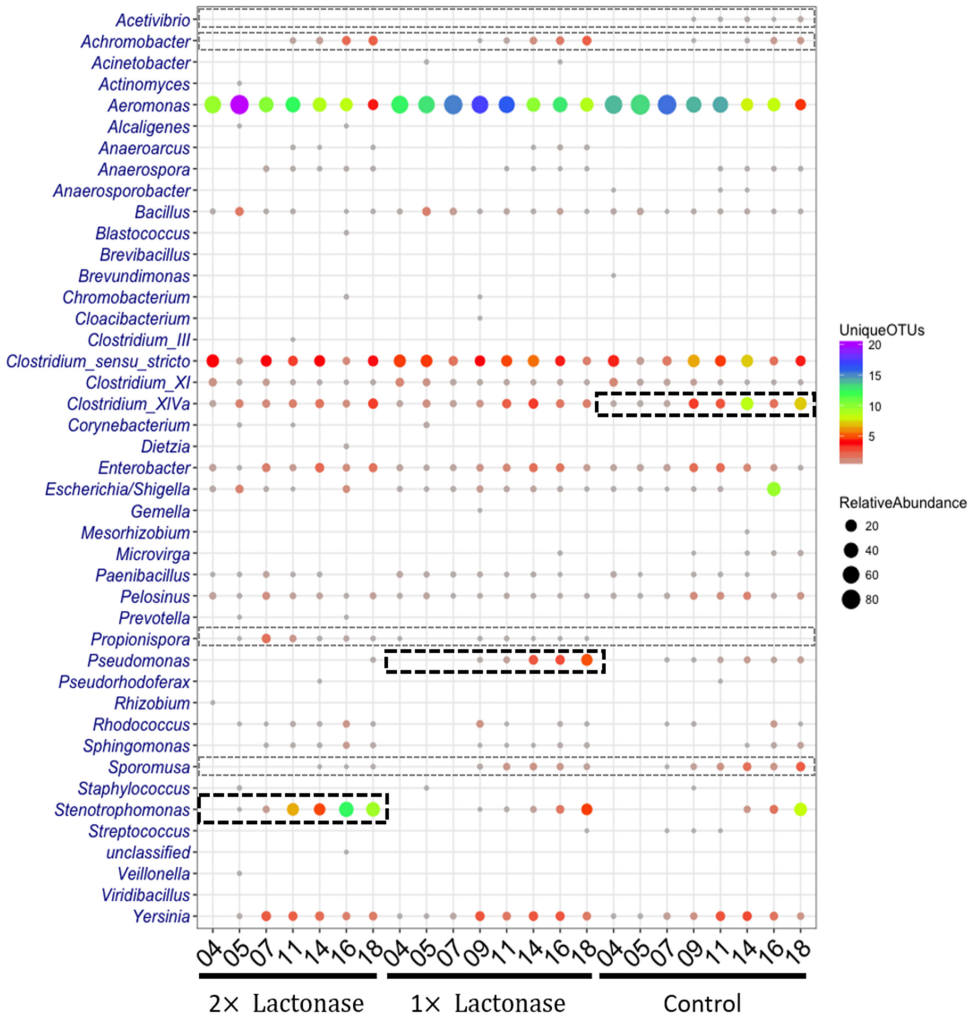

FIGURE 6 | The shift of relative abundance and diversity of bacterial taxa as a function of lactonase concentration and time at the genus level. The color represents the number of unique OTUs and the size of the circles is propositional to the total number of sequences for each given taxonomic group and sample. Abundant and less abundant genera showing difference in the bioreactors are shown in bold black-hashed boxes and light gray hashed boxes, respectively.

absence of quorum quencher are so different that comparisons between communities are difficult. Nevertheless, we observe again that *Pseudomonas* are more abundant in the presence of the lactonase than in the control experiments (24.9% versus 14%; $p < 0.05$). These experiments reveal that the effects of signal disruption using the lactonase *Sso*Pox W263I robustly alters the composition of the treated microbial community and that changes are not limited to biofilms, but also affect suspension communities.

Presence of a Lactonase Modulates Diversity Within Genera but Not the Community Diversity

Analysis of the relative abundance and diversity of genera distinctly highlighted population changes as a function of lactonase concentration and time of incubation (**Figure 6**). Overall, this analysis showed that while the presence of the lactonase induced changes in the relative abundance and diversity of some bacterial genera, it did not significantly alter overall community diversity. This is further evidenced by Shannon indices and observed species counts that are both slowly increasing over the time course of the experiments in all three bioreactors in a similar way (**Supplementary Figure S9**). Additionally, this analysis (**Figure 6**) highlights that *Stenotrophomonas*, *Pseudomonas* and *Clostridium XIVa* are specifically enriched over time in the 2× lactonase (Pearson correlation, $r = 0.95$, $P = 0.001$), the 1× lactonase (Pearson correlation, $r = 0.90$, $P = 0.002$), and the control bioreactors (Pearson correlation, $r = 0.77$, $P = 0.027$), respectively. This abundance increase is concomitant with an increase in their diversity.

Bacterial community compositions revealed that a few genera in low abundance were specific to treatments. For example, *Propionispora* were only detected in flow systems using lactonase in the filtration cartridge, whereas *Acetivibrio* were only detected

in the control bioreactor. Other microbial community biases were also noted: *Achromobacter* was more abundant in tanks using lactonases, as compared to controls. In contrast, the abundance and diversity of *Sporomusa* decreased as the concentration of lactonase increased.

Changes in microbial communities in the presence of lactonase were recently observed in the context of membrane biofouling (Jo et al., 2016), as well as fish gut microbiomes (Zhou et al., 2016). In this study, we show the dynamics of community composition changes in a water recirculating system and observe that these changes are concomitant with biofilm inhibition. Furthermore, these changes depend on the enzyme concentration and are related to the abundance and diversity of genera, but not the overall diversity of the community. The mechanism(s) underpinning the ability of QQ lactonases to affect complex microbial communities are unknown. Complete QS circuits (a synthase and a receptor) were previously reported to be found only in Proteobacteria (Case et al., 2008). Within the bacterial genera detected in this study, some are known to: (1) produce AHLs and utilize them for sensing [i.e., *Pseudomonas, Aeromonas, Yersinia,* (Venturi, 2005; Medina-Martínez et al., 2007; Ortori et al., 2007; Khajanchi et al., 2011)], (2) be capable of producing AHLs [i.e., *Enterobacter* (Yin et al., 2012; Ochiai et al., 2013)], and (3) be capable of sensing AHLs [i.e., *Stenotrophomonas, Escherichia, Shigella* (Soares and Ahmer, 2011; Martínez et al., 2015; Taghadosi et al., 2015; Lu et al., 2017)] (**Supplementary Table S3**). Others, however, are known to not produce, use, or sense AHLs (i.e., *Clostridium*). Additionally, the relationship between the AHL signal disruption by a lactonase and some genera is not straight forward as indicated by the increase of *Pseudomonas* in the community present in the 1× lactonase system. Furthermore, it is intriguing to note that *Clostridium* XIVa, despite being a Gram-positive bacterium that does not produce and/or sense AHLs, is reduced in the presence of the lactonase. This observation might echo previous studies describing the ability of lactonase to inhibit the biofilm of *Staphylococcus aureus* and *Escherichia coli* (Ivanova et al., 2015a; Mayer et al., 2015). Mechanisms explaining these observations are lacking. Yet, this study is a first comprehensive, time-resolved, statistically significant description on the effects of a lactonase on microbial community structures, and will inform the understanding of these complex interactions.

CONCLUSION

Our study demonstrates that lactonase-containing beads reduce biofilm formation by a complex soil microbial community, in a dose-dependent manner. Biofilm inhibition was observed, despite the presence of abundant microbes that are not known for using or sensing AHLs, such as *Clostridium*. Sequencing analysis revealed that biofilm inhibition was concomitant to a change in the microbial community composition on the surface. Dynamic population analysis shows that the bias introduced by AHL signal disruption occurs rapidly and is persistent over the time course of the experiment. We show in three independent experiments that signal disruption using a lactonase robustly and significantly changes the composition of microbial communities. We show that changes related to the relative proportion of some genera, but may also reflect in the observed specific presence or absence of genera in the biofilm. Therefore, signal disruption using a lactonase may have global effects on microbial populations, and not only inhibit bacteria utilizing AHLs for signaling.

Additionally, we find that signal disruption also lead to changes in the composition of suspension communities. This suggests that the importance of AHLs signaling extends beyond biofilm formation. In fact, this unexpected finding likely points to the importance of signaling in the competition between bacteria within communities (Diggle et al., 2007; Sandoz et al., 2007; Defoirdt et al., 2010).

Finally, the system used in this study provides a unique platform to study the importance of bacterial signaling, and the effects of signal disruption on complex microbial communities of multiple origins. We strongly feel that these findings and tools will pave the way for future investigations exploring the potential use of QQ enzymes in the water treatment arena, as well as the importance of signaling in complex microbial communities.

DATA AVAILABILITY

The datasets generated for this study can be found in Sequence Read Archive, SRP156219.

AUTHOR CONTRIBUTIONS

ME conceived and designed the work. MS, CB, and JS performed the experiments. ME, MS, CB, CS, QZ, MJS, and AA analyzed the data. QZ, MJS, and CS performed the statistical analysis. ME, CB, and MS wrote the first draft. ME, MS, JS, QZ, and CS wrote sections of the manuscript. ME, MJS, and AA critically revised the manuscript. All authors read and approved the final manuscript.

FUNDING

This work was supported by the MnDrive Initiative, the MnDrive demonstration grant, the BTI Biocatalysis Initiative, and the BARD grant IS-4960-16 FR to ME.

ACKNOWLEDGMENTS

We thank the University of Minnesota Genomics Center for the deep sequencing. We also thank Dr. David Daude and Dr. Eric Chabriere for fruitful discussions.

SUPPLEMENTARY MATERIAL

The Supplementary Material for this article can be found online at: https://www.frontiersin.org/articles/10.3389/fmicb.2019.00611/full#supplementary-material

REFERENCES

Afriat, L., Roodveldt, C., Manco, G., and Tawfik, D. S. (2006). The latent promiscuity of newly identified microbial lactonases is linked to a recently diverged phosphotriesterase. *Biochemistry* 45, 13677–13686. doi: 10.1021/bi061268r

Aislabie, J., Deslippe, J. R., and Dymond, J. (2013). "Soil microbes and their contribution to soil services," in *Ecosystem Sevices in New Zealand-Conditions and Trends*, ed. J. R. Dymond (Lincoln: Manaaki Whenua Press), 143–161.

Anderson, M. J., and Willis, T. J. (2003). Canonical analysis of principal coordinates: a useful method of constrained ordination for ecology. *Ecology* 84, 511–525. doi: 10.1890/0012-9658(2003)084[0511:CAOPCA]2.0.CO;2

Aronesty, E. (2013). Comparison of sequencing utility programs. *Open Bioinform. J.* 7, 1–8. doi: 10.2174/1875036201307010001

Aukema, K. G., Kasinkas, L., Aksan, A., and Wackett, L. P. (2014). Use of silica-encapsulated *Pseudomonas* sp. Strain NCIB 9816-4 in biodegradation of novel hydrocarbon ring structures found in hydraulic fracturing waters. *Appl. Environ. Microbiol.* 80, 4968–4976. doi: 10.1128/AEM.01100-14

Bassler, B. L. (1999). How bacteria talk to each other: regulation of gene expression by quorum sensing. *Curr. Opin. Microbiol.* 2, 582–587. doi: 10.1016/S1369-5274(99)00025-9

Benson, J. J., Sakkos, J. K., Radian, A., Wackett, L. P., and Aksan, A. (2018). Enhanced biodegradation of atrazine by bacteria encapsulated in organically modified silica gels. *J. Colloid Interface Sci.* 510, 57–68. doi: 10.1016/j.jcis.2017.09.044

Bergonzi, C., Schwab, M., Chabriere, E., and Elias, M. (2017). The quorum-quenching lactonase from Alicyclobacter acidoterrestris: purification, kinetic characterization, crystallization and crystallographic analysis. *Acta Crystallogr. Sect. F Struct. Biol. Commun.* 73(Pt 8), 476–480. doi: 10.1107/S2053230X17010640

Bergonzi, C., Schwab, M., and Elias, M. (2016). The quorum-quenching lactonase from Geobacillus caldoxylosilyticus: purification, characterization, crystallization and crystallographic analysis. *Acta Crystallogr F Struct. Biol. Commun.* 72, 681–686. doi: 10.1107/S2053230X16011821

Bergonzi, C., Schwab, M., Naik, T., Daudé, D., Chabrière, E., and Elias, M. (2018). Structural and biochemical characterization of AaL, a quorum quenching lactonase with unusual kinetic properties. *Sci. Rep.* 8:11262. doi: 10.1038/s41598-018-28988-5

Bray, J. R., and Curtis, J. T. (1957). An ordination of the upland forest communities of southern Wisconsin. *Ecol. Monogr.* 27, 325–349. doi: 10.2307/1942268

Bzdrenga, J., Daudé, D., Rémy, B., Jacquet, P., Plener, L., Elias, M., et al. (2016). Biotechnological applications of quorum quenching enzymes. *Chem. Biol. Interact.* 267, 104–115. doi: 10.1016/j.cbi.2016.05.028

Bzdrenga, J., Hiblot, J., Gotthard, G., Champion, C., Elias, M., and Chabriere, E. (2014). SacPox from the thermoacidophilic crenarchaeon *Sulfolobus acidocaldarius* is a proficient lactonase. *BMC Res. Notes* 7:333. doi: 10.1186/1756-0500-7-333

Cao, Y., He, S., Zhou, Z., Zhang, M., Mao, W., Zhang, H., et al. (2012). Orally administered thermostable N-acyl homoserine lactonase from Bacillus sp. strain AI96 attenuates Aeromonas hydrophila infection in zebrafish. *Appl. Environ. Microbiol.* 78, 1899–1908. doi: 10.1128/AEM.06139-11

Case, R. J., Labbate, M., and Kjelleberg, S. (2008). AHL-driven quorum-sensing circuits: their frequency and function among the *Proteobacteria*. *ISME J.* 2:345. doi: 10.1038/ismej.2008.13

Chow, J. Y., Yang, Y., Tay, S. B., Chua, K. L., and Yew, W. S. (2014). Disruption of biofilm formation by the human pathogen *Acinetobacter baumannii* using engineered quorum-quenching lactonases. *Antimicrob. Agents Chemother.* 58, 1802–1805. doi: 10.1128/AAC.02410-13

Clarke, K. R. (1993). Non-parametric multivariate analyses of changes in community structure. *Aust. Ecol.* 18, 117–143. doi: 10.1111/j.1442-9993.1993.tb00438.x

Cole, J. R., Wang, Q., Cardenas, E., Fish, J., Chai, B., Farris, R. J., et al. (2008). The ribosomal database project: improved alignments and new tools for rRNA analysis. *Nucleic Acids Res.* 37, D141–D145. doi: 10.1093/nar/gkn879

Costerton, J. W., Stewart, P. S., and Greenberg, E. P. (1999). Bacterial biofilms: a common cause of persistent infections. *Science* 284, 1318–1322. doi: 10.1126/science.284.5418.1318

Defoirdt, T., Boon, N., and Bossier, P. (2010). Can bacteria evolve resistance to quorum sensing disruption? *PLoS Pathog.* 6:e1000989. doi: 10.1371/journal.ppat.1000989

Del Vecchio, P., Elias, M., Merone, L., Graziano, G., Dupuy, J., Mandrich, L., et al. (2009). Structural determinants of the high thermal stability of SsoPox from the hyperthermophilic archaeon Sulfolobus solfataricus. *Extremophiles* 13, 461–470. doi: 10.1007/s00792-009-0231-9

Diggle, S. P., Griffin, A. S., Campbell, G. S., and West, S. A. (2007). Cooperation and conflict in quorum-sensing bacterial populations. *Nature* 450:411. doi: 10.1038/nature06279

Dong, Y. H., Wang, L. H., Xu, J. L., Zhang, H. B., Zhang, X. F., and Zhang, L. H. (2001). Quenching quorum-sensing-dependent bacterial infection by an N-acyl homoserine lactonase. *Nature* 411, 813–817. doi: 10.1038/35081101

Dong, Y. H., Xu, J. L., Li, X. Z., and Zhang, L. H. (2000). AiiA, an enzyme that inactivates the acylhomoserine lactone quorum-sensing signal and attenuates the virulence of Erwinia carotovora. *Proc. Natl. Acad. Sci. U.S.A.* 97, 3526–3531. doi: 10.1073/pnas.97.7.3526

Edgar, R. C., Haas, B. J., Clemente, J. C., Quince, C., and Knight, R. (2011). UCHIME improves sensitivity and speed of chimera detection. *Bioinformatics* 27, 2194–2200. doi: 10.1093/bioinformatics/btr381

Elias, M., Dupuy, J., Merone, L., Lecomte, C., Rossi, M., Masson, P., et al. (2007). Crystallization and preliminary X-ray diffraction analysis of the hyperthermophilic Sulfolobus solfataricus phosphotriesterase. *Acta Crystallogr. Sect. F Struct. Biol. Cryst. Commun.* 63, 553–555. doi: 10.1107/S1744309107023512

Elias, M., Dupuy, J., Merone, L., Mandrich, L., Porzio, E., Moniot, S., et al. (2008). Structural basis for natural lactonase and promiscuous phosphotriesterase activities. *J. Mol. Biol.* 379, 1017–1028. doi: 10.1016/j.jmb.2008.04.022

Elias, M., and Tawfik, D. S. (2012). Divergence and convergence in enzyme evolution: parallel evolution of Paraoxonases from quorum-quenching lactonases. *J. Biol. Chem.* 287, 11–20. doi: 10.1074/jbc.R111.257329

Excoffier, L., Smouse, P. E., and Quattro, J. M. (1992). Analysis of molecular variance inferred from metric distances among DNA haplotypes: application to human mitochondrial DNA restriction data. *Genetics* 131, 479–491.

Gorski, L. (2012). Selective enrichment media bias the types of *Salmonella enterica* strains isolated from mixed strain cultures and complex enrichment broths. *PLoS One* 7:e34722. doi: 10.1371/journal.pone.0034722

Gotthard, G., Hiblot, J., Gonzalez, D., Elias, M., and Chabriere, E. (2013). Structural and enzymatic characterization of the phosphotriesterase OPHC2 from *Pseudomonas* pseudoalcaligenes. *PLoS One* 8:e77995. doi: 10.1371/journal.pone.0077995

Guendouze, A., Plener, L., Bzdrenga, J., Jacquet, P., Rémy, B., Elias, M., et al. (2017). Effect of quorum quenching lactonase in clinical isolates of *Pseudomonas aeruginosa* and comparison with quorum sensing inhibitors. *Front. Microbiol.* 8:227. doi: 10.3389/fmicb.2017.00227

Hiblot, J., Bzdrenga, J., Champion, C., Chabriere, E., and Elias, M. (2015). Crystal structure of VmoLac, a tentative quorum quenching lactonase from the extremophilic crenarchaeon *Vulcanisaeta* moutnovskia. *Sci. Rep.* 5:8372. doi: 10.1038/srep08372

Hiblot, J., Gotthard, G., Chabriere, E., and Elias, M. (2012a). Characterisation of the organophosphate hydrolase catalytic activity of SsoPox. *Sci. Rep.* 2:779. doi: 10.1038/srep00779

Hiblot, J., Gotthard, G., Chabriere, E., and Elias, M. (2012b). Structural and enzymatic characterization of the lactonase SisLac from *Sulfolobus islandicus*. *PLoS One* 7:e47028. doi: 10.1371/journal.pone.0047028

Hiblot, J., Gotthard, G., Elias, M., and Chabriere, E. (2013). Differential active site loop conformations mediate promiscuous activities in the lactonase SsoPox. *PLoS One* 8:e75272. doi: 10.1371/journal.pone.0075272

Hraiech, S., Hiblot, J., Lafleur, J., Lepidi, H., Papazian, L., Rolain, J. M., et al. (2014). Inhaled lactonase reduces *Pseudomonas aeruginosa* quorum sensing and mortality in rat pneumonia. *PLoS One* 9:e107125. doi: 10.1371/journal.pone.0107125

Huse, S. M., Welch, D. M., Morrison, H. G., and Sogin, M. L. (2010). Ironing out the wrinkles in the rare biosphere through improved OTU clustering. *Environ. Microbiol.* 12, 1889–1898. doi: 10.1111/j.1462-2920.2010.02193.x

Ivanova, K., Fernandes, M. M., Francesko, A., Mendoza, E., Guezguez, J., Burnet, M., et al. (2015a). Quorum-quenching and matrix-degrading enzymes in multilayer coatings synergistically prevent bacterial biofilm formation on

urinary catheters. *ACS Appl. Mater. Interfaces* 7, 27066–27077. doi: 10.1021/acsami.5b09489

Ivanova, K., Fernandes, M. M., Mendoza, E., and Tzanov, T. (2015b). Enzyme multilayer coatings inhibit *Pseudomonas aeruginosa* biofilm formation on urinary catheters. *Appl. Microbiol. Biotechnol.* 99, 4373–4385. doi: 10.1007/s00253-015-6378-7

Jacquet, P., Hiblot, J., Daudé, D., Bergonzi, C., Gotthard, G., Armstrong, N., et al. (2017). Rational engineering of a native hyperthermostable lactonase into a broad spectrum phosphotriesterase. *Sci. Rep.* 7:16745. doi: 10.1038/s41598-017-16841-0

Jo, S. J., Kwon, H., Jeong, S.-Y., Lee, S. H., Oh, H.-S., Yi, T., et al. (2016). Effects of quorum quenching on the microbial community of biofilm in an anoxic/oxic MBR for wastewater treatment. *J. Microbiol. Biotechnol.* 26, 1593–1604. doi: 10.4014/jmb.1604.04070

Khajanchi, B. K., Kirtley, M. L., Brackman, S. M., and Chopra, A. K. (2011). Immunomodulatory and protective roles of quorum-sensing signaling molecules N-acyl homoserine lactones during infection of mice with *Aeromonas hydrophila*. *Infect. Immun.* 79, 2646–2657. doi: 10.1128/IAI.00096-11

Kim, S.-R., Lee, K.-B., Kim, J.-E., Won, Y.-J., Yeon, K.-M., Lee, C.-H., et al. (2015). Macroencapsulation of quorum quenching bacteria by polymeric membrane layer and its application to MBR for biofouling control. *J. Membr. Sci.* 473, 109–117. doi: 10.1016/j.memsci.2014.09.009

Kim, S.-R., Oh, H.-S., Jo, S.-J., Yeon, K.-M., Lee, C.-H., Lim, D.-J., et al. (2013). Biofouling control with bead-entrapped quorum quenching bacteria in membrane bioreactors: physical and biological effects. *Environ. Sci. Technol.* 47, 836–842. doi: 10.1021/es303995s

LaSarre, B., and Federle, M. J. (2013). Exploiting quorum sensing to confuse bacterial pathogens. *Microbiol. Mol. Biol. Rev.* 77, 73–111. doi: 10.1128/MMBR.00046-12

Lee, S., Park, S.-K., Kwon, H., Lee, S. H., Lee, K., Nahm, C. H., et al. (2016). Crossing the border between laboratory and field: bacterial quorum quenching for anti-biofouling strategy in an MBR. *Environ. Sci. Technol.* 50, 1788–1795. doi: 10.1021/acs.est.5b04795

Lu, Y., Zeng, J., Wu, B., Wang, L., Cai, R., Zhang, N., et al. (2017). Quorum sensing N-acyl homoserine lactones-SdiA suppresses *Escherichia coli-Pseudomonas aeruginosa* conjugation through inhibiting traI expression. *Front. Cell. Infect. Microbiol.* 7:7. doi: 10.3389/fcimb.2017.00007

Martínez, P., Huedo, P., Martinez-Servat, S., Planell, R., Ferrer-Navarro, M., Daura, X., et al. (2015). *Stenotrophomonas maltophilia* responds to exogenous AHL signals through the LuxR solo SmoR (Smlt1839). *Front. Cell. Infect. Microbiol.* 5:41. doi: 10.3389/fcimb.2015.00041

Mascarenhas, R., Thomas, P. W., Wu, C.-X., Nocek, B. P., Hoang, Q. Q., Liu, D., et al. (2015). Structural and biochemical characterization of AidC, a quorum-quenching lactonase with atypical selectivity. *Biochemistry* 54, 4342–4353. doi: 10.1021/acs.biochem.5b00499

Mayer, C., Romero, M., Muras, A., and Otero, A. (2015). Aii20J, a wide-spectrum thermostable N-acylhomoserine lactonase from the marine bacterium tenacibaculum sp. 20J, can quench AHL-mediated acid resistance in *Escherichia coli*. *Appl. Microbiol. Biotechnol.* 99, 9523–9539. doi: 10.1007/s00253-015-6741-8

McClean, K. H., Winson, M. K., Fish, L., Taylor, A., Chhabra, S. R., Camara, M., et al. (1997). Quorum sensing and *Chromobacterium violaceum*: exploitation of violacein production and inhibition for the detection of N-acylhomoserine lactones. *Microbiology* 143, 3703–3711. doi: 10.1099/00221287-143-12-3703

Medina-Martínez, M., Uyttendaele, M., Meireman, S., and Debevere, J. (2007). Relevance of N-acyl-L-homoserine lactone production by *Yersinia enterocolitica* in fresh foods. *J. Appl. Microbiol.* 102, 1150–1158.

Merone, L., Mandrich, L., Rossi, M., and Manco, G. (2005). A thermostable phosphotriesterase from the archaeon Sulfolobus solfataricus: cloning, overexpression and properties. *Extremophiles* 9, 297–305. doi: 10.1007/s00792-005-0445-4

Miller, M. B., and Bassler, B. L. (2001). Quorum sensing in bacteria. *Annu. Rev. Microbiol.* 55, 165–199. doi: 10.1146/annurev.micro.55.1.165

Mutlu, B. R., Yeom, S., Tong, H.-W., Wackett, L. P., and Aksan, A. (2013). Silicon alkoxide cross-linked silica nanoparticle gels for encapsulation of bacterial biocatalysts. *J. Mater. Chem. A* 1, 11051–11060. doi: 10.1039/c3ta12303k

Mutlu, B. R., Yeom, S., Wackett, L. P., and Aksan, A. (2015). Modelling and optimization of a bioremediation system utilizing silica gel encapsulated whole-cell biocatalyst. *Chem. Eng. J.* 259, 574–580. doi: 10.1016/j.cej.2014.07.130

Ochiai, S., Morohoshi, T., Kurabeishi, A., Shinozaki, M., Fujita, H., Sawada, I., et al. (2013). Production and degradation of N-acylhomoserine lactone quorum sensing signal molecules in bacteria isolated from activated sludge. *Biosci. Biotechnol. Biochem.* 77, 2436–2440. doi: 10.1271/bbb.130553

Oh, H.-S., Yeon, K.-M., Yang, C.-S., Kim, S.-R., Lee, C.-H., Park, S. Y., et al. (2012). Control of membrane biofouling in MBR for wastewater treatment by quorum quenching bacteria encapsulated in microporous membrane. *Environ. Sci. Technol.* 46, 4877–4884. doi: 10.1021/es204312u

Ortori, C. A., Atkinson, S., Chhabra, S. R., Cámara, M., Williams, P., and Barrett, D. A. (2007). Comprehensive profiling of N-acylhomoserine lactones produced by *Yersinia pseudotuberculosis* using liquid chromatography coupled to hybrid quadrupole–linear ion trap mass spectrometry. *Anal. Bioanal. Chem.* 387, 497–511. doi: 10.1007/s00216-006-0710-0

Parsek, M. R., and Greenberg, E. P. (2005). Sociomicrobiology: the connections between quorum sensing and biofilms. *Trends Microbiol* 13, 27–33. doi: 10.1016/j.tim.2004.11.007

Pruesse, E., Quast, C., Knittel, K., Fuchs, B. M., Ludwig, W., Peplies, J., et al. (2007). SILVA: a comprehensive online resource for quality checked and aligned ribosomal RNA sequence data compatible with ARB. *Nucleic Acids Res.* 35, 7188–7196. doi: 10.1093/nar/gkm864

Reátegui, E., Reynolds, E., Kasinkas, L., Aggarwal, A., Sadowsky, M. J., Aksan, A., et al. (2012). Silica gel-encapsulated AtzA biocatalyst for atrazine biodegradation. *Appl. Microbiol. Biotechnol.* 96, 231–240. doi: 10.1007/s00253-011-3821-2

Rémy, B., Plener, L., Poirier, L., Elias, M., Daudé, D., and Chabrière, E. (2016). Harnessing hyperthermostable lactonase from Sulfolobus solfataricus for biotechnological applications. *Sci. Rep.* 6:37780. doi: 10.1038/srep37780

Sakkos, J. K., Kieffer, D. P., Mutlu, B. R., Wackett, L. P., and Aksan, A. (2016). Engineering of a silica encapsulation platform for hydrocarbon degradation using *Pseudomonas* sp. NCIB 9816-4. *Biotechnol. Bioeng.* 113, 513–521. doi: 10.1002/bit.25821

Sakkos, J. K., Mutlu, B. R., Wackett, L. P., and Aksan, A. (2017). Adsorption and biodegradation of aromatic chemicals by bacteria encapsulated in a hydrophobic silica gel. *ACS Appl. Mater. Interfaces* 9, 26848–26858. doi: 10.1021/acsami.7b06791

Sandoz, K. M., Mitzimberg, S. M., and Schuster, M. (2007). Social cheating in *Pseudomonas aeruginosa* quorum sensing. *Proc. Natl. Acad. Sci. U.S.A.* 104, 15876–15881. doi: 10.1073/pnas.0705653104

Schloss, P. D., Westcott, S. L., Ryabin, T., Hall, J. R., Hartmann, M., Hollister, E. B., et al. (2009). Introducing mothur: open-source, platform-independent, community-supported software for describing and comparing microbial communities. *Appl. Environ. Microbiol.* 75, 7537–7541. doi: 10.1128/AEM.01541-09

Soares, J. A., and Ahmer, B. M. (2011). Detection of acyl-homoserine lactones by *Escherichia* and *Salmonella*. *Curr. Opin. Microbiol.* 14, 188–193. doi: 10.1016/j.mib.2011.01.006

Staley, C., Gould, T. J., Wang, P., Phillips, J., Cotner, J. B., and Sadowsky, M. J. (2015). Evaluation of water sampling methodologies for amplicon-based characterization of bacterial community structure. *J. Microbiol. Methods* 114, 43–50. doi: 10.1016/j.mimet.2015.05.003

Stewart, P. S., and Costerton, J. W. (2001). Antibiotic resistance of bacteria in biofilms. *Lancet* 358, 135–138. doi: 10.1016/S0140-6736(01)05321-1

Tabacchioni, S., Chiarini, L., Bevivino, A., Cantale, C., and Dalmastri, C. (2000). Bias caused by using different isolation media for assessing the genetic diversity of a natural microbial population. *Microb. Ecol.* 40, 169–176.

Taghadosi, R., Shakibaie, M. R., and Masoumi, S. (2015). Biochemical detection of N-Acyl homoserine lactone from biofilm-forming uropathogenic *Escherichia coli* isolated from urinary tract infection samples. *Rep. Biochem. Mol. Biol.* 3:56.

Tang, K., Su, Y., Brackman, G., Cui, F., Zhang, Y., Shi, X., et al. (2015). MomL, a novel marine-derived N-acyl homoserine lactonase from Muricauda olearia. *Appl. Environ. Microbiol.* 81, 774–782. doi: 10.1128/AEM.02805-14

Uroz, S., Dessaux, Y., and Oger, P. (2009). Quorum sensing and quorum quenching: the yin and yang of bacterial communication. *ChemBioChem* 10, 205–216. doi: 10.1002/cbic.200800521

Venturi, V. (2005). Regulation of quorum sensing in *Pseudomonas*. *FEMS Microbiol. Rev.* 30, 274–291. doi: 10.1111/j.1574-6976.2005.00012.x

Yin, W.-F., Purmal, K., Chin, S., Chan, X.-Y., Koh, C.-L., Sam, C.-K., et al. (2012). N-acyl homoserine lactone production by *Klebsiella pneumoniae* isolated from human tongue surface. *Sensors* 12, 3472–3483. doi: 10.3390/s120303472

Zhang, L. H. (2003). Quorum quenching and proactive host defense. *Trends Plant Sci.* 8, 238–244. doi: 10.1016/S1360-1385(03)00063-3

Zhang, Y., Brackman, G., and Coenye, T. (2017). Pitfalls associated with evaluating enzymatic quorum quenching activity: the case of MomL and its effect on *Pseudomonas aeruginosa* and *Acinetobacter baumannii* biofilms. *PeerJ* 5:e3251. doi: 10.7717/peerj.3251

Zhou, S., Zhang, A., Yin, H., and Chu, W. (2016). Bacillus sp. QSI-1 modulate quorum sensing signals reduce Aeromonas hydrophila level and alter gut microbial community structure in fish. *Front. Cell. Infect. Microbiol.* 6:184. doi: 10.3389/fcimb.2016.00184

Conflict of Interest Statement: The authors declare that the research was conducted in the absence of any commercial or financial relationships that could be construed as a potential conflict of interest.

frontiers in Microbiology

ORIGINAL RESEARCH
published: 17 April 2019
doi: 10.3389/fmicb.2019.00823

Discovering, Characterizing, and Applying Acyl Homoserine Lactone-Quenching Enzymes to Mitigate Microbe-Associated Problems Under Saline Conditions

*Tian-Nyu Wang[1], Qing-Tian Guan[2], Arnab Pain[2], Anna H. Kaksonen[3] and Pei-Ying Hong[1]**

[1] Water Desalination and Reuse Center, Biological and Environmental Science and Engineering Division, King Abdullah University of Science and Technology, Thuwal, Saudi Arabia, [2] Pathogen Genomics Laboratory, Division of Biological and Environmental Science and Engineering, King Abdullah University of Science and Technology, Thuwal, Saudi Arabia, [3] CSIRO Land and Water, Floreat, WA, Australia

OPEN ACCESS

Edited by:
Ana Maria Otero,
University of Santiago de Compostela, Spain

Reviewed by:
Xiuzhu Dong,
Institute of Microbiology (CAS), China
Manuel Romero,
University of Nottingham, United Kingdom

***Correspondence:**
Pei-Ying Hong
peiying.hong@kaust.edu.sa

Specialty section:
This article was submitted to Antimicrobials, Resistance and Chemotherapy, a section of the journal Frontiers in Microbiology

Received: 19 December 2018
Accepted: 01 April 2019
Published: 17 April 2019

Citation:
Wang T-N, Guan Q-T, Pain A, Kaksonen AH and Hong P-Y (2019) Discovering, Characterizing, and Applying Acyl Homoserine Lactone-Quenching Enzymes to Mitigate Microbe-Associated Problems Under Saline Conditions. Front. Microbiol. 10:823. doi: 10.3389/fmicb.2019.00823

Quorum quenching (QQ) is proposed as a new strategy for mitigating microbe-associated problems (e.g., fouling, biocorrosion). However, most QQ agents reported to date have not been evaluated for their quenching efficacies under conditions representative of seawater desalination plants, cooling towers or marine aquaculture. In this study, bacterial strains were isolated from Saudi Arabian coastal environments and screened for acyl homoserine lactone (AHL)-quenching activities. Five AHL quenching bacterial isolates from the genera *Pseudoalteromonas*, *Pontibacillus,* and *Altererythrobacter* exhibited high AHL-quenching activity at a salinity level of 58 g/L and a pH of 7.8 at 50°C. This result demonstrates the potential use of these QQ bacteria in mitigating microbe-associated problems under saline and alkaline conditions at high (>37°C) temperatures. Further characterizations of the QQ efficacies revealed two bacterial isolates, namely, *Pseudoalteromonas* sp. L11 and *Altererythrobacter* sp. S1-5, which could possess enzymatic QQ activity. The genome sequences of L11 and S1-5 with a homologous screening against reported AHL quenching genes suggest the existence of four possible QQ coding genes in each strain. Specifically, two novel AHL enzymes, $AiiA_{S1-5}$ and Est_{S1-5} from *Altererythrobacter* sp. S1-5, both contain signal peptides and exhibit QQ activity over a broad range of pH, salinity, and temperature values. In particular, $AiiA_{S1-5}$ demonstrated activity against a wide spectrum of AHL molecules. When tested against three bacterial species, namely, *Aeromonas hydrophila*, *Pseudomonas aeruginosa,* and *Vibrio alginolyticus*, $AiiA_{S1-5}$ was able to inhibit the motility of all three species under saline conditions. The biofilm formation associated with *P. aeruginosa* was also significantly inhibited by $AiiA_{S1-5}$. $AiiA_{S1-5}$ also reduced the quorum sensing-mediated virulence traits of *A. hydrophila*, *P. aeruginosa*, and *V. alginolyticus* during the mid and late exponential phases of cell growth. The enzyme did not impose any detrimental effects on cell growth, suggesting a lower potential

for the target bacterium to develop resistance over long-term exposure. Overall, this study suggested that some QQ enzymes obtained from the bacteria that inhabit saline environments under high temperatures have potential applications in the mitigation of microbe-associated problems.

Keywords: quorum quenching enzyme, biofouling, salinity, virulence inhibition, AHL, bacterial motility, *Altererythrobacter*

INTRODUCTION

Seawater is increasingly being used as an alternative water resource for various purposes to alleviate water demands in water-stressed countries (Elimelech and Phillip, 2011). However, marine microorganisms can attach onto surfaces, propagate and establish biofilm matrices, and frequently, this attachment can result in detrimental consequences. For example, biofilm formation can foul membranes in a seawater desalination plant, in turn reducing the flux (Al-Ahmad et al., 2000). Biofilm formation can also accelerate the biocorrosion of metal pipelines (Enning et al., 2012). Marine pathogens form biofilms on fish and shrimp, which can lead to the mortality and morbidity of these livestock and cause economic losses in marine aquaculture (Mizan et al., 2015). In all instances, biofilm formation increases the capital and operational costs associated with seawater usage.

Conventional antifouling strategies include the use of toxic biocides and coating materials such as tributyltin, copper, chlorine and ozone (Amara et al., 2018). However, there are health, safety and environmental concerns associated with the incessant use of these chemicals. Recently, a quorum quenching (QQ) strategy was proposed as an eco-friendly way to inhibit biofouling by blocking the cell-to-cell communication ability of bacteria (which is also known as quorum sensing, or QS). QS is a cell density-dependent regulatory mechanism used by bacteria to coordinate group behavior in response to QS signals secreted by the cell population. The concentration of QS signals increases as the cell population grows, which, upon reaching a certain threshold value, will trigger the expression of certain genes, including one related to pathogenicity, biofilm formation, spore germination and other functions (Defoirdt, 2018). QQ bacteria and QQ enzymes have been demonstrated to be effective in the membrane fouling mitigation of lab-scale membrane bioreactors (MBRs) used for wastewater treatment (Lee et al., 2018; Oh and Lee, 2018), and in a pilot-scale MBR (Lee et al., 2016).

Several studies have also presented the QQ strategy for mitigating biofouling in marine environments or in seawater desalination plants (Dobretsov et al., 2011; Katebian et al., 2016, 2018). The QQs discovered and applied to date have primarily been restricted to QS inhibitors (e.g., vanillin, cinnamaldehyde, and kojic acid). Nevertheless, several QQ bacteria were tested for biocontrol in marine environments. Tinh et al. (2008) enriched a complex bacterial consortium that exhibited AHL degradation activity, and they introduced this enrichment culture to colonize larval fish guts and demonstrated an improved survival rate from AHL-induced virulence traits by opportunistic bacteria. Torres et al. (2016) further screened for QQ enzymatic activity among 450 bacterial strains that were isolated from a mollusk hatchery, and they identified *Alteromonas stellipolaris* PQQ-42 as a potential AHL-degrading bacterium that increased the survival rate of corals against *Vibrio*. QQ bacteria and enzymes were subsequently shown to be widely distributed in marine sources (Romero et al., 2011, 2012). Marine isolates belonging to the *Erythrobacter*, *Labrenzia,* and *Bacterioplanes* genera were capable of degrading AHL molecules (Rehman and Leiknes, 2018). However, none of these studies took advantage of the special traits of marine QQ enzyme-secreting bacteria to mitigate marine biofouling. Moreover, these studies did not evaluate if the QQ enzymes were able to mitigate biofouling under the harsh environmental conditions representative of industrial seawater applications. These environmental conditions include high salinity (of up to 58 g/L), high temperatures (of up to 45°C) and an alkaline pH ranging from 7.2 to 8.0 (Scarascia et al., 2016).

To address this knowledge gap, during this study, bacteria isolated from a Saudi coastal habitat and the Red Sea were first screened for their AHL-quenching ability. Five AHL-quenching bacterial isolates from the genera *Pseudoalteromonas*, *Pontibacillus*, and *Altererythrobacter* were determined to exhibit high AHL quenching at a salinity value of 58 g/L and a pH of 7.8 at 50°C. The genomes of two bacterial isolates were sequenced, and the potential QQ genes from the genomes were screened based on their homologies with reported QQ genes. The possible AHL-quenching genes were verified by expressing the potential QQ genes in recombinant *E. coli* to obtain enzymatically active recombinant proteins for testing. Subsequently, two enzymes (*N*-acyl homoserine lactonase, AiiA and esterase, Est) from *Altererythrobacter* sp. S1-5 were biochemically characterized at different pH, salinity and temperature. The AiiA from *Altererythrobacter* sp. S1-5 was further demonstrated to inhibit marine biofilm formation and the virulence of the opportunistic bacteria *Aeromonas hydrophila, Pseudomonas aeruginosa,* and *Vibrio alginolyticus* under saline conditions. The findings from this study demonstrate the potential feasibility of using QQ bacteria and enzymes to mitigate biofouling under saline conditions. Specifically, it is the first study to demonstrate the presence of AHL-quenching activity in *Altererythrobacter*.

MATERIALS AND METHODS

Sample Collection, Strain Isolation, and Identification

High-salinity artificial seawater (**HSAS**: 51.5 g/L NaCl, 0.74 g/L KCl, 0.99 g/L $CaCl_2$, 2.85 g/L $MgCl_2$, and 1.92 g/L $MgSO_4$;

salinity: 58 g/L), high-salinity marine broth medium (**HSMB**: **HSAS** containing 1 g/L yeast extract, 5 g/L peptone), and high-salinity marine agar (**HSMA**: **HSMB** with 15 g/L agar) were used for strain isolation and screening. Marine aquaculture sludge from the Jeddah Fisheries Research Center (JFRC) as well as beach sand and seawater from the Red Sea were collected for the isolation of AHL-quenching bacteria. A 50 mL aliquot of seawater was transferred into a sterile flask. For the sludge and sand, 15 g of each sample was individually poured into separate sterile flasks that contained 50 mL of sterile **HSAS** and 2 g of glass beads (Sigma, St. Louis, MO, United States; diameter: 5 mm). All the inoculated flasks were cultivated at 40°C and 180 rpm for 24 h. Following that incubation, the cultures were serially diluted with **HSAS** and plated onto **HSMA** plates. The agar plates were further incubated at 40°C for 24 h. Colonies showing different morphologies were picked and purified by plate streaking.

The bacterial isolates were identified through partial length 16S rRNA gene sequencing. A single colony of marine isolates was scraped with sterile toothpicks, suspended in 20 μL of sterile water and heated at 95°C for 5 min to achieve cell lysis. One microliter of supernatant was used as the DNA template for polymerase chain reactions (PCRs). A partial 16S rRNA gene was amplified using the universal primers 11F (5′-GTTYGATYCTGG CTCAG-3′) and 1492R (5′-GGYTACCTTGTTACGACTT-3′). The PCR was performed at 95°C for 5 min, followed by 35 cycles of 30 s at 95°C, 30 s at 52°C and 2 min at 72°C, and a final elongation for 5 min at 72°C. The PCR products were purified using a Wizard SV Gel and PCR Clean-Up System (Promega, Madison, WI, United States) and submitted to the KAUST Bioscience core lab for Sanger-based sequencing using the primers 11F, 1492R, 338F (5′-ACTCCTACGGGAGGCAGCAG-3′), and 592R (5′-GWATTACCGCGGCKGCTG-3′). The sequences were paired and searched against the NCBI GenBank database using the BLASTn search algorithm.

Screening for AHL Quenching Strains From Marine Isolates Under High Salinity

Single colonies of tested strains were inoculated into individual wells of sterile 96-well microtiter plates, and each well contained 200 μL of autoclaved **HSMB** medium. The 96-well plates were incubated at 50°C and 120 rpm for 24 h. After the incubation, the plates were centrifuged at 2,300 × *g* for 10 min. The supernatant in each well was discarded and the cell pellet was washed once with HSAS. The centrifugation process was repeated and the resulting cell pellets were individually resuspended in 200 μL of **HSAS** containing an AHL mixture (0.29 mM C4-HSL, 0.25 mM C6-HSL, 0.22 mM C8-HSL and 0.17 mM 3-oxo-C12-HSL). After incubating at 50°C for 24 h, the culture was centrifuged again at 2300 × *g* for 10 min. Ten microliters of supernatant was collected for residual AHL quantification using an *Agrobacterium tumefaciens* bioassay (Tang et al., 2013). In brief, *A. tumefaciens* NT1 (traR, tra::lacZ749) (Piper et al., 1993) was grown in **AT** minimal medium (10.7 g/L KH_2PO_4, 2 g/L $(NH4)_2SO_4$, 78 mg/L $MgSO_4$, 13 mg/L $CaCl_2.H_2O$, 5 mg/L $FeSO_4.7H_2O$, 1.4 mg/L $MnSO_4.H_2O$, pH 6.7, and 0.5% filtered glucose, pH = 6.7) at 28°C and 150 rpm overnight. The culture was diluted 1:500 into fresh **AT** minimal medium containing 250 μg/mL 5-bromo-4-chloro-3-indolyl-β-D-galactopyranoside (X-gal, Sigma, St. Louis, MO, United States) to make the *A. tumefaciens* bioassay solution. Ten microliters of each sample used to analyze the residual AHL concentrations were pipetted into individual wells of a sterile 96-well-plate, with each well containing 190 μL of *A. tumefaciens* bioassay solution. After an incubation at 28°C for 12 h, the absorbance of each well at 492 nm and 630 nm was recorded using a SpectraMax 340 PC 384 microplate reader (Molecular Devices LLC, San Jose, CA, United States). The absorbances at 492 nm and 630 nm are a combination of absorption and light scattering by indigo (which is an X-gal degradation product) and biosensor cells (Tang et al., 2013). The residual AHL activity in each sample was expressed as normalized β-galactosidase activity as described in Tang et al. (2013). The quantification was performed in triplicate. The same concentration of AHL mixture in abiotic HSAS solution was incubated under the same conditions described above and used as a negative control when determining the residual AHL activity. The relative AHL quenching efficiency (QE) for each strain was determined using Eq. (1) as follows:

$$QE = \frac{AHLn - AHLs}{AHLn} \times 100\% \quad (1)$$

where AHLn denotes the residual AHL activity of the negative control after the reaction and AHLs denotes the residual AHL activity of bacterial samples after the reaction with potential QQ enzymes. It was previously shown that AHLs can be rather unstable in alkaline and high temperature environments (Yates et al., 2002). Therefore, to eliminate the instability of AHLs caused by abiotic factors after long-term reactions and to denote the AHL activity changes arising from the potential QQ enzymes more accurately, we use AHLn instead of the initial AHL activity spiked into the prior reaction mixture. Strains with a relative AHL QE ≥ 90% were selected for further QQ enzyme screening.

Localization of AHL Quenching Enzyme in AHL Quenching Isolates

Artificial seawater (**AS**: 29.5 g/L NaCl, 0.74 g/L KCl, 0.99 g/L $CaCl_2$, 2.85 g/L $MgCl_2$, and 1.92 g/L $MgSO_4$; salinity: 36 g/L), marine broth medium (**MB**: **AS** with 1 g/L yeast extract, 5 g/L peptone), and marine agar (**MA**: **MB** with 15 g/L agar) were used for the AHL quenching enzyme experiment. Selected strains were grown in **MB** medium at 37°C overnight. To obtain the potential AHL quenching enzymes present in the intracellular fraction of each bacterial isolate, 5 mL of pure culture was centrifuged at 20,000 × *g* for 10 min, and the cell pellet was suspended in phosphate-buffered saline (PBS) (Fisher Scientific, Hampton, NH, United States). The cells were lysed using a Q500 sonicator (Qsonica, Newtown, CT, United States) at a 45% amplitude for 5 min, with repetitive 15 s pulsating sonication at 45 s intervals. The fraction was centrifuged at 10,000 × *g* for 10 min and filtered through a 0.2 μm cellulose acetate membrane to obtain the lysed cellular extract as filtrate. To obtain the potential AHL-quenching enzymes secreted extracellularly by the bacterial isolates, a cell pellet made from 5 mL of overnight

culture was resuspended in 5 mL of **AS**. The cell suspension was incubated at 37°C for 12 h and centrifuged at 20,000 × *g* for 10 min to obtain the supernatant fraction. The cellular extract and supernatant fraction of each strain were fractionated separately using centrifugal filters (MWCO: 10 kDa, Merck, Darmstadt, Germany) prior to the determination of the potential AHL-quenching activity. To demonstrate whether the quenching activity arose from enzymatic activity, the cellular extract and supernatant fraction were also heat-inactivated at 100°C for 30 min and tested for AHL quenching activity. Each sample was mixed with an AHL mixture (0.15 mM C4-HSL, 0.13 mM C6-HSL, 0.11 mM C8-HSL, and 0.08 mM 3-oxo-C12-HSL) and incubated at 37°C for 18 h for the residual AHL determination. PBS buffer and **AS** were used to replace the cell extract and supernatant to create the negative control.

Genome Sequencing of AHL-Quenching Strains

Two strains (L11 and S1-5) that exhibit potential enzymatic AHL-quenching activity were sequenced for protein-coding genes (CDS) that encode the AHL quenching enzyme. The genomic DNA from L11 and S1-5 was extracted with a QIAGEN Genomic Tips kit (Qiagen, Hilden, Germany). A 20 kb DNA library was prepared for each strain by genomic DNA fragmentation with a Pippin HT size-selection system (Sage Science, Beverly, MA, United States). Single molecular real-time (SMRT) sequencing was performed with a PacBio RS II platform (Pacific Biosciences, Menlo Park, CA, United States). The raw reads were assembled into contigs using a Canu assembler (Koren et al., 2017). The assembled contigs were examined for integrity using dotplots with a GEnome PAir-Rapid Dotter tool (Krumsiek et al., 2007). The assembled contigs were annotated with a RASTtk server (Brettin et al., 2015). The potential AHL quenching ORFs in L11 and S1-5 were screened with NCBI tBLASTn using published AHL quenching genes as reference genes. A structure-based multiple sequence alignment of potential ORFs and published QQ sequences was performed using ESPript (Gouet et al., 1999). Highly homologous ORFs (identify ≥ 25%, coverage ≥ 40%) that share a conserved domain with the reported QQ protein were selected for gene expression evaluation and to test for quenching activity.

Expression of AHL Quenching Genes in *Escherichia coli*

Eight potential QQ gene sequences from strains L11 and S1-5 were amplified with Q5-hot start polymerase (New England BioLabs, Beverly, MA, United States) using the primers listed in **Supplementary Table 1**. The PCR amplicons of the QQ genes were either ligated into a pTrcHis A vector (Thermo Fisher, Waltham, MA, United States) by T4 DNA ligase (Thermo Fisher Waltham, MA, United States) or into pET-20b (+) vectors (Merck, Darmstadt, Germany) by Gibson Assembly Master Mix (New England BioLabs, Beverly, MA, United States). Recombinant pTricHis A and pET-20b(+) vectors with correct insertions were transformed into *E. coli* TOP10 (Thermo Fisher, Waltham, MA, United States) and *E. coli* BL21 (DE3) (Merck, Darmstadt, Germany), respectively, for protein expression. The blank vectors pTricHisA and pET-20b(+) were also transformed into *E. coli* TOP10 and *E. coli* BL21 (DE3) and denoted as negative recombinant controls (NC-1 and NC-2). The AiiA gene from *Bacillus mycoides* ATCC 6462 was inserted into pET-20b(+) and expressed in *E. coli* BL21 (DE3) as a positive control sample for QQ activity evaluation.

Overnight cultures of recombinant strains were diluted 1:100 into fresh LB medium supplemented with 100 μg/mL ampicillin (Sigma, St. Louis, MO, United States). The culture was incubated at 30°C and 160 rpm until the cells reached exponential growth (OD_{600} = 0.8). Subsequently, induction was initiated by adding 0.1 mM isopropyl β-D-1-thiogalactopyranoside (IPTG, Thermo Fisher, Waltham, MA, United States) to the culture prior to further incubation at 30°C 120 rpm for 16 h. After the induction, the cell pellet was collected and suspended in PBS buffer. The cell suspension was sonicated, and the supernatant was passed through a 0.2 μm filter to remove any cell debris. The crude enzyme was subjected to SDS-PAGE (sodium dodecyl sulfate - polyacrylamide gel electrophoresis) analysis. Each target protein band was excised from the SDS-PAGE gel and fragmented into short peptides by in-gel digestion treatment with trypsin (Promega, Madison, WI, United States). The digested peptides were subjected to NanoLC MS/MS analysis using a nanopump UltiMate 3000 ultra-high-performance liquid chromatography (UHPLC) binary HPLC system coupled to a Q-Exactive HF mass spectrometer (Thermo Fisher, Waltham, MA, United States). The target proteins were identified by searching against the Swiss-Prot protein sequence database using the Mascot v 2.6 search engine from Matrix Science.

To evaluate the quenching performance of recombinant QQ enzymes, a reaction system containing 10 μM 3-oxo-C12-HSL, 50 μL of crude enzyme, and PBS buffer was incubated at 37°C for 3 h. Ten microliters of reaction mixture was tested for residual AHL activity using the *A. tumefaciens* bioassay. The crude extract of the control strain (NC-1 and NC-2) was used as a negative control. The substrate specificity of the crude enzyme was tested with C4-HSL, C6-HSL, C8-HSL, C10-HSL, C12-HSL, 3-oxo-C6-HSL, 3-oxo-C8-HSL, and 3-oxo-C12-HSL (Sigma, St. Louis, MO, United States). The crude enzyme was mixed with different AHL molecules in PBS buffer, and after the reaction at 37°C, the residual AHL was determined by bioassay.

Purification of Recombinant QQ Enzyme

The recombinant strain that was verified to possess AHL-quenching activity was induced in 100 mL of LB medium. The crude enzyme was prepared as described above and the recombinant enzyme was purified by affinity chromatography using a 5 mL HisTrap HP column (GE Healthcare, Piscataway, NJ, United States). The column was equilibrated with binding buffer (20 mM sodium phosphate, pH 7.4, 0.5 M NaCl, and 20 mM imidazole). The crude enzyme was diluted with binding buffer and loaded onto the column. The target protein was eluted with 200 mM imidazole; the eluted fractions were pooled and dialyzed in a dialysis tubing (Fisher Scientific, Hampton, NH, United States) with a molecular weight cutoff (MWCO) of 3.5 kDa. The PBS buffer was used as the dialysis medium, and

the entire procedure was performed three times to remove the extra imidazole and salt. The solution was then concentrated using a centrifugal filter with a MWCO of 3.5 kDa (Merck, Darmstadt, Germany).

Biochemical Characterization of Recombinant QQ Enzymes

The optimal pH of the QQ enzyme was tested by incubating a purified enzyme with 5 μM oxo-C12-HSL in 0.1 M citrate-phosphate buffer (pH 3.0–8.0) and 0.1 M glycine-NaOH buffer (pH 9.0–10.0) at 37°C for 1 h. The effect of the salinity on the enzyme activity was evaluated by incubating the enzyme with 5 μM oxo-C12-HSL in PBS buffer (pH 7.4) under different concentrations of sodium chloride (0 M, 0.1 M, 0.5 M, 1 M, 1.5 M, and 2 M) for 1 h. The optimal temperature for the recombinant enzyme activity was determined by mixing the enzyme with 5 μM oxo-C12-HSL under the optimal pH for each enzyme and under different temperatures ranging from 20 to 100°C for 10 min. The same amount of PBS buffer was used instead of the purified enzyme as a negative control for each test. After the reaction, the residual AHL was quantified using a liquid chromatography-tandem mass spectrometry (LC-MS/MS) system. All the reactions were performed in triplicate. For the biochemical characterization of the NAD(P)-dependent enzymes SDR_{S1-5} and SDR_{L11}, 1 mM NADPH or NADH (Sigma, St. Louis, MO, United States) was added to each reaction to facilitate the enzymatic activity.

AHL Quantification by LC-MS/MS

The AHL molecule oxo-C12-HSL was determined with an Agilent 1260 Infinity quaternary liquid chromatograph (Agilent, Santa Clara, CA, United States) equipped with an Agilent Pursuit C18 column (3 μm particle size, 2.0 × 150 mm) and SCIEX Q-TRAP 5500 mass spectrometer (AB SCIEX, Foster City, CA, United States). The separation was performed at room temperature at a mobile phase flow rate of 250 μL/min using the following gradient elution profile: t = 0 min, 95% solution A (LC-MS grade water with 0.1% formic acid), 5% solution B (LC-MS grade methanol); t = 2 min, 95% solution A, 5% solution B; t = 4 min, 50% solution A, 50% solution B; t = 6 min, 5% solution A, 95% solution B; t = 10 min, 5% solution A, 95% solution B; t = 12 min, 95% solution A, 5% solution B; t = 18 min, 95% solution A, 5% solution B. The detection was performed in positive ion mode using the parameters listed in **Supplementary Table 2**.

Enzymatic Effect on the Motility and Biofilm Formation of Opportunistic Marine Pathogens

The effect of $AiiA_{S1-5}$ on the motility and biofilm formation of *Aeromonas hydrophila, Pseudomonas aeruginosa,* and *Vibrio alginolyticus* (**Supplementary Table 3**), was investigated. Five microliters of overnight culture for each marine strain was spotted in the center of the plate containing marine broth-soft agar (0.3% and 0.5% agar) prior to the addition of 5 μL of purified $AiiA_{S1-5}$ (0.2 μg). The plate was cultured at 40°C overnight. The slightly higher mesophilic temperature of 40°C was chosen to mimic the temperature experienced by bacteria during industrial processes (e.g., in cooling towers, seawater desalination plants and tropical marine aquaculture). The experiment was repeated six times. The migration of the culture was evaluated by calculating the diameters of the haloes around the spotted area. In addition, the effect of the $AiiA_{S1-5}$ on the biofilm formation was also evaluated. Single colonies of *A. hydrophila*, *P. aeruginosa*, and *V. alginolyticus* were cultured in **AS** with 2% peptone and incubated at 40°C overnight. Thereafter, 2×10^9 colony forming units (CFU)/mL of cells were mixed with purified $AiiA_{S1-5}$ (0, 5, 10, and 20 μg/mL). The cultures were transferred into 96-well microtiter plates and further incubated at 40°C for 24 h. Thereafter, the supernatants were carefully removed, and the biofilms were stained with 0.2% crystal violet at room temperature for 30 min. Extra dye was removed with **AS** and the stained cells were solubilized with 200 μL of 30% acetic acid (O'Toole, 2011). The absorbance of the solution was measured at 595 nm. PBS buffer was used instead of purified $AiiA_{S1-5}$ as a negative control.

Transcription of Virulence Genes in Marine Strains in the Presence of Purified $AiiA_{S1-5}$

A. hydrophila, *P. aeruginosa*, and *V. alginolyticus* were grown in marine media at 37°C and 180 rpm overnight. The overnight culture was diluted 1:100 in **MB** medium as mentioned before (salinity: 36 g/L), and 50 μg/mL of purified $AiiA_{S1-5}$ was added to the pathogenic strain culture at the inoculation time. The bacterial cultures were grown at 37°C and 180 rpm. The growth curve of the marine strain with $AiiA_{S1-5}$ or PBS buffer was monitored based on the optical density at 600 nm. The bacterial cultures were sampled at the mid-exponential, late exponential and stationary phases of growth. The samples were used for RNA extraction (RNeasy Mini Kit, Qiagen). cDNA was synthesized with a SuperScript III First-Strand Synthesis Supermix (Thermo Fisher, Waltham, MA, United States). The transcriptional level of each gene (**Supplementary Table 4**) was calculated using the relative standard curve method. To obtain the standard curve, the PCR amplification product of each gene was first cloned into a PCR Blunt II-TOPO vector (Thermo Fisher, Waltham, MA, United States). Plasmid DNA containing the target gene was serially diluted based on the copy number and used as the standard. Real-time PCR was performed on a 7900HT Fast Real-Time PCR system (Thermo Fisher, Waltham, MA, United States). The reaction system contained 5 μL of Fast SYBR Green master mix (Thermo Fisher, Waltham, MA, United States), 0.2 μL each of the forward and reverse primers (10 μM), and 2 μL of cDNA template (2 ng/μL). The quantification of the target gene was normalized to the reference gene (*rpoB*) in each sample.

Statistical Analysis

The statistical analysis was performed with Minitab 17. A paired t-test was used to determine the statistical significance of the difference. The difference was defined as statistically significant when $P < 0.05$.

RESULTS

Bacterial Screening From Marine Sources and the AHL Quenching Test

A total of 51 bacterial isolates that can grow at a high salinity (58 g/L) and a high temperature of 50°C were obtained for QQ screening (**Supplementary Table 5**). The AHL mixture (0.29 mM C4-HSL, 0.25 mM C6-HSL, 0.22 mM C8-HSL and 0.17 mM 3-oxo-C12-HSL) was used to screen the QQ bacteria under high salinity (58 g/L) and a high temperature (50°C). These AHL quenchers belong to the following three phyla: Firmicutes (*Staphylococcus*, *Bacillus*, *Halobacillus*, *Virgibacillus*, *Pontibacillus*, *Aquibacillus*, and *Thalassobacillus*), Bacteroidetes (*Tamlana*, *Tenacibaculum*, *Vibrio*, and *Mesoflavibacter*), and Proteobacteria (*Delftia*, *Bacterioplanes*, *Altererythrobacter*, *Devosia*, *Halomonas*, and *Pseudoalteromonas*). Among the QQ isolates, five showed ≥90% relative AHL QE toward AHL mixtures (**Supplementary Table 1** and **Supplementary Figure 1**). These five QS-quenching bacteria belong to the Pseudomonadaceae (Proteobacteria), Bacillaceae (Firmicutes), and Erythrobacteraceae (Proteobacteria), with three of them belonging to the genus *Altererythrobacter* in the Erythrobacteraceae (**Table 1**).

Size Fractionation of the Bacterial Cell Extract and Supernatant Contents to Identify the AHL-Quenching Enzymes

Both the cell extract and supernatant fraction obtained from the five bacterial isolates showed the ability to inhibit AHL (**Figure 1**), with the cell extract having a higher AHL inhibition performance than the supernatant (**Figures 1A,C**). After heat inactivation, the cell extracts of L11 and S1-5 showed decreased AHL inhibition activity, while no decrease in AHL inhibition activity was detected for the other isolates (**Figure 1A**). This result corresponds with the size fraction experiment for the L11 and S1-5 cell extract (**Figure 1B**), in which a higher relative AHL QE was observed in the >10 kDa portion. This size fraction was generally found to contain potential QQ enzymes (Czajkowski and Jafra, 2009). For the other isolates, the relative AHL quenching activity was higher in the <10 kDa portion, suggesting the presence of quorum signal inhibitors (QSIs). The supernatant of the isolates maintained the same AHL quenching activity before and after heat inactivation (**Figure 1C**), and the <10 kDa fractions in the supernatant contributed more to the quenching effect than the larger size fractions (**Figure 1D**). Both the cell extract and the supernatant of the five strains showed similar QQ performance at 50°C (**Supplementary Figures 2A,C**) except for the presence of QQ activity found in the >3 kDa fraction of the S1-5 supernatant (**Supplementary Figures 2B,D**).

Genomic Sequencing of the Two Bacterial Isolates S1-5 and L11 That Potentially Possess Enzymatic QQ Activity

One closed contig was assembled from S1-5 raw reads, and it had a sequence length of 3.35 Mbp and a GC content of 66.3%. Two contigs were assembled from the L11 raw reads; both contigs were predicted to be closed, with no gap detected (**Supplementary Figure 3**). Contig 1 has a sequence length of 2.89 Mbp (GC content of 46%) and Contig 2 has a full length of 0.64 Mbp (GC content of 45.2%). The sequencing files were deposited in the European Nucleotide Archive (ENA) under study accession number PRJEB30480. Eight potential QQ enzyme genes from S1-5 and L11 (**Table 2**) were classified as *N*-acyl homoserine lactonase (AiiA), oxidoreductase (SDR), esterase (Est), hydrolase (Hyd), a penicillin acylase family protein (PvdQ) and a hypothetical protein (HP). These ORFs all shared a conserved motif with the reference AHL-quenching enzymes (**Supplementary Figure 4**).

Verification of Identified QQ Enzymes for AHL Quenching Activity and Specificity

The identified ORFs were expressed in recombinant *Escherichia coli*. The crude enzyme and cell lysate from recombinant *E. coli*, along with the *E. coli* host that contained blank expression vectors (NC-1 and NC-2), were individually mixed with 5 μM 3-oxo-C12-HSL and tested for residual AHL concentration. Four ORFs, namely, $AiiA_{S1-5}$, SDR_{S1-5}, $Ests_{1-5}$ and SDR_{L11}, were verified to be AHL quenchers. The enzymes showed 26.5%, 40.1%, 13.8%, and 38.0% relative AHL QE compared with the negative controls (**Figure 2**). The positive control made up of AiiA from *B. mycoides* ATCC 6462 showed a 37.9% relative AHL QE compared with the negative control. The level of activity exhibited by the positive control was comparable to that observed for both SDRs from L11 and S1-5. The AHL specificity test further showed that $AiiA_{S1-5}$ showed catalytic activity toward all the tested AHLs, and Est_{S1-5} can quench all the AHLs except C4-HSL and C6-HSL. Both SDR_{S1-5} and SDR_{L11} can quench all

TABLE 1 | Marine bacteria that showed 90–100% relative AHL quenching efficiency under saline condition and at high temperature.

Strain name	Best matched 16S rRNA gene identification	Accession number for 16S rRNA gene sequences	*E*-value	Similarity percentage
L11	*Pseudoalteromonas* sp. (JQ237129.1)	MK575497	0.0	98%
L12	*Pontibacillus* sp. (MG252492.1)	MK575888	0.0	99%
S1-1	*Altererythrobacter marinus* (MF716636.1)	MK578236	0.0	99%
S1-5	*Altererythrobacter* sp. (KC169804.1)	MK574878	0.0	98%
S1-6	*Altererythrobacter marinus* (NR_116432.1)	MK578235	0.0	99%

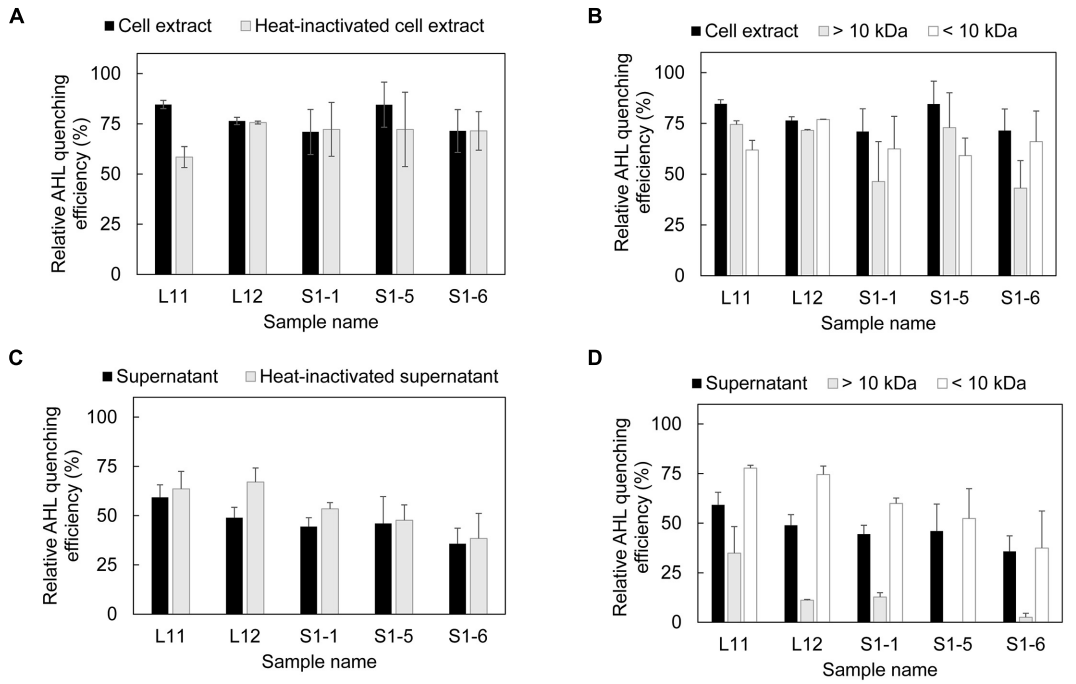

FIGURE 1 | Presence of AHL quenching enzymes in each fraction of AHL quenching bacteria. **(A)** Evaluation of AHL quenching activity in cell extracts and heat-inactivated cell extracts, **(B)** separation of cell extract based on molecular size (10 kDa) and evaluation of the AHL quenching effect in each fraction, **(C)** detection of AHL quenching activity in bacterial supernatant and heat-inactivated supernatant, and **(D)** separation of bacterial supernatant based on the molecular size and evaluation of the AHL quenching effect in each fraction. Each fraction was mixed with AHL mixture (0.15 mM C4-HSL, 0.13 mM C6-HSL, 0.11 mM C8-HSL and 0.08 mM 3-oxo-C12-HSL) and incubated at 37°C for 18 h for residual AHL determination using a biosensor. The relative AHL quenching efficiency of each sample was calculated based on Eq. (1), as stated in the section "Materials and Methods." PBS buffer and AS were used to replace the cell extract and supernatant to create the negative control. Three biological replicates were performed, and the results were expressed as the means ± standard error.

the 3-oxo-AHLs. Moreover, SDR_{L11} showed a quenching effect on C8-HSL (**Supplementary Table 6**).

Biochemical Characterization of Recombinant QQ Enzymes

$AiiA_{S1-5}$ and Est_{S1-5}, SDR_{S1-5} and SDR_{L11} were further induced and purified for biochemical characterization at varying pH values, salt concentrations and temperatures. However, during the course of this 1-month experiment, the purified SDR_{S1-5} and SDR_{L11} did not exhibit good stability while they were in storage compared to $AiiA_{S1-5}$ and Est_{S1-5}. The purified SDR_{S1-5} and SDR_{L11} consistently did not show any AHL-quenching activity after storage despite the addition of NADH or NADPH (data not shown). Hence, the biochemical characterization of only $AiiA_{S1-5}$ and Est_{S1-5} was performed using 3-oxo-C12-HSL as the substrate. $AiiA_{S1-5}$ exhibited >25% relative activity against 3-oxo-C12-HSL between pH 7 and 9, with the highest activity observed at pH 8.0 (**Figure 3A**). $AiiA_{S1-5}$ showed the maximum relative activity in PBS buffer, but it was still able to retain more than 63% of its activity at 0.1–2 M NaCl concentrations (**Figure 3B**). $AiiA_{S1-5}$ showed the highest activity at 0.5 M KCl, and it maintained >70% activity at 0–2 M KCl (**Supplementary Figure 5A**). The relative activity of $AiiA_{S1-5}$ increased from 10 to 50°C (the optimal temperature range) before decreasing rapidly to 7.8%, when the temperature was further increased to 70°C. The enzyme was fully inactivated at 80°C (**Figure 3C**). Est_{S1-5} exhibited the highest relative activity at pH 9.0, and it retained 26.9% of its activity at pH 10.0 (**Figure 3D**). Est_{S1-5} showed optimal activity at 0.1 M NaCl, and it retained more than 83% of its activity at NaCl concentrations between 0 and 0.5 M (**Figure 3E**). The relative activity of Est_{S1-5} decreased with the increasing KCl concentration (**Supplementary Figure 5B**). The enzyme showed the highest activity at both 30 and 40°C, and it was still able to maintain >30% of its relative activity at high temperatures of 50 and 60°C (**Figure 3F**).

Effect of Purified $AiiA_{S1-5}$ on Marine Bacteria

Purified $AiiA_{S1-5}$ was selected for further testing due to its stability, broad substrate specificity and high enzymatic activity in comparison to Est_{S1-5}. The swarming and swimming of *A. hydrophila*, *P. aeruginosa*, and *V. alginolyticus* all decreased in the presence of $AiiA_{S1-5}$ compared with the negative control (**Figure 4A** and **Supplementary Figure 6**). Purified $AiiA_{S1-5}$ reduced swarming more significantly than swimming. There were observed reductions of 48.9%, 35.4%, and 70.2% in swarming in *A. hydrophila*, *P. aeruginosa*, and *V. alginolyticus*, respectively, compared to their respective controls, which were not exposed to the enzyme. Purified $AiiA_{S1-5}$ reduced swimming

TABLE 2 | Screening of potential ORFs from strains L11 and S1-5 using the reported AHL quenching enzymes.

Strain name	ORF name	Protein size (kDa)	Signal peptide prediction	Asp + Glu (%)	Hypothetical function	Superfamily	References QQ ORF	Coverage	Identity	*E*-value
S1-5	$AiiA_{S1-5}$	29.6	√	13.2	N-acyl homoserine lactonase (AiiA)	Metallo-hydrolase-like_MBL-fold superfamily	AiiA *Bacillus thuringiensis* (Liu et al., 2008)	84%	26%	2e-24
	SDR_{S1-5}	25.3	–	10.2	NAD(P)-dependent oxidoreductase (SDR)	Short-chain dehydrogenase/reductase (SDR) family	BpiB09 soil metagenome (Bijtenhoorn et al., 2011)	95%	41%	1e-45
	Est_{S1-5}	31.8	√	9.9	Esterase (Est)	α/β hydrolase family	dlhR *Rhizobium sp.* NGR234 (Krysciak et al., 2011)	45%	36%	4e-07
	Hyd_{S1-5}	38.3	–	11.9	α/β hydrolase (Hyd)	α/β hydrolase family	AidH *Ochrobactrum* sp. (Mei et al., 2010)	49%	28%	1E-11
L11	Hyd_{L11}	28.8	–	13.3	α/β hydrolase (Hyd)	α/β hydrolase family	Est816 soil metagenome (Fan et al., 2012)	83%	25%	1e-16
	$PvdQ_{L11}$	83.8	–	11.3	Penicillin acylase family protein (PvdQ)	Ntn_hydrolase superfamily	QuiP *P. aeruginosa* PAO1 (Huang et al., 2006)	96%	25%	2e-43
	SDR_{L11}	26.8	–	12.0	Oxidoreductase (SDR)	SDR family NAD(P)-dependent oxidoreductase	BpiB09 soil metagenome (Bijtenhoorn et al., 2011)	98%	32%	6e-42
	HP_{L11}	36.0	–	10.8	Hypothetical protein (HP)	DUF523 and DUF1722 domain-containing protein	QQ-16d *Pseudoalteromonas* sp. (Weiland-Bräuer et al., 2015)	99%	48%	8e-106

Potential QQ ORFs were screened by tBLASTn using known QQ enzymes published as references.

consistently by only 20% for all three strains compared to the controls (**Figure 4A**). An inhibitory effect on biofilm formation was observed in *P. aeruginosa,* in which $AiiA_{S1-5}$ significantly inhibited biofilm formation by 46.9%, 79.8%, and 77.0% at 5 μg/mL, 10 μg/mL, and 20 μg/mL of enzyme ($p < 0.001$ compared to the control). The *P. aeruginosa* biofilm inhibitory effects at 10 μg/mL and 20 μg/mL $AiiA_{S1-5}$ were similar ($p > 0.05$). By contrast, a 32.2% biofilm inhibition in *V. alginolyticus* was only observed when 20 μg/mL of $AiiA_{S1-5}$ was applied ($p = 0.04$). $AiiA_{S1-5}$ has no effect on *A. hydrophila* at all the tested levels of the purified enzyme (p-value > 0.05 compared to the control, **Figure 4B**).

Transcription of the Virulence Gene in Marine Strains in the Presence of $AiiA_{S1-5}$

The growth curve of three marine bacteria (*A. hydrophila, P. aeruginosa*, and *V. alginolyticus*) showed no difference in the presence or absence of purified $AiiA_{S1-5}$ (**Figure 5A**). At mid-exponential phase, the transcription levels of the QS-mediated global regulators AhyR and LasR for *A. hydrophila* (**Figure 5B**) and *P. aeruginosa* (**Figure 5C**) were not significantly inhibited by $AiiA_{S1-5}$ ($p > 0.05$). However, $AiiA_{S1-5}$ significantly inhibited AhyR and LasR expression by 56.1% ($p < 0.0001$) and 69.0% ($p = 0.0003$) compared to the sample treated with PBS (control) during the late exponential phase. However, the inhibitory effects on both regulators were no longer observed during the stationary phase. The downstream virulence traits AprA, LasB, and ToxA were regulated by the global regulator *LsrR*, and therefore, they exhibited a similar trend as that observed for LasR in *P. aeruginosa* (**Figure 5C**). AprA is an exception to this trend, in which an inhibition of 22.5% was still observed at the stationary phase (**Figure 5C**, $p = 0.01$). By contrast, for *V. alginolyticus,* an inhibitory effect was only observed on LuxR transcription at the mid-exponential phase and not at the late exponential and stationary phases. This result likewise detrimentally affected the expression of the *Pep* virulence gene in *V. alginolyticus* only at the mid-exponential phase ($p = 0.02$) (**Figure 5D**).

DISCUSSION

Microbe-associated problems in the marine environment (e.g., seawater desalination plants, seawater cooling towers, and aquaculture) are conventionally mitigated by means of biocides or antibiotics that cause health, safety and environmental concerns. QS inhibitors are increasingly being explored as alternative agents to mitigate these problems (Dobretsov et al., 2011). However, research has shown that bacteria can develop resistance to QS inhibitors (Maeda et al., 2012; García-Contreras et al., 2013), rendering the treatment ineffective over the long term. In comparison, QQ enzymes that degrade extracellular QS signals are viewed as imposing less of a burden on cellular metabolism (Fetzner, 2015), and hence, they minimize the development of resistance toward these greener inhibitory agents. In most instances, QQ enzymes or bacteria with enzymatic activity from marine sources (Huang et al., 2012; Mayer et al.,

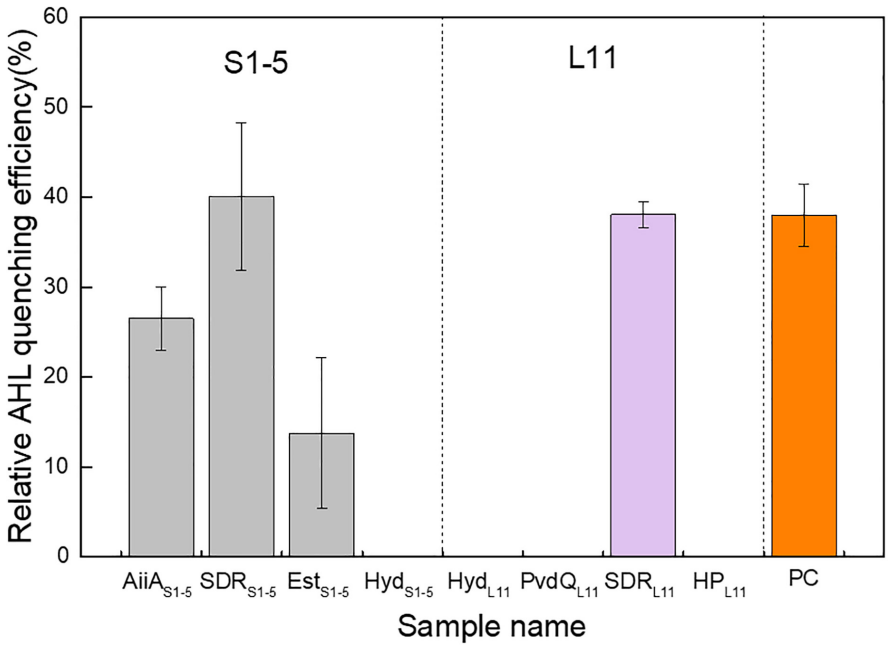

FIGURE 2 | AHL quenching activity comparison of eight potential protein-coding genes expressed in recombinant *Escherichia coli* cells. The relative AHL quenching efficiency of each sample was calculated based on Eq. (1), as stated in the "Materials and Methods" section. The *E. coli* TOP10 carrying vector pTricHisA and *E. coli* BL21 (DE3) carrying pET-20b(+) were used as negative controls. AiiA$_{S1-5}$ (acyl homoserine lactonase), SDR$_{S1-5}$ (oxidoreductase), Est$_{S1-5}$ (esterase), and Hyd$_{S1-5}$ (hydrolase) are possible AHL quenching ORFs from *Altererythrobacter* sp. S1-5; Hyd$_{L11}$ (hydrolase), PvdQ$_{L11}$ (penicillin acylase family protein), SDR$_{L11}$ (oxidoreductase), and H$_{PL11}$ (hypothetical protein) are possible AHL quenching ORFs from *Pseudoalteromonas* sp. L11. PC denotes a positive control, which is obtained by inserting an AiiA gene from *Bacillus mycoides* ATCC 6462 into pET-20b(+) and expressing it in *E. coli* BL21 (DE3). Two independent biological replicates with three technical replicates in each biological replicate were performed for this experiment.

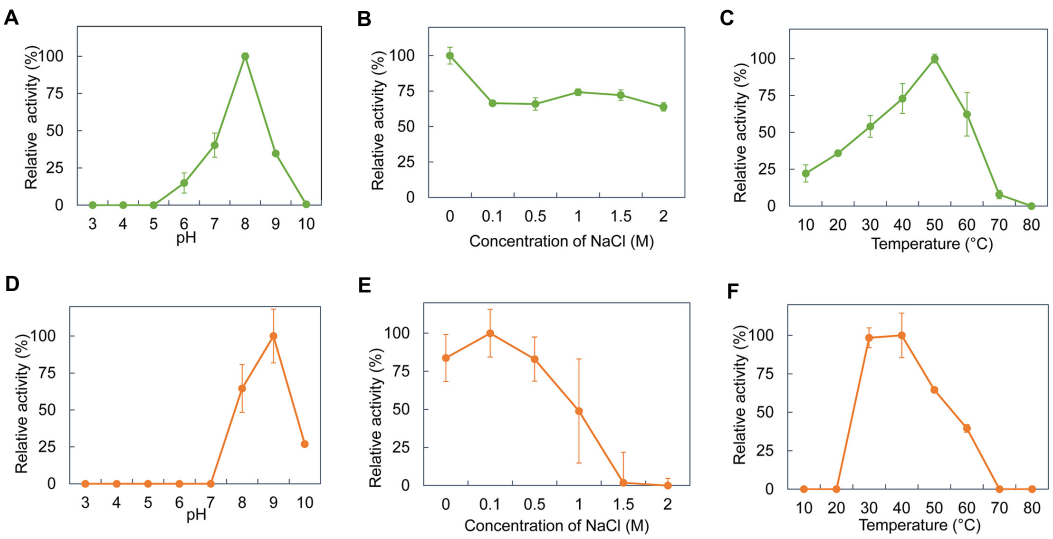

FIGURE 3 | Biochemical properties of purified AiiA$_{S1-5}$ and Est$_{S1-5}$. The relative enzyme activity of AiiA$_{S1-5}$ in/at different **(A)** pH buffers (0.1 M citrate-phosphate buffer, pH 3.0–8.0; 0.1 M glycine-NaOH buffer, pH 9.0–10.0), **(B)** NaCl concentrations (0, 0.1, 0.5, 1, and 2 M), and **(C)** temperatures of 10–80°C. The relative enzyme activity of Est$_{S1-5}$ in/at different **(D)** pH buffers, **(E)** NaCl concentrations, and **(F)** temperatures. The relative enzyme activity of the purified enzymes was normalized using the activity of the purified enzymes at the optimal pH, salinity, and temperature.

2015; Tang et al., 2015; Liu et al., 2017; Rehman and Leiknes, 2018) were demonstrated for their efficiencies to quench QS in only minimal or nutrient medium, which deviate significantly from conditions in marine industrial systems such as seawater desalination plants (salinity: 46,400 ppm, temperature: 22–33°C, and pH 8.1–8.3) (Khawaji et al., 2007) and cooling

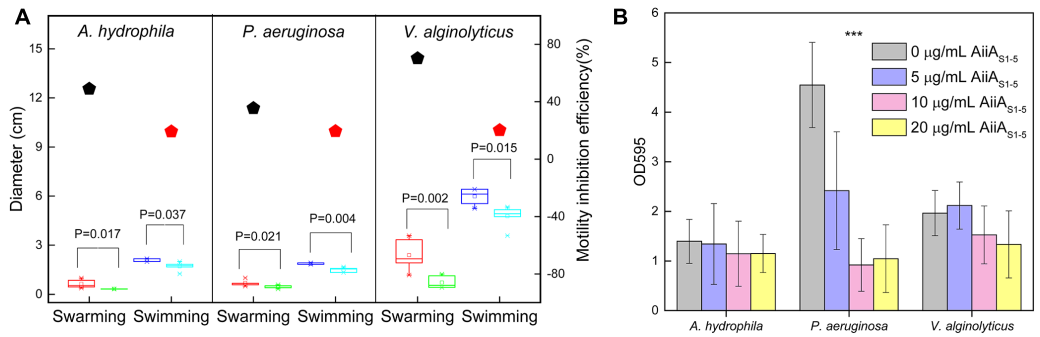

FIGURE 4 | Effect of purified AiiA$_{S1-5}$ on the motility and biofilm formation of marine strains. **(A)** Swarming and swimming of *A. hydrophila*, *P. aeruginosa*, and *V. alginolyticus* on soft MB agar (MB medium with 0.3% and 0.5% agar) in the presence of PBS or 0.2 μg of purified AiiA$_{S1-5}$ at 40°C for 12 h. The red and green boxes represent the swarming diameters of the marine strains in the presence of PBS and AiiA$_{S1-5}$. The blue and magenta boxes represent the swimming diameters of the marine strains in the presence of PBS and AiiA$_{S1-5}$. The inhibition efficiency of AiiA$_{S1-5}$ on the swarming and swimming of the strains under saline conditions is shown in the right *y*-axis, and the inhibition efficiency was calculated using the following equation: (*Pm* – *Em*)/*Pm* × 100%, where *Pm* and *Em* represent the motility halos of each strain in centimeters in the presence of PBS buffer and the purified enzyme AiiA$_{S1-5}$. **(B)** The effect of 0, 5, 10, and 20 μg/mL of purified AiiA$_{S1-5}$ on the biofilm formation of *A. hydrophila*, *P. aeruginosa*, and *V. alginolyticus*. The biofilm formation of the marine bacteria was developed on artificial seawater (**AS**) with 2% peptone extracted from casein in 96-well polystyrene plates at 40°C for 24 h. $^{*}P < 0.05$; $^{**}P < 0.01$; $^{***}P < 0.001$.

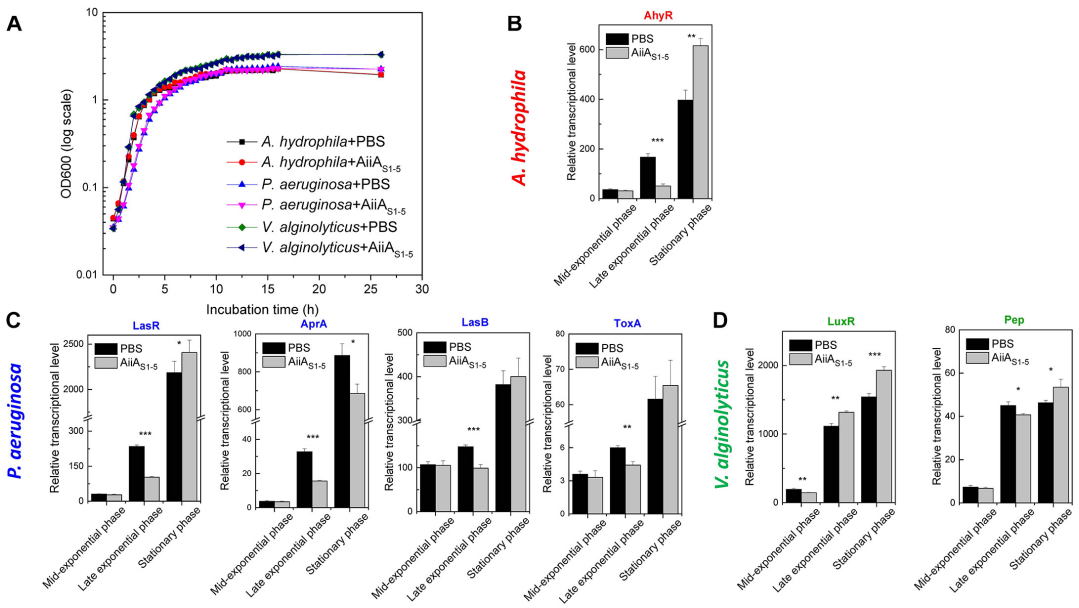

FIGURE 5 | RT-qPCR analysis on the relative expression of selected virulence-associated genes in *A. hydrophila*, *P. aeruginosa*, and *V. alginolyticus* on MB medium in the presence of PBS (negative control) or AiiA$_{S1-5}$ at 37°C. **(A)** Growth curves of *A. hydrophila*, *P. aeruginosa* and *V. alginolyticus* in the presence of PBS or AiiA$_{S1-5}$. The relative transcription levels of genes from **(B)** *A. hydrophila*, **(C)** *P. aeruginosa*, and **(D)** *V. alginolyticus* in the presence of PBS and purified AiiA$_{S1-5}$. The transcriptional levels of pathogenicity-related genes at different growth stages were normalized to the reference gene *rpoB*. Information on these genes can be found in **Supplementary Table 4**. The results are presented as the means ± standard deviation ($n = 3$). $^{*}P < 0.05$; $^{**}P < 0.01$; $^{***}P < 0.001$.

towers (e.g., salinity: >35,000 ppm, and temperature 32–48°C) (Al-Bloushi et al., 2018).

In this study, five bacterial isolates belonging to *Pseudoalteromonas*, *Pontibacillus*, and *Altererythrobacter* demonstrated high QQ activity at a salinity of 58 g/L, 50°C, and a pH of 7.8. To the best of our knowledge, this is the first report on the existence of QQ activity in *Pontibacillus and Altererythrobacter*. The enzymatic QQ activity was primarily discovered in the intracellular fraction of *Pseudoalteromonas* sp. L11 and to a certain extent, it was also found in *Altererythrobacter* sp. S1-5 (**Figure 1**). So far, many bacteria with either intracellular or extracellular QQ enzymatic activity (Kim et al., 2014; Fetzner, 2015) have been reported, but the extracellular activity is more feasible. For example, Cheong et al. (2013) entrapped the bacteria in a vessel that allows only the extracellular enzymes to pass through and react with AHL in a lab-scale membrane bioreactor used for wastewater treatment. This exclusion eliminated the need for an additional step of lysing the bacterial hosts to retrieve

the intracellular enzymes. However, no similar demonstration has been performed in saline environments.

To look for possible QQ enzymes for marine application purposes, the genes identified in L11 and S1-5 that shared homologies with the existing known QQ genes were first expressed in recombinant *E. coli*, purified and characterized further. Using this approach, we found four protein coding genes that shared high homology with the existing QQ genes in *Altererythrobacter* sp. S1-5, but only three demonstrated QQ enzymatic activity when expressed in recombinant *E. coli.* Similarly, we found four homologous QQ ORFs in L11. Both $PvdQ_{L11}$ and HP_{L11} shared 24% and 48% of their identity with the reported pfmA and QQ-16d enzymes from the same genera (Weiland-Bräuer et al., 2015; Liu et al., 2017). However, a further examination of each of the individual purified enzymes from L11 showed that only $SDRL_{11}$ was positive for AHL quenching activity. This may be because the enzyme from the halophilic microorganism was folded incorrectly or maintained poor stability during recombinant expression in its mesophilic host under low-salt conditions (Madern et al., 2000). Among the three ORFs in *Altererythrobacter* S1-5 that showed QQ activity, an N-terminal peptide was predicted for both $AiiA_{S1-5}$ and Est_{S1-5}, suggesting the possibility that the extracellular enzymes would be feasible for use in practical applications. Most QQ enzymes reported thus far do not have a signal peptide, except for AiiA in the marine organisms *Muricauda olearia* (Tang et al., 2015) and *Erythrobacter flavus* (Rehman and Leiknes, 2018) and dlhR in *Rhizobium* sp. (Krysciak et al., 2011).

After purification, only the $AiiA_{S1-5}$ and Est_{S1-5} belonging to the AHL lactonase showed a capacity to degrade AHL. To date, the reported AHL lactonases primarily belong to the metallo-β-lactamase superfamily, the phosphotriesterase family and the α/β hydrolase family. The phosphotriesterase family from the archaeon *Sulfolobus solfataricus* and the crenarchaeon *Vulcanisaeta moutnovskia* (Hiblot et al., 2015) are the most thermophilic QQ enzyme group discovered so far, and they display activity at temperatures of 85–95°C (Merone et al., 2005; Hiblot et al., 2012). The Est816 from the α/β hydrolase family screened from the Turban Basin metagenome can degrade AHL at an optimal temperature of 60°C. Compared to the other two families of AHL lactonases, the metallo-β-lactamase superfamily has a mild optimal catalytic temperature range from 30 to 50°C (Seo et al., 2011; Cao et al., 2012; Sakr et al., 2013; Pedroza et al., 2014; Vinoj et al., 2014; Tang et al., 2015). The AiiT from the thermophilic bacteria *Thermaerobacter marianensis* is an exception, in that it exhibited optimal QQ activity at 60–80°C (Morohoshi et al., 2015). Similarly, the purified $AiiA_{S1-5}$ and Est_{S1-5} obtained during this study can degrade AHL at temperatures of 50°C and 30–40°C, respectively.

To assess if these enzymes can work under saline conditions, the activity of the two enzymes was tested in different concentrations of NaCl and KCl. The $AiiA_{S1-5}$ maintained >63% and >70% relative activity in the presence of 0–2 M NaCl and KCl, respectively (**Figure 3** and **Supplementary Figure 5**), which implied high enzyme robustness under saline conditions. Halophilic proteins usually share common physical features, namely, a high percentage of negatively charged amino acids along the surface area, a high number of salt bridges, low hydrophobicity, and a flexible protein structure (Madern et al., 2000; Takahashi et al., 2018). The 3D structural modeling of $AiiA_{S1-5}$ (without a signal sequence) suggested that there was a high percentage of negatively charged amino acids along the surface area (**Supplementary Figure 7**). Twenty-four salt bridges were predicted from $AiiA_{S1-5}$ (**Supplementary Table 7**), which is higher than that predicted from the AiiA described in an earlier study (Easwaran et al., 2015). This physical property of $AiiA_{S1-5}$ can perhaps account for its ability to exhibit activity under saline conditions, and it is consistent with that of another AiiA (TSAWB) from *Bacillus* sp. that can tolerate up to a 5% salt solution (Easwaran et al., 2015).

$AiiA_{S1-5}$ outperformed the other enzymes discovered in this study, and it was further chosen to demonstrate its QQ efficacy against *A. hydrophila*, *P. aeruginosa*, and *V. alginolyticus.* Both *P. aeruginosa* and *A. hydrophila* were previously reported to be commonly associated with fouled membranes in a seawater desalination plant (Hong et al., 2016; Yap et al., 2017; Nagaraj et al., 2018), while *V. alginolyticus* (Bermont-Bouis et al., 2007) and *P. aeruginosa* (Hamzah et al., 2014) were reportedly possibly linked to pipeline biocorrosion by seawater. Furthermore, these three bacterial species constitute the dominant pathogenic bacterial group reported in marine aquaculture (Sindermann, 1984). It was observed that $AiiA_{S1-5}$ did not impose detrimental effects on cell growth, which reiterates its lower possibility of developing resistance against QQ enzymes over long-term usage. Instead, purified $AiiA_{S1-5}$ showed an inhibitory effect against bacterial motility, biofilm formation and virulence transcription in three marine bacteria under saline conditions (salinity: 36 g/L). The biofilm inhibitory effect of $AiiA_{S1-5}$ in *P. aeruginosa* is more significant than that of the other two bacteria. This distinction was likely caused by the substrate affinity of $AiiA_{S1-5}$ toward the different AHLs secreted by the tested strains (**Supplementary Table 3**). A 10 μg/mL concentration of $AiiA_{S1-5}$ inhibited the biofilm formation of *P. aeruginosa* to ca. 80% under saline conditions. Similarly, purified AHL-lactonase (100 μg/mL) from *Enterobacter aerogenes* VT66 inhibited >70% of the *P. aeruginosa* PAO1 biofilm (Rajesh and Rai, 2015). *Labrenzia* sp. VG12 cells with AHL lactonase activity also reduced the *P. aeruginosa* biofilm by 25% (Rehman and Leiknes, 2018), although the exact enzymatic concentration used here was not made known. These earlier studies, along with that reported here, demonstrated the inhibition effect of AHL lactonases on QS-regulated biofilm formation in *P. aeruginosa*.

In most instances, the transcribed levels of QS-coordinated receptor genes and virulence genes were significantly decreased by $AiiA_{S1-5}$ at the late exponential phases of *A. hydrophila* and *P. aeruginosa* (**Figure 5**). However, the inhibitory effect was no longer observed at the stationary phase. This observation is consistent with that reported in an earlier study (Park et al., 2005; Sivakumar et al., 2019), and it was probably due

to the accumulation of enzymatic inhibitors in the culture over time, or to a decrease in the metabolic activities of the cultures at the stationary phase. QQ enzymes should therefore be deployed as an environmentally benign approach for controlling microbe-associated problems at the early stages of growth and biofilm formation.

CONCLUSION

In this study, bacterial species that proliferate under saline conditions were isolated and screened to select the ones that are positive for QQ under high salinity and high temperatures. Further genomic and biochemical characterization revealed a particularly promising AiiA from the *Altererythrobacter* sp. S1-5 that demonstrated a broad AHL substrate specificity range and enzymatic activity at an optimal pH of 8 and 50°C. $AiiA_{S1-5}$ was also able to maintain good relative QQ activity with increasing salt concentrations up to 2 M. Its QQ efficacy against *P. aeruginosa*, *A. hydrophila*, and *V. alginolyticus* was further demonstrated, in that the motility traits and virulence gene cascades were detrimentally impacted, especially at the mid to late exponential phases of bacterial growth.

These findings collectively suggest that this QQ enzyme would be feasible for use in mitigating membrane biofouling under saline conditions and/or QS-associated pathogenic infections in marine aquaculture.

AUTHOR CONTRIBUTIONS

T-NW designed and performed the experiments, performed the data analysis, and wrote the manuscript with P-YH, who also supervised the research and provided reagents and materials. Q-TG and AP assisted with the genomic DNA sequence assembly. AK helped to write the manuscript.

FUNDING

This work was funded by the King Abdullah University of Science and Technology (KAUST) Competitive Research Grant 2017 (URF/1/2982-01-01) awarded to P-YH.

ACKNOWLEDGMENTS

AK thanked for the support by CSIRO Land and Water.

SUPPLEMENTARY MATERIAL

The Supplementary Material for this article can be found online at: https://www.frontiersin.org/articles/10.3389/fmicb.2019.00823/full#supplementary-material

REFERENCES

Al-Ahmad, M., Aleem, F. A. A., Mutiri, A., and Ubaisy, A. (2000). Biofuoling in RO membrane systems Part 1: fundamentals and control. *Desalination* 132, 173–179. doi: 10.1016/S0011-9164(00)00146-6

Al-Bloushi, M., Saththasivam, J., Al-Sayeghc, S., Jeong, S., Ng, K. C., Amy, G. L., et al. (2018). Performance assessment of oxidants as a biocide for biofouling control in industrial seawater cooling towers. *J. Ind. Eng. Chem.* 59, 127–133. doi: 10.1016/j.jiec.2017.10.015

Amara, I., Miled, W., Slama, R. B., and Ladhari, N. (2018). Antifouling processes and toxicity effects of antifouling paints on marine environment. A review. *Environ. Toxicol. Pharmacol.* 57, 115–130. doi: 10.1016/j.etap.2017.12.001

Bermont-Bouis, D., Janvier, M., Grimont, P. A. D., Dupont, I., and Vallaeys, T. (2007). Both sulfate-reducing bacteria and *Enterobacteriaceae* take part in marine biocorrosion of carbon steel. *J. Appl. Microbiol.* 102, 161–168. doi: 10.1111/j.1365-2672.2006.03053.x

Bijtenhoorn, P., Mayerhofer, H., Muller-Dieckmann, J., Utpatel, C., Schipper, C., Hornung, C., et al. (2011). A novel metagenomic short-chain dehydrogenase/reductase attenuates *Pseudomonas aeruginosa* biofilm formation and virulence on *Caenorhabditis elegans*. *PLoS One* 6:e26278. doi: 10.1371/journal.pone.0026278

Brettin, T., Davis, J. J., Disz, T., Edwards, R. A., Gerdes, S., Olsen, G. J., et al. (2015). RASTtk: a modular and extensible implementation of the RAST algorithm for building custom annotation pipelines and annotating batches of genomes. *Sci. Rep.* 5:8365. doi: 10.1038/srep08365

Cao, Y., He, S., Zhou, Z., Zhang, M., Mao, W., Zhang, H., et al. (2012). Orally administered thermostable N-acyl homoserine lactonase from *Bacillus* sp. strain AI96 attenuates *Aeromonas hydrophila* infection in zebrafish. *Appl. Environ. Microbiol.* 78, 1899–1908. doi: 10.1128/AEM.06139-11

Cheong, W.-S., Lee, C.-H., Moon, Y.-H., Oh, H.-S., Kim, S.-R., Lee, S. H., et al. (2013). Isolation and identification of indigenous quorum quenching bacteria,*Pseudomonas* sp. 1A1, for biofouling control in MBR. *Ind. Eng. Chem. Res.* 52, 10554–10560. doi: 10.1021/ie303146f

Czajkowski, R., and Jafra, S. (2009). Quenching of acyl-homoserine lactone-dependent quorum sensing by enzymatic disruption of signal molecules. *Acta Biochim. Pol.* 56, 1–16. doi: 10.18388/abp.2009_2512

Defoirdt, T. (2018). Quorum-Sensing systems as targets for antivirulence therapy. *Trends Microbiol.* 26, 313–328. doi: 10.1016/j.tim.2017.10.005

Dobretsov, S., Teplitski, M., Bayer, M., Gunasekera, S., Proksch, P., and Paul, V. J. (2011). Inhibition of marine biofouling by bacterial quorum sensing inhibitors. *Biofouling* 27, 893–905. doi: 10.1080/08927014.2011.609616

Easwaran, N., Karthikeyan, S., Sridharan, B., and Gothandam, K. M. (2015). Identification and analysis of the salt tolerant property of AHL lactonase (AiiATSAWB) of *Bacillus* species. *J. Basic Microbiol.* 55, 579–590. doi: 10.1002/jobm.201400013

Elimelech, M., and Phillip, W. A. (2011). The future of seawater desalination: energy, technology, and the environment. *Science* 333, 712–717. doi: 10.1126/science.1200488

Enning, D., Venzlaff, H., Garrelfs, J., Dinh, H. T., Meyer, V., Mayrhofer, K., et al. (2012). Marine sulfate-reducing bacteria cause serious corrosion of iron under electroconductive biogenic mineral crust. *Environ. Microbiol.* 14, 1772–1787. doi: 10.1111/j.1462-2920.2012.02778.x

Fan, X. J., Liu, X. L., and Liu, Y. H. (2012). The cloning and characterization of one novel metagenome-derived thermostable esterase acting on N-acylhomoserine lactones. *J. Mol. Catal. B Enzym.* 83, 29–37. doi: 10.1016/j.molcatb.2012.07.006

Fetzner, S. (2015). Quorum quenching enzymes. *J. Biotechnol.* 201, 2–14. doi: 10.1016/j.jbiotec.2014.09.001

García-Contreras, R., Martínez-Vázquez, M., Velázquez Guadarrama, N., Villegas Pañeda, A. G., Hashimoto, T., Maeda, T., et al. (2013). Resistance to the quorum-quenching compounds brominated furanone C-30 and 5-fluorouracil in *Pseudomonas aeruginosa* clinical isolates. *Pathog. Dis.* 68, 8–11. doi: 10.1111/2049-632X.12039

Gouet, P., Courcelle, E., Stuart, D. I., and Métoz, F. (1999). ESPript: analysis of multiple sequence alignments in PostScript. *Bioinformatics* 15, 305–308. doi: 10.1093/bioinformatics/15.4.305

Hamzah, E., Hussain, M. F., Ibrahim, Z., and Abdolahi, A. (2014). Corrosion behaviour of carbon steel in sea water medium in presence of *P. aeruginosa* Bacteria. *Arab. J. Sci. Eng.* 39, 6863–6870. doi: 10.1007/s13369-014-1264-7

Hiblot, J., Bzdrenga, J., Champion, C., Chabriere, E., and Elias, M. (2015). Crystal structure of VmoLac, a tentative quorum quenching lactonase from the extremophilic crenarchaeon *Vulcanisaeta moutnovskia*. *Sci. Rep.* 5:8372. doi: 10.1038/srep08372

Hiblot, J., Gotthard, G., Chabriere, E., and Elias, M. (2012). Structural and enzymatic characterization of the lactonase SisLac from *Sulfolobus islandicus*. *PLoS One* 7:e47028. doi: 10.1371/journal.pone.0047028

Hong, P.-Y., Moosa, N., and Mink, J. (2016). Dynamics of microbial communities in an integrated ultrafiltration reverse osmosis desalination pilot plant located at the Arabian Gulf. *Desalination Water Treat.* 57, 16310–16323. doi: 10.1080/19443994.2015.1083483

Huang, J. J., Petersen, A., Whiteley, M., and Leadbetter, J. R. (2006). Identification of QuiP, the product of gene PA1032, as the second acyl-homoserine lactone acylase of *Pseudomonas aeruginosa* PAO1. *Appl. Environ. Microbiol.* 72, 1190–1197. doi: 10.1128/Aem.72.2.1190-1197.2006

Huang, W., Lin, Y., Yi, S., Liu, P., Shen, J., Shao, Z., et al. (2012). QsdH, a novel AHL lactonase in the RND-type inner membrane of marine *Pseudoalteromonas byunsanensis* strain 1A01261. *PLoS One* 7:e46587. doi: 10.1371/journal.pone.0046587

Katebian, L., Gomez, E., Skillman, L., Li, D., Ho, G., and Jiang, S. C. (2016). Inhibiting quorum sensing pathways to mitigate seawater desalination RO membrane biofouling. *Desalination* 393, 135–143. doi: 10.1016/j.desal.2016.01.013

Katebian, L., Hoffmann, M. R., and Jiang, S. C. (2018). Incorporation of quorum sensing inhibitors onto reverse osmosis membranes for biofouling prevention in seawater desalination. *Environ. Eng. Sci.* 35, 261–269. doi: 10.1089/ees.2017.0129

Khawaji, A. D., Kutubkhanah, I. K., and Wie, J. M. (2007). A 13.3 MGD seawater RO desalination plant for Yanbu Industrial City. *Desalination* 203, 176–188. doi: 10.1016/j.desal.2006.02.018

Kim, A. L., Park, S. Y., Lee, C. H., Lee, C. H., and Lee, J. K. (2014). Quorum quenching bacteria isolated from the sludge of a wastewater treatment plant and their application for controlling biofilm formation. *J. Microbiol. Biotechnol.* 24, 1574–1582. doi: 10.4014/jmb.1407.07009

Koren, S., Walenz, B. P., Berlin, K., Miller, J. R., Bergman, N. H., and Phillippy, A. M. (2017). Canu: scalable and accurate long-read assembly via adaptive k-mer weighting and repeat separation. *Genome Res.* 27, 722–736. doi: 10.1101/gr.215087.116

Krumsiek, J., Arnold, R., and Rattei, T. (2007). Gepard: a rapid and sensitive tool for creating dotplots on genome scale. *Bioinformatics* 23, 1026–1028. doi: 10.1093/bioinformatics/btm039

Krysciak, D., Schmeisser, C., Preuss, S., Riethausen, J., Quitschau, M., Grond, S., et al. (2011). Involvement of multiple loci in quorum quenching of autoinducer I molecules in the nitrogen-fixing symbiont *Rhizobium* (*Sinorhizobium*) sp. strain NGR234. *Appl. Environ. Microbiol.* 77, 5089–5099. doi: 10.1128/AEM.00112-11

Lee, K., Yu, H., Zhang, X., and Choo, K. H. (2018). Quorum sensing and quenching in membrane bioreactors: opportunities and challenges for biofouling control. *Bioresour. Technol.* 270, 656–668. doi: 10.1016/j.biortech.2018.09.019

Lee, S., Park, S. K., Kwon, H., Lee, S. H., Lee, K., Nahm, C. H., et al. (2016). Crossing the border between laboratory and field: bacterial quorum quenching for anti-biofouling strategy in an MBR. *Environ. Sci. Technol.* 50, 1788–1795. doi: 10.1021/acs.est.5b04795

Liu, D., Momb, J., Thomas, P. W., Moulin, A., Petsko, G. A., Fast, W., et al. (2008). Mechanism of the quorum-quenching lactonase (AiiA) from *Bacillus thuringiensis*. 1. Product-bound structures. *Biochemistry* 47, 7706–7714. doi: 10.1021/bi800368y

Liu, N., Yu, M., Zhao, Y., Cheng, J., An, K., and Zhang, X. H. (2017). PfmA, a novel quorum-quenching N-acylhomoserine lactone acylase from *Pseudoalteromonas flavipulchra*. *Microbiology* 163, 1389–1398. doi: 10.1099/mic.0.000535

Madern, D., Ebel, C., and Zaccai, G. (2000). Halophilic adaptation of enzymes. *Extremophiles* 4, 91–98. doi: 10.1007/s007920050142

Maeda, T., Garcia-Contreras, R., Pu, M., Sheng, L., Garcia, L. R., Tomas, M., et al. (2012). Quorum quenching quandary: resistance to antivirulence compounds. *ISME J.* 6, 493–501. doi: 10.1038/ismej.2011.122

Mayer, C., Romero, M., Muras, A., and Otero, A. (2015). Aii20J, a wide-spectrum thermostable N-acylhomoserine lactonase from the marine bacterium *Tenacibaculum* sp. 20J, can quench AHL-mediated acid resistance in *Escherichia coli*. *Appl. Microbiol. Biotechnol.* 99, 9523–9539. doi: 10.1007/s00253-015-6741-8

Mei, G. Y., Yan, X. X., Turak, A., Luo, Z. Q., and Zhang, L. Q. (2010). AidH, an Alpha/Beta-Hydrolase Fold Family Member from an *Ochrobactrum* sp. Strain, Is a novel N-Acylhomoserine Lactonase. *Appl. Environ. Microbiol.* 76, 4933–4942. doi: 10.1128/Aem.00477-10

Merone, L., Mandrich, L., Rossi, M., and Manco, G. (2005). A thermostable phosphotriesterase from the archaeon *Sulfolobus solfataricus*: cloning, overexpression and properties. *Extremophiles* 9, 297–305. doi: 10.1007/s00792-005-0445-4

Mizan, M. F. R., Jahid, I. K., and Ha, S. D. (2015). Microbial biofilms in seafood: a food-hygiene challenge. *Food Microbiol.* 49, 41–55. doi: 10.1016/j.fm.2015.01.009

Morohoshi, T., Tominaga, Y., Someya, N., and Ikeda, T. (2015). Characterization of a novel thermostable N-acylhomoserine lactonase from the thermophilic bacterium *Thermaerobacter marianensis*. *J. Biosci. Bioeng.* 120, 1–5. doi: 10.1016/j.jbiosc.2014.11.014

Nagaraj, V., Skillman, L., Li, D., and Ho, G. (2018). Review - Bacteria and their extracellular polymeric substances causing biofouling on seawater reverse osmosis desalination membranes. *J. Environ. Manage.* 223, 586–599. doi: 10.1016/j.jenvman.2018.05.088

Oh, H. S., and Lee, C. H. (2018). Origin and evolution of quorum quenching technology for biofouling control in MBRs for wastewater treatment. *J. Membrane Sci.* 554, 331–345. doi: 10.1016/j.memsci.2018.03.019

O'Toole, G. A. (2011). Microtiter dish biofilm formation assay. *J. Vis. Exp.* 47:2437. doi: 10.3791/2437

Park, S. Y., Kang, H. O., Jang, H. S., Lee, J. K., Koo, B. T., and Yum, D. Y. (2005). Identification of extracellular N-acylhomoserine lactone acylase from a *Streptomyces* sp. and its application to quorum quenching. *Appl. Environ. Microbiol.* 71, 2632–2641. doi: 10.1128/AEM.71.5.2632-2641.2005

Pedroza, C. J., Florez, A. M., Ruiz, O. S., and Orduz, S. (2014). Enzymatic hydrolysis of molecules associated with bacterial quorum sensing using an acyl homoserine lactonase from a novel *Bacillus thuringiensis* strain. *Antonie Van Leeuwenhoek* 105, 253–264. doi: 10.1007/s10482-013-0072-5

Piper, K. R., Beck von Bodman, S., and Farrand, S. K. (1993). Conjugation factor of *Agrobacterium tumefaciens* regulates Ti plasmid transfer by autoinduction. *Nature* 362, 448–450. doi: 10.1038/362448a0

Rajesh, P. S., and Rai, V. R. (2015). Purification and antibiofilm activity of AHL-lactonase from endophytic *Enterobacter aerogenes* VT66. *Int. J. Biol. Macromol.* 81, 1046–1052. doi: 10.1016/j.ijbiomac.2015.09.048

Rehman, Z. U., and Leiknes, T. (2018). Quorum-quenching bacteria isolated from red sea sediments reduce biofilm formation by *Pseudomonas aeruginosa*. *Front. Microbiol.* 9:1354. doi: 10.3389/fmicb.2018.01354

Romero, M., Martin-Cuadrado, A. B., and Otero, A. (2012). Determination of whether quorum quenching is a common activity in marine bacteria by analysis of cultivable bacteria and metagenomic sequences. *Appl. Environ. Microbiol.* 78, 6345–6348. doi: 10.1128/AEM.01266-12

Romero, M., Martin-Cuadrado, A. B., Roca-Rivada, A., Cabello, A. M., and Otero, A. (2011). Quorum quenching in cultivable bacteria from dense marine coastal microbial communities. *FEMS Microbiol. Ecol.* 75, 205–217. doi: 10.1111/j.1574-6941.2010.01011.x

Sakr, M. M., Aboshanab, K. M., Aboulwafa, M. M., and Hassouna, N. A. (2013). Characterization and complete sequence of lactonase enzyme from *Bacillus weihenstephanensis* isolate P65 with potential activity against acyl homoserine lactone signal molecules. *Biomed. Res. Int.* 2013:192589. doi: 10.1155/2013/192589

Scarascia, G., Wang, T., and Hong, P. Y. (2016). Quorum sensing and the use of quorum quenchers as natural biocides to inhibit sulfate-reducing bacteria. *Antibiotics* 5:39. doi: 10.3390/antibiotics5040039

Seo, M. J., Lee, B. S., Pyun, Y. R., and Park, H. (2011). Isolation and characterization of N-acylhomoserine lactonase from the thermophilic bacterium, *Geobacillus caldoxylosilyticus* YS-8. *Biosci. Biotechnol. Biochem.* 75, 1789–1795. doi: 10.1271/bbb.110322

Sindermann, C. J. (1984). Disease in marine aquaculture. *Helgoländer Meeresuntersuchungen* 37, 505–532. doi: 10.1007/BF01989327

Sivakumar, K., Scarascia, G., Zaouri, N., Wang, T., Kaksonen, A. H., and Hong, P. Y. (2019). Salinity-mediated increment in sulfate reduction, biofilm formation, and quorum sensing: a potential connection between quorum sensing and sulfate reduction? *Front. Microbiol.* 10:188. doi: 10.3389/fmicb.2019.00188

Takahashi, M., Takahashi, E., Joudeh, L. I., Marini, M., Das, G., Elshenawy, M. M., et al. (2018). Dynamic structure mediates halophilic adaptation of a DNA polymerase from the deep-sea brines of the Red Sea. *FASEB J.* 32, 3346–3360. doi: 10.1096/fj.201700862RR

Tang, K., Su, Y., Brackman, G., Cui, F., Zhang, Y., Shi, X., et al. (2015). MomL, a novel marine-derived N-acyl homoserine lactonase from *Muricauda olearia*. *Appl. Environ. Microbiol.* 81, 774–782. doi: 10.1128/AEM.02805-14

Tang, K., Zhang, Y., Yu, M., Shi, X., Coenye, T., Bossier, P., et al. (2013). Evaluation of a new high-throughput method for identifying quorum quenching bacteria. *Sci. Rep.* 3:2935. doi: 10.1038/srep02935

Tinh, N. T. N., Yen, V. H. N., Dierckens, K., Sorgeloos, P., and Bossier, P. (2008). An acyl homoserine lactone-degrading microbial community improves the survival of first-feeding turbot larvae (*Scophthalmus maximus* L.). *Aquaculture* 285, 56–62. doi: 10.1016/j.aquaculture.2008.08.018

Torres, M., Rubio-Portillo, E., Antón, J., Ramos-Esplá, A. A., Quesada, E., and Llamas, I. (2016). Selection of the *N*-acylhomoserine lactone-degrading bacterium *Alteromonas stellipolaris* PQQ-42 and of its potential for biocontrol in aquaculture. *Front. Microbiol.* 7:646. doi: 10.3389/fmicb.2016.00646

Vinoj, G., Vaseeharan, B., Thomas, S., Spiers, A. J., and Shanthi, S. (2014). Quorum-quenching activity of the AHL-lactonase from *Bacillus licheniformis* DAHB1 inhibits Vibrio biofilm formation in vitro and reduces shrimp intestinal colonisation and mortality. *Mar. Biotechnol.* 16, 707–715. doi: 10.1007/s10126-014-9585-9

Weiland-Bräuer, N., Pinnow, N., and Schmitz, R. A. (2015). Novel reporter for identification of interference with acyl homoserine lactone and autoinducer-2 quorum sensing. *Appl. Environ. Microbiol.* 81, 1477–1489. doi: 10.1128/AEM.03290-14

Yap, S. A., Scarascia, G., and Hong, P. Y. (2017). Bacterial cell numbers and community structures of seawater biofilms depend on the attachment substratum. *Desalination Water Treatment* 97, 41–71. doi: 10.5004/dwt.2017.21600

Yates, E. A., Philipp, B., Buckley, C., Atkinson, S., Chhabra, S. R., Sockett, R. E., et al. (2002). N-Acylhomoserine lactones undergo lactonolysis in a pH-, temperature-, and acyl chain length-dependent manner during growth of *Yersinia pseudotuberculosis* and *Pseudomonas aeruginosa*. *Infect. Immun.* 70, 5635–5646. doi: 10.1128/iai.70.10.5635-5646.2002

Conflict of Interest Statement: The authors declare that the research was conducted in the absence of any commercial or financial relationships that could be construed as a potential conflict of interest.

frontiers in Microbiology

ORIGINAL RESEARCH
published: 24 April 2019
doi: 10.3389/fmicb.2019.00867

Effect of Quercetin Rich Onion Extracts on Bacterial Quorum Sensing

B. X. V. Quecan[1], J. T. C. Santos[1], M. L. C. Rivera[1], N. M. A. Hassimotto[1], F. A. Almeida[2] and U. M. Pinto[1]†*

[1] Food Research Center (FoRC), Faculty of Pharmaceutical Sciences, University of São Paulo, São Paulo, Brazil,
[2] Department of Nutrition, Federal University of Juiz de Fora, Governador Valadares, Brazil

OPEN ACCESS

Edited by:
Ana Maria Otero, University of Santiago de Compostela, Spain

Reviewed by:
Jin Zhou, Tsinghua University, China
Tania Pozzo, University of California, Davis, United States

***Correspondence:**
U. M. Pinto
uelintonpinto@usp.br;
uelintonpinto@gmail.com

†Present address:
U. M. Pinto, Harvard Medical School, Massachusetts General Hospital, Boston, MA, United States

Specialty section:
This article was submitted to Antimicrobials, Resistance and Chemotherapy, a section of the journal Frontiers in Microbiology

Received: *04 February 2019*
Accepted: *04 April 2019*
Published: *24 April 2019*

Citation:
Quecan BXV, Santos JTC, Rivera MLC, Hassimotto NMA, Almeida FA and Pinto UM (2019) Effect of Quercetin Rich Onion Extracts on Bacterial Quorum Sensing. Front. Microbiol. 10:867. doi: 10.3389/fmicb.2019.00867

Quorum sensing (QS) regulates bacterial gene expression and studies suggest quercetin, a flavonol found in onion, as a QS inhibitor. There are no studies showing the anti-QS activity of plants containing quercetin in its native glycosylated forms. This study aimed to evaluate the antimicrobial and anti-QS potential of organic extracts of onion varieties and its representative phenolic compounds quercetin aglycone and quercetin 3-β-D-glucoside in the QS model bacteria *Chromobacterium violaceum* ATCC 12472, *Pseudomonas aeruginosa* PAO1, and *Serratia marcescens* MG1. Three phenolic extracts were obtained: red onion extract in methanol acidified with 2.5% acetic acid (RO-1), white onion extract in methanol (WO-1) and white onion extract in methanol ammonium (WO-2). Quercetin 4-*O*-glucoside and quercetin 3,4-*O*-diglucoside were identified as the predominant compounds in both onion varieties using HPLC-DAD and LC-ESI-MS/MS. However, quercetin aglycone, cyanidin 3-*O*-glucoside and quercetin glycoside were identified only in RO-1. The three extracts showed minimum inhibitory concentration (MIC) values equal to or above 125 μg/ml of dried extract. Violacein production was significantly reduced by RO-1 and quercetin aglycone, but not by quercetin 3-β-D-glucoside. Motility in *P. aeruginosa* PAO1 was inhibited by RO-1, while WO-2 inhibited *S. marcescens* MG1 motility only in high concentration. Quercetin aglycone and quercetin 3-β-D-glucoside were effective at inhibiting motility in *P. aeruginosa* PAO1 and *S. marcescens* MG1. Surprisingly, biofilm formation was not affected by any extracts or the quercetins tested at sub-MIC concentrations. *In silico* studies suggested a better interaction and placement of quercetin aglycone in the structures of the CviR protein of *C. violaceum* ATCC 12472 than the glycosylated compound which corroborates the better inhibitory effect of the former over violacein production. On the other hand, the two quercetins were well placed in the AHLs binding pockets of the LasR protein of *P. aeruginosa* PAO1. Overall onion extracts and quercetin presented antimicrobial activity, and interference on QS regulated production of violacein and swarming motility.

Keywords: quorum sensing, antimicrobial activity, onion, quorum quenching, phenolic compounds, glycosylation

INTRODUCTION

Quorum sensing (QS) is a bacterial communication that uses signaling molecules known as autoinducers that accumulate in the medium according to population density (Fuqua et al., 1994; Whitehead et al., 2001; Lazdunski et al., 2004; Waters and Bassler, 2005). Signaling in Gram-positive microorganisms is mediated by low molecular weight peptides known as autoinducer peptides (AIPs) (Miller and Bassler, 2001). Other molecules such as autoinducer-2 (AI-2) are associated with most bacterial species allowing intra and interspecific communication (Miller and Bassler, 2001; Fuqua and Greenberg, 2002; Bai and Rai, 2011). Molecules such as quinolones, diketopiperazines and indole hydroxyketones can also function as communication cues (Waters and Bassler, 2005; Platt and Fuqua, 2010; Papenfort and Bassler, 2016).

In Gram-negative bacteria, signaling is usually mediated by acyl homoserine lactone (AHL) molecules, known as autoinducer-1 (AI-1) (Skandamis and Nychas, 2012). These molecules are composed of a fatty acid chain attached to a lactone ring by an amide bond. The variation that exists between the molecules of AHL occurs both by the size and the composition of the fatty acids that have a variation from 4 to 18 carbons and have some substitutions in the chain (Whitehead et al., 2001; Lazdunski et al., 2004; La Sarre and Federle, 2013). This mechanism was described in the 1970s in two species of bioluminescent marine bacteria: *Allivibrio fischeri* and *Vibrio harveyi* (Nealson and Hastings, 1979). In addition to these bacteria, there are other model microorganisms such as *Chromobacterium violaceum, Pseudomonas aeruginosa, Agrobacterium tumefaciens, Erwinia carotovora,* and *Serratia liquefaciens* in which QS has been well elucidated (Miller and Bassler, 2001; Waters and Bassler, 2005). There is great interest in these microorganisms as models to study QS, since many of the phenotypes are easily measured and are specifically regulated by QS.

In several bacteria QS regulates a range of phenotypes, coordinating a group behavior that controls the expression of virulence factors, extracellular enzymes, biofilm formation, secondary metabolites, motility, among others (Whitehead et al., 2001; Waters and Bassler, 2005; Skandamis and Nychas, 2012). Many of these phenotypes can impact food spoilage, making the product undesirable or unacceptable for consumption. As an example, the expression of some microbial extracellular enzymes like proteases, pectinases and lipases is regulated by QS (Ammor et al., 2008; Martins et al., 2018). Therefore, researchers have tried to find strategies to disrupt this communication using inhibitory compounds and consequently improve food quality and safety (Bai and Rai, 2011; Skandamis and Nychas, 2012).

Many studies have shown the potential of plant organic extracts rich in phenolic compounds to interfere with QS in different bacteria. These compounds constitute a diverse group of chemical substances, with different chemical activities, important for plant reproduction, growth, and protection against pathogens attack (Martínez et al., 2002). They can be classified depending on the ring number and the type of elements that bind them into phenolic acids, stilbenes, lignans, and flavonoids (Rodrigues et al., 2016).

The last group is an important class of natural products with polyphenol structure, widely found in fruits and vegetables (Panche et al., 2016). Its basic structural feature is the 2-phenyl-benzo-α-pyran compound which consists in two benzene rings (A and B) attached through a heterocyclic pyran ring (C) (Cushnie and Lamb, 2005). There is great interest in flavonoids because of their anti-inflammatory, antimicrobial, antioxidant and antitumor properties, among others (Cushnie and Lamb, 2005; Silveira, 2012; Rodrigues et al., 2016). In addition, flavonoids have also gained importance as potential inhibitors of the QS system. Different flavonoids such as taxifolin, kaempferol, naringenin, apigenin, baicalein, and others have demonstrated their ability to interfere in the QS system of microorganisms such as *P. aeruginosa* PAO1 and *C. violaceum* CV026 (Vandeputte et al., 2011), changing the transcription of QS-controlled target promoters and inhibiting the production of virulence factors (Paczkowski et al., 2017).

One of the most representative flavonoids found in high concentrations in foods, especially onion (284–486 mg/kg) is quercetin (Behling et al., 2008). Different studies showed the inhibitory potential of this compound against some microorganisms with phenotypes regulated by QS. A research performed by Gopu et al. (2015) evaluated the ability of quercetin against the QS biosensor strain *C. violaceum* CV026 and tested the anti-biofilm property of the compound against food-borne pathogens such as *Bacillus* spp., *Pseudomonas* spp. *Salmonella* spp., *Campylobacter jejuni,* and *Yersinia enterocolitica*. The results showed that quercetin inhibited violacein production in all the concentrations tested and additionally had a significant reduction of other phenotypes such as biofilm formation, exopolysaccharides, alginate production and motility in the compound's presence (Gopu et al., 2015). Another study showed the effect of quercetin on biofilm formation and virulence factors' production by *P. aeruginosa* PAO1 (Ouyang et al., 2016). The authors observed that quercetin had a significant inhibition on biofilm formation, pyocyanin, protease and elastase production. It was also observed that the expression of *lasI, lasR, rhII,* and *rhIR* genes was significantly reduced in response to quercetin (Ouyang et al., 2016).

Different types of quercetins such as quercetin aglycone, quercetin 4-glucoside, quercetin 3,4-*O*-diglucoside, quercetin 7,4-diglucoside, quercetin 3-glucosideglucoside and quercetin 5-glucoside are found in onion (*Allium cepa* Lineu). The anthocyanin cyanidin has also been identified in purple onion cultivars that give reddish or purple coloration to the bulbs (Lombard et al., 2005). The amount of quercetin in onions varies according to the color and type of bulb, being distributed mainly in the skins and outer rings (Arabbi et al., 2004; Lombard et al., 2005; Corzo Martínez et al., 2007; Kwak et al., 2017).

Studies have suggested that quercetin, a flavonol present in high concentrations in onion (*Allium cepa*), presents anti-QS properties against some Gram-negative microorganisms.

However, there are no studies showing the anti-QS activity of plants containing quercetin in its native glycosylated forms. Thus, the objective of this work was to assess the potential presented by onion extracts to interfere with bacterial cell-to-cell communication.

MATERIALS AND METHODS

Bacterial Strains and Culture Conditions

The microorganisms used in this work were *Chromobacterium violaceum* ATCC 12472 (30°C/24 h), *Pseudomonas aeruginosa* PAO1 (37°C/24 h), and *Serratia marcescens* MG1 (30°C/24 h). All cultures were grown in Luria Bertani (LB) agar or broth containing peptone 1%, yeast extract 0.5%, sodium chloride 0.5% with 1.2% agar, as needed.

Preparation, Extraction, and Characterization of Phenolic Compounds of Onion Varieties

Preparation of Extracts

The extracts were prepared in the Laboratory of Chemistry, Biochemistry and Molecular Biology of Food in the Faculty of Pharmaceutical Sciences of the University of São Paulo. Samples of 5 kg of white and red onion (*Allium cepa*) were purchased from *Companhia de Entrepostos e Armazéns Gerais de São Paulo* (CEAGESP) warehouse. The samples were selected, cut and frozen with liquid nitrogen and stored at −80°C until use. For the analysis, 20 g of each onion variety were homogenized for 1 min using Ultra-Turrax (Polytron-Kinematica GmbH, Kriens-Luzern, Switzerland) in 100 ml of 70% methanol for white onion and 70% methanol acidified with 5% acetic acid for red onion due to its content of anthocyanins. Then, the samples were vacuum filtered, and the residue was recovered, repeating the process twice using 50 ml of the respective solvent. The obtained extracts were pooled and concentrated in a rotary evaporator (Rotavapor 120, Büchi, Flawil, Switzerland) at a temperature of 40°C until complete methanol removal, in order to use it for the solid phase separation step.

Solid Phase Extraction

Methanol free samples were loaded in a column with 1 g of polyamide (CC 6, Macherey-Nagel, Germany), prepared in a syringe of 6 ml and preconditioned passing 20 ml of methanol and 60 ml of distilled water. After application of the white onion extract, the column was washed with 20 ml of water and the elution of the flavonoids was performed with 50 ml of methanol and 50 ml of methanol: ammonium (95.5: 0.5 v/v), named WO-1 and WO-2 extracts, respectively. For red onion, the elution of the flavonoids was performed with 50 ml methanol acidified with 2.5% acetic acid, naming the extract as RO-1. The obtained eluates were completely dried in a rotary evaporator at 40°C and suspended in 1 ml of methanol. These extracts were used for the identification and quantification of total phenolic compounds using high-performance liquid chromatography with diode array detector (HPLC-DAD) and liquid chromatography-electrospray ionization-tandem mass spectrometry (LC-ESI-MS/MS).

High-Performance Liquid Chromatography With Diode Array Detector (HPLC-DAD)

Quantification and partial identification of flavonoids were conducted using HPLC-DAD. The chromatograph (Infinity 1120 model, Agilent, Germany) used was equipped with automatic sample injector, quaternary pump and DAD, controlled by Agilent's own software. The column used was Prodigy 5 (ODS3 250 × 4.60 mm, Phenomenex Ltd., United Kingdom) with a flow rate of 1 ml/min, 25°C. The elution was performed with a solvent gradient with the following elements: A: water with 0.5% formic acid; B: Acetonitrile with 0.5% formic acid. The concentration gradient of the solvents was made with 8% of B at the beginning, 10% in 5 min, 17% in 10 min, 25% in 15 min, 50% in 25 min, 90% in 30 min, 50% in 32 min, and 8% in 35 min (running time, 35 min). The run was monitored with the following wavelengths: 270, 370, and 525 nm and peak identification was performed comparing the retention time and similarity with the absorption spectra of commercial patterns and the spectra contained in the equipment library, previously inserted in the method. The identification was also performed according to the sequence of elution according to Pérez Gregorio et al. (2011). For the quantification the following flavonoid standards were used: quercetin 3-*O*-glucoside, isorhamnetin and cyanidin 3-*O*-glucoside (Extrasynthese, Genay, France). All quercetin derivates were quantified and values expressed as quercetin 3-*O*-glucoside. All isorhamnetin derivates were quantified and values expressed as isorhamnetin equivalent. Cyanidin 3-*O*-glucoside was quantified, and value expressed as cyanidin 3-*O*-glucoside.

Liquid Chromatography-Electrospray Ionization-Tandem Mass Spectrometry (LC-ESI-MS/MS)

The identification of flavonoids and other phenolic compounds was conducted in the liquid chromatography (LC) (Prominence model, Shimadzu, Japan) linked to a mass spectrometer ion trap (Esquire HCT model, Bruker Daltonics, Germany) and electrospray ionization interface (ESI). The separation conditions were the same as those used for the HPLC-DAD, described in section High-Performance Liquid Chromatography With Diode Array Detector (HPLC-DAD). After passage through the DAD, the flow was changed to 0.2 ml/min to the passage in the mass spectrometer. The ESI was maintained in positive mode. The mass detector was programmed to perform full scan between *m/z* 100–1000. The ionization energy for the positive mode was 3500 V. The identity of the compounds was evaluated by comparing the mass spectrum obtained with the commercial standards and, or literature data (Lee and Mitchell, 2011). To confirm the identity, the HPLC retention time of commercial flavonoid standards (quercetin 3-*O*-glucoside, quercetin aglycone, and cyanidin 3-*O*-glucoside) was used for comparison.

Antimicrobial Activity of the Extracts and Isolated Compounds of Onions

Minimal Inhibitory Concentration of the Extracts

The minimal inhibitory concentration (MIC) of each extract was determined using the broth microdilution method, according to

the methodology of Wiegand et al. (2008), with modifications. The extracts suspended in LB broth were tested in a 96-well plate. Cultures of *C. violaceum* ATCC 12472, *P. aeruginosa* PAO1, and *S. marcescens* MG1 were grown overnight on plates with LB agar, suspended in saline solution 0.85% and adjusted using a solution of McFarland 0.5 to reach a concentration of approximately 1×10^8 CFU/ml. Subsequently, each culture was diluted in LB broth in a proportion of 1:100 and 50 μl of this dilution were placed in each well, to attain the final concentration ranging from 31.2 to 125 μg/ml of extract. The controls were bacterial culture in LB broth without extracts, the broth with each of the extracts in each of the concentrations tested without bacteria, and a sterility control. The QS inhibition tests were prepared with sub-MIC concentrations to ensure that the extracts did not interfere with bacterial growth. Bacterial growth was evaluated following the same procedure for the MIC. Optical density at 595 nm (OD 595 nm) was determined each 3 h during a total time of 24 h using the spectrophotometer (Multiskan FC, Thermo Fisher Scientific, Finland). Quercetin aglycone and quercetin 3-β-D-glucoside were also evaluated as onion's representative isolated compounds.

Quorum Sensing Modulation Assays by Extracts and Isolated Compounds of Onions

Violacein Production in *C. violaceum* ATCC 12472

The test was performed according to Tan et al. (2012, 2013), with modifications. *C. violaceum* ATCC 12472 was grown overnight following the same parameters as in the section Minimal Inhibitory Concentration of the Extracts. In concentrations ranging from 7.8 to 31.2 μg/ml. A 96-well plate was incubated at 30°C, 120 rpm for 24 h and then the plates were completely dried at 60°C. Subsequently, 100 μl of dimethyl sulfoxide (DMSO) were added to each well, keeping the plate with agitation at 120 rpm for 12 h, approximately. The OD 595 nm was measured using the spectrophotometer (Multiskan FC, Thermo Fisher Scientific, Finland). The controls used in the test were the same as in the section Minimal Inhibitory Concentration of the Extracts. Quercetin aglycone and quercetin 3-β-D-glucoside were also evaluated for their anti-QS activity for being representative isolated compounds found in the extracts.

Swarming Motility by *P. aeruginosa* PAO1 and *S. marcescens* MG1

Swarming motility was tested using semi-solid LB medium prepared with 0.5% agar, as described by Oliveira et al. (2016). Aliquots of the extracts giving final concentrations of 31.2, 62.5, and 125 μg/ml were placed in sterile Petri dishes of 49 × 9 mm and then 10 ml of the molten agar were added. For the swarming test 2 μl of the overnight grown bacteria were point inoculated at the center of the agar. Once the inoculum was dried, about 20 min after inoculation, the plates were closed and incubated at 37°C for 24 h for *P. aeruginosa* PAO1 and at 30°C for 24 h for *S. marcescens* MG1. Inhibition of swarming motility was considered when a visual reduction of the swarm was observed in presence of the extracts. Quercetin aglycone and quercetin 3-β-D-glucoside were also evaluated for their anti-QS activity. Synthetic furanone C-30 (≥97.0% of purity; Sigma-Aldrich, Brazil) (Z-)-4-Bromo-5-(bromomethylene)-2(5H)-furanone, was used as positive control for motility inhibition at 100 μM (Oliveira et al., 2016).

Biofilm Formation in *P. aeruginosa* PAO1 and *S. marcescens* MG1

The effect of onion extracts on biofilm formation was assessed in a 96-well plate as it was described by Borges et al. (2012), with modifications. An aliquot of 20 μl of the overnight cultures adjusted according to McFarland solution 0.5 were inoculated into LB broth with 31.2, 62.5, and 125 μg/ml of extract, completing a final volume of 200 μl. The cultures were incubated at 37°C for 24 h when using *P. aeruginosa* PAO1 and at 30°C for 24 h when evaluating *S. marcescens* MG1. Thereafter, non-adherent bacteria were removed by washing with 200 μl of saline solution 0.85% and adherent bacteria were fixed with 200 μl of methanol 99% for 15 min, following removal of the solvent. Then 200 μl of crystal violet solution 0.3% (w/v) were added to the well for 5 min. The wells were washed with sterile water to remove excess stain and the crystal violet bound to the biofilm was extracted with glacial acetic acid 33% (v/v). The OD 595 nm of the crystal violet solution was measured using the spectrophotometer (Multiskan FC, Thermo Fisher Scientific, Finland). Quercetin aglycone and quercetin 3-β-D-glucoside were also evaluated.

To confirm biofilm production in the case of the microorganism *P. aeruginosa* PAO1, a test was performed according to Minei et al. (2008) with modifications. The 96-well plates with cultures grown overnight in LB broth and the different compounds to be tested were incubated, as previously mentioned. Planktonic cells were removed with 200 μl of sterile saline solution 0.85%. Shortly, the adhered cells and biofilm were removed manually scrubbing the walls of each well with a sterile swab until the biofilm was completely removed, and then the swab was transferred to a tube containing 10 ml of saline solution 0.85% and vortexed for 1 min. Serial dilutions were made, and an inoculum of 20 μl was plated using the drop plate method in LB agar following incubation at 37°C monitoring the plates until the appearance of the micro-colonies. After that, cells were counted, and the results were expressed as Log_{10} CFU/biofilm formed into the well.

Molecular Docking of Quercetin Molecules With CviR and LasR Proteins

Docking studies were performed according to Almeida et al. (2016) and Almeida et al. (2018). In brief, the crystallized structures of CviR protein of *C. violaceum* ATCC 12472 (PDB: 3QP6 and 3QP8; Chen et al., 2011) and LasR protein of *P. aeruginosa* PAO1 (PDB: 2UV0, 6D6A, 6D6L, 6D6O, and 6D6P; Bottomley et al., 2007; O'Reilly et al., 2018) with different ligands were obtained in the RCSB Protein Data

Bank database (PDB)[1]. Then, the molecular docking was performed between these proteins and *N*-(3-hydroxydecanoyl)-DL-homoserine lactone (3-OH-C10-HSL; Pubchem CID: 71353010), *N*-(3-oxododecanoyl)-L-homoserine lactone (3-oxo-C12-HSL; Pubchem CID: 3246941), quercetin (quercetin aglycone; Pubchem CID: 5280343), quercetin 3,4-*O*-diglucoside (quercetin 3-β-D-glucoside; Pubchem CID: 5280804) and 4-bromo-5-(bromomethylene)-2(5H)-furanone (Furanone C-30; Pubchem CID: 10131246) using the "Dock Ligands" tool of the CLC Drug Discovery Workbench 4.0 software[2], with 1000 interactions for each compound and the conformation of the compounds was changed during the docking via rotation around flexible bonds. The generated score mimics the potential energy change when the protein and the compound come together based on hydrogen bonds, metal ions and steric interactions, where lower scores (more negative) correspond to higher binding affinities. The five best scores of the docking of each compound were selected, allowing the inspection of the binding sites of CviR and LasR proteins with each compound (Almeida et al., 2016, 2018).

Statistical Analysis

All experiments were performed at least three times. The data represent the means of the repetitions and their differences with respect to the controls. All data were subjected to analysis of variance (ANOVA) followed by Tukey's test using the Statistical Analysis System and Genetics Software (Ferreira, 2011). A $p < 0.05$ was considered to be statistically significant.

RESULTS

Characterization of the Phenolic Compounds Present in Onion Samples

Chromatograms obtained by HPLC-DAD of flavonoids from red and white onion extracts are shown in **Figure 1** and their respective identification detailed in **Table 1**. The LC-ESI-MS/MS spectra of chromatographic peaks obtained from red and white onions are also shown in **Supplementary Figure S1**. The major flavonol identified in the two onion varieties was quercetin 4-*O*-glucoside. The second major flavonol found was identified as quercetin 3,4-*O*-diglucoside. In addition, an anthocyanin in RO-1 extract was found. Cyanidin 3-*O*-glucoside, responsible for purple pigmentation of red onion, was presented with molecular ion [M]+ at *m/z* 449 and characteristic MS2 fragment at m/z 287 ($[M]^+ - 162$). Concentrations of flavonoids from red and white onion extracts are shown in **Table 2**. Quercetin 4-*O*-glucoside and quercetin 3,4-*O*-diglucoside corresponded to 52 and 37% of total flavonoids in the WO-1 extract. The WO-2 extract was primarily composed of quercetin 4-*O*-glucoside. On the other hand, in RO-1 extract, the main flavonoids were quercetin 4-*O*-glucoside and quercetin aglycone, representing 57 and 20% of total flavonoids.

[1]http://www.rcsb.org/pdb/home/home.do

[2]https://www.qiagenbioinformatics.com/

Determination of Minimum Inhibitory Concentration (MIC) and Microbial Growth Curves in the Presence of Extracts and Isolated Compounds of Onions

The MIC results of red and white onion extract of *C. violaceum* ATCC 12472, *P. aeruginosa* PAO1, and *S. marcescens* MG1 are presented in **Table 3**. For QS inhibition experiments we used sub-MIC concentrations that did not affect microbial growth, according to growth curves. For *C. violaceum* ATCC 12472 both the RO-1 and the WO-2 extract had an inhibitory effect in a concentration of 125 μg/ml. In addition, bacterial multiplication was slightly affected in relation to the control for the two types of onion extracts in the concentration of 62 μg/ml, showing a partial inhibition of the growth. Thus, QS inhibition experiments were performed using concentrations below 62 μg/ml to avoid toxic effects. In the case of *P. aeruginosa* PAO1 bacteria grew, similarly, to the control in almost all extract concentrations tested. Only the WO-2 extract had a delayed exponential phase, compared to the control at 125 μg/ml. A similar trend was observed for *S. marcescens* MG1.

Growth curves were also performed in order to check the effect of quercetin aglycone and quercetin 3-β-D-glucoside on the microorganisms used in this study (**Table 3**). These compounds were chosen because the first one was found in the literature as a potential QS inhibitor besides being present in the RO-1 extract and the second as a representative compound of the glycosylated forms of quercetin found in both types of onion in the present study. The MIC for the two compounds was greater than 125 μg/ml. Additionally, for *C. violaceum* ATCC 12472 a partial inhibition of growth was observed at the concentration of 125 μg/ml of quercetin 3-β-D-glucoside, therefore we used lower concentrations to avoid toxic effects.

Determination of Anti-QS Activity of Extracts and Isolated Compounds of Onions

Effect on Violacein Production in *C. violaceum* ATCC 12472

Figure 2 shows the effect of white and red onion extracts on violacein production in *C. violaceum* ATCC 12472. The production of violacein was statistically inhibited in the presence of 31.2 μg/ml of RO-1 extract when compared to the control ($p < 0.05$). On the other hand, WO-1 and WO-2 extracts did not influence the production of violacein, even though WO-1 presented an inhibitory tendency. It is noteworthy that only the RO-1 extract contains quercetin aglycone (**Table 2**).

As quercetin aglycone and quercetin 3-β-D-glucoside were molecules identified in the extracts and as the aglycone form has been reported as a potential QS inhibitor, the effect of onion extracts was compared to the effect of these two molecules **Figure 2**. For the aglycone form, the results showed that there was a significant inhibition of violacein production ($p < 0.05$). In contrast, quercetin 3-β-D-glucoside showed no significant inhibition of pigment production, even though a tendency

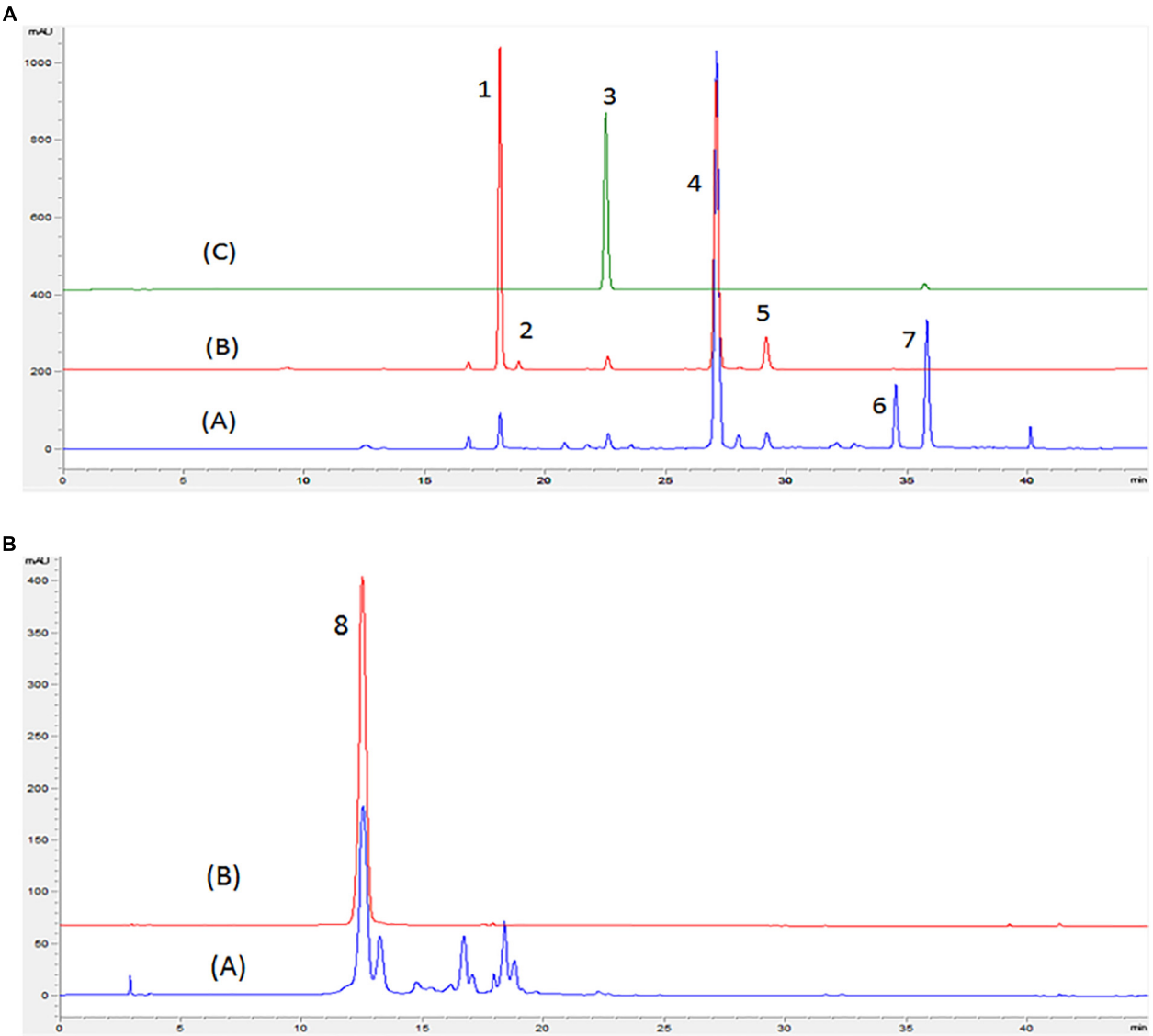

FIGURE 1 | Chromatogram obtained by HPLC-DAD in wavelengths of 370 **(A)** and 525 nm **(B)** of red and white onion. (A) Red onion, (B) White onion, (C) Quercetin 3-*O*-glucoside standard. Peaks identified: peak 1 – Quercetin 3,4-*O*-diglucoside; peak 2 – Isorhamnetin 3,4′-diglucoside, peak 3 – Quercetin 3-*O*-glucoside; peak 4 – Quercetin 4′-*O*-glucoside; peak 5 – Isorhamnetin 4- glucoside; peak 6 – Quercetin glycoside; peak 7 – Quercetin aglycone; peak 8 –Cyanidin 3-*O* glucoside. Identification shown in **Table 1**.

TABLE 1 | Mass spectra of flavonoids in positive mode from red and white onion extracts obtained by LC-ESI-MS/MS.

Peak	RT (min)	Molecular ion (*m/z*)	MS2 (*m/z*)	Flavonoids	Red onion	White onion
1	18.1	627	465/303	Quercetin 3,4-*O*-diglucoside	✓	✓
2	19.0	641	479/317	Isorhamnetin3,4′-diglucoside		✓
3	22.7	465	303	Quercetin 3-*O*-glucoside*	✓	✓
4	27	465	303	Quercetin 4′-*O*-glucoside	✓	✓
5	29.5	479	317	Isorhamnetin4-glucoside	✓	✓
6	34.4	507	303	Quercetin glycoside	✓	
7	35.2	303	257/229/165/137	Quercetin aglycone*	✓	
8	11.9	449	287	Cyanidin 3-*O*-glucoside*	✓	

*RT, retention time. *Identity confirmed with commercial standard.*

TABLE 2 | Flavonoids content in red and white onion extracts.

	Red onion	White onion	
	RO-1	**WO-1**	**WO-2**
FLAVONOL			
Quercetin 3,4-*O*-diglucoside	0.684 ± 0.001	**7.846 ± 0.080**	–
Isorhamnetin3,4-diglucoside	–	0.191 ± 0.001	–
Quercetin 3-*O*-glucoside	0.359 ± 0.001	0.413 ± 0.001	–
Quercetin 4-*O*-glucoside	**10.546 ± 0.020**	**11.032 ± 0.010**	**1.478 ± 0.005**
Isorhamnetin4-glucoside	0.500 ± 0.001	1.263 ± 0.008	–
Quercetin glycoside	1.44 ± 0.004	–	–
Quercetin aglycone	**3.741 ± 0.050**	–	–
Total flavonol	17.272	20.738	1.478
ANTHOCYANIN			
Cyanidin 3-*O*-glucoside	**1.162 ± 0.007**	–	–

–, not detected; RO-1, red onion extract in methanol acidified with 2.5% acetic acid; WO-1, white onion extract in methanol; WO-2, white onion extract in methanol ammonium. All quercetin derivates were expressed as equivalents of quercetin 3-O-glucoside. All isorhamnetin derivates were expressed as isorhamnetin. All results were expressed as mg/100 mg of dry extract. In bold, the major compounds identified.

TABLE 3 | Minimum inhibitory concentration of onion extracts.

Microorganism	MIC (μg/ml)				
	RO-1	**WO-1**	**WO-2**	**Quercetin aglycone**	**Quercetin 3-β-D-glucoside**
C. violaceum ATCC 12472	125	>125	125	>125	125
P. aeruginosa PAO1	>125	>125	>125	>125	>125
S. marcescens MG1	125	>125	>125	>125	>125

RO-1, red onion extract in methanol acidified with 2.5% acetic acid; WO-1, white onion extract in methanol; WO-2, white onion extract in methanol ammonium.

can be observed, possibly explaining the low anti-QS activity of the extracts that had glycosylated forms of quercetin as major compounds.

Effect on Swarming Motility of *P. aeruginosa* PAO1 and *S. marcescens* MG1

The results of the effect of onion extracts on swarming motility of *P. aeruginosa* PAO1 are shown in **Figure 3A**. The RO-1 extract significantly reduced motility in the tested concentrations, and the control with furanone C-30 demonstrated the best phenotype inhibition. The other extracts did not present significant inhibition in this assay.

For *S. marcescens* MG1, inhibition of swarming motility was clearly observed at the concentration of 125 μg/ml of the WO-2 extract **Figure 3B**. The other extracts showed no significant inhibition, despite a trend observed in higher concentrations. Additionally, our assays with quercetin aglycone and quercetin 3-β-D-glucoside revealed a significant inhibition of swarming motility in both bacteria ($p < 0.05$) (**Figures 3A,B**). The violacein production tests showed that quercetin aglycone had better inhibitory activity than the glycosylated quercetin in *C. violaceum* ATCC12472. However, the results from the swarming motility assay showed that both types of quercetin were able to inhibit bacterial motility on agar plates.

Effect on Biofilm Formation of *P. aeruginosa* PAO1 and *S. marcescens* MG1

Biofilm production was not significantly inhibited by any of the extracts as shown in **Figure 4A** for *P. aeruginosa* PAO1 and **Figure 4C** for *S. marcescens* MG1. Tests with quercetin aglycone and quercetin 3-β-D-glucoside in *P. aeruginosa* PAO1 showed inhibition at some concentrations, but paradoxically no inhibition was observed in the highest concentration tested. As

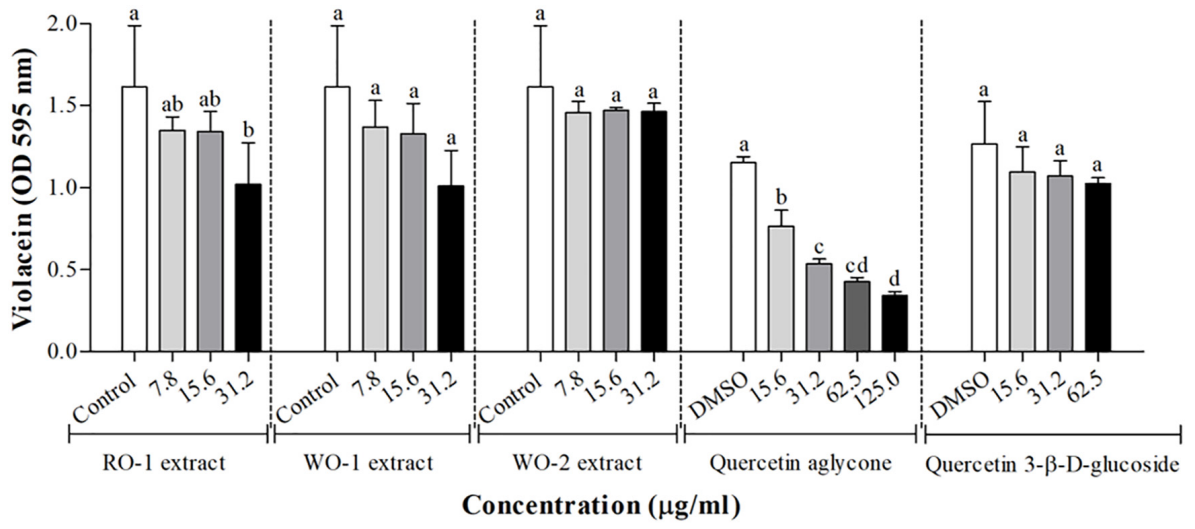

FIGURE 2 | Violacein production in *C. violaceum* ATCC 12472 in the presence of RO-1 (Red onion extract in methanol acidified with 2.5% acetic acid), WO-1 (White onion extract in methanol), WO-2 (White onion extract in methanol ammonium), quercetin aglycone and quercetin 3-β-D-glucoside. Control, bacterial growth in LB; DMSO, bacterial control in LB plus DMSO; Means followed by different letters differ statistically ($p < 0.05$).

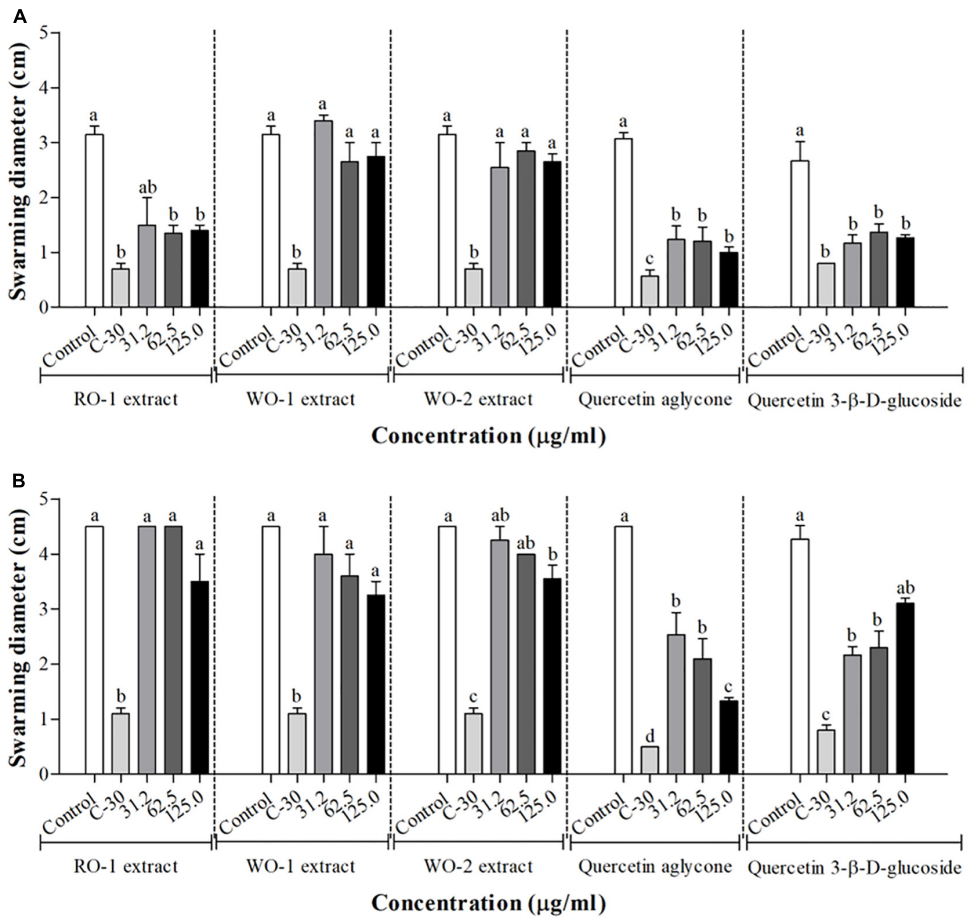

FIGURE 3 | Swarming motility in *P. aeruginosa* PAO1 **(A)** and *S. marcescens* MG1 **(B)** in the presence of RO-1 (Red onion extract in methanol acidified with 2.5% acetic acid), WO-1 (White onion extract in methanol), WO-2 (White onion extract in methanol ammonium), quercetin aglycone and quercetin 3-β-D-glucoside. Control, bacterial growth in LB; C-30, Furanone C-30 with bacterium; Means followed by different letters differ statistically ($p < 0.05$).

this result was somewhat contradictory, we decided to use an additional technique to measure biofilm formation by counting viable cells recovered from the biofilms. However, the results of these counts did not reveal any inhibition of biofilm formation in any of the tested concentrations (**Figure 4B**), meaning that there was no difference in the counts of viable cells recovered from the biofilms at different concentrations of both types of quercetins. **Figure 4C**, shows the results of biofilm formation of *S. marcescens* MG1, revealing little to no inhibition by the tested molecules.

Molecular Docking of Quercetin Molecules With CviR and LasR Protein

All the evaluated compounds were able to bind in the evaluated structures of the CviR and LasR proteins and the binding affinities and binding residues are shown in **Tables 4**, **5**. The 3-OH-C10-HSL presented the highest binding affinities for the two structures of CviR protein of *C. violaceum* ATCC 12472, 3QP6, and 3QP8. The quercetin aglycone presented lower binding affinities than this AHL and higher than quercetin 3-β-D-glucoside and furanone C-30 (**Table 4**). The quercetin aglycone bound to M135 and S155 residues from the two structures of the CviR protein evaluated, differently from quercetin 3-β-D-glucoside that bound at different sites (**Table 4** and **Figure 5**). In addition, the S155 residue was a common binding site for quercetin aglycone and 3-OH-C10-HSL in these structures (**Table 4** and **Figures 5A,B**). In 3QP8 structure, the flavonoid structure of quercetin 3-β-D-glucoside bound in the S89 residue and glucoside structure in residue Y88, N92, and A94 (**Table 4**). On the other hand, the different structures of the LasR protein of *P. aeruginosa* PAO1 showed variations of the binding affinities for the four evaluated compounds. The 3-oxo-C12-HSL showed the highest binding affinities for the structures 2UV0 and 6D6A and the quercetin 3-β-D-glucoside the highest binding affinities for the structures 6D6L, 6D6O, and 6D6P (**Table 5**). The T75, T115, and S129 residues were common binding sites for the two quercetins, 3-oxo-C12-HSL and furanone C-30 (**Table 5** and **Figure 6**). These residues were also common binding sites for flavonoid structure of quercetin 3-β-D-glucoside (**Table 5**). On the other hand, the glucoside structure of this quercetin was able to bind in specific amino acid residues, such as G38, Y47, Y64, V76, L125, and A127 (**Table 5**). However, the inspection of the binding sites of CviR and LasR protein with these compounds showed that

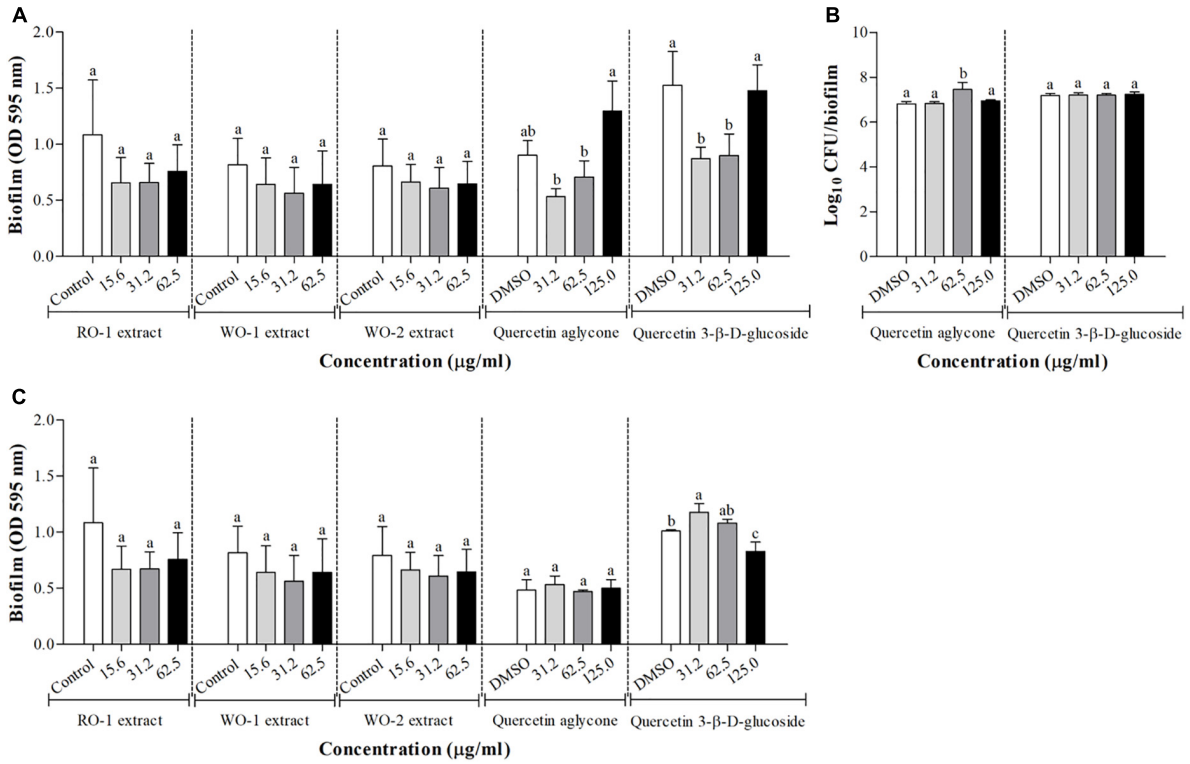

FIGURE 4 | Biofilm formation in *P. aeruginosa* PAO1 **(A)** and *S. marcescens* MG1 **(C)** in the presence of RO-1 (Red onion extract in methanol acidified with 2.5% acetic acid), WO-1 (White onion extract in methanol), WO-2 (White onion extract in methanol ammonium), quercetin aglycone and quercetin 3-β-D-glucoside. DMSO, bacterial control in LB plus DMSO; Means followed by different letters differ statistically ($p < 0.05$); **(B)** Surface-adhered cell and cell in biofilm count after 24 h of incubation of *P. aeruginosa* PAO1 in the presence of quercetin aglycone and quercetin 3-β-D-glucoside.

TABLE 4 | Results from molecular docking of structures of CviR protein of *C. violaceum* ATCC 12472 with selected compounds.

Compound	Pubchem CID	Structures of CviR protein of *C. violaceum* ATCC 12472					
		3QP6			3QP8		
		Binding residue	Score	Rank	Binding residue	Score	Rank
3-OH-C10-HSL	71353010	Y80, W84, Y88, D97, S155	−85.11	1	Y80, W84, Y88, D97, S155	−81.54	1
Quercetin aglycone	5280343	M135, S155	−52.95	2	M135, S155	−53.87	2
Quercetin 3-β-D-glucoside	5280804	Y88, S89	−45.81	3	**Y88**, S89, **N92**, **A94**	−53.40	3
Furanone C-30	10131246	Y80, T140, S155	−34.42	4	W84	−33.58	4

Amino acid residues that bind only to the glucoside structure of quercetin 3-β-D-glucoside are in bold.

quercetin 3-β-D-glucoside was unable to accommodate in the pocket of the two structures of CviR protein of *C. violaceum* ATCC 12472 (**Figures 5**, **6**).

DISCUSSION

Different cellular functions that affect food spoilage are influenced by signaling molecules accumulated as a function of QS. Consequently, many researchers have attempted to find alternatives that can inhibit this communication using natural sources that may reduce the virulence capacity of microorganisms. In the present study, we evaluated the effect of onion organic extracts and representative isolated compounds in QS model bacteria.

First, we identified the different phenolic compounds present in the organic extracts. The results showed that different types of glycosylated quercetin were found in both onion varieties. Studies have shown that flavonoids such as quercetin 4-*O*-glucoside and quercetin 3,4-*O*-diglucoside are the major compounds found in onion and compounds derived from kaempferol and isorhamnetin were identified as minor flavonoids (Slimestad et al., 2007; Lee et al., 2011; Pérez Gregorio et al., 2011). In addition, cyanidin 3-*O*-glucoside was the

TABLE 5 | Results from molecular docking of structures of LasR protein of *P. aeruginosa* PAO1 with selected compounds.

Compound	Pubchem CID	Structures of LasR protein of *P. aeruginosa* PAO1											
		2UV0			6D6A		6D6L		6D6O		6D6P		
		Binding residue	Score	Rank	Binding residue	Score	Rank	Binding residue	Score	Rank	Binding residue	Score	Rank	Binding residue	Score	Rank
3-oxo-C12-HSL	3246941	Y56, T75, S129	−81.85	1	Y56, S129	−75.07	1	Y56, W60, D73	−76.40	2	Y56, S129	−76.80	2	T75, T115, S129	−78.90	2
Quercetin aglycone	5280343	T75, T115, L125, S129	−61.09	2	T75, Y93, L110, T115, S129	−70.07	3	R61, D65, T75, T115, S129	−70.37	3	R61, D65, T75, T115, S129	−69.56	3	R61, D65, T75, T115, S129	−67.13	3
Quercetin 3-β-D-glucoside	5280804	Y47, W60, Y64, T75, **V76**, T115, **L125**, S129	−47.80	3	**G38**, R61, T75, T115, **A127**, S129	−71.21	2	**Y47**, R61, **Y64**, D65, T75, T115, S129	−88.24	1	**Y47**, R61, **Y64**, D65, T115, S129	−84.24	1	**Y47**, R61, **Y64**, D65, T115, S129	−81.89	1
Furanone C-30	10131246	T75, T115, S129	−37.88	4	T75, T115, S129	−38.08	4	T75, T115, S129	−45.78	4	T75, T115, S129	−46.44	4	T75, T115, S129	−44.87	4

Amino acid residues that bind only to the glucoside structure of quercetin 3-β-D-glucoside are in bold.

main anthocyanin present in red onion (Pérez Gregorio et al., 2011). Another study by Arabbi et al. (2004) has also shown that significant amounts of quercetin aglycone are found in concentrations of 48–56 mg/100 g on white onions and amounts of 38–94 mg/100 g in red onions. In addition, they reported that anthocyanin cyanidin was found in varieties of red onion contributing with 9.2% of total flavonoids (Arabbi et al., 2004).

The MIC of the extracts was equal to or greater than 125 μg/ml of dry extract for all the evaluated microorganisms. These results are related to those of Gopu et al. (2015), in which quercetin aglycone, one of the compounds found in the present study, showed a MIC value of 120 μg/ml for *C. violaceum* CV026. Another study by Al-Yousef et al. (2017) evaluated the ethyl acetate fraction of onion peel and its major compound quercetin 4-O-β-D-glucopyranoside as a possible QS inhibitor, finding a MIC value for *C. violaceum* ATCC 12472 of 500 μg/ml (Al-Yousef et al., 2017). Thus, it is possible that higher concentrations of onion extracts and quercetin are needed in order to fully inhibit the growth of the bacteria evaluated in the present study.

Quorum sensing regulates violacein production, a characteristic violet pigment produced by *C. violaceum,* which is induced by some types of *N*-acyl homoserine lactone molecules (Stauff and Bassler, 2011). Curiously, the strain used in the present work, *C. violaceum* ATCC 12472, is induced by *N*-(3-hydroxydecanoyl)-L-homoserine lactone, differing from the biosensor strain *C. violaceum* CV026 which is induced by *N*-hexanoyl-L-homoserine lactone (Morohoshi et al., 2008). We observed that neither WO-1 and WO-2 extracts nor quercetin 3-β-D-glucoside significantly inhibited violacein production, even though a tendency for an inhibitory effect can be observed (**Figure 2**). On the other hand, the RO-1 extract and quercetin aglycone significantly inhibited violacein production.

Several studies indicated violacein inhibition by different extracts. For instance, Oliveira et al. (2016) showed that the phenolic extract of *Rubus rosaefolius* (wild strawberry) reduced violacein production by up to 88%, especially in the concentration of 118.60 mg GAE/L, showing a higher inhibition than furanone, positive control for this experiment, which inhibited 68.6%. The same authors found that the enriched extract in phenolic compounds of *Malpighia emarginata* (*acerola*) significantly inhibited violacein production in all sub-MIC concentrations evaluated (Oliveira et al., 2017). Rodrigues et al. (2016) also showed that the phenolic extract of *Eugenia brasiliensis* (*grumixama*) presented a significant inhibition of violacein production in *C. violaceum* ATCC 6357. However, in these studies, no identification of which phenolic compounds specifically inhibited the phenotypes was performed. Therefore, the compounds that inhibited violacein production are likely different from those of the present study. In a work by Song et al. (2018), coral symbiotic bacteria were screened for their ability to inhibit violacein production in *C. violaceum* ATCC 12472, with 15% of the isolates presenting QS inhibition. Furthermore, the authors showed that rhodamine isothiocyanate which is produced by one of the isolates characterized as *Vibrio alginolyticus* was involved in the disruption of QS in *P. aeruginosa* PAO1.

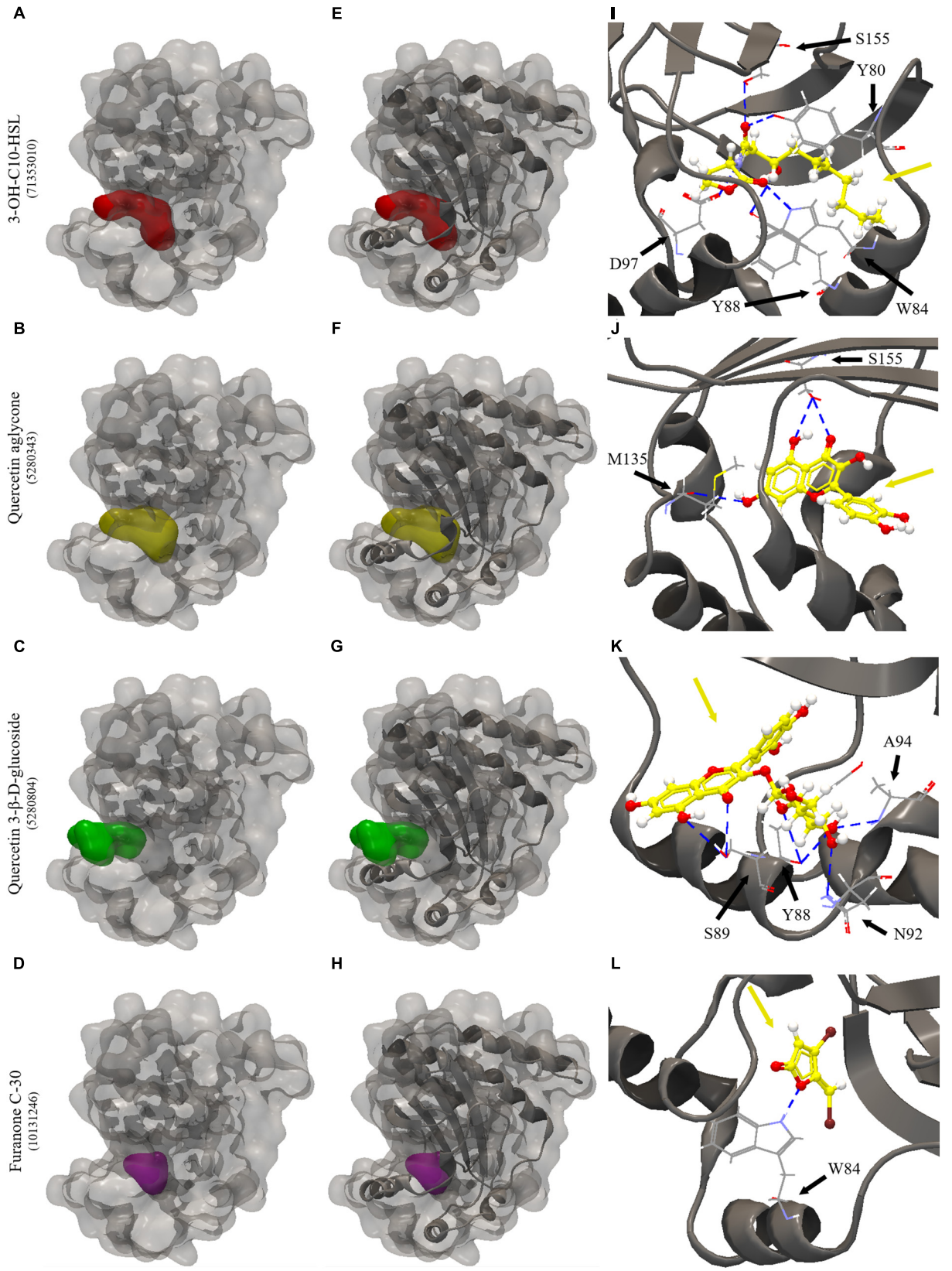

FIGURE 5 | Continued

FIGURE 5 | Molecular docking of 3QP8 structure of CviR protein of *C. violaceum* ATCC 12472 with 3-OH-C10-HSL, quercetin aglycone, quercetin 3-β-D-glucoside and furanone C-30. **(A–D)** surface representation of 3QP8 structure of CviR protein of *C. violaceum* ATCC 12472, **(E–H)** surface and backbone representations and **(I–L)** backbone representation with hydrogen bond between the amino acid residues and compounds evaluated. Gray surface representation, CviR protein; Red surface representation, 3-OH-C10-HSL; Yellow surface representation, quercetin aglycone; Green surface representation, quercetin 3-β-D-glucoside; Purple surface representation, furanone C-30; Gray backbone representation, CviR protein; Black arrow indicates the binding site; Yellow arrow, 3-OH-C10-HSL or quercetin aglycone or quercetin 3-β-D-glucoside or furanone C-30; Blue dashed line, hydrogen bond.

For quercetin aglycone, the results showed that there was a significant inhibition of violacein production ($p < 0.05$). The results were comparable to those found by Gopu et al. (2015), who reported that in the presence of quercetin aglycone violacein production in *C. violaceum* CV026 was inhibited by up to 83.2% in a concentration of 80 μg/ml. We found inhibition in a concentration ranging from 15.6 to 125 μg/ml, even though we used a different strain of *C. violaceum* ATCC 12472. In contrast, quercetin 3-β-D-glucoside showed no significant inhibition of pigment production, possibly explaining the low anti-QS activity of the extracts that had glycosylated forms of quercetin as major compounds. This result indicates that the glycosylation of the molecule, or even other types of changes in the structure, could modify the antimicrobial and anti-QS activity of a phenolic compound. This hypothesis is supported by other studies reporting that changes in the flavone structure influence the biological activity of flavonoids (Xiao et al., 2014; Paczkowski et al., 2017; Xiao, 2017).

We have also performed molecular docking of quercetin aglycone and quercetin 3-β-D-glucoside with the QS transcription activator CviR protein of *C. violaceum* ATCC 12472 (**Figure 5**). The quercetin aglycone accommodates in the structure of the protein in a similar fashion to the autoinducer 3-OH-C10-HSL (**Figures 5A,B**), while the glycosylated quercetin presents an overall different molecular interaction with the protein, as observed by a larger portion of the bulky glycosylated quercetin molecule being exposed to the exterior of the structure (**Figure 5C**). In addition, the two quercetins bound at different amino acid residues, as well as the glucoside structure of quercetin 3-β-D-glucoside bound to other specific residues (**Figures 5B,C**). However, only quercetin aglycone and 3-OH-C10-HSL showed common binding site, suggesting that these compounds can compete to bind to the CviR protein of *C. violaceum* ATCC 12472 (**Figures 5A,B**).

The effect of the extracts on swarming motility was also evaluated. The expression of some virulence factors such as biofilm formation is associated with motility (Al-Yousef et al., 2017). Therefore, interferences in this phenotype can affect a microorganism's pathogenicity. We observed for *P. aeruginosa* PAO1 a motility inhibition by RO-1 in all tested concentrations. On the other hand, *S. marcescens* MG1 swarming was inhibited by WO-2 only in the concentration of 125 μg/ml. Furanone C-30 was used as a positive control for swarming motility inhibition in the concentration of 100 μM and, as expected, presented the best phenotype inhibition, corroborating previous findings (Manefield et al., 2002; Hentzer et al., 2003). The other extracts did not present significant inhibition of the phenotype. These results are related to those obtained by Husain et al. (2015) in which the essential oil of *Mentha piperita* inhibited the swarming motility of *P. aeruginosa* PAO1. Vattem et al. (2007) also evaluated the effect of sub-lethal concentrations of phytochemicals of common fruits, herbs and spice extracts, demonstrating that they decreased *P. aeruginosa* PAO1 swarming motility by approximately 50% (Vattem et al., 2007). This behavior was also replicated in other bacteria, as in the study of Oliveira et al. (2016), which demonstrated that wild strawberry phenolic extract inhibited the swarming motility of a strain of *S. marcescens* and *A. hydrophila*, two bacteria found in refrigerated food products, besides inhibiting the production of prodigiosin, a red pigment found in *S. marcescens*, regulated by QS (Oliveira et al., 2016).

Our results also revealed that the two types of quercetin showed swarming inhibitory activity in *P. aeruginosa* PAO1 and *S. marcescens* MG1. Molecular docking of these quercetins with LasR protein of *P. aeruginosa* PAO1 revealed that they all could interact and accommodate in the pocket of the different structures of this protein (**Figures 6B,C**). The two quercetins and 3-oxo-C12-HSL, an autoinducer synthesized by *P. aeruginosa* PAO1, showed common binding sites (**Figures 6A–C**). In quercetin 3-β-D-glucoside, the flavonoid structure bound to these common amino acid residues, unlike its glucoside structure (**Table 5**). These results suggest that these quercetins could compete with autoinducer to bind to the LasR protein of *P. aeruginosa* PAO1. Our results confirm a previous docking study performed by Gopu et al. (2015) with quercetin aglycone and LasR protein. Biochemical studies such as those performed by Paczkowski et al. (2017) with purified LasR protein and different types of quercetin molecules should be performed in order to confirm these findings.

It is important to highlight that no study has evaluated in detail the effects of red and white onion extracts on QS regulated phenotypes. In a work by Rasmussen et al. (2005), libraries of plant extracts and isolated chemical compounds were created to evaluate which of these had anti-QS activity, using a selection system of QS inhibitors called QSIS. They evaluated extracts of spring and brown onion but there was no apparent QS inhibition in their assays. The answer to the absence of inhibition may be related to the extracts concentration, identity of the extracted compounds, extraction method and the systems used to detect the anti-QS activity. It could also point to the fact that their extract could be enriched in glycosylated phenolic compounds which we suggest have lower anti-QS activity.

Finally, we analyzed the effect of the extracts on biofilm production. Biofilms are known as microbial communities that adhere to surfaces and are protected by an adherent polymeric matrix (Hentzer et al., 2002). Studies have shown that QS communication plays an important role in the maturation process of these cellular aggregates (Hammer and Bassler, 2003;

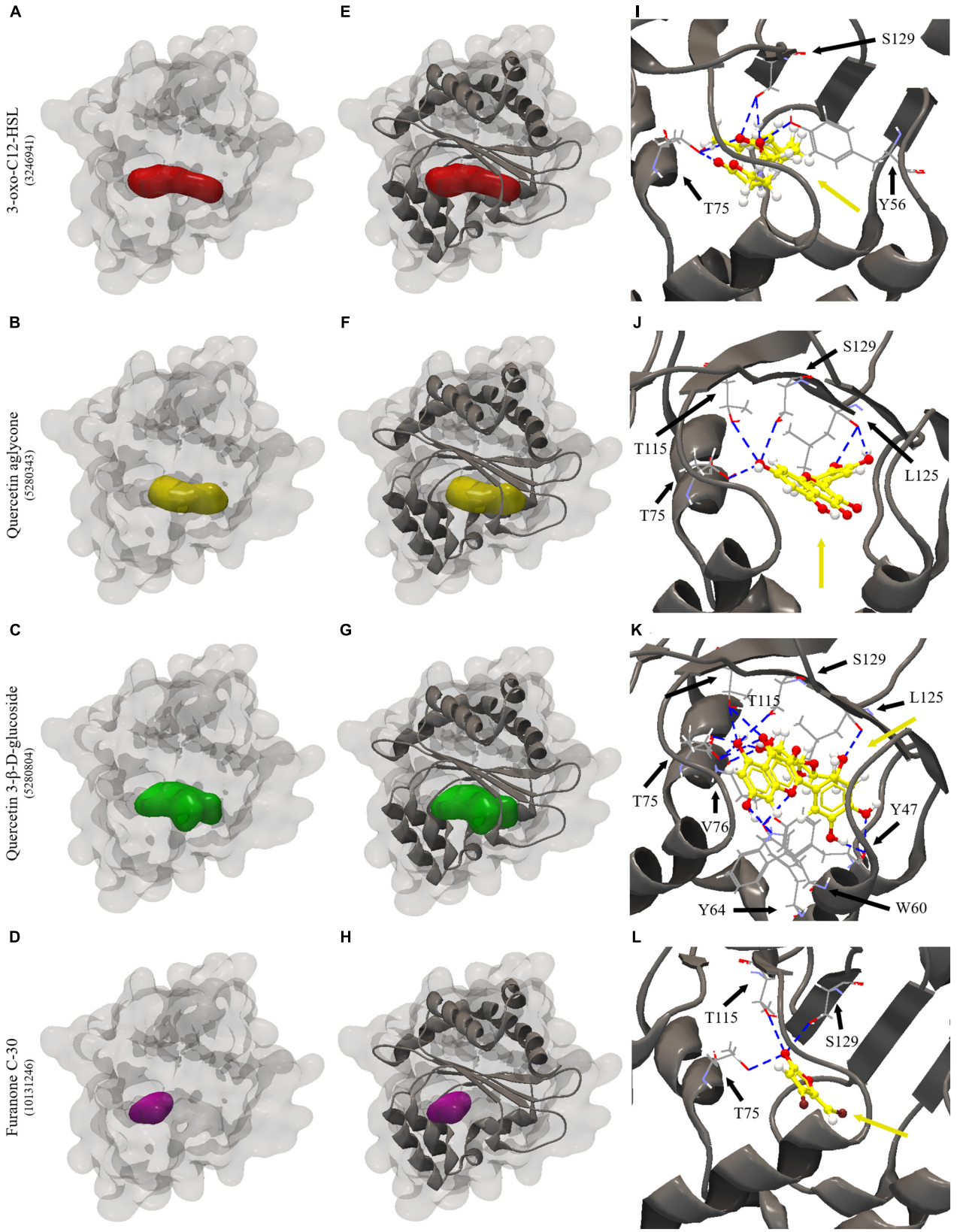

FIGURE 6 | Continued

FIGURE 6 | Molecular docking of 2UV0 structure of LasR protein of *P. aeruginosa* PAO1 with 3-oxo-C12-HSL, quercetin aglycone, quercetin 3-β-D-glucoside and furanone C-30. **(A–D)** surface representation of 2UV0 structure of LasR protein of *P. aeruginosa* PAO1, **(E–H)** surface and backbone representations and **(I–L)** backbone representation with hydrogen bond between the amino acid residues and compounds evaluated. Gray surface representation, LasR protein; Red surface representation, 3-oxo-C12-HSL; Yellow surface representation, quercetin aglycone; Green surface representation, quercetin 3-β-D-glucoside; Purple surface representation, furanone C-30; Gray backbone representation, LasR protein; Black arrow indicates the binding site; Yellow arrow, 3-oxo-C12-HSL or quercetin aglycone or quercetin 3-β-D-glucoside or furanone C-30; Blue dashed line, hydrogen bond.

Morohoshi et al., 2007). Our experiments indicate that the extracts did not inhibit biofilm formation by *P. aeruginosa* PAO1 and *S. marcescens* MG1 at any given concentration (**Figures 4A,C**). However, experiments with quercetin and quercetin 3-β-D-glucoside showed conflicting results. For instance, the crystal violet assay suggested inhibition at concentration of 31.2 and 62.5 μg/ml of the glycosylated quercetin, and with the motility assay we also observed inhibition by both types of quercetins in the two evaluated microorganisms. But in the case of *P. aeruginosa* PAO1 there was no inhibition of biofilm at the concentration of 125 μg/ml (**Figure 4A**). We attempted to confirm these results by counting viable cells recovered from biofilms under these conditions, but no inhibition was observed at any of the tested concentrations (**Figure 4B**). Overall, these results suggest that neither the extracts, nor the quercetins evaluated in this study presented potential to inhibit biofilm formation at concentrations that supposedly inhibit QS. Therefore, we encourage the use of different methods in order to confirm a possible QS inhibiting candidate.

Generally, our results disagree with those of Al-Yousef et al. (2017). These authors evaluated the ethyl acetate fraction of onion peel and its major compound quercetin 4-*O*-β-D-glucopyranoside and found an inhibition of up to 64% in biofilm formation by *P. aeruginosa*. Interestingly, they used higher concentrations of extract and quercetin (up to 400 μg/ml) than in the present study where the highest concentration tested in QS inhibition experiments was 125 μg/ml. Additionally, it is important to note that in the Al-Yousef study, the major compound identified was quercetin 4-*O*-β-D-glucopyranoside, which in its structure has a sugar molecule attached to C4 of B ring in the flavone group, while the majority of glycosylated compounds present in the onion extracts evaluated in the present work have a sugar moiety attached to C3, taking into account that these structural changes would interfere with the effectiveness of the compound as an inhibitor.

Ouyang et al. (2016) evaluated the effect of quercetin aglycone on biofilm formation of *P. aeruginosa* PAO1 in sub-MIC concentrations. Their results showed that quercetin aglycone inhibited biofilm formation in concentrations ranging from 8 to 64 μg/ml. The concentration of 16 μg/ml had the best inhibitory effect (around 50% inhibition), similarly to azithromycin at 32 μg/ml, an antibiotic used in clinical treatments (Ouyang et al., 2016). Interestingly, when comparing their data to the results of the present study, inhibition was not consistent. For instance, concentrations of 32 and 64 μg/ml of quercetin presented less inhibition than 16 μg/ml. The reasons for these inconsistent results could be related to the hormesis effect (Calabrese, 2008), even though more studies are needed to confirm such hypothesis.

Another research conducted by Paczkowski et al. (2017) showed that different flavonoids, including quercetin, could specifically inhibit QS in *P. aeruginosa* PAO1. Structure-activity analyses demonstrated that the presence of two hydroxyl groups on the A ring of flavone, one at position 7 and at least one at any other position, are required for a potent inhibition of LasR/RhIR receptors. In addition, the authors have shown that rings B and C can accommodate many substitutions, with exception of methyl groups in B ring, which are not tolerated, because they are too bulky. Biochemical analysis revealed that flavonoids function in a non-competitive way to prevent binding of QS receptors to DNA, altering the transcription of QS-controlled target promoters and suppressing the production of virulence factors (Paczkowski et al., 2017). However, the study evaluated non-glycosylated compounds; therefore, the question whether these modifications would work for compounds that have sugar substitutions attached to any of the flavonoid rings still remains.

Overall, quercetin aglycone had better inhibitory activity over QS in *C. violaceum* ATCC 12472 than quercetin 3-β-D-glucoside. On the other hand, the two quercetins inhibited motility of *P. aeruginosa* PAO1 and *S. marcescens* MG1. The results of the biological and *in silico* analyses confirmed that the structure of the compounds interferes with anti-QS activity indicating that the low activities of organic extracts of onion varieties may be related to the glycosylation of phenolic compounds. In addition, the response of the tested bacteria may be different as a function of the amino acid variations and structures of the receptor QS proteins. It would be interesting to test different phenolic compounds with or without modifications and in different bacteria to strengthen these findings. Xiao et al. (2014) and Xiao (2017) demonstrated that glycosylation generally reduces the bioactivity of flavonoids. This phenomenon has been observed for different properties including antioxidant, anti-inflammatory, antibacterial and antifungal activities.

CONCLUSION

The effect of organic extracts of red and white onion and their major constituents on QS controlled phenotypes has been evaluated. Different glycosylated quercetins were found in both onion varieties. The onion organic extracts showed inhibition of violacein production and swarming motility. Violacein production was significantly inhibited by quercetin aglycone, while glycosylated and quercetin aglycone inhibited motility of *P. aeruginosa* PAO1 and *S. marcescens* MG1. *In silico* studies suggested a better interaction and accommodation of quercetin aglycone in the structures of the CviR protein of *C. violaceum* ATCC 12472 than the glycosylated compound.

On the other hand, the two quercetins were able to bind and accommodate in the pocket of LasR protein of *P. aeruginosa* PAO1. Surprisingly, biofilm formation was not affected by any extracts or the quercetins tested in this study. These results suggest that the extracts and isolated compounds of onions could interfere in the antimicrobial and anti-QS activity, but interference on QS was limited to violacein production and swarming motility.

AUTHOR CONTRIBUTIONS

All authors listed have made a substantial, direct and intellectual contribution to the work, and approved it for publication.

FUNDING

This research was funded by a grant from CNPq-Brazil (457794/2014-3) and supported by the Food Research Center – FoRC (2013/07914-8).

ACKNOWLEDGMENTS

UP acknowledges a grant from CNPq-Brazil (457794/2014-3). We thank the São Paulo Research Foundation (FAPESP) for financial support to the Food Research Center – FoRC (2013/07914-8). BQ and MR thank CNPq-Brazil for providing scholarships. We acknowledge the CLC bio of the QIAGEN Company which licensed the CLC Drug Discovery Workbench 4.0 software.

SUPPLEMENTARY MATERIAL

The Supplementary Material for this article can be found online at: https://www.frontiersin.org/articles/10.3389/fmicb.2019.00867/full#supplementary-material

FIGURE S1 | LC(ESI)-MS/MS spectra of chromatographic peaks obtained from red and white onions. **(A)** Peak 1 – Quercetin 3,4-*O*-diglucoside; **(B)** peak 2 – Isorhamnetin 3,4′-diglucoside; **(C)** peak 3 – Quercetin 3-*O*-glucoside; **(D)** peak 4 – Quercetin 4′-*O*-glucoside; **(E)** peak 5 – Isorhamnetin4-glucoside; **(F)** peak 6 –Quercetin glycoside; **(G)** peak 7 – Quercetin aglycone, and **(H)** peak 8 – Cyanidin 3-*O*-glucoside in positive ion mode.

REFERENCES

Almeida, F. A., Pinto, U. M., and Vanetti, M. C. D. (2016). Novel insights from molecular docking of SdiA from *Salmonella* Enteritidis and *Escherichia coli* with quorum sensing and quorum quenching molecules. *Microb. Pathog.* 99, 178–190. doi: 10.1016/j.micpath.2016.08.024

Almeida, F. A., Vargas, E. L. G., Carneiro, D. G., Pinto, U. M., and Vanetti, M. C. D. (2018). Virtual screening of plant compounds and nonsteroidal anti-inflammatory drugs for inhibition of quorum sensing and biofilm formation in *Salmonella*. *Microb. Pathog.* 121, 369–388. doi: 10.1016/j.micpath.2018.05.014

Al-Yousef, H. M., Ahmed, A. F., Al-Shabib, N. A., Laeeq, S., Khan, R. A., Rehman, M. T., et al. (2017). Onion peel ethyl acetate fraction and its derived constituent quercetin 4′-O-β-D glucopyranoside attenuates quorum sensing regulated virulence and biofilm formation. *Front. Microbiol.* 8:1675. doi: 10.3389/fmicb.2017.01675

Ammor, M. S., Michaelidis, C., and Nychas, G. J. E. (2008). Insights into the role of quorum sensing in food spoilage. *J. Food Prot.* 71, 1510–1525. doi: 10.4315/0362-028X-71.7.1510

Arabbi, P. R., Genovese, M. I., and Lajolo, F. M. (2004). Flavonoids in vegetable foods commonly consumed in Brazil and estimated ingestion by the Brazilian population. *J. Agric. Food Chem.* 52, 1124–1131. doi: 10.1021/jf0499525

Bai, A. J., and Rai, V. R. (2011). Bacterial quorum sensing and food industry. *Compr. Rev. Food Sci. Food Saf.* 10, 183–193. doi: 10.1111/j.1541-4337.2011.00150.x

Behling, E., Sendão, M. C., Francescato, H. D. C., Antunes, L. M. G., and Bianchi, M. D. L. P. (2008). Flavonóide quercetina: aspectos gerais e ações biológicas. *Alim. Nutr. Araraquara* 15, 285–292.

Borges, A., Saavedra, M. J., and Simões, M. (2012). The activity of ferulic and gallic acids in biofilm prevention and control of pathogenic bacteria. *Biofouling* 28, 755–767. doi: 10.1080/08927014.2012.706751

Bottomley, M. J., Muraglia, E., Bazzo, R., and Carfi, A. (2007). Molecular insights into quorum sensing in the human pathogen *Pseudomonas aeruginosa* from the structure of the virulence regulator LasR bound to its autoinducer. *J. Biol. Chem.* 282, 13592–13600. doi: 10.1074/jbc.M700556200

Calabrese, E. J. (2008). Hormesis: why it is important to toxicology and toxicologists. *Environ. Toxicol. Chem.* 27, 1451–1474. doi: 10.1897/07-541.1

Chen, G., Swem, L. R., Swem, D. L., Stauff, D. L., O'Loughlin, C. T., Jeffrey, P. D., et al. (2011). A strategy for antagonizing quorum sensing. *Mol. Cell* 42, 199–209. doi: 10.1016/j.molcel.2011.04.003

Corzo Martínez, M., Corzo, N., and Villamiel, M. (2007). Biological properties of onions and garlic. *Trends Food Sci. Technol.* 18, 609–625. doi: 10.1016/j.tifs.2007.07.011

Cushnie, T. P. T., and Lamb, A. J. (2005). Antimicrobial activity of flavonoids. *Int. J. Antimicrob. Agents* 26, 343–356. doi: 10.1016/j.ijantimicag

Ferreira, D. F. (2011). Sisvar: a computer statistical analysis system. *Ciênc. Agrotecnol.* 35, 1039–1042. doi: 10.1590/S1413-70542011000600001

Fuqua, C., and Greenberg, E. P. (2002). Listening in on bacteria: acyl-homoserine lactone signaling. *Nat. Rev. Mol. Cell Biol.* 3, 685–695. doi: 10.1038/nrm907

Fuqua, W. C., Winans, S. C., and Greenberg, E. P. (1994). Quorum sensing in bacteria: the LuxR-LuxI family of cell density-responsive transcriptional regulators. *J. Bacteriol.* 176, 269–275. doi: 10.1128/jb.176.2.269-275.1994

Gopu, V., Meena, C. K., and Shetty, P. H. (2015). Quercetin influences quorum sensing in food borne bacteria: in-vitro and in-silico evidence. *PLoS One* 10:e0134684. doi: 10.1371/journal.pone.0134684

Hammer, B. K., and Bassler, B. L. (2003). Quorum sensing controls biofilm formation in *Vibrio cholerae*. *Mol. Microbiol.* 50, 101–114. doi: 10.1046/j.1365-2958.2003.03688.x

Hentzer, M., Riedel, K., Rasmussen, T. B., Heydorn, A., Andersen, J. B., Parsek, M. R., et al. (2002). Inhibition of quorum sensing in *Pseudomonas aeruginosa* biofilm bacteria by a halogenated furanone compound. *Microbiology* 148, 87–102. doi: 10.1099/00221287-148-1-87

Hentzer, M., Wu, H., Andersen, J. B., Riedel, K., Rasmussen, T. B., Bagge, N., et al. (2003). Attenuation of *Pseudomonas aeruginosa* virulence by quorum sensing inhibitors. *EMBO J.* 22, 3803–3815. doi: 10.1093/emboj/cdg366

Husain, F., Ahmad, I., Khan, M. S., Ahmad, E., Tahseen, Q., Khan, M. S., et al. (2015). Sub-MICs of *Mentha piperita* essential oil and menthol inhibits AHL mediated quorum sensing and biofilm of Gram-negative bacteria. *Front. Microbiol.* 6:420. doi: 10.3389/fmicb.2015.00420

Kwak, J.-H., Seo, J. M., Kim, N.-H., Arasu, M. V., Kim, S., Yoon, M. K., et al. (2017). Variation of quercetin glycoside derivatives in three onion (*Allium cepa* L.) varieties. *Saudi J. Biol. Sci.* 24, 1387–1391. doi: 10.1016/j.sjbs.2016.05.014

La Sarre, B., and Federle, M. J. (2013). Exploiting quorum sensing to confuse bacterial pathogens. *Microbiol. Mol. Biol. Rev.* 77, 73–111. doi: 10.1128/MMBR.00046-12

Lazdunski, A. M., Ventre, I., and Sturgis, J. N. (2004). Regulatory circuits and communication in Gram-negative bacteria. *Nat. Rev. Microbiol.* 2, 581–592. doi: 10.1038/nrmicro924

Lee, J., and Mitchell, A. E. (2011). Quercetin and isorhamnetin glycosides in onion (*Allium cepa* L.): varietal comparison, physical distribution, coproduct

evaluation, and long-term storage stability. *J. Agric. Food Chem.* 59, 857–863. doi: 10.1021/jf1033587

Lee, K. A., Kim, K. T., Nah, S. Y., Chung, M.-S., Cho, S., and Paik, H.-D. (2011). Antimicrobial and antioxidative effects of onion peel extracted by the subcritical water. *Food Sci. Biotechnol.* 20, 543–548. doi: 10.1007/s10068-011-0076-8

Lombard, K., Peffley, E., Geoffriau, E., Thompson, L., and Herring, A. (2005). Quercetin in onion (*Allium cepa* L.) after heat-treatment simulating home preparation. *J. Food Compost. Anal.* 18, 571–581. doi: 10.1016/j.jfca.2004.03.027

Manefield, M., Rasmussen, T. B., Henzter, M., Andersen, J. B., Steinberg, P., Kjelleberg, S., et al. (2002). Halogenated furanones inhibit quorum sensing through accelerated LuxR turnover. *Microbiology* 148, 1119–1127. doi: 10.1099/00221287-148-4-1119

Martínez, F. S., González, G. J., Culebras, J. M., and Tuñón, M. J. (2002). Los flavonoides: propiedades y acciones antioxidantes. *Nutr. Hosp.* 17, 271–278.

Martins, M. L., Pinto, U. M., Riedel, K., and Vanetti, M. C. D. (2018). Quorum sensing and spoilage potential of psychrotrophic *Enterobacteriaceae* isolated from milk. *Biomed Res. Int.* 2018:2723157. doi: 10.1155/2018/2723157

Miller, M. B., and Bassler, B. L. (2001). Quorum sensing in bacteria. *Annu. Rev. Microbiol.* 55, 165–199. doi: 10.1146/annurev.micro.55.1.165

Minei, C., Gomes, B., Ratti, R., D'angelis, C. E. M., and De Martinis, E. C. P. (2008). Influence of peroxyacetic acid and nisin and coculture with *Enterococcus faecium* on *Listeria monocytogenes* biofilm formation. *J. Food Prot.* 71, 634–638. doi: 10.4315/0362-028X-71.3.634

Morohoshi, T., Kato, M., Fukamachi, K., Kato, N., and Ikeda, T. (2008). N-acylhomoserine lactone regulates violacein production in *Chromobacterium violaceum* type strain ATCC 12472. *FEMS Microbiol. Lett.* 279, 124–130. doi: 10.1111/j.1574-6968.2007.01016.x

Morohoshi, T., Shiono, T., Takidouchi, K., Kato, M., Kato, N., Kato, J., et al. (2007). Inhibition of quorum sensing in *Serratia marcescens* AS-1 by synthetic analogs of N-Acylhomoserine lactone. *Appl. Environ. Microbiol.* 73, 6339–6344. doi: 10.1128/AEM.00593-07

Nealson, K. H., and Hastings, J. W. (1979). Bacterial bioluminescence: its control and ecological significance. *Microbiol. Rev.* 43, 496–518.

Oliveira, B. D. A., Rodrigues, A. C., Bertoldi, M. C., Taylor, J. G., and Pinto, U. M. (2017). Microbial control and quorum sensing inhibition by phenolic compounds of acerola (*Malpighia emarginata*). *Int. Food Res. J.* 24, 2228–2237.

Oliveira, B. D. A., Rodrigues, A. C., Cardoso, B. M. I., Ramos, A. L. C. C., Bertoldi, M. C., Taylor, J. G., et al. (2016). Antioxidant, antimicrobial and anti-quorum sensing activities of *Rubus rosaefolius* phenolic extract. *Ind. Crops Prod.* 84, 59–66. doi: 10.1016/j.indcrop.2016.01.037

O'Reilly, M. C., Dong, S.-H., Rossi, F. M., Karlen, K. M., Kumar, R. S., Nair, S. K., et al. (2018). Structural and biochemical studies of non-native agonists of the LasR quorum-sensing receptor reveal an L3 loop "out" conformation for LasR. *Cell Chem. Biol.* 25, 1128–1139. doi: 10.1016/j.chembiol.2018.06.007

Ouyang, J., Sun, F., Feng, W., Sun, Y., Qiu, X., Xiong, L., et al. (2016). Quercetin is an effective inhibitor of quorum sensing, biofilm formation and virulence factors in *Pseudomonas aeruginosa*. *J. Appl. Microbiol.* 120, 966–974. doi: 10.1111/jam.13073

Paczkowski, J. E., Mukherjee, S., McCready, A. R., Cong, J. P., Aquino, C. J., Kim, H., et al. (2017). Flavonoids suppress *Pseudomonas aeruginosa* virulence through allosteric inhibition of quorum-sensing receptors. *J. Biol. Chem.* 292, 4064–4076. doi: 10.1074/jbc.M116.770552

Panche, A. N., Diwan, A. D., and Chandra, S. R. (2016). Flavonoids: an overview. *J. Nutr. Sci.* 5:e47. doi: 10.1017/jns.2016.41

Papenfort, K., and Bassler, B. L. (2016). Quorum sensing signal–response systems in Gram-negative bacteria. *Nat. Rev. Microbiol.* 14, 576–588. doi: 10.1038/nrmicro.2016.89

Pérez Gregorio, M. R., González-Barreiro, C., Rial-Otero, R., and Simal-Gándara, J. (2011). Comparison of sanitizing technologies on the quality appearance and antioxidant levels in onion slices. *Food Control* 22, 2052–2058. doi: 10.1016/j.foodcont.2011.05.028

Platt, T. G., and Fuqua, C. (2010). What's in a name? The semantics of quorum sensing. *Trends Microbiol.* 18, 383–387. doi: 10.1016/j.tim.2010.05.003

Rasmussen, T. B., Bjarnsholt, T., Skindersoe, M. E., Hentzer, M., Kristoffersen, P., Köte, M., et al. (2005). Screening for quorum-sensing inhibitors (QSI) by use of a novel genetic system, the QSI selector. *J. Bacteriol.* 187, 1799–1814. doi: 10.1128/JB.187.5.1799-1814.2005

Rodrigues, A. C., Oliveira, B. D., Silva, E. R. D., Sacramento, N. T. B., Bertoldi, M. C., and Pinto, U. M. (2016). Anti-quorum sensing activity of phenolic extract from *Eugenia brasiliensis* (Brazilian cherry). *Food Sci. Technol.* 36, 337–343. doi: 10.1590/1678-457X.0089

Silveira, S. M. D. (2012). *Avaliação da Atividade Antimicrobiana e Antioxidante de Extratos Vegetais e Óleos Essenciais e Aplicação do Óleo Essencial de Louro (L. nobilis) Como Agente Conservador Natural em Embutido Cárneo Frescal*. Available at: https://repositorio.ufsc.br/handle/123456789/100520 (accessed October 6, 2018).

Skandamis, P. N., and Nychas, G. J. E. (2012). Quorum sensing in the context of food microbiology. *Appl. Environ. Microbiol.* 78, 5473–5482. doi: 10.1128/AEM.00468-12

Slimestad, R., Fossen, T., and Vågen, I. M. (2007). Onions: a source of unique dietary flavonoids. *J. Agric. Food Chem.* 55, 10067–10080. doi: 10.1021/jf0712503

Song, Y., Cai, Z. H., Lao, Y. M., Jin, H., Ying, K. Z., Lin, G. H., et al. (2018). Antibiofilm activity substances derived from coral symbiotic bacterial extract inhibit biofouling by the model strain *Pseudomonas aeruginosa* PAO1. *Microbiol. Biotechnol.* 11, 1090–1105.

Stauff, D. L., and Bassler, B. L. (2011). Quorum sensing in *Chromobacterium violaceum*: DNA recognition and gene regulation by the CviR receptor. *J. Bacteriol.* 193, 3871–3878. doi: 10.1128/JB.05125-11

Tan, L., Yin, W. F., and Chan, K. G. (2013). *Piper nigrum*, *Piper betle* and *Gnetum gnemon* - Natural food source with anti-quorum sensing properties. *Sensors* 13, 3975–3985. doi: 10.3390/s130303975

Tan, L. Y., Yin, W. F., and Chan, K. G. (2012). Silencing quorum sensing through extracts of *Melicope lunu*-ankenda. *Sensors* 12, 4339–4351. doi: 10.3390/s120404339

Vandeputte, O. M., Kiendrebeogo, M., Rasamiravaka, T., Stevigny, C., Duez, P., Rajaonson, S., et al. (2011). The flavanone naringenin reduces the production of quorum sensing-controlled virulence factors in *Pseudomonas aeruginosa* PAO1. *Microbiology* 157, 2120–2132. doi: 10.1099/mic.0.049338-0

Vattem, D. A., Mihalik, K., Crixell, S. H., and McLean, R. J. C. (2007). Dietary phytochemicals as quorum sensing inhibitors. *Fitoterapia* 78, 302–310. doi: 10.1016/j.fitote.2007.03.009

Waters, C. M., and Bassler, B. L. (2005). Quorum sensing: cell-to-cell communication in bacteria. *Annu. Rev. Cell Dev. Biol.* 21, 319–346. doi: 10.1146/annurev.cellbio.21.012704.131001

Whitehead, N. A., Barnard, A. M. L., Slater, H., Simpson, N. J. L., and Salmond, G. P. C. (2001). Quorum-sensing in Gram-negative bacteria. *FEMS Microbiol. Rev.* 25, 365–404. doi: 10.1111/j.1574-6976.2001.tb00583.x

Wiegand, I., Hilpert, K., and Hancock, R. E. W. (2008). Agar and broth dilution methods to determine the minimal inhibitory concentration (MIC) of antimicrobial substances. *Nat. Protoc.* 3, 163–175. doi: 10.1038/nprot.2007.521

Xiao, J. (2017). Dietary flavonoid aglycones and their glucosides: which show better biological significance? *Crit. Rev. Food Sci. Nutr.* 57, 1874–1905. doi: 10.1080/10408398.2015.1032400

Xiao, J., Chen, T., and Cao, H. (2014). Flavonoid glycosylation and biological benefits. *Biotechnol. Adv.* doi: 10.1016/j.biotechadv.2014.05.004 [Epub ahead of print].

Conflict of Interest Statement: The authors declare that the research was conducted in the absence of any commercial or financial relationships that could be construed as a potential conflict of interest.

frontiers in Microbiology

REVIEW
published: 07 June 2019
doi: 10.3389/fmicb.2019.01100

Relationship Between Quorum Sensing and Secretion Systems

Rocio Trastoy Pena[1†], Lucia Blasco[1†], Antón Ambroa[1], Bertha González-Pedrajo[2], Laura Fernández-García[1], Maria López[1], Ines Bleriot[1], German Bou[1], Rodolfo García-Contreras[3†], Thomas Keith Wood[4] and Maria Tomás[1*†]*

[1] Deapartamento de Microbiología y Parasitología, Complejo Hospitalario Universitario A Coruña (CHUAC), Instituto de Investigación Biomédica (INIBIC), Universidad de A Coruña (UDC), A Coruña, Spain, [2] Departamento de Genética Molecular, Instituto de Fisiología Celular, Universidad Nacional Autónoma de México, Mexico City, Mexico, [3] Departamento de Microbiología y Parasitología, Facultad de Medicina, Universidad Nacional Autónoma de México, Mexico City, Mexico, [4] Department of Chemical Engineering, Pennsylvania State University, University Park, PA, United States

OPEN ACCESS

Edited by:
Tom Defoirdt,
Ghent University, Belgium

Reviewed by:
Romé Voulhoux,
UMR7255 Laboratoire d'Ingénierie des Systèmes Macromoléculaires (LISM), France
Jin Zhou,
Tsinghua University, China

***Correspondence:**
Rodolfo García-Contreras
rgarc@bq.unam.mx
Maria Tomás
MA.del.Mar.Tomas.Carmona@sergas.es

[†] These authors have contributed equally to this work

Specialty section:
This article was submitted to Microbial Physiology and Metabolism, a section of the journal Frontiers in Microbiology

Received: 20 February 2019
Accepted: 30 April 2019
Published: 07 June 2019

Citation:
Pena RT, Blasco L, Ambroa A, González-Pedrajo B, Fernández-García L, López M, Bleriot I, Bou G, García-Contreras R, Wood TK and Tomás M (2019) Relationship Between Quorum Sensing and Secretion Systems. Front. Microbiol. 10:1100. doi: 10.3389/fmicb.2019.01100

Quorum sensing (QS) is a communication mechanism between bacteria that allows specific processes to be controlled, such as biofilm formation, virulence factor expression, production of secondary metabolites and stress adaptation mechanisms such as bacterial competition systems including secretion systems (SS). These SS have an important role in bacterial communication. SS are ubiquitous; they are present in both Gram-negative and Gram-positive bacteria and in *Mycobacterium* sp. To date, 8 types of SS have been described (T1SS, T2SS, T3SS, T4SS, T5SS, T6SS, T7SS, and T9SS). They have global functions such as the transport of proteases, lipases, adhesins, heme-binding proteins, and amidases, and specific functions such as the synthesis of proteins in host cells, adaptation to the environment, the secretion of effectors to establish an infectious niche, transfer, absorption and release of DNA, translocation of effector proteins or DNA and autotransporter secretion. All of these functions can contribute to virulence and pathogenesis. In this review, we describe the known types of SS and discuss the ones that have been shown to be regulated by QS. Due to the large amount of information about this topic in some pathogens, we focus mainly on *Pseudomonas aeruginosa* and *Vibrio* spp.

Keywords: quorum, secretion, virulence, motility, competence

INTRODUCTION

Microorganisms coexist in competitive environments with other species, and they must develop different survival strategies to compete for space, nutrients and ecological niches. Bacteria have developed several molecular mechanisms that enable them to survive under stress conditions in different environments. The general stress response (RpoS) (Battesti et al., 2011), tolerance to reactive oxygen species (ROS) (Zhao and Drlica, 2014; Van den Bergh et al., 2017), energy metabolism (cytochrome *bd* complex) (Korshunov and Imlay, 2010) and Tau metabolism (Javaux et al., 2007), drug efflux pumps (Blanco et al., 2016), SOS response (Baharoglu and Mazel, 2014), (p)ppGpp signaling under starvation conditions (Hauryliuk et al., 2015), toxin-antitoxin (TA) systems (Wood et al., 2013) and quorum sensing (QS), which we will discuss in detail in this review, are the main molecular mechanisms of tolerance and bacterial persistence (Harms et al., 2016; Trastoy et al., 2018).

Quorum sensing acts by monitoring cell density through chemical signals that allow communication between bacteria in order to regulate the expression of genes involved in virulence, competition, pathogenicity and resistance (Nealson et al., 1970; Hawver et al., 2016; Paul et al., 2018). In general, QS systems are species-dependent and contribute to processes such as cell maintenance, biofilm formation and horizontal gene transfer. QS also plays a role in other events involving the synchronization of the whole population such as antibiotic production (Abisado et al., 2018), natural competence (Shanker and Federle, 2017), sporulation (Rai et al., 2015) and the expression of secretion systems (SS). In this review, we will focus on the relationship between QS networks and SS in two important bacterial pathogens *Pseudomonas aeruginosa* and *Vibrio* spp.

QS NETWORK

To explain the structure and functioning of the QS network, we will focus on Gram-negative bacteria, in which the signaling pathways are better described. In general terms, QS systems are composed of synthase proteins that produce QS signals, QS signals, and response regulators that bind QS signals and reprogram gene expression (Ng and Bassler, 2009). *N*-acyl homoserine lactones (AHLs) are the most common QS signals in Gram-negative bacteria (Geske et al., 2008). Other QS signals include autoinducer-2 (AI-2) in *Vibrio harveyi* (Surette et al., 1999), PQS (*Pseudomonas* quinolone signal) (Pesci et al., 1999), DSF (diffusible signaling factor) in *Xanthomonas campestris* (Barber et al., 1997), indole in *Escherichia coli* (Lee and Lee, 2010), and PAME (hydroxyl-palmitic acid methyl ester) in *Ralstonia solanacearum* (Flavier et al., 1997). The LuxI/LuxR QS system of *Vibrio fischeri* is the prototypical model system for Gram-negative bacteria (Engebrecht et al., 1983; Engebrecht and Silverman, 1984). Homologs of *luxI* (which encode synthase proteins) and *luxR* (which encode response regulators) are present in many bacteria (Case et al., 2008). AHL signals are produced inside the cell and most of them are transported freely to the local environment. When the concentration of AHL reaches a certain level outside of the cell, the molecule re-enters the cell (or binds surface receptors) and binds/activates the LuxR-type receptor to alter gene expression. AHL signals with small structural differences are involved in the process of gene regulation (Fuqua et al., 1994; Whiteley et al., 2017; Paul et al., 2018).

Pseudomonas aeruginosa possesses three well-known QS systems: LasI/LasR, RhlI/RhlR, and PQS (*Pseudomonas* quinolone signal)/PqsR (MvfR). The Las system consists of LasI, a synthase protein which produces the AHL *N*-(3-oxododecanoyl)-L-homoserine lactone (3O-C12-HSL), and LasR, the transcriptional regulator (Seed et al., 1995; Stintzi et al., 1998; Kariminik et al., 2017). Likewise, the RhlI/RhlR system produces the N-hexanoyl-L-homoserine lactone (C4-HSL) signal and the RhlR transcriptional regulator. Finally, the PQS system comprises 2-heptyl-3-hydroxy-4(1H)-quinolone (PQS signal) and the PqsR (MvfR) receptor (Xiao et al., 2006; Jimenez et al., 2012). In 2016, James and collaborators, analyzed the role of a new binding receptor for PQS signals, i.e., MexG, an inner membrane protein of the *mexGHI-opmD* operon and a component of a resistance-nodulation-cell division (RND) efflux pump (Hodgkinson et al., 2016).

Quorum quenching (QQ) enzymes have also been shown to be important in the functioning of QS systems (Zhang and Dong, 2004; Dong et al., 2007; Bzdrenga et al., 2017). Our research group has recently described a new QQ enzyme (AidA) which participates in the QS network in *Acinetobacter baumannii* clinical strains (Lopez et al., 2017b, 2018).

SECRETION SYSTEMS

Bacterial pathogens secrete proteins through their cell membranes in a fundamental process that enables them to attack other microorganisms, evade the host immune system, produce tissue damage and invade the host cells. Secreted proteins can act as virulence factors that generate toxic products to the host cells and may also facilitate adhesion to these cells. Translocation of proteins across the phospholipid membranes is carried out by several types of SS (Green and Mecsas, 2016). SS play a significant role in bacterial communication. To date, 8 types of SS (T1SS, T2SS, T3SS, T4SS, T5SS, T6SS, T7SS, and T9SS) have been made defined on their structure, composition and activity (**Figure 1**). These differences can be attributed to the differences between Gram-negative and Gram-positive bacteria (Desvaux et al., 2009; Sato et al., 2010; Costa et al., 2015). The characteristics of each type of SS are described in detail below.

T1SS

The type I secretion system is widely distributed in Gram-negative bacteria such as *P. aeruginosa*, *Salmonella enterica*, *Neisseria meningitidis,* and *E. coli* (Thomas et al., 2014).

The type I secretion system (T1SS), which has three structural elements (ABC transporter protein, a membrane fusion protein and an outer membrane factor), can transfer substrates across both bacterial membranes in Gram negative bacteria in a one-step process (Green and Mecsas, 2016). T1SS uses proteins as substrates, e.g., proteases and lipases of different sizes and with different functions; these proteins have a C-terminal uncleaved secretion signal which is recognized by the ABC transporter protein to form the translocation complex (Delepelaire, 2004; Kanonenberg et al., 2013).

There are two systems described so far that regulate the expression and secretion of substrates of T1SS, the Has system of *S. marcescens* and *P. aeruginosa,* and the hemolysins of *Vibrio cholerae*, *N. meningitidis* and in particular of uropathogenic *E. coli* (Thomas et al., 2014).

T2SS

The type II secretion system (T2SS), which is conserved in most Gram negative bacteria, is responsible for secreting folded proteins from the periplasm. These proteins are first transported through the IM by the general secretory (Sec) or twin-arginine translocation (Tat) pathways, and then secreted from the periplasm into the extracellular medium by the T2SS (Nivaskumar and Francetic, 2014; Green and Mecsas, 2016).

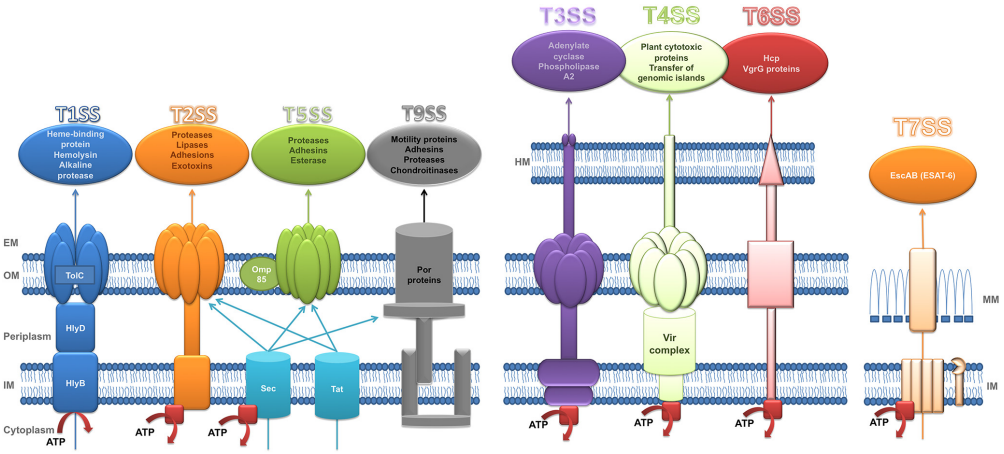

FIGURE 1 | Structure of secretion systems. Schematic representation of secretory systems: type I (T1SS), type II (T2SS), type V (T5SS), type IX (T9SS), type III (T3SS), type IV (T4SS), type VI (T6SS), and type VII (T7SS). The type I pathway is exemplified by hemolysin A (HlyA) secretion in *E. coli* where TolC, HlyD, and HlyB are the three components which constitute the channel to transport HlyA to extracellular space. Sec (general secretion route) and Tat (twin-arginine translocation pathway) transfer the substrates of T2SS and T5SS across the inner membrane. Sec also participates in the transport of T9SS substrates across de inner membrane. T9SS is also called Por Secretion System (PoSS). T4SS is represented by VirB/D system of *Agrobacterium tumefaciens*. The T7SS is based on a system in Mycobacteria. Red squares represent the ATPases. HM, host membrane; EM, extracellular medium; OM, outer membrane; IM, inner membrane; MM, mycomembrane. Substrates secreted by each secretory system are included in a circle in the top of the figure. Adapted from Tseng et al. (2009).

The Sec pathway consists of three structural parts: a protein targeting component, a motor protein and a membrane integrated conducting channel called SecYEG translocase. This mechanism transports unfolded proteins with a hydrophobic sequence at the N-terminus. Moreover, the secreted protein either remains in the periplasm or is transported to the extracellular space. The proteins may contain a SecB-specific signal sequence for transport to the periplasm or the extracellular milieu; however, if it has the signal recognition particle (SRP) signal it can follow the SRP pathway and remain in the inner membrane (Green and Mecsas, 2016; Tsirigotaki et al., 2017).

By contrast, the Tat secretion pathway consists of 2–3 subunits, TatA and TatB, which form a unique multifunctional protein in Gram-positive bacteria, and TatC. This mechanism translocates folded proteins with a twin-arginine motif. In Gram-positive bacteria, most proteins are transported out of the cell, while in Gram-negative bacteria the protein can remain in the periplasm or it can be translocated to the extracellular space by the T2SS (Patel et al., 2014; Green and Mecsas, 2016).

The T2SS, a complex structure composed of 15 proteins, named general secretion pathway proteins (Gsp) in *E. coli* (Korotkov et al., 2012), Eps in *V. cholera* (Abendroth et al., 2009; Sloup et al., 2017) and Xcp in *P. aeruginosa* (Filloux et al., 1998; Robert et al., 2005), has a wide range of substrates with diverse functions, although all share one feature, an N-terminal signal which enables them pass to the periplasm via the Sec or Tat secretion mechanisms (Nivaskumar and Francetic, 2014; Green and Mecsas, 2016).

The main function of the T2SS is to acquire nutrients (Nivaskumar and Francetic, 2014). It is responsible for secreting numerous exoproteins, most of which are hydrolytic enzymes and other proteins such as toxins, adhesins and cytochromes that have various roles in respiration, biofilm formation and motility (Nivaskumar and Francetic, 2014). The T2SS has been described in various environmental strains and also human pathogens such as *V. cholera* (Overbye et al., 1993), *P. aeruginosa, Aeromonas* sp. and enterotoxigenic *Escherichia coli* (ETEC) (Nivaskumar and Francetic, 2014).

T3SS

The type III secretion system (T3SS) or injectisome, is a double-membrane-embedded apparatus found in multiple pathogenic Gram-negative bacteria such as *Salmonella* spp., *Yersinia* spp., enteropathogenic and enterohemorrhagic *E. coli*, *Shigella* spp. and *Pseudomonas* spp. (Cornelis, 2006; Gaytan et al., 2016; Deng et al., 2017). This complex nanomachine promotes the transfer of virulence proteins called effectors from the bacterial cytoplasm into the eukaryotic cell in a single step (Galan and Waksman, 2018).

The T3SS is composed of approximately 25 proteins assembled in three main structures: the basal body, a set of rings spanning the two membranes of the bacterium; a hollow needle-shaped component through which the semi-unfolded effectors are transported (these first two structures are collectively called "needle complex"); and the translocon, made up of a hydrophilic protein that serves as a scaffold for forming a translocation pore, constituted by two hydrophobic proteins, which is inserted into the host cell membrane and through which effectors are directly translocated. A unique set of effectors is delivered by each pathogen, which subverts specific host-cell signaling pathways to allow bacterial colonization (Izore et al., 2011; Notti and Stebbins, 2016; Deng et al., 2017).

The export apparatus associated with the basal body is formed by five poly topic inner membrane proteins that are essential

for substrate secretion. This protein complex, together with a cytoplasmic sorting platform and the ATPase complex are responsible for substrate recruitment and classification, and for energizing the secretion process enabling chaperone-effector dissociation and protein unfolding for initial entry into the T3SS central channel that serves as the secretion pathway. These components are highly conserved between different T3SS systems and with the flagella, which is evolutionarily related to the injectisome (Abby and Rocha, 2012; Galan and Waksman, 2018; Lara-Tejero and Galan, 2019).

Several effectors of T3SS have been described such as ExoS, ExoT, ExoU, and ExoY in *P. aeruginosa*; Tir and EspE in *E. coli* and YopE, YopH, YopM, YopJ/P, YopO/YpkA, and YopT in *Yersinia* sp. (Cornelis and Van Gijsegem, 2000).

T4SS

The type IV secretion system family is found in Gram-negative and Gram-positive bacteria as well as in *Archaea*. T4SS is the most cosmopolitan secretion system and differs from other SS as it is able to transfer DNA in addition to proteins (Cascales and Christie, 2003). More specifically, T4SS is capable of performing contact-dependent secretion of effector molecules into eukaryotic cells, conjugative transfer of mobile DNA elements and also exchange of DNA without any contact with the outside of the cell (Green and Mecsas, 2016; Grohmann et al., 2018). T4SS can be divided on the basis of its functionality into two subfamilies: conjugation systems and effector translocators. Conjugation systems are responsible for the transfer of antibiotic resistance genes and virulence determinants among bacteria. The effector translocators introduce virulence factors into the host cell (Christie, 2016). However, in Gram-negative bacteria T4SS has been divided into two different subfamilies: IVA and IVB. The *E. coli* conjugation apparatuses and VirB/D system of *Agrobacterium tumefaciens* are the models used to study the structure of type IVA of T4SS (Grohmann et al., 2018). The VirB/D apparatus consists of 12 proteins which form a complex envelope-spanning structure that facilitate the translocation function. Two of these proteins, VirB2 and VirB5, make up the pilus, while another three proteins act as ATPases, and VirB1 is a lytic transglycosylase (Costa et al., 2015; Green and Mecsas, 2016). The *Legionella pneumophila* Dot/Icm (Defective for organelle trafficking/Intracellular multiplication) system is the model used to study the IVB subfamily of T4SS (Nagai and Kubori, 2011; Grohmann et al., 2018).

T5SS

The type V secretion system is unique because its substrates transport themselves across the outer membrane. The substrates use the Sec translocase to pass through the inner membrane to the periplasm space. Various different types of T5SS have been identified: autotransporters (T5aSS), two-partner passenger-translocators (T5bSS), trimeric autotransporters (T5cSS), hybrid autotransporters (T5dSS) and inverted autotransporters (T5eSS) (Henderson et al., 2004; Leo et al., 2012; Rojas-Lopez et al., 2017). In general, the T5SS transports proteins across the asymmetric outer membrane (OM) that contains lipopolysaccharides, through their own C-terminal translocation domain that inserts into the OM as a β-barrel to complete the secretion of the N-terminal passenger domain via the barrel pore. Several periplasmic chaperones also participate in transport through the OM, specifically the β-barrel assembly machinery (BAM complex) and the translocation and assembly module (TAM complex) facilitate protein secretion (Rojas-Lopez et al., 2017).

A T5SS has been described in human pathogens such as *Bordetella pertussis* and *Haemophilus influenzae*, which have two-partner SS and uropathogenic *E. coli*, which has chaperone-usher systems (Costa et al., 2015; Green and Mecsas, 2016).

YadA of *Yersinia enterocolitica* and SadA of *Salmonella* are T5SS type c (Leo et al., 2012). Intimin of *E. coli* and invasin of enteropathogenic *Yersinia* spp. are type Ve SS (Leo et al., 2012).

A self-transporter (T5aSS) (Wilhelm et al., 2007) and three T5bSS: LepA /LepB system (Kida et al., 2008), the CupB system (Ruer et al., 2008) and PdtA/PdtB system (Faure et al., 2014), have been reported in *P. aeruginosa*. In *B. cenocepacia,* four T5SS (Holden et al., 2009) have been found, two with pertactin domains and two with haemagglutinin autotransporters; this last type is also present in *S. maltophilia* (Ryan et al., 2009).

T6SS

The type VI secretion system is widely represented in Gram-negative bacteria (Coulthurst, 2013; Gallique et al., 2017b). T6SS is an integrated secretion device within the membrane and it transfers substrates, which are toxic effectors to eukaryotic (Pukatzki et al., 2007) and prokaryotic cells (Russell et al., 2014). It plays a crucial role in the pathogenesis and competition among bacteria (Ho et al., 2014; Zoued et al., 2014; Costa et al., 2015; Gallique et al., 2017a). The origin of T6SS is related to bacteriophages (Leiman et al., 2009). T6SS is a huge apparatus and consists of 13 core components organized into a *trans*-membrane complex, a baseplate-like structure at the cytoplasmic face of the inner membrane, and a sheathed inner tube, which is the effector delivery module that is ejected to the target cell. The tube-sheath complex is assembled from the baseplate in the cytoplasm and the hollow tube is built from hexamers of the hemolysin co-regulated protein (Hcp). The sheath contracts and pushes the tube with the associated effectors into targeted cells, using a puncturing mechanism similar to the one used by the contractile tails of phages (Russell et al., 2011, 2014; Cianfanelli et al., 2016; Green and Mecsas, 2016; Galan and Waksman, 2018).

T7SS

Type VII secretory system has been described in some Gram-positive bacteria such as *Staphylococcus aureus* and in species of *Mycobacterium* and *Corynebacterium*. This SS was reported for the first time in 2003 in *Mycobacterium tuberculosis* and it was called ESX-1 (Stanley et al., 2003), which is an important virulence factor in *M. tuberculosis*. To date, five T7SS have been identified in *Mycobacterium* sp. but the transport mechanisms across the mycobacterial membrane are almost unknown (Costa et al., 2015; Ates et al., 2016; Green and Mecsas, 2016).

Most of the substrates of T7SS belong to EscAB clan which includes six protein families: Esx, PE, PPE, LXG, DUF2563,

and DUF2580. ESAT-6 is a *M. tuberculosis* protein which belongs to Esx family and which is secreted with EsxB (CFP-10) (Ates et al., 2016).

T9SS

The type IX secretion system (T9SS) or Por secretion system (PorSS) is the most recently discovered system (Lasica et al., 2017). Its function is to transport molecules across the outer membrane. Its substrates must include a Sec signal, which allows transfer of proteins through the inner membrane with the aid of the Sec system. The T9SS system has been described in almost all members of the phylum *Bacteroidetes,* but it has mainly been studied in oral pathogens such as *Porphyromonas gingivalis* and *Tannerella forsythia.* In *P. gigivalis*, the T9SS system consists of 16 proteins with structural and functional activity, and another two proteins involved in the regulation of the transport process (Sato et al., 2010; Lasica et al., 2017).

REGULATION OF SECRETION SYSTEMS BY QUORUM SENSING NETWORKS (TABLE 1)

Pseudomonas aeruginosa

T1SS

Transcriptional studies in *P. aeruginosa* suggest that in this bacterium T1SS is positively regulated by QS, since the expression of its effector, the alkaline protease AprA, depends on QS. In addition, the genes of the AprA inhibitor *aprI* and the structural genes *aprDEF* also appear to be positively regulated by QS (Hentzer et al., 2003; Schuster et al., 2003; Wagner et al., 2003).

T2SS

Three T2SS systems, the Xcp, Hxc and Txc systems, have been described in *P. aeruginosa*. The first of these, Xcp, secretes the QS regulated virulence factors elastase A and B (LasA and LasB) as well as the exotoxin A (ExoA) and it is itself positively regulated by QS (**Figure 2**). Accordingly, recently it was demonstrated by ChIPseq analysis that MvfR (the receptor of the PQS autoinducer) is able to directly bind *xcpQ-xcpP-xcpR* regions and this is related to their induction in the presence of MvfR (Maura et al., 2016).

The second T2SS, Hxc, is regulated by the availability of phosphate and secretes LapA a low-molecular weight alkaline phosphatase (Wagner et al., 2003; Michel et al., 2007). Two genes, *xphA* and *xqhA*, which encode the PaQa subunit of the Xcp functional hybrid system, have been described. These genes, which are located outside the *xcp* locus, are regulated by environmental conditions but not by QS, in contrast to what occurs with the rest of the Xcp system (Michel et al., 2007, 2011). In contrast to the first two systems, the third system Txc has just recently been described and so far only identified in a region of genome plasticity of the strain PA7; it is regulated by a two component system (TtsSR) and secretes the chitin binding protein CpbE (Cadoret et al., 2014).

T3SS

Current evidence suggest that as in *Vibrio* spp., QS in *P. aeruginosa* negatively regulates the expression of T3SS, specifically the RhlI/RhlR system, as transcription of the T3SS genes and secretion of ExoS increase significantly in a *rhlI* mutant and return to basal levels on the addition of exogenous C4-HSL (Bleves et al., 2005; Kong et al., 2009; **Figure 2**). In agreement, the expression of *exoS* is also negatively regulated by QS, specifically by the RhlI/RhlR system, as well as by the stationary phase sigma factor RpoS (Hogardt et al., 2004).

The fact that the T3SS genes do not appear to be repressed by QS in some global transcriptomic studies with mutants may be explained by the presence of high calcium concentrations in the media, or by the lack of resolution of DNA microarrays (Hentzer et al., 2003; Schuster et al., 2003). More striking is the fact that some QS inhibitors like 6-gingerol and coumarin inhibit rather than increase the expression of T3SS (Zhang et al., 2018). Nevertheless, these studies were done in the presence of high calcium, and QS-independent inhibition of T3SS has not been ruled out. Moreover, a recent study in the PA01 strain, using a *lasR rhlR* double mutant, demonstrated that it remains virulent in a murine abscess model, despite that it does not produce QS-dependent virulence factors and that the secretion of ExoT and ExoS is fully functional in this mutant. Hence the authors hypothesized that T3SS is the cause of the remaining virulence (Soto-Aceves et al., 2019).

The *P. aeruginosa* QS network and its T3SS are also related by the fact that VqsM, an AraC-family transcription factor, binds to both the promoter region of *lasI* and the promoter of *exsA*, which encodes a master regulator of the T3SS, regulating both mechanisms (Liang et al., 2014; **Figure 2**).

T6SS

The T6SS is involved in iron transport, and a connection has been observed between T6SS and QS through the TseF protein, which is a substrate of T6SS and interacts with PQS (Lin et al., 2017; **Figure 2**).

In *P. aeruginosa,* three loci which encode T6SS have been found to be regulated by QS proteins (LasR and MvfR) (Lesic et al., 2009). Expression of the second loci, H2-T6SS, is regulated by the Las and Rhl QS systems in PAO1 strains (Sana et al., 2012; **Figure 2**) and by the direct binding of MvfR in PA14 (Maura et al., 2016).

Vibrio sp.

T2SS

The formation of biofilms has multifactorial regulation in *V. cholerae* as in other pathogens. The QS network controls directly biofilm production which is related to type II secretion system in *V. cholerae* (Teschler et al., 2015). Several proteins such as RbmA, RbmC and Bap1, which are involved in the formation of biofilms, are transported by T2SS. In addition, mutant strains with inactivated T2SS have reduced biofilm formation (Johnson et al., 2014; Teschler et al., 2015).

TABLE 1 | Pathogens and QS elements related to secretion systems.

Type secretion system	SS element	QS regulation	QS element	Microorganisms	References
T1SS	Lip	+	*Swr*	*Serratia liquefaciens*	Riedel et al., 2001
T2SS	Xcp	+	*lasR/lasI rhLR/rhlI*	*Pseudomonas aeruginosa*	Wagner et al., 2003; Michel et al., 2007
			DSF-type	*Xanthomonas* species	Qian et al., 2013
T3SS	LEE operon	+	*luxS*	*Escherichia coli*	Sperandio et al., 1999
		−		*Vibrio parahaemolyticus Vibrio harveyi*	Henke and Bassler, 2004
	ExsA		*lasI*	*Pseudomonas aeruginosa*	Liang et al., 2014
	Yop-Ysc	+	Hfq	*Yersinia pseudotuberculosis Yersinia pestis*	Schiano et al., 2014
T4SS	VirB/D	+	VjbR (LuxR-type QS)	*Brucella abortus*	Arocena et al., 2010; Li et al., 2017
		+	*luxI*	Roseobacter group	Patzelt et al., 2013, 2016
T6SS				*Vibrio alginolyticus*	Yang et al., 2018
	Hcp		HapR and LuxO	*Vibrio cholerae*	Ishikawa et al., 2009; Zheng et al., 2010; Kitaoka et al., 2011; Leung et al., 2011
				Burkholderia thailandensis	Majerczyk et al., 2016
			AHL	*Pseudomonas fluorescens*	Gallique et al., 2017b
	TseF		PQS	*Pseudomonas* spp.	Lin et al., 2017
			LasR and MvfR	*Pseudomonas aeruginosa*	Lesic et al., 2009
	VipA,Hcp-1, VipB		AbaR/AbaI	*Acinetobacter baumannii*	Lopez et al., 2017b

T3SS

In *V. parahaemolyticus* and *V. harveyi* (unlike in *E. coli*), both the HAI-1 and AI-2 QS systems inhibit the expression of T3SS genes (Henke and Bassler, 2004). QS also represses T3SS during *V. harveyi* infections of gnotobiotic brine shrimp (Ruwandeepika et al., 2015). Waters et al. (2010) have described the regulatory pathway by which QS controls T3SS. At low cell density when LuxR is repressed, which entails the derepression of two promoters of the *exsBA* operon and the *exsA* operon, ExsA activates the expression of genes that encode the structural proteins of the type III secretion system. However, when the cell density is high, LuxR directly represses transcription of the PB promoter, preventing the production of ExsA and consequently decreasing the expression of structural genes of T3SS (Waters et al., 2010; Ball et al., 2017). OpaR inhibits the T3SS1 in *V. parahaemolyticus* which is the most important factor in its cytotoxicity (Gode-Potratz and McCarter, 2011).

T6SS

Several researchers have demonstrated the regulation of T6SS by QS networks in *Vibrio* spp. We present the main findings in this field here. In *V. alginolyticus*, activation of T6SS and the QS network has been found to be coordinated by the serine/threonine kinase PpkA cascade (Yang et al., 2018). PpkA2 is autophosphorylation and it transfers the phosphate group to VstR. Phosphorylated VstR promotes the expression of both of the T6SS in *V. alginolyticus* through the inhibition of LuxO activity, which acts to impede the expression of LuxR, a promoter of the T6SS. LuxR inhibits the expression of the first T6SS (T6SS1) or promotes the expression of the second T6SS (T6SS2) (Yang et al., 2018).

At low cell population density, LuxO is phosphorylated, which activates the expression of specific small regulatory RNAs (sRNAs) in conjunction with alternative sigma factor σ^{54} (Sheng et al., 2012). sRNAs inhibit the expression of LuxR with the help of RNA chaperone Hfq (Liu et al., 2011). However, at high cell population density, LuxO is dephosphorylated turning off the transcription of the sRNAs and allowing the translation of LuxR (Waters and Bassler, 2005; Milton, 2006). Sheng et al. (2012) also demonstrated that the expression of the *hcp* T6SS gene is growth phase-dependent and the QS regulators controls the haemolysin co-regulated protein, which is one of the main proteins of the T6SS functioning as an effector of the system and/or an effector binding protein (**Figure 2**). The phosphatase PppA also acts on the QS (modulating the transcription of LuxR) and the expression and secretion of *hcp1* and *hcp2* (Sheng et al., 2013). It is important to highlight that PppA permits the cross-talk between the two T6SS in *V. alginolyticus* (Sheng et al., 2013).

Rpo N (σ^{54}) collaborates with QS in the regulation of T6SS genes. It is involved in the regulation of the expression of *hcp* and *vgrG3* operons that encode T6SS secreted molecules, but does not control the genes that encode the structural and sheath components of T6SS (Ishikawa et al., 2009; Dong and Mekalanos, 2012).

There are a few more studies in *V. cholerae* related to this topic than other species. Two QS autoinducers, CAI-I (cholerae autoinducer) and AI-2 (autoinducer-2), co-operate to control the gene expression depending on the cell density

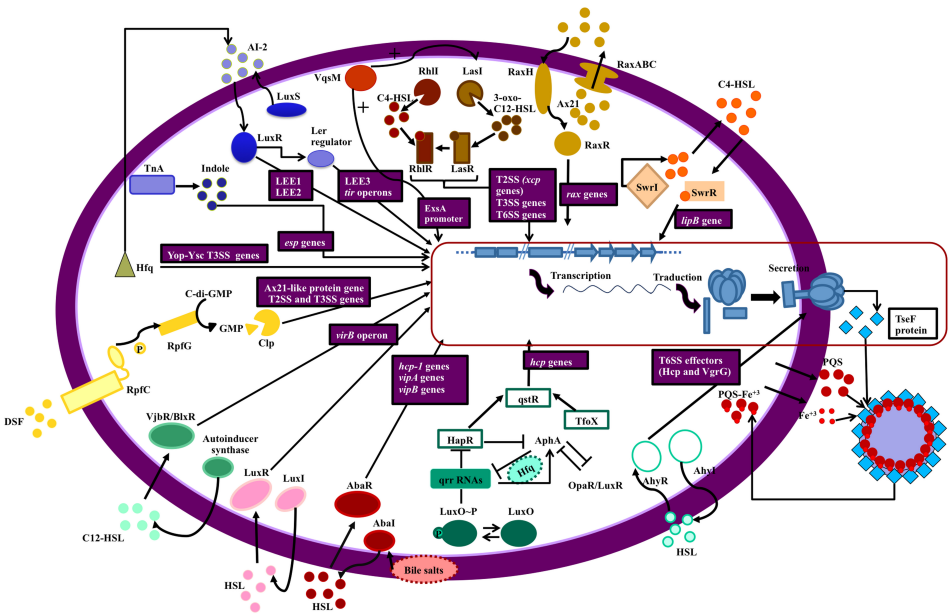

FIGURE 2 | Secretion systems and QS network elements. The figure shows the relationship between QS networks and expression of secretion systems (blue squares). The genes regulated by QS are in purple boxes. Each QS network is represented by a different color. Starting at the top right of the figure: The swr QS system of *S. liquefaciens* controls the *lipB* genes of the T1SS (orange); Ax21 (QS effector) and QS system Rax regulate RaxABC TOSS (T1SS) in gram negative bacteria (ochre); QS (RhlIR and LasIR) regulates expression of T2SS, T3SS, and T6SS in *P. aeruginosa* (brown); VqsM (an AraC family transcription factor) interacts with the LasIR and ExsA promoters (a master regulator of T3SS) in *P. aeruginosa* (dark orange); T2SS is regulated by LuxS/LuxI/AI-2 QS in *E. coli* and indole production by TnA (tryptophanase) regulates *esp* genes expression (T2SS) in this bacterium (blue); in *Yersinia* sp. the Hfq chaperone is connected with QS (AI-2) and regulates the Yop-Ysc type III secretion system (T3SS) (green); in *Xanthomonas* sp. T2SS and T3SS are regulated by DSF (diffusible signal factor) which is a quorum sensing signal (yellow); T4SS (*virB* operon) is regulated by VjbR (LuxR like protein) and LuxI in *Brucella* (turquoise) and *Roseobacter* (pink), respectively; a connection between *Acinetobacter baumanii* QS (AbaI/AbaR, controlled by bile salts) and T6SS has been established (maroon); in *Vibrio* sp. there is a complex network which relates QS (LuxO/HapR/TfoX) with T6SS (aquamarine); AhyRI (a QS network) in *Aeromonas* sp. and *P. atrosepticum* is involved in Hcp and VgrG secretion (sky blue) and finally, iron is transported across the cell membrane accompanied by PQS, a quorum sensing signal in *P. aeruginosa*, and this process depend on Tse a substrate of T6SS, which binds to OMVs (outer membrane vesicles) containing PQS- Fe^{3+}.

(Ng and Bassler, 2009). Two enzymes are necessary for the biosynthesis of these autoinducers: CqsA and LuxS, respectively (Schauder et al., 2001; Miller et al., 2002; Chen et al., 2002; Higgins et al., 2007). These signal molecules are detected by two sensor kinases, LuxQ (sensor of CAI-I) and CqsS (sensor of AI-2). Both pathways merge on LuxU, a phosphotranfer protein. At low cell density (LCD), the two sensor kinases phosphorylate LuxU due to the absence of their respective autoinducers. There are two histidine kinases which also contribute to the phosphorylation of LuxU: VpsS and CqsR (Jung et al., 2015). Then, LuxU transfers the phosphorylate group to a DNA-binding response regulator protein called LuxO. Phosphorylated LuxO activates the expression of sRNA molecules (known as qrr1-4) when the cell density is low thanks to the interaction with the alternative sigma factor σ^{54} (Freeman et al., 2000; Lenz et al., 2004). In conjunction with the RNA-binding protein Hfq, LuxO represses the expression of HapR (Lenz et al., 2004), a TetR-family global transcriptional regulator which acts on QstR (Tsou et al., 2009; Shao and Bassler, 2014; Watve et al., 2015; **Figure 2**). HapR is accumulated when the cell density is high (Lenz et al., 2004) because LuxO is not phosphorylated and transcription of the sRNAs is blocked. QstR is a master regulator of the T6SS belonging to the LuxR-type family of regulators (Jaskólska et al., 2018). QstR binds to the promoter region of the T6SS cluster inducing the expression of the genes. The regulation of the T6SS by cAMP-CRP pathway is not clear, but it is possible that it influences T6SS genes through regulation of QS and chitin-induced competency (Liang et al., 2007; Blokesch, 2012). It is known that CRP positively regulates T6SS (Ishikawa et al., 2009). Apart from the activation of QstR via QS, it is also regulated by chitin and arabinose (Lo Scrudato and Blokesch, 2012, 2013).

The expression of the three T6SS gene clusters in *V. cholerae* requires TfoX, CytR, HapR, and QstR for the highest level of expression (Watve et al., 2015). CytR and TfoX are required for the expression of the T6SS genes but their regulatory effects are only mediated by QstR (**Figure 2**).

Other Pathogens

T1SS

The *swr* QS system, which controls swarming motility, regulates the Lip secretion system, a T1SS responsible for the secretion of lipases, metalloproteases and S-layer proteins in *Serratia liquefaciens* MG1 (Riedel et al., 2001). The *swr* QS system consists of SwrI, which synthesizes C4-HSL, and SwrR, which regulates gene transcription after binding the diffusible signal C4-HSL.

QS-mediated regulation of *lipB*, which encodes the LipB exporter, was demonstrated in *swrI* mutants with *luxAB* insertions, in which the level of secreted proteins was lower (Riedel et al., 2001; **Figure 2**). Other relationships between T1SS and QS have also been observed. The rice pathogen recognition XA21 receptor recognizes a sulphated peptide (axY^S22) derived from the Ax21 protein (activator of XA21-mediated immunity) and confers resistance to *Xanthomonas oryzae* strains. Ax21 may have a key biological role because it is conserved in *Xanthomonas* spp., *Xylella fastidiosa,* and *Stenotrophomonas maltophilia*. Ax21 requires RaxABC TOSS (type I secretion system) for secretion and activity. The expression of *rax* genes which encode T1SS has been demonstrated to be QS-dependent due to the cell-density dependency (Han et al., 2011). These data indicate that Ax21 could have a role as a signaling molecule and a direct relationship between the QS network and T1SS is established (**Figure 2**; Lee et al., 2006).

T2SS

In *Xanthomonas* species, QS is mediated by the diffusible signal factor (DSF). A proteomic analysis conducted in 2013 revealed 33 proteins that are controlled by DSF. Their putative functions are associated with QS and include cellular processes, intermediary metabolism, oxidative adaption, macromolecule metabolism, cell-structure, protein catabolism, and hypothetical functions (Qian et al., 2013). In this study, it was observed that three genes encoding T2SS-dependent proteins and one gene which encodes Ax21 (activator of XA21-mediated immunity)-like protein are regulated by QS and are essential for virulence-associated functions, including extracellular protease, cell motility, antioxidative ability, extracellular polysaccharide biosynthesis (EPS), colonization, and biofilm (Qian et al., 2013; **Figure 2**).

T3SS

The relationship between QS and T3SS in *E. coli* was first demonstrated by Sperandio et al. (1999), who showed that expression of the locus of enterocyte effacement (LEE) operons that encode the T3SS is activated by QS in both enterohemorrhagic (EHEC) and enteropathogenic (EPEC) *E. coli* due to transcriptional control of the LEE operons by LuxS, which directly activates the LEE1 and LEE2 operons and indirectly activates (via the Ler regulator) the LEE3 and *tir* operons (**Figure 2**). These researchers proposed that activation of the T3SS by the AI-2 autoinducer synthesized by commensal *E. coli* resident in the large intestine could explain the high infectivity of *E. coli* O157: H7, which has an infectious dose of about 50 bacterial cells (Sperandio et al., 1999).

The major virulence factors of EHEC and EPEC are intimin (T5eSS), Tir (the receptor for intimin) and the three secreted proteins EspA, EspB and EspD. T3SS functions in the secretion of the Tir and Esp proteins. The LuxR-type response regulator SdiA negatively regulates the expression of EspD and intimin in the same bacterium, indicating multifactorial regulation of the T3SS by bacterial QS signals (Kanamaru et al., 2000).

Indole, which is produced by tryptophanase (TnA) in enteric bacteria and reaches high concentrations in the gut, is another signaling molecule that influences expression of T3SS in *E. coli* (Lee et al., 2007, 2008). Indole increases the production and secretion of the translocators EspA and EspB in EHEC O157:H7 (Hirakawa et al., 2009; **Figure 2**); hence, indole promotes the development of attaching and effacing (A/E) lesions in HeLa cells.

The involvement of the RNA chaperone protein Hfq, which also participates in QS, in T3SS expression was demonstrated in *Yersinia pseudotuberculosis* and *Yersinia pestis* (Schiano et al., 2014; **Figure 2**). Moreover, Schiano et al., 2014 have demonstrated the regulation of T3SS by QS through virulence regulators LcrF and YmoA in *Y. pseudotuberculosis* (Amy, 2018).

In *Aeromonas hydrophila*, an unique QS system, encoded in *ahyR/ahyI* loci, has been described (Vilches et al., 2009; Garde et al., 2010). Vilches et al. (2009) have used the *A. hydrophila* AH-3 strain to study the T3SS regulation. AH-3: ahyI and AH-3: ahyR mutants have reduced activity of the *aopN-aopB* promoter (promoter of T3SS components) compared to the wild-type strain (**Figure 2**). So they concluded that QS could be involved in the positive regulation of the production of the T3SS component in the AH-3 strain (Vilches et al., 2009).

T4SS

In *Brucella abortus,* there is a clear relationship between the QS network and T4SS. For the *virB* operon, which encodes the T4SS regulated by VjbR, a LuxR-type QS is responsible for the virulence characteristics of *B. abortus* (Li et al., 2017). The *virB* operon is responsible for establishing the replicative niche of the bacterium once it enters the host cell. The T4SS in *B. abortus,* as in other bacteria, translocates effector proteins into the host cell to avoid the immune defense mechanisms, making it one of the two main virulence factors for *Brucella.* Arocena et al. (2010) described the binding site of VjbR to the *virB* operon (Li et al., 2017). Otherwise, the conjugation process between two members of the *Roseobacter* group mediated by T4SS, encoded in RepABC-type plasmids, is controlled by the QS network. This was demonstrated by construction of *luxI* mutant and the addition of external long chain AHLs, which restored the phenotype (Patzelt et al., 2013, 2016; **Figure 2**).

T6SS

Quorum sensing has been reported to control expression of T6SS toxin-immunity systems in *Burkholderia thailandensis*. Moreover, a new role for T6SS in constraining the proliferation of QS mutants has been described in *B. thailandensis* (Majerczyk et al., 2016). Interestingly, it has been observed that T6SS effectors function as cell-to-cell signals in a *Pseudomonas fluorescens* MFE01 strain lacking the AHL QS pathway (Gallique et al., 2017b).

In *A. hydrophila*, Hcp and VgrG- two of the "core" proteins and also effectors of the T6SS- secretion have been suggested to be regulated by the AhyRI QS regulon (Khajanchi et al., 2009; **Figure 2**). Finally, our research group has described the association between T6SS machinery and the activation of the QS system by bile salts in *A. baumannii* clinical strains (Lopez et al., 2017a; **Figure 2**).

T7SS

As with other bacteria, *Mycobacterium* spp regulate biofilm formation by QS (Virmani et al., 2018). The second messenger c-di-cGMP, an intracellular signaling molecule, coordinates

biofilm production and QS signaling (Sharma et al., 2014). Both *M. tuberculosis* (Kulka et al., 2012) and diverse species of non-tuberculous mycobacteria (*M. smegmatis, M. marinum, M. fortuitum, M. chelonae, M. ulcerans, M. abscessus, M. avium,* and *M. bovis*) produce biofilm depending on certain environmental conditions such as the availability of nutrients or the pH of the medium (Hall-Stoodley et al., 1998; Bardouniotis et al., 2003; Ojha et al., 2005; Marsollier et al., 2007; Johansen et al., 2009; Rhoades et al., 2009).

In the recent work of Lai et al. (2018) it was demonstrated that *the espE, espF, espG,* and *espH* genes, located in the T7SS ESX-1 operon, are crucial for sliding motility and biofilm formation in *M. marinum*. Esp proteins, which regulate substrate transport, are involved also in virulence. This paper clearly demonstrates the role of *M. marinum* T7SS in the production of biofilm which, as already mentioned, is related to QS (Lai et al., 2018).

The T7SS of *S. aureus*, a virulence factors export machinery, plays a key role in the promotion of bacterial survival and long-term persistence of subpopulations of staphylococci. The expression of T7SS is regulated by the bacterial interaction with host tissues (Lopez et al., 2017c) mediated by the secondary sigma factor (σB) (Schulthess et al., 2012). Schulthess et al. (2012) reported that the repression of *esxA* by σB is due to the transcription of *sarA* induced by σB, which leads to a strong repression of *esxA*. The activation of the *esxA* transcript, on the other hand, is stimulated by *arlR*, the response regulator of the ArlRS two-component system, SpoVG, a σ-dependent element, and the Agr quorum detection system (Schulthess et al., 2012). Agr QS system is composed by AIP (self-activating peptide), the inducer ligand of AgrC which is the receptor of the agr signal. In the case of the QS Agr system, the effector of global gene regulation is an important regulatory RNA, RNAIII (Novick and Geisinger, 2008).

T9SS

Moreover, an important relationship between T9SS and biofilm formation has been observed in periodontopathogenic pathogens such as *Capnocytophaga ochracea*, *Porphyromonas* spp., *Fusobacterium* spp. and *Prevotella* spp. (Kita et al., 2016). In the study by Kita et al. (2016), the participation of T9SS in the formation of biofilm of *C. ochracea* is demonstrated. The formation of biofilm of *C. ochracea* is crucial for the development of dental plaque and the same happens with other periodontal pathogens, in which it has also been seen that genes related to T9SS are present. Therefore, the components of the T9SS could be potential targets to inhibit the formation of biofilm and thus avoid the formation of dental plaque (McBride and Zhu, 2013; Kita et al., 2016). However, in depth analysis of the relationship between T9SS and QS network in different pathogens is required.

DISCUSSION

To date, the T1SS, T2SS, T3SS, T4SS, T6SS, T7SS, and T9SS SS have been found to have important relationships with QS networks. The involvement of the T1SS system (Lip B which is part of the Lip exporter) in the QS network (*swr* quorum system) of *S. liquefaciens* MG1 has been investigated (Riedel et al., 2001). In *P. aeruginosa,* two QS systems (*lasR/lasI* and *rhLR/rhlI*) are linked to T2SS system by microarrays and proteomic studies (Chapon-Herve et al., 1997; Wagner et al., 2003; Michel et al., 2007), and DSF-type systems are also linked to T2SS in *Xanthomonas* species through proteome analysis (Qian et al., 2013). The QS signal AI-2 has been associated with a T3SS system in *E. coli* (Sperandio et al., 1999) and *Vibrio* spp. (Henke and Bassler, 2004). Moreover, this T3SS system has been related to QS proteins in another two pathogens, *P. aeruginosa* and *Yersinia* spp. (Liang et al., 2014; Schiano et al., 2014).

Several T4SS (*virB* operon) are controlled by VjbR protein which is a LuxR-type quorum-sensing regulator in *B. abortus* (Arocena et al., 2010; Li et al., 2017). Moreover, in the *Roseobacter* group, the conjugation of plasmids, which encode T4SS, is QS-controlled and the QS system may detect a broad range of long-chain AHLs at the cell surface (Patzelt et al., 2013, 2016).

There is a wealth of information relating the T6SS to QS in pathogens such as *Vibrio* spp. For example, Hcp and VasH from the T6SS system in *V. cholerae* are involved in QS (Ishikawa et al., 2009; Zheng et al., 2010; Kitaoka et al., 2011; Leung et al., 2011; Yang et al., 2018). For *Pseudomonas* spp,. there are numerous works where the different T6SS are regulated by QS networks (Lesic et al., 2009; Gallique et al., 2017b; Lin et al., 2017). In other pathogens as *Burkholderia thailandensis* (Majerczyk et al., 2016), and in *A. baumannii,* the relationship between QS and SS has begun to be studied (Lopez et al., 2017a).

In *M. marinum,* the relationship between biofilm formation, which is tightly connected with QS, and T7SS, has been demonstrated (Lai et al., 2018). Also in *S. aureus,* the Agr QS network has been related to T7SS (Schulthess et al., 2012). An important relationship between T9SS and biofilm formation has been observed in periodontopathogenic pathogens (Kita et al., 2016). Finally, although the involvement of T5SS secretion system in virulence, motility and competence is well-known, these systems and their association with QS must be studied in greater depth in order to clarify their roles.

Taking *P. aeruginosa* as a reference point, the positive effect of QS in the expression of T1SS and T2SS could be related to the fact that this organism secretes exoproducts that are public goods (proteases and lipases); hence, it is better to produce and secrete these compounds when a high cell density is reached, since these products are costly and the benefits associated to their production are higher at high cell densities. Similarly, the T6SS, which is involved in killing competitors by contact, will be more efficient at high cell densities since the probability of finding target bacteria is higher. In contrast, the T3SS appears to be negatively regulated by QS, and this may be related to its role in an acute infection and its "inhibition by QS" may be a way to facilitate the transition to a chronic infection state. In addition to its well established role in infections, T3SS has a broader ecological role suggested by its role in killing biofilm associated *Acanthamoeba castellanii* amoeba (Matz et al., 2008). Furthermore, it was recently demonstrated that T3SS is susceptible of cheating by mutants that do not produce it, allowing their establishment in infections (Czechowska et al., 2014); hence, the selective forces that act over T3SS are complex.

Therefore, research into the relationship between QS and SS must be further developed in order to better understand human infections.

AUTHOR CONTRIBUTIONS

RTP, LB, AA, BG-P, LF-G, ML, IB, and GB developed the redaction of the manuscript, figures and table. RG-C, TW, and MT designed the review, assigned writing tasks to co-authors, contributed to writing and proofread the final version.

FUNDING

This study was funded by grant PI16/01163 awarded to MT within the State Plan for R+D+I 2013–2016 (National Plan for Scientific Research, Technological Development and Innovation 2008–2011) and co-financed by the ISCIII-Deputy General Directorate for Evaluation and Promotion of Research – European Regional Development Fund "A way of making Europe" and Instituto de Salud Carlos III FEDER, Spanish Network for the Research in Infectious Diseases (REIPI, RD16/0016/0001 and RD16/0016/0006) and by the Study Group on Mechanisms of Action and Resistance to Antimicrobials, GEMARA (SEIMC, http://www.seimc.org/). MT was financially supported by the Miguel Servet Research Programme (SERGAS and ISCIII). RTP and LF-G were financially supported by, respectively, a post-speciality grant awarded by the Fundación Novoa Santos (CHUAC-SERGAS, Galicia) and predoctoral fellowship from the Xunta de Galicia (GAIN, Axencia de Innovación). RG-C research is supported by the grant PAPIIT-UNAM number IN214218. BG-P was supported by grants PAPIIT-UNAM IN209617 and CONACYT 284081.

REFERENCES

Abby, S. S., and Rocha, E. P. (2012). The non-flagellar type III secretion system evolved from the bacterial flagellum and diversified into host-cell adapted systems. *PLoS Genet.* 8:e1002983. doi: 10.1371/journal.pgen.1002983

Abendroth, J., Mitchell, D. D., Korotkov, K. V., Johnson, T. L., Kreger, A., Sandkvist, M., et al. (2009). The three-dimensional structure of the cytoplasmic domains of EpsF from the type 2 secretion system of *Vibrio cholerae*. *J. Struct. Biol.* 166, 303–315. doi: 10.1016/j.jsb.2009.03.009

Abisado, R. G., Benomar, S., Klaus, J. R., Dandekar, A. A., and Chandler, J. R. (2018). Bacterial quorum sensing and microbial community interactions. *mBio* 9:e02331-17. doi: 10.1128/mBio.02331-17

Amy, S. (2018). *Unraveling the Regulatory Relationship between Quorum Sensing and the Type III Secretion System in Yersinia pseudotuberculosis*. Ph.D. thesis, University of Nottingham, Nottingham.

Arocena, G. M., Sieira, R., Comerci, D. J., and Ugalde, R. A. (2010). Identification of the quorum-sensing target DNA sequence and N-Acyl homoserine lactone responsiveness of the *Brucella abortus* virB promoter. *J. Bacteriol.* 192, 3434–3440. doi: 10.1128/JB.00232-10

Ates, L. S., Houben, E. N., and Bitter, W. (2016). Type VII secretion: a highly versatile secretion system. *Microbiol. Spectr.* 4. doi: 10.1128/microbiolspec.VMBF-0011-2015

Baharoglu, Z., and Mazel, D. (2014). SOS, the formidable strategy of bacteria against aggressions. *FEMS Microbiol. Rev.* 38, 1126–1145. doi: 10.1111/1574-6976.12077

Ball, A. S., Chaparian, R. R., and van Kessel, J. C. (2017). Quorum sensing gene regulation by LuxR/HapR master regulators in vibrios. *J. Bacteriol.* 199:e00105-17. doi: 10.1128/JB.00105-17

Barber, C. E., Tang, J. L., Feng, J. X., Pan, M. Q., Wilson, T. J., Slater, H., et al. (1997). A novel regulatory system required for pathogenicity of *Xanthomonas campestris* is mediated by a small diffusible signal molecule. *Mol. Microbiol.* 24, 555–566. doi: 10.1046/j.1365-2958.1997.3721736.x

Bardouniotis, E., Ceri, H., and Olson, M. E. (2003). Biofilm formation and biocide susceptibility testing of *Mycobacterium fortuitum* and *Mycobacterium marinum*. *Curr. Microbiol.* 46, 28–32. doi: 10.1007/s00284-002-3796-4

Battesti, A., Majdalani, N., and Gottesman, S. (2011). The RpoS-mediated general stress response in *Escherichia coli*. *Annu. Rev. Microbiol.* 65, 189–213. doi: 10.1146/annurev-micro-090110-102946

Blanco, P., Hernando-Amado, S., Reales-Calderon, J. A., Corona, F., Lira, F., Alcalde-Rico, M., et al. (2016). Bacterial multidrug efflux pumps: much more than antibiotic resistance determinants. *Microorganisms* 4:E14. doi: 10.3390/microorganisms4010014

Bleves, S., Soscia, C., Nogueira-Orlandi, P., Lazdunski, A., and Filloux, A. (2005). Quorum sensing negatively controls type III secretion regulon expression in *Pseudomonas aeruginosa* PAO1. *J. Bacteriol.* 187, 3898–3902. doi: 10.1128/JB.187.11.3898-3902.2005

Blokesch, M. (2012). Chitin colonization, chitin degradation and chitin-induced natural competence of *Vibrio cholerae* are subject to catabolite repression. *Environ. Microbiol.* 14, 1898–1912. doi: 10.1111/j.1462-2920.2011.02689.x

Bzdrenga, J., Daudé, D., Rémy, B., Jacquet, P., Plener, L., Elias, M., et al. (2017). Biotechnological applications of quorum quenching enzymes. *Chem. Biol. Interact.* 267, 104–115. doi: 10.1016/j.cbi.2016.05.028

Cadoret, F., Ball, G., Douzi, B., and Voulhoux, R. (2014). Txc, a new type II secretion system of *Pseudomonas aeruginosa* strain PA7, is regulated by the TtsS/TtsR two-component system and directs specific secretion of the CbpE chitin-binding protein. *J. Bacteriol.* 196, 2376–2386. doi: 10.1128/JB.01563-14

Cascales, E., and Christie, P. J. (2003). The versatile bacterial type IV secretion systems. *Nat. Rev. Microbiol.* 1, 137–149. doi: 10.1038/nrmicro753

Case, R. J., Labbate, M., and Kjelleberg, S. (2008). AHL-driven quorum-sensing circuits: their frequency and function among the *Proteobacteria*. *ISME J.* 2, 345–349. doi: 10.1038/ismej.2008.13

Chapon-Herve, V., Akrim, M., Latifi, A., Williams, P., Lazdunski, A., and Bally, M. (1997). Regulation of the xcp secretion pathway by multiple quorum-sensing modulons in *Pseudomonas aeruginosa*. *Mol. Microbiol.* 24, 1169–1178. doi: 10.1046/j.1365-2958.1997.4271794.x

Chen, X., Schauder, S., Potier, N., Van Dorsselaer, A., Pelczer, I., Bassler, B. L., et al. (2002). Structural identification of a bacterial quorum-sensing signal containing boron. *Nature* 415, 545–549. doi: 10.1038/415545a

Christie, P. J. (2016). The mosaic type IV secretion systems. *Ecosal Plus* 7. doi: 10.1128/ecosalplus.ESP-0020-2015

Cianfanelli, F. R., Monlezun, L., and Coulthurst, S. J. (2016). Aim, load, fire: the type VI secretion system, a bacterial nanoweapon. *Trends Microbiol.* 24, 51–62. doi: 10.1016/j.tim.2015.10.005

Cornelis, G. R. (2006). The type III secretion injectisome. *Nat. Rev. Microbiol.* 4, 811–825. doi: 10.1038/nrmicro1526

Cornelis, G. R., and Van Gijsegem, F. (2000). Assembly and function of type III secretory systems. *Annu. Rev. Microbiol.* 54, 735–774. doi: 10.1146/annurev.micro.54.1.735

Costa, T. R., Felisberto-Rodrigues, C., Meir, A., Prevost, M. S., Redzej, A., Trokter, M., et al. (2015). Secretion systems in Gram-negative bacteria: structural and mechanistic insights. *Nat. Rev. Microbiol.* 13, 343–359. doi: 10.1038/nrmicro3456

Coulthurst, S. J. (2013). The Type VI secretion system - a widespread and versatile cell targeting system. *Res. Microbiol.* 164, 640–654. doi: 10.1016/j.resmic.2013.03.017

Czechowska, K., McKeithen-Mead, S., Al Moussawi, K., and Kazmierczak, B. I. (2014). Cheating by type 3 secretion system-negative *Pseudomonas aeruginosa*

during pulmonary infection. *Proc. Natl. Acad. Sci. U.S.A.* 111, 7801–7806. doi: 10.1073/pnas.1400782111

Delepelaire, P. (2004). Type I secretion in gram-negative bacteria. *Biochim. Biophys. Acta* 1694, 149–161. doi: 10.1016/j.bbamcr.2004.05.001

Deng, W., Marshall, N. C., Rowland, J. L., McCoy, J. M., Worrall, L. J., Santos, A. S., et al. (2017). Assembly, structure, function and regulation of type III secretion systems. *Nat. Rev. Microbiol.* 15, 323–337. doi: 10.1038/nrmicro.2017.20

Desvaux, M., Hebraud, M., Talon, R., and Henderson, I. R. (2009). Secretion and subcellular localizations of bacterial proteins: a semantic awareness issue. *Trends Microbiol.* 17, 139–145. doi: 10.1016/j.tim.2009.01.004

Dong, T. G., and Mekalanos, J. J. (2012). Characterization of the RpoN regulon reveals differential regulation of T6SS and new flagellar operons in *Vibrio cholerae* O37 strain V52. *Nucleic Acids Res.* 40, 7766–7775. doi: 10.1093/nar/gks567

Dong, Y. H., Wang, L. Y., and Zhang, L. H. (2007). Quorum-quenching microbial infections: mechanisms and implications. *Philos. Trans. R. Soc. Lond. B Biol. Sci.* 362, 1201–1211. doi: 10.1098/rstb.2007.2045

Engebrecht, J., Nealson, K., and Silverman, M. (1983). Bacterial bioluminescence: isolation and genetic analysis of functions from *Vibrio fischeri*. *Cell* 32, 773–781. doi: 10.1016/0092-8674(83)90063-6

Engebrecht, J., and Silverman, M. (1984). Identification of genes and gene products necessary for bacterial bioluminescence. *Proc. Natl. Acad. Sci. U.S.A.* 81, 4154–4158. doi: 10.1073/pnas.81.13.4154

Faure, L. M., Garvis, S., de Bentzmann, S., and Bigot, S. (2014). Characterization of a novel two-partner secretion system implicated in the virulence of *Pseudomonas aeruginosa*. *Microbiology* 160(Pt 9), 1940–1952. doi: 10.1099/mic.0.079616-0

Filloux, A., Michel, G., and Bally, M. (1998). GSP-dependent protein secretion in gram-negative bacteria: the Xcp system of *Pseudomonas aeruginosa*. *FEMS Microbiol. Rev.* 22, 177–198. doi: 10.1111/j.1574-6976.1998.tb00366.x

Flavier, A. B., Clough, S. J., Schell, M. A., and Denny, T. P. (1997). Identification of 3-hydroxypalmitic acid methyl ester as a novel autoregulator controlling virulence in *Ralstonia solanacearum*. *Mol. Microbiol.* 26, 251–259. doi: 10.1046/j.1365-2958.1997.5661945.x

Freeman, J. A., Lilley, B. N., and Bassler, B. L. (2000). A genetic analysis of the functions of LuxN: a two-component hybrid sensor kinase that regulates quorum sensing in *Vibrio harveyi*. *Mol. Microbil.* 35, 139–149. doi: 10.1046/j.1365-2958.2000.01684.x

Fuqua, W. C., Winans, S. C., and Greenberg, E. P. (1994). Quorum sensing in bacteria: the LuxR-LuxI family of cell density-responsive transcriptional regulators. *J. Bacteriol.* 176, 269–275. doi: 10.1128/jb.176.2.269-275.1994

Galan, J. E., and Waksman, G. (2018). Protein-injection machines in bacteria. *Cell* 172, 1306–1318. doi: 10.1016/j.cell.2018.01.034

Gallique, M., Bouteiller, M., and Merieau, A. (2017a). The type VI secretion system: a dynamic system for bacterial communication? *Front. Microbiol.* 8:1454. doi: 10.3389/fmicb.2017.01454

Gallique, M., Decoin, V., Barbey, C., Rosay, T., Feuilloley, M. G., Orange, N., et al. (2017b). Contribution of the *Pseudomonas fluorescens* MFE01 type VI secretion system to biofilm formation. *PLoS One* 12:e0170770. doi: 10.1371/journal.pone.0170770

Garde, C., Bjarnsholt, T., Givskov, M., Jakobsen, T. H., Hentzer, M., Claussen, A., et al. (2010). Quorum sensing regulation in *Aeromonas hydrophila*. *J. Mol. Biol.* 396, 849–857. doi: 10.1016/j.jmb.2010.01.002

Gaytan, M. O., Martinez-Santos, V. I., Soto, E., and Gonzalez-Pedrajo, B. (2016). Type three secretion system in attaching and effacing pathogens. *Front. Cell. Infect. Microbiol.* 6:129. doi: 10.3389/fcimb.2016.00129

Geske, G. D., O'Neill, J. C., and Blackwell, H. E. (2008). Expanding dialogues: from natural autoinducers to non-natural analogues that modulate quorum sensing in Gram-negative bacteria. *Chem. Soc. Rev.* 37, 1432–1447. doi: 10.1039/b703021p

Gode-Potratz, C. J., and McCarter, L. L. (2011). Quorum sensing and silencing in *Vibrio parahaemolyticus*. *J. Bacteriol.* 193, 4224–4237. doi: 10.1128/JB.00432-11

Green, E. R., and Mecsas, J. (2016). Bacterial secretion systems: an overview. *Microbiol. Spectr.* 4. doi: 10.1128/microbiolspec.VMBF-0012-2015

Grohmann, E., Christie, P. J., Waksman, G., and Backert, S. (2018). Type IV secretion in Gram-negative and Gram-positive bacteria. *Mol. Microbiol.* 107, 455–471. doi: 10.1111/mmi.13896

Hall-Stoodley, L., Keevil, C. W., and Lappin-Scott, H. M. (1998). *Mycobacterium fortuitum* and *Mycobacterium chelonae* biofilm formation under high and low nutrient conditions. *J. Appl. Microbiol.* 85(Suppl. 1), 60s–69s. doi: 10.1111/j.1365-2672.1998.tb05284.x

Han, S. W., Sriariyanun, M., Lee, S. W., Sharma, M., Bahar, O., Bower, Z., et al. (2011). Small protein-mediated quorum sensing in a Gram-negative bacterium. *PLoS One* 6:e29192. doi: 10.1371/journal.pone.0029192

Harms, A., Maisonneuve, E., and Gerdes, K. (2016). Mechanisms of bacterial persistence during stress and antibiotic exposure. *Science* 354:aaf4268. doi: 10.1126/science.aaf4268

Hauryliuk, V., Atkinson, G. C., Murakami, K. S., Tenson, T., and Gerdes, K. (2015). Recent functional insights into the role of (p)ppGpp in bacterial physiology. *Nat. Rev. Microbiol.* 13, 298–309. doi: 10.1038/nrmicro3448

Hawver, L. A., Jung, S. A., and Ng, W. L. (2016). Specificity and complexity in bacterial quorum-sensing systems. *FEMS Microbiol. Rev.* 40, 738–752. doi: 10.1093/femsre/fuw014

Henderson, I. R., Navarro-Garcia, F., Desvaux, M., Fernandez, R. C., and Ala'Aldeen, D. (2004). Type V protein secretion pathway: the autotransporter story. *Microbiol. Mol. Biol. Rev.* 68, 692–744. doi: 10.1128/MMBR.68.4.692-744.2004

Henke, J. M., and Bassler, B. L. (2004). Quorum sensing regulates type III secretion in *Vibrio harveyi* and *Vibrio parahaemolyticus*. *J. Bacteriol.* 186, 3794–3805. doi: 10.1128/JB.186.12.3794-3805.2004

Hentzer, M., Wu, H., Andersen, J. B., Riedel, K., Rasmussen, T. B., Bagge, N., et al. (2003). Attenuation of *Pseudomonas aeruginosa* virulence by quorum sensing inhibitors. *EMBO J.* 22, 3803–3815. doi: 10.1093/emboj/cdg366

Higgins, D. A., Pomianek, M. E., Kraml, C. M., Taylor, R. K., Semmelhack, M. F., and Bassler, B. L. (2007). The major *Vibrio cholerae* autoinducer and its role in virulence factor production. *Nature* 450, 883–886. doi: 10.1038/nature06284

Hirakawa, H., Kodama, T., Takumi-Kobayashi, A., Honda, T., and Yamaguchi, A. (2009). Secreted indole serves as a signal for expression of type III secretion system translocators in enterohaemorrhagic *Escherichia coli* O157:H7. *Microbiology* 155(Pt 2), 541–550. doi: 10.1099/mic.0.020420-0

Ho, B. T., Dong, T. G., and Mekalanos, J. J. (2014). A view to a kill: the bacterial type VI secretion system. *Cell Host Microbe* 15, 9–21. doi: 10.1016/j.chom.2013.11.008

Hodgkinson, J. T., Gross, J., Baker, Y. R., Spring, D. R., and Welch, M. (2016). A new *Pseudomonas* quinolone signal (PQS) binding partner: MexG. *Chem. Sci.* 7, 2553–2562. doi: 10.1039/c5sc04197j

Hogardt, M., Roeder, M., Schreff, A. M., Eberl, L., and Heesemann, J. (2004). Expression of *Pseudomonas aeruginosa exoS* is controlled by quorum sensing and RpoS. *Microbiology* 150(Pt 4), 843–851. doi: 10.1099/mic.0.26703-0

Holden, M. T., Seth-Smith, H. M., Crossman, L. C., Sebaihia, M., Bentley, S. D., Cerdeno-Tarraga, A. M., et al. (2009). The genome of *Burkholderia cenocepacia* J2315, an epidemic pathogen of cystic fibrosis patients. *J. Bacteriol.* 191, 261–277. doi: 10.1128/JB.01230-08

Ishikawa, T., Rompikuntal, P. K., Lindmark, B., Milton, D. L., and Wai, S. N. (2009). Quorum sensing regulation of the two *hcp* alleles in *Vibrio cholerae* O1 strains. *PLoS One* 4:e6734. doi: 10.1371/journal.pone.0006734

Izore, T., Job, V., and Dessen, A. (2011). Biogenesis, regulation, and targeting of the type III secretion system. *Structure* 19, 603–612. doi: 10.1016/j.str.2011.03.015

Jaskólska, M., Stutzmann, S., Stoudmann, C., and Blokesch, M. (2018). QstR-dependent regulation of natural competence and type VI secretion in *Vibrio cholerae*. *Nucleic Acids Res.* 46, 10619–10634. doi: 10.1093/nar/gky717

Javaux, C., Joris, B., and De Witte, P. (2007). Functional characteristics of TauA binding protein from TauABC *Escherichia coli* system. *Protein J.* 26, 231–238. doi: 10.1007/s10930-006-9064-x

Jimenez, P. N., Koch, G., Thompson, J. A., Xavier, K. B., Cool, R. H., and Quax, W. J. (2012). The multiple signaling systems regulating virulence in *Pseudomonas aeruginosa*. *Microbiol. Mol. Biol. Rev.* 76, 46–65. doi: 10.1128/MMBR.05007-11

Johansen, T. B., Agdestein, A., Olsen, I., Nilsen, S. F., Holstad, G., and Djonne, B. (2009). Biofilm formation by *Mycobacterium avium* isolates originating from humans, swine and birds. *BMC Microbiol.* 9:159. doi: 10.1186/1471-2180-9-159

Johnson, T. L., Fong, J. C., Rule, C., Rogers, A., Yildiz, F. H., and Sandkvist, M. (2014). The Type II secretion system delivers matrix proteins for biofilm formation by *Vibrio cholerae*. *J. Bacteriol.* 196, 4245–4252. doi: 10.1128/JB.01944-14

Jung, S. A., Chapman, C. A., and Ng, W. L. (2015). Quadruple quorum-sensing inputs control *Vibrio cholerae* virulence and maintain system robustness. *PLoS Pathog.* 11:e1004837. doi: 10.1371/journal.ppat.1004837

Kanamaru, K., Tatsuno, I., Tobe, T., and Sasakawa, C. (2000). SdiA, an *Escherichia coli* homologue of quorum-sensing regulators, controls the expression of virulence factors in enterohaemorrhagic *Escherichia coli* O157:H7. *Mol. Microbiol.* 38, 805–816. doi: 10.1046/j.1365-2958.2000.02171.x

Kanonenberg, K., Schwarz, C. K., and Schmitt, L. (2013). Type I secretion systems - a story of appendices. *Res. Microbiol.* 164, 596–604. doi: 10.1016/j.resmic.2013.03.011

Kariminik, A., Baseri-Salehi, M., and Kheirkhah, B. (2017). *Pseudomonas aeruginosa* quorum sensing modulates immune responses: an updated review article. *Immunol. Lett.* 190, 1–6. doi: 10.1016/j.imlet.2017.07.002

Khajanchi, B. K., Sha, J., Kozlova, E. V., Erova, T. E., Suarez, G., Sierra, J. C., et al. (2009). N-acylhomoserine lactones involved in quorum sensing control the type VI secretion system, biofilm formation, protease production, and in vivo virulence in a clinical isolate of *Aeromonas hydrophila*. *Microbiology* 155(Pt 11), 3518–3531. doi: 10.1099/mic.0.031575-0

Kida, Y., Higashimoto, Y., Inoue, H., Shimizu, T., and Kuwano, K. (2008). A novel secreted protease from *Pseudomonas aeruginosa* activates NF-kappaB through protease-activated receptors. *Cell Microbiol.* 10, 1491–1504. doi: 10.1111/j.1462-5822.2008.01142.x

Kita, D., Shibata, S., Kikuchi, Y., Kokubu, E., Nakayama, K., Saito, A., et al. (2016). Involvement of the type IX secretion system in *Capnocytophaga ochracea* gliding motility and biofilm formation. *Appl. Environ. Microbiol.* 82, 1756–1766. doi: 10.1128/AEM.03452-15

Kitaoka, M., Miyata, S. T., Brooks, T. M., Unterweger, D., and Pukatzki, S. (2011). VasH is a transcriptional regulator of the type VI secretion system functional in endemic and pandemic *Vibrio cholerae*. *J. Bacteriol.* 193, 6471–6482. doi: 10.1128/JB.05414-11

Kong, W., Liang, H., Shen, L., and Duan, K. (2009). [Regulation of type III secretion system by Rhl and PQS quorum sensing systems in *Pseudomonas aeruginosa*]. *Wei Sheng Wu Xue Bao* 49, 1158–1164.

Korotkov, K. V., Sandkvist, M., and Hol, W. G. (2012). The type II secretion system: biogenesis, molecular architecture and mechanism. *Nat. Rev. Microbiol.* 10, 336–351. doi: 10.1038/nrmicro2762

Korshunov, S., and Imlay, J. A. (2010). Two sources of endogenous hydrogen peroxide in *Escherichia coli*. *Mol. Microbiol.* 75, 1389–1401. doi: 10.1111/j.1365-2958.2010.07059.x

Kulka, K., Hatfull, G., and Ojha, A. K. (2012). Growth of *Mycobacterium tuberculosis* biofilms. *J. Vis. Exp.* 60:3820. doi: 10.3791/3820

Lai, L. Y., Lin, T. L., Chen, Y. Y., Hsieh, P. F., and Wang, J. T. (2018). Role of the *Mycobacterium marinum* ESX-1 secretion system in sliding motility and biofilm formation. *Front. Microbiol.* 9:1160. doi: 10.3389/fmicb.2018.01160

Lara-Tejero, M., and Galan, J. E. (2019). The injectisome, a complex nanomachine for protein injection into mammalian cells. *Ecosal Plus* 8. doi: 10.1128/ecosalplus.ESP-0039-2018

Lasica, A. M., Ksiazek, M., Madej, M., and Potempa, J. (2017). The type IX secretion system (T9SS): highlights and recent insights into its structure and function. *Front. Cell. Infect. Microbiol.* 7:215. doi: 10.3389/fcimb.2017.00215

Lee, J., Bansal, T., Jayaraman, A., Bentley, W. E., and Wood, T. K. (2007). Enterohemorrhagic *Escherichia coli* biofilms are inhibited by 7-hydroxyindole and stimulated by isatin. *Appl. Environ. Microbiol.* 73, 4100–4109. doi: 10.1128/AEM.00360-07

Lee, J., Zhang, X-S., Hegde, M., Bentley, W. E., Jayaraman, A., and Wood, T. K. (2008). Indole cell signaling occurs primarily at low temperatures in *Escherichia coli*. *ISME J.* 2, 1007–1023. doi: 10.1038/ismej.2008.54

Lee, J. H., and Lee, J. (2010). Indole as an intercellular signal in microbial communities. *FEMS Microbiol. Rev.* 34, 426–444. doi: 10.1111/j.1574-6976.2009.00204.x

Lee, S. W., Han, S. W., Bartley, L. E., and Ronald, P. C. (2006). From the academy: colloquium review. Unique characteristics of *Xanthomonas oryzae* pv. *oryzae* AvrXa21 and implications for plant innate immunity. *Proc. Natl. Acad. Sci. U.S.A.* 103, 18395–18400. doi: 10.1073/pnas.0605508103

Leiman, P. G., Basler, M., Ramagopal, U. A., Bonanno, J. B., Sauder, J. M., Pukatzki, S., et al. (2009). Type VI secretion apparatus and phage tail-associated protein complexes share a common evolutionary origin. *Proc. Natl. Acad. Sci. U.S.A.* 106, 4154–4159. doi: 10.1073/pnas.0813360106

Lenz, D. H., Mok, K. C., Lilley, B. N., Kulkarni, R. V., Wingreen, N. S., and Bassler, B. L. (2004). The small RNA chaperone Hfq and multiple small RNAs control quorum sensing in *Vibrio harveyi* and *Vibrio cholerae*. *Cell* 118, 69–82. doi: 10.1016/j.cell.2004.06.009

Leo, J. C., Grin, I., and Linke, D. (2012). Type V secretion: mechanism(s) of autotransport through the bacterial outer membrane. *Philos. Trans. R. Soc. Lond. B Biol. Sci.* 367, 1088–1101. doi: 10.1098/rstb.2011.0208

Lesic, B., Starkey, M., He, J., Hazan, R., and Rahme, L. G. (2009). Quorum sensing differentially regulates *Pseudomonas aeruginosa* type VI secretion locus I and homologous loci II and III, which are required for pathogenesis. *Microbiology* 155(Pt 9), 2845–2855. doi: 10.1099/mic.0.029082-0

Leung, K. Y., Siame, B. A., Snowball, H., and Mok, Y. K. (2011). Type VI secretion regulation: crosstalk and intracellular communication. *Curr. Opin. Microbiol.* 14, 9–15. doi: 10.1016/j.mib.2010.09.017

Li, P., Tian, M., Bao, Y., Hu, H., Liu, J., Yin, Y., et al. (2017). *Brucella* rough mutant induce macrophage death via activating IRE1alpha pathway of endoplasmic reticulum stress by enhanced T4SS secretion. *Front. Cell. Infect. Microbiol.* 7:422. doi: 10.3389/fcimb.2017.00422

Liang, H., Deng, X., Li, X., Ye, Y., and Wu, M. (2014). Molecular mechanisms of master regulator VqsM mediating quorum-sensing and antibiotic resistance in *Pseudomonas aeruginosa*. *Nucleic Acids Res.* 42, 10307–10320. doi: 10.1093/nar/gku586

Liang, W., Pascual-Montano, A., Silva, A. J., and Benitez, J. A. (2007). The cyclic AMP receptor protein modulates quorum sensing, motility and multiple genes that affect intestinal colonization in *Vibrio cholerae*. *Microbiology* 153(Pt 9), 2964–2975. doi: 10.1099/mic.0.2007/006668-0

Lin, J., Zhang, W., Cheng, J., Yang, X., Zhu, K., Wang, Y., et al. (2017). A *Pseudomonas* T6SS effector recruits PQS-containing outer membrane vesicles for iron acquisition. *Nat. Commun.* 8:14888. doi: 10.1038/ncomms14888

Liu, H., Wang, Q., Liu, Q., Cao, X., Shi, C., and Zhang, Y. (2011). Roles of Hfq in the stress adaptation and virulence in fish pathogen *Vibrio alginolyticus* and its potential application as a target for live attenuated vaccine. *Appl. Microbiol. Biotechnol.* 91, 353–364. doi: 10.1007/s00253-011-3286-3

Lo Scrudato, M., and Blokesch, M. (2012). The regulatory network of natural competence and transformation of *Vibrio cholerae*. *PLoS Genet.* 8:e1002778. doi: 10.1371/journal.pgen.1002778

Lo Scrudato, M., and Blokesch, M. (2013). A transcriptional regulator linking quorum sensing and chitin induction to render *Vibrio cholerae* naturally transformable. *Nucleic Acids Res.* 41, 3644–3658. doi: 10.1093/nar/gkt041

Lopez, M., Blasco, L., Gato, E., Perez, A., Fernandez-Garcia, L., Martinez-Martinez, L., et al. (2017a). Response to bile salts in clinical strains of *Acinetobacter baumannii* lacking the AdeABC efflux pump: virulence associated with quorum sensing. *Front. Cell. Infect. Microbiol.* 7:143. doi: 10.3389/fcimb.2017.00143

Lopez, M., Mayer, C., Fernandez-Garcia, L., Blasco, L., Muras, A., Ruiz, F. M., et al. (2017b). Quorum sensing network in clinical strains of *A. baumannii*: aidA is a new quorum quenching enzyme. *PLoS One* 12:e0174454. doi: 10.1371/journal.pone.0174454

Lopez, M. S., Tan, I. S., Yan, D., Kang, J., McCreary, M., Modrusan, Z., et al. (2017c). Host-derived fatty acids activate type VII secretion in *Staphylococcus aureus*. *Proc. Natl. Acad. Sci. U.S.A.* 114, 11223–11228. doi: 10.1073/pnas.1700627114

Lopez, M., Rueda, A., Florido, J. P., Blasco, L., Fernandez-Garcia, L., Trastoy, R., et al. (2018). Evolution of the Quorum network and the mobilome (plasmids and bacteriophages) in clinical strains of *Acinetobacter baumannii* during a decade. *Sci. Rep.* 8:2523. doi: 10.1038/s41598-018-20847-7

Majerczyk, C., Schneider, E., and Greenberg, E. P. (2016). Quorum sensing control of Type VI secretion factors restricts the proliferation of quorum-sensing mutants. *eLife* 5:e14712. doi: 10.7554/eLife.14712

Marsollier, L., Brodin, P., Jackson, M., Kordulakova, J., Tafelmeyer, P., Carbonnelle, E., et al. (2007). Impact of *Mycobacterium ulcerans* biofilm on transmissibility to ecological niches and Buruli ulcer pathogenesis. *PLoS Pathog.* 3:e62. doi: 10.1371/journal.ppat.0030062

Matz, C., Moreno, A. M., Alhede, M., Manefield, M., Hauser, A. R., Givskov, M., et al. (2008). *Pseudomonas aeruginosa* uses type III secretion system to kill biofilm-associated amoebae. *ISME J.* 2, 843–852. doi: 10.1038/ismej.2008.47

Maura, D., Hazan, R., Kitao, T., Ballok, A. E., and Rahme, L. G. (2016). Evidence for direct control of virulence and defense gene circuits by the *Pseudomonas*

aeruginosa quorum sensing regulator, MvfR. *Sci. Rep.* 6:34083. doi: 10.1038/srep34083

McBride, M. J., and Zhu, Y. (2013). Gliding motility and Por secretion system genes are widespread among members of the phylum bacteroidetes. *J. Bacteriol.* 195, 270–278. doi: 10.1128/JB.01962-12

Michel, G. P., Aguzzi, A., Ball, G., Soscia, C., Bleves, S., and Voulhoux, R. (2011). Role of fimV in type II secretion system-dependent protein secretion of *Pseudomonas aeruginosa* on solid medium. *Microbiology* 157(Pt 7), 1945–1954. doi: 10.1099/mic.0.045849-0

Michel, G. P., Durand, E., and Filloux, A. (2007). XphA/XqhA, a novel GspCD subunit for type II secretion in *Pseudomonas aeruginosa*. *J. Bacteriol.* 189, 3776–3783. doi: 10.1128/JB.00205-07

Miller, M. B., Skorupski, K., Lenz, D. H., Taylor, R. K., and Bassler, B. L. (2002). Parallel quorum sensing systems converge to regulate virulence in *Vibrio cholerae*. *Cell* 110, 303–314. doi: 10.1016/S0092-8674(02)00829-2

Milton, D. L. (2006). Quorum sensing in vibrios: complexity for diversification. *Int. J. Med. Microbiol.* 296, 61–71. doi: 10.1016/j.ijmm.2006.01.044

Nagai, H., and Kubori, T. (2011). Type IVB secretion systems of *Legionella* and other gram-negative bacteria. *Front. Microbiol.* 2:136. doi: 10.3389/fmicb.2011.00136

Nealson, K. H., Platt, T., and Hastings, J. W. (1970). Cellular control of the synthesis and activity of the bacterial luminescent system. *J. Bacteriol.* 104, 313–322.

Ng, W. L., and Bassler, B. L. (2009). Bacterial quorum-sensing network architectures. *Annu. Rev. Genet.* 43, 197–222. doi: 10.1146/annurev-genet-102108-134304

Nivaskumar, M., and Francetic, O. (2014). Type II secretion system: a magic beanstalk or a protein escalator. *Biochim. Biophys. Acta* 1843, 1568–1577. doi: 10.1016/j.bbamcr.2013.12.020

Notti, R. Q., and Stebbins, C. E. (2016). The structure and function of type III secretion systems. *Microbiol. Spectr.* 4. doi: 10.1128/microbiolspec.VMBF-0004-2015

Novick, R. P., and Geisinger, E. (2008). Quorum sensing in staphylococci. *Annu. Rev. Genet.* 42, 541–564. doi: 10.1146/annurev.genet.42.110807.091640

Ojha, A., Anand, M., Bhatt, A., Kremer, L., Jacobs, W. R. Jr., and Hatfull, G. F. (2005). GroEL1: a dedicated chaperone involved in mycolic acid biosynthesis during biofilm formation in mycobacteria. *Cell* 123, 861–873. doi: 10.1016/j.cell.2005.09.012

Overbye, L. J., Sandkvist, M., and Bagdasarian, M. (1993). Genes required for extracellular secretion of enterotoxin are clustered in *Vibrio cholerae*. *Gene* 132, 101–106. doi: 10.1016/0378-1119(93)90520-D

Patel, R., Smith, S. M., and Robinson, C. (2014). Protein transport by the bacterial Tat pathway. *Biochim. Biophys. Acta* 1843, 1620–1628. doi: 10.1016/j.bbamcr.2014.02.013

Patzelt, D., Michael, V., Pauker, O., Ebert, M., Tielen, P., Jahn, D., et al. (2016). Gene flow across genus barriers - conjugation of *Dinoroseobacter shibae*'s 191-kb killer plasmid into *Phaeobacter inhibens* and AHL-mediated expression of type IV secretion systems. *Front. Microbiol.* 7:742. doi: 10.3389/fmicb.2016.00742

Patzelt, D., Wang, H., Buchholz, I., Rohde, M., Grobe, L., Pradella, S., et al. (2013). You are what you talk: quorum sensing induces individual morphologies and cell division modes in *Dinoroseobacter shibae*. *ISME J.* 7, 2274–2286. doi: 10.1038/ismej.2013.107

Paul, D., Gopal, J., Kumar, M., and Manikandan, M. (2018). Nature to the natural rescue: silencing microbial chats. *Chem. Biol. Interact.* 280, 86–98. doi: 10.1016/j.cbi.2017.12.018

Pesci, E. C., Milbank, J. B., Pearson, J. P., McKnight, S., Kende, A. S., Greenberg, E. P., et al. (1999). Quinolone signaling in the cell-to-cell communication system of *Pseudomonas aeruginosa*. *Proc. Natl. Acad. Sci. U.S.A.* 96, 11229–11234. doi: 10.1073/pnas.96.20.11229

Pukatzki, S., Ma, A. T., Revel, A. T., Sturtevant, D., and Mekalanos, J. J. (2007). Type VI secretion system translocates a phage tail spike-like protein into target cells where it cross-links actin. *Proc. Natl. Acad. Sci. U.S.A.* 104, 15508–15513. doi: 10.1073/pnas.0706532104

Qian, G., Zhou, Y., Zhao, Y., Song, Z., Wang, S., Fan, J., et al. (2013). Proteomic analysis reveals novel extracellular virulence-associated proteins and functions regulated by the diffusible signal factor (DSF) in *Xanthomonas oryzae* pv. *oryzicola*. *J. Proteome Res.* 12, 3327–3341. doi: 10.1021/pr4001543

Rai, N., Rai, R., and Kareenhalli, V. (2015). "Quorum sensing in competence and sporulation", in *Quorum Sensing vs Quorum Qenching: A Battle with No End in Sight*, ed. K. Vipin Chandra (New Delhi: Springer), 61–64.

Rhoades, E. R., Archambault, A. S., Greendyke, R., Hsu, F. F., Streeter, C., and Byrd, T. F. (2009). *Mycobacterium abscessus* Glycopeptidolipids mask underlying cell wall phosphatidyl-myo-inositol mannosides blocking induction of human macrophage TNF-alpha by preventing interaction with TLR2. *J. Immunol.* 183, 1997–2007. doi: 10.4049/jimmunol.0802181

Riedel, K., Ohnesorg, T., Krogfelt, K. A., Hansen, T. S., Omori, K., Givskov, M., et al. (2001). N-acyl-L-homoserine lactone-mediated regulation of the lip secretion system in *Serratia liquefaciens* MG1. *J. Bacteriol.* 183, 1805–1809. doi: 10.1128/JB.183.5.1805-1809.2001

Robert, V., Filloux, A., and Michel, G. P. (2005). Subcomplexes from the Xcp secretion system of *Pseudomonas aeruginosa*. *FEMS Microbiol. Lett.* 252, 43–50. doi: 10.1016/j.femsle.2005.08.029

Rojas-Lopez, M., Zorgani, M. A., Kelley, L. A., Bailly, X., Kajava, A. V., Henderson, I. R., et al. (2017). Identification of the autochaperone domain in the type va secretion system (T5aSS): prevalent feature of autotransporters with a beta-helical passenger. *Front. Microbiol.* 8:2607. doi: 10.3389/fmicb.2017.02607

Ruer, S., Ball, G., Filloux, A., and de Bentzmann, S. (2008). The 'P-usher', a novel protein transporter involved in fimbrial assembly and TpsA secretion. *EMBO J.* 27, 2669–2680. doi: 10.1038/emboj.2008.197

Russell, A. B., Hood, R. D., Bui, N. K., LeRoux, M., Vollmer, W., and Mougous, J. D. (2011). Type VI secretion delivers bacteriolytic effectors to target cells. *Nature* 475, 343–347. doi: 10.1038/nature10244

Russell, A. B., Peterson, S. B., and Mougous, J. D. (2014). Type VI secretion system effectors: poisons with a purpose. *Nat. Rev. Microbiol.* 12, 137–148. doi: 10.1038/nrmicro3185

Ruwandeepika, H. A., Karunasagar, I., Bossier, P., and Defoirdt, T. (2015). Expression and quorum sensing regulation of type III secretion system genes of *Vibrio harveyi* during infection of gnotobiotic brine shrimp. *PLoS One* 10:e0143935. doi: 10.1371/journal.pone.0143935

Ryan, R. P., Monchy, S., Cardinale, M., Taghavi, S., Crossman, L., Avison, M. B., et al. (2009). The versatility and adaptation of bacteria from the genus *Stenotrophomonas*. *Nat. Rev. Microbiol.* 7, 514–525. doi: 10.1038/nrmicro2163

Sana, T. G., Hachani, A., Bucior, I., Soscia, C., Garvis, S., Termine, E., et al. (2012). The second type VI secretion system of *Pseudomonas aeruginosa* strain PAO1 is regulated by quorum sensing and Fur and modulates internalization in epithelial cells. *J. Biol. Chem.* 287, 27095–27105. doi: 10.1074/jbc.M112.376368

Sato, K., Naito, M., Yukitake, H., Hirakawa, H., Shoji, M., McBride, M. J., et al. (2010). A protein secretion system linked to bacteroidete gliding motility and pathogenesis. *Proc. Natl. Acad. Sci. U.S.A.* 107, 276–281. doi: 10.1073/pnas.0912010107

Schauder, S., Shokat, K., Surette, M. G., and Bassler, B. L. (2001). The LuxS family of bacterial autoinducers: biosynthesis of a novel quorum-sensing signal molecule. *Mol. Microbiol.* 41, 463–476. doi: 10.1046/j.1365-2958.2001.02532.x

Schiano, C. A., Koo, J. T., Schipma, M. J., Caulfield, A. J., Jafari, N., and Lathem, W. W. (2014). Genome-wide analysis of small RNAs expressed by *Yersinia pestis* identifies a regulator of the Yop-Ysc type III secretion system. *J. Bacteriol.* 196, 1659–1670. doi: 10.1128/JB.01456-13

Schulthess, B., Bloes, D. A., and Berger-Bachi, B. (2012). Opposing roles of sigmaB and sigmaB-controlled SpoVG in the global regulation of *esxA* in *Staphylococcus aureus*. *BMC Microbiol.* 12:17. doi: 10.1186/1471-2180-12-17

Schuster, M., Lostroh, C. P., Ogi, T., and Greenberg, E. P. (2003). Identification, timing, and signal specificity of *Pseudomonas aeruginosa* quorum-controlled genes: a transcriptome analysis. *J. Bacteriol.* 185, 2066–2079. doi: 10.1128/JB.185.7.2066-2079.2003

Seed, P. C., Passador, L., and Iglewski, B. H. (1995). Activation of the *Pseudomonas aeruginosa lasI* gene by LasR and the *Pseudomonas* autoinducer PAI: an autoinduction regulatory hierarchy. *J. Bacteriol.* 177, 654–659. doi: 10.1128/jb.177.3.654-659.1995

Shanker, E., and Federle, M. J. (2017). Quorum sensing regulation of competence and bacteriocins in *Streptococcus pneumoniae* and *mutans*. *Genes* 8:E15. doi: 10.3390/genes8010015

Shao, Y., and Bassler, B. L. (2014). Quorum regulatory small RNAs repress type VI secretion in *Vibrio cholerae*. *Mol. Microbiol.* 92, 921–930. doi: 10.1111/mmi.12599

Sharma, I. M., Petchiappan, A., and Chatterji, D. (2014). Quorum sensing and biofilm formation in mycobacteria: role of c-di-GMP and methods to study this second messenger. *IUBMB Life* 66, 823–834. doi: 10.1002/iub.1339

Sheng, L., Gu, D., Wang, Q., Liu, Q., and Zhang, Y. (2012). Quorum sensing and alternative sigma factor RpoN regulate type VI secretion system I (T6SSVA1) in fish pathogen *Vibrio alginolyticus*. *Arch. Microbiol.* 194, 379–390. doi: 10.1007/s00203-011-0780-z

Sheng, L., Lv, Y., Liu, Q., Wang, Q., and Zhang, Y. (2013). Connecting type VI secretion, quorum sensing, and c-di-GMP production in fish pathogen *Vibrio alginolyticus* through phosphatase PppA. *Vet. Microbiol.* 162, 652–662. doi: 10.1016/j.vetmic.2012.09.009

Sloup, R. E., Konal, A. E., Severin, G. B., Korir, M. L., Bagdasarian, M. M., Bagdasarian, M., et al. (2017). Cyclic Di-GMP and VpsR induce the expression of type II secretion in *Vibrio cholerae*. *J. Bacteriol.* 199:e00106-17. doi: 10.1128/JB.00106-17

Soto-Aceves, M. P., Cocotl-Yanez, M., Merino, E., Castillo-Juarez, I., Cortes-Lopez, H., Gonzalez-Pedrajo, B., et al. (2019). Inactivation of the quorum-sensing transcriptional regulators LasR or RhlR does not suppress the expression of virulence factors and the virulence of *Pseudomonas aeruginosa* PAO1. *Microbiology* 165, 425–432. doi: 10.1099/mic.0.000778

Sperandio, V., Mellies, J. L., Nguyen, W., Shin, S., and Kaper, J. B. (1999). Quorum sensing controls expression of the type III secretion gene transcription and protein secretion in enterohemorrhagic and enteropathogenic *Escherichia coli*. *Proc. Natl. Acad. Sci. U.S.A.* 96, 15196–15201. doi: 10.1073/pnas.96.26.15196

Stanley, S. A., Raghavan, S., Hwang, W. W., and Cox, J. S. (2003). Acute infection and macrophage subversion by *Mycobacterium tuberculosis* require a specialized secretion system. *Proc. Natl. Acad. Sci. U.S.A.* 100, 13001–13006. doi: 10.1073/pnas.2235593100

Stintzi, A., Evans, K., Meyer, J. M., and Poole, K. (1998). Quorum-sensing and siderophore biosynthesis in *Pseudomonas aeruginosa*: *lasR/lasI* mutants exhibit reduced pyoverdine biosynthesis. *FEMS Microbiol. Lett.* 166, 341–345. doi: 10.1111/j.1574-6968.1998.tb13910.x

Surette, M. G., Miller, M. B., and Bassler, B. L. (1999). Quorum sensing in *Escherichia coli*, *Salmonella typhimurium*, and *Vibrio harveyi*: a new family of genes responsible for autoinducer production. *Proc. Natl. Acad. Sci. U.S.A.* 96, 1639–1644. doi: 10.1073/pnas.96.4.1639

Teschler, J. K., Zamorano-Sanchez, D., Utada, A. S., Warner, C. J., Wong, G. C., Linington, R. G., et al. (2015). Living in the matrix: assembly and control of *Vibrio cholerae* biofilms. *Nat. Rev. Microbiol.* 13, 255–268. doi: 10.1038/nrmicro3433

Thomas, S., Holland, I. B., and Schmitt, L. (2014). The Type 1 secretion pathway - the hemolysin system and beyond. *Biochim. Biophys. Acta* 1843, 1629–1641. doi: 10.1016/j.bbamcr.2013.09.017

Trastoy, R., Manso, T., Fernandez-Garcia, L., Blasco, L., Ambroa, A., Perez Del Molino, M. L., et al. (2018). Mechanisms of bacterial tolerance and persistence in the gastrointestinal and respiratory environments. *Clin. Microbiol. Rev.* 31:e00023-18. doi: 10.1128/CMR.00023-18

Tseng, T.-T., Tyler, B. M., and Setubal, J. C. (2009). Protein secretion systems in bacterial-host associations, and their description in the Gene Ontology. *BMC Microbiol.* 9:S2. doi: 10.1186/1471-2180-9-S1-S2

Tsirigotaki, A., De Geyter, J., Sostaric, N., Economou, A., and Karamanou, S. (2017). Protein export through the bacterial Sec pathway. *Nat. Rev. Microbiol.* 15, 21–36. doi: 10.1038/nrmicro.2016.161

Tsou, A. M., Cai, T., Liu, Z., Zhu, J., and Kulkarni, R. V. (2009). Regulatory targets of quorum sensing in *Vibrio cholerae*: evidence for two distinct HapR-binding motifs. *Nucleic Acids Res.* 37, 2747–2756. doi: 10.1093/nar/gkp121

Van den Bergh, B., Fauvart, M., and Michiels, J. (2017). Formation, physiology, ecology, evolution and clinical importance of bacterial persisters. *FEMS Microbiol. Rev.* 41, 219–251. doi: 10.1093/femsre/fux001

Vilches, S., Jimenez, N., Tomas, J. M., and Merino, S. (2009). *Aeromonas hydrophila* AH-3 type III secretion system expression and regulatory network. *Appl. Environ. Microbiol.* 75, 6382–6392. doi: 10.1128/AEM.00222-09

Virmani, R., Hasija, Y., and Singh, Y. (2018). Effect of homocysteine on biofilm formation by mycobacteria. *Indian J. Microbiol.* 58, 287–293. doi: 10.1007/s12088-018-0739-8

Wagner, V. E., Bushnell, D., Passador, L., Brooks, A. I., and Iglewski, B. H. (2003). Microarray analysis of *Pseudomonas aeruginosa* quorum-sensing regulons: effects of growth phase and environment. *J. Bacteriol.* 185, 2080–2095. doi: 10.1128/JB.185.7.2080-2095.2003

Waters, C. M., and Bassler, B. L. (2005). Quorum sensing: cell-to-cell communication in bacteria. *Annu. Rev. Cell Dev. Biol.* 21, 319–346. doi: 10.1146/annurev.cellbio.21.012704.131001

Waters, C. M., Wu, J. T., Ramsey, M. E., Harris, R. C., and Bassler, B. L. (2010). Control of the type 3 secretion system in *Vibrio harveyi* by quorum sensing through repression of ExsA. *Appl. Environ. Microbiol.* 76, 4996–5004. doi: 10.1128/AEM.00886-10

Watve, S. S., Thomas, J., and Hammer, B. K. (2015). CytR is a global positive regulator of competence, type VI secretion, and chitinases in *Vibrio cholerae*. *PLoS One* 10:e0138834. doi: 10.1371/journal.pone.0138834

Whiteley, M., Diggle, S. P., and Greenberg, E. P. (2017). Progress in and promise of bacterial quorum sensing research. *Nature* 551, 313–320. doi: 10.1038/nature24624

Wilhelm, S., Gdynia, A., Tielen, P., Rosenau, F., and Jaeger, K. E. (2007). The autotransporter esterase EstA of *Pseudomonas aeruginosa* is required for rhamnolipid production, cell motility, and biofilm formation. *J. Bacteriol.* 189, 6695–6703. doi: 10.1128/JB.00023-07

Wood, T. K., Knabelm, S. J., and Kwan, B. W. (2013). Bacterial persister cell formation and dormancy. *Appl. Environ. Microbiol.* 79, 7116–7121. doi: 10.1128/AEM.02636-13

Xiao, G., Déziel, E., He, J., Lépine, F., Lesic, B., Castonguay, M. H., et al. (2006). MvfR, a key *Pseudomonas aeruginosa* pathogenicity LTTR-class regulatory protein, has dual ligands. *Mol. Microbiol.* 62, 1689–1699. doi: 10.1111/j.1365-2958.2006.05462.x

Yang, Z., Zhou, X., Ma, Y., Zhou, M., Waldor, M. K., Zhang, Y., et al. (2018). Serine/threonine kinase PpkA coordinates the interplay between T6SS2 activation and quorum sensing in the marine pathogen *Vibrio alginolyticus*. *Environ. Microbiol.* 20, 903–919. doi: 10.1111/1462-2920.14039

Zhang, L. H., and Dong, Y. H. (2004). Quorum sensing and signal interference: diverse implications. *Mol. Microbiol.* 53, 1563–1571. doi: 10.1111/j.1365-2958.2004.04234.x

Zhang, Y., Sass, A., Van Acker, H., Wille, J., Verhasselt, B., Van Nieuwerburgh, F., et al. (2018). Coumarin reduces virulence and biofilm formation in *Pseudomonas aeruginosa* by affecting quorum sensing, type III secretion and C-di-GMP levels. *Front. Microbiol.* 9:1952. doi: 10.3389/fmicb.2018.01952

Zhao, X., and Drlica, K. (2014). Reactive oxygen species and the bacterial response to lethal stress. *Curr. Opin. Microbiol.* 21, 1-6. doi: 10.1016/j.mib.2014.06.008

Zheng, J., Shin, O. S., Cameron, D. E., and Mekalanos, J. J. (2010). Quorum sensing and a global regulator TsrA control expression of type VI secretion and virulence in *Vibrio cholerae*. *Proc. Natl. Acad. Sci. U.S.A.* 107, 21128–21133. doi: 10.1073/pnas.1014998107

Zoued, A., Brunet, Y. R., Durand, E., Aschtgen, M. S., Logger, L., Douzi, B., et al. (2014). Architecture and assembly of the Type VI secretion system. *Biochim. Biophys. Acta* 1843, 1664–1673. doi: 10.1016/j.bbamcr.2014.03.018

Conflict of Interest Statement: The authors declare that the research was conducted in the absence of any commercial or financial relationships that could be construed as a potential conflict of interest.

frontiers in Microbiology

ORIGINAL RESEARCH
published: 07 June 2019
doi: 10.3389/fmicb.2019.01246

Elucidating the Hot Spot Residues of Quorum Sensing Peptidic Autoinducer PapR by Multiple Amino Acid Replacements

*Avishag Yehuda[1], Leyla Slamti[2], Einav Malach[1], Didier Lereclus[2] and Zvi Hayouka[1]**

[1] Institute of Biochemistry, Food Science and Nutrition, The Hebrew University of Jerusalem, Rehovot, Israel, [2] Micalis Institute, INRA, AgroParisTech, Université Paris-Saclay, Jouy-en-Josas, France

The quorum sensing (QS) system of *Bacillus cereus,* an opportunistic human pathogen, utilizes the autoinducing PapR peptide signal that mediates the activation of the pleiotropic virulence regulator PlcR. A set of synthetic 7-mer PapR-derived peptides ($PapR_7$; ADLPFEF) have been shown to inhibit efficiently the PlcR regulon activity and the production of virulence factors, reflected by a loss in hemolytic activity without affecting bacterial growth. Interestingly, these first potent synthetic inhibitors involved D-amino acid or alanine replacements of three amino acids; proline, glutamic acid, and phenylalanine of the heptapeptide PapR. To better understand the role of these three positions in PlcR activity, we report herein the second generation design, synthesis, and characterization of $PapR_7$-derived combinations, alternate double and triple alanine and D-amino acids replacement at these positions. Our findings generate a new set of non-native $PapR_7$-derived peptides that inhibit the PlcR regulon activity and the production of virulence factors. Using the amino acids substitution strategy, we revealed the role of proline and glutamic acid on PlcR regulon activation. Moreover, we demonstrated that the D-Glutamic acid substitution was crucial for the design of stronger PlcR antagonists. These peptides represent potent synthetic inhibitors of *B. cereus* QS and constitute new and readily accessible chemical tools for the study of the PlcR system. Our method might be applied to other quorum sensing systems to design new anti-virulence agents.

Keywords: quorum sensing, quorum quenching, PlcR antagonists, *B. cereus* group, anti-virulence peptides

OPEN ACCESS

Edited by:
Tom Defoirdt,
Ghent University, Belgium

Reviewed by:
Evelien Wynendaele,
Ghent University, Belgium
Johann Mignolet,
Catholic University of Louvain, Belgium

****Correspondence:***
Zvi Hayouka
zvi.hayouka@mail.huji.ac.il

Specialty section:
This article was submitted to Infectious Diseases, a section of the journal Frontiers in Microbiology

Received: *12 March 2019*
Accepted: *20 May 2019*
Published: *07 June 2019*

Citation:
Yehuda A, Slamti L, Malach E, Lereclus D and Hayouka Z (2019) Elucidating the Hot Spot Residues of Quorum Sensing Peptidic Autoinducer PapR by Multiple Amino Acid Replacements. Front. Microbiol. 10:1246. doi: 10.3389/fmicb.2019.01246

INTRODUCTION

Quorum sensing (QS) is a cell-cell communication mechanism used to coordinate bacterial group behaviors (conjugation, virulence, sporulation, or competence) by assessing cell density through the production, secretion, and detection of small signaling molecules (Dunny and Leonard, 1997; Miller and Bassler, 2001; Slamti et al., 2014). Gram-negative bacteria appear to predominantly respond to *N*-acyl homoserine lactones, while QS in Gram-positive species mainly relies on the secretion of auto-inducing oligopeptides to bind and activate their cognate quorum sensors. In the past decade, a rapid increase of interest in bacterial quorum sensing peptides (QSPs) has emerged. Therefore, new QSPs databases are being established to provide chemical structures overview, microbial origin

and functionality responses of these QS-derived signaling peptides (Gray et al., 2013; Wynendaele et al., 2013; Rajput et al., 2016).

The QSPs binding to their cognate quorum sensors occurs either on the outside of the bacterium (by interacting with a sensor in the membrane) or in the cytoplasm of the bacterial cell. In the latter case, the quorum-sensing regulators are controlled by direct interaction with a internalized signaling peptide (Dunny and Leonard, 1997; Lazazzera et al., 1997; Gominet et al., 2001; Miller and Bassler, 2001). They have been grouped in a new family of quorum sensors termed Rap-Rgg-NprR-PrgX-PlcR (RRNPP; Declerck et al., 2007; Neiditch et al., 2017). These quorum sensors are characterized by the presence of structural tetratricopeptide repeats (TPRs) forming a peptide binding domain (Blatch and Lässle, 1999), and a helix-turn-helix (HTH) DNA-binding domain (Wintjens and Rooman, 1996) in the case of transcriptional regulators. The PrgX – cCF10 system regulates conjugation in *Enterococcus faecalis* (Suzuki et al., 1984; Shi et al., 2005), the Rap phosphatases-Phr peptides system control competence and sporulation in *Bacillus subtilis* (Lazazzera et al., 1997; Perego and Brannigan, 2001; Perego, 2013), the transcriptional regulator/peptide pairs PlcR – PapR and NprR – NprX of the *Bacillus cereus* group are required for virulence and necrotrophism gene expression, respectively (Slamti and Lereclus, 2002; Perchat et al., 2011; Dubois et al., 2012; Grenha et al., 2013) and the archetype transcriptional regulator of the Rgg family, namely ComR that controls competence in most mutans, suis, pyogenes, bovis and salivarius *streptococci* (Mashburn-Warren et al., 2010; Fontaine et al., 2015) and predation in *S. salivarius* (Mignolet et al., 2018). The last discovered RRNPP transcriptional regulators are the PlcRa that activate the oxidative stress response and cysteine metabolism in transition state cells in *B. cereus* (Huillet et al., 2012) and aimR, which coordinates viruses of SPbeta group lysis-lysogeny decisions during infection of its *Bacillus* host cell (Erez et al., 2017).

The RRNPP family has an important role in adaptive and virulence processes in several bacteria (Slamti et al., 2014; Neiditch et al., 2017). This clearly identifies these regulators as major targets for the search of novel strategies against bacterial infections beyond conventional treatments. Antimicrobial therapy based on quorum quenching (QQ) can interfere or block all the processes involved in quorum sensing (Amara et al., 2011; Kalia, 2013; Grandclément et al., 2015). In contrast to antibiotics or antimicrobial agents, which aim at killing bacteria or inhibiting their growth, blocking cell-to-cell signaling mechanism, could attenuate bacterial pathogenicity without imposing the level of selective pressure on a bacterial population to develop resistance (Suga and Smith, 2003; Rasmussen and Givskov, 2006). A wide range of promising molecules have been already identified to inhibit QS-controlled virulence genes in Gram-negative bacteria (Hentzer et al., 2003; Galloway et al., 2012). On the other hand, except for strategies that have been investigated to inhibit the two component QS system Agr of *Staphylococcus*, which uses a peptide-thiolactone as the extracellular signal, the design of molecules modulating QS systems in Gram-positive bacteria has been poorly explored (Fontaine et al., 2010; Zheng et al., 2011; Tal-Gan et al., 2013a, 2014, 2016; Sully et al., 2014).

Bacillus cereus is a human opportunistic, Gram-positive spore-forming bacterial pathogen belonging to the *B. cereus* group (Stenfors Arnesen et al., 2008). This group comprises a number of highly phenotypically and genetically indistinguishable related species, including *Bacillus thuringiensis*, an insect pathogen, and *Bacillus anthracis*, the aetiological agent of anthrax (Helgason et al., 2000). The widespread presence of *B. thuringiensis* and *B. cereus* in soil and food, and their close relationship with *B. anthracis* make this group an important threat to public health (Rasko et al., 2005; Rossi et al., 2018), and a potential source of new pathogens. Indeed, *B. cereus* is generally regarded as a pathogen causing foodborne infections due to the production of enterotoxins such as Hbl and Nhe (Stenfors Arnesen et al., 2008), and nosocomial infections in an immuno-compromised patients (Granum and Lund, 1997; Kotiranta et al., 2000; Chu et al., 2001; Gaur et al., 2001; Bottone, 2010). *B. cereus* strains were also found to be responsible for severe infections resembling anthrax (Hoffmaster et al., 2004; Klee et al., 2006).

The QS system of *B. cereus* plays an important role in virulence (Agaisse et al., 1999; Gohar et al., 2008). *B. cereus* uses QS to establish infections by producing an arsenal of virulence factors, such as enterotoxins, pore-forming haemolysins, cytotoxins and various degradative enzymes (Granum and Lund, 1997; Vilas-Boas et al., 2002; Stenfors Arnesen et al., 2008; Ramarao and Sanchis, 2013). Production of most of these exported virulence factors is activated by PlcR, a 34 kDa protein that acts as a *B. cereus* group main virulence transcription factor (Lereclus et al., 1996; Agaisse et al., 1999; ØKstad et al., 1999; Gohar et al., 2008). Activity of PlcR depends on the binding of the signaling C-terminal heptapeptide $PapR_7$ (ADLPFEF) at the end of the exponential growth stage. $PapR_7$ is imported by the oligopeptide permease system (OppABCDF; Gominet et al., 2001), binds the tetratricopeptide repeat (TPR)-type regulatory domain of PlcR (Grenha et al., 2013) and promotes recognition of the PlcR box to transcriptional activation of the target genes (Lereclus et al., 1996; Gominet et al., 2001; Slamti and Lereclus, 2002; Bouillaut et al., 2008). This triggers a positive feedback loop that up-regulates the expression of *plcR*, *papR* and various virulence genes (Agaisse et al., 1999; Ivanova et al., 2003; Gohar et al., 2008).

The structural and molecular basis for the activation of PlcR by PapR has been the focus of several studies, which have revealed interesting insights on the PlcR – PapR interactions. The PlcR – PapR relationship has been shown to be strain specific; comparison of the amino acid sequences of PlcR and PapR from 29 different strains demonstrated the existence of four classes (I to IV) of PlcR – PapR pairs, defining four distinct pherotypes in the *B. cereus* group. While PapR sequences from different strains of the *B. cereus* group showed divergences in their three N-terminal residues, the PFEF core was more conserved (Slamti and Lereclus, 2005). In 2007, the crystal structure of the complex formed between the protein PlcR (from group I) and the C-terminal $PapR_5$ pentapeptide (LPFEF) was published (Declerck et al., 2007). According to RRNPP conserved features, each subunit of PlcR is formed of an N-terminal HTH DNA-binding domain, and a C-terminal regulatory domain

composed of five degenerated TPRs forming a peptide binding domain. Binding of PapR triggers an allosteric mechanism that leads to a drastic conformational change of the HTH domains upon the two half sites of the DNA binding site, known as PlcR-box. The LPFEF pentapeptide, $PapR_5$ was identified as the minimal peptide size required for PlcR activation (Slamti and Lereclus, 2002). However, the physiologically relevant heptapeptide $PapR_7$ displays a slightly better affinity for PlcR (Bouillaut et al., 2008; Grenha et al., 2013). In 2008, Bouillaut and co-workers established a molecular model for the complex formed between PlcR and the heptapeptide $PapR_7$ based on the crystal structure of $PapR_5$-bound PlcR (Declerck et al., 2007; Bouillaut et al., 2008). Structural analysis and directed mutagenesis of PlcR residues suggested that: a) activation of PlcR by $PapR_7$ is triggered by the hydrophobic interactions of the leucine, and two phenylalanines with helices 5 and 7 of the TPR-containing domain of PlcR b) the central proline residue may be required for the PapR peptides to fit into the binding groove on PlcR and c) the glutamic acid of the FEF $PapR_7$ core motif may function to selectively allow PapR to bind PlcR by ionic interactions with Lys87 and 89. In a follow up study in 2013, Grenha and co-workers, have determined the crystal structure of the ternary complex DNA-PlcR-$PapR_7$. It has been reported that both $PapR_7$ phenylalanine residues are located in hydrophobic pockets and the only specific interactions are made between the glutamate of $PapR_7$ and residues Lys89, Gln237, and Tyr275 of PlcR.

Binding of PapR to PlcR is essential to trigger QS-mediated functions in *B. cereus*. Thus, we recently studied the PlcR – PapR activation in *B. cereus* and *B. thuringiensis* at the molecular level. We designed, synthesized and characterized synthetic PapR 7-mer derived peptides to determine the contribution of each residue within PlcR – $PapR_7$ interactions. Our findings reveal the first set of non-native peptides that can repress the PlcR regulon and thus relevant virulence factors. Moreover, we could demonstrate that the repression is mediated by QS and regulation of PlcR expression without affecting bacterial growth (Yehuda et al., 2018). Interestingly, these first potent synthetic inhibitors involved D-amino acid or alanine replacements of either proline (P) glutamic acid (E) or phenylalanine (F) of the heptapeptide PapR (ADLPFEF). To better understand the role of these three crucial positions in PlcR activation, we report herein the second generation design, synthesis, and characterization of $PapR_7$-derived combinations, alternate double and triple alanine and D-amino acids replacement at these positions. We propose this systematic replacement approach to elucidate other quorum quenching agents in Gram-positive bacteria.

MATERIALS AND METHODS

Bacterial Strains and Growth Conditions

Bacterial strains used in this study: *B. thuringiensis* 407 Cry^- *plcA′Z* (Bt A'Z) and the PapR null-mutant 407 Cry^- Δ*papR plcA'Z* (Bt ΔpapR A'Z) strains, containing a transcriptional fusion between the promoter of *plcA* and the *lacZ* reporter gene (as described previously; Gominet et al., 2001; Slamti and Lereclus, 2002); *B. cereus* strain ATCC 14579 (Ivanova et al., 2003). Unless otherwise noted, cells were grown in modified LB medium (16 g/L tryptone, 8 g/L yeast extract, 5 g/L NaCl) at 37°C and stored at −80°C in LB containing 25% glycerol. Kanamycin (200 μg/mL) was used for the selection of *B. thuringiensis*.

Solid Phase Peptide Synthesis Methodology (SPPS)

All the peptides were synthesized using standard Fmoc-based solid-phase peptide synthesis (SPPS), microwave irradiation, procedures on Rink Amide resin (substitution 0.5 mmol/g, 25 μmol) in SPE polypropylene Single-Fritted tubes. The Fmoc-protecting group was then removed by treating the resin with 20% (v/v) piperidine diluted in dimethylformamide (DMF) followed by heating to 80°C in the microwave (MARS, CEM, United States; 2-min ramp to 80°C, 2-min hold at 80°C) with stirring. To couple each amino-acid, Fmoc-protected amino acids (4 equiv. relative to the overall loading of the resin), were dissolved in DMF and mixed with 2-(1H-benzotriazol-1-yl)-1,1,3,3-tetramethyluronium hexafluorophosphate (HBTU; 4 equiv.) and diisopropylethylamine (DIEA; 4 equiv.). The solution was allowed to pre-activate for 5 min before being added to the resin, and heated to 70°C in a multimode microwave (2-min ramp to 70°C, 4-min hold at 70°C) with stirring. After each coupling/deprotection cycle the resin was drained and washed with DMF (3 × 5 mL). Once peptide synthesis was completed, the peptide was cleaved from the resin, by mixing the resin with 3 mL cleavage cocktail of 95% trifluoroacetic acid (TFA), 2.5% triisopropylsilane (TIPS), and 2.5% deionized water for 3 h with agitation. The peptide mixture was precipitated from the TFA solution by the addition of cold ether and collected by centrifugation (Eppendorf R5810 8000 rpm for 10 min). The ether was then removed, and the peptide was dried under a stream of nitrogen, and lyophilized, before high-performance liquid chromatography (HPLC) purification.

Peptide Purification

Crude peptides were purified and characterized with Reverse-Phase (RP)-HPLC. The crude peptides were diluted to a final concentration of 10 mg/ml in a solution of 20% acetonitrile (ACN) in water (v/v) or dimethyl sulfoxide (DMSO). A semi-preparative Phenomenex Kinetex C18 (5 μm, 10 × 250 mm) was used for preparative RP-HPLC work. An analytical Phenomenex Gemini C18 column (5 μm, 4.6 mm × 250 mm, 110 Å) was used for analytical RP-HPLC work (**Supplementary Figure S1**). Standard RP-HPLC conditions were as follows: flow rates = 5 mL min^{-1} for semi-preparative separations and 1 mL min^{-1} for analytical separations; mobile phase *A* = 18 MΩ water + 0.1% TFA; mobile phase *B* = ACN. Purities were determined by integration of peaks with UV detection at 220 nm using a linear gradient (first prep 5% B → 65% B over 60 min and second prep 26% B → 36% B over 20 min). The purity of the tested peptides was determined using a linear gradient (5% B → 65% B

over 60 min). MALDI-TOF spectrometry (Bruker Daltonik, Germany) was used to validate the synthesized peptides molecular weight (**Supplementary Table S1**). The purified peptides were lyophilized and stored at −20°C.

Analysis of PlcR Regulon Expression Using β-Galactosidase Assay

PlcR Activation Studies

Bt ΔpapR A'Z cells were grown overnight in LB medium with selective antibiotic. The cells were diluted 10^{-3} in modified LB to a final volume of 1 liter and incubated at 37°C with shaking (200 rpm) until onset of the stationary phase of bacterial growth (OD_{600} 3 ± 0.5). Various concentrations of synthetic peptides were added to 2 ml aliquots of culture, which were incubated for 1 h before centrifugation (Eppendorf centrifuge R5810, 4000 rpm for 5 min) and quantification of β-galactosidase.

Competition Studies of $PapR_7$-Derived Peptides

Bt A'Z cells were grown overnight in LB medium. The cells were diluted 10^{-3} in modified LB to a final volume of 1 L and incubated at 37°C with shaking (200 rpm) until the end of the lag or late-exponential of bacterial growth (OD_{600} 0.1 ± 0.03; 1.8 ± 0.1, respectively). Different concentrations of synthetic peptides were added to 2 ml aliquots of culture and incubated for various times (1–24 h) before centrifugation (Eppendorf centrifuge R5810, 4000 rpm for 5 min) and quantification of β-galactosidase activity.

β-Galactosidase Assay

β-galactosidase activity was measured as described previously (Yang et al., 2017), with minor modifications. Briefly, 200 μL aliquots from 2 ml treated cultures were added in triplicate to a clear 96-well microtiter plate, and then OD_{600} was measured and β-galactosidase activity was assayed. The final results were reported as percentage of activation, which is the ratio between the Miller units obtained after addition of the $PapR_7$ analogs. In Bt ΔpapR A'Z strain, the plcA promoter activity was very low and considered as a baseline. In Bt A'Z strain, the untreated bacteria were considered as 100% of activation and the results were normalized accordingly. Each assay was repeated at least three times.

Hemolytic Assay Toward Human Red Blood Cells

Bt A'Z or *B. cereus* ATCC 14579 cells were grown overnight in LB medium. The cells were diluted 10^{-3} in modified LB to a final volume of 1 liter and incubated at 37°C with shaking (200 rpm) until the end of the lag phase of bacterial growth (OD_{600} 0.1 ± 0.03). Different concentrations of synthetic peptides were added to 2 ml aliquots of culture and incubated for 2.5 h before centrifugation (Eppendorf centrifuge R5810, 4000 rpm for 5 min), separation and filtration (0.2 μm filter) of the supernatants of the treated cultures. Analyses of hemolytic activity were conducted as previously described using human red blood cells (Tal-Gan et al., 2013b; Lobel et al., 2015). Bacterial supernatants were serially diluted in Tris-buffered saline (pH 7.2, 10 mM Tris–HCl, 155 mM NaCl) with 1% human red blood cells (hRBC) suspension and were incubated for 30 min at 37°C. Hemolytic activities were measured by monitoring the absorbance at 420 nm.

Statistical Analysis

Unless otherwise noted, the results are presented as the mean ± SEM. One-way analysis ANOVA of variance, followed by Tukey *post hoc* analysis was used for statistical analysis. The results were considered to be statistically significant if $p < 0.01$.

RESULTS

We have previously reported the first five synthetic peptidic inhibitors of *B. cereus* PlcR-PapR QS system; three independent alanine amino acid replacements ($PapR_7$ – P4A, E6A, and F7A) and two D-amino acid substitutions ($PapR_7$ – dE_6 and dF_7) showed great reduction of PlcR regulon expression and virulence factor secretion (Yehuda et al., 2018).

We initiated the current study by evaluating the three crucial positions of the heptapeptide PapR -proline (Pro4), glutamic acid (Glu6) and phenylalanine (Phe7) through systematic single or/and multiple amino acid substitution strategy. We designed, synthesized and purified a second generation set of $PapR_7$-derived peptide combinations to further explore the structure–activity relationship delineated previously for the first-generation of peptidic analogs. This set included twelve peptides with double and triple alanine and D-amino acid replacements, at the crucial Pro4, Glu6 and Phe7 residues (**Supplementary Table S1**, **Supplementary Figure S1** and **Figure 1**).

We scanned each of $PapR_7$-derived peptide combinations for its ability to modulate the expression of the PlcR regulon using *B. thuringiensis* 407 Cry^- (Bt 407^-) as a model bacterium for the *B. cereus* group. This strain cured of its plasmid is acrystalliferous and shows high phylogenic similarity with the *B. cereus* reference strain ATCC 14579 (Lereclus et al., 1989; Priest et al., 1994; Slamti and Lereclus, 2005). Two *lacZ*-based reporter strains were used in the current study, *B. thuringiensis* 407^- *plcA′Z* (Bt A'Z) and PapR-null mutant *B. thuringiensis* 407^- Δ*papR plcA′Z* (Bt ΔpapR A'Z). Both reporter strains contain a transcriptional fusion between the *plcA* promoter region and the *lacZ* gene. *plcA* is a member of the PlcR regulon and its expression directly reflects the activity of PlcR. The activity of each $PapR_7$-derived peptide combination was evaluated and compared to the previously described five *B. cereus* inhibitory synthetics $PapR_7$-derived peptides ($PapR_7$-P4A; E6A; F7A; dE_6 and dF_7; Yehuda et al., 2018).

We first conducted an initial screening of all the analogs at high peptide concentration (5 μM) in order to evaluate their ability to activate the PlcR regulon to a level comparable to the synthetic $PapR_7$ signal peptide (**Figure 2**). Both first and second generations of $PapR_7$ analogous were classified by their number of amino acid replacements (alanine or D-amino); single, double and triple. Similar to our first-generation single replacement inhibitors, none of the new $PapR_7$-derived peptide combinations were capable of activating the PlcR regulon. These findings revealed that any alanine and D-amino acid replacements, at the

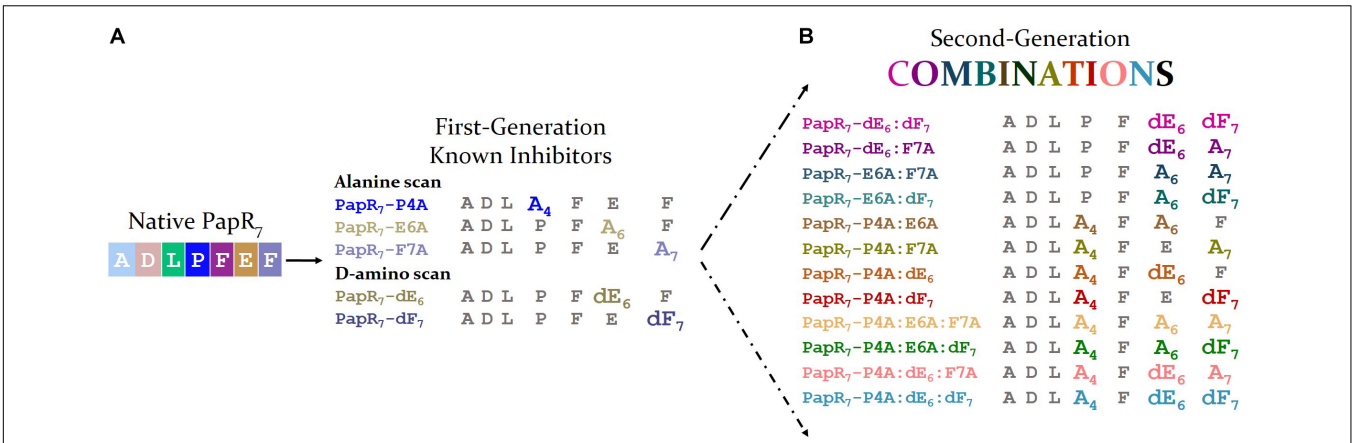

FIGURE 1 | Second generation of PapR$_7$-derived peptide combinations. **(A)** Sequences of first generation potent synthetic inhibitors 7-mer PapR-derived peptides (PapR$_7$; ADLPFEF) involved D-amino acid or alanine replacements at three positions; proline (P) glutamic (E), and phenylalanine (F) of the heptapeptide PapR. **(B)** Sequences of second generation of PapR$_7$-derived peptide combinations, involved double and triple alanine and D-amino acids replacement.

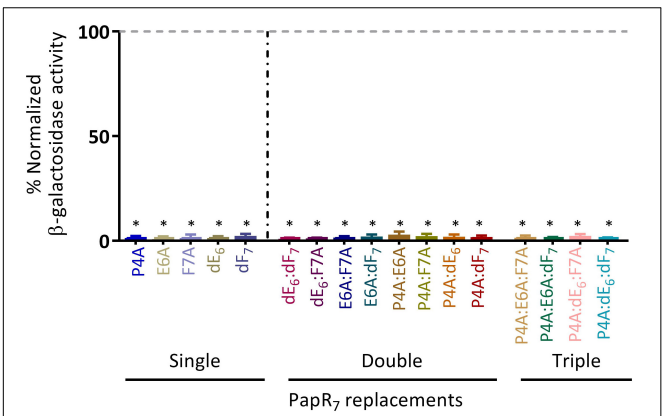

FIGURE 2 | PlcR regulon activation by the new PapR$_7$-derived peptide combinations. β-galactosidase activity of Bt ΔpapR A'Z induced by the addition of 5 μM PapR$_7$-derived peptides normalized to synthetic PapR$_7$ signal peptide at onset of the stationary phase of bacterial growth (OD$_{600}$ of 3 ± 0.5, mean ± SEM, n = 9). *p < 0.01 indicates a statistically significant difference between addition of synthetic PapR$_7$ peptide and PapR$_7$-derived peptides.

positions Pro4, Glu6 and Phe7 of PapR$_7$ derivatives, are critical for PlcR regulon activation. These derivatives can therefore be classified as potential candidates for the development of potent second-generation PlcR inhibitors.

We next scrutinized their ability to compete with the endogenous PapR signal peptide (in Bt A'Z reporter strain) for reducing the activation of the PlcR regulon in late-exponential phase of bacterial growth (OD$_{600}$ of 1.8 ± 0.1). As shown in **Figure 3A**; PapR$_7$ derivatives activities were classified by D-amino acid enantiomer or Ala replacements at either of the three PapR$_7$ crucial positions (Pro4, Glu6 and Phe7). The previously reported inhibitors, PapR$_7$-P4A; E6A; F7A; dE$_6$ and dF$_7$, were also included for comparison. Peptides PapR$_7$ – P4A:E6A, P4A:E6A:F7A and P4A:E6A:dF$_7$ did not show any reduction in *plcA'Z* activity. PapR$_7$ – E6A:F7A, E6A:dF$_7$, P4A:F7A, P4A:dE$_6$, P4A:dF$_7$, PapR$_7$ – P4A:dE$_6$:dF$_7$ and P4A:dE$_6$:F7A were able to reduce *plcA'Z* activity by approximately 40%. We identified two candidate peptides that inhibited *plcA'Z* activation when added at late-exponential phase. Indeed, PapR$_7$ – dE$_6$:dF$_7$ and dE$_6$:F7A reduced *plcA'Z* activity by 71 and 65 %, respectively, similarly to the inhibitory activity of their parent reporter inhibitors PapR$_7$ – dE$_6$, dF$_7$ and F7A (65, 63, and 70%, respectively). To confirm PapR$_7$ – dE$_6$:dF$_7$ and dE$_6$:F7A potent inhibition, we repeated the experiment with several concentrations of these inhibitors in order to determine their IC$_{50}$ values (**Figures 3B,C**). The results show that the new inhibitory peptides have IC$_{50}$ values in the low micromolar range, almost comparable to their parent reporter inhibitors IC$_{50}$ values (**Table 1**). Overall, we identified new potent inhibitors, PapR$_7$ – dE$_6$:dF$_7$ and dE$_6$:F7A, which were able to compete with endogenous PapR and inhibit PlcR regulon activity very effectively. Interestingly, these two potent inhibitors contain D-Glutamic acid replacement at position 6 of the PapR heptapeptide.

We have previously reported that inhibition through PapR$_7$ inhibitory peptidic derivatives is cell density dependent (Slamti and Lereclus, 2002; Yehuda et al., 2018). To examine the effect of bacterial cell density on the inhibition of the PlcR regulon expression, each derivative was added to Bt A'Z cells at OD$_{600}$ 0.1 ± 0.03, which corresponds to the early stage of exponential phase. PlcR-dependent gene expression was then quantified after 2.5 h (**Figure 4**) and after 24 h in order to assess their activity and stability over time (**Supplementary Figure S2**). As has been reported recently, all of our known parent PapR$_7$ inhibitors were able to completely block *plcA'Z* activation for up to 24 h under these conditions (Yehuda et al., 2018). We observed similar results with PapR$_7$ – dE$_6$:dF$_7$ and dE$_6$:F7A; these peptides blocked *plcA'Z* activation compared to the parent peptidic inhibitors for 2.5 h and up to 24 h (**Figure 4** and **Supplementary Figure S2**). Combining them with additional alanine replacement at Pro4, PapR$_7$ – P4A:dE$_6$:dF$_7$ and P4A:dE$_6$: F7A showed a

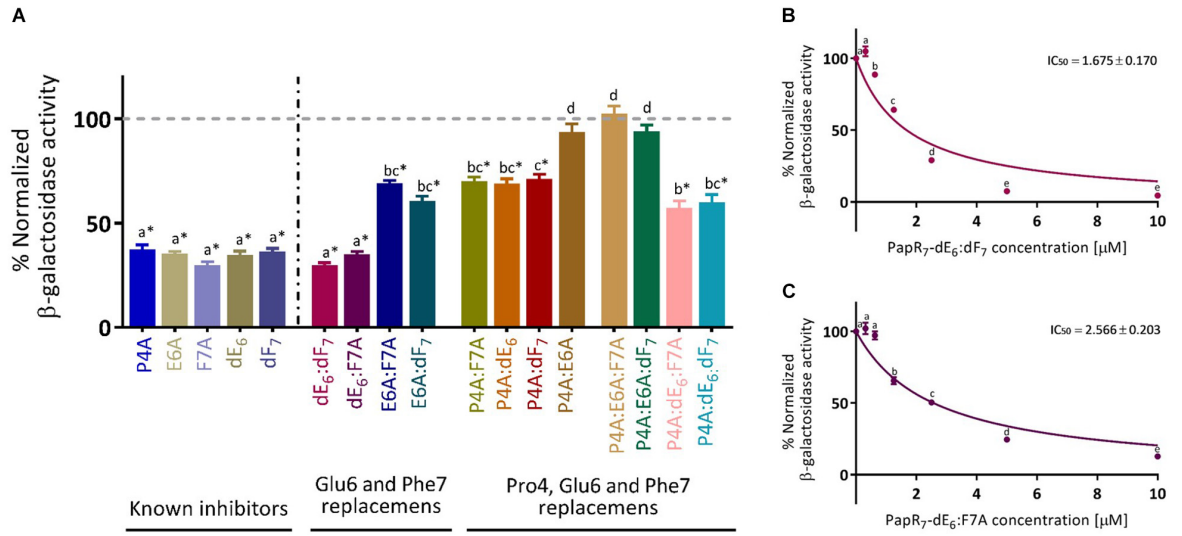

FIGURE 3 | Competition studies with new $PapR_7$-derived peptide combinations. **(A)** β-galactosidase activity of Bt A'Z induced by the addition of 2.5 μM $PapR_7$-derived peptides, **(B)** $PapR_7$- dE_6:dF_7, and **(C)** $PapR_7$-dE_6:F7A derivatives in several concentrations normalized to untreated bacterial cells at late-exponential of bacterial growth (OD_{600} of 1.8 ± 0.1, mean ± SEM, $n = 9$). *$p < 0.01$ indicates a statistically significant difference between untreated Bt A'Z and addition of $PapR_7$-derived peptides. Different letters indicate statistically significant differences between $PapR_7$-derived peptide treatments ($p < 0.01$).

reduction of ∼75% in *plcA'Z* activation. The addition of $PapR_7$ derivatives as $PapR_7$- E6A:F7A, E6A:dF_7, P4A:F7A, P4A:dE_6 and P4A:dF_7 in the early stages of the bacterial growth led to drastic reduction in *plcA'Z* activity, revealing a series of new peptidic inhibitors. In contrast, the non-inhibitory peptidic combinations ($PapR_7$- P4A:E6A, P4A:E6A:F7A and P4A:E6A:dF_7) did not reduce the PlcR regulon expression even in low bacterial density. Importantly, the bacterial growth was not affected by the addition of all the examined peptides (data not shown).

Throughout these competition studies, we identified a group of three non-inhibitory peptidic combinations ($PapR_7$- P4A:E6A, P4A:E6A:F7A and P4A:E6A:dF_7), seven variants of $PapR_7$ containing multiple replacements combinations with median to high inhibitory activities ($PapR_7$- P4A:dE_6:F7A, P4A:dE_6:dF_7, E6A:F7A, E6A:dF_7, P4A:F7A, P4A:dE_6 and P4A:dF_7) and two very potent inhibitors that abolish activation of *plcA'lacZ* ($PapR_7$ – dE_6:dF_7 and dE_6:F7A) and compete with endogenous PapR. These two peptides are proposed as quorum quenchers that do not affect the bacterial growth but inhibit the expression of the PlcR regulon.

After observing this inhibitory activity, we expanded our study to explore the effect of these second generation $PapR_7$ analogs on the production of a representative virulence factor under the control of PlcR in wild-type bacteria. Previous studies have shown that the activity of hemolysins in *B. cereus* is regulated by the PlcR – PapR QS system (Salamitou et al., 2000; Slamti and Lereclus, 2002; Slamti et al., 2004). Therefore, we studied

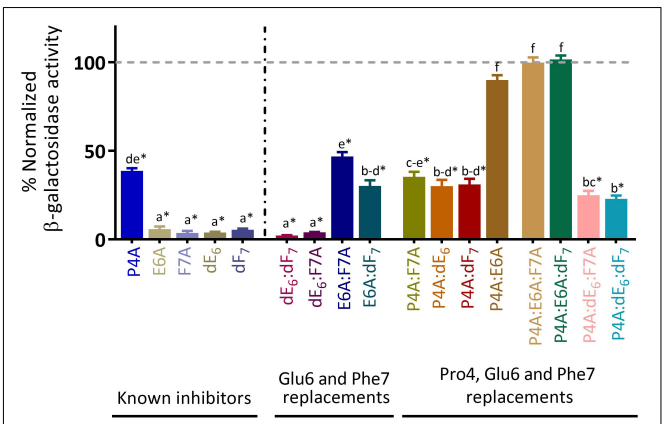

FIGURE 4 | Exploring the effect of bacterial cell density on the $PapR_7$-derived peptide combinations activity. β-galactosidase activity of Bt A'Z induced by the addition of 10 μM $PapR_7$-derived peptides normalized to untreated bacterial cells at end lag phase of bacterial growth (OD_{600} of 0.1 ± 0.03; mean ± SEM, $n = 9$). *$p < 0.01$ indicates a statistically significant difference between untreated Bt A'Z and addition of $PapR_7$-derived peptides. Different letters indicate statistically significant differences between $PapR_7$-derived peptide treatments ($p < 0.01$).

TABLE 1 | Comparison between IC_{50} values of new $PapR_7$-derived peptide combinations and their parent inhibitors, as determined by the *lacZ*-based reporter assay.

	IC_{50}[μM]*		
$PapR_7$-dE_6:dF_7	1.675 ± 0.170[a]	$PapR_7$-dE_6	0.977 ± 0.042[c]
$PapR_7$-dE_6:F7A	2.566 ± 0.203[b]	$PapR_7$-dF_7	1.223 ± 0.072[ac]
		$PapR_7$-F7A	1.675 ± 0.102[a]

*IC_{50} values were calculated by GraphPad Prism 8, using the non-linear inhibitor vs. normalized response method. Different letters indicate statistically significant differences between IC_{50} values of $PapR_7$-derived peptide combinations ($p < 0.01$).

the effect of the new $PapR_7$ derivatives on the production of hemolysins in *B. cereus* strain ATCC 14579, a representative member of the *B. cereus sensu stricto* species.

We performed hemolytic activity assays toward human red blood cells in the presence of the synthetic derivatives (**Figure 5A**). From these results, we identified $PapR_7$ inhibitory peptidic analogs that were able to reduce the hemolytic activity of wild type *B. cereus* ATCC 14579. Interestingly, these analogs reduced the expression of hemolysin (**Figure 5A**) even more efficiently than the inhibition that was observed for Bt 407$^-$ PlcR-dependent gene expression (as shown in **Figure 4**). We quantified the hemolytic activity of the strong inhibitors group by determining their IC_{50} values. In addition to the two strong inhibitors derivatives ($PapR_7$ – dE_6:dF_7, dE_6:F7A), we observed great activity also for $PapR_7$ – P4A:dE_6:dF_7 and P4A:dE_6:F7A analogs. Regard to $PapR_7$ – dE_6:dF_7 and dE_6:F7A derivatives, the relative IC_{50} value trends were highly similar to those in the *lacZ*-reporter assays results (**Figure 5B** and **Tables 1**, **2**). In comparison to their parent single inhibitors $PapR_7$ – dF_7 and F7A, the relative IC_{50} values were in the same range (**Figures 5B,C** and **Table 2**); addition of D- Glutamic acid in the parent peptide $PapR_7$ – dF_7 ($PapR_7$ – dE_6:dF_7) slightly improved its IC_{50} (IC_{50} value was reduced to 1.382 compared to 3.041), while alanine substituted at position Phe7 ($PapR_7$ – dE_6:F7A) did not show any effect. $PapR_7$– P4A:dE6:dF7 and P4A:dE6:F7A exhibited lower IC_{50} values compared to their parent single inhibitors $PapR_7$– P4A, dF_7 and F7A but a higher IC_{50} value compared to the parent peptide $PapR_7$–dE_6 (**Table 2**). We observed another key feature in the new $PapR_7$ combinations; sharing specific substitutions at $PapR_7$ sequence influence their ability to inhibit PlcR activity; for example, all non-inhibitory peptidic combinations included alanine substitutions at positions Pro4 and Glu6 of $PapR_7$ peptide, while all strong inhibitors group members share replacement of Glu6 by its D-isomer. All these new $PapR_7$ combinations activity profiles may shed light on PlcR and PapR interaction. To better understand their role in PlcR activity, we divided the delineated above (**Figure 5**) $PapR_7$-derived peptidic combinations hemolytic activities on human red blood cells to three different sets (**Figures 6A–C**).

TABLE 2 | Comparison between IC_{50} values of new $PapR_7$-derived peptide combinations and their parent inhibitors, as determined by the hemolytic assay.

	IC.$_{50}$ values [μM]*		
$PapR_7$-dE_6:dF_7	1.382 ± 0.117^{ab}	$PapR_7$-dE_6	1.053 ± 0.089^{a}
$PapR_7$-dE_6:F7A	2.497 ± 0.212^{cd}	$PapR_7$-dF_7	3.041 ± 0.206^{cd}
		$PapR_7$-F7A	2.725 ± 0.239^{d}
$PapR_7$ - P4A: dE_6: dF_7	$2.141 \pm 0.148^{b-d}$	$PapR_7$-P4A	4.391 ± 0.288^{e}
$PapR_7$-P4A: dE_6: F7A	$1.994 \pm 0.184^{a-c}$	$PapR_7$-dE_6	1.053 ± 0.089^{a}
		$PapR_7$-dF_7	3.041 ± 0.206^{cd}
		$PapR_7$-F7A	2.725 ± 0.239^{d}

**IC_{50} values were calculated by GraphPad Prism 8, using the non-linear inhibitor vs. normalized response method. Different letters indicate statistically significant differences between IC_{50} values of $PapR_7$-derived peptide combinations ($p < 0.01$).*

SUMMARY

Role of Individual and Combined Pro4 or Glu6 Residue Replacements

Replacing both Pro4 and Glu6 in $PapR_7$ with alanine yielded non-active peptidic combinations regardless of other modifications in Phe7 position ($PapR_7$- P4A:E6A, P4A:E6A:F7A, and P4A:E6A:dF_7; **Figure 6A**). $PapR_7$- **P4A:E6A**:F7A and **P4A:E6A** are non-inhibitory peptides, while $PapR_7$- **E6A**:F7A and **P4A**:F7A defined as medium inhibitors, reduce the hemolytic activity by ∼60%. The same trend was observed with other two non-inhibitory peptidic combinations; $PapR_7$- **P4A:E6A**:dF_7 and $PapR_7$- **P4A:E6A** compared to their disassembled peptidic combinations $PapR_7$- **E6A**:dF_7, **P4A**:dF_7 and $PapR_7$- **P4A**, **E6A,** respectively. These findings verified the dependence of proline and glutamic acid residues in $PapR_7$ inhibitory activity. By modifying these two residues together to alanine the $PapR_7$-derived inhibitors lost their antagonist features and their ability to prevent native PapR-PlcR interaction. This is in agreement with previous study (Bouillaut et al., 2008; Grenha et al., 2013), which emphasizes that both proline and glutamic acid have an important role in PlcR activation.

Effect of Phe7 Replacement

Crystal structure of $PapR_7$- PlcR complex showed that both $PapR_7$ phenylalanine residues (Positions 5 and 7) are located in hydrophobic pockets (Grenha et al., 2013), and involved in hydrophobic interactions with PlcR. We examined the effect of replacing Phe7 with alanine or D-amino acid on the inhibitory activities of the designed peptides. Introducing D-Phenylalanine at position 7, regardless to the modifications at position 4 and 6, enhances the inhibitory activity of PlcR (**Figure 6B**). Replacing F7 in alanine ($PapR_7$ – E6A:**F7A** or P4A:**F7A)** reduced hemolysis of red blood cells by 60%. However, these replacements combined with D-Phenylalanine yielded analogs ($PapR_7$ – E6A:**dF**$_7$ and P4A:**dF**$_7$) with stronger antagonistic activities (approximately 83% inhibition). These results indicate that the inclusion of D-Phenylalanine may contribute to hydrophobic interactions with PlcR by preserving the aromatic ring side chain interaction.

Importance of Glu6 and Its Stereoisomer Substitution

We observed that all the strong inhibitor group members contain the replacement of Glu6 to its D-enantiomer (**Figure 5A**). $PapR_7$ – **dE**$_6$:F7A and **dE**$_6$:dF_7 displayed similar inhibitory effect, regardless of other modifications (D-amino or alanine replacements) in position Phe7 (**Figure 6C**). In contrast, replacing Glu6 with alanine yielded two weaker PlcR antagonists, when either Phe7 combined substitutions with alanine or D-amino ($PapR_7$ – **E6A**:F7A and **E6A**:dF_7). $PapR_7$ – P4A:**dE**$_6$:F7A and P4A:**dE**$_6$:dF_7 fully prevented hemolysis of red blood cells, however, replacing only Glu6 with alanine yielded two non-inhibitory peptidic combinations $PapR_7$-P4A:**E6A**:F7A and P4A:**E6A**:dF_7 as was supported by IC_{50} values (**Figure 6D**).

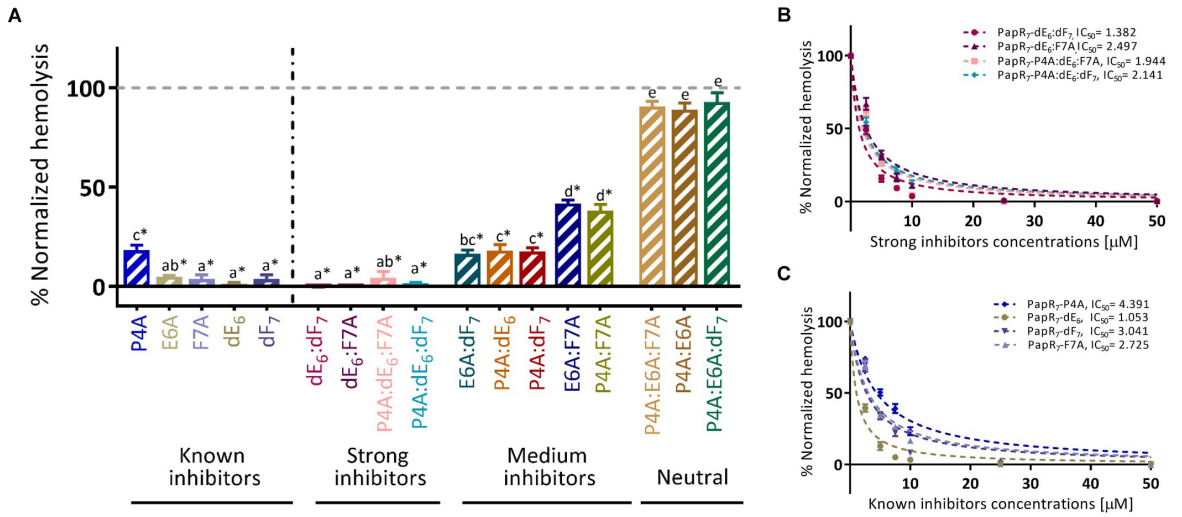

FIGURE 5 | New $PapR_7$-derived peptide combinations inhibit Bc virulence factor. **(A)** Hemolytic activity on human red-blood cells of supernatant *B. cereus* ATCC 14579 treated cultures in 10 μM of $PapR_7$-derived peptides normalized to untreated bacterial cells at end lag phase of bacterial growth (OD_{600} of 0.1 ± 0.03; mean ± SEM, $n = 9$). Hemolysis inhibition dose response curves of *B. cereus* ATCC 14579 treated supernatant cultures in different concentrations of **(B)** $PapR_7$ – dE_6:dF_7, dE_6:F7A, P4A:dE_6:dF_7, and P4A:dE_6:F7A and **(C)** known inhibitors normalized to untreated bacterial culture (mean ± SEM, $n = 9$). *$p < 0.01$ indicates a statistically significant difference between untreated *B. cereus* ATCC 14579 and addition of $PapR_7$-derived peptides. Different letters indicate statistically significant differences between $PapR_7$-derived peptide treatments ($p < 0.01$).

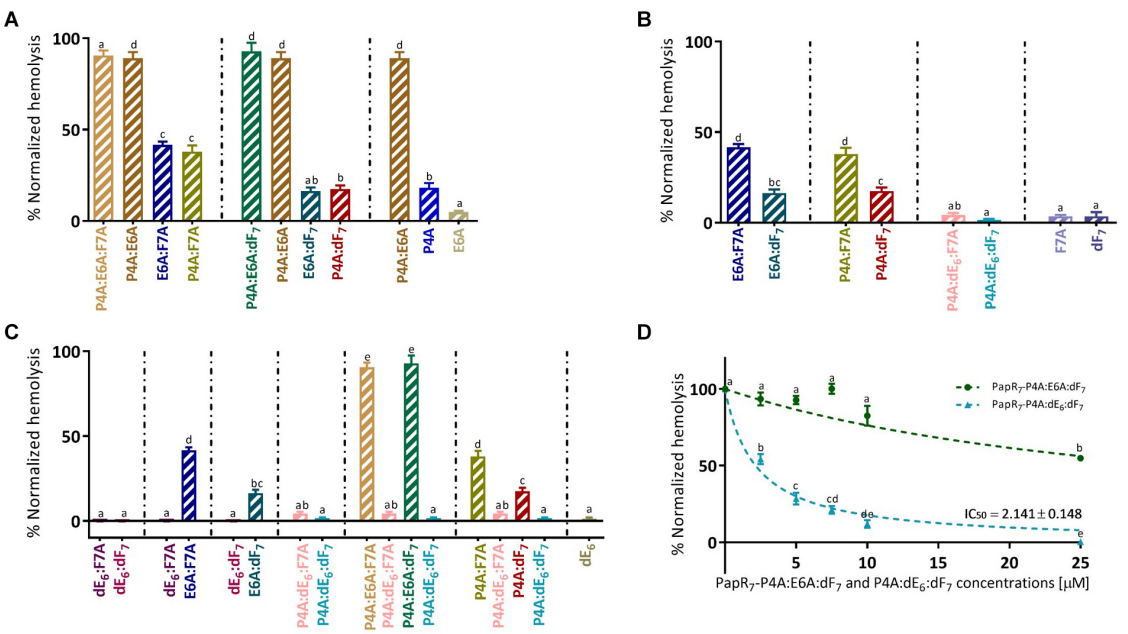

FIGURE 6 | Exploring specific combination replacements effect on Bc virulence inhibition. Hemolytic activity of supernatant *B. cereus* ATCC 14579 treated cultures in 10 μM of $PapR_7$-derived peptides normalized to untreated supernatants of bacterial cells at end lag phase of bacterial growth (OD_{600} of 0.1 ± 0.03; mean ± SEM, $n = 9$). Hemolytic activities on human red blood cells were classified by exploring the role of three $PapR_7$ crucial positions in PlcR activity; **(A)** Role of individual and combined Pro4 or Glu6 residue replacements. **(B)** Effect of Phe7 replacement. **(C)** Importance of Glu6 and its stereoisomer substitution. Hemolysis inhibition dose response curves of *B. cereus* ATCC 14579 treated supernatant cultures in different concentrations of **(D)** $PapR_7$ – P4A:E6A:dF_7 and P4A:dE_6:dF_7 normalized to untreated bacterial culture (mean ± SEM, $n = 9$). Different letters indicate statistically significant differences between $PapR_7$-derived peptide treatments ($p < 0.01$).

Interestingly, in an earlier study (Bouillaut et al., 2008; Grenha et al., 2013) the authors characterized the function and specific interactions of PapR glutamic acid with conserved residues in PlcR. These findings support our results about the important role of Glu6 in the activity of PlcR regulon. Indeed, replacement of L-glutamic acid of $PapR_7$- P4A:F7A and P4A:dF_7

(corresponding ADLAF**E**A and ADLAF**E**dF), with D-glutamic acid yielded two potent PlcR antagonists; $PapR_7$- P4A:**dE**$_6$:F7A and P4A:**dE**$_6$:dF_7. Overall, these three sets of new $PapR_7$-derived peptide combinations support previous published studies and reveal the important role of three crucial positions at designing potent PlcR antagoinsts; Pro4, Phe7 and especially Glu6 that may function to selectively allow PapR, but not other similar autoinducers, to bind PlcR.

CONCLUSION

The PapR-PlcR QS system is extensively involved in the pathogenesis of *B. cereus*, highlighting this system as an attractive target for an alternative treatment to prevent infection. We have previously reported the first five potent synthetic peptidic inhibitors of *B. cereus* PlcR-PapR QS system (Yehuda et al., 2018); three independent alanine amino acid replacements ($PapR_7$ - P4A, E6A, and F7A) and two D-amino acid substitutions ($PapR_7$ – dE_6 and dF_7). We concluded that the critical residues for $PapR_7$ –PlcR interaction and PlcR activation were proline, glutamic acid and phenylalanine. To further understand their role in PlcR activity, a new set of $PapR_7$ analogs with double and triple alanine and D-amino acid replacements at these positions were designed and synthesized. Multiple amino acid substitutions revealed that any replacement at these positions Pro4, Glu6 and Phe7 of $PapR_7$ derivatives, is critical for PlcR regulon activation in the Δ*papR* mutant strain. A comprehensive competition study of all $PapR_7$-derived peptides combinations in late-exponential phase identified four promising QS peptidic inhibitors candidates; $PapR_7$ – dE_6:dF_7 and dE_6:F7A and two other analogs with additional alanine substituted $PapR_7$ – P4A:dE_6:dF_7 and P4A:dE_6:F7A, all contained D-Glutamic acid at position 6 of the C-terminus of heptapeptide PapR. The two potent inhibitors $PapR_7$ – dE_6:dF_7 and dE_6:F7A generated similar inhibitory activity as their parent single replacement reported inhibitors $PapR_7$ – dE_6, dF_7 and F7A with comparable IC_{50} values ≅ 1–2.6 μM. Our results verified previous reports that inhibition through $PapR_7$ derivatives is cell density dependent (Slamti and Lereclus, 2002; Yehuda et al., 2018). We showed that all of our new four promising QS peptidic inhibitors candidates blocked the PlcR regulon activity even after 24-h period, when they were added at an early stage of bacterial growth ($PapR_7$ – dE_6:dF_7, dE_6:F7A, $PapR_7$ – P4A:dE_6:dF_7, and P4A:dE_6:F7A). Moreover, by exposing the bacterial cells to these analogs at earlier stage (OD_{600} 0.1 ± 0.03) we discovered a new series of inhibitors ($PapR_7$-E6A:F7A, E6A:dF_7, P4A:F7A, P4A:dE_6, and P4A:dF_7). Similar to the parent peptidic inhibitors, we hypothesized that the positive autoregulatory loop was blocked and quorum quenching was achieved throughout growth by the inhibitory multiple combinations $PapR_7$ derivatives.

We next used a human red-blood cells hemolytic assay as a direct method to assess a QS-related phenotype linked to virulence in wild-type *B. cereus*. The inhibitory $PapR_7$ peptidic analogs identified using the lacZ-reporter assays were even more efficient in reducing the hemolytic activity of wild type *B. cereus* ATCC 14579.

Our findings both corroborate and extend previous observations regarding the role of the $PapR_7$ in PlcR receptor recognition; first, we showed the important role of proline or glutamic acid residues in PapR- PlcR interactions and as key in designing strong inhibitors. Second, we demonstrated that inclusion of D-Phenylalanine at Phe7 contribute to $PapR_7$ derivatives inhibitory activities probably due to its hydrophobic features. Moreover, by interfering this Glu6 specific interactions with PlcR, we found the potential of D-Glutamic substitution at designing potent PlcR antagonist. These findings are consistent with previous study (Slamti and Lereclus, 2005) which investigated specificity and polymorphism of PlcR – PapR in the *B. cereus* group. Interestingly, while all the PapR sequences from different strains of the *B. cereus* group showed divergences in their three N-terminal residues, the E6 position was conserved. In the current study we highlighted the precise and unpredictable engineering of natural pheromone in our effort to develop new Quorum Quenching agents, reflecting the trade-off between good peptide binding and lower activation. These new non-native peptides inhibitors may be applied as chemical tools to further study the role of PlcR and other QS in all *B. cereus* group members. Further, our method of single and multiple amino acid replacements might be applied to other QS system to design new anti-virulence agents.

DATA AVAILABILITY

No datasets were generated or analyzed for this study.

AUTHOR CONTRIBUTIONS

AY, LS, and EM performed the research. DL and ZH analyzed the data and wrote the manuscript.

FUNDING

This research project was supported by UHJ-France and the Scopus Foundation.

ACKNOWLEDGMENTS

We would like to thank Dr. John Karas for reading and improving this manuscript.

SUPPLEMENTARY MATERIAL

The Supplementary Material for this article can be found online at: https://www.frontiersin.org/articles/10.3389/fmicb.2019.01246/full#supplementary-material

REFERENCES

Agaisse, H., Gominet, M., Okstad, O. A., Kolstø, A. B., and Lereclus, D. (1999). PlcR is a pleiotropic regulator of extracellular virulence factor gene expression in *Bacillus thuringiensis*. *Mol. Microbiol.* 32, 1043–1053. doi: 10.1046/j.1365-2958.1999.01419.x

Amara, N., Krom, B. P., Kaufmann, G. F., and Meijler, M. M. (2011). Macromolecular Inhibition of quorum sensing: enzymes, antibodies, and beyond. *Chem. Rev.* 111, 195–208. doi: 10.1021/cr100101c

Blatch, G. L., and Lässle, M. (1999). The tetratricopeptide repeat: a structural motif mediating protein-protein interactions. *BioEssays* 21, 932–939. doi: 10.1002/(sici)1521-1878(199911)21:11<932::aid-bies5>3.3.co;2-e

Bottone, E. J. (2010). *Bacillus cereus*, a volatile human pathogen. *Clin. Microbiol. Rev.* 23, 382–398. doi: 10.1128/CMR.00073-79

Bouillaut, L., Perchat, S., Arold, S., Zorrilla, S., Slamti, L., Henry, C., et al. (2008). Molecular basis for group-specific activation of the virulence regulator PlcR by PapR heptapeptides. *Nucleic Acids Res.* 36, 3791–3801. doi: 10.1093/nar/gkn149

Chu, W. P., Wong, S. N., Que, T. L., and Lee, W. K. (2001). Meningoencephalitis caused by *Bacillus cereus* in a neonate. *Hong Kong Med. J.* 7, 89–92.

Declerck, N., Bouillaut, L., Chaix, D., Rugani, N., Slamti, L., Hoh, F., et al. (2007). Structure of PlcR: insights into virulence regulation and evolution of quorum sensing in gram-positive bacteria. *Proc. Natl. Acad. Sci. U.S.A.* 104, 18490–18495. doi: 10.1073/pnas.0704501104

Dubois, T., Faegri, K., Perchat, S., Lemy, C., Buisson, C., Nielsen-LeRoux, C., et al. (2012). Necrotrophism is a quorum-sensing-regulated lifestyle in *Bacillus thuringiensis*. *PLoS Pathog.* 8:e1002629. doi: 10.1371/journal.ppat.1002629

Dunny, G. M., and Leonard, B. A. (1997). Cell-cell communication in gram-positive bacteria. *Ann. Rev. Microbiol.* 51, 527–564. doi: 10.1146/annurev.micro.51.1.527

Erez, Z., Steinberger-Levy, I., Shamir, M., Doron, S., Stokar-Avihail, A., Peleg, Y., et al. (2017). Communication between viruses guides lysis-lysogeny decisions. *Nature* 541, 488–493. doi: 10.1038/nature21049

Fontaine, L., Boutry, C., De Frahan, M. H., Delplace, B., Fremaux, C., Horvath, P., et al. (2010). A novel pheromone quorum-sensing system controls the development of natural competence in *Streptococcus thermophilus* and *Streptococcus salivarius*. *J. Bacteriol.* 192, 1444–1454. doi: 10.1128/JB.01251-1259

Fontaine, L., Wahl, A., Fléchard, M., Mignolet, J., and Hols, P. (2015). Regulation of competence for natural transformation in *streptococci*. *Infect. Genet. Evol.* 33, 343–360. doi: 10.1016/j.meegid.2014.09.010

Galloway, W. R., Hodgkinson, J. T., Bowden, S., Welch, M., and Spring, D. R. (2012). Applications of small molecule activators and inhibitors of quorum sensing in Gram-negative bacteria. *Trends Microbiol.* 20, 449–458. doi: 10.1016/j.tim.2012.06.003

Gaur, H., Patrick, C. C., McCullers, J. A., Flynn, P. M., Pearson, T. A., Razzouk, B. I, et al. (2001). *Bacillus cereus* bacteremia and meningitis in immunocompromised children. *Clin. Infect. Dis.* 32, 1456–1462. doi: 10.1086/320154

Gohar, M., Faegri, K., Perchat, S., Ravnum, S., Økstad, O. A., Gominet, M., et al. (2008). The PlcR virulence regulon of *Bacillus cereus*. *PLoS One* 30:e2793. doi: 10.1371/journal.pone.0002793

Gominet, M., Slamti, L., Gilois, N., Rose, M., and Lereclus, D. (2001). Oligopeptide permease is required for expression of the *Bacillus thuringiensis* plcR regulon and for virulence. *Mol. Microbiol.* 40, 963–975. doi: 10.1046/j.1365-2958.2001.02440.x

Grandclément, C., Tannières, M., Moréra, S., Dessaux, Y., and Faure, D. (2015). Quorum quenching: role in nature and applied developments. *FEMS Microbiol. Rev.* 40, 86–116. doi: 10.1093/femsre/fuv038

Granum, P. E., and Lund, T. (1997). *Bacillus cereus* and its food poisoning toxins. *FEMS Microbiol. Lett.* 157, 223–228. doi: 10.1016/s0378-1097(97)00438-2

Gray, B., Hall, P., and Gresham, H. (2013). Targeting agr- and agr-like quorum sensing systems for development of common therapeutics to treat multiple gram-positive bacterial infections. *Sensors* 13, 5130–5166. doi: 10.3390/s130405130

Grenha, R., Slamti, L., Nicaise, M., Refes, Y., Lereclus, D., and Nessler, S. (2013). Structural basis for the activation mechanism of the PlcR virulence regulator by the quorum-sensing signal peptide PapR. *Proc. Natl. Acad. Sci.* 110, 1047–1052. doi: 10.1073/pnas.1213770110

Helgason, E., Okstad, O. A., Caugant, D. A., Johansen, H. A., Fouet, A., Mock, M., et al. (2000). *Bacillus anthracis*, *Bacillus cereus*, and *Bacillus thuringiensis*–one species on the basis of genetic evidence. *Appl. Environ. Microbiol.* 66, 2627–2630. doi: 10.1128/AEM.66.6.2627-2630.2000

Hentzer, M., Wu, H., Andersen, J. B., Riedel, K., Rasmussen, T. B., Bagge, N., et al. (2003). Attenuation of *Pseudomonas aeruginosa* virulence by quorum sensing inhibitors. *EMBO J.* 22, 3803–3815. doi: 10.1093/emboj/cdg366

Hoffmaster, A. R., Ravel, J., Rasko, D. A., Chapman, G. D., Chute, M. D., Marston, C. K., et al. (2004). Identification of anthrax toxin genes in a *Bacillus cereus* associated with an illness resembling inhalation anthrax. *Proc. Natl. Acad. Sci. U.S.A.* 101, 8449–8454. doi: 10.1073/pnas.0402414101

Huillet, E., Tempelaars, M. H., André-Leroux, G., Wanapaisan, P., Bridoux, L., Makhzami, S., et al. (2012). PlcRa, a new quorum-sensing regulator from *bacillus cereus*, plays a role in oxidative stress responses and cysteine metabolism in stationary phase. *PLoS One* 7:e51047. doi: 10.1371/journal.pone.0051047

Ivanova, N., Sorokin, A., Anderson, I., Galleron, N., Candelon, B., Kapatral, V., et al. (2003). Genome sequence of *Bacillus cereus* and comparative analysis with *Bacillus anthracis*. *Nature* 423, 87–91. doi: 10.1038/nature01582

Kalia, V. C. (2013). Quorum sensing inhibitors: an overview. *Biotechnol. Adv.* 31, 224–245. doi: 10.1016/j.biotechadv.2012.10.004

Klee, S. R., Özel, M., Appel, B., Boesch, C., Ellerbrok, H., Jacob, D., et al. (2006). Characterization of *Bacillus anthracis*-like bacteria isolated from wild great apes from Cŏte d'Ivoire and Cameroon. *J. Bacteriol.* 188, 5333–5344. doi: 10.1128/JB.00303-306

Kotiranta, A., Lounatmaa, K., and Haapasalo, M. (2000). Epidemiology and pathogenesis of *Bacillus cereus* infections. *Microb. Infect.* 2, 189–198. doi: 10.1016/S1286-4579(00)00269-260

Lazazzera, B. A., Solomon, J. M., and Grossman, A. D. (1997). An exported peptide functions intracellularly to contribute to cell density signaling in *B. subtilis*. *Cell* 89, 917–925. doi: 10.1016/S0092-8674(00)80277-80279

Lereclus, D., Agaisse, H., Gominet, M., Salamitou, S., and Sanchis, V. (1996). Identification of a *Bacillus thuringiensis* gene that positively regulates transcription of the phosphatidylinositol-specific phospholipase C gene at the onset of the stationary phase. *J. Bacteriol.* 178, 2749–2756. doi: 10.1128/jb.178.10.2749-2756.1996

Lereclus, D., Arantès, O., Chaufaux, J., and Lecadet, M. (1989). Transformation and expression of a cloned delta-endotoxin gene in *Bacillus thuringiensis*. *FEMS Microbiol. Lett.* 51, 211–217. doi: 10.1016/0378-1097(89)90511-9

Lobel, L., Sigal, N., Borovok, I., Belitsky, B. R., Sonenshein, A. L., and Herskovits, A. A. (2015). The metabolic regulator CodY links *Listeria monocytogenes* metabolism to virulence by directly activating the virulence regulatory gene prfA. *Mol. Microbiol.* 95, 624–644. doi: 10.1111/mmi.12890

Mashburn-Warren, L., Morrison, D. A., and Federle, M. J. (2010). A novel double-tryptophan peptide pheromone controls competence in *Streptococcus* spp. via an Rgg regulator. *Mol. Microbiol.* 78, 589–606. doi: 10.1111/j.1365-2958.2010.07361.x

Mignolet, J., Fontaine, L., Sass, A., Nannan, C., Mahillon, J., Coenye, T., et al. (2018). Circuitry rewiring directly couples competence to predation in the gut dweller *Streptococcus salivarius*. *Cell Rep.* 22, 1627–1638. doi: 10.1016/j.celrep.2018.01.055

Miller, M. B., and Bassler, B. L. (2001). Quorum sensing in bacteria. *Ann. Rev. Microbiol.* 55, 165–199. doi: 10.1146/annurev.micro.55.1.165

Neiditch, M. B., Capodagli, G. C., Prehna, G., and Federle, M. J. (2017). Genetic and structural analyses of RRNPP intercellular peptide signaling of gram-positive bacteria. *Ann. Rev. of Genet.* 51, 311–333. doi: 10.1146/annurev-genet-120116-123507

ØKstad, O. A., Gominet, M., Purnelle, B., Rose, M., Lereclus, D., and Kolstø, A. B. (1999). Sequence analysis of three *Bacillus cereus* loci carrying PlcR-regulated genes encoding degradative enzymes and enterotoxin. *Microbiology* 145, 3129–3138. doi: 10.1099/00221287-145-11-3129

Perchat, S., Dubois, T., Zouhir, S., Gominet, M., Poncet, S., Lemy, C., et al. (2011). A cell-cell communication system regulates protease production during sporulation in bacteria of the *Bacillus cereus* group. *Mol. Microbiol.* 82, 619–633. doi: 10.1111/j.1365-2958.2011.07839.x

Perego, M. (2013). Forty years in the making: understanding the molecular mechanism of peptide regulation in bacterial development. *PLoS Biol.* 11:e1001516. doi: 10.1371/journal.pbio.1001516

Perego, M., and Brannigan, J. A. (2001). Pentapeptide regulation of aspartyl-phosphate phosphatases. *Peptides* 22, 1541–1547. doi: 10.1016/S0196-9781(01)00490-499

Priest, F. G., Kaji, D. A., Rosato, Y. B., and Canhos, V. P. (1994). Characterization of *Bacillus thuringiensis* and related bacteria by ribosomal RNA gene restriction fragment length polymorphisms. *Microbiology* 140, 1015–1022. doi: 10.1099/13500872-140-5-1015

Rajput, A., Kaur, K., and Kumar, M. (2016). SigMol: repertoire of quorum sensing signaling molecules in prokaryotes. *Nucleic Acids Res.* 44, D634–D639. doi: 10.1093/nar/gkv1076

Ramarao, N., and Sanchis, V. (2013). The pore-forming haemolysins of *Bacillus cereus*: a review. *Toxins* 5, 1119–1139. doi: 10.3390/toxins5061119

Rasko, D. A., Altherr, M. R., Han, C. S., and Ravel, J. (2005). Genomics of the *Bacillus cereus* group of organisms. *FEMS Microbiol. Rev.* 29, 303–329. doi: 10.1016/j.femsre.2004.12.005

Rasmussen, T. B., and Givskov, M. (2006). Quorum sensing inhibitors: a bargain of effects. *Microbiology* 152, 895–904. doi: 10.1099/mic.0.28601-28600

Rossi, G. A. M., Aguilar, C. E. G., Silva, H. O., and Vidal, A. M. C. (2018). *Bacillus cereus* group: genetic aspects related to food safety and dairy processing. *Arquivos do Instituto Biológico* 85, e0232017. doi: 10.1590/1808-1657000232017

Salamitou, S., Ramisse, F., Brehelin, M., Bourguet, D., Gilois, N., Gominet, M., et al. (2000). The plcR regulon is involved in the opportunistic properties of *Bacillus thuringiensis* and *Bacillus cereus* in mice and insects. *Microbiology* 146, 2825–2832. doi: 10.1099/00221287-146-11-2825

Shi, K., Brown, C. K., Gu, Z.-Y., Kozlowicz, B. K., Dunny, G. M., Ohlendorf, D. H., et al. (2005). Structure of peptide sex pheromone receptor PrgX and PrgX/pheromone complexes and regulation of conjugation in *Enterococcus faecalis*. *Proc. Natl. Acad. Sci. U.S.A.* 102, 18596–18601. doi: 10.1073/pnas.0506163102

Slamti, L., and Lereclus, D. (2002). A cell-cell signaling peptide activates the PlcR virulence regulon in bacteria of the *Bacillus cereus* group. *EMBO J.* 21, 4550–4559. doi: 10.1093/emboj/cdf450

Slamti, L., and Lereclus, D. (2005). Specificity and polymorphism of the PlcR-PapR quorum-sensing system in the *Bacillus cereus* group specificity and polymorphism of the PlcR-PapR quorum-sensing system in the *Bacillus cereus* Group. *J. Bacteriol.* 187, 1182–1187. doi: 10.1128/JB.187.3.1182

Slamti, L., Perchat, S., Gominet, M., Vilas-Bôas, G., Fouet, A., Mock, M., et al. (2004). Distinct mutations in PlcR explain why some strains of the *Bacillus cereus* group are nonhemolytic. *J. Bacteriol.* doi: 10.1128/JB.186.11.3531-3538.2004

Slamti, L., Perchat, S., Huillet, E., and Lereclus, D. (2014). Quorum sensing in *Bacillus thuringiensis* is required for completion of a full infectious cycle in the insect. *Toxins* 6, 2239–2255. doi: 10.3390/toxins6082239

Stenfors Arnesen, L. P., Fagerlund, A., and Granum, P. E. (2008). From soil to gut: *Bacillus cereus* and its food poisoning toxins. *FEMS Microbiol. Rev.* 32, 579–606. doi: 10.1111/j.1574-6976.2008.00112.x

Suga, H., and Smith, K. M. (2003). Molecular mechanisms of bacterial quorum sensing as a new drug target. *Curr. Opin. Chem. Biol.* 7, 586–591. doi: 10.1016/j.cbpa.2003.08.001

Sully, E. K., Malachowa, N., Elmore, B. O., Alexander, S. M., Femling, J. K., Gray, B. M., et al. (2014). Selective chemical inhibition of agr quorum sensing in *Staphylococcus aureus* promotes host defense with minimal impact on resistance. *PLoS Pathog.* 10:e1004174. doi: 10.1371/journal.ppat.1004174

Suzuki, A., Mori, M., Sakagami, Y., Isogai, A., Fujino, M., Kitada, C., et al. (1984). Isolation and structure of bacterial sex pheromone, cPD1. *Science* 226, 849–850. doi: 10.1126/science.6436978

Tal-Gan, Y., Ivancic, M., Cornilescu, G., Cornilescu, C. C., and Blackwell, H. E. (2013a). Structural characterization of native autoinducing peptides and abiotic analogues reveals key features essential for activation and inhibition of an agrc quorum sensing receptor in *Staphylococcus aureus*. *J. Am. Chem. Soc.* 135, 18436–18444. doi: 10.1021/ja407533e

Tal-Gan, Y., Stacy, D. M., Foegen, M. K., Koenig, D. W., and Blackwell, H. E. (2013b). Highly potent inhibitors of quorum sensing in *Staphylococcus aureus* revealed through a systematic synthetic study of the group-III autoinducing peptide. *J. Am. Chem. Soc.* 135, 7869–7882. doi: 10.1021/ja3112115

Tal-Gan, Y., Ivancic, M., Cornilescu, G., Yang, T., and Blackwell, H. E. (2016). Highly stable, amide-bridged autoinducing peptide analogues that strongly inhibit the AgrC quorum sensing receptor in *Staphylococcus aureus*. *Angew. Chem. Int. Ed. Engl.* 55, 8913–8917. doi: 10.1002/anie.201602974

Tal-Gan, Y., Stacy, D. M., and Blackwell, H. E. (2014). N-Methyl and peptoid scans of an autoinducing peptide reveal new structural features required for inhibition and activation of AgrC quorum sensing receptors in *Staphylococcus aureus*. *Chem. Commun.* 50, 3000–3003. doi: 10.1039/c4cc00117f

Vilas-Boas, G., Sanchis, V., Lereclus, D., Lemos, M. V., and Bourguet, D. (2002). Genetic differentiation between sympatric populations of *Bacillus cereus* and *Bacillus thuringiensis*. *Appl. Environ. Microbiol.* 68, 1414–1424. doi: 10.1128/AEM.68.3.1414

Wintjens, R., and Rooman, M. (1996). Structural classification of HTH DNA-binding domains and protein-DNA interaction modes. *J. Mol. Biol.* 262, 294–313. doi: 10.1006/jmbi.1996.0514

Wynendaele, E., Bronselaer, A., Nielandt, J., D'Hondt, M., Stalmans, S., Bracke, N., et al. (2013). Quorumpeps database: chemical space, microbial origin and functionality of quorum sensing peptides. *Nucleic Acids Res.* 41, D655–D659. doi: 10.1093/nar/gks1137

Yang, Y., Koirala, B., Sanchez, L. A., Phillips, N. R., Hamry, S. R., and Tal-Gan, Y. (2017). Structure-activity relationships of the competence stimulating peptides (CSPs) in *Streptococcus pneumoniae* reveal motifs critical for intra-group and cross-group ComD receptor activation. *ACS Chem. Biol.* 12, 1141–1151. doi: 10.1021/acschembio.7b00007

Yehuda, A., Slamti, L., Bochnik-Tamir, R., Malach, E., Lereclus, D., and Hayouka, Z. (2018). Turning off *Bacillus cereus* quorum sensing system with peptidic analogs. *Chem. Commun.* 54, 9777–9780. doi: 10.1039/c8cc05496g

Zheng, F., Ji, H., Cao, M., Wang, C., Feng, Y., Li, M., et al. (2011). Contribution of the Rgg transcription regulator to metabolism and virulence of *Streptococcus suis* serotype 2. *Infect. Immun.* 79, 1319–1328. doi: 10.1128/IAI.00193-10

Conflict of Interest Statement: The authors declare that the research was conducted in the absence of any commercial or financial relationships that could be construed as a potential conflict of interest.

frontiers in Microbiology

ORIGINAL RESEARCH
published: 18 June 2019
doi: 10.3389/fmicb.2019.01230

*Lb*DSF, the *Lysobacter brunescens* Quorum-Sensing System Diffusible Signaling Factor, Regulates Anti-*Xanthomonas* XSAC Biosynthesis, Colony Morphology, and Surface Motility

Jun Ling[1†], Runjie Zhu[1†], Pedro Laborda[2], Tianping Jiang[1], Yifan Jia[1], Yangyang Zhao[1] and Fengquan Liu[1,3]*

[1] Institute of Plant Protection, Jiangsu Academy of Agricultural Sciences, Jiangsu Key Laboratory for Food Quality and Safety-State Key Laboratory Cultivation Base of Ministry of Science and Technology, Nanjing, China, [2] School of Life Sciences, Nantong University, Nantong, China, [3] Institute of Life Sciences, Jiangsu University, Zhenjiang, China

OPEN ACCESS

Edited by:
Cristina García-Aljaro, University of Barcelona, Spain

Reviewed by:
Meriyem Aktas, Ruhr-Universität Bochum, Germany
Shaohua Chen, South China Agricultural University, China

***Correspondence:**
Fengquan Liu
fqliu20011@sina.com

[†] These authors have contributed equally to this work

Specialty section:
This article was submitted to Microbial Physiology and Metabolism, a section of the journal Frontiers in Microbiology

Received: 14 February 2019
Accepted: 17 May 2019
Published: 18 June 2019

Citation:
Ling J, Zhu R, Laborda P, Jiang T, Jia Y, Zhao Y and Liu F (2019) LbDSF, the Lysobacter brunescens Quorum-Sensing System Diffusible Signaling Factor, Regulates Anti-Xanthomonas XSAC Biosynthesis, Colony Morphology, and Surface Motility. Front. Microbiol. 10:1230. doi: 10.3389/fmicb.2019.01230

Lysobacter species are emerging as novel sources of antibiotics, but the regulation of these antibiotics has not been thoroughly elucidated to date. In this work, we identified a small diffusible signaling factor (DSF) molecule (*Lb*DSF) that regulates the biosynthesis of a novel *Xanthomonas*-specific antibiotic compound (XSAC) in *Lysobacter brunescens* OH23. *Lb*DSF was isolated from the culture broth of *L. brunescens* OH23, and the chemical structure of the molecule was determined by NMR and MS. The *Lb*DSF compound induced GUS expression in a reporter strain of *Xanthomonas campestris* pv. *campestris* FE58, which contained the *gus* gene under the control of a DSF-inducible *engXCA* promoter. *Lb*DSF production was found to be linked to the enoyl-CoA hydratase RpfF and dependent on the two-component regulatory system RpfC (hybrid sensor histidine kinase)/RpfG (response regulator), and *Lb*DSF production was increased 6.72 times in the Δ*rpfC* compared to wild-type OH23. *Lb*DSF-regulated XSAC production was dramatically decreased in Δ*rpfF*, Δ*rpfC*, and Δ*rpfG*. Additionally, a significant reduction in surface motility and a number of changes in colony morphology was observed in the Δ*rpfF*, Δ*rpfC*, and Δ*rpfG* compared to the wild-type OH23. The exogenous *Lb*DSF significantly increased XSAC production in wild-type OH23 and recovered the XSAC biosynthetic ability in Δ*rpfF*. Taken together, these results showed that *Lb*DSF is a fatty-acid-derived DSF that positively regulates XSAC biosynthesis, cell morphology, and surface motility. Moreover, the RpfC/RpfG quorum-sensing signal transduction pathway mediates XSAC biosynthesis. These findings may facilitate antibiotic production through genetic engineering in *Lysobacter* spp.

Keywords: diffusible signaling factor, anti-*Xanthomonas* compound, colony morphology, surface motility, *Lysobacter brunescens*

INTRODUCTION

The gliding Gram-negative *Lysobacter* bacteria are ubiquitous freshwater and soil microorganisms; because they are fast-growing, simple to maintain, and genetically amenable for bioengineering, they are a promising source of novel bioactive natural antibiotics (Christensen and Cook, 1978; Xie et al., 2012). Some *Lysobacter* species have been demonstrated to be capable of producing antibiotics, including cyclodepsipeptides, cyclic lipodepsipeptides, cephem-type β-lactams, polycyclic tetramate macrolactams, phenazines, and lactivicins, which can inhibit the growth of plant pathogens.

Lysobactin is a cyclodepsipeptide that was first reported by O'Sullivan et al. (1988). The structure of lysobactin contains five natural amino acid residues and six non-proteinogenic amino acids, forming a macrocycle. Conversely, two families of cyclic lipodepsipeptides have been isolated from *Lysobacter* species (Kato et al., 1997; Hashizume et al., 2001; Zhang et al., 2011), both of which contain a β-hydroxyl fatty acid linked to the peptide moiety. The WAP-8294A family consists of 12 amino acid macrocycles, whereas the tripopeptin family is formed by eight amino acid cycles and a branched acyl group varying in length from 11 to 16 carbons (Xie et al., 2012). Cephem-type β-lactam antibiotics include cephalosporins, cephabacins, and cephamycins, but only cephabacins have been isolated from *Lysobacter* species (Harada et al., 1984; Ono et al., 1984). Cephabacins contain a cephem nucleus, which is linked to a non-ribosomal peptide by an ester linkage. Three different polycyclic tetramate macrolactams, xanthobacin, dihydromaltophilin (HSAF), and maltophilin, have been isolated from *Lysobacter gummosus* OH17 and *Lysobacter enzymogenes* OH11. All three of these polycyclic tetramate macrolactams contain γ-butyrolactam, which is involved in the macrocyclic structure (Meyers et al., 1985; Lou et al., 2011; Qian et al., 2013; Wang et al., 2013). *Lysobacter* cephabacins were shown to employ a novel mode of antibacterial action. These cephabacins specifically interfere with the biosynthesis of sphingolipids by targeting ceramide synthase, which causes thickening of the cell wall due to the accumulation of sphingolipid promoters that increase the degradation of chitin and block the elongation of the hyphal tips (Li et al., 2009). Several phenazines, including myxin and iodinin, have been found in *Lysobacter antibioticus* OH13 (Zhao et al., 2016). These phenazines differ not only in the presence of an *N*-oxide bond but also in the substituent at position 1 of the heterocycle. Finally, it is worth mentioning that lactivicin has a unique structure composed of a cycloserine ring linked to a γ-lactone ring (Harada et al., 1986). HSAF was shown to have a wide range of biological activities, including antibiotic, antifungal, and anticancer activities. Our research group also described a new cyclic lipodepsipeptide, WAP-8294A2, from *L. enzymogenes*, which exhibits strong inhibitory activity against methicillin-resistant *Staphylococcus aureus* (Zhang et al., 2011). WAP-8294A2 is currently in phase I/II clinical studies. WAP-8294A2 is produced by a large non-ribosomal peptide synthetase complex of 12 modules, which forms the linear assembly of amino acids. The biosynthetic pathway leading to the formation of 6 bioactive phenazines in *L. antibioticus*, starting from chorismic acid, was also reported by our research group (Zhao et al., 2016). After isolation of the compounds using reverse-phase HPLC, it was demonstrated that these phenazines exhibited strong activity against several bacteria, including *Escherichia coli*, *Bacillus subtilis*, and *Xanthomonas* spp.

In some prokaryotic systems, bacteria produce exogenous chemical signaling molecules to monitor population density and regulate a wide range of biological functions, such as secondary metabolite biosynthesis, biofilm formation, colony morphology, surface motility, and virulence (Abisado et al., 2018). LuxI/LuxR-type quorum-sensing systems are very common in Gram-negative bacteria, where they regulate the expression of genes through small chemical auto-inducers (Van Houdt et al., 2007). LuxI proteins are responsible for the synthesis of *N*-acyl homoserine lactone (AHL) quorum-sensing signals, and LuxR proteins are considered to be the main regulatory component of AHL quorum-sensing systems. These two proteins share two conserved regions, an AHL-binding domain and a DNA-binding domain (Maddocks and Oyston, 2008). Another group of quorum-sensing signals, the diffusible signaling factor (DSF) family, has recently been reported in a range of plant and human bacterial pathogens, including *Xanthomonas campestris* pv. *campestris* (*Xcc*), *Xylella fastidiosa*, *Stenotrophomonas maltophilia*, and *L. enzymogenes* (Barber et al., 1997; Deng et al., 2011; Robert and Dow, 2011; Han et al., 2015). In the DSF system, the putative enoyl-CoA hydratase RpfF is responsible for the synthesis of the DSF, and the RpfC/RpfG two-component system is involved in sensing and transducing DSF signals through a conserved phosphorelay mechanism (Holly et al., 2000). Different types of DSF signal molecules have been identified by electrospray ionization mass spectrometry (ESI-MS), gas chromatography, and nuclear magnetic resonance (NMR) analysis, such as *cis*-11-methyl-2-dodecenoic acid (DSF), *cis*-dodecenoic acid (BDSF), *cis*-11-methyldodeca-2,5-dienoic acid (CDSF), and 13-methyltetradecanoic acid (Wang et al., 2004; He et al., 2010; Han et al., 2015). Functional analysis of *rpfF* and *rpfC* mutants in different bacterial species suggests that the general role of the DSF-signaling system in virulence modulation is conserved, but the regulatory mechanisms and DSF-dependent traits may differ among taxa (Holly et al., 2000).

In this study, we isolated a novel *Lysobacter brunescens* strain, OH23, and active compounds from the culture supernatant of OH23 were shown to have strong specific activity against *Xanthomonas* species, whereas other bacteria and fungi, including *Pseudomonas syringae* pv. *glycinea*, *P. syringae* pv. *lachrymans*, *Acidovorax citrulli*, *E. coli*, *Erwinia amylovora*, *Botryosphaeria dothidea*, *Phytophthora capsica*, *Valsa ambiens* var. *Pyri*, and *Colletotrichum gloeosporioide*, remained unaltered (**Supplementary Figure S1**). We found that the genome of *L. brunescens* OH23 contained gene homologs to the regulation of pathogenicity factor (*rpf*) gene clusters of quorum-sensing genes from *L. enzymogenes* OH11. DSF signaling has been shown to be involved in the synthesis of metabolites with high pharmaceutical interest in *L. enzymogenes* OH11. This finding prompted us to investigate whether a DSF-dependent quorum-sensing signaling pathway was also responsible for the production of *Xanthomonas*-specific antibiotic compounds

(XSAC). To this end, we developed single in-frame mutants of the homolog DSF genes *rpfF*, *rpfC*, and *rpfG* and tested their ability to both produce DSF signals and synthesize XSAC. Our results revealed that *L. brunescens* uses an autoregulatory mechanism similar to *L. enzymogenes* to control DSF biosynthesis, suggesting the production of a DSF-like molecule in *L. brunescens* (Holly et al., 2000). We characterized the *L. brunescens* DSF signal as 13-methyltetradecanoic acid and demonstrated that this molecule regulates XSAC biosynthesis, surface motility, and cell morphology through the RpfC/RpfG signaling pathway.

MATERIALS AND METHODS

Bacterial Strains, Vectors, and Culture Conditions

The bacterial strains and plasmids used in this study are listed in **Table 1**. *E. coli* DH5α λpir, K-12, and S17-1 λpir were grown in LB (10 g tryptone, 5 g yeast extract, and 10 g sodium chloride, pH 7.0–7.2, in 1 L of distilled water) at 37°C (Sambrook, 2001). *L. brunescens* OH23 (stored at China General Microbiological Culture Collection Center, Beijing, CGMCC No. 13677) and the genetically engineered Δ*rpfF*, Δ*rpfC*, and Δ*rpfG* mutants were grown in nutrient broth (NB) medium (5 g peptone, 1 g yeast extract, 3 g beef extract, and 10 g sucrose, pH 7.0–7.2, in 1 L of distilled water) or in nutrient broth–yeast extract–glucose (NYG) medium (5 g peptone, 3 g yeast extract, and 20 g glycerol, pH 7.0–7.2, in 1 L of distilled water) at 28°C (Atlas, 1997). *X. campestris* pv. *campestris* FE58, *Xanthomonas oryzae* pv. *oryzae* PXO99^{A}, *X. oryzae* pv. *oryzae* RS105, *X. oryzae* pv. *oryzae* KACC10331, *X. campestris* pv. *campestris* 8004, *Xanthomonas axonopodis* pv. *glycines* 12-2, *P. syringae* pv. *glycinea* PG4180, *A. citrulli* DSM17060, *P. syringae* pv. *lachrymans* 814/98, and *E. amylovora* ATCC15580 were also grown in nutrient broth (NB) medium at 28°C. All solid media contained 1.5% agar, and antibiotics were added at the following concentrations: 20 μg/ml rifampicin and 8 μg/ml gentamicin for *L. brunescens*, 50 μg/ml rifampicin, and 10 μg/ml tetracycline for *X. campestris* pv. *campestris* FE58, and 20 μg/ml gentamicin for *E. coli*. Sucrose was added at a final concentration of 4% for the counter-selection of in-frame deletion strains.

TABLE 1 | Bacterial strains and plasmids used in this study.

Strain/plasmid	Description	Source or references
Lysobacter brunescens		
OH23	Wild-type symbiotic strain	Lab strain
OH23 Rif	Spontaneous Rif^{R} mutant of OH23, Rif^{R}	
Δ*rpfF*	*rpfF* gene in-frame deletion mutant	This study
Δ*rpfG*	*rpfG* gene in-frame deletion mutant	This study
Δ*rpfC*	*rpfC* gene in-frame deletion mutant	This study
Xanthomonas		
Xanthomonas campestris pv. *campestris* FE58	DSF biosensor strain, Rif^{R}, Tc^{R}	Wang et al., 2004
Xanthomonas oryzae pv. *oryzae* PXO99^{A}	Plant pathogen, causes bacterial leaf blight disease in rice	Steven et al., 2008
E. coli		
DH5α λpir	*supE44 Dlacu169 (f80 lacZDM15) hsdR17 recA1 endA1 gyrA96 thi-1 relA1* λpir	Lab strain
S17-1 λpir	Tp^{R} Sm^{R} *recA thi pro hsdR*$^{-}$M^{++} *recA*::RP4-2-Tc::Mu Km::Tn7 λpir	Lab strain
Plasmid		
pJQ200SK	Suicide cloning vector, Gm^{R}	Quandt and Hynes, 1993
pJQ-*rpfF*	pJQ200SK derivative carrying two flanking fragments of *rpfF*, Gm^{R}	This study
pJQ-*rpfG*	pJQ200SK derivative carrying two flanking fragments of *rpfG*, Gm^{R}	This study
pJQ-*rpfC*	pJQ200SK derivative carrying two flanking fragments of *rpfC*, Gm^{R}	This study

Generation of In-Frame Deletion Mutants

In-frame deletion plasmids were constructed by amplifying the flanking regions of specific genes by polymerase chain reaction (PCR) using Tks Gflex DNA Polymerase (TaKaRa Bio Inc., Kusatsu, Japan) and OH23 genomic DNA as the template according to the manufacturer's instructions. Briefly, PCR amplification was performed using 30 PCR cycles consisting of denaturation at 98°C for 10 s, annealing at 55°C for 15 s, and elongation at 68°C for 1 min on a Bio-Red S1000 thermal cycler. The suicide vector pJQ200SK was digested with *Xba*I and *Bam*HI (Thermo Fisher Scientific), and the target PCR fragments were ligated into the suicide vector using In-Fusion HD Cloning Plus (TaKaRa Bio Inc.). The recombinant vectors were transformed into *E. coli* DH5αλpir and confirmed using the universal primers M13F/M13R. The resulting plasmids were introduced into *L. brunescens* by conjugation. The deletion mutants Δ*rpfF*, Δ*rpfC*, and Δ*rpfG* were selected for double homologous recombination events because the suicide vector contained a *sacB* counter-selectable marker (Quandt and Hynes, 1993). Finally, all mutants were confirmed by PCR using specific primers (**Table 2**).

Growth Measurements

Lysobacter brunescens OH23 and the *rpf* mutants were cultured in NB medium at 28°C with shaking at 180 rpm until the OD_{600} was approximately 1.0 [which corresponds to approximately 10^9 CFU/ml (Colony Forming Units/ml)]. Then, 1 ml of culture for each strain was transferred into 50 ml of new liquid NB medium. The cultures were then incubated at 28°C with shaking at 180 rpm. To measure the growth, the OD_{600} value was determined every 12 h for each culture using a BioPhotometer Plus (Eppendorf, Germany) until each culture reached stationary stage. Three replicates were performed for each treatment, and the experiment was repeated three times.

Bioassay for DSF Activities in a DSF Reporter Strain

The fermentation and isolation of *Lb*DSF was assessed as previously described (Han et al., 2015). After extracting the DSF-dependent quorum-sensing signals in *L. brunescens* OH23,

TABLE 2 | Primers used in this study.

Primer name	Sequence (5′ → 3′)	Amplicon size (bp)	Usage
rpfF-1	CGAATTCCTGCAGCCCGGGGGATCCGCTGCTGCCATCGCGCAAGC	535	*rpfF* deletion
rpfF-2	GGCATCAGGCCGACATGCGAGTGGAAGTAGAG		
rpfF-3	TCGCATGTCGGCCTGATGCCGATGATCACGGATCCGGACC	535	
rpfF-4	CTGCCGCGGCAGCGGCCGCTCTAGATCGCATCGATCGCTGC		
rpfG-1	CGAATTCCTGCAGCCCGGGGGATCCACCGGCCAGCAGACCCCAGGA	535	*rpfG* deletion
rpfG-2	GTGGGGCAATGGGCTGGAGTGAACGCGCTGCGCGCCGCCTAC		
rpfG-3	ACTCCAGCCCATTGCCCCACATGCGGATAC	535	
rpfG-4	CTGCCGCGGCAGCGGCCGCTCTAGACCTCGGTGTCGGCATCGACCG		
rpfC-1	TCCTGCAGCCCGGGGGATCCTCGAAGGCGACGCGTTGGGTG	528	*rpfC* deletion
rpfC-2	TGAACGCGTGATCATCGGCATCAGGCCGTGGCGGCATCG		
rpfC-3	GATGATCACGCGTTCACTCCAGCCCCGGCCGTTG	528	
rpfC-4	GCGGCAGCGGCCGCTCTAGAATGCCCGAGGACGAGGTCCG		
M13-F	TGTAAAACGACGGCCAGT		Confirmation of vector construction
M13-R	CAGGAAACAGCTATGACC		
RT-$pilA_1$-F	AAGCCGAACGTCCAGATATC	127	$pilA_1$ expression detection
RT-$pilA_1$-R	GGCTGGAATTCGAGGAATAC		
RT-*recA*-F	GTCACCGAAATCCTCTATGG	164	
RT-recA-R	GGGTTGTCCTTCATGTACTG		

we performed a DSF bioassay, as described previously with modifications (Wang et al., 2004). Briefly, *L. brunescens* OH23 and the Δ*rpfF*, Δ*rpfC*, and Δ*rpfG* mutants were grown in NB liquid medium (25 L liquid medium in a CRJ-50D fermenter, twice, for a total of 50 L) at 28°C at 180 rpm until the culture reached 2×10^9 CFU/ml (OD_{600} = approximately 2.0). The culture broth was centrifuged at 12,000 rpm for 10 min, and the supernatant was extracted with the same volume of ethyl acetate. The extracted organic phase was evaporated at 47°C, and the dry crude extract was partitioned using methanol and petroleum ether (100 ml each, three times). The petroleum ether phase was evaporated at 47°C, and the resulting oil (2.1 g) was dissolved in 10 ml of dimethyl sulfoxide (DMSO). The DSF-reporter strain, *Xcc* FE58, was grown in liquid NYG medium (5.0 g peptone, 3.0 g yeast extract, 20.0 g glycerol, and 1.0 L water, pH 7.2) for 2 days until the culture reached 3×10^9 CFU/ml (OD_{600} = approximately 3.0).

The bioassay plates were prepared using the following steps. First, 0.8 g agarose powder was added to 100 ml 0.5 × NYG liquid medium. The medium was heated until the agarose was resolved, at which point 60 μl of X-gluc (60 mg/ml) and 2 ml of the reporter strain *Xcc* FE58 culture (3×10^9 CFU/ml) were added into the NYG agarose medium (the medium was cooled to 42°C before use). This medium was used to prepare the 90-mm bioassay plates. Then, 5 μl of the DSF crude extract (10 mg crude extract resuspended in 200 μl of DMSO) from *L. brunescens* OH23, Δ*rpfF*, Δ*rpfC*, or Δ*rpfG* mutants was added to each well. The bioassay plates were incubated at 28°C for 24 h. The quantification of *Lb*DSF was assessed as previously described (Wang et al., 2004). In brief, DSF activity was confirmed by the presence of a blue halo around the well and measured using the formula DSF (unit/ml) = $0.134 \times e^{(1.9919W)}$, where *W* is the diameter of the blue halo zone and the width of the blue halo zone was increased while adding more exogenous *Lb*DSF (**Figure 2B**).

One unit of DSF is equivalent to a 1-cm-diameter blue halo zone formed by the addition of 0.18 ± 0.07 μg exogenous *Lb*DSF. We also added DMSO to the bioassay plate as a negative control. Three replicates were performed for each treatment, and the experiment was repeated three times.

Isolation and Identification of *Lb*DSF

The crude DSF extract was purified using HPLC. The HPLC detection conditions were as follows: reverse-phase HPLC (Shimadzu MS-2020, Tokyo, Japan) at 210 nm using a C-18 column (250 × 4.6 mm, Phenomenex). The mobile phase was 80% methanol in H_2O from 0 to 13 min, 100% methanol in H_2O from 13 to 20 min, and 80% methanol in H_2O from 20 to 30 min (H_2O containing 0.04% trifluoroacetic acid). The fraction corresponding to *Lb*DSF appeared at 11.5 min.

Fractions containing the desired compound were evaporated to dryness under reduced pressure. The purified compound (4.3 mg) was dissolved in chloroform and characterized by mass spectrometry and NMR. High-resolution ESI-MS of the purified compound was performed in an AB (QTRAP 6500) instrument. The samples were directly infused into a mass spectrometer and analyzed in negative ion mode using a Turbo Ion Spray source. The NMR spectra (^{1}H NMR and ^{13}C NMR) were recorded in CD_3OD using an AVANCE 600 (Bruker Company, Germany) instrument with a standard pulse program.

^{1}H NMR (600 MHz, $CDCl_3$): δ 2.35 (t, 2H, *J* = 7.8 Hz), 1.63 (qt, 2H, *J* = 7.2 Hz), 1.51 (sept, 1 H, *J* = 6.6 Hz), 1.37–1.24 (m, 16 H), 1.15 (m, 2 H), and 0.86 (d, 6 H, *J* = 6.6 Hz).

^{13}C NMR (150 MHz, $CDCl_3$): 179.97, 39.05, 34.01, 29.93, 29.69, 29.63, 29.59, 29.42, 29.23, 29.05, 27.97, 27.41, 24.67, and 22.65.

MS (ESI): calculated for $C_{15}H_{29}O_2$ $[M\text{-}H]^-$ 241.2173, found 241.2.

Effect of the DSF-Dependent Quorum-Sensing System on XSAC Production

The ability of the wild-type and DSF mutants to produce XSAC was measured by an anti-*Xanthomonas* activity assay (diameter of inhibition zone) and analyzed using the agar diffusion method as described below. Pathogenic strains of *Xanthomonas*, including *X. oryzae* pv. *oryzae* PXO99^{A}, *X. oryzae* pv. *oryzae* RS105, *X. oryzae* pv. *oryzae* KACC10331, *X. campestris* pv. *campestris* 8004, and *X. axonopodis* pv. *glycines* 12-2, were individually incubated in NB liquid medium until the culture OD_{600} was approximately 1.0. *L. brunescens* OH23, and its derived mutants (Δ*rpfF*, Δ*rpfC*, and Δ*rpfG* mutants) were incubated in NB liquid medium or NB liquid medium supplemented with 2 μM *Lb*DSF until approximately 1.5–2.0 × 10^9 CFU/ml (OD_{600} = approximately 1.5–2.0). The cultures of *L. brunescens* OH23, Δ*rpfF*, Δ*rpfC*, and Δ*rpfG* were centrifuged, and the supernatants were incubated at 85°C for 30 min. For each pathogenic strain of *Xanthomonas* (**Table 1** and **Supplementary Table S1**), 100 ml of liquefied NB solid medium was incubated at 45°C for 30 min, mixed with 10^8 cells, and then poured into plates. Then, 30 μl of supernatant from the cultures was spotted onto the selective plates. All plates were cultured at 28°C, and the zones of inhibition on the plates were photographed and compared after 2 days. XSAC production was confirmed by the diameter of the inhibition zone, and all of the data regarding the inhibition zone were subtracted from the diameter of the oxford cup. Three replicates were performed for each treatment, and the experiment was repeated three times.

Pathogenicity Assays *in vivo*

Oryza sativa ssp. *indica* rice cultivars IR24 and *X. oryzae* pv. *oryzae* PXO99^{A} were used in the pathogenicity assay. *O. sativa* ssp. *indica* rice cultivars IR24 were grown under a 12-h light/dark cycle at 25°C with approximately 70% relative humidity for 2 months. The preparation of the supernatants from cultures of *L. brunescens* OH23, Δ*rpfF*, Δ*rpfC*, and Δ*rpfG* is described above. The leaves of IR24 plants were detached and dipped in the liquid culture of *X. oryzae* pv. *oryzae* PXO99^{A} at a concentration of approximately 0.5 × 10^9 CFU/ml (OD_{600} = approximately 0.5) for 1 h. To determine the XSAC production and activity of wild-type OH23, Δ*rpfF*, Δ*rpfC*, and Δ*rpfG*, and chemically complemented strains, *X. oryzae* pv. *oryzae* PXO99^{A}-infected rice leaves were treated with the respective supernatants every 24 h. For the negative control, *X. oryzae* pv. *oryzae* PXO99^{A}-infected rice leaves were treated with NB medium. IR24 plants were grown in a glasshouse with the same conditions as above, and lesion lengths were measured and photographed at 7 dpi. Three replicates were performed for each treatment, and the experiment was repeated three times.

Detection and Comparison of Colony Morphology in *L. brunescens*

Single colonies of wild-type OH23, Δ*rpfF*, Δ*rpfC*, and Δ*rpfG* strains were inoculated on NYG plates or NYG plates containing 5 μM *Lb*DSF for 3 days at 28°C. Then, the colony morphology of each strain was photographed and compared. Three replicates were used for each treatment, and the experiment was repeated three times.

Observation of Surface Motility

The surface motility assay of *L. brunescens* wild-type OH23, Δ*rpfF*, Δ*rpfC*, and Δ*rpfG* strains was performed as previously described (Song et al., 2017). Briefly, NB semi-solid medium containing 0.3% agar was used for surface motility assays, and 2.5 μl of *L. brunescens* wild-type OH23 or the derived mutants (10^9 CFU/ml, OD_{600} was approximately 1.0 for all strains) was spotted onto the surface of NB semi-solid medium plates or NB semi-solid medium plates containing 5 μM *Lb*DSF. The plates were incubated at 28°C for 4 days, and then the surface motility of each strain was photographed, measured, and compared. Three replicates were performed for each treatment, and the experiment was repeated three times.

RNA Extraction, Reverse Transcription PCR, and Real-Time-PCR

Lysobacter brunescens OH23, Δ*rpfF*, Δ*rpfC*, and Δ*rpfG* mutants were each grown in 5 ml of NA medium to an OD_{600} of approximately 1.0. Three milliliters of cells was transferred into a sterile centrifuge tube and centrifuged for 3 min at 12,000 rpm. RNA was extracted from the strains using TRIzol solution (TaKaRa Biocompany) following the manufacturer's instructions. For DNA removal and reverse transcription PCR, the PrimerScript RT Reagent Kit with the gDNA Eraser Kit (TaKaRa Biocompany) was used in this study. For the real-time PCR assay, a QuantStudio 6 Flex Real-Time PCR System (Thermo Fisher Scientific) was used to detect gene expression. The gene expression was calculated by the $2^{-\Delta\Delta CT}$ method. The primers for real-time PCR are listed in **Supplementary Table S2**. Three replicates were performed for each treatment, and the experiment was repeated three times.

Data Analysis

Statistical analyses were calculated using SPSS (Statistical Package, Version 21.0). The variables were subjected to Student's *t*-test and tested for significance at $P < 0.05$ (*), $P < 0.01$ (**), $P < 0.001$ (***), and $P < 0.0001$ (****).

RESULTS AND DISCUSSION

Identification of the Small Signaling Molecule *Lb*DSF in *L. brunescens*

To identify the structure of the DSF signal in *L. brunescens* OH23, we harvested the *L. brunescens* culture from a 50-L fermenter system (CRJ-50D), collecting 25 L each time for a total of 50 L, and we extracted the crude DSF from the supernatant using the same method as previously described (Han et al., 2015). The methods of separation and identification of the DSF from OH23 were described previously (Wang et al., 2004). Briefly, we collected samples every 2 min from HPLC, concentrated every fraction by evaporation, and added 1 μg of every sample

into the DSF bioassay plates containing *Xcc* FE58 and X-gluc. The formation of a blue halo in the plates indicated the induction ability of each fraction. The results showed that the samples from 10.01 to 12.00 min induced *gusA* expression (**Figures 1A,B**). The DSF activity from 10.01 to 12.00 min was 0.53 ± 0.20 units. Furthermore, P_{engXCA}-*gusA* was minimally induced by the addition of the samples from 0.01–10.00 or 12.01–16.00 min, and blue halo zones were not observed. To further confirm these results, we purified 1 μg of compound from these four fractions and detected the induction abilities of each fraction using the DSF bioassay system. The results of this assay revealed that P_{engXCA}-*gusA* activation was induced only by adding the purified compound from fraction c, which exhibited a DSF activity of 1.98 ± 0.69 units.

We also examined whether the compound from these fractions enhanced the anti-*Xanthomonas* activity in *L. brunescens* OH23. We collected, dried, and dissolved every fraction in DMSO. The supernatant from strain OH23 formed a zone of inhibition in the growth of *X. oryzae* pv. *oryzae* RS105 that was 2.15 ± 0.09 cm in diameter. The zone of inhibition increased to 2.77 ± 0.12 cm after the addition of 2.0 μM purified fraction c (**Supplementary Figure S3**). Moreover, the zone of inhibition did not significantly increase when the purified compounds from fraction a, fraction b, fraction d, or the DMSO control were added (**Supplementary Figure S3**). These results demonstrated that only the compounds from fraction c, collected at 11.5 min, enhanced the inhibition activities in strain OH23 (**Supplementary Figure S3**).

To identify the structure of the unidentified DSF compounds, we first collected approximately 2.6 mg of the compounds exhibiting the highest DSF activity (fraction c, 11.5 min) from 50 L of crude supernatant and resuspended it in chloroform for NMR analysis. After purification of the compounds from fraction c, mass spectrometry analysis of the purified compound revealed a main *m/z* fraction at 241.2 Da, which was consistent with the expected molecular weight of *Le*DSF3, $[M\text{-}H]^-$ = 241.2173 Da (**Figure 1C**). In contrast with most DSFs, the structure of *Le*DSF3 consisted of a saturated aliphatic chain, which was formed by a tetradecanoic acid structure with a methyl group linked to carbon 13. To confirm the presence of *Le*DSF3, ^{1}H and ^{13}C NMR spectra were collected, and all signals were assigned (**Supplementary Figures S2A,B**). In agreement with the expected structure, no signal was detected between 7 and 5 ppm in the ^{1}H NMR spectrum, indicating that the purified compound was not an unsaturated aliphatic chain. A doublet with a 6.6-Hz coupling constant appeared at 0.86 ppm in the ^{1}H NMR spectrum, corresponding to the methyl groups. The protons in the alpha and beta position to the carboxylic acid were observed at 2.35 and 1.63 ppm as a triple and a quintuplet, respectively, whereas the proton of carbon **13** appeared at 1.51 ppm as a septuplet. ^{13}C NMR revealed a signal at 179.97 ppm, corresponding to the carboxylic acid. Carbon **2** was detected at 34.01 ppm, whereas the methyl groups appeared at 22.65 ppm in the ^{13}C NMR spectrum. In agreement with the ^{1}H NMR spectrum, no signal was detected between 180 and 120 ppm in the ^{13}C NMR spectrum, discarding the possibility of an unsaturated chain. Therefore, the primary compound from fraction c, named *Lb*DSF, was determined to be 13-methyltetradecanoic acid (**Figure 1C**), which was originally reported in *L. enzymogenes* (Han et al., 2015).

Identification of the *rpf* Gene Cluster in *L. brunescens*

As mentioned above, DSF family signals have been reported in different *Xanthomonas* bacteria. As a result, we compared and sequenced the genome of OH23 to identify genes potentially related to the *Lb*DSF biosynthesis pathway. By blasting all *rpf* operon protein sequences[1], we found that *rpf* proteins were highly conserved in *Lysobacter* spp. NCBI BLASTp analysis revealed that the Rpf proteins from *L. brunescens* had the highest homology to those of *L. enzymogenes* (taxid: 69), and the levels of protein identity were 72% (*rpfF*), 61% (*rpfC*), and 89% (*rpfG*). According to our BLASTp results, RpfF is an enoyl-CoA hydratase involved in the biosynthesis of DSF (**Figure 2A**). Accordingly, the DSF activity by wild-type OH23 was 0.88 ± 0.28 units, and the mutation of the *rpfF* gene abolished DSF production in *L. brunescens* (**Figure 2B**). RpfC is the hybrid histidine sensor kinase of the Rpf two-component regulatory system, which negatively regulates DSF production. Therefore, DSF accumulated in the Δ*rpfC* mutant (**Figures 2A,B**), and DSF production of Δ*rpfC* was 5.91 ± 2.29 units. RpfG is the response regulator of the Rpf two-component regulatory system and is responsible for signal transduction. Compared to wild-type OH23, DSF production was not altered in the Δ*rpfG* mutant (**Figures 2A,B**), and the DSF activity of the Δ*rpfG* was 0.63 ± 0.14 units.

Mutation of *rpfF* abolished the ability to produce DSFs in *X. campestris* pv *campestris*, which suggested that *rpfF* were essential for DSF production (Deng et al., 2011). In *X. oryzae* pv *oryzae*, the DSF production increased in the mutant of *rpfC*, and the DSF sensor kinase RpfC negatively regulated the biosynthesis of DSF (He et al., 2010; Deng et al., 2011). Taken together, these results indicate that the model for DSF production and signal transduction in *L. brunescens* is highly similar to that of *L. enzymogenes* and *X. oryzae* pv *oryzae* (He et al., 2010; Qian et al., 2013). In addition, the growth of wild-type OH23 and the *rpf* mutants was measured. The results demonstrated that the *rpf* mutants had growth similar to that of the wild-type strain under the tested conditions (**Figure 2C**).

DSF-Dependent Quorum-Sensing System Positively Regulates Antibiotic Biosynthesis Through the Small Signaling Molecule *Lb*DSF and the RpfC/RpfG Two-Component System

In previous findings, the genus *Xanthomonas* and several Gram-negative bacteria used the DSF-dependent quorum-sensing system to mediate a diverse range of physiological activities related to virulence, motility, biofilm, and extracellular enzyme, and the DSF-dependent quorum-sensing system was also required for the biosynthesis of HSAF in *L. enzymogenes* (Qian et al., 2013; Guo et al., 2019). To investigate the

[1]https://blast.ncbi.nlm.nih.gov/Blast.cgi

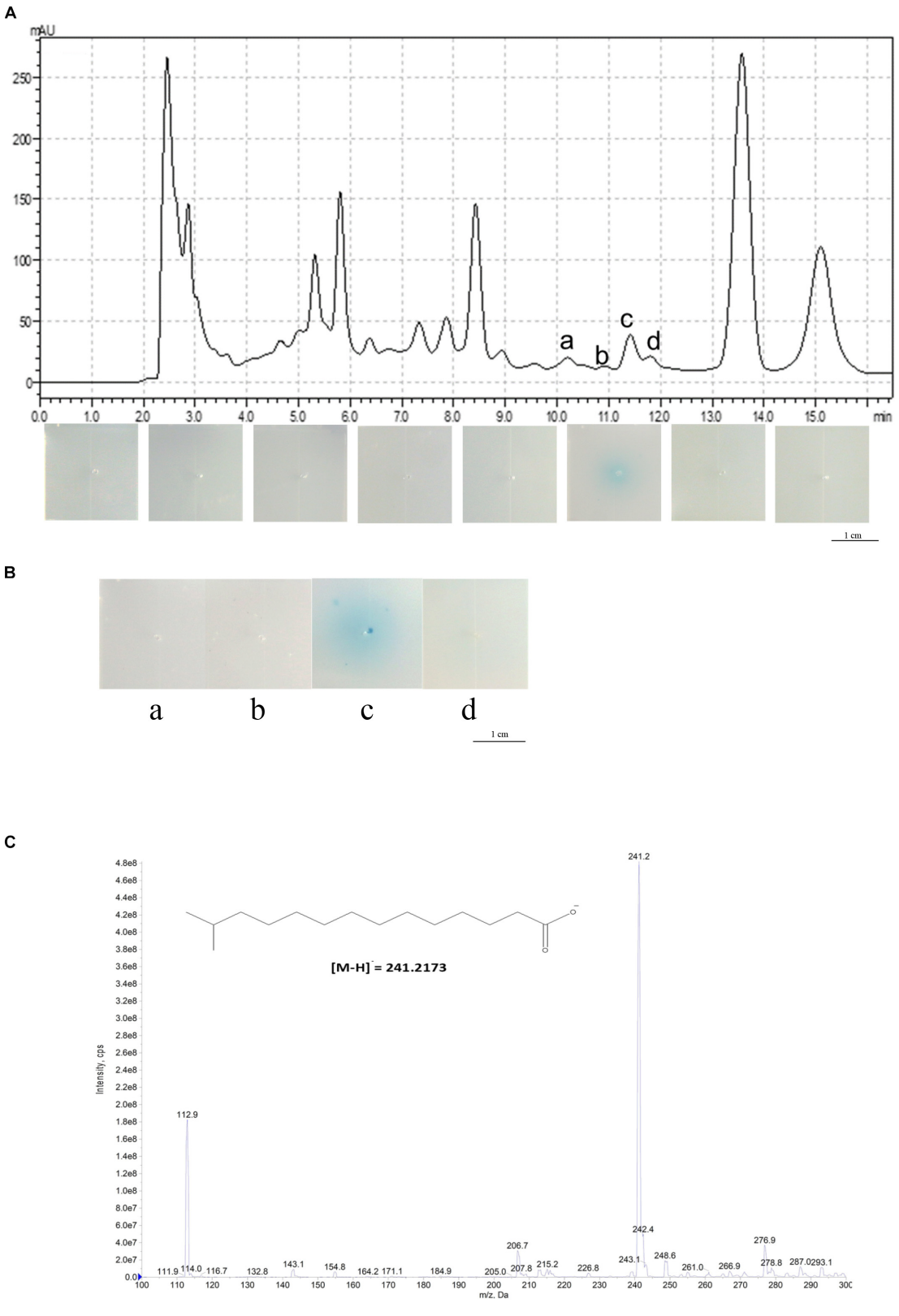

FIGURE 1 | Structural determination of the DSF from *L. brunescens* OH23. **(A)** HPLC analysis of the *L. brunescens* crude supernatant. **(B)** Bioassay of the four purified HPLC fractions a, b, c, and d from 10 to 12 min. The blue halo indicates DSF activity. **(C)** Mass spectrometry analysis of *Le*DSF3 (calculated $[M-H]^-$ = 241.2173 Da, observed 241.2 Da).

A

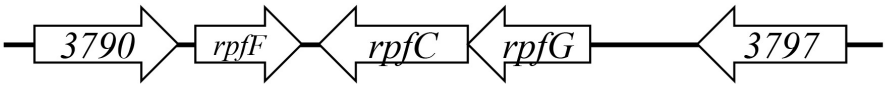

Gene	#nucleotides	#aa	Blastp Homologue	Identity	E-value	GenBank accession number
rpfF	4319513-4320454	313	enoyl-CoA hydratase	72%	1e-154	MK532476
rpfC	4322701-4320464	745	hybrid sensor histidine kinase	61%	0.0	MK532477
rpfG	4323771-4322698	357	response regulator	89%	0.0	MK532478

B

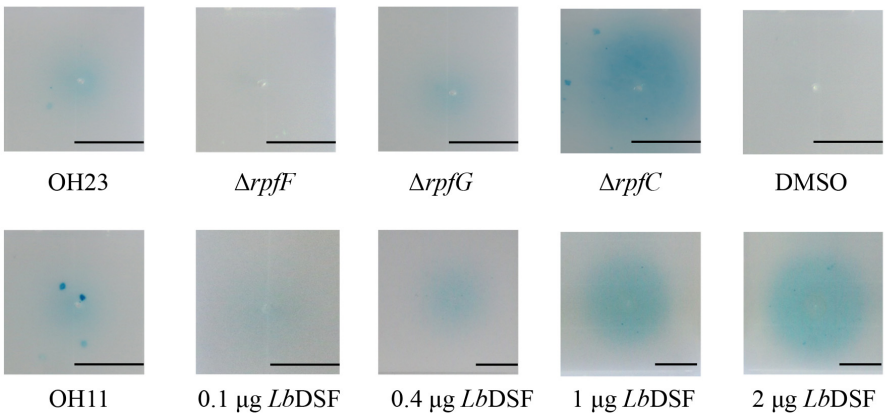

C

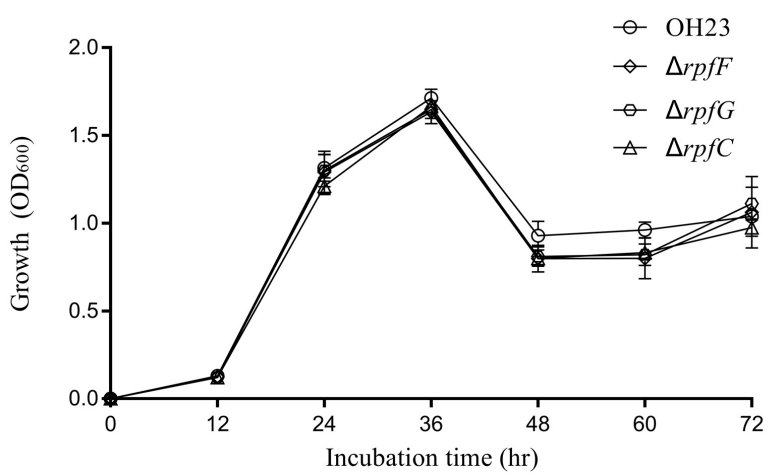

FIGURE 2 | Location of the *rpf* genes in the genome of *L. brunescens* OH23 and the DSF activity of the different *L. brunescens* OH23, *rpf* mutants, or *L. enzymogenes* OH11. **(A)** BLASTp comparison between the proteins encoded by the *rpf* genes (*rpfF*, *rpfC*, and *rpfG*) of *L. brunescens* and *L. enzymogenes*. The protein similarity was compared using BioEdit7.0.9.0. **(B)** The DSF production ability of strain OH23 and its corresponding *rpf* mutants. **(C)** The growth of wild-type OH23 and its corresponding *rpf* mutants.

function of the DSF-dependent quorum-sensing system in the biosynthesis of XSAC, we tested the anti-*Xanthomonas* abilities of the OH23 wild-type, Δ*rpfF*,Δ*rpfG*, Δ*rpfC*, and chemically complemented strains (mutants supplemented with *Lb*DSF). As shown in **Figures 3A,B** and **Supplementary Figures S4–S7**, wild-type OH23 inhibited the growth of *X. oryzae* pv. *oryzae*

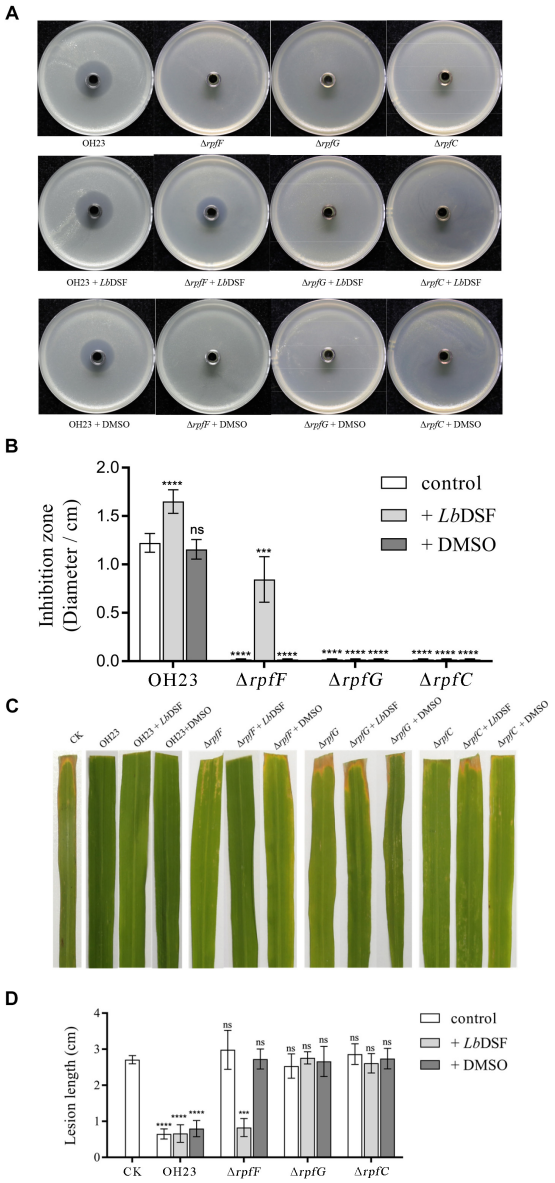

FIGURE 3 | Anti-*Xanthomonas* activity of *L. brunescens* OH23 and its corresponding *rpf* mutants with or without *Lb*DSF addition. **(A)** Supernatants from *L. brunescens* OH23 or *rpf* mutant cultures with or without exogenous *Lb*DSF supplementation were tested for their antimicrobial activity against *X. oryzae* pv. *oryzae* PXO99^{A}. **(B)** The analysis of the images of *X. oryzae* pv. *oryzae* PXO99^{A} growth inhibition zones shown in A. **(C)** Representative images of IR24 leaves infected with *X. oryzae* pv. *oryzae* PXO99^{A} and treated with test supernatants. CK is the control, which was treated with water every 24 h. Images were taken 7 days post-inoculation (dpi). **(D)** Analysis of the lesion lengths on IR24 rice leaves caused by *X. oryzae* pv. *oryzae* PXO99^{A} infection with or without treatment with test supernatants, as shown in **C**. Different numbers of star (*) above the bars indicate a significant difference between the wild-type strain OH23 and mutant strains (ns: not sigificant, $^{***}P < 0.001$; $^{****}P < 0.001$, *t*-test).

PXO99^{A} (*Xoo* PXO99^{A}), *X. oryzae* pv. *oryzae* RS105 (*Xoo* RS105), *X. oryzae* pv. *oryzae* KACC 10331 (*Xoo* KACC 10331), *X. campestris* pv. *campestris* 8004 (Xcc 8004), and *X. axonopodis* pv. *glycines* 12-2 (*Xag* 12-2). The diameters of the inhibition zones were 1.22 ± 0.10 cm, 1.75 ± 0.15 cm, 1.95 ± 0.24 cm, 0.29 ± 0.09 cm, and 1.50 ± 0.14 cm, respectively. The Δ*rpfF*,Δ*rpfG*, and Δ*rpfC* mutants lost the ability to inhibit all tested *Xanthomonas* strains, demonstrating that these mutants were impaired in the biosynthesis of XSAC (**Figure 3A** and **Supplementary Figures S4–S7**). To determine the genes relevant to the XSAC biosynthesis, we analyzed the putative operon that related to the biosynthesis of XSAC (data not shown), and 8 genes of 13 genes were indispensable for the biosynthesis of XSAC (**Supplementary Figures S8A,B**). Furthermore, the q-PCR results shown that the expression of all 13 genes, the genes for XSAC biosynthesis, were dramatically reduced in the Δ*rpfF* mutant (**Supplementary Figure S8C**).

In *L. enzymogenes*, HSAF biosynthesis gene *pks-nrps* expression was reduced ∼10 times, and HSAF production was also dramatically reduced in the Δ$rpfF_{OH11}$ mutant (Qian et al., 2013). Taken together, the DSF quorum-sensing XSAC biosynthesis regulation model in *L. brunescens* OH23 was similar to the DSF quorum-sensing HSAF biosynthesis regulation model in *L. enzymogenes* OH11, and the DSF quorum-sensing system positively regulated the biosynthesis of XSAC (Qian et al., 2013; Han et al., 2015).

To further address whether the small signaling molecule *Lb*DSF restored XSAC biosynthesis in the *rpf* mutants, we added *Lb*DSF (2 μM) to the mutant culture in liquid NB medium, incubated the culture at 28°C at 180 rpm, and then tested the anti-*Xanthomonas* activity of the supernatant. When *Lb*DSF was added into the cultures, the growth inhibitory ability of wild-type OH23 increased 35.01, 19.54, 8.97, 16.86, and 27.15% against *Xoo* PXO99^{A}, *Xoo* RS105, *Xoo* KACC 10331, *Xcc* 8004, and *Xag* 12-2, respectively (**Figure 3A** and **Supplementary Figures S4–S7**). *Lb*DSF addition restored the anti-*Xanthomonas* activity in the Δ*rpfF*, and the diameter of the zones of inhibition were 0.84 ± 0.22 cm, 1.71 ± 0.16 cm, 0.36 ± 0.10 cm, 0.25 ± 0.11 cm, and 1.18 ± 0.16 cm against *Xoo* PXO99^{A}, *Xoo* RS105, *Xoo* KACC 10331, *Xcc* 8004, and *Xag* 12-2, respectively (**Figure 3A** and **Supplementary Figures S4–S7**). Additionally, exogenous *Lb*DSF had no effect on the anti-*Xanthomonas* activity in Δ*rpfC* and Δ*rpfG* (**Figure 3A**). These results were consistent with the fact that the small signaling molecule *Lb*DSF is a transduction signal in the *L. brunescens rpf* system, where RpfF is involved in DSF biosynthesis, and RpfC/RpfG is the two-component system involved in signal transduction.

We then investigated whether all of the supernatants mentioned above had inhibitory activities *in vivo*. *Xoo* PXO99^{A}-infected IR24 rice leaves were treated with the supernatants every 24 h, and lesion lengths were measured at 7 dpi. As shown in **Figures 3C,D**, the negative control was only treated with NB medium, and the lesion length was 2.92 ± 0.41 cm. However, the wild-type OH23 treatment group showed significantly decreased lesion lengths (0.70 ± 0.21 cm). The addition of exogenous *Lb*DSF or DMSO to the culture of wild-type OH23 was shown to significantly influence the lesion length relative to the negative control. For the Δ*rpfF* treatment group, exogenous *Lb*DSF restored the anti-*Xanthomonas* activity, and the lesion length was 0.83 ± 0.23 cm. However, both the Δ*rpfG* and Δ*rpfC* treatment

groups exhibited similar lesion lengths as the negative control. The results from the *in vivo* plant assays were consistent with the results from the anti-*Xanthomonas* ability on plates.

In *L. enzymogenes*, *Le*DSF3 was 13-methyltetradecanoic acid, and acted as an extracellular signal to positively regulate the biosynthesis of HSAF; the two-component regulatory system RpfC/RpfG sensed and transduced *Le*DSF3; and the global regulator Clp was downstream of the *Le*DSF quorum-sensing system and also played a positive role in regulating the biosynthesis of HSAF and WAP-8294A2 (Han et al., 2015; Xu et al., 2016). To further investigate the function of *clp* in *L. brunescens* OH23, the Clp_{OH11} amino acid sequence was compared with the draft genome sequence of *L. brunescens* OH23, and Peg.2300 (Clp) shared 83% similarity to that of Clp_{OH11} at the amino acid level (**Supplementary Figure S9A**). Next, the anti-*Xanthomonas* abilities of Δ*clp* and its complementary strain were tested, and *clp* had no significant effect on biosynthesis of XSAC (**Supplementary Figure S9B**), which revealed that Clp was not involved in the regulation of XSAC biosynthesis. Taken together, these findings indicate that the structure of *Lb*DSF and the regulation of RpfC/RpfG *L. brunescens* were similar to the *Le*DSF quorum-sensing HSAF biosynthesis regulation model in *L. enzymogenes* and a potential novel transcription regulator in the DSF-dependent quorum-sensing system that regulated XSAC biosynthesis in *L. brunescens*.

DSF-Dependent Quorum-Sensing System Affects Colony Morphology in *L. brunescens*

The DSF quorum-sensing system was shown to influence colony morphology in *L. enzymogenes* (Qian et al., 2013). To investigate the function of the DSF-dependent quorum-sensing system in modulating colony morphology in *L. brunescens*, we tested the wild-type OH23 strain and the Δ*rpfF*, Δ*rpfC*, and Δ*rpfG* mutants. As shown in **Figure 4**, the wild-type OH23 displayed round colonies with lobular and spiculated boundaries on NYG plates with an average diameter size of 1.87 ± 0.05 cm. However, the Δ*rpfF*, Δ*rpfC*, and Δ*rpfG* mutants showed smooth colony appearance with an average diameter size of 0.64 ± 0.08 cm under the same growth conditions.

Exogenous *Lb*DSF (2 μM) restored the colony morphology in the Δ*rpfF* when compared to the wild-type OH23 with an average diameter size of 1.32 ± 0.08 cm, whereas the addition of exogenous *Lb*DSF did not influence the colony morphology of the Δ*rpfC* and Δ*rpfG* (**Figure 4**). These results indicate that the DSF-dependent quorum-sensing system is involved in the regulation of colony morphology in *L. brunescens*.

DSF Signaling Controls Surface Motility Through Type IV Pili (T4P) in *L. brunescens*

The DSF-dependent quorum-sensing system was also shown to affect cell motility in *L. enzymogenes* (Qian et al., 2013). To investigate the function of the DSF-dependent quorum-sensing system in regulating motility in *L. brunescens*, we tested

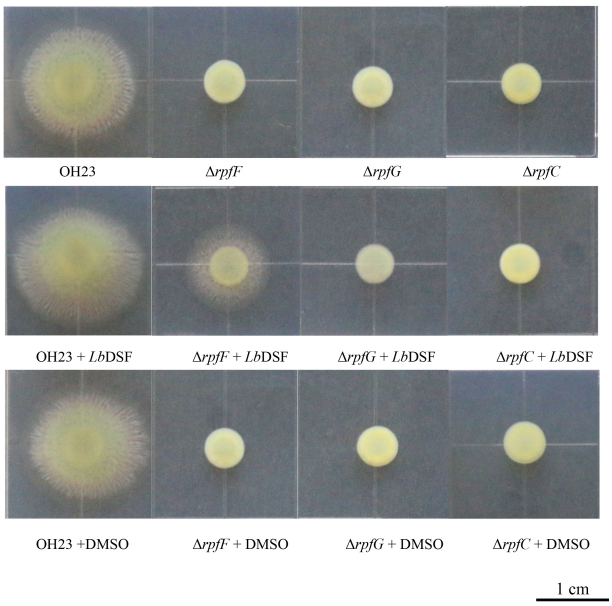

FIGURE 4 | Colony morphology of wild-type OH23 and the *rpf* mutants on NYG plates with or without the exogenous addition of *Lb*DSF. Each strain was grown in NYG liquid medium until the OD_{600} was approximately 1.0. Then, 3 μl of each strain was inoculated onto the surface of NYG plates. The plates were incubated at 28°C for 4 days. For the *Lb*DSF treatment group, the strains were grown in NYG liquid medium containing 2 μM *Lb*DSF, and the NYG plates contained 5 μM *Lb*DSF. Each treatment was completed in triplicate, and the experiment was repeated three times.

the motility of the wild-type OH23, Δ*rpfF*, Δ*rpfC*, and Δ*rpfG* strains. Since OH23, unlike *L. enzymogenes* OH11, does not exhibit twitching motility (data not shown), we analyzed the surface motility of wild-type OH23 and its derivative mutants on NB semi-solid (0.3% agar) motility medium plates for 4 days incubated at 28°C.

As shown in **Figure 5A**, the wild-type OH23 strain was motile in motility medium plates with a typical circular dissemination pattern from the point of inoculation that was 2.78 ± 0.33 cm in size. However, the surface motility of Δ*rpfF*, Δ*rpfC*, or Δ*rpfG* was substantially reduced. These mutants only reached an average surface motility diameter of approximately 0.82 ± 0.11 cm in 4 days, indicating that the mutants had a 73.72% reduction in the diameter of their surface motility zone compared to the wild-type OH23. Exogenous *Lb*DSF (2 μM) restored surface motility in the Δ*rpfF* strain compared to the wild-type OH23 strain with an average surface motility diameter of 2.42 ± 0.10 cm. However, exogenous *Lb*DSF did not exhibit any effect on the surface motility in the Δ*rpfC* and Δ*rpfG* mutants. These results indicate that the DSF-dependent quorum-sensing system is involved in the regulation of surface motility in *L. brunescens*.

Type IV Pili has been shown to be important for surface motility in diverse bacteria. Since the *pilA* gene encodes the major pilin subunit of T4P (Mattick, 2002; Burdman et al., 2011; Wang et al., 2014), we measured $pilA_1$ expression in the wild-type OH23, Δ*rpfF*, Δ*rpfC*, and Δ*rpfG*. As shown

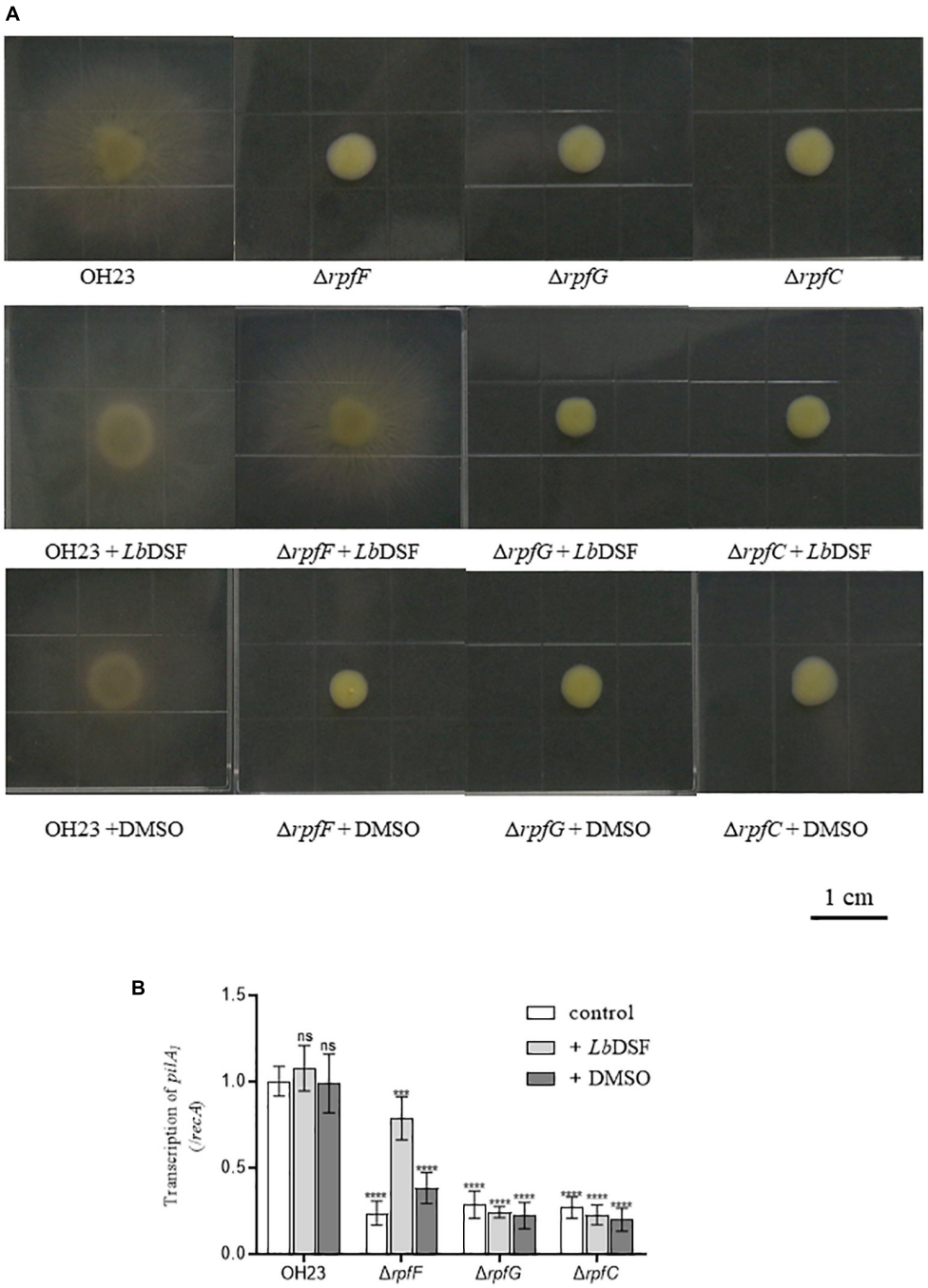

FIGURE 5 | Surface motility of wild-type OH23 and the *rpf* mutants with or without the exogenous addition of *Lb*DSF. **(A)** Surface motility of wild-type OH23 and the *rpf* mutants with or without the exogenous addition of *Lb*DSF. Each strain was grown in liquid NB medium until the culture reached an OD_{600} of approximately 1.0. Then, 3 μl of strain was inoculated onto the surface of NB plates. The plates were inoculated at 28°C for 4 days. For the *Lb*DSF treatment group, the strains were grown in NYG liquid medium containing 2 μM *Lb*DSF. **(B)** $pilA_1$ expression in wild-type OH23 and the *rpf* mutants with or without the exogenous addition of *Lb*DSF. Different numbers of star (*) above the bars indicate a significant difference between the wild-type strain OH23 and mutant strains (ns: not sigificant, ***$P < 0.001$; ****$P < 0.001$, *t*-test).

in **Figure 5B**, $pilA_1$ expression was dramatically decreased in Δ*rpfF*, Δ*rpfC*, and Δ*rpfG*. The addition of exogenous *Lb*DSF (2 μM) partially restored $pilA_1$ expression in the Δ*rpfF* compared to wild-type OH23, while exogenous *Lb*DSF did not influence $pilA_1$ expression in the Δ*rpfC* and Δ*rpfG*. These results indicate that the DSF-dependent quorum-sensing system is involved in the regulation of $pilA_1$ expression in *L. brunescens*.

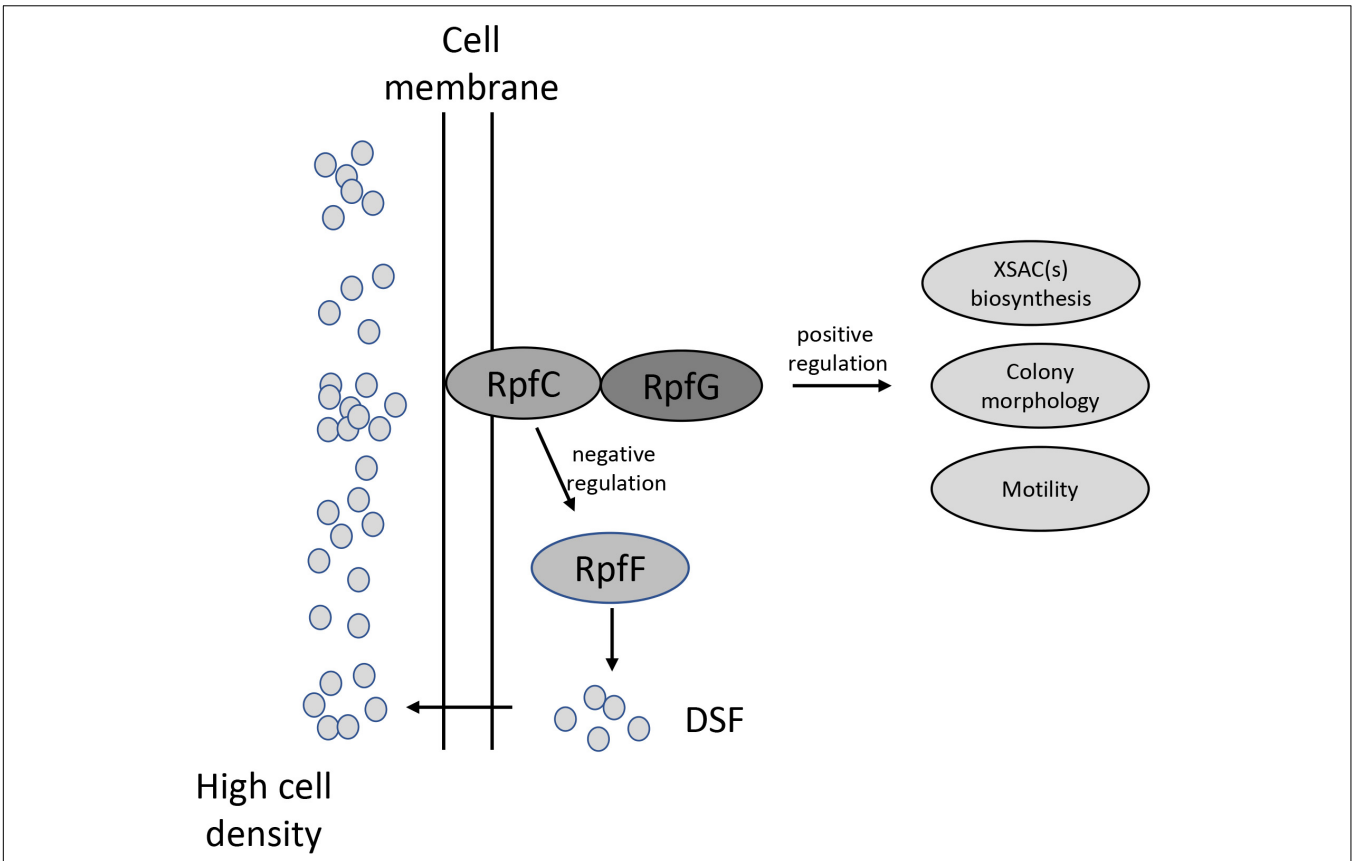

FIGURE 6 | Schematic model of the DSF quorum-sensing system in *L. brunescens*. *Lb*DSF biosynthesis was found to be linked to RpfF (enoyl-CoA hydratase) and was dependent on the two-component regulatory system RpfC (hybrid sensor histidine kinase)/RpfG (response regulator). *Lb*DSF positively regulates XSAC biosynthesis, surface motility, and cell morphology.

The DSF-dependent quorum-sensing system in the *Xanthomonas* genus differs substantially between species and has been shown to positively regulate virulence, biofilm formation, EPS biosynthesis, and adaption. Moreover, specific DSF molecules were related to specific antibiotic HSAF biosynthesis (He et al., 2010; Han et al., 2015). The Rpf system was shown to be activated by adding specific DSF molecules, and EPS production, extracellular xylanase activity, or antibiotic HSAF biosynthesis were restored (He et al., 2010; Han et al., 2015).

CONCLUSION

In this study, we report the role of a quorum-sensing system in the production of a novel XSAC in the ubiquitous environmental bacterium *L. brunescens* (**Figure 6**). Our data revealed that *L. brunescens* OH23 uses a DSF-dependent quorum-sensing molecule to regulate XSAC production. We characterized this DSF compound as 13-methyltetradecanoic acid. This extracellular signal is produced by RpfF and transduced by the RpfC/RpfG two-component regulatory system. This molecule also regulates surface motility and colony morphology. Our findings will be useful in applied genetics and molecular biotechnology, thereby facilitating the improvement of antibiotic production in *Lysobacter* spp., which can potentially be used in the agricultural industry. Furthermore, the tight control that our identified DSF molecule exerts on XSAC expression suggests that *Lysobacter* spp. may produce other quorum-sensing signals that can induce the production of additional novel bioactive compounds.

DATA AVAILABILITY

The datasets generated for this study can be found in Genbank, MK532476, MK532477, and MK532478.

AUTHOR CONTRIBUTIONS

JL, RZ, PL, TJ, YJ, and YZ conducted the experiments. FL designed and conducted the experiments. JL, PL, and FL contributed to the writing of the manuscript. FL revised the manuscript.

FUNDING

This study was supported by the Jiangsu Agricultural Science and Technology Innovation Funds [CX (16) 1049], the Jiangsu

Provincial Key Technology Support Programme (BE2015354), the "948" Project of the Ministry of Agriculture (2014-Z24), the Earmarked Fund for China Agriculture Research System (CARS-28-16), and the China Postdoctoral Science Foundation (2017M610310).

SUPPLEMENTARY MATERIAL

The Supplementary Material for this article can be found online at: https://www.frontiersin.org/articles/10.3389/fmicb.2019.01230/full#supplementary-material

REFERENCES

Abisado, R. G., Benomar, S., Klaus, J. R., Dandekar, A. A., and Chandler, J. R. (2018). Bacterial quorum sensing and microbial community interactions. *mBio* 9:e02331-17. doi: 10.1128/mBio.02331-17

Atlas, R. M. (1997). Handbook of microbiological media. *Q. Rev. Biol.* 2, 364–365.

Barber, C. E., Tang, J. L., Feng, J. X., Pan, M. Q., Wilson, T. J., Slater, H., et al. (1997). A novel regulatory system required for pathogenicity of *Xanthomonas campestris* is mediated by a small diffusible signal molecule. *Mol. Microbiol.* 24, 555–566. doi: 10.1046/j.1365-2958.1997.3721736.x

Burdman, S., Bahar, O., Parker, J. K., and De La Fuente, L. (2011). Involvement of type IV pili in pathogenicity of plant pathogenic bacteria. *Genes* 2, 706–735. doi: 10.3390/genes2040706

Christensen, P., and Cook, F. D. (1978). Lysobacter, a new genus of nonfruiting, gliding bacteria with a high base ratio. *Int. J. Syst. Bacteriol.* 28, 367–393. doi: 10.1099/00207713-28-3-367

Deng, Y. Y., Wu, J. E., Tao, F., and Zhang, L. H. (2011). Listening to a new language: DSF-based quorum sensing in gram-negative bacteria. *Chem. Rev.* 111, 160–173. doi: 10.1021/cr100354f

Guo, W., Gao, J., Chen, Q., Ma, B., Fang, Y., Liu, X., et al. (2019). Crp-like protein (Clp) plays both positive and negative roles in regulating the pathogenicity of bacterial pustule pathogen *Xanthomonas axonopodis* pv. glycines. *Phytopathology* doi: 10.1094/PHYTO-07-18-0225-R [Epub ahead of print].

Han, Y., Wang, Y., Tombosa, S., Wright, S., Huffman, J., Yuen, G., et al. (2015). Identification of a small molecule signaling factor that regulates the biosynthesis of the antifungal polycyclic tetramate macrolactam HSAF in *Lysobacter enzymogenes*. *Appl. Microbiol. Biotechnol.* 99, 801–811. doi: 10.1007/s00253-014-6120-x

Harada, S., Tsubotani, S., Hida, T., Ono, H., and Okazaki, H. (1986). Structure of lactivicin, an antibiotic having a new nucleus and similar biological activities to β-lactam antibiotics. *Tetrahedron. Lett.* 27, 6229–6232. doi: 10.1016/s0040-4039(00)85439-8

Harada, S., Tsubotani, S., Ono, H., and Okazaki, H. (1984). Cephabacins, new cephem antibiotics of bacterial origin. *J. Antibiot.* 37, 1536–1545. doi: 10.7164/antibiotics.37.1536

Hashizume, H., Igarashi, M., Hattori, S., Hori, M., Hamada, M., and Takeuchi, T. (2001). Tripropeptins, novel antimicrobial agents produced by *Lysobacter* sp. I. taxonomy, isolation and biological activities. *J. Antibiot.* 54, 1054–1059. doi: 10.7164/antibiotics.54.1054

He, Y. W., Wu, J. E., Cha, J. S., and Zhang, L. H. (2010). Rice bacterial blight pathogen *Xanthomonas oryzae* pv. oryzae produces multiple DSF-family signals in regulation of virulence factor production. *BMC Microbiol.* 10:187. doi: 10.1186/1471-2180-10-187

Holly, S., Ariel, A. M., Christine, E. B., Michael, J. D., and Dow, J. M. (2000). A two-component system involving an HD-GYP domain protein links cell-cell signalling to pathogenicity gene expression in *Xanthomonas campestris*. *Mol. Microbiol.* 38, 986–1003. doi: 10.1046/j.1365-2958.2000.02196.x

Kato, A., Nakaya, S., Ohashi, Y., and Hirata, H. (1997). WAP-8294A(2), a novel anti-MRSA antibiotic produced by *Lysobacter* sp. *J. Am. Chem. Soc.* 119, 6680–6681. doi: 10.1021/ja970895o

Li, S. J., Calvo, A. M., Yuen, G. Y., Du, L. C., and Harris, S. D. (2009). Induction of cell wall thickening by the antifungal compound dihydromaltophilin disrupts fungal growth and is mediated by sphingolipid biosynthesis. *J. Eukaryot. Microbiol.* 56, 182–187. doi: 10.1111/j.1550-7408.2008.00384.x

Lou, L. L., Qian, G. L., Xie, Y. X., Hang, J., Chen, H., Zaleta-Rivera, K., et al. (2011). Biosynthesis of HSAF, a tetramic acid-containing macrolactam from *Lysobacter enzymogenes*. *J. Am. Chem. Soc.* 133, 643–645. doi: 10.1021/ja105732c

Maddocks, S. E., and Oyston, P. C. F. (2008). Structure and function of the LysR-type transcriptional regulator (LTTR) family proteins. *Microbiol.* 154, 3609–3623. doi: 10.1099/mic.0.2008/022772-0

Mattick, J. S. (2002). Type IV pili and twitching motility. *Ann. Rev. Microbiol.* 56, 289–314. doi: 10.1146/annurev.micro.56.012302.160938

Meyers, E., Cooper, R., Dean, L., Johnson, J. H., Slusarchyk, D. S., Trejo, W. H., et al. (1985). Catacandins, novel anticandidal antibiotics of bacterial origin. *J. Antibiot.* 38, 1642–1648. doi: 10.7164/antibiotics.38.1642

Ono, H., Nozaki, Y., Katayama, N., and Okazaki, H. (1984). Cephabacins, new cephem antibiotics of bacterial origin. *J. Antibiot.* 37, 1528–1535. doi: 10.7164/antibiotics.37.1528

O'Sullivan, J., Mccullough, J. E., Tymiak, A. A., Kirsch, D. R., Trejo, W. H., Principe, P. A., et al. (1988). Lysobactin, a novel antibacterial agent produced by *Lysobacter* sp. I taxonomy, isolation and partial characterization. *J. Antibiot.* 41, 1740–1744. doi: 10.7164/antibiotics.41.1740

Qian, G. L., Wang, Y. L., Liu, Y. R., Xu, F., He, Y. W., Du, L., et al. (2013). *Lysobacter enzymogenes* uses two distinct cell–cell signaling systems for differential regulation of secondary-metabolite biosynthesis and colony morphology. *Appl. Environ. Microbiol.* 79, 6604–6616. doi: 10.1128/AEM.01841-13

Quandt, J., and Hynes, M. F. (1993). Versatile suicide vectors which allow direct selection for gene replacement in gram-negative bacteria. *Gene* 127, 15–21. doi: 10.1016/0378-1119(93)90611-6

Robert, P. R., and Dow, J. M. (2011). Communication with a growing family: diffusible signal factor (DSF) signaling in bacteria. *Trends Microbiol.* 19, 145–152. doi: 10.1016/j.tim.2010.12.003

Steven, L. S., Daniel, D. S., Michael, C. S., Adam, M. P., Pablo, D. R., Seiji, T. (2008). Genome sequence and rapid evolution of the rice pathogen *Xanthomonas oryzae* pv. oryzae PXO99A. *BMC Genomics* 9:204. doi: 10.1186/1471-2164-9-204

Sambrook, J. (2001). *Molecular Cloning, a Laboratory Manual*. New York, NY: Hamlet.

Song, Z. W., Zhao, Y. C., Qian, G. L., Odhiambo, B. O., and Liu, F. (2017). Novel insights into the regulatory roles of gene hshB in *Xanthomonas* oryzae pv. oryzicola. *Res. Microbiol.* 168, 165–173. doi: 10.1016/j.resmic.2016.10.007

Van Houdt, R., Moons, P., Aertsen, A., Jansen, A., Vanoirbeek, K., Daykin, M., et al. (2007). Characterization of a luxI/luxR-type quorum sensing system and *N*-acyl-homoserine lactone-dependent regulation of exo-enzyme and antibacterial component production in Serratia plymuthica RVH1. *Res. Microbiol.* 158, 150–158. doi: 10.1016/j.resmic.2006.11.008

Wang, L. H., He, Y., Gao, Y., Wu, J. E., Dong, Y. H., He, C., et al. (2004). A bacterial cell–cell communication signal with cross-kingdom structural analogues. *Mol. Microbiol.* 51, 903–912. doi: 10.1046/j.1365-2958.2003.03883.x

Wang, Y., Qian, G. L., Liu, F. Q., Shen, Y., and Du, L. (2013). Facile method for site-specific gene integration in *Lysobacter enzymogenes* for yield improvement of the anti-MRSA antibiotics WAP-8294A and the antifungal antibiotic HSAF. *ACS Synth. Biol.* 2, 670–678. doi: 10.1021/sb4000806

Wang, Y. S., Zhao, Y. X., Zhang, J., Zhao, Y., Shen, Y., Su, Z., et al. (2014). Transcriptomic analysis reveals new regulatory roles of Clp signaling in secondary metabolite biosynthesis and surface motility in *Lysobacter enzymogenes* OH11. *Appl. Microbiol. Biotechnol.* 98, 9009–9020. doi: 10.1007/s00253-014-6072-1

Xie, Y., Stephen, W., Shen, Y. M., and Du, L. C. (2012). Bioactive natural products from Lysobacter. *Nat. Prod. Rep.* 29, 1277–1287. doi: 10.1039/c2np20064c

Xu, G., Shi, X. F., Wang, R. P., Xu, H. Y., Du, L. C., Chou, S.-H., et al. (2016). Insights into the distinct cooperation between the transcription factor Clp and LeDSF signaling in the regulation of antifungal factors in *Lysobacter*

enzymogenes OH11. *Biol. Control* 120, 52–58. doi: 10.1016/j.biocontrol.2016.08.006

Zhang, W., Li, Y., Qian, G. L., Wang, Y., Chen, H., Li, Y. Z., et al. (2011). Identification and characterization of the anti-methicillin-resistant *Staphylococcus aureus* WAP-8294A2 biosynthetic gene cluster from *Lysobacter* enzymogenes OH 11. *Antimicrob. Agents Chemother.* 55, 5581–5589. doi: 10.1128/aac.05370-11

Zhao, Y. Y., Qian, G. L., Ye, Y. H., Wright, S., Chen, H., Shen, Y., et al. (2016). Heterocyclic aromatic N-oxidation in the biosynthesis of phenazine antibiotics from *Lysobacter* antibioticus. *Org. Lett.* 18, 2495–2498. doi: 10.1021/acs.orglett.6b01089

Conflict of Interest Statement: The authors declare that the research was conducted in the absence of any commercial or financial relationships that could be construed as a potential conflict of interest.

frontiers in Microbiology

ORIGINAL RESEARCH
published: 19 June 2019
doi: 10.3389/fmicb.2019.01330

AHLs Regulate Biofilm Formation and Swimming Motility of *Hafnia alvei* H4

Yao lei Zhu[1,2], *Hong man Hou*[1,2]*, *Gong liang Zhang*[1,2], *Yi fang Wang*[1,2] and *Hong shun Hao*[2]

[1] School of Food Science and Technology, Dalian Polytechnic University, Dalian, China, [2] Liaoning Key Lab for Aquatic Processing Quality and Safety, Dalian, China

The aim of this study was to evaluate the role of *N*-acyl homoserine lactones (AHLs) in the regulation of swimming motility of *Hafnia alvei* H4 and its biofilm formation on 96-well plate, glass and stainless-steel surfaces. The *luxI* gene, which codes for an enzyme involved in AHL synthesis, was deleted to generate a *luxI* mutant (Δ*luxI*). The mutant produced no AHL, and the relative expression of the *luxR* gene was significantly ($P < 0.05$) decreased. In addition, *q*RT-PCR analysis showed that the relative expression of the *luxR* gene in Δ*luxI* was stimulated by the presence of exogenous AHLs (C4-HSL, C6-HSL, and 3-o-C8-HSL) added at concentrations ranging from of 50–250 μg/ml. Among the three AHLs, C6-HSL had the strongest effect. The ability of Δ*luxI* to form biofilm on 96-well plate, glass and stainless-steel surfaces was significantly reduced ($P < 0.05$) compared with the wild type (WT), but was increased when provided with 150 μg/ml C4-HSL, whereas C6-HSL and 3-o-C8-HSL had no effect. Scanning electron microscopy analysis of the biofilm revealed less bacteria adhering to the surface of stainless-steel and fewer filaments were found binding to the cells compared with the WT. Furthermore, Δ*luxI* also exhibited significant ($P < 0.05$) decrease in the expression of biofilm- and swimming motility-related genes, *flgA*, *motA* and *cheA*, consistent with the results observed for biofilm formation and swimming motility. Taken together, the results suggested that in *H. alvei* H4, C4-HSL may act as an important molecular signal through regulating the ability of the cells to form biofilm, as well as through regulating the swimming motility of the cell, and this could provide a new way to control these phenotypes of *H. alvei* in food processing.

Keywords: *Hafnia alvei*, AHLs, quorum sensing, biofilm, swimming motility

OPEN ACCESS

Edited by:
Tom Defoirdt,
Ghent University, Belgium

Reviewed by:
Maria Cristina D. Vanetti,
Universidade Federal de Viçosa, Brazil
Julia Van Kessel,
Indiana University Bloomington, United States

***Correspondence:**
Hong man Hou
houhongman@dlpu.edu.cn

Specialty section:
This article was submitted to Microbial Physiology and Metabolism, a section of the journal Frontiers in Microbiology

Received: *29 November 2018*
Accepted: *28 May 2019*
Published: *19 June 2019*

Citation:
Zhu Yl, Hou Hm, Zhang Gl, Wang Yf and Hao Hs (2019) AHLs Regulate Biofilm Formation and Swimming Motility of Hafnia alvei H4. Front. Microbiol. 10:1330. doi: 10.3389/fmicb.2019.01330

INTRODUCTION

Quorum sensing (QS) is a cell-to-cell communication system used by bacteria, and it is widely by both Gram-negative and Gram-positive bacteria (Ammor et al., 2008). Bacteria secret several kinds of chemical compounds that can act as signaling molecules [autoinducers (AIs)]. *N*-acyl homoserine lactone (AHL), also known as AI-1, is secreted by Gram-negative bacteria, and the communication mechanism of this compound involves AHL synthase (LuxI) and the transcription factor LuxR, which is responsible for controlling gene expression in the presence of AHLs. The

LuxI/LuxR system has become the model system of AHLs-mediated quorum sensing, and the quorum-sensing system of Gram-negative is based on this system. LuxI synthesizes AHLs and it is encoded by the *luxI* gene. LuxR is encoded by the *luxR* gene, and it acts by binding to AHLs, thereby stimulating the expression of these genes in the presence of AHLs. The LuxI/LuxR complex is responsible for the up- or down-regulation of multiple target genes, such as those that code for pectinase, cellulase, and protease (Swift et al., 2001). Autoinducer-2 (AI-2) is synthesized from 4,5-dihydroxy-2,3-pentanedione (DPD) by LuxS, and it is used by Gram-negative and Gram-positive bacteria in interspecies communication. Peptides and derived peptides, generally serve as signaling molecules in Gram-positive bacteria (Bai and Rai, 2011).

Biofilm is a bacterial self-protection growth pattern and it is formed by the aggregation of bacterial cells within an extracellular matrix, which is mainly made of exopolimers (EPS) (Wang J. et al., 2016), and the adherence of bacterial cells to a solid surface depends on the EPS that the cells secret (Jung et al., 2013). In general, some pathogens and spoilage bacteria can adhere to the solid surfaces that can come into contact with food, such as the surfaces of food processing machines and packaging materials. These bacteria may then form biofilms, and the biofilms will allow the cells to become more resistant to cleaning treatments, and enable them to contaminate the food during subsequent processing (Gounadaki et al., 2008; Bai and Rai, 2011). This will effectively facilitate the transmission of the bacteria to the consumers via the contaminated food, eventually causing infections. Biofilms have been recognized as a frequent source of bacterial infections (Costerton et al., 1999). According to a report by Janssens et al. (2008), nearly 80% of persistent bacterial infections in the US were found to be related to biofilms. The formation of biofilm is a multi-step process, which consists of initial attachment, irreversible attachment, early development of biofilm architecture (microcolony formation), maturation and dispersion (Srey et al., 2013). Quorum sensing appears to be involved in all the steps of the process. Promotion and inhibition of biofilm formation by exogenous AHLs have been reported for *Shewanella baltica* (Zhao et al., 2016), *Serratia* A2 and *Aeromonas* B1 (Zhang et al., 2016), *Vibrio parahaemolyticus* (Bai and Rai, 2016), and *Pseudomonas* sp. HF-1 (Wang et al., 2012), suggesting that QS has a regulatory role in biofilm formation.

H. alvei is a Gram-negative, short-rod-shaped, flagellated bacterium that belongs to the family *Enterobacteriaceae*, which is considered as an opportunistic pathogen of humans and animals (Tan et al., 2014). However, despite being classified as a member of the *Enterobacteriaceae* family, *H. alvei* is still far from being virulent and pathogenic (Vivas et al., 2008). *H. alvei* is a common bacterial food contaminant (Liu et al., 2006), and it has been frequently isolated from spoiled food products, especially in chill-stored proteinaceous raw food, like refrigerated spherical fish paste (Tan et al., 2014), vacuum-packed beef (Bruhn et al., 2004) and raw milk (Viana et al., 2009). The strong tendency of *H. alvei* to adhere to solid surface and to form biofilm has been reported by Viana et al. (2009) and Hou et al. (2017), and it is considered to be a potentially important factor that causes food contamination and food spoilage. Therefore, it is necessary to look for effective ways to control biofilm formation. To our knowledge, fewer studies have studied the regulatory mechanism of quorum sensing of *H. alvei* with respect to biofilm formation and the motility of the cells in an artificial medium. Understanding more about the mechanism by which quorum sensing can impact biofilm formation will open up a new way to tackle the problem of food contamination by bacteria, and help safeguard better food quality and prevent food-poising.

In our previous study, we isolated a strain of *H. alvei* (*H. alvei* H4) from spoiled instant sea cucumber, and identified three kinds of AHLs secreted by this bacterium. These AHLs are C4-HSL, C6-HSL, and 3-o-C8-HSL. In addition, we also detected a significant influence of AHLs on the biofilm formation of *H. alvei* H4 (Hou et al., 2017). In this study, a *luxI* mutant of *H. alvei* H4 was constructed to conduct further research on the regulatory roles of C4-HSL, C6-HSL, and 3-o-C8-HSL in biofilm formation and swimming motility of *H. alvei* H4.

MATERIALS AND METHODS

Bacterial Strains and Culture Conditions

The bacterial strains used in this study are presented in **Table 1**. *Chromobacterium violaceum* CV026, and *H. alvei* H4 were routinely cultured at 30°C, while *Escherichia coli* was grown at 37°C. All strains were grown in LB medium (Luria Bertani, 10 g/l tryptone, 5 g/l yeast extract, 10 g/l NaCl) supplemented with antibiotics where appropriate (50 μg/ml ampicillin and 34 μg/ml chloramphenicol in the case of *E. coli* culture or 20 μg/ml chloramphenicol for the *H. alvei* H4 mutant).

Construction of Δ*luxI* Strain

To construct a *luxI*-deficient strain of *H. alvei* H4, a chloramphenicol resistance marker (Cm^R) was inserted into the genomic DNA of *H. alvei* H4 at the *luxI* locus. Briefly, a 608-bp upstream homologous recombination arm and a 654-bp downstream homologous recombination arm of the *luxI* gene were amplified from the gDNA of *H. alvei* H4 and then cloned into the plasmid pUC19 to yield the construct pUC19-Δ*luxI*. The two DNA fragments were linked by a *Bam*HI restriction

TABLE 1 | Strains and plasmids used in this study.

Strains and plasmids	Relevant characteristic(s)	Source/references
C. violaceum CV026	mini-Tn-5 mutant of ATCC31532, violacein reporter, Km^R	McClean et al. (1997)
H. alvei H4	Wild type	This study
Δ*luxI*	H4 derivative, Δ*luxI*::Cm^R	This study
*E. coli*β2155	Cm^R	Purchased from Takara
E. coli TOP10	General cloning strain, Str^R	Purchased from Takara
PCVD442	Suicide plasmid, SacB, oriT, Am^R	Songon
Puc19	Am^R	Purchased from Takara

site. The chloramphenicol resistance maker (Cm^R) was amplified from the plasmid pKD3, and then cloned into pUC19-Δ*luxI* at a site between the upstream and downstream homologous recombination arm fragments, yielding the construct pUC19-Δ*luxI*::Cm. Target fragment in pUC19-Δ*luxI*::Cm was subcloned and ligated into the suicide plasmid pCVD442 to yield the construct pCVD442-Δ*luxI*::Cm, which was then introduced into *E. coli*β2155 by electroplating. Conjugation between *E. coli*β2155 harboring pCVD442-Δ*luxI*::Cm and *H. alvei* H4 was then performed. The mutant colonies obtained were verified by PCR and DNA sequencing. Primers used in this section see **Table 2**.

AHLs Production

Chromobacterium violaceum CV026 was used as the biosensor strain to detect the production of AHLs by *H. alvei* H4 WT and Δ*luxI,* since in the presence of AHLs, *C. violaceum* CV026 would produce a purple pigment that could be easily detected. This assay was performed as described by Viana et al. (2009). Briefly, AHLs were extracted from the corresponding bacterial culture. Aliquot (100 ml) of an overnight culture was centrifuged at 8000 × *g* for 15 min at 4°C, and the supernatant was added to an equal volume of ethyl acetate containing 0.1% acetic acid (v/v) followed by thorough mixing. The mixture was then incubated at 25°C for 2 h with shaking at 180 rpm. After that, the ethyl acetate layer was removed and freeze-dried under vacuum, and the residue was dissolved in 1 ml ultra-pure water. To prepare the plates for the assay, 80 ml LB agar medium was cooled to about 60°C, mixed with 20 ml overnight culture of CV026, and then poured into sterile plates (20 ml per plate). Holes were punched into the solidified medium at the center of each plate using a sterile 1 ml pipette tip, and 60 μl of the AHL extract was dispensed into the hole. The plates was incubated at 30°C until the purple zone appeared around the point of AHL application.

Biofilm Formation on 96-Well-Plate

Biofilm formation was measured using the microplate assay as described by Hou et al. (2017), but with some modifications. Briefly, culture of *H. alvei* H4 WT and Δ*luxI* were grown to an $OD_{600\ nm}$ value of 1.0, and then diluted 100-fold in LB medium. The diluted culture was dispensed into a 96-well plate polypropylene microtiter plate (Corning, NY, United States) using 200 μl per well. After incubation at 30°C for 24 h, the $OD_{600\ nm}$ of the culture was measured. After that, the culture medium was removed and washed off unattached cells by washing each well with 250 μl of 10 mM PBS (pH 7.2). A total of three washes were performed. This was followed by the addition of 250 μl anhydrous methanol and a 15-min incubation to fix the cells. Subsequently, 250 μl of 0.1% (v/v) crystal violet solution was added to each well and the plate was incubated at room temperature for 15 min and rinsed three times with deionized water (250 μl per rinse). The crystal violet was dissolved by the addition of 200 μl 33% glacial acetic acid followed by shaking at 300 rpm for 15 min. Biofilm formation was finally analyzed by measuring the absorbance of the plate at $OD_{590\ nm}$ using a Spectra M2 spectrophotometer (Molecular Devices, United States). Biofilm formed by Δ*luxI* in the presence of 150 μg/ml C4-HSL, 200 μg/ml C6-HSL, or 100 μg/ml 3-o-C8-HSL was detected essentially as described above.

Biofilm Formation on Glass Surface

To examine the effect of quorum sensing on biofilms formed by *H. alvei* H4 on the glass surface, biofilm formation was investigated as described by Cai et al. (2018) with some modifications. Briefly, an overnight bacterial culture was diluted 100-fold in fresh LB medium, and 2 ml of the diluted culture was added to a glass tube (1 cm × 10 cm). As a control, 2 ml of LB was added to a separate glass tube. Both tubes were incubated at 30°C for 24 h without shaking. After incubation, the culture medium was gently removed, and each tube was washed three times with 2.5 ml PBS, and then with 2.5 ml anhydrous methanol followed by drying at 60°C for 15 min. The tube was then stained with 2.5 ml 0.1% CV (v/v) for 15 min at room temperature followed by three washes with 2.5 ml ultra-pure water and drying at 60°C. The remaining CV on the inner surface of the tube was dissolved in 1.0 ml of 33% glacial acetic acid (v/v) with vortexing, and 200 μl of the sample was transferred to a new 96-well plate and the optical density of the sample at 590 nm was measured with a microplate reader (Spectra M2; Molecular Devices, Sunnyvale, CA, United States).

Biofilm Formation on Stainless Steel

Stainless steels (type: 304) were cut into strips (1 cm × 3 cm × 0.2 mm) and processed as described by Tapia-Rodriguez et al. (2017). An overnight culture of *H. alvei* H4 WT and Δ*luxI* were diluted 100-fold with LB medium to a cell density of about 10^6 CFU/ml. Aliquot (10 ml) of the diluted culture was placed in a test tube (1.5 cm × 10 cm) containing

TABLE 2 | Primers used for the construction of Δ*luxI*.

Primer name	Primer sequences
Upstream of *luxI*	ATAGAATTCGTCGACATCACATTGATGTCAGACCTCAAGATTTC (*Eco*RI-*Sal*I)
	ATAGGATCCATATCTGAGTGAGGATGAGCGAATTTATC (*Bam*HI)
Downstream of *luxI*	ATAGGATCCATCACCTTGATTACATTTTAGTTACTATCC (*Bam*HI)
	ATAGCATGCGTCGACTACTGCCCTTGCTTTCTCAATGAC (*Sph*I-*Sal*I)
Chloramphenicol resistance gene region	ATAGGATCCATATGAATATCCTCCTTAGTTCCTATTC (*Bam*HI)
	ATAGGATCCGAGCTGCTTCGAAGTTCCTA (*Bam*HI)

The underlined are restriction sites.

a stainless-steel strip and incubated at 30°C for 24 h without shaking. After incubation, the strip was transferred to a small test tube (1.5 cm × 5 cm) containing 5 ml PBS to wash off unattached cells. This washing step was repeated three times and the strip was then transferred to a 10 ml-tube and sonicated for 1.5 min in an ultrasonication bath (power, 300 W, 37 kHz 37; Elma; Elmasonic P; Germany) to disperse the biofilm as previously described (Jahid et al., 2015). Finally, the bacterial suspension was vortexed and serially diluted with 0.85% NaCl solution, and then spread onto an LB agar plate. The plate was incubated at 30°C for 24 h and the colonies appearing on the plate were then counted.

Biofilms Detected by SEM

H. alvei H4 WT and Δ*luxI* were separately incubated in LB medium for 16 h at 30°C with shaking at 150 rpm. The culture was then diluted to a final density of about 1.0×10^7 CFU/ml. First, 1 ml of the diluted culture was dispensed onto a sterile stainless steel (1 cm × 1 cm × 0.2 mm) placed inside a 24-well microtiter plate and cultured at 30°C for 24 h. The biofilm deposited on the stainless steel was then was prepared for scanning electron microscopy (SEM) analysis according to the method described by Nithya et al. (2010). Briefly, the stainless steel was gently washed with sterile 0.1 M PBS, and the biofilm was fixed with 2.5% glutaraldehyde solution for 2 h followed by washing with 0.1 M PBS. The stainless steel was subjected to dehydration under a graded series of tert-butanol. This was followed by critical point drying, gold sputtering and SEM observation (Quanta 450, Waltham, MA, United States) performed at 3.0 kV under 5000 and 50000× magnifications as described previously (Hou et al., 2018).

Swimming Motility Assay

To measure the swimming motility of *H. alvei* H4 and Δ*luxI*, motility agar (2.6 g/l agar, 10 g/l tryptone, 5 g/l NaCl) (Zhu and Winans, 1998) was used. *H. alvei* H4 or Δ*luxI* was incubated in LB medium at 30°C until the $OD_{600\ nm}$ of the cultures reached 1.0. Aliquot (3 μL) of the culture was spotted at the center of the motility agar plate followed by incubation at 30°C. The extent of motility was assessed by measuring the diameter of the zone spread from the point of inoculation. To detect the effect of AHLs on the swimming motility of Δ*luxI,* C4-HSL, C6-HSL, and 3-o-C8-HSL were added to separate motility agar plates. The final concentrations of C4-HSL, C6-HSL, and 3-o-C8-HSL in the plates were 150, 200, and 100 μg/ml, respectively. Swimming motility was determined as described above.

Real-Time PCR Assay

H. alvei H4 WT and Δ*luxI* was cultured in LB medium the absence or presence of AHLs (C4-HSL, C6-HSL, and 3-o-C8-HSL) at 30°C with shaking at 150 rpm for 16 h. When the $OD_{600\ nm}$ of the cultures reached 1.65, the cells were harvested and subjected to total RNA extraction using a RNAprep Pure Bacteria Kit (DP430, TIANGEN, Beijing). About 500 ng of total RNA was reversely transcribed into cDNA using a PrimeScript™ Reagent kit (RR047, Takara, Japan). The reaction mixture consisted of 2 μL template cDNA, 12.5 μL SYBR Premix Ex Taq™ (RR420, Takara, Japan), 0.5 μL each of the forward and reverse primers (10 mM) (**Table 3**), and 9.5 μL RNA free water. Amplification was performed with a Step-One Thermal Cycler (Applied Biosystems, United States) and consisted of 40 cycles of denaturation at 95°C for 15 s, annealing at 95°C for 30 s, and extension at 60°C for 45 s. The *16S rRNA* gene was used as housekeeping control. The result was analyzed by $2^{-\Delta\Delta CT}$ method (Schmittgen and Livak, 2008).

Statistical Analysis

Three replicate trials were carried out for each sample, and all the experiments were repeated three times. Data were analyzed by one-way analysis of variance (ANOVA) using SPSS18.0 software, and expressed as means ± standard deviations (SDs). Statistical significance was considered at the $P < 0.05$ level. All graphs were drawn with OriginPro 8.6 software.

RESULTS

AHLs Production by *luxI* Mutant

Pigment production assay showed a violet zone in the center of the plate when CV026 was incubated with the ethyl acetate extract prepared from the culture supernatant of *H. alvei* H4 but not from the culture supernatant of Δ*luxI* (**Figure 1**), indicating the lack of AHLs production by Δ*luxI*. The assay demonstrated the dependence of AHLs production on a functional *luxI* gene.

TABLE 3 | Primers used for RT-PCR.

Primer name	Function	Primer sequences
16S rRNA	16S ribosomal RNA	5′-TAGCGGTGAAATGCGTAG-3′
		5′-TCGTTTACAGCGTGGACTA-3′
flgA	Flagella basal body P-ring formation protein	5′-GGGTTATCACCAATCCTG-3′
		5′-GGTAATGGGTTGTAAATCG-3′
cheA	Chemotaxis protein	5′-CCAACTTCGTCGTCGGTCATG-3′
		5′-GAACATCAGGGCGGCAAT-3′
motA	Flagellar motor protein	5′-TTCATGTTGCCGCTTACC-3′
		5′-ACCCGCAAGAAAGTGAAC-3′
luxR	AHLs receptor	5′-CTTTATTGGGCGAGTATGG-3′
		5′-TTGTCGGGCGTTGCTTAC-3′

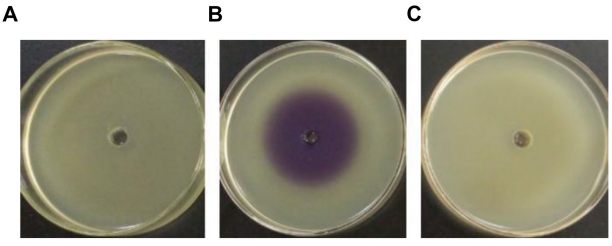

FIGURE 1 | Detection of AHL production via the biosensor strain CV026. CV026 was cultured in the absence of ethyl acetate extract prepared from LB medium **(A)**, *H. alvei* H4 culture supernatant **(B)**, and Δ*luxI* culture supernatant **(C)**.

Response of *luxR* to AHLs

The effect of *luxI* mutation was further investigated by measuring the level of *luxR* mRNA in Δ*luxI* and compared it with that of WT strain. Δ*luxI* exhibited about fivefold reduction in the level of *luxR* mRNA relative the WT (**Figure 2A**), which clearly suggested that the expression of the *luxR* gene in the mutant was significantly ($P < 0.05$) inhibited. However, in the presence of exogenous AHLs, the level of *luxR* mRNA gradually increased with increasing concentrations of AHLs, suggesting that the expression of *luxR* could be stimulated by the presence of AHLs (**Figure 2B**). Maximum increase in *luxR* mRNA level stimulated by AHL ranged from 5.5-fold in the case of C4-HSL to 6.5-fold in the case of C6-HSL, while 3-o-C8-HSL yielded somewhat lower increase (4.5-fold). Thus, C6-HSL appeared to exert the strongest stimulatory effect on the expression of *luxR*.

Biofilm Formation

Growth of *H. alvei* H4 was not affected by the deletion of the *lux*I gene, as shown by the similar growth curves between WT and Δ*luxI* in the absence of AHLs (**Figure 3A**). Furthermore, the addition of AHLs to the culture of Δ*luxI* also had not obvious effect on its growth. This suggested that growth of the bacterial cells was not dependent on the product of the *luxI* gene. However, deletion of the *luxI* gene had a significant effect on biofilm formation by *H. alvei* H4, as shown by the significantly higher level of biofilm formed by the wild type (WT) compared with Δ*luxI* (**Figure 3B**). Addition of AHLs to the culture of Δ*luxI* appeared to cause increase in biofilm formation. The extent of biofilm formation of Δ*luxI* in the presence of C4-HSL was significantly ($P < 0.05$) enhanced and almost similar to that of the WT strain. However, C6-HSL seemed to

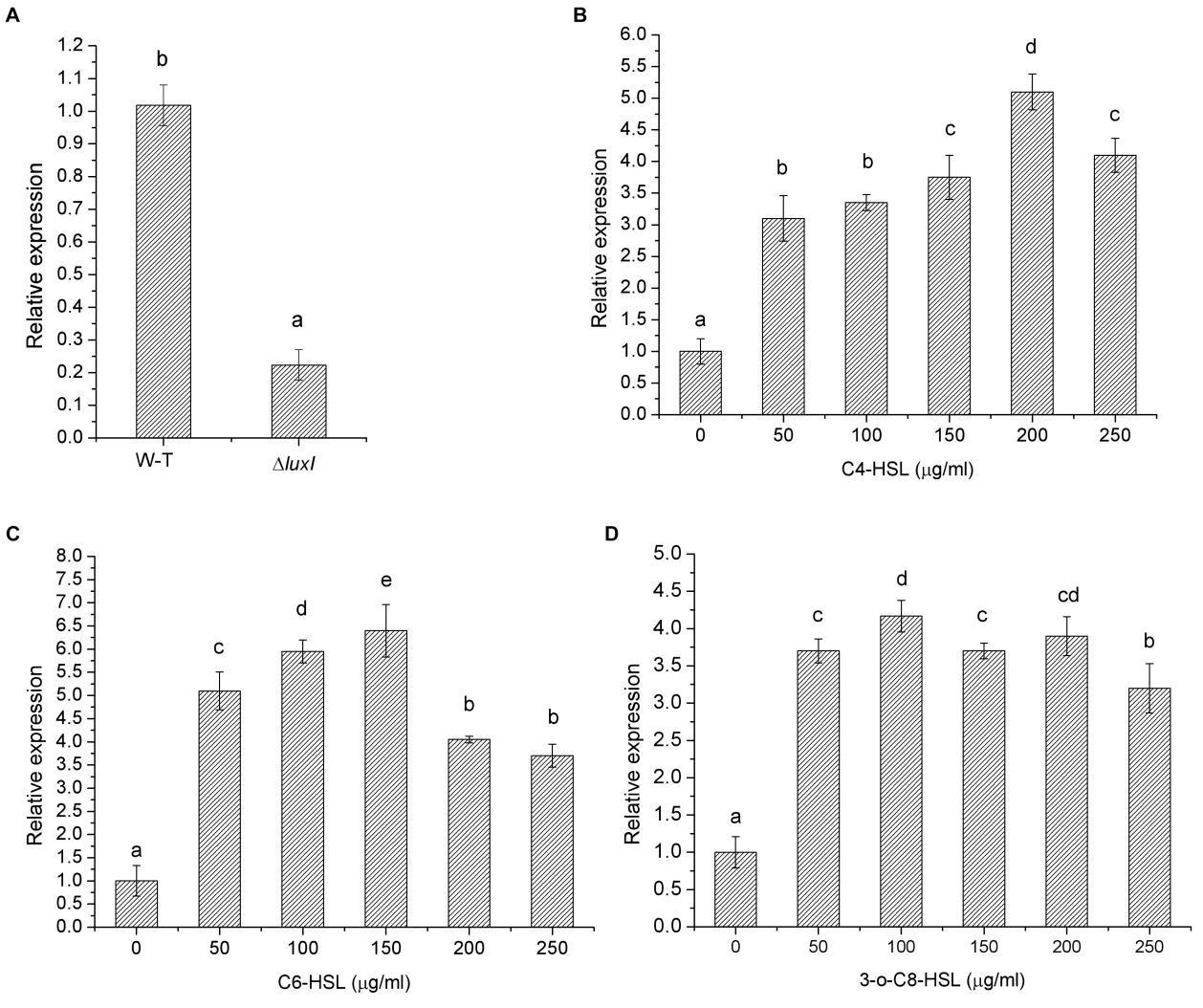

FIGURE 2 | Relative expression of the *luxR* gene by *H. alvei* H4 cultured in the absence and presence of AHLs. **(A)** *H. alvei* H4 and Δ*luxI* cultured in the absence of AHLs. Δ*luxI* cultured in the presence of C4-HSL **(B)**, C6-HSL **(C)**, and 3-o-C8-HSL **(D)**. The mRNA level of the *luxR* gene was determined by *q*RT-PCR. Data are the means ± SEMs ($n = 3$). Different letters above the columns indicate significant differences at the $P < 0.05$ level.

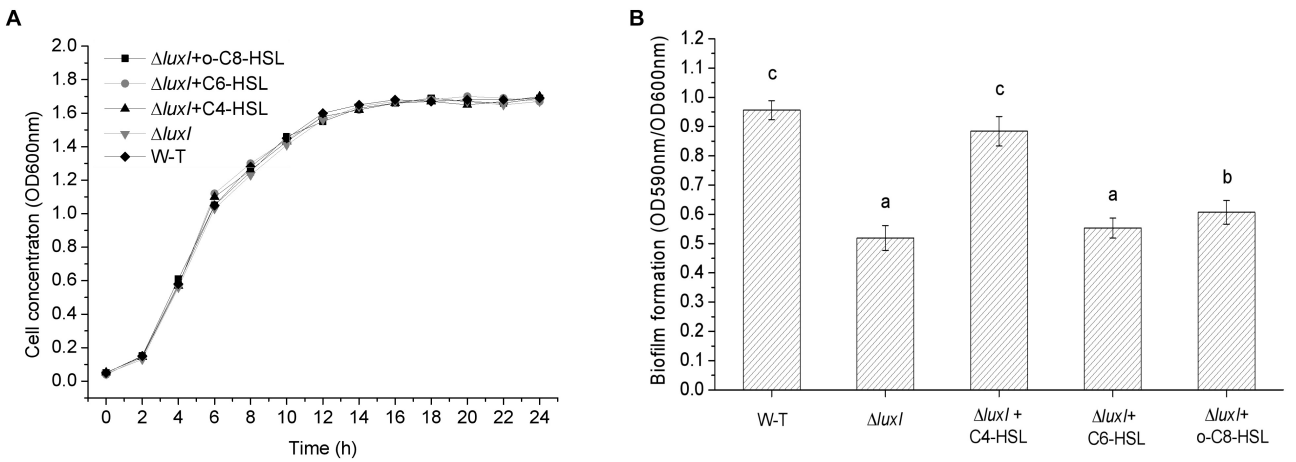

FIGURE 3 | Growth curve and biofilm formation of wild type (WT) *H. alvei* H4. **(A)** Growth curve; **(B)** Biofilm formation. Wild type *H. alvei* H4 was cultured in the absence of AHL only. Δ*luxI* was cultured both in the absence and presence of the indicated AHLs (150 μg/ml C4-HSL, 200 μg/ml C6-HSL and 100 μg/ml 3-o-C8-HSL), respectively. Data are the means ± SEMs (n = 3). Different letters above the columns indicate differences at the $P < 0.05$ level.

have no effect on the biofilm formation of Δ*luxI*, causing no significant increase. Obvious promotion ($P < 0.05$) of biofilm formation on Δ*luxI* were also achieved at the presence of 3-o-C8-HSL, but still far less than that of C4-HSL on Δ*luxI* and WT strain. The result suggested that C4-HSL could be the AHL with major influence on biofilm formation.

Biofilms on Glass

An intense zone of purple stain was found on the wall of the glass tube used to culture WT strain, indicating the presence of biofilm (**Figure 4A**). On the other hand, only very slight purple staining was found on the wall of the glass tube that was used to culture Δ*luxI*, suggesting a lack of biofilm being formed by Δ*luxI*. Addition of C4-HSL to the Δ*luxI* culture resulted in obvious enhancement of the purple zone, but this did not occur when either C6-HSL or 3-o-C8-HSL was added to the culture. The result clearly suggested that the capacity of Δ*luxI* to form biofilm was greatly reduced compared with its WT strain counterpart, and that only C4-HSL was able to restore its biofilm formation capacity.

Biofilms on Stainless Steel

The mutant Δ*luxI* was also compared with its WT counterpart in term of the ability to form biofilm on the surface of stainless steel. Significantly ($P < 0.05$) less colonies of Δ*luxI* were found on the surface of the stainless steel compared with the WT strain, but when Δ*luxI* was cultured in the presence of C4-HSL, the number of colonies found on the surface of the stainless steel was significantly ($P < 0.05$) increased, and being comparable with that of WT strain (**Figure 5**). However, as in the case of biofilm formed on glass surface, C6-HSL and 3-o-C8-HSL had no obvious effect on the ability of Δ*luxI* to form biofilm on stainless steel surface.

Biofilm by SEM

Biofilm formation of *H. alvei* H4 WT and Δ*luxI* on stainless-steel surface was detected by SEM. Obvious reduction in the number of Δ*luxI* cells on stainless-steel

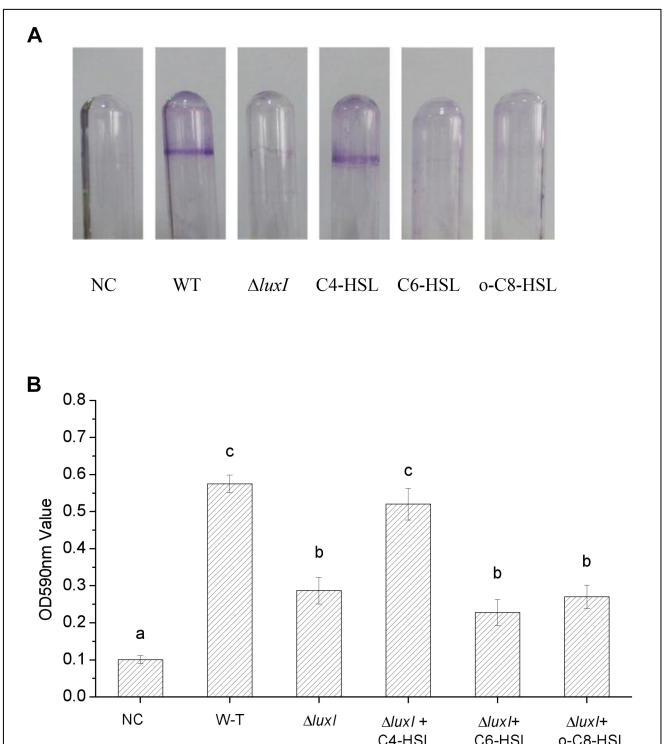

FIGURE 4 | Biofilm formation by *H. alvei* strains. The image shows the biofilms formed on glass surface by WT and Δ*luxI* with and without AHLs. The plot shows the extent of biofilm formed on the glass surface as quantitated by $OD_{590\ nm}$. NC, negative control. Data are the means ± SEMs (n = 3). Different letters above the columns indicate differences at the $P < 0.05$ level.

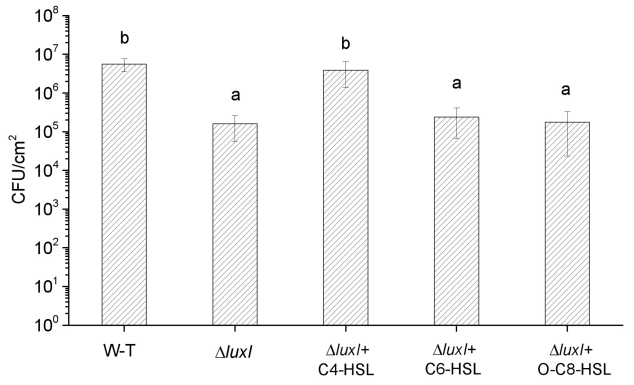

FIGURE 5 | Biofilm dormation of *H. alvei* H4 on stainless steel surface. *H. alvei* H4 and its mutant Δ*luxI* were allowed to form biofilm on stainless-steel surface with and without AHLs (C4-HSL, C6-HSL, and o-C8-HSL). The cells were then washed and counted. Data are the means ± SEMs (n = 3). Different letters above the columns indicate significant differences at the $P < 0.05$ level.

surface was observed, but the number of Δ*luxI* cells was restored when supplied with 150 μg/ml C4-HSL (**Figure 6**). In addition, WT cells appeared to aggregate and adhered to the surface, and produced evident EPS filaments. In contrast, Δ*luxI* tended to adhere to the surface as individual cells. When Δ*luxI* was exposed to 150 μg/ml C4-HSL, the cells also formed aggregates and adhered to the surface of stainless steel, these cells also produced a lot of EPS.

Swimming Motility

As shown in **Figures 2B–D**, the concentrations of AHLs, which induce the relative expression of *luxR* gene to the maximum respectively, were chosen for swimming motility assay, and swimming motility was determined by the expansion of the bacterial colony from the point of application to a greater diameter on the surface of an agar plate. Compared with WT, Δ*luxI* suffered significant ($P < 0.05$) loss in swimming motility in the absence of exogenous AHLs (**Figure 7**). However, upon addition of C4-HSL, the swimming motility of Δ*luxI* increased and became significantly higher than the level of WT. Addition of C6-HSL also had some enhancing effect on the swimming motility of Δ*luxI*, but it remained obviously reduced compared with WT. In contrast, the addition of 3-o-C8-HSL appeared to have no real effect on the swimming motility of Δ*luxI*.

Expression of *flgA*, *motA*, and *cheA*

To further study the molecular mechanism of quorum sensing on biofilm formation, three biofilm formation and swimming motility related genes, *flgA*, *motA* and *cheA*, were chosen for analysis using *q*RT-PCR. The mRNA levels of all three genes in Δ*luxI* in the absence of exogenous AHLs were significantly ($P < 0.05$) reduced compared with those of the WT, with *motA* being the most severely affected gene (**Figure 8**). Addition of C4-HSL (150 μg/ml) to the Δ*luxI* culture restored the mRNA levels of the three genes to the levels comparable with those of the WT strain, except for the *cheA* gene, which showed lesser, but still significant increase. Similarly, the addition of C6-HSL (200 μg/ml) had some enhancing effect on the mRNA levels of *motA* and *cheA*, whereas the addition of 3-o-C8-HSL (100 μg/ml)

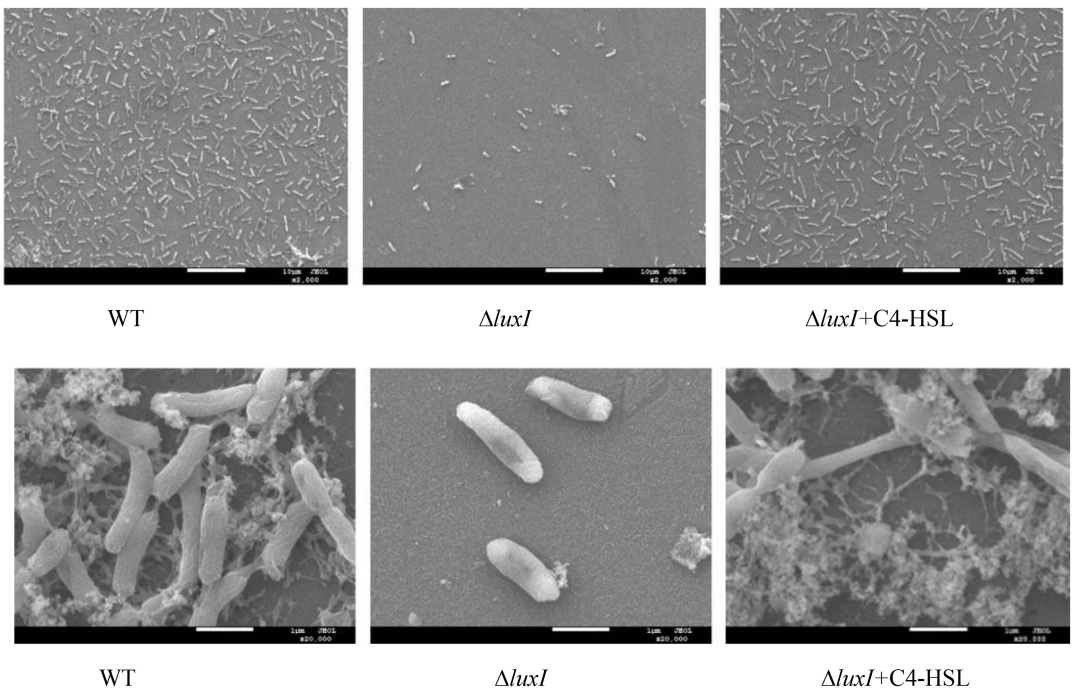

FIGURE 6 | Scanning electron micrographs showing the appearance of biofilms formed by wild type *H. alvei* H4, Δ*luxI,* and Δ*luxI*+C4-HSL.

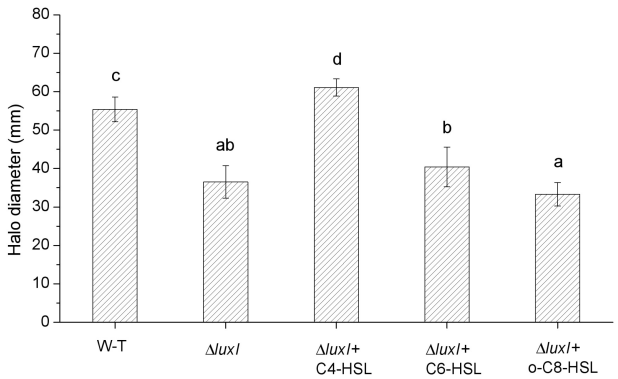

FIGURE 7 | Swimming motility of wild type and mutant *H. alvei* H4. Swimming motility was conducted in the absence or exogenous AHLs in the case of WT or both in the absence and presence of AHLs in the case of Δ*luxI*. The concentrations of C4-HSL, C6-HSL, o-C8-HSL used were 150, 200, and 100 μg/ml respectively. Data are the means ± SEMs ($n = 3$). Different letters above the columns indicate significant differences at the $P < 0.05$ level.

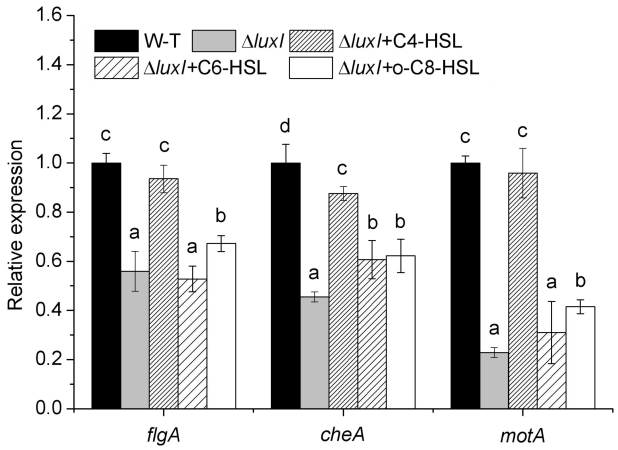

FIGURE 8 | Relative expression of several genes related to biofilm formation and swimming motility of *H. alvei* H4. Expression of the *flgA*, *motA,* and *cheA* genes in WT cultured in the absence of exogenous AHL was compared with those of Δ*luxI* mutant cultured in the absence and in the presence of 150 μg/ml C4-HSL, 200 μg/ml C6-HSL, or 100 μg/ml 3-o-C8-HSL. The mRNA levels of the genes were measured by *q*RT-PCR. Data are the means ± SEMs ($n = 3$). Different letters above the columns indicate significant differences at the $P < 0.05$ level.

appeared to increase the mRNA levels of all three genes, but the increases still fell short of those achieved by C4-HSL. The result suggested that AHL could stimulate the expression of the *motA* and *cheA* genes, and to a lesser extent, the expression of the *flgA* gene.

DISCUSSION

Mutant strain of *H. alvei* H4 with defective *luxI* gene was successfully constructed in this study, and the effect of this mutation on the quorum-sensing system was characterized with respect to AHL production, biofilm formation, and swimming motility. The *luxI* gene was generally recognized as AHL synthase gene, which controls the synthesis of AHLs (Waters and Bassler, 2005; Morohoshi et al., 2007). Indeed, the *luxI* mutant produced no detectable AHLs as assayed with the biosensor strain CV026 (**Figure 1**), consistent with the results reported for *Aeromonas hydrophila* and *Acinetobacter nosocomialis* (Khajanchi et al., 2009; Oh and Choi, 2015). The complementing strain of *luxI* was also constructed, and no differences in AHLs production, biofilm formation and swimming motility were found between comp-Δ*luxI* and WT strain (**Supplementary Figure 1**).

It is known to us that when local concentration of AHLs is high enough, AHLs would diffuse back into the cell, and induce the expression of *luxR* gene (Waters and Bassler, 2005; Bai and Rai, 2011). Expression of the *luxR* gene in the AHL-deficient strain of *H. alvei* H4 was found to decrease significantly, suggesting that expression of the *luxR* gene might require induction by AHLs. This hypothesis was confirmed by significant increase in *luxR* expression in the mutant when it was cultured in the presence of exogenous AHL (C4-HSL, C6-HSL, or 3-o-C8-HSL). The stimulating effect on *luxR* gene increased with the increase of AHLs concentration, causing the increase in *luxR* gene expression consequently. Similar result has also been obtained for *Aliivibrio fischeri*, whereby expression of the *luxR* gene was observed in the presence of 3-o-C6-HSL, with higher concentrations of the compound leading to more expression of the gene (Ramalho et al., 2016). In addition, there is also a threshold concentration of AHLs, and QS regulon is depressed when the concentration of AHLs exceeds this threshold, as a result of causing the reduction of *luxR* gene expression (Swift et al., 2001). Similar changes of *sinR* gene expression affected by AHLs were also obtained by Gao et al. (2012) in *Sinorhizobium meliloti*. Besides, response of CviR to autoinducer were found depressed when exposed to high concentration AHLs (Swem et al., 2009) in *C. violaceum,* consistent to the results achieved in the present study (**Figures 2B–D**).

Biofilm formation by the *luxI* mutant was inhibited, and since the mutant was deficient in AHL, this indicated that biofilm formation might be modulated by AHLs, and is associated with AHL-mediated QS. As reported by Ammor et al. (2008), bacterial phenotype such as resistance to antimicrobial compounds, biofilm formation, bioluminescence; pigment production, virulence gene expression, swimming motility and production of degradative extracellular proteases are regulated by the QS system. Furthermore, the addition of C4-HSL to the Δ*luxI* culture restored the ability of the mutant cells to form biofilm, while the addition of C6-HSL and 3-o-C8-HSL appeared to have no significant effect, suggesting that the C4-HSL might play an important role in the regulation of biofilm formation in *H. alvei* H4. Similar result has been reported for *A. hydrophila*, in which biofilm formation and protease activity, which are inhibited in an AHL-deficient strain, can be stimulated by the addition of C4-HSL to the culture (Khajanchi et al., 2009). Niu et al. (2008) investigated the regulatory role of C12-HSL in the biofilm formation of *Acinetobacter baumannii* M2 and showed that biofilm formation is obviously inhibited in an

abaI mutant, but can be restored by the addition of C12-HSL to the culture. Similarly, in *Acinetobacter* sp. strain DR1, C12-HSL was also found to play the same role as in *A. baumannii* M2 (Kang and Park, 2010). In *P. aeruginosa*, the LasR protein (a LuxR homologous protein) is soluble and stable only when it is produced in the presence of its cognate AHL ligand 3-o-C12-HSL, as the protein is becoming less soluble if it is produced in the presence of a different AHL, such as 3-o-C8-HSL or 3-o-C6-HSL, while soluble form is not produced in the presence of C4-HSL (Bottomley et al., 2007). Hence, C4-HSL might be the cognate ligand of LuxR in *H. alvei* H4, and it may possibly bind to the LuxR protein and play a regulatory role. In *P. syringae* and *S. meliloti,* the production of extracellular polysaccharide has been shown to be regulated by QS (Marketon et al., 2003; Quiñones et al., 2005). Therefore, the reduction in the numbers Δ*luxI* cells adhering to polystyrene, glass and stainless-steel surfaces that we observed (**Figures 3–5**) might be caused by the reduction in biofilm formation and extracellular polysaccharide secretion. According to the results achieved in the present research and the studies reported by Nasser et al. (1998) and Andersson et al. (2000), different AHLs in bacteria may regulate different phenotypes, for *H. alvei* H4, C4-HSL seems to have a more important effect on regulating biofilm formation and swimming motility than C6-HSL and 3-o-C8-HSL, however, in other phenotypes regulated by quorum sensing system, C6-HSL and 3-o-C8-HSL might act as regulators.

Another important factor in the biofilm formation of bacteria is the extent of swimming motility, which contributes to the early development of the biofilm architecture (microcolony formation) (Srey et al., 2013). Bacterial motility depends mainly on the movement of flagella and Brownian motion (Li et al., 2008). Furthermore, some genes such as the *flgA*, *motA,* and *cheA* genes have been shown to be involved in biofilm formation and swimming motility (Lee et al., 2015). The data on swimming motility assay and *q*RT-PCR analysis of the expression of these three motility-related and biofilm-related genes, *flgA*, *motA,* and *cheA* (**Figure 8**), appeared to suggest that swimming motility might be regulated by regulating the expression of these genes. Since Δ*luxI* exhibited significantly less swimming motility and lower expression of the *flgA*, *motA,* and *cheA* genes than WT strain in the absence of exogenous AHLs, these two factors might also be the cause of poor biofilm formation displayed by the mutant. Similar results have also been reported by Gurich and González (2009), whereby deletion of the *sinI* gene in *S. meliloti* can result in significant reduction in the expression of the motility genes *flaA* and *flaB*, but such reduction can be reversed by the presence of AHLs. In contrast to our data, Wang T. et al. (2016) demonstrated that in *Acidovorax citrulli*, biofilm formation, motility and adherence of bacterial cells to a solid surface can be significantly promoted when the *accR/I* gene is defective. Furthermore, in *A. nosocomialis,* both biofilm formation and motility were found to be modulated by the *luxR* homologous gene *anoR* (Oh and Choi, 2015), and not the *anoI* gene. Therefore, the regulation of QS in biofilm formation their swimming motility might be different for different bacteria.

CONCLUSION

In *H. alvei*, AHL-mediated QS system plays a key part in swimming motility and biofilm formation on different solid surfaces. We have shown here that among the different AHLs tested, C4-HSL appeared to exert a more significant impact on the modulation of these properties of the cells. Further study focusing on the regulation mechanism of the *luxR/I* gene, and the screening of effective QS inhibitors for *H. alvei,* and the application of these inhibitors to food production may bring about economic benefits as well as preventing the spread of food-related incident of infection among the public.

AUTHOR CONTRIBUTIONS

HMH and GZ designed this study. YZ conducted the experiments. YZ, HMH, and YW performed the data analyses. HSH, GZ, and YZ drafted and revised the manuscript. All authors read and approved the final version of this manuscript.

FUNDING

This work was supported financially by "The National Natural Science Foundation of China (Grant No. 31871895)."

SUPPLEMENTARY MATERIAL

The Supplementary Material for this article can be found online at: https://www.frontiersin.org/articles/10.3389/fmicb.2019.01330/full#supplementary-material

REFERENCES

Ammor, M. S., Michaelidis, C., and Nychas, G. J. E. (2008). Insights into the role of quorum sensing in food spoilage. *J. Food protect.* 71, 1510–1525. doi: 10.4315/0362-028x-71.7.1510

Andersson, R. A., Eriksson, A. R. B., Heikinheimo, R., Mäe, A., Pirhonen, M., Kõiv, V., et al. (2000). Quorum sensing in the plant pathogen *Erwinia carotovora* subsp, carotovora: the role of expR$_{Ecc}$. *Mol. Plant Microbe Interact.* 13, 384–393. doi: 10.1094/MPMI.2000.13.4.384

Bai, A. J., and Rai, V. R. (2011). Bacterial quorum sensing and food industry. *Compr. Rev. Food Sci. F.* 10, 183–193. doi: 10.1111/j.1541-4337.2011.00150.x

Bai, J. and Rai, R. V. (2016). Effect of small chain N-acyl homoserine lactone quorum sensing signals on biofilms of food-borne pathogens. *J. Food Sci. Tech.* 53, 3609–3614. doi: 10.1007/s13197-016-2346-1

Bottomley, M. J., Muraglia, E., Bazzo, R., and Carfì, A. (2007). Molecular insights into quorum sensing in the human pathogen *Pseudomonas aeruginosa* from the structure of the virulence regulator LasR bound to its autoinducer. *J. Biol. Chem.* 282, 13592–13600. doi: 10.1074/jbc.m700556200

Bruhn, J. B., Christensen, A. B., Flodgaard, L. R., Nielsen, K. F., Larsen, T. O., Givskov, M., et al. (2004). Presence of acylated homoserine lactones (AHLs) and AHL-producing bacteria in meat and potential role of AHL in spoilage of meat. *Appl. Environ. Microbiol.* 70, 4293–4302. doi: 10.1128/aem.70.7.4293-4302.2004

Cai, S., Cheng, H., Pang, H., Jian, J., and Wu, Z. (2018). AcfA is an essential regulator for pathogenesis of fish pathogen *Vibrio alginolyticus*. *Vet. Microbiol.* 213, 35–41. doi: 10.1016/j.vetmic.2017.11.016

Costerton, J. W., Stewart, P. S., and Greenberg, E. P. (1999). Bacterial biofilms: a common cause of persistent infections. *Science* 284, 1318–1322. doi: 10.1126/science.284.5418.1318

Gao, M., Coggin, A., Yagnik, K., and Teplitski, M. (2012). Role of specific quorum-sensing signals in the regulation of exopolysaccharide II production within *Sinorhizobium meliloti* spreading colonies. *PLoS One* 7:e42611. doi: 10.1371/journal.pone.0042611

Gounadaki, A. S., Skandamis, P. N., Drosinos, E. H., and Nychas, G. J. E. (2008). Microbial ecology of food contact surfaces and products of small-scale facilities producing traditional sausages. *Food Microbiol.* 25, 313–323. doi: 10.1016/j.fm.2007.10.001

Gurich, N., and González, J. E. (2009). Role of quorum sensing in *Sinorhizobium meliloti*-alfalfa symbiosis. *J. Bacteriol.* 191, 4372–4382. doi: 10.1128/jb.00376-09

Hou, H. M., Wang, Y. F., Zhang, G. L., Zhu, Y. L., Xu, L. Q., Hao, H. S., et al. (2018). Effects of sulfide flavors on AHL-mediated quorum sensing and biofilm formation of *Hafnia alvei*. *J. Food Sci.* 83, 2550–2559. doi: 10.1111/1750-3841.14345

Hou, H. M., Zhu, Y. L., Wang, J. Y., Jiang, F., Qu, W. Y., Zhang, G. L., et al. (2017). Characteristics of N-Acylhomoserine lactones produced by *Hafnia alvei* H4 isolated from spoiled instant sea cucumber. *Sensors* 17:E772. doi: 10.3390/s17040772

Jahid, I. K., Mizan, M. F. R., Ha, A. J., and Ha, S. D. (2015). Effect of salinity and incubation time of planktonic cells on biofilm formation, motility, exoprotease production, and quorum sensing of *Aeromonas hydrophila*. *Food Microbiol.* 49, 142–151. doi: 10.1016/j.fm.2015.01.016

Janssens, J. C. A., Steenackers, H., Robijns, S., Gellens, E., Levin, J., Zhao, H., et al. (2008). Brominated furanones inhibit biofilm formation by *Salmonella enterica* serovar typhimurium. *Appl. Environ. Microbiol.* 74, 6639–6648. doi: 10.1128/aem.01262-08

Jung, J. H., Choi, N. Y., and Lee, S. Y. (2013). Biofilm formation and exopolysaccharide (EPS) production by *Cronobacter sakazakii* depending on environmental conditions. *Food Microbiol.* 34, 70–80. doi: 10.1016/j.fm.2012.11.008

Kang, Y. S., and Park, W. (2010). Contribution of quorum-sensing system to hexadecane degradation and biofilm formation in *Acinetobacter sp.* strain DR1. *J Appl. Microbiol.* 109, 1650–1659. doi: 10.1111/j.1365-2672.2010.04793.x

Khajanchi, B. K., Sha, J., Kozlova, E. V., Erova, T. E., Suarez, G., Sierra, J. C., et al. (2009). N-acylhomoserine lactones involved in quorum sensing control the type VI secretion system, biofilm formation, protease production, and in vivo virulence in a clinical isolate of *Aeromonas hydrophila*. *Microbiol.* 155, 3518–3531. doi: 10.1099/mic.0.031575-0

Lee, J. H., Kim, Y. G., Baek, K. H., Cho, M. H., and Lee, J. (2015). The multifaceted roles of the interspecies signalling molecule indole in *Agrobacterium tumefaciens*. *Environ. Microbiol.* 17, 1234–1244. doi: 10.1111/1462-2920.12560

Li, G., Tam, L. K., and Tang, J. X. (2008). Amplified effect of brownian motion in bacterial near-surface swimming. *Proc. Natl. Acad. Sci. U.S.A.* 105, 18355–18359. doi: 10.1073/pnas.0807305105

Liu, M., Gray, J. M., and Griffiths, M. W. (2006). Occurrence of proteolytic activity and N-acyl-homoserine lactone signals in the spoilage of aerobically chill-stored proteinaceous raw foods. *J. Food Protect.* 69, 2729–2737. doi: 10.4315/0362-028x-69.11.2729

Marketon, M. M., Glenn, S. A., Eberhard, A., and González, J. E. (2003). Quorum sensing controls exopolysaccharide production in *Sinorhizobium meliloti*. *J. Bacteriol.* 185, 325–331. doi: 10.1128/jb.185.1.325-331.2003

McClean, K. H., Winson, M. K., Fish, L., Taylor, A., Chhabra, S. R., Camara, M., et al. (1997). Quorum sensing and *Chromobacterium violaceum*: exploitation of violacein production and inhibition for the detection of *N*-acylhomoserine lactones. *Microbiol* 143, 3703–3711. doi: 10.1099/00221287-143-12-3703

Morohoshi, T., Nakamura, Y., Yamazaki, G., Ishida, A., Kato, N., and Ikeda, T. (2007). The plant pathogen Pantoea ananatis produces N-acylhomoserine lactone and causes center rot disease of onion by quorum sensing. *J. Bacteriol.* 189, 8333–8338. doi: 10.1128/jb.01054-07

Nasser, W., Bouillant, M. L., Salmond, G., and Reverchon, S. (1998). Characterization of the *Erwinia chrysanthemi* expl-expR locus directing the synthesis of two N-acyl-homoserine lactone signal molecules. *Mol. Microbiol.* 29, 1391–1405. doi: 10.1046/j.1365-2958.1998.01022.x

Nithya, C., Begum, M. F., and Pandian, S. K. (2010). Marine bacterial isolates inhibit biofilm formation and disrupt mature biofilms of *Pseudomonas aeruginosa* PAO_1. *Appl. Microbiol. Biot.* 88, 341–358. doi: 10.1007/s00253-010-2777-y

Niu, C., Clemmer, K. M., Bonomo, R. A., and Rather, P. N. (2008). Isolation and characterization of an autoinducer synthase from *Acinetobacter baumannii*. *J. Bacteriol.* 190, 3386–3392. doi: 10.1128/jb.01929-07

Oh, M. H., and Choi, C. H. (2015). Role of LuxIR homologue AnoIR in acinetobacter nosocomialis and the effect of virstatin on the expression of anoR Gene. *J. Microbiol. Biotechnol.* 25, 1390–1400. doi: 10.4014/jmb.1504.04069

Quiñones, B., Dulla, G., and Lindow, S. E. (2005). Quorum sensing regulates exopolysaccharide production, motility, and virulence in *Pseudomonas syringae*. *Mol. Plant Microbe. Interact.* 18, 682–693. doi: 10.1094/mpmi-18-0682

Ramalho, T., Meyer, A., Muckl, A., Kapsner, K., Gerland, U., and Simmel, F. C. (2016). Single cell analysis of a bacterial sender-receiver system. *PLoS One* 11:e0145829. doi: 10.1371/journal.pone.0145829

Schmittgen, T. D., and Livak, K. J. (2008). Analyzing real-time PCR data by the comparative CT method. *Nat. Protoc.* 3, 1101–1108. doi: 10.1038/nprot.2008.73

Srey, S., Jahid, I. K., and Ha, S. D. (2013). Biofilm formation in food industries: a food safety concern. *Food Control* 31, 572–585. doi: 10.1016/j.foodcont.2012.12.001

Swem, L. R., Swem, D. L., O'Loughlin, C. T., Gatmaitan, R., Zhao, B., Ulrich, S. M., et al. (2009). A quorum-sensing antagonist targets both membrane-bound and cytoplasmic receptors and controls bacterial pathogenicity. *Mol. Cell* 35, 143–153. doi: 10.1016/j.molcel.2009.05.029

Swift, S., Downie, J. A., Whitehead, N. A., Barnard, A. M., Salmond, G. P., and Williams, P. (2001). Quorum sensing as a population-density-dependent determinant of bacterial physiology. *Adv. Microb. Physiol.* 45, 199–270. doi: 10.1016/s0065-2911(01)45005-3

Tan, J. Y., Yin, W. F., and Chan, K. G. (2014). Quorum sensing activity of *Hafnia alvei* isolated from packed food. *Sensors* 14, 6788–6796. doi: 10.3390/s140406788

Tapia-Rodriguez, M. R., Hernandez-Mendoza, A., Gonzalez-Aguilar, G. A., Martinez-Tellez, M. A., Martins, C. M., and Ayala-Zavala, J. F. (2017). Carvacrol as potential quorum sensing inhibitor of *Pseudomonas aeruginosa* and biofilm production on stainless steel surfaces. *Food Control* 75, 255–261. doi: 10.1016/j.foodcont.2016.12.014

Viana, E. S., Campos, M. E., Ponce, A. R., Mantovani, H. C., and Vanetti, M. C. (2009). Biofilm formation and acyl homoserine lactone production in *Hafnia alvei* isolated from raw milk. *Biol. Res.* 42, 427–436. doi: 10.4067/S0716-97602009000400004

Vivas, J., Padilla, D., Real, F., Bravo, J., Grasso, V., and Acosta, F. (2008). Influence of environmental conditions on biofilm formation by *Hafnia alvei* strains. *Vet. microbiol* 129, 150–155. doi: 10.1016/j.vetmic.2007.11.007

Wang, J., Stanford, K., McAllister, T. A., Johnson, R. P., Chen, J., Hou, H., et al. (2016). Biofilm formation, virulence gene profiles, and antimicrobial resistance of nine serogroups of Non-O157 shiga toxin-producing *Escherichia coli*. *Foodborne Pathog. Dis.* 13, 316–324. doi: 10.1089/fpd.2015.2099

Wang, M. Z., Zheng, X., He, H. Z., Shen, D. S., and Feng, H. J. (2012). Ecological roles and release patterns of acylated homoserine lactones in *Pseudomonas sp*. HF-1 and their implications in bacterial bioaugmentation. *Bioresour. Technol.* 125, 119–126. doi: 10.1016/j.biortech.2012.08.116

Wang, T., Guan, W., Huang, Q., Yang, Y., Yan, W., Sun, B., et al. (2016). Quorum-sensing contributes to virulence, twitching motility, seed attachment and biofilm formation in the wild type strain Aac-5 of *Acidovorax citrulli*. *Microb. Pathog.* 100, 133–140. doi: 10.1016/j.micpath.2016.08.039

Waters, C. M., and Bassler, B. L. (2005). Quorum sensing: cell-to-cell communication in bacteria. *Annu. Rev. Cell Dev. Biol.* 21, 319–346. doi: 10.4016/9468.01

Zhang, C., Zhu, S., Jatt, A. N., and Zeng, M. (2016). Characterization of N-acyl homoserine lactones (AHLs) producing bacteria isolated from vacuum-packaged refrigerated turbot (*Scophtluxmus maximus*) and possible influence

of exogenous AHLs on bacterial phenotype. *J. Gen. Appl. Microbiol.* 62, 60–67. doi: 10.2323/jgam.62.60

Zhao, A., Zhu, J., Ye, X., Ge, Y., and Li, J. (2016). Inhibition of biofilm development and spoilage potential of *Shewanella baltica* by quorum sensing signal in cell-free supernatant from *Pseudomonas fluorescens*. *Int. J. Food Microbiol.* 230, 73–80. doi: 10.1016/j.ijfoodmicro.2016.04.015

Zhu, J., and Winans, S. C. (1998). Activity of the quorum-sensing regulator TraR of *Agrobacterium tumefaciens* is inhibited by a truncated, dominant defective TraR-like protein. *Mol. Microbiol.* 27, 289–297. doi: 10.1046/j.1365-2958.1998.00672.x

Conflict of Interest Statement: The authors declare that the research was conducted in the absence of any commercial or financial relationships that could be construed as a potential conflict of interest.

frontiers in Microbiology

HYPOTHESIS AND THEORY
published: 23 July 2019
doi: 10.3389/fmicb.2019.01582

Can Biofilm Be Reversed Through Quorum Sensing in *Pseudomonas aeruginosa*?

*Shaomin Yan and Guang Wu**

State Key Laboratory of Non-Food Biomass and Enzyme Technology, National Engineering Research Center for Non-Food Biorefinery, Guangxi Key Laboratory of Biorefinery, Guangxi Biomass Engineering Technology Research Center, Guangxi Academy of Sciences, Nanning, China

Pseudomonas aeruginosa is a Gram-negative bacterium causing diseases in plants, animals, and humans, and its drug resistance is a major concern in medical care. Biofilms play an important role in *P. aeruginosa* drug resistance. Three factors are most important to induce biofilm: quorum sensing (QS), bis-(3′-5′)-cyclic diguanosine monophosphate (c-di-GMP), and small RNAs (sRNAs). *P. aeruginosa* has its own specific QS system (PQS) besides two common QS systems, LasI–LasR and RhlI–RhlR, in bacteria. PQS is interesting not only because there is a negative regulation from RhlR to *pqsR* but also because the null mutation in PQS leads to a reduced biofilm formation. Furthermore, *P. aeruginosa* dispersed cells have physiological features that are distinct between the planktonic cells and biofilm cells. In response to a low concentration of c-di-GMP, *P. aeruginosa* cells can disperse from the biofilms to become planktonic cells. These raise an interesting hypothesis of whether biofilm can be reversed through the QS mechanism in *P. aeruginosa*. Although a single factor is certainly not sufficient to prevent the biofilm formation, it necessarily explores such possibility. In this hypothesis, the literature is analyzed to determine the negative regulation pathways, and then the transcriptomic data are analyzed to determine whether this hypothesis is workable or not. Unexpectedly, the transcriptomic data reveal a negative regulation between *lasI* and *psqR*. Also, the individual cases from transcriptomic data demonstrate the negative regulations of PQS with *lasII, lasIR*, *rhlI,* and *rhlR* under different experiments. Based on our analyses, possible strategies to reverse biofilm formation are proposed and their clinic implications are addressed.

Keywords: biofilm, *P. aeruginosa*, quorum sensing, transcriptome, positive feedback, negative feedback

OPEN ACCESS

Edited by:
Cristina García-Aljaro, University of Barcelona, Spain

Reviewed by:
Rodolfo García-Contreras, National Autonomous University of Mexico, Mexico
Akanksha Singh, Central Institute of Medicinal and Aromatic Plants (CIMAP), India

***Correspondence:**
Guang Wu
hongguanglishibahao@yahoo.com; hongguanglishibahao@gxas.cn

Specialty section:
This article was submitted to Antimicrobials, Resistance and Chemotherapy, a section of the journal Frontiers in Microbiology

Received: *02 April 2019*
Accepted: *25 June 2019*
Published: *23 July 2019*

Citation:
Yan S and Wu G (2019) Can Biofilm Be Reversed Through Quorum Sensing in Pseudomonas aeruginosa? Front. Microbiol. 10:1582. doi: 10.3389/fmicb.2019.01582

INTRODUCTION

Pseudomonas aeruginosa is a Gram-negative bacterium living in soil and water. Being an opportunistic pathogen, *P. aeruginosa* can cause the bacterial soft rot in plants (Rahme et al., 2000; Walker et al., 2004), and diseases in animals (Ferris et al., 2017; Vingopoulou et al., 2018) and humans, including eye (Willcox, 2007), burn wound (Church et al., 2006), acute and chronic pulmonary infections, where cystic fibrosis is associated with substantial morbidity and mortality (Elborn, 2016; Klockgether and Tümmler, 2017).

Therefore, *P. aeruginosa* is a major concern in medical care because of its drug resistance against the traditional antibiotic therapy (Buhl et al., 2015; Oliver et al., 2015), that is particularly problematic for immunocompromised patients and the elderly in nosocomial environments (Xia et al., 2016). *P. aeruginosa* brings about its drug resistance through hydrolyzation of antibiotics with carbapenemases or extended-spectrum β-lactamases or ApmR (Vatcheva-Dobrevska et al., 2013; Fisher and Mobashery, 2014; Hakemi Vala et al., 2014), the low permeability of outer membrane (Eren et al., 2013; Zgurskaya et al., 2015), the multidrug efflux (Poole, 2004; Aghazadeh et al., 2014), etc. Also, the biofilm is an important player in *P. aeruginosa* drug resistance (Mah et al., 2003) because the dense extracellular matrix of biofilms reduces the efficacy of detergents and antibiotics (Mah et al., 2003). Such resistance could be increased a thousand times in some cases (Stewart and Costerton, 2001).

The dispersal of cells from the biofilm colony is a crucial and unique stage for biofilms to spread and colonize new surfaces (Monroe, 2007) and for the transition of dispersed cells from the biofilm to the planktonic growth phase. Could it be possible to stop the biofilm from happening, or reserve the biofilm back to the planktonic phenotype, or eradicate the biofilm in bacteria?

Theoretically, this hypothesis could be possible for *P. aeruginosa*, because its dispersed cells have physiological features that are distinct between the planktonic and the biofilm cells (Chua et al., 2014, 2015). In response to a low concentration of c-di-GMP, *P. aeruginosa* cells can disperse from the biofilm to become the planktonic cells. The drug resistance is not stronger in the biofilm cells than in the stationary-phase planktonic cells, but is stronger than in the logarithmic-phase planktonic cells (Spoering and Lewis, 2001). Additionally, *P. aeruginosa* produces *cis*-2-decenoic acid, which is a fatty acid messenger and induces dispersion and inhibits the growth of biofilm colonies (Davies and Marques, 2009). Furthermore, nitric oxide triggers the dispersal of biofilms in *P. aeruginosa* (Barraud et al., 2006), leading to the treatment of chronic infections in cystic fibrosis (Howlin et al., 2017).

The formation of biofilm is induced and regulated by numerous genes and environmental factors (Fazli et al., 2014), of which three are most important. The first one is the quorum sensing (QS), because QS controls about 10% genes in *P. aeruginosa* (Wagner et al., 2003), including many genes that are actively involved in the biofilm development and dispersal, although they are unlikely to be involved in the attachment and the initial of biofilm growth (Davies et al., 1998). The second one is the bis-(3′-5′)-cyclic diguanosine monophosphate (c-di-GMP), because its signaling network is the most complex secondary signaling system in bacteria (Hengge, 2009) and has the responsibility to decide whether bacteria adopt either planktonic or biofilm phenotype (Jenal and Malone, 2006). The third one is the small RNAs (sRNAs) although their role in biofilm is yet to be clear (Wolska et al., 2016).

Indeed, QS has a close relationship with biofilm (Wolska et al., 2016). It controls the synthesis of rhamnolipids that maintain the channels (Stoodley et al., 1994) for distributing nutrient and oxygen and removing waste products in mushroom-shaped structures (Davey and O'Toole, 2000). The channels can help in the release of a large amount of eDNA due to the autolysis of subpopulation of bacteria (Allesen-Holm et al., 2006) at the late stage of biofilm development. Various components of the biofilm matrix, such as extracellular DNA (eDNA), exopolysaccharides (EPS) and glucan, are closely related to biofilm matrix dynamics and bacterial virulence (Rainey et al., 2019). Also, there are other virulence factors, which play an important role in the QS regulation and biofilm formation. For example, pyocyanin promotes eDNA release and facilitates the biofilm formation (Klare et al., 2016).

It is worth reviewing literature to explore whether the biofilm is theoretically reversible through QS in *P. aeruginosa*, not only because *P. aeruginosa* is a causal organism of important health ailments but also because *P. aeruginosa* is a commonly used biofilm model organism (Rasamiravaka et al., 2015). More importantly, the synthesis of rhamnolipid in *P. aeruginosa* occurs at its late-exponential and stationary phases (Guerra-Santos et al., 1986). Rhamnolipid helps bacteria to utilize long-chain fatty acids as sources of carbon (Ochsner et al., 1994a) so it plays an important role in the biofilm formation (Stoodley et al., 1994; Davey and O'Toole, 2000; Allesen-Holm et al., 2006).

Reversing of biofilms could be plausible because QS is a target in many different circumstances such as attenuate virulence (Chan et al., 2015), bacterial metabolism (Goo et al., 2015), bacterial response to antibiotics (Rasamiravaka and El Jaziri, 2016), and therapy (LaSarre and Federle, 2013). Besides, the mechanism to form biofilms in *P. aeruginosa* is definitely different from other bacteria such as *P. putida*, *P. fluorescens*, *Staphylococcus aureus*, and *Vibrio cholera* (Wolska et al., 2016).

Needless to say, the reversing of biofilms is related to multiple factors, so a single factor such as QS could have very limited effects. However, we should theoretically explore those possibilities one by one at initial stage in view of the importance of biofilms in clinical meanings.

POSITIVE AND NEGATIVE REGULATIONS IN QS

If we wish to reverse the biofilm through the QS, we need to find out whether the QS is reversible or not. So far overwhelmed evidence suggests that the QS is a positive feedback system, which implies that it is impossible to stop the QS once the QS is initiated. However, we have yet to know whether the ending point of QS is the biofilm formation? If this is the case, the stop of QS will either reverse the biofilm or stop the biofilm formation. To answer this issue, it is necessary to find out the negative regulation (feedback) in QS.

The QS is a cell-to-cell communication by means of production, detection, and response of chemical compounds, autoinducers, and thus the QS changes an individual or a population behavior upon the concentration of autoinducers, which are subject to the cell density (Fuqua et al., 1994).

Pseudomonas aeruginosa has three QS systems. (i) LasI–LasR that is related to the synthesis and the use of *N*-(3-oxo-dodecanoyl)-L-homoserine lactone ($3OC_{12}$-HL) (Passador et al., 1993; Pearson et al., 1994), whose concentration is ranged from

1 to 5 μM (Pearson et al., 1994, 1995) (brown color items in **Figure 1**). (ii) RhlI-RhlR that is related to the synthesis and the use of *N*-(butyryl)-L-homoserine lactone (BHL) (Pearson et al., 1995), whose concentration is about 10 μM (Pearson et al., 1995) (yellow color items in **Figure 1**). (iii) Pseudomonas quinolone signal (PQS)-based QS, PqsABCDH-PqsR that is related to the synthesis and the use of 2-heptyl-3-hydroxy-4-quinolone (HHQ) (Mashburn-Warren et al., 2008; Kulkarni and Jagannadham, 2014), whose concentration is about 6 μM (Pesci et al., 1999) (green color items in **Figure 1**). The first two QS systems essentially are *N*-acylated homoserine lactone (AHL)-based QS systems (Pesci et al., 1997) and exist in many bacteria.

The sophisticated QS systems in *P. aeruginosa* are described as follows. (i) LasI produces $3OC_{12}$-HL, which acts on LasR (Gambello and Iglewski, 1991; Pearson et al., 1994) (the upward brown arrow from *lasR* to LasR on the left side of **Figure 1**). (ii) LasR acts on *aprA* (Gambello et al., 1993), *lasA* (Toder et al., 1991) and *toxA* (Gambello and Iglewski, 1991; Gambello et al., 1993; Passador et al., 1993) (the downward brown arrow on the far left side in **Figure 1**). (iii) Both LasI and LasR act on *lasB* (Pearson et al., 1994, 1995) through $3OC_{12}$-HL, whose half-maximal expression needs 1.0 nM (Seed et al., 1995) (brown symbols on the left side of **Figure 1**). (iv) RhlI produces BHL, which acts on RhlR (Pearson et al., 1995, 1997) (the bright yellow arrow on the right side of **Figure 1**). (v) RhlR acts on pyocyanin synthesis (Meighen, 1991; Ochsner et al., 1994b; Brint and Ohman, 1995) (the long yellow arrow on the middle of **Figure 1**), *lasA* (Brint and Ohman, 1995) (the yellow arrow on the middle left of **Figure 1**), and *rpoS* (Latifi et al., 1996) (the yellow arrow on the upper right corner of **Figure 1**). (vi) Both RhlI and RhlR act on *lasB* through BHL (Brint and Ohman, 1995) (the yellow arrow on the upper right part of **Figure 1**), and *rhlABR* (Ochsner and Reiser, 1995) (the small yellow arrow on the middle of **Figure 1**), where *rhlAB* encodes rhamnosyltransferase (Ochsner et al., 1994a) (two yellow arrows on the upper middle part of **Figure 1**) together with *rhlR* positively regulate rhamnolipid synthesis (Ochsner et al., 1994b) (the yellow arrow on the middle upper part of **Figure 1**). (vii) LasR and RhlR positively regulate the synthesis of hydrogen cyanide (Pessi and Haas, 2000) (the downward yellow arrow on the lower middle part of **Figure 1**).

Still, **Figure 1** displays the effects of PQS-based QS on their targets. (i) PqsABCDH produces HHQ requiring *phnA* and *phnB* through anthranilate (Gallagher et al., 2002) (the green curly lines on the middle right part of **Figure 1**), then HHQ acts on PqsR (Cao et al., 2001), regulating the production of elastase, PA-IL lectin, pyocyanin and rhamnolipid (Pesci et al., 1999; McKnight et al., 2000; Gallagher et al., 2002; Lee and Zhang, 2015) (the green lines from the lower right corner in **Figure 1**). (ii) PqsE positively acts on biosynthesis of various virulent factors, which is independent of HHQ or any compounds produced related to the function of *pqsABCDE* operon although the expression of *pqsE* and PqsE are controlled by HHQ and PqsR (Farrow, et al., 2008) (dashed green line on the lower right part of **Figure 1**). (iii) PqsR–HHQ is involved in iron homeostasis (Bredenbruch et al., 2006; Oglesby et al., 2008) (the lowest green line in **Figure 1**).

A positive feedback can be found in each of three QS systems. (i) The first positive feedback goes from LasR–$3OC_{12}$-HL to LasI through *lasI*, whose half-maximal expression needs 0.1 nM $3OC_{12}$-HL (Seed et al., 1995) (light gray ellipse on the left part of **Figure 1**). (ii) The second positive feedback goes from RhlR–HL to RhlI through *rhlI* (Ochsner and Reiser, 1995) (light gray ellipse on the upper right part of **Figure 1**). (iii) The third positive feedback goes from PqsR–HHQ to *pqsABCDE* and *phnAB* operons (Cao et al., 2001; Gallagher et al., 2002; Wade et al., 2005) (light gray ellipse on the middle right part of **Figure 1**).

The relationship among three QS systems in *P. aeruginosa* is positive in the following regulations. (i) LasR positively regulates HHQ through the complex LasR–$3OC_{12}$-HL on *pqsH* (Pesci et al., 1999; Schertzer et al., 2009) (brown arrow on the right middle part of **Figure 1**). (ii) RhlR positively regulates HHQ through *PqsE* (Pesci et al., 1999) (two arrow-blue lines on the middle right part of **Figure 1**). (iii) LasR positively regulates *rhlR* through the complex LasR–$3OC_{12}$-HL (Latifi et al., 1996; Pesci et al., 1997) and *rhlI* (Latifi et al., 1996) (the brown horizontal line with two arrows in **Figure 1**). (iv) HHQ strongly acts on *rhlI* with BHL (two arrow-blue lines in middle right part of **Figure 1**) but weakly acts on *lasR* and *rhlR* (McKnight et al., 2000). (v) RhlR positively regulates PqsE, whose overexpression leads to a high rhamnolipid production (Farrow, et al., 2008) (the yellow arrow on the right middle part of **Figure 1**). (vi) PqsE changes the function of RhlR rather than that of BHL (Farrow, et al., 2008) (two arrow-blue lines on the middle right part of **Figure 1**). (vii) LasR/$3OC_{12}$-HL controls *pqsR* (Camilli and Bassler, 2006) (the end arrow of brown horizontal line in **Figure 1**).

In fact, there is a negative regulation among QS systems, namely, RhlR negatively regulates *pqsR* in *P. aeruginosa* (Pesci et al., 1997; Wade et al., 2005), or RhlR and BHL together negatively affect the production of HHQ and other quinolones through *pqsR* to *pqsABCDE* operon transcription (McGrath et al., 2004; Jensen et al., 2006; Xiao et al., 2006b) (the yellow arrow from RhlR–BHL to the yellow horizontal line to the right end with downward dash end in **Figure 1**). On the other hand, a negatively regulatory pathway is not so sure (the yellow end line highlighted with a red star on the middle of **Figure 1**).

CAN THIS NEGATIVE REGULATION WORK?

As PQS-based QS is so particularly relevant to *Pseudomonas*, its significance should not be ignored. This is because the null mutation in PQS leads to a reduced biofilm formation and decreased the productions of pyocyanin, elastase, PA-IL lectin and rhamnolipids (Rahme et al., 1997, 2000; Cao et al., 2001; Diggle et al., 2003). Indeed, PQS directly or indirectly controls 92 or 143 genes as shown in two transcriptomic analyses (Deziel et al., 2005; Bredenbruch et al., 2006). By contrast, the other two QS systems together influence the expression in 200-plus genes (Whiteley et al., 1999).

For PQS, it does not reach its maximal production until the late stationary phase of growth (McKnight et al., 2000). This implies that HHQ is not involved in sensing the cell density, so the observation that the QS response is not reversed for

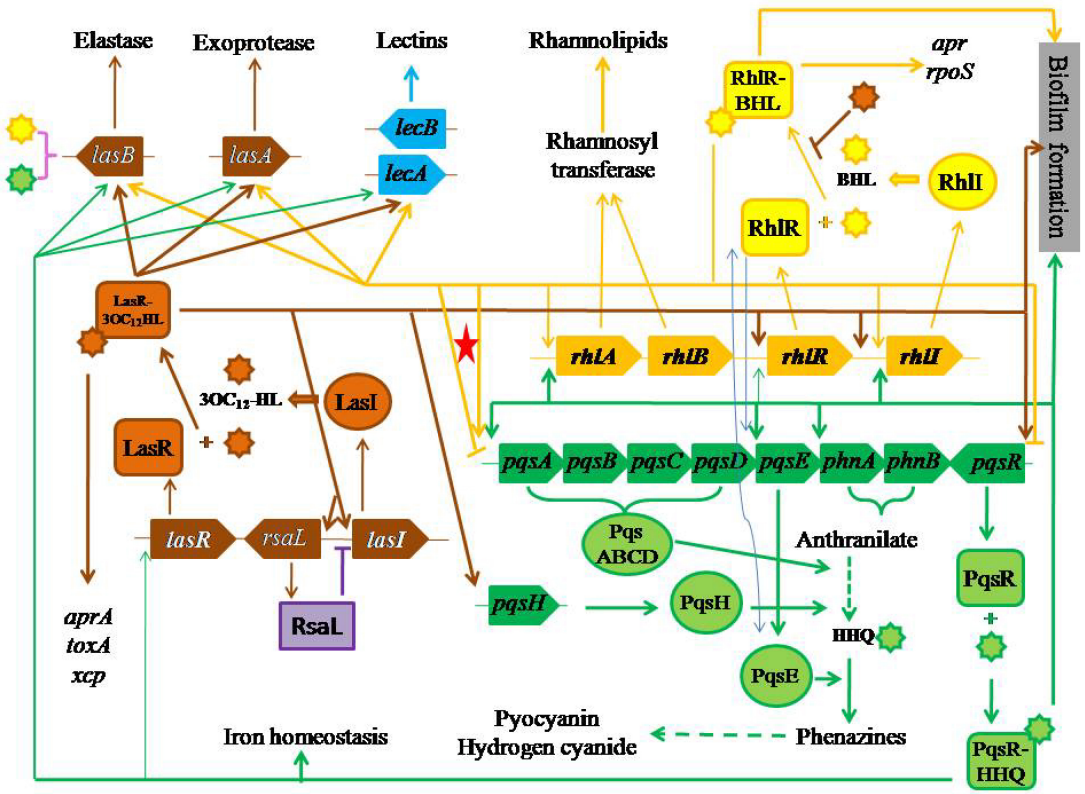

FIGURE 1 | Three QS systems with their effects and regulatory pathways. The red star highlights bi-functional regulation of RhlI–RhlR system to PQS synthesis.

small decreases in population density in *P. aeruginosa* (Williams and Camara, 2009) is not the failure of PQS. An important time interval appears between QS systems, i.e., BHL is produced during the log phase of growth but HHQ is produced during late time in the stationary phase of growth (McKnight et al., 2000), so the positive regulation of HHQ on *rhlI* is more likely to be related to the second round of RhlI cycle. If HHQ would not function at this time interval, perhaps the QS would stop.

Another promising point is that the phenazine production requires HHQ in *P. aeruginosa* (McKnight et al., 2000; Mavrodi et al., 2001). In fact, phenazines may have a significant ecological impact on the biofilm formation in *P. aeruginosa* as well as other bacteria persisting in biofilms mixed with *P. aeruginosa*. Through affecting H_2O_2 generation, phenazines bring about the lysis of competing bacterial cells in mixed biofilms and the subsequent eDNA release (Das and Manefield, 2013).

Perhaps, one of the best ways to explore the possibility of whether the QS is reversible through PQS in *P. aeruginosa* is to analyze the transcriptomic data in order to find some common patterns. Accordingly, we analyzed the transcriptomic data on Affymetrix *P. aeruginosa* array with 5549 *P. aeruginosa* genes, platform GPL84, from Gene Expression Omnibus (GEO) (Edgar et al., 2002; Barrett et al., 2013), including all the data in 104 publications (**Supplementary Information**) with 274 datasets. Each dataset represents the response to a specifically experimental condition. With these all available transcriptomic data, we wish to determine if PQS could be depressed under different experimental conditions.

Table 1 shows correlation coefficients between any two genes of three QS systems. The rationale is that there are up-regulations and down-regulations in transcriptomic data. The correlation between two genes, which are both up-regulated or both down-regulated, would suggest a positive regulation with a positive correlation coefficient. By contrast, the correlation between two genes, which are regulated oppositely, would suggest a negative regulation with a negative correlation coefficient.

Based upon the correlations within a single QS system in **Table 1**, the correlations between *lasI* and *lasR*, and between *rhlI* and *rhlR* confirm their auto-induction relationships (Gambello and Iglewski, 1991; Pearson et al., 1994) within each QS system. No negative correlation is found between the QS genes in the same QS system. As *pqsR* is named *mvfR* in gene bank, the auto-induction relationship with the rest of PQS genes are not very evident as the paired correlations between *pdsA*, *pqsB*, *pqsC*, *pqsD*, *pqsE,* but all paired correlations suggest a positive regulation within PQS system (Gallagher et al., 2002). Based upon the correlations between two QS systems in **Table 1**, the results conform there is a positive regulation between *lasI–lasR* and *rhlI–rhlR*, and between *rhlI-rhlR* and *pqsABCDE*. However, an undocumented negative regulation is revealed between *lasI*

TABLE 1 | Correlation coefficient between any two genes of three QS systems using transcriptomic data.

Gene		*lasI*	*lasR*	*rhlI*	*rhlR*	*rhl*	*pqsA*	*pqsB*	*pqsC*	*pqsD*	*pqsE*	*pqsH*	*pqsR/mvfR*
		PA1432	PA1430	PA3476	PA3477	PA3861	PA0996	PA0997	PA0998	PA0999	PA1000	PA2587	PA1003
lasI	PA1432	1	0.62	0.37	0.37	0.16	0.06	0.04	−0.02	−0.01	0.01	0.17	−0.38
lasR	PA1430		1	0.51	0.33	0.52	0.15	0.12	0.11	0.13	0.10	0.14	−0.03
rhlI	PA3476			1	0.89	0.29	0.73	0.76	0.58	0.67	0.58	0.20	0.17
rhlR	PA3477				1	0.13	0.84	0.88	0.66	0.76	0.68	0.05	−0.04
rhl	PA3861					1	0.15	0.14	0.19	0.22	0.14	0.16	0.24
pqsA	PA0996						1	0.97	0.85	0.95	0.82	−0.05	0.25
pqsB	PA0997							1	0.89	0.96	0.84	−0.03	0.24
pqsC	PA0998								1	0.90	0.87	−0.03	0.28
pqsD	PA0999									1	0.81	0.00	0.30
pqsE	PA1000										1	−0.07	0.23
pqsH	PA2587											1	0.27
pqsR/mvfR	PA1003												1

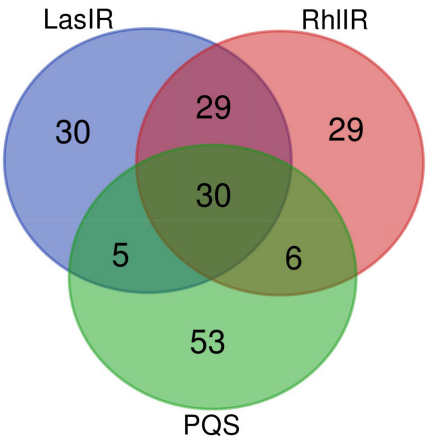

FIGURE 2 | Number of transcriptomic studies affecting QS in *P. aeruginosa* PAO1. The figure was made using online server at http://bioinformatics.psb.ugent.be/webtools/Venn/.

and *pqsR/mvfR* using these transcriptomic data. Could it be a potential pathway to reverse the biofilm formation?

Furthermore, the responses of QS systems are analyzed under different transcriptomic experiments, and classified as down-regulation, down-regulation/no response, no response, no response/up-regulation, up-regulation and mixed responses. **Figure 2** shows such analysis according to 94 transcriptomic experiments. No response on three QS systems was found in 30 transcriptomic experiments (the intersection of three circles in **Figure 2**). Both LasI-LasR and RhlI-RhlR have the same response in 29 transcriptomic experiments (the intersection of two upper circles in **Figure 2**), suggesting a good cooperation between them. By the contrast, only five and six transcriptomic experiments show the same response for PQS with LasI-LasR and RhlI-RhlR (the intersection of two upper and lower circles in **Figure 2**), respectively. The same response in both LasI-LasR and PQS systems includes no response in GSE24784, GSE26142, GSE35248, and GSE39044, and no response/up-regulation in GSE22684, indicating few positive impact of LasI-LasR on PQS. The same response in both RhlI-RhlR and PQS systems includes: down-regulation in GSE9255; down-regulation/no response in GSE5887; no response in GSE17179 and GSE61925; and no response/up-regulation in GSE65882 and GSE7402. Thus, the results from Venn diagram indicate that RhlI-RhlR has weak impacts on PQS. **Figure 2** demonstrates the responses of 30, 29, and 53 transcriptomic experiments solely in LasI-LasR, RhlI-RhlR, and PQS, respectively, of which their response ranges from down-regulation to mixed response.

Finally, the negative regulation between different QS systems is found in four transcriptomic experiments (GSE4152, GSE8408, GSE6122, and GSE17296). In the study on Australian clonal strain (AES-1) in patients with cystic fibrosis in GSE6122 (Manos et al., 2009), *lasI*, *rhlI,* and *rhlR* were down-regulated while *pqsA*, *pqsB*, *pqsC*, *pqsD*, and *pqsE* were up-regulated. This highlights the PQS remarkable effect on the biofilm formation and enhanced infectivity. Another three

transcriptomic experiments show that *pqsA*, *pqsB*, *pqsC*, *pqsD*, and *pqsE* were down-regulated whereas *rhlI* and *rhlR* were up-regulated (Teitzel et al., 2006; Tralau et al., 2007; Kawakami et al., 2010), of which *lasI* was up-regulated in copper-stressed (Teitzel et al., 2006), and both *lasI* and *lasR* were up-regulated in sulfate limitation (Tralau et al., 2007). Therefore, RhlI-RhlR does have a negative regulation on PQS (McGrath et al., 2004; Wade et al., 2005; Xiao et al., 2006a).

CONCLUSION

In this hypothesis, we apply the transcriptomic data to verify the hypothesis of whether the biofilm can be reversed in *P. aeruginosa* through QS because there are negative regulations between PQS and RhlI-RhlR. Interestingly, the transcriptomic data from 104 publications reveal a negative regulation between *lasI* and *psqR*, rendering a support to the hypothesis. Individual cases from transcriptomic data under different experiments demonstrate the negative regulations of PQS with *laslI, laslR*, *rhlI,* and *rhlR*.

In general, the relationships among different QS systems reveal positive regulations, which act together to promote the biofilm formation. However, the present analyses from literature and transcriptomic data provide the evidence that both LaslI-LaslR and RhlI-RhlR systems have negatively regulatory effects on PQS system. This is very important because these negative regulations lay the foundation for the biofilm reversion through QS. Although the exact pathways are still not fully discovered, the *N*-acylated homoserine lactone (AHL)-based QS systems can influence PQS-based QS system by inhibiting the expression of *pqsABCDE* operon and *pqsR*, resulting in the reduction of HHQ and PqsR synthesis. Consequently, the low concentration of PQS related products cannot maintain the biofilm, leading to its reversion. On the other hand, the down-regulated PQS-based QS system cannot perform well their function of positive regulations on LaslI-LaslR and RhlI-RhlR systems, which will further affect the biofilm formation, especially in the second round of RhlI cycle. Surely, there are other factors that play roles in the formation of drug-resistant multicellular biofilms, such as c-di-GMP. As mentioned in section "Introduction," this signal can govern bacterial cells to adopt either planktonic phenotype or biofilm formation (Hengge, 2009). Recent study demonstrates that high levels of cAMP lead to the decrease of c-di-GMP content, which inhibits the biofilm formation in *P. aeruginosa* (Almblad et al., 2019).

In clinic therapeutics for infectious diseases, antibiotic resistance has been spreading widely and rapidly, which becomes a major challenge for modern medicine. The strategy of interfering the biofilm formation is effective through bacterial cell-to-cell communication, especially with QS system (Soheili et al., 2019). More recently, QS inhibitors are drawing great attention in blocking the pathogenicity from *P. aeruginosa* (Calvert et al., 2018; Schütz and Empting, 2018). The transcriptional regulator PqsR becomes an attractive object and is considered to be one of the most appropriate targets. Currently, QS regulation mechanism in *P. aeruginosa* is mainly related to positive and negative regulation between QS systems. Clearly, exploration of regulation beyond QS should get attention in future.

DATA AVAILABILITY

All datasets generated or analyzed for this study are included in the manuscript and the **Supplementary Files**.

AUTHOR CONTRIBUTIONS

GW designed the work. Both authors prepared and approved the manuscript.

FUNDING

This work was partly supported by the National Natural Science Foundation of China (Nos. 31460296 and 31560315) and the Key Project of Guangxi Scientific Research and Technology Development Plan (AB17190534).

SUPPLEMENTARY MATERIAL

The Supplementary Material for this article can be found online at: https://www.frontiersin.org/articles/10.3389/fmicb.2019.01582/full#supplementary-material

REFERENCES

Aghazadeh, M., Hojabri, Z., Mahdian, R., Nahaei, M. R., Rahmati, M., Hojabri, T., et al. (2014). Role of efflux pumps: MexAB-OprM and MexXY(-OprA), AmpC cephalosporinase and OprD porin in non-metallo-β-lactamase producing *Pseudomonas aeruginosa* isolated from cystic fibrosis and burn patients. *Infect. Genet. Evol.* 24, 187–192. doi: 10.1016/j.meegid.2014.03.018

Allesen-Holm, M., Barken, K. B., Yang, L., Klausen, M., Webb, J. S., Kjelleberg, S., et al. (2006). A characterization of DNA release in *Pseudomonas aeruginosa* cultures and biofilms. *Mol. Microbiol.* 59, 1114–1128. doi: 10.1111/j.1365-2958.2005.05008.x

Almblad, H., Rybtke, M., Hendiani, S., Andersen, J. B., Givskov, M., and Tolker-Nielsen, T. (2019). High levels of cAMP inhibit *Pseudomonas aeruginosa* biofilm formation through reduction of the c-di-GMP content. *Microbiology* 165, 324–333. doi: 10.1099/mic.0.000772

Barraud, N., Hassett, D. J., Hwang, S. H., Rice, S. A., Kjelleberg, S., and Webb, J. S. (2006). Involvement of nitric oxide in biofilm dispersal of *Pseudomonas aeruginosa*. *J. Bacteriol.* 188, 7344–7353. doi: 10.1128/jb.00779-06

Barrett, T., Wilhite, S. E., Ledoux, P., Evangelista, C., Kim, I. F., Tomashevsky, M., et al. (2013). NCBI GEO: archive for functional genomics data sets–update. *Nucleic Acids Res.* 41, D991–D995. doi: 10.1093/nar/gks1193

Bredenbruch, F., Geffers, R., Nimtz, M., Buer, J., and Haussler, S. (2006). The *Pseudomonas aeruginosa* quinolone signal (PQS) has an iron-chelating activity. *Environ. Microbiol.* 8, 81318–81329.

Brint, J. M., and Ohman, D. E. (1995). Synthesis of multiple exoproducts in *Pseudomonas aeruginosa* is under the control of RhlR-RhlI, another set of regulators in strain PAO1 with homology to the autoinducer-responsive LuxR-LuxI family. *J. Bacteriol.* 177, 7155–7163. doi: 10.1128/jb.177.24.7155-7163.1995

Buhl, M., Peter, S., and Willmann, M. (2015). Prevalence and risk factors associated with colonization and infection of extensively drug-resistant *Pseudomonas aeruginosa*: a systematic review. *Expert. Rev. Anti. Infect. Ther.* 13, 1159–1170. doi: 10.1586/14787210.2015.1064310

Calvert, M. B., Jumde, V. R., and Titz, A. (2018). Pathoblockers or antivirulence drugs as a new option for the treatment of bacterial infections. *Beilstein J. Org. Chem.* 14, 2607–2617. doi: 10.3762/bjoc.14.239

Camilli, A., and Bassler, B. L. (2006). Bacterial small-molecule signaling pathways. *Science* 311, 1113–1116. doi: 10.1126/science.1121357

Cao, H., Krishnan, G., Goumnerov, B., Tsongalis, J., Tompkins, R., and Rahme, L. G. (2001). A quorum sensing-associated virulence gene of *Pseudomonas aeruginosa* encodes a LysR-like transcription regulator with a unique self-regulatory mechanism. *Proc. Natl. Acad. Sci. U.S.A.* 98, 14613–14618. doi: 10.1073/pnas.251465298

Chan, K. G., Liu, Y. C., and Chang, C. Y. (2015). Inhibiting N-acyl-homoserine lactone synthesis and quenching *Pseudomonas* quinolone quorum sensing to attenuate virulence. *Front. Microbiol.* 6:1173. doi: 10.3389/fmicb.2015.01173

Chua, S. L., Hultqvist, L. D., Yuan, M., Rybtke, M., Nielsen, T. E., Givskov, M., et al. (2015). In vitro and in vivo generation and characterization of *Pseudomonas aeruginosa* biofilm-dispersed cells via c-di-GMP manipulation. *Nat. Protoc.* 10, 1165–1180. doi: 10.1038/nprot.2015.067

Chua, S. L., Liu, Y., Yam, J. K., Chen, Y., Vejborg, R. M., Tan, B. G., et al. (2014). Dispersed cells represent a distinct stage in the transition from bacterial biofilm to planktonic lifestyles. *Nat. Commun.* 5:4462. doi: 10.1038/ncomms5462

Church, D., Elsayed, S., Reid, O., Winston, B., and Lindsay, R. (2006). Burn wound infections. *Clin. Microbiol. Rev.* 19, 403–434.

Das, T., and Manefield, M. (2013). Phenazine production enhances extracellular DNA release via hydrogen peroxide generation in *Pseudomonas aeruginosa*. *Commun. Integr. Biol.* 6:e23570. doi: 10.4161/cib.23570

Davey, M. E., and O'Toole, G. A. (2000). Microbial biofilms: from ecology to molecular genetics. *Microbiol. Mol. Biol. Rev.* 64, 847–867. doi: 10.1128/mmbr.64.4.847-867.2000

Davies, D. G., and Marques, C. N. (2009). A fatty acid messenger is responsible for inducing dispersion in microbial biofilms. *J. Bacteriol.* 191, 1393–1403. doi: 10.1128/JB.01214-08

Davies, D. G., Parsek, M. R., Pearson, J. P., Iglewski, B. H., Costerton, J. W., and Greenberg, E. P. (1998). The involvement of cell-to-cell signals in the development of a bacterial biofilm. *Science* 280, 295–298. doi: 10.1126/science.280.5361.295

Deziel, E., Gopalan, S., Tampakaki, A. P., Lepine, F., Padfield, K. E., Saucier, M., et al. (2005). The contribution of MvfR to *Pseudomonas aeruginosa* pathogenesis and quorum sensing circuitry regulation: multiple quorum sensing-regulated genes are modulated without affecting lasRI, rhlRI or the production of N-acyl-l-homoserine lactones. *Mol. Microbiol.* 55, 998–1014. doi: 10.1111/j.1365-2958.2004.04448.x

Diggle, S. P., Winzer, K., Chhabra, S. R., Worrall, K. E., Camara, M., and Williams, P. (2003). The *Pseudomonas aeruginosa* quinolone signal molecule overcomes the cell density-dependency of the quorum sensing hierarchy, regulates rhl-dependent genes at the onset of stationary phase and can be produced in the absence of LasR. *Mol. Microbiol.* 50, 29–43. doi: 10.1046/j.1365-2958.2003.03672.x

Edgar, R., Domrachev, M., and Lash, A. E. (2002). Gene expression omnibus: NCBI gene expression and hybridization array data repository. *Nucleic Acids Res.* 30, 207–210. doi: 10.1093/nar/30.1.207

Elborn, J. S. (2016). Cystic fibrosis. *Lancet* 388, 2519–2531. doi: 10.1016/S0140-6736(16)00576-6

Eren, E., Parkin, J., Adelanwa, A., Cheneke, B., Movileanu, L., Khalid, S., et al. (2013). Toward understanding the outer membrane uptake of small molecules by *Pseudomonas aeruginosa*. *J. Biol. Chem.* 288, 12042–12053. doi: 10.1074/jbc.M113.463570

Farrow, J. M. III, Sund, Z. M., Ellison, M. L., Wade, D. S., Coleman, J. P., and Pesci, E. C. (2008). PqsE functions independently of PqsR-*Pseudomonas* quinolone signal and enhances the rhl quorum-sensing system. *J. Bacteriol.* 190, 7043–7051. doi: 10.1128/JB.00753-08

Fazli, M., Almblad, H., Rybtke, M. L., Givskov, M., Eberl, L., and Tolker-Nielsen, T. (2014). Regulation of biofilm formation in *Pseudomonas* and Burkholderia species. *Environ. Microbiol.* 16, 1961–1981. doi: 10.1111/1462-2920.12448

Ferris, R. A., McCue, P. M., Borlee, G. I., Glapa, K. E., Martin, K. H., Mangalea, M. R., et al. (2017). Model of chronic equine endometritis involving a *Pseudomonas aeruginosa* biofilm. *Infect. Immun.* 85:e00332-17. doi: 10.1128/IAI.00332-17

Fisher, J. F., and Mobashery, S. (2014). The sentinel role of peptidoglycan recycling in the β-lactam resistance of the Gram-negative *Enterobacteriaceae* and *Pseudomonas aeruginosa*. *Bioorg. Chem.* 56, 41–48. doi: 10.1016/j.bioorg.2014.05.011

Fuqua, W. C., Winans, S. C., and Greenberg, E. P. (1994). Quorum sensing in bacteria: the LuxR-LuxI family of cell density-responsive transcriptional regulators. *J. Bacteriol.* 176, 269–275. doi: 10.1128/jb.176.2.269-275.1994

Gallagher, L. A., McKnight, S. L., Kuznetsova, M. S., Pesci, E. C., and Manoil, C. (2002). Functions required for extracellular quinolone signaling by *Pseudomonas aeruginosa*. *J. Bacteriol.* 184, 6472–6480. doi: 10.1128/jb.184.23.6472-6480.2002

Gambello, M. J., and Iglewski, B. H. (1991). Cloning and characterization of the *Pseudomonas aeruginosa* lasR gene, a transcriptional activator of elastase expression. *J. Bacteriol.* 173, 3000–3009. doi: 10.1128/jb.173.9.3000-3009.1991

Gambello, M. J., Kaye, S., and Iglewski, B. H. (1993). LasR of *Pseudomonas aeruginosa* is a transcriptional activator of the alkaline protease gene (apr) and an enhancer of exotoxin A expression. *Infect. Immun.* 61, 1180–1184.

Goo, E., An, J. H., Kang, Y., and Hwang, I. (2015). Control of bacterial metabolism by quorum sensing. *Trends Microbiol.* 23, 567–576. doi: 10.1016/j.tim.2015.05.007

Guerra-Santos, L., Käppeli, O., and Fiechter, A. (1986). Dependence of *Pseudomonas aeruginosa* continuous culture biosurfactant production on nutritional and environmental factors. *Appl. Microbiol. Biotechnol.* 24, 443–448.

Hakemi Vala, M., Hallajzadeh, M., Hashemi, A., Goudarzi, H., Tarhani, M., Sattarzadeh Tabrizi, M., et al. (2014). Detection of Ambler class A, B and D ß-lactamases among *Pseudomonas aeruginosa* and *Acinetobacter baumannii* clinical isolates from burn patients. *Ann. Burns Fire Disasters* 27, 8–13.

Hengge, R. (2009). Principles of c-di-GMP signalling in bacteria. *Nat. Rev. Microbiol.* 7, 263–273. doi: 10.1038/nrmicro2109

Howlin, R. P., Cathie, K., Hall-Stoodley, L., Cornelius, V., Duignan, C., Allan, R. N., et al. (2017). Low-dose nitric oxide as targeted anti-biofilm adjunctive therapy to treat chronic *Pseudomonas aeruginosa* infection in cystic fibrosis. *Mol. Ther.* 25, 2104–2116. doi: 10.1016/j.ymthe.2017.06.021

Jenal, U., and Malone, J. (2006). Mechanisms of cyclic-di-GMP signaling in bacteria. *Annu. Rev. Genet.* 40, 385–407. doi: 10.1146/annurev.genet.40.110405.090423

Jensen, V., Lons, D., Zaoui, C., Bredenbruch, F., Meissner, A., Dieterich, G., et al. (2006). RhlR expression in *Pseudomonas aeruginosa* is modulated by the *Pseudomonas* quinolone signal via PhoB-dependent and -independent pathways. *J. Bacteriol.* 188, 8601–8606. doi: 10.1128/jb.01378-06

Kawakami, T., Kuroki, M., Ishii, M., Igarashi, Y., and Arai, H. (2010). Differential expression of multiple terminal oxidases for aerobic respiration in *Pseudomonas aeruginosa*. *Environ. Microbiol.* 12, 1399–1412. doi: 10.1111/j.1462-2920.2009.02109.x

Klare, W., Das, T., Ibugo, A., Buckle, E., Manefield, M., and Manos, J. (2016). Glutathione-disrupted biofilms of clinical *Pseudomonas aeruginosa* strains exhibit an enhanced antibiotic effect and a novel biofilm transcriptome. *Antimicrob. Agents Chemother.* 60, 4539–4551. doi: 10.1128/AAC.02919-15

Klockgether, J., and Tümmler, B. (2017). Recent advances in understanding *Pseudomonas aeruginosa* as a pathogen. *F1000Res.* 6:1261. doi: 10.12688/f1000research.10506.1

Kulkarni, H. M., and Jagannadham, M. V. (2014). Biogenesis and multifaceted roles of outer membrane vesicles from Gram-negative bacteria. *Microbiology* 160, 2109–2121. doi: 10.1099/mic.0.079400-0

LaSarre, B., and Federle, M. J. (2013). Exploiting quorum sensing to confuse bacterial pathogens. *Microbiol. Mol. Biol. Rev.* 77, 73–111. doi: 10.1128/MMBR.00046-12

Latifi, A., Foglino, M., Tanaka, K., Williams, P., and Lazdunski, A. (1996). A hierarchical quorum-sensing cascade in *Pseudomonas aeruginosa* links the transcriptional activators LasR and RhlR (VsmR) to expression of the stationary-phase sigma factor RpoS. *Mol. Microbiol.* 21, 1137–1146. doi: 10.1046/j.1365-2958.1996.00063.x

Lee, J., and Zhang, L. (2015). The hierarchy quorum sensing network in *Pseudomonas aeruginosa*. *Protein Cell* 6, 26–41. doi: 10.1007/s13238-014-0100-x

Mah, T. F., Pitts, B., Pellock, B., Walker, G. C., Stewart, P. S., and O'Toole, G. A. (2003). A genetic basis for *Pseudomonas aeruginosa* biofilm antibiotic resistance. *Nature* 426, 306–310. doi: 10.1038/nature02122

Manos, J., Arthur, J., Rose, B., Bell, S., Tingpej, P., Hu, H., et al. (2009). Gene expression characteristics of a cystic fibrosis epidemic strain of *Pseudomonas aeruginosa* during biofilm and planktonic growth. *FEMS Microbiol. Lett.* 292, 107–114. doi: 10.1111/j.1574-6968.2008.01472.x

Mashburn-Warren, L., Howe, J., Garidel, P., Richter, W., Steiniger, F., Roessle, M., et al. (2008). Interaction of quorum signals with outer membrane lipids: insights into prokaryotic membrane vesicle formation. *Mol. Microbiol.* 69, 491–502. doi: 10.1111/j.1365-2958.2008.06302.x

Mavrodi, D. V., Bonsall, R. F., Delaney, S. M., Soule, M. J., Phillips, G., and Thomashow, L. S. (2001). Functional analysis of genes for biosynthesis of pyocyanin and phenazine-1-carboxamide from *Pseudomonas aeruginosa* PAO1. *J. Bacteriol.* 183, 6454–6465. doi: 10.1128/jb.183.21.6454-6465.2001

McGrath, S., Wade, D. S., and Pesci, E. C. (2004). Dueling quorum sensing systems in *Pseudomonas aeruginosa* control the production of the *Pseudomonas* quinolone signal (PQS). *FEMS Microbiol. Lett.* 230, 27–34. doi: 10.1016/s0378-1097(03)00849-8

McKnight, S. L., Iglewski, B. H., and Pesci, E. C. (2000). The *Pseudomonas* quinolone signal regulates rhl quorum-sensing in *Pseudomonas aeruginosa*. *J. Bacteriol.* 182, 2702–2708. doi: 10.1128/jb.182.10.2702-2708.2000

Meighen, E. A. (1991). Molecular biology of bacterial bioluminescence. *Microbiol. Rev.* 55, 123–142.

Monroe, D. (2007). Looking for chinks in the armor of bacterial biofilms. *PLoS Biol.* 5:e307. doi: 10.1371/journal.pbio.0050307

Ochsner, U. A., Fiechter, A., and Reiser, J. (1994a). Isolation, characterization, and expression in *Escherichia coli* of the *Pseudomonas aeruginosa* rhlAB genes encoding a rhamnosyltransferase involved in rhamnolipid biosurfactant synthesis. *J. Biol. Chem.* 269, 19787–19795.

Ochsner, U. A., Koch, A. K., Fiechter, A., and Reiser, J. (1994b). Isolation and characterization of a regulatory gene affecting rhamnolipid biosurfactant synthesis in *Pseudomonas aeruginosa*. *J. Bacteriol.* 176, 2044–2054. doi: 10.1128/jb.176.7.2044-2054.1994

Ochsner, U. A., and Reiser, J. (1995). Autoinducer-mediated regulation of rhamnolipid biosurfactant synthesis in *Pseudomonas aeruginosa*. *Proc. Natl. Acad. Sci. U.S.A.* 92, 6424–6428. doi: 10.1073/pnas.92.14.6424

Oglesby, A. G., Farrow, J. M. I. I. I., Lee, J. H., Tomaras, A. P., Greenberg, E. P., Pesci, E. C., et al. (2008). The influence of iron on *Pseudomonas aeruginosa* physiology: a regulatory link between iron and quorum sensing. *J. Biol. Chem.* 283, 28315558–28315567. doi: 10.1074/jbc.M707840200

Oliver, A., Mulet, X., López-Causapé, C., and Juan, C. (2015). The increasing threat of *Pseudomonas aeruginosa* high-risk clones. *Drug Resist. Update* 2, 41–59. doi: 10.1016/j.drup.2015.08.002

Passador, L., Cook, J. M., Gambello, M. J., Rust, L., and Iglewski, B. H. (1993). Expression of *Pseudomonas aeruginosa* virulence genes requires cell-to-cell communication. *Science* 260, 1127–1130. doi: 10.1126/science.8493556

Pearson, J. P., Gray, K. M., Passador, L., Tucker, K. D., Eberhard, A., Iglewski, B. H., et al. (1994). Structure of the autoinducer required for expression of *Pseudomonas aeruginosa* virulence genes. *Proc. Natl. Acad. Sci. U.S.A.* 91, 197–201. doi: 10.1073/pnas.91.1.197

Pearson, J. P., Passador, L., Iglewski, B. H., and Greenberg, E. P. (1995). A second N-acylhomoserine lactone signal produced by *Pseudomonas aeruginosa*. *Proc. Natl. Acad. Sci. U.S.A.* 92, 1490–1494. doi: 10.1073/pnas.92.5.1490

Pearson, J. P., Pesci, E. C., and Iglewski, B. H. (1997). Roles of *Pseudomonas aeruginosa* las and rhl quorum-sensing systems in control of elastase and rhamnolipid biosynthesis genes. *J. Bacteriol.* 179, 5756–5767. doi: 10.1128/jb.179.18.5756-5767.1997

Pesci, E. C., Milbank, J. B., Pearson, J. P., McKnight, S., Kende, A. S., Greenberg, E. P., et al. (1999). Quinolone signaling in the cell-to-cell communication system of *Pseudomonas aeruginosa*. *Proc. Natl. Acad. Sci. U.S.A.* 96, 11229–11234. doi: 10.1073/pnas.96.20.11229

Pesci, E. C., Pearson, J. P., Seed, P. C., and Iglewski, B. H. (1997). Regulation of las and rhl quorum sensing in *Pseudomonas aeruginosa*. *J. Bacteriol.* 179, 3127–3132. doi: 10.1128/jb.179.10.3127-3132.1997

Pessi, G., and Haas, D. (2000). Transcriptional control of the hydrogen cyanide biosynthetic genes hcnABC by the anaerobic regulator ANR and the quorum-sensing regulators LasR and RhlR in *Pseudomonas aeruginosa*. *J. Bacteriol.* 182, 6940–6949. doi: 10.1128/jb.182.24.6940-6949.2000

Poole, K. (2004). Efflux-mediated multiresistance in Gram-negative bacteria. *Clin. Microbiol. Infect.* 10, 12–26. doi: 10.1111/j.1469-0691.2004.00763.x

Rahme, L. G., Ausubel, F. M., Cao, H., Drenkard, E., Goumnerov, B. C., Lau, G. W., et al. (2000). Plants and animals share functionally common bacterial virulence factors. *Proc. Natl. Acad. Sci. U.S.A.* 97, 8815–8821. doi: 10.1073/pnas.97.16.8815

Rahme, L. G., Tan, M. W., Le, L., Wong, S. M., Tompkins, R. G., Calderwood, S. B., et al. (1997). Use of model plant hosts to identify *Pseudomonas aeruginosa* virulence factors. *Proc. Natl. Acad. Sci. U.S.A.* 94, 13245–13250. doi: 10.1073/pnas.94.24.13245

Rainey, K., Michalek, S. M., Wen, Z. T., and Wu, H. (2019). Glycosyltransferase-mediated biofilm matrix dynamics and virulence of *Streptococcus* mutans. *Appl. Environ. Microbiol.* 85:e02247-18. doi: 10.1128/AEM.02247-18

Rasamiravaka, T., and El Jaziri, M. (2016). Quorum-sensing mechanisms and bacterial response to antibiotics in *P. aeruginosa*. *Curr. Microbiol.* 73, 747–753. doi: 10.1007/s00284-016-1101-1

Rasamiravaka, T., Labtani, Q., Duez, P., and El Jaziri, M. (2015). The formation of biofilms by *Pseudomonas aeruginosa*: a review of the natural and synthetic compounds interfering with control mechanisms. *Biomed. Res. Int.* 2015:759348. doi: 10.1155/2015/759348

Schertzer, J. W., Boulette, M. L., and Whiteley, M. (2009). More than a signal: non-signaling properties of quorum sensing molecules. *Trends Microbiol.* 17, 189–195. doi: 10.1016/j.tim.2009.02.001

Schütz, C., and Empting, M. (2018). Targeting the *Pseudomonas* quinolone signal quorum sensing system for the discovery of novel anti-infective pathoblockers. *Beilstein J. Org. Chem.* 14, 2627–2645. doi: 10.3762/bjoc.14.241

Seed, P. C., Passador, L., and Iglewski, B. H. (1995). Activation of the *Pseudomonas aeruginosa* lasI gene by LasR and the *Pseudomonas* autoinducer PAI: an autoinduction regulatory hierarchy. *J. Bacteriol.* 177, 654–659. doi: 10.1128/jb.177.3.654-659.1995

Soheili, V., Tajani, A. S., Ghodsi, R., and Bazzaz, B. S. F. (2019). Anti-PqsR compounds as next-generation antibacterial agents against *Pseudomonas aeruginosa*: a review. *Eur. J. Med. Chem.* 172, 26–35. doi: 10.1016/j.ejmech.2019.03.049

Spoering, A. L., and Lewis, K. (2001). Biofilms and planktonic cells of *Pseudomonas aeruginosa* have similar resistance to killing by antimicrobials. *J. Bacteriol.* 183, 6746–6751. doi: 10.1128/jb.183.23.6746-6751.2001

Stewart, P. S., and Costerton, J. W. (2001). Antibiotic resistance of bacteria in biofilms. *Lancet* 358, 135–138. doi: 10.1016/s0140-6736(01)05321-1

Stoodley, P., Debeer, D., and Lewandowski, Z. (1994). Liquid flow in biofilm systems. *Appl. Environ. Microbiol.* 60, 2711–2716.

Teitzel, G. M., Geddie, A., De Long, S. K., Kirisits, M. J., Whiteley, M., and Parsek, M. R. (2006). Survival and growth in the presence of elevated copper: transcriptional profiling of copper-stressed *Pseudomonas aeruginosa*. *J. Bacteriol.* 188, 7242–7256. doi: 10.1128/jb.00837-06

Toder, D. S., Gambello, M. J., and Iglewski, B. H. (1991). *Pseudomonas aeruginosa* LasA: a second elastase under the transcriptional control of lasR. *Mol. Microbiol.* 5, 2003–2010. doi: 10.1111/j.1365-2958.1991.tb00822.x

Tralau, T., Vuilleumier, S., Thibault, C., Campbell, B. J., Hart, C. A., and Kertesz, M. A. (2007). Transcriptomic analysis of the sulfate starvation response of *Pseudomonas aeruginosa*. *J. Bacteriol.* 189, 6743–6750. doi: 10.1128/jb.00889-07

Vatcheva-Dobrevska, R., Mulet, X., Ivanov, I., Zamorano, L., Dobreva, E., Velinov, T., et al. (2013). Molecular epidemiology and multidrug resistance mechanisms of *Pseudomonas aeruginosa* isolates from Bulgarian hospitals. *Microb. Drug Resist.* 19, 355–361. doi: 10.1089/mdr.2013.0004

Vingopoulou, E. I., Delis, G. A., Batzias, G. C., Kaltsogianni, F., Koutinas, A., Kristo, I., et al. (2018). Prevalence and mechanisms of resistance to fluoroquinolones in *Pseudomonas aeruginosa* and *Escherichia coli* isolates recovered from dogs suffering from otitis in Greece. *Vet. Microbiol.* 213, 102–107. doi: 10.1016/j.vetmic.2017.11.024

Wade, D. S., Calfee, M. W., Rocha, E. R., Ling, E. A., Engstrom, E., Coleman, J. P., et al. (2005). Regulation of *Pseudomonas* quinolone signal synthesis in *Pseudomonas aeruginosa*. *J. Bacteriol.* 187, 4372–4380.

Wagner, V. E., Bushnell, D., Passador, L., Brooks, A. I., and Iglewski, B. H. (2003). Microarray analysis of *Pseudomonas aeruginosa* quorum-sensing regulons: effects of growth phase and environment. *J. Bacteriol.* 185, 2080–2095. doi: 10.1128/jb.185.7.2080-2095.2003

Walker, T. S., Bais, H. P., Déziel, E., Schweizer, H. P., Rahme, L. G., Fall, R., et al. (2004). *Pseudomonas aeruginosa*-plant root interactions. Pathogenicity, biofilm formation, and root exudation. *Plant Physiol.* 134, 320–331. doi: 10.1104/pp.103.027888

Whiteley, M., Lee, K. M., and Greenberg, E. P. (1999). Identification of genes controlled by quorum sensing in *Pseudomonas aeruginosa*. *Proc. Natl. Acad. Sci. U.S.A.* 96, 13904–13909.

Willcox, M. D. (2007). *Pseudomonas aeruginosa* infection and inflammation during contact lens wear: a review. *Optom. Vis. Sci.* 84, 273–278. doi: 10.1097/opx.0b013e3180439c3e

Williams, P., and Camara, M. (2009). Quorum sensing and environmental adaptation in *Pseudomonas aeruginosa*: a tale of regulatory networks and multifunctional signal molecules. *Curr. Opin. Microbiol.* 12, 182–191. doi: 10.1016/j.mib.2009.01.005

Wolska, K. I., Grudniak, A. M., Rudnicka, Z., and Markowska, K. (2016). Genetic control of bacterial biofilms. *J. Appl. Genet.* 57, 225–238. doi: 10.1007/s13353-015-0309-2

Xia, J., Gao, J., and Tang, W. (2016). Nosocomial infection and its molecular mechanisms of antibiotic resistance. *Biosci. Trends* 10, 14–21. doi: 10.5582/bst.2016.01020

Xiao, G., Deziel, E., He, J., Lepine, F., Lesic, B., Castonguay, M. H., et al. (2006a). MvfR, a key *Pseudomonas aeruginosa* pathogenicity LTTR-class regulatory protein, has dual ligands. *Mol. Microbiol.* 62, 1689–1699. doi: 10.1111/j.1365-2958.2006.05462.x

Xiao, G., He, J., and Rahme, L. G. (2006b). Mutation analysis of the *Pseudomonas aeruginosa* mvfR and pqsABCDE gene promoters demonstrates complex quorum-sensing circuitry. *Microbiology* 152, 1679–1686. doi: 10.1099/mic.0.28605-0

Zgurskaya, H. I., Löpez, C. A., and Gnanakaran, S. (2015). Permeability barrier of gram-negative cell envelopes and approaches to bypass it. *ACS Infect. Dis.* 1, 512–522. doi: 10.1021/acsinfecdis.5b00097

Conflict of Interest Statement: The authors declare that the research was conducted in the absence of any commercial or financial relationships that could be construed as a potential conflict of interest.

frontiers in Microbiology

ORIGINAL RESEARCH
published: 31 July 2019
doi: 10.3389/fmicb.2019.01693

Bacterial–Fungal Interactions in the Kelp Endomicrobiota Drive Autoinducer-2 Quorum Sensing

Anne Tourneroche[1], Raphaël Lami[2], Cédric Hubas[3], Elodie Blanchet[2], Marine Vallet[1], Karine Escoubeyrou[4], Alain Paris[1] and Soizic Prado[1]**

[1] Unité Molécules de Communication et Adaptation des Microorganismes (MCAM), Muséum National d'Histoire Naturelle (MNHN), Centre National de la Recherche Scientifique (CNRS), CP 54, Paris, France, [2] CNRS, Laboratoire de Biodiversité et Biotechnologies Microbiennes (LBBM), USR3579, Observatoire Océanologique de Banyuls, Sorbonne Université, Banyuls-sur-Mer, France, [3] Muséum National d'Histoire Naturelle, UMR BOREA 7208 MNHN-Sorbonne Université-CNRS-UCN-UA-IRD, Station Marine de Concarneau, Paris, France, [4] CNRS, Observatoire Océanologique de Banyuls, Sorbonne Université, FR3724, Banyuls-sur-Mer, France

Brown macroalgae are an essential component of temperate coastal ecosystems and a growing economic sector. They harbor diverse microbial communities that regulate algal development and health. This algal holobiont is dynamic and achieves equilibrium *via* a complex network of microbial and host interactions. We now report that bacterial and fungal endophytes associated with four brown algae (*Ascophyllum nodosum*, *Pelvetia canaliculata*, *Laminaria digitata*, and *Saccharina latissima)* produce metabolites that interfere with bacterial autoinducer-2 quorum sensing, a signaling system implicated in virulence and host colonization. Additionally, we performed co-culture experiments combined to a metabolomic approach and demonstrated that microbial interactions influence production of metabolites, including metabolites involved in quorum sensing. Collectively, the data highlight autoinducer-2 quorum sensing as a key metabolite in the complex network of interactions within the algal holobiont.

Keywords: quorum sensing (QS), AI-2, bacterial–fungal interaction, kelp microbiota, algal holobiont

OPEN ACCESS

Edited by:
Tom Defoirdt,
Ghent University, Belgium

Reviewed by:
Qian Yang,
Yellow Sea Fisheries Research Institute (CAFS), China
Natrah Fatin Mohd Ikhsan,
Putra Malaysia University, Malaysia

***Correspondence:**
Raphaël Lami
lami@obs-banyuls.fr
Soizic Prado
soizic.prado@mnhn.fr

Specialty section:
This article was submitted to Microbial Physiology and Metabolism, a section of the journal Frontiers in Microbiology

Received: *16 April 2019*
Accepted: *09 July 2019*
Published: *31 July 2019*

Citation:
Tourneroche A, Lami R, Hubas C, Blanchet E, Vallet M, Escoubeyrou K, Paris A and Prado S (2019) Bacterial–Fungal Interactions in the Kelp Endomicrobiota Drive Autoinducer-2 Quorum Sensing. Front. Microbiol. 10:1693. doi: 10.3389/fmicb.2019.01693

INTRODUCTION

Large marine brown algae, i.e., kelp, are an essential component of temperate coastal ecosystems. Indeed, these organisms are important primary producers that generate a specific habitat and thereby shape coastal marine life (Egan et al., 2013). In addition, kelp farming has been a growing economic sector over the last decades (FAO, 2018).

Like most eukaryotes, macroalgae are colonized by various microorganisms (the microbiota) that interact with them throughout the life cycle, and that modify their physiology (Wahl et al., 2012; Egan et al., 2013; Singh and Reddy, 2014). For example, commensal bacteria have profound effects on seaweed development, nutrition, and defense (Wahl et al., 2012; Singh and Reddy, 2014; Tapia et al., 2016). Algal tissues are also asymptomatically colonized by filamentous fungi (Debbab et al., 2012), although these fungi and their role are yet to be fully characterized (Fries, 1979; Zuccaro et al., 2003, 2008; Loque et al., 2010; Jones et al., 2012). Previously, we isolated and characterized the molecular diversity of cultivable fungi in different parts of the brown algae *Ascophyllum nodosum*, *Pelvetia canaliculata*, *Laminaria digitata*, and *Saccharina latissima*. We also found that metabolites produced by endophytic fungi are key mediators of interactions among macroalgae, their fungal microbiota, and protistan pathogens (Vallet et al., 2018).

Endophytic bacteria are likely to interact with fungi in the algal host to maintain the host-microbiota equilibrium and thus contribute to host health (Deveau et al., 2018; Hassani et al., 2018). Indeed, structural changes in the microbiota, i.e., dysbiosis, have been linked to disease in marine organisms and seaweeds (Fernandes et al., 2012; Zozaya-Valdes et al., 2015; Egan and Gardiner, 2016). However, the mechanisms underlying bacterial–fungal homeostasis remain unclear, although they appear crucial to macroalgal physiology not only in nature but also in farms, highlighting their importance in light of intensifying algal culture (Gachon et al., 2010).

Bacterial–fungal interactions consist of multiple and concomitant mechanisms ranging from nutrient competition to antibiosis, many of which depend on chemical signaling. Quorum sensing, which allows bacteria to coordinate gene expression based on the density of specific signaling molecules, is of particular interest, since it is essential for virulence, colonization, biofilm formation, and toxin production (Atkinson and Williams, 2009). Indeed, various types of quorum signals, also known as auto-inducers (AI), are already known. Some have been found in only one genus whereas others, such as type 1 (AI-1) or type 2 (AI-2), are present in various bacterial genera. Indeed, AI-2 molecules appear widespread among prokaryotes, and is produced by over 50% of sequenced bacterial species, including both Gram-positive and Gram-negative species (Hammer and Bassler, 2003; Federle, 2009). AI-2 molecules are derived from a common precursor, (*S*)-4,5-dihydroxypentane-2,3-dione (DPD), which is synthesized by the enzyme LuxS. By spontaneous cyclization, this precursor is transformed to 4-hydroxy-5-methyl-3(*2H*)furanone, (*2R*,*4S*)-2-methyl-2,3,3,4-tetrahydroxytetrahydrofuran, and, especially in marine environments, to the furanosyl borate diester (Hardie and Heurlier, 2008).

Various marine bacteria were found to produce AI-2 (Bodor et al., 2008; Doberva et al., 2015; Pérez-Rodríguez et al., 2015), although it is considered in some species to be a metabolic by product and not a signaling molecule (Rezzonico and Duffy, 2008). Nevertheless, many studies showed that AI-2 regulates niche-specific behaviors in commensal and pathogenic bacteria, including biofilm formation or dispersion, cell division, virulence, bioluminescence, and motility (Hammer and Bassler, 2003; Hardie and Heurlier, 2008; Federle, 2009). Accordingly, secreted AI-2 is now recognized as a key signaling molecule that affects bacterial behavior at species and community level (Whiteley et al., 2017).

Strikingly, quorum sensing molecules are not exclusively produced by bacteria. Indeed, these compounds were also shown to regulate fungal morphogenesis, germination, apoptosis, biofilm development, or pathogenicity (Wongsuk et al., 2016). Importantly, some recent studies showed that both bacterial and fungal quorum sensing compounds mediate cross-kingdom signaling. For instance, eukaryotes may interfere with bacterial quorum sensing (Martín-Rodríguez et al., 2014; Ismail et al., 2016), while bacteria may react to fungal quorum signals (Cugini et al., 2007; Fourie et al., 2016). Cross-kingdom signaling is also modulated by quorum sensing inhibitors, i.e., quorum quenchers (Grandclément et al., 2016; Rolland et al., 2016). To date, halogenated furanones synthesized by the marine red algae *Delisea pulchra* are the best-studied naturally occurring quorum sensing inhibitors in eukaryotes. These compounds regulate bacterial colonization of algal surfaces by interfering with AI-1 and AI-2 (Defoirdt et al., 2007; Harder et al., 2012).

Despite these breakthroughs, the role of AI-2 quorum sensing in marine environments in general, and in holobionts in particular, remains poorly characterized (Doberva et al., 2015; Hmelo, 2017). One important shortcoming is the lack of quantitative measurements, since AI-2 itself is difficult to quantify (Wang et al., 2018). In this study, we hypothesized that AI-2 quorum sensing is involved in interspecies chemical signaling among endophytic fungi and bacteria in seaweeds. Accordingly, we first isolated and molecularly characterized the cultivable bacteria associated with the brown algae *A. nodosum*, *P. canaliculata*, *L. digitata*, and *S. latissima*. These bacteria were then investigated for their ability to produce or inhibit production of AI-2 along with fungi previously isolated from the same samples (Vallet et al., 2018). Co-cultures experiments, between several fungal and bacterial endophytic strains isolated from *S. latissima* microbiota combined with metabolomics approach pointed out that inter-species interactions involve metabolites production that modulates AI-2 production. Altogether these results suggest that dynamic interactions driven by microbial metabolites may occur within the microbiota and impact AI-2 QS signaling.

MATERIALS AND METHODS

Sampling and Endophyte Isolation

Fungi and bacteria were previously isolated from the brown algae *L. digitata*, *S. latissima*, *A. nodosum*, and *P. canaliculata*. *L. digitata,* and *A. nodosum* were collected in triplicate in Roscoff, France, in January 2013. Samples of all four species were also collected in triplicate in Oban, Scotland, in July 2013. Algae were surface-sterilized with 70% ethanol and 0.1% sodium hypochlorite, and cut into small pieces. Around 4,600 of these pieces were then aseptically transferred to different solid media, using at least 10 replicates from each algal part on each type of medium (**Supplementary Table S1**). Resulting cultures were then grown and preserved following previously described protocols (Vallet et al., 2018).

Taxonomic Identification of Endophytic Bacteria

Genomic DNA was extracted with Wizard® Genomic DNA Purification Kit (Promega, Charbonnières-les-Bains, France) from single colonies of 209 bacterial isolates that were grown in marine broth. 16S rRNA genes were then amplified using 2× KAPA2G Ready Mix (Clinisciences, Nanterre, France), 1 μL bacterial DNA, and the universal primers 27F mod (5′-AGRGTTTGATCMTGGCTCAG-3′) and 1492R mod (5′-TACGGYTACCTTGTTAYGACTT-3′). Targets were amplified over one cycle of denaturation at 94°C for 5 min, 35 cycles at 94°C for 15 s, 50°C for 15 s, and 72°C for 20 s, and final extension at 72°C for 10 min. PCR products were sequenced

by Sanger sequencing on the Bio2Mar platform (Observatoire Océanologique, Banyuls-sur-Mer, France), using primer 907R (Eurofins MWG Operon, Ebersberg, Germany).

The quality of each sequence was checked manually and the closest match in NCBI databases was determined by BLAST (Altschul et al., 1990). Further, sequences were aligned in Muscle, as implemented in MEGA 7.0 (Edgar, 2004; Kumar et al., 2016). Alignments were reviewed manually to verify mismatches, and a phylogenetic tree was constructed by maximum likelihood using the K2, G+I model. The reliability of each node in the tree was assessed by bootstrapping over 500 replicates.

Screening for the Production of Quorum Sensing Mediators

The QS bioluminescent reporter strain *Vibrio campbellii* MM32 (***luxN***::Cm, ***luxS***::Tn5Kan) was used to detect AI-2 in bacterial and fungal extracts, as previously described (Miller et al., 2004). The receptor *luxN* is mutated in this strain to abolish sensing of acyl homoserine lactones, while the synthase gene *luxS* is mutated to abolish AI-2 production but not sensing. It was previously constructed by introducing *luxS*::Tn5Kan onto the chromosome of strain JAF305 (*luxN*::Cm) (Bassler et al., 1993; Freeman and Bassler, 1999).

To obtain bacterial supernatants, 1 mL was collected from each of 209 bacterial cultures grown for 24 h at 22°C in marine broth. Samples were then centrifuged at 17,000 × *g* for 10 min, and resulting supernatants were filtered at 0.22 μm. To obtain fungal extracts, 43 fungal isolates were grown for 3 weeks at 19°C in MEA/ASW medium, and extracted three times with ethyl acetate. A detailed recipe of the medium is provided in **Supplementary Table S1**. Extracts were tested at a final concentration of 250 μg/mL, with final concentration of DMSO 2.5%.

Bacterial supernatants and fungal extracts were tested for the production of molecules interfering with AI-2 quorum sensing. Briefly, 20 μL of test samples and corresponding controls were mixed with 180 μL of *V. campbellii* MM32 diluted 1:5,000 and incubated at 30°C and 100 rpm. Luminescence and cell density (OD_{620}) were measured after 24 h. Data were collected in triplicate, and luminescence change was calculated as $(lumi_{SN/E} - lumi_{Control})/lumi_{Control}$, where $lumi_{SN/E}$ is bioluminescence (normalized to cell density) from the reporter strain in the presence of supernatant or extract, and $lumi_{Control}$ is bioluminescence (normalized to cell density) in the presence of either marine broth (when supernatants are tested) or DMSO (when extracts are tested).

Quantification of AI-2 Precursor by LC–MS/MS

Due to low ionization potential and instability, AI-2 and DPD are not directly detectable by mass spectrometry (MS). However, quinoxaline derivatives of DPD, obtained by reaction with 4,5-dimethyl-1,2-phenylenediamine, are detectable by LC–MS/MS. DPD was thus quantified in bacterial supernatants after performing a derivatization reaction as described (Xu et al., 2017). Briefly, triplicate DPD standard solutions with concentration 2.6 nM–26 μM were obtained by diluting a stock solution of DPD (16.64 nM) in marine broth. To obtain quinoxaline derivatives, 250 μL of standard solution or supernatant was reacted with 250 μL of 0.1 mg/mL 4,5-dimethyl-1,2-phenylenediamine (Sigma, St. Louis, MO, United States) in 0.1M HCl. Samples were thoroughly mixed for 1 min, and incubated for 5 h at 25°C with agitation. Samples were then desalted with two volumes of water using Sep-Pak C18 SPE cartridges (Waters, Beverly, MA, United States), and eluted with two volumes of acetonitrile. Subsequently, samples were analyzed by LC–MS/MS on a Dionex Ultimate 3000 HPLC system coupled to a Q Exactive™ Focus mass spectrometer (Thermo Fisher Scientific, Waltham, MA, United States) and fitted with an electrospray ionization source and a Hypersil GOLD C18 column (2.1 mm × 150 mm, 1.9 μm particle size; Thermo Scientific, Waltham, MA, United States) operating at 20°C. In this system, eluates are introduced directly into the mass spectrometer. LC–MS parameters are detailed in **Supplementary Table S1**. Data were collected using Xcalibur, in parallel reaction monitoring mode targeting the precursor ion at *m/z* 233.1285. The product ion at *m/z* 186.1140 was used for quantification.

AI-2 Antagonist Activity in Fungal Extracts

To test AI-2 antagonist activity in fungal extracts, 20 μL samples were reacted as described with 180 μL of *V. campbellii* MM32 diluted 1:5,000 in marine broth and supplemented with 2 μM DPD (purchased from Rita Ventura's research group at ITQB, Oeiras, Portugal). To confirm that loss of luminescence, if any, was not due to cytotoxicity, 100 μL of culture was reacted with 30 μL of 0.01% resazurin (Graça et al., 2013) immediately after measurement of luminescence, and fluorescence (λ_{ex}: 530 nm, λ_{em}: 590 nm) was measured after incubating for 4 h at 30°C with agitation. As control, a 96-well plate containing 20 μL of fungal extract in marine broth was assayed in the same manner to assess background luminescence, fluorescence, and absorbance.

Co-culture Experiment: Culture Conditions and Impact on Quorum Sensing

Fungal and bacterial isolates were co-cultured in triplicate in marine broth supplemented with 10% malt extract, 4% glucose, and 1.5% agar, adjusted to pH 7, and plated. Plates were inoculated with 2 mL of a mixture of 2×10^4 fungal spores and bacteria diluted to OD 0.1. Corresponding monocultures were prepared in triplicate in the same manner. Cultures were then incubated for 21 days at 19°C and on a 12-h light/dark cycle. Petri dishes containing only culture medium ($n = 3$) were used as blank. Cultures and corresponding controls were extracted with ethyl acetate for 30 min, in a sonicator at room temperature. Samples were then filtered through a filter paper, and dried under vacuum using a centrifugal evaporator. Extracts were tested for their impact on quorum sensing at a final concentration of 250 μg/mL, with final concentration of DMSO 2.5%. Briefly, 20 μL of extract were mixed with 180 μL of *V. campbellii* MM32 diluted 1:5,000 and incubated at 30°C and

100 rpm. Luminescence and cell density (OD_{620}) were measured after 24 h. Data were collected in triplicate, and luminescence change was calculated as $(lumi_E - lumi_{Control})/lumi_{Control}$, where $lumi_E$ is bioluminescence (normalized to cell density) from the reporter strain in the presence of extract, and $lumi_{Control}$ is bioluminescence (normalized to cell density) in the presence of DMSO. To assess the viability of the biosensor, 100 µL of culture was reacted with 30 µL of 0.01% resazurin (Graça et al., 2013) immediately after measurement of luminescence, and fluorescence (λ_{ex}: 530 nm, λ_{em}: 590 nm) was measured after incubating for 4 h at 30°C with agitation.

Co-culture Experiment: LC–MS-Based Metabolomic Analysis

Dried extracts were solubilized in methanol at 0.5 mg/mL, and analyzed by HPLC–MS in one batch and in a random sequence. Samples were loaded onto a Dionex Ultimate 3000 HPLC system fitted with a C18 Acclaim™ RSLC PolarAdvantage II column (2.1 mm × 100 mm, 2.2 µm pore size; Thermo Scientific, Waltham, MA, United States) operating at 40°C, and coupled to a Maxis II™ QTOF mass spectrometer (Bruker, Bellerica, MA, United States) with an electrospray ionization source. Data were acquired with Data Analysis software. LC–MS parameters are listed in **Supplementary Table S1**. Raw LC–MS data were calibrated and converted to netCDF format using Data Analysis software (Bruker), and processed using the R package XCMS (Smith et al., 2006). Based on analytical conditions and raw data characteristics, final peak picking parameters were method = 'centWave,' ppm = 10, and peak width = c(5,20), while final grouping parameters were bw = 5, mzwid = 0.015, and retention time correction method = 'obiwarp.' Other parameters were set to default values. To limit noise from compounds already present in culture media, the dataset was filtered with an in-house script to retain only those features with intensity in at least one sample more than fivefold its average intensity in blank samples.

Statistical Procedures

All analyses and graphs were performed using the R statistical framework (R Core Team, 2019). Van der Waerden tests followed by a *post hoc* test using the Fischer's Least Significant Difference (LSD) criterion was performed to test the contrasting effect of mono and co-culture on QS activity. Multivariate analyses were done using the R library mixOmics (Rohart et al., 2017).

RESULTS

Diversity of Cultivable Endophytic Bacteria From Brown Algae

A total of 209 bacterial isolates was obtained, and classified based according to 16S rRNA genes into 4 phyla, 12 orders, 19 families, 27 genera, and 88 taxonomically unique units (**Figures 1**, **2** and **Supplementary Table S2**). The most abundant phyla in *L. digitata* and *S. latissima* were *Firmicutes* (comprising 47 and 35% of all isolates, respectively) and *Proteobacteria* (39 and 53%). In *P. canaliculata*, *Proteobacteria,* and *Actinobacteria* were

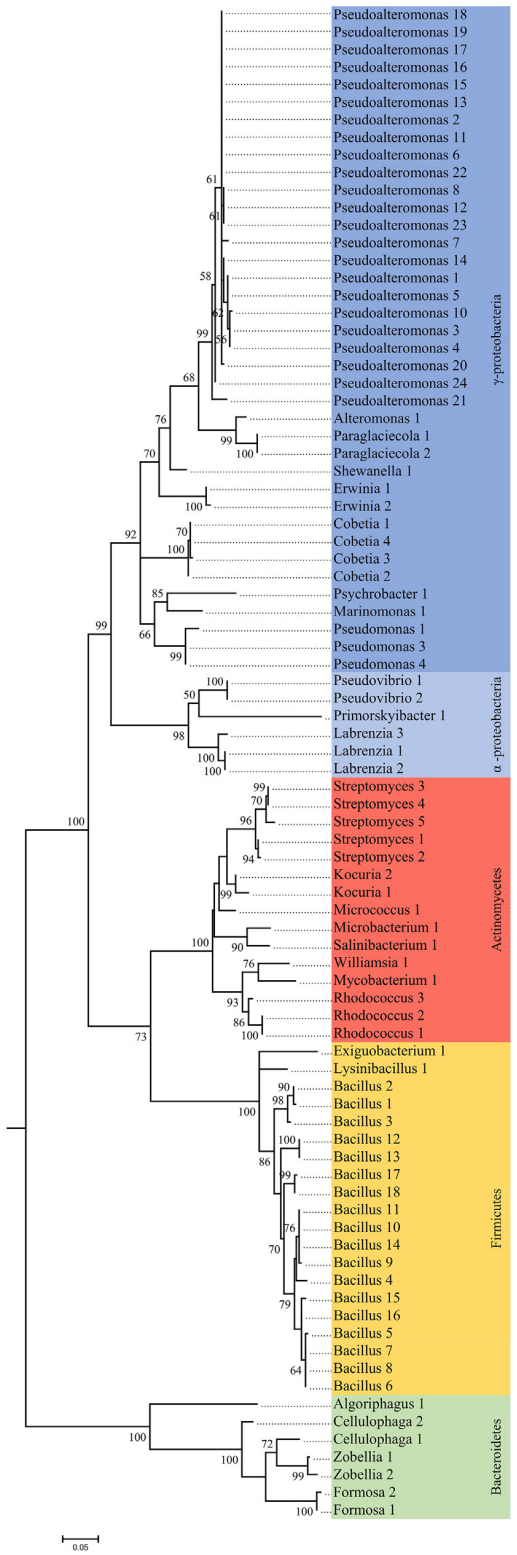

FIGURE 1 | Phylogenetic tree of unique 16S rRNA sequences from bacteria isolated from four algal species. The tree was constructed by maximum likelihood using the K2, G+I model. The reliability of each node was assessed by bootstrapping over 500 replicates.

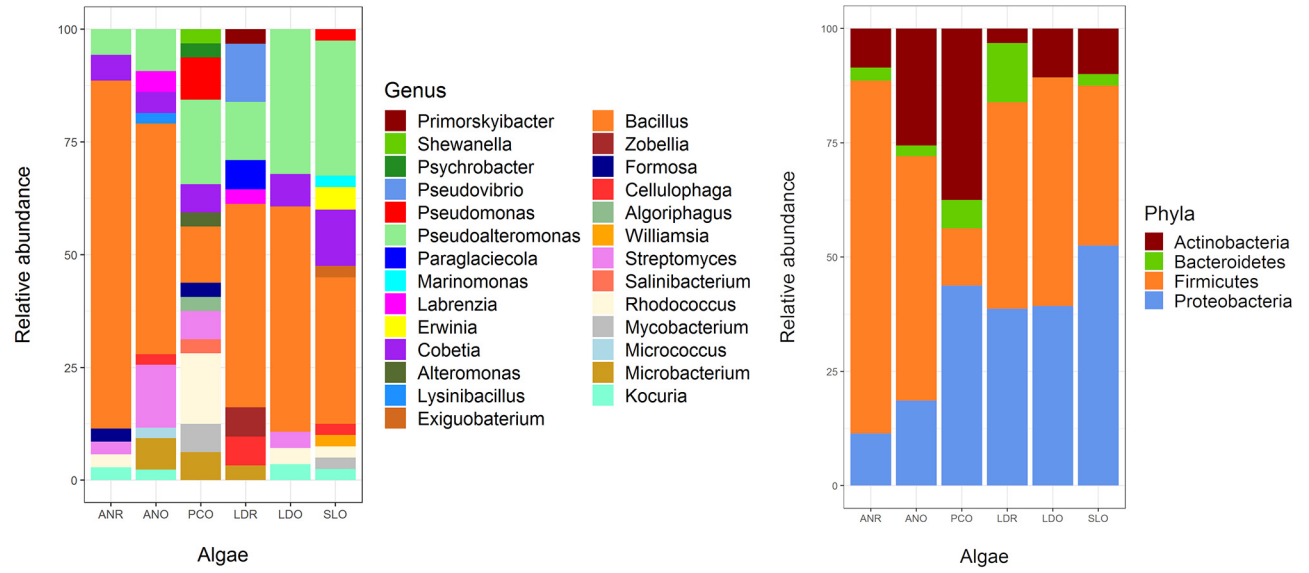

FIGURE 2 | Abundance of cultivable bacterial genus (left) and phyla (right) by algal host and sampling site. ANR, *Ascophylum nodosum* from Roscoff; ANO, *A. nodosum* from Oban; PCO, *Pelvetia canaliculata* from Oban; LDR, *Laminaria digitata* from Roscoff; LDO, *L. digitata* from Oban; SLO, *Saccharina latissima* from Oban.

predominant (44 and 38%), whereas *Firmicutes* accounted for 77% of bacteria isolated from *A. nodosum*. *Gammaproteobacteria* was between 50 and 100% of all *Proteobacteria* depending on algal species, although *Alphaproteobacteria* was occasionally present. On the other hand, *Bacillus* and *Pseudoalteromonas* were the most abundant genera in *S. latissima* (33 and 30%) and *L. digitata* (47 and 22%). Isolates from *P. canaliculata* were mostly *Pseudoalteromonas*, *Rhodococcus*, and *Bacillus* (19, 16, and 13%), whereas *Bacillus* was dominant in *A. nodosum* (63%). *Rhodococcus*, *Bacillus*, *Cobetia*, and *Pseudoalteromonas* were isolated from all four algal species.

Production of AI-2 Compounds by Bacterial Endophytes

Most (86%) bacterial endophytes isolated from brown algae elicited an increase in luminescence from *V. campbellii* MM32, a quorum sensing reporter strain (**Table 1** and **Supplementary Data S1**). Strikingly, 10% of isolates boosted luminescence by over 50%, including a *Kocuria* isolate, six *Bacillus* isolates, and 13 *Proteobacteria*. Indeed, a *Marinomonas* isolate and five *Cobetia* isolates increased luminescence by at least 100%. In contrast, all but one *Pseudoalteromonas* isolate increased luminescence by less than 50%.

To confirm these results, DPD production by *Marinomonas* 424 and *Cobetia* 352b, two of the strongest inducers of luminescence, was quantified by LC–MS/MS. For comparison, DPD production was also quantified in *Pseudoalteromonas* 352a, which was co-isolated with *Cobetia* 352b and is a weak inducer of luminescence. Interestingly, culture supernatants from *Marinomonas* 424 and *Cobetia* 352b contained similar levels of DPD (692 and 585 nM, respectively), whereas a lower amount was found in the supernatant from *Pseudoalteromonas* 352a (66 nM). Thus, our results based on LC–MS/MS confirmed the quorum sensing patterns observed using the biosensor-based approach (**Figure 3**).

Impact of Metabolites of Endophytic Fungi on Quorum Sensing

As presented in **Figure 4**, extracts from 13 fungi boosted the luminescence from the biosensor. Of these, eight (*Verticillium biguttatum* AN130T, *Chaetomium globosum* LD13H, *Microsphaeropsis olivacea* LD50H, *Botryotinia fuckeliana* LD535H, *Leptosphaeria marina* SL457T, and *Diaporthe eres* SL473T) increased the luminescence by over 50%. Conversely, extracts from 30 fungi strongly diminished the luminescence, as shown in **Figure 5**. For 14 of these extracts, the loss of luminescence was due to toxicity against the biosensor *V. campbellii* MM32. In contrast, the other 16 extracts evidently inhibited AI-2, blocking the effects of 2 μM DPD but with very limited impact on the biosensor *V. campbellii* MM32 metabolism (**Figure 5**).

Impact of Bacterial–Fungal Interactions on Quorum Sensing

Metabolites produced in co-cultures of *Cladosporium* SL405T with *Pseudoalteromonas* 352a or *Cobetia* 352b reduced luminescence from *V. campbellii* MM32 by 44 and 20%, respectively. In contrast, metabolites from monocultures of *Cladosporium* SL405T decreased luminescence only slightly (12%), whereas metabolites from monocultures of either bacterium elicited a stronger decrease in luminescence (49%) (**Supplementary Data S3**). These results highlight the contrasting effects of co-cultures and monocultures on quorum sensing supported by a non-parametric test for independent

TABLE 1 | Induction of luminescence in the biosensor *V. campbellii* MM32 by bacterial supernatants.

Genus	No induction	Induction inferior to 50%	Induction between 50 and 100%	Induction superior or equal to 100%
Kocuria	1	2	1	0
Microbacterium	1	5	0	0
Micrococcus	0	1	0	0
Mycobacterium	1	2	0	0
Rhodococcus	3	5	0	0
Salinibacterium	0	1	0	0
Streptomyces	3	7	0	0
Williamsia	0	1	0	0
Algoriphagus	1	0	0	0
Cellulophaga	2	2	0	0
Formosa	0	2	0	0
Zobellia	2	0	0	0
Bacillus	1	88	6	0
Exiguobacterium	0	1	0	0
Lysinibacillus	0	1	0	0
Alteromonas	0	1	0	0
Cobetia	0	2	5	5
Erwinia	0	1	1	0
Labrenzia	1	2	0	0
Marinomonas	0	0	0	1
Paraglaciecola	2	0	0	0
Pseudoalteromonas	9	27	1	0
Pseudomonas	0	4	0	0
Pseudovibrio	3	1	0	0
Psychrobacter	0	1	0	0
Shewanella	0	1	0	0
Primorskyibacter	0	1	0	0

Numbers are bacterial isolates per genus.

samples (Van Der Waerden test), followed by a *post hoc* test using the Fischer's Least Significant Difference (LSD) criterion (**Figure 6**). Furthermore, the partial least squares discriminant analysis of samples covering the different co-culture conditions characterized through 4,221 metabolomic features collected by LC–MS showed that each monoculture or co-culture is characterized by a specific set of features corresponding to a unique set of metabolites (**Supplementary Data S2**). Sparse partial least squares discriminant analysis also identified four latent variables of 180 features (720 features in total) that discriminate a culture from all others (**Supplementary Data S2**). In a second round of partial least squares discriminant analysis based only on these 720 features (**Figure 7**), the co-cultures were differentiated in the third dimension both from each other and from every monoculture. Analysis of variance of scores get on the 3rd dimension confirmed that selected features significantly separate co-cultures from each other and from monocultures ($F_{2,12} = 167.2$, $p < 1.7 \times 10^{-9}$). This result implies that bacterial–fungal interactions impact very significantly metabolite production in specific ways.

Features that distinguish a culture and that are altered more than 10-fold over other cultures are listed in **Supplementary Table S3**. When compared to the corresponding monocultures, 28 and 5 of such features were identified in co-cultures of *Cladosporium* SL405T with *Cobetia* 352b and *Pseudoalteromonas* 352a, respectively. Conversely, 120 and 87 of such features were identified in *Cobetia* 352b and *Pseudoalteromonas* 352a monocultures when compared to the corresponding co-cultures with *Cladosporium* SL405T. Moreover, 93 features diminished by at least a factor of 10 in co-cultures when compared to *Cladosporium* SL405T monocultures. Unfortunately, top-ranked metabolites were not identified by annotation against ISDB (Allard et al., 2016), GNPS, and MassBank. Similarly, identification against SIRIUS 4.0. (Böcker and Rasche, 2008) and Pubchem was inconclusive.

Search of a Multivariate Link Between Luminescence Measurements and MS Metabolomic Variables

A link between the global response given by the luminescence representing an integrated measurement of the QS and the metabolome in the different mono or co-culture conditions was obtained thanks a PLS-based regression (**Figure 8**).

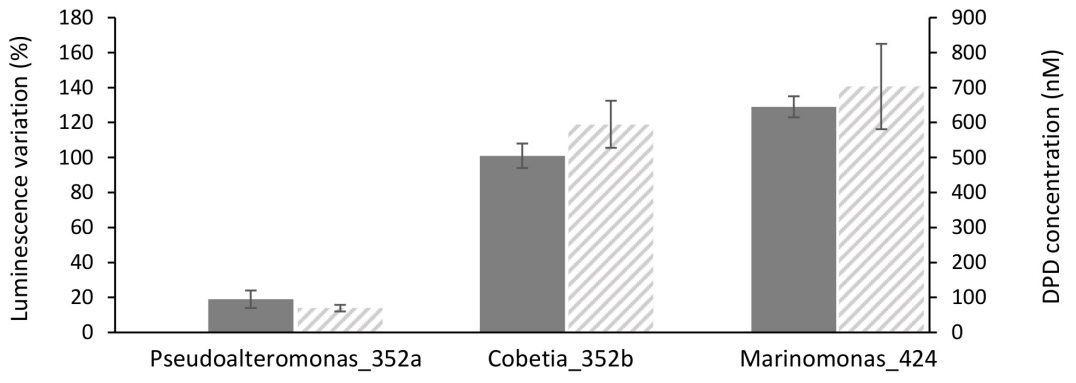

FIGURE 3 | Induction of luminescence in the biosensor *Vibrio campbellii* MM32 by (gray bars), and DPD concentration in three bacterial supernatants (hatched bars). Luminescence induction was quantified as described in Section "Materials and Methods." Error bars indicate standard deviation.

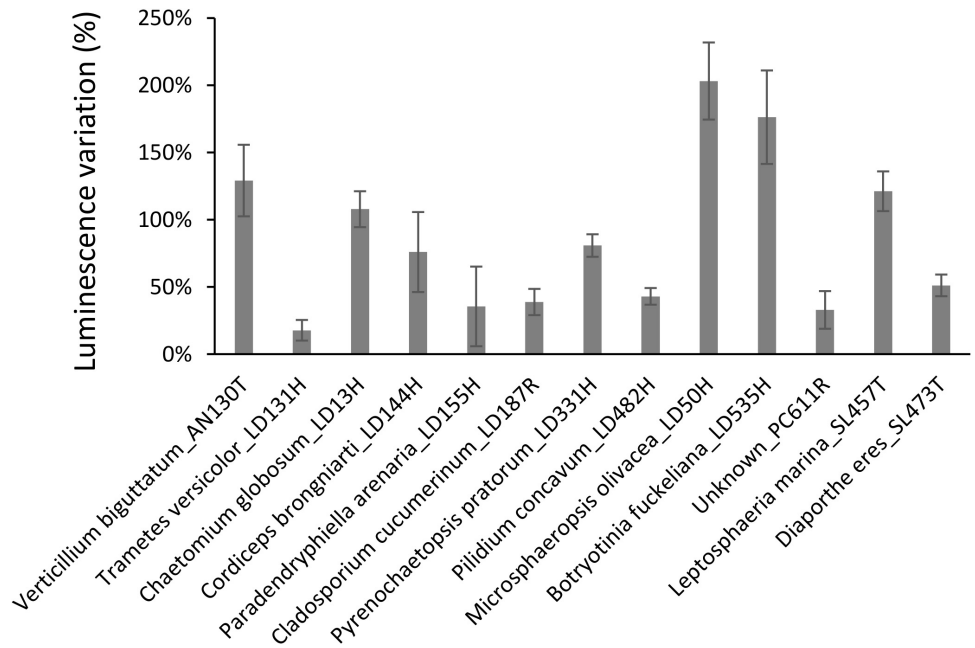

FIGURE 4 | Induction of luminescence in the biosensor *V. campbellii* MM32 by fungal extracts. Error bars indicate standard deviation.

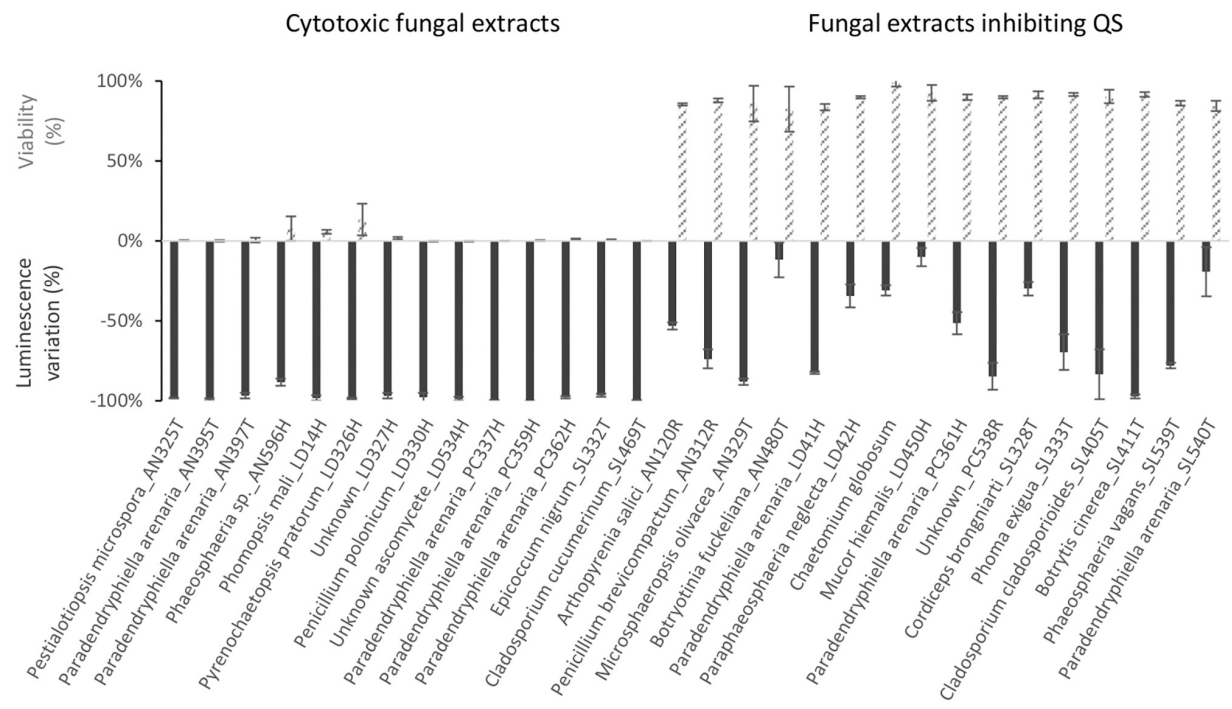

FIGURE 5 | Impact of fungal extracts on quorum sensing in and viability of the biosensor *V. campbellii* MM32, as measured, respectively, by inhibition of luminescence in the presence of 2 μM DPD and by resazurin test. Assays are described in Section "Materials and Methods." Error bars indicate standard deviation.

Complementary filters such as (i) VIP above 1.20 with a VIP standard error coming from repeated cross-validation calculus lower than the VIP value for the variable, and (ii) absolute value of the correlation between primary metabolomic variables and the predicted luminescence response above 0.75, were used to select from the initial set of 4221 variables a subset of 521 variables. The comprehensive heatmap obtained (**Figure 9**) showcased nine and one variables displaying a significantly higher mean

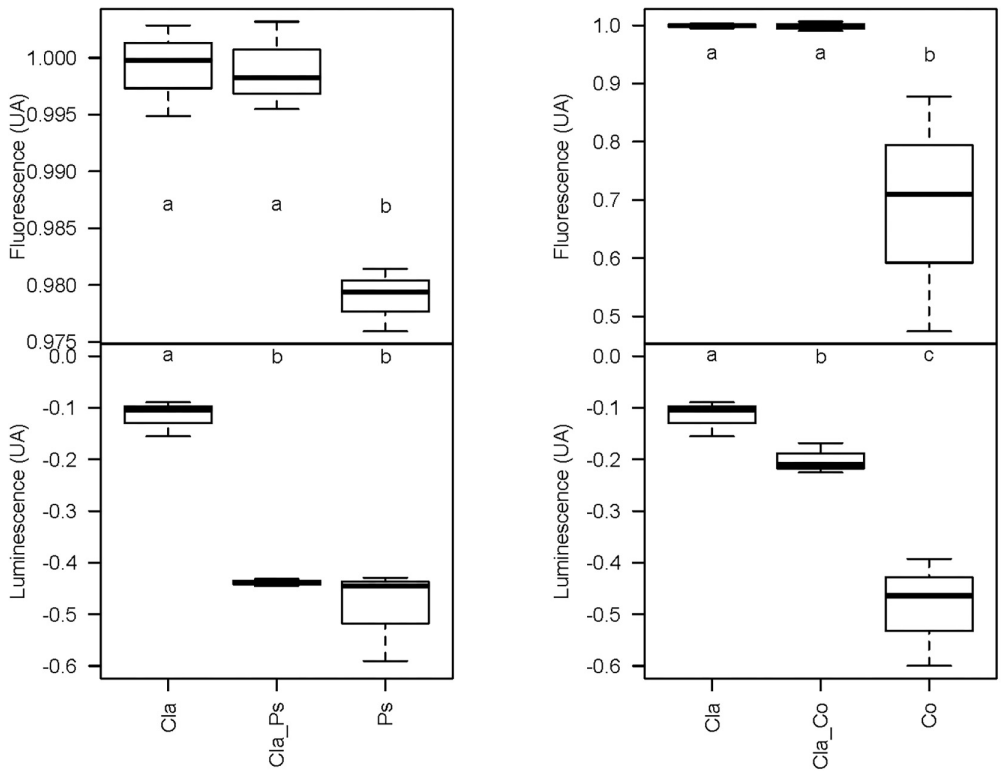

FIGURE 6 | Box plot representing the variation of the luminescence and viability (fluorescence) of the biosensor *V. campbellii* MM32 by the bacterial or the fungal monoculture and the co-culture. Cla, Cladosporium monocultures; Cla_Co, Cladosporium-*Cobetia* co-cultures; Co, *Cobetia* monocultures; Cla_Ps, Cladosporium-*Pseudoalteromonas* co-cultures; Ps, *Pseudoalteromonas* monocultures. Error bars represent standard deviation for three replicates. Different letters indicate statistically significant differences between groups [mean ± SEM, $N = 3$, Van Der Waerden test followed by a *post hoc* test using the Fischer's least significant difference (LSD), $p < 0.05$].

value for co-culture between Cla and Co and Cla and Ps, respectively (**Figure 10**). All these 10 significant variables are supposed to be induced in these co-culture conditions when compared to mono-culture conditions as revealed by the multiple comparison of means based on the Student-Newman-Keuls test. Indeed, these variables are of prime importance candidates that would be putatively involved in some metabolic pathways explaining the QS event.

DISCUSSION

The data highlight the large diversity of cultivable bacterial endophytes associated with healthy *L. digitata*, *S. latissima*, *A. nodosum*, and *P. canaliculata* (**Figures 1**, **2**). The four phyla (*Proteobacteria*, *Firmicutes*, *Actinobacteria*, and *Bacteroidetes*) and 27 genera that were identified are consistent with previous surveys of cultivable bacteria associated with macroalgae (Wiese et al., 2009; Hollants et al., 2013; KleinJan et al., 2017). Notably, the cultivable fraction of bacterial communities appears to vary depending on algal species, sampling site, and algal tissue. Nevertheless, bacteria classified as *Cobetia* and *Pseudoalteromonas* were isolated from every algal species, tissue, and sampling site. Moreover, these genera are the most frequently isolated from *S. latissima*, apart from *Bacillus*. Of note, *Vibrio* and *Flavobacterium* were not isolated from our samples, even though these are frequently isolated from brown algae (Hollants et al., 2013; Albakosh et al., 2016).

Among the isolated bacterial endophytes, 86% were found to produce AI-2, which triggers quorum sensing in the reporter strain *V. campbellii* MM32 (**Table 1**). *Cobetia, Marinomonas*, and *Erwinia* were the strongest inducers (>100% induction) of quorum sensing, whereas 93 and 73% of isolated *Bacillus* and *Pseudoalteromonas* induced quorum sensing only weakly (<50% induction). These results were confirmed by quantifying DPD, an AI-2 precursor, in bacterial supernatants using tandem mass spectrometry. As shown in **Figure 3**, *Cobetia* 352b and *Marinomonas* 424 produced around 700 nM of DPD, suggesting that these strains engage neighboring bacteria with AI-2 receptors. *Pseudoalteromonas* 352a also produced DPD but to a lesser extent (66 nM). Interestingly, fungal endophytes isolated along with these bacteria positively or negatively modulated AI-2 quorum sensing (**Figures 4**, **5**). These results provide more evidence that AI-2 quorum sensing is involved in interkingdom signaling.

While inhibitory activity against quorum sensing was previously detected in marine fungi (Martín-Rodríguez et al., 2014), this is the first demonstration, to the best of our

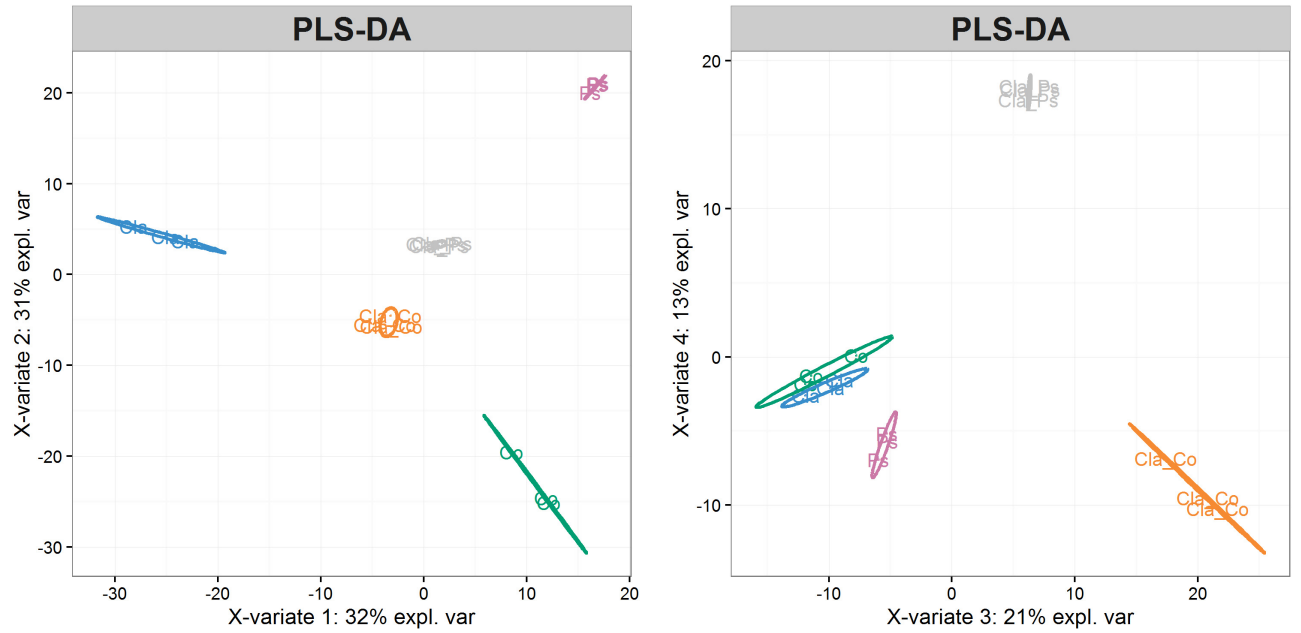

FIGURE 7 | Visualization of samples using the first four latent variables from partial least squares discriminant analysis of 720 selected features. Ps, *Pseudoalteromonas* monocultures (violet); Co, *Cobetia* monocultures (green); Cla, *Cladosporium* monocultures (blue); Cla-Ps, *Cladosporium-Pseudoalteromonas* co-cultures (gray); Cla-Co, *Cladosporium-Cobetia* co-cultures (orange). Ellipses represent 95% confidence intervals.

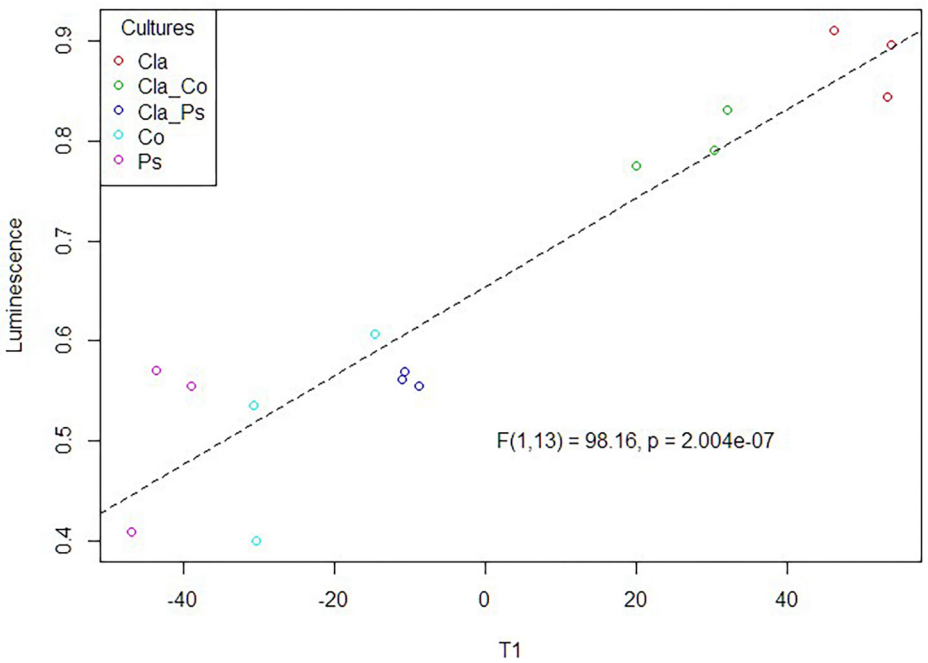

FIGURE 8 | PLS-based regression between the luminescence measurement (QS activity) and the metabolomic profiles obtained in the different culture or co-culture conditions.

knowledge, that fungal metabolites may also enhance quorum sensing. However, such result is not surprising, as this effect was previously observed in metabolites from some other types of eukaryotes such as *Chlamydomonas reinhardtii* and *Chlorella* spp. microalgae (Rolland et al., 2016). Collectively, these findings suggest a key role for AI-2 signaling among endophytes of brown algae. On the other hand, we note that 14 fungal endophytes are strongly antimicrobial against the *Vibrio* biosensor (**Figure 5**),

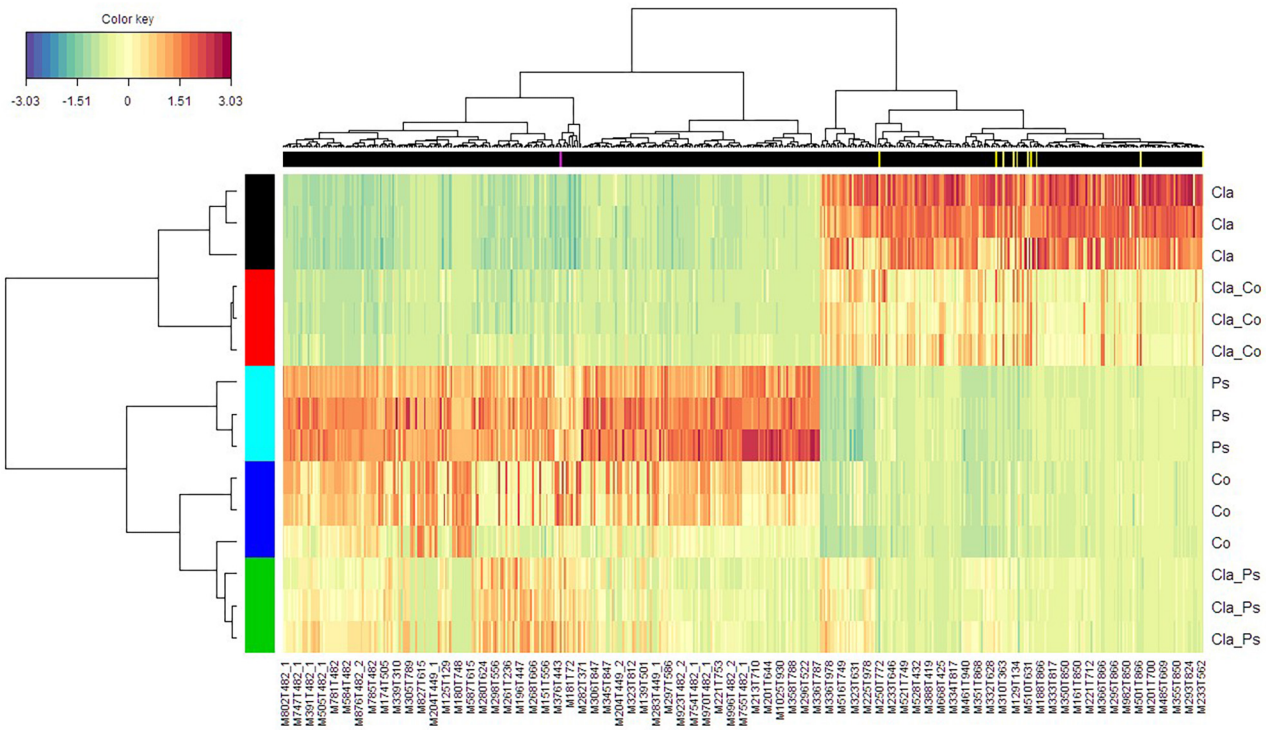

FIGURE 9 | Heatmap displaying both the culture clusters in rows and the clusters of variables (*m/z*) in columns. Ps, *Pseudoalteromonas*; Co, *Cobetia* monocultures; Cla, *Cladosporium* monocultures; Cla-Ps, *Cladosporium-Pseudoalteromonas* co-cultures; Cla-Co, *Cladosporium-Cobetia* co-cultures. For convenience, not all variables are labeled. In the black banner are given variables marked in yellow and pink vertical lines for Cla-Co and Cla-Ps co-cultures, respectively, which were significantly filtered according to (i) a VIP value above 1.20 (and with respective SE values lower than VIP), and (ii) an absolute value of the correlation between the variables selected at the previous step and the PLS component which is above 0.75.

and thus may be similarly active against *V. harveyi*, a prominent pathogen in aquaculture (Zhang and Li, 2016).

As the fungus *Cladosporium* SL405T and the bacteria *Pseudoalteromonas* 352a and *Cobetia* 352b were isolated from the same holobiont (*S. latissima*), they were characterized in monoculture and in co-culture, with a view to assess the impact of fungal–bacterial interactions on metabolite production and quorum sensing. The data indicate that these isolates produce quorum sensing or quorum sensing-modulating compounds. Of note, these genera are frequently isolated from macroalgae (Hollants et al., 2013; Hulikere et al., 2016; Li et al., 2017). *Pseudoalteromonas* is of particular interest, as it was shown to produce antimicrobials or bioactive molecules against algal spores, invertebrate larvae, fungi, and other bacteria. Such molecules may help the host against surface colonization by these organisms (Holmström et al., 2002; Richards et al., 2017). Also, *Pseudoalteromonas* was implicated in Hole-Rotten disease (Wang et al., 2007).

As shown in **Figures 6**, **7**, co-cultures of Cladosporium SL405T with two different bacteria produce different metabolites. These metabolites are also different from those produced by corresponding monocultures. For example, 28 and 5 metabolic features were at least 10-fold more abundant in co-cultures of *Cladosporium* SL405T with *Cobetia* 352b and *Pseudoalteromonas* 352a than in corresponding monocultures. This result implies that microbial interactions induce production of specific metabolites (**Supplementary Table S3**). Conversely, 120 and 87 features were at least 10-fold more abundant in *Cobetia* 352b monocultures and *Pseudoalteromonas* 352a monocultures than in co-cultures, suggesting either that production of these metabolites is inhibited by microbial interaction, or that these metabolites are degraded in co-cultures. Similarly, 105 and 108 features (of which 93 are common) were at least 10-fold more abundant in *Cladosporium* SL405T monocultures than in co-cultures with *Cobetia* 352b and *Pseudoalteromonas* 352a.

Taken together, these results demonstrate that metabolomes in co-cultures fundamentally differ from metabolomes in monocultures due to microbial interactions. Unfortunately, chemical characterization of culture-specific metabolites was not possible since none matched known natural products. Identification of the source of metabolites in co-cultures also remains a major challenge, since the structure of such metabolites and other related biochemical information would be required (Xu et al., 2018). Nevertheless, we found that different cultures have variable impact on quorum sensing (**Figure 6**), such that metabolites obtained from co-cultures of the same fungus with two different bacteria clearly display contrasting effects on quorum sensing (**Figure 6**). For instance, metabolites from

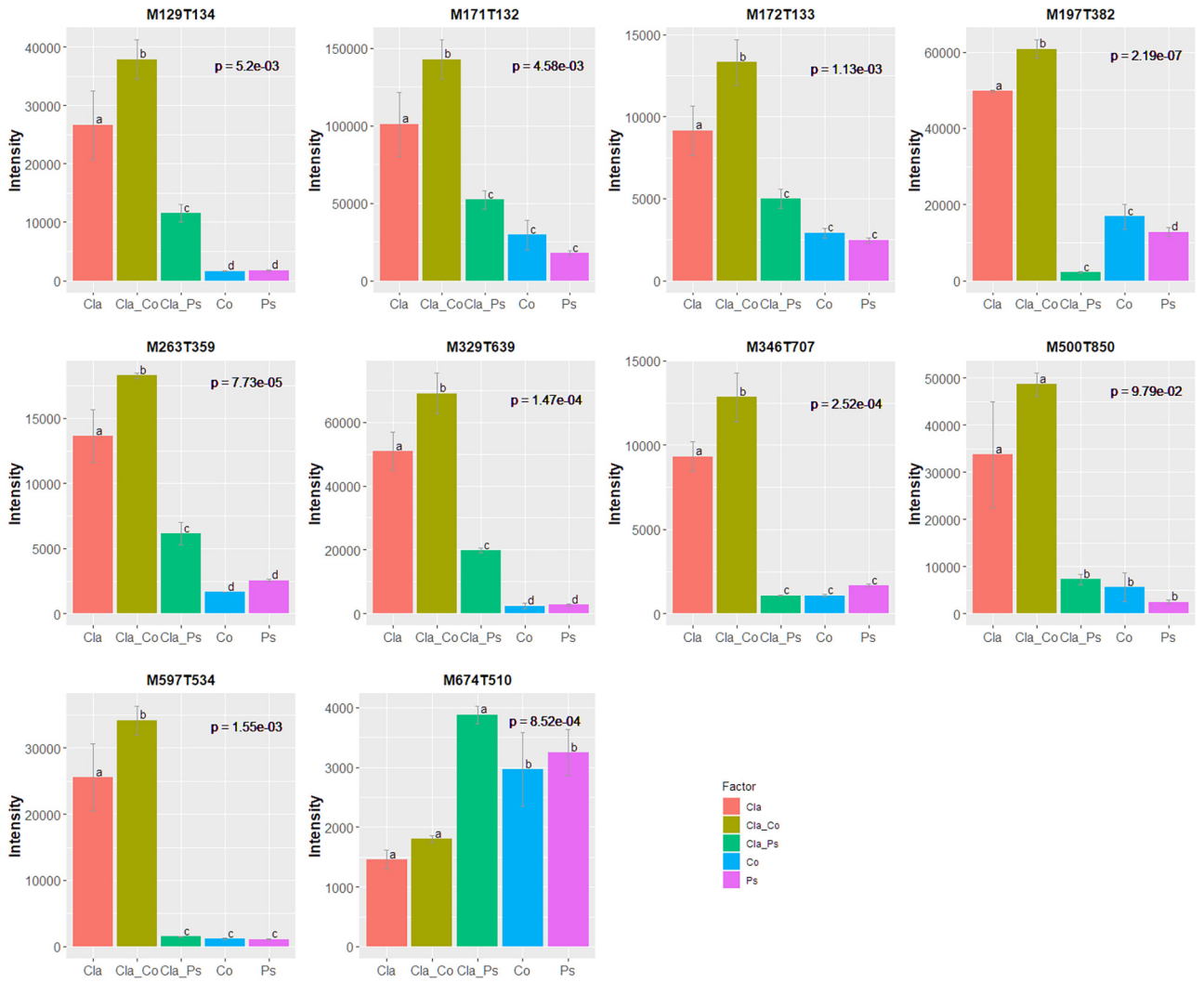

FIGURE 10 | 10 variables displaying a correlation with the predicted luminescence response above 0.75 and a higher mean value in co-culture conditions compared to other mono-culture conditions or the alternate co-culture condition. *p*-Values coming from ANOVA are stringently corrected for the false discovery rate when considering the initial set of 4221 variables. Multiple comparisons of means used the Student-Newman-Keuls test.

a co-culture of *Cladosporium* SL405T and *Pseudoalteromonas* 352a diminish luminescence from the biosensor by 40%, while metabolites from a co-culture of *Cladosporium* SL405T and *Cobetia* 352b led to a loss of only 20%. The link between the impact on quorum sensing and the metabolites present in different culture conditions was strengthened by the PLS-regression based analysis highlighting 10 variables, highly correlated with the predicted luminescence response (absolute value of the correlation above 0.75), and specially induced in the co-culture conditions when compared to mono-culture conditions (**Figure 10**).

Collectively, our data provide the first evidence of quorum sensing and quorum quenching in bacterial and fungal endophytes of brown algae. These results highlight the importance of chemical communication among microbial components of a holobiont. Indeed, our laboratory model clearly demonstrates the impact of interspecies interactions on the production of metabolites, including metabolites involved in quorum quenching or in antagonizing other microorganisms. Our model also demonstrates the various phenotypes that may be observed in a given fungal or bacterial strain depending on environmental conditions. Hence, these results provide a glimpse of the complexity of molecular dialogs in the holobiont, and how this may impact host fitness.

Accordingly, the data also highlight the need to fully understand the functional role of all microbial members in the seaweed holobiont and their impact on algal fitness either in nature or in farms. Indeed, quorum sensing is already known to significantly affect the expression of virulence genes in aquaculture pathogens (Zhao et al., 2015). Quorum sensing was also demonstrated to control microbial colonization in the red algae *Delisea pulchra,* notably by release of halogenated furanone,

which inhibits pathogenic epiphytic bacteria such as *Nautella* sp. (Harder et al., 2012). Hence, quorum sensing represents a very promising target in future studies of approaches to limit pathogenic effects in algae.

DATA AVAILABILITY

The datasets generated for this study can be found in GenBank, SUB4670131.

AUTHOR CONTRIBUTIONS

AT carried out the experiments. AT, AP, RL, CH, KE, and SP analyzed the data. AT, RL, and SP wrote the manuscript. All authors conceived this study.

FUNDING

This work was supported by ATM "Microorganisms" grant from the Natural History Museum of Paris (SP), EMBRC project No. 262280 and PEPS ExoMod CNRS grant (SP), EC2CO Roseocom CNRS grant (RL), and the Convergence Sorbonne Université program (RL and SP). This work was funded through the IDEX SUPER (AT).

ACKNOWLEDGMENTS

We acknowledge the Scottish Association for Marine Science (SAMS) and the Biological Station of Roscoff for hosting the field missions. We would like to greatly thank Philippe Potin (Marine Biology Station of Roscoff, France) for taxonomic identification of the brown macroalgae species during the field mission. We are grateful to the Bio2Mar platform (http://bio2mar.obs-banyuls.fr) for providing technical help and support.

SUPPLEMENTARY MATERIAL

The Supplementary Material for this article can be found online at: https://www.frontiersin.org/articles/10.3389/fmicb.2019.01693/full#supplementary-material

REFERENCES

Albakosh, M. A., Naidoo, R. K., Kirby, M., and Bauer, R. (2016). Identification of epiphytic bacterial communities associated with the brown alga *Splachnidium rugosum*. *J. Appl. Phycol.* 28, 1891–1901. doi: 10.1007/s10811-015-0725-z

Allard, P. M., Péresse, T., Bisson, J., Gindro, K., Marcourt, L., Pham, V. C., et al. (2016). Integration of molecular networking and in-silico MS/MS fragmentation for natural products dereplication. *Anal. Chem.* 88, 3317–3323. doi: 10.1021/acs.analchem.5b04804

Altschul, S. F., Gish, W., Miller, W., Myers, E. W., and Lipman, D. J. (1990). Basic local alignment search tool. *J. Mol. Biol.* 215, 403–410. doi: 10.1016/S0022-2836(05)80360-2

Atkinson, S., and Williams, P. (2009). Quorum sensing and social networking in the microbial world. *J. R. Soc.* 6, 959–978. doi: 10.1098/rsif.2009.0203

Bassler, B. L., Wright, M., Showalter, R. E., and Silverman, M. R. (1993). Intercellular signalling in *Vibrio harveyi*: sequence and function of genes regulating expression of luminescence. *Mol. Microbiol.* 9, 773–786. doi: 10.1111/j.1365-2958.1993.tb01737.x

Böcker, S., and Rasche, F. (2008). Towards de novo identification of metabolites by analyzing tandem mass spectra. *Bioinformatics* 24, i49–i55. doi: 10.1093/bioinformatics/btn270

Bodor, A., Elxnat, B., Thiel, V., Schulz, S., and Wagner-Döbler, I. (2008). Potential for LuxS related signalling in marine bacteria and production of autoinducer-2 in the genus *Shewanella*. *BMC Microbiol.* 8:13. doi: 10.1186/1471-2180-8-13

R Core Team (2019). *R: A Language and Environment for Statistical Computing*. Vienna: R Foundation for Statistical Computing.

Cugini, C., Calfee, M. W., Farrow, J. M., Morales, D. K., Pesci, E. C., and Hogan, D. A. (2007). Farnesol, a common sesquiterpene, inhibits PQS production in *Pseudomonas aeruginosa*. *Mol. Microbiol.* 65, 896–906. doi: 10.1111/j.1365-2958.2007.05840.x

Debbab, A., Aly, A. H., and Proksch, P. (2012). Endophytes and associated marine derived fungi—ecological and chemical perspectives. *Fungal Divers.* 57, 45–83. doi: 10.1007/s13225-012-0191-8

Defoirdt, T., Miyamoto, C. M., Wood, T. K., Meighen, E. A., Sorgeloos, P., Verstraete, W., et al. (2007). The natural furanone (5Z)-4-bromo-5-(Bromomethylene)-3-butyl-2(5H)-furanone disrupts quorum sensing-regulated gene expression in *Vibrio Harveyi* by decreasing the DNA-binding activity of the transcriptional regulator protein LuxR. *Environ. Microbiol.* 9, 2486–2495. doi: 10.1111/j.1462-2920.2007.01367.x

Deveau, A., Bonito, G., Uehling, J., Paoletti, M., Becker, M., Bindschedler, S., et al. (2018). Bacterial–fungal interactions: ecology, mechanisms and challenges. *FEMS Microbiol. Rev.* 42, 335–352. doi: 10.1093/femsre/fuy008

Doberva, M., Ferandin, S. S., Toulza, E., Lebaron, P., and Lami, R. (2015). Diversity of quorum sensing autoinducer synthases in the global ocean sampling metagenomic database. *Aquat. Microb. Ecol.* 74, 107–119. doi: 10.3354/ame01734

Edgar, R. C. (2004). MUSCLE: multiple sequence alignment with high accuracy and high throughput. *Nucleic Acids Res.* 32, 1792–1797. doi: 10.1093/nar/gkh340

Egan, S., and Gardiner, M. (2016). Microbial dysbiosis: rethinking disease in marine ecosystems. *Front. Microbiol.* 7:991. doi: 10.3389/fmicb.2016.00991

Egan, S., Harder, T., Burke, C., Steinberg, P., Kjelleberg, S., and Thomas, T. (2013). The Seaweed holobiont: understanding seaweed–bacteria interactions. *FEMS Microbiol. Rev.* 37, 462–476. doi: 10.1111/1574-6976.12011

FAO (2018). *The State of World Fisheries and Aquaculture*. Rome: Food and Agriculture Organization of the United Nations.

Federle, M. J. (2009). "Autoinducer-2-based chemical communication in bacteria: complexities of interspecies signaling," in *Contributions to Microbiology*, Vol. 16, eds M. Collin and R. Schuch (Basel: KARGER), 18–32. doi: 10.1159/000219371

Fernandes, N., Steinberg, P., Rusch, D., Kjelleberg, S., and Thomas, T. (2012). Community structure and functional gene profile of bacteria on healthy and diseased thalli of the red seaweed *Delisea Pulchra*. *PloS One* 7:e50854. doi: 10.1371/journal.pone.0050854

Fourie, R., Ells, R., Swart, C. W., Sebolai, O. M., Albertyn, J., and Pohl, C. H. (2016). *Candida albicans* and *Pseudomonas aeruginosa* interaction, with focus on the role of eicosanoids. *Front. Physiol.* 7:64. doi: 10.3389/fphys.2016.00064

Freeman, J. A., and Bassler, B. L. (1999). Sequence and function of LuxU: a two-component phosphorelay protein that regulates quorum sensing in *Vibrio Harveyi*. *J. Bacteriol.* 181, 899–906.

Fries, N. (1979). Physiological characteristics of *Mycosphaerella ascophylli*, a fungal endophyte of the marine brown alga *Ascophyllum nodosum*. *Physiol. Plant.* 45, 117–121. doi: 10.1111/j.1399-3054.1979.tb01674.x

Gachon, C. M., Sime-Ngando, T., Strittmatter, M., Chambouvet, A., and Kim, G. H. (2010). Algal diseases: spotlight on a black box. *Trends Plant Sci.* 15, 633–640. doi: 10.1016/j.tplants.2010.08.005

Graça, A. P., Bondoso, J., Gaspar, H., Xavier, J. R., Monteiro, M. C., de la Cruz, M., et al. (2013). Antimicrobial activity of heterotrophic bacterial communities from the marine sponge *Erylus discophorus* (*Astrophorida, Geodiidae*). *PLoS One* 8:e78992. doi: 10.1371/journal.pone.0078992

Grandclément, C., Tannières, M., Moréra, S., Dessaux, Y., and Faure, D. (2016). Quorum quenching: role in nature and applied developments. *FEMS Microbiol. Rev.* 40, 86–116. doi: 10.1093/femsre/fuv038

Hammer, B. K., and Bassler, B. L. (2003). Quorum sensing controls biofilm formation in *Vibrio cholerae*. *Mol. Microbiol.* 50, 101–104. doi: 10.1046/j.1365-2958.2003.03688.x

Harder, T., Campbell, A. H., Egan, S., and Steinberg, P. D. (2012). "Chemical mediation of ternary interactions between marine holobionts and their environment as exemplified by the red alga *Delisea pulchra*."*J. Chem. Ecol. C* 38, 442–450. doi: 10.1007/s10886-012-0119-5

Hardie, K. R., and Heurlier, K. (2008). Establishing bacterial communities by'word of mouth': luxS and autoinducer 2 in biofilm development. *Nat. Rev. Microbiol.* 6, 635–643. doi: 10.1038/nrmicro1916

Hassani, M. A., Durán, P., and Hacquard, S. (2018). Microbial interactions within the plant holobiont. *Microbiome* 6:58. doi: 10.1186/s40168-018-0445-0

Hmelo, L. R. (2017). Quorum sensing in marine microbial environments. *Ann. Rev. Marine. Sci.* 9, 257–281. doi: 10.1146/annurev-marine-010816-060656

Hollants, J., Leliaert, F., De Clerck, O., and Willems, A. (2013). What we can learn from sushi: a review on seaweed-bacterial associations. *FEMS Microbiol. Ecol.* 83, 1–16. doi: 10.1111/j.1574-6941.2012.01446.x

Holmström, C., Egan, S., Franks, A., McCloy, S., and Kjelleberg, S. (2002). Antifouling activities expressed by marine surface associated *Pseudoalteromonas* species. *FEMS Microbiol. Ecol.* 41, 47–58. doi: 10.1111/j.1574-6941.2002.tb00965.x

Hulikere, M. M., Joshi, C. G., Ananda, D., Poyya, J., and Nivya, T. (2016). Antiangiogenic, wound healing and antioxidant activity of *Cladosporium cladosporioides* (Endophytic fungus) isolated from seaweed (*Sargassum wightii*). *Mycology* 7, 203–211. doi: 10.1080/21501203.2016.1263688

Ismail, A. S., Valastyan, J. S., and Bassler, B. L. (2016). A host-produced autoinducer-2 mimic activates bacterial quorum sensing. *Cell Host Microbe* 19, 470–480. doi: 10.1016/j.chom.2016.02.020

Jones, E. B. G., Pang, K. L., and Stanley, S. J. (2012). "Fungi from marine algae," in *Marine Fungi: And Fungal-Like Organisms*, eds E. B. G. Jones and K.-L. Pang (Berlin: Walter de Gruyter).

KleinJan, H., Jeanthon, C., Boyen, C., and Dittami, S. M. (2017). Exploring the cultivable *Ectocarpus* microbiome. *Front. Microbe* 8:2456. doi: 10.3389/fmicb.2017.02456

Kumar, S., Stecher, G., and Tamura, K. (2016). MEGA7: molecular evolutionary genetics analysis version 7.0 for bigger datasets. *Mol. Biol. Evol.* 33, 1870–1874. doi: 10.1093/molbev/msw054

Li, H. L., Li, X. M., Mándi, A., Antus, S., Li, X., Zhang, P., et al. (2017). Characterization of cladosporols from the marine algal-derived endophytic fungus *Cladosporium Cladosporioides* EN-399 and configurational revision of the previously reported cladosporol derivatives. *J. Org. Chem.* 82, 9946–9954. doi: 10.1021/acs.joc.7b01277

Loque, C. P., Medeiros, A. O., Pellizzari, F. M., Oliveira, E. C., Rosa, C. A., and Rosa, L. H. (2010). Fungal community associated with marine macroalgae from Antarctica. *Polar Biol.* 33, 641–648. doi: 10.1007/s00300-009-0740-0

Martín-Rodríguez, A. J., Reyes, F., Martín, J., Pérez-Yépez, J., León-Barrios, M., Couttolenc, A., et al. (2014). Inhibition of bacterial quorum sensing by extracts from aquatic fungi: first report from marine endophytes. *Mar. Drugs* 12, 5503–5526. doi: 10.3390/md12115503

Miller, S. T., Xavier, K. B., Campagna, S. R., Taga, M. E., Semmelhack, M. F., Bassler, B. L., et al. (2004). *Salmonella typhimurium* recognizes a chemically distinct form of the bacterial quorum-sensing signal AI-2. *Mol. Cell* 15, 677–687. doi: 10.1016/j.molcel.2004.07.020

Pérez-Rodríguez, I., Bolognini, M., Ricci, J., Bini, E., and Vetriani, C. (2015). From deep-sea volcanoes to human pathogens: a conserved quorum-sensing signal in epsilon *proteobacteria*. *ISME J.* 9, 1222–1234. doi: 10.1038/ismej.2014.214

Rezzonico, F., and Duffy, B. (2008). Lack of genomic evidence of AI-2 receptors suggests a non-quorum sensing role for LuxS in most bacteria. *BMC Microbiol.* 8:154. doi: 10.1186/1471-2180-8-154

Richards, G. P., Watson, M. A., Needleman, D. S., Uknalis, J., Boyd, E. F., and Fay, J. P. (2017). Mechanisms for *Pseudoalteromonas piscicida*-induced killing of *Vibrios* and other bacterial pathogens. *Appl. Environ. Microbiol.* 83, e175–e117. doi: 10.1128/AEM.00175-17

Rohart, F., Gautier, B., Singh, A., and Le Cao, K.-A. (2017). mixOmics: an R package for 'omics feature selection and multiple data integration. *PLoS Comput. Biol.* 13:e1005752. doi: 10.1371/journal.pcbi.1005752

Rolland, J. L., Stien, D., Sanchez-Ferandin, S., and Lami, R. (2016). Quorum sensing and quorum quenching in the phycosphere of phytoplankton: a case of chemical interactions in ecology. *J. Chem. Ecol.* 42, 1201–1211. doi: 10.1007/s10886-016-0791-y

Singh, R. P., and Reddy, C. R. K. (2014). Seaweed-microbial interactions: key functions of seaweed-associated bacteria. *FEMS Microbiol. Ecol.* 88, 213–230. doi: 10.1111/1574-6941.12297

Smith, C. A., Want, E. J., O'Maille, G., Abagyan, R., and Siuzdak, G. (2006). XCMS: processing mass spectrometry data for metabolite profiling using nonlinear peak alignment, matching, and identification. *Anal. Chem.* 78, 779–787. doi: 10.1021/ac051437y

Tapia, J. E., González, B., Goulitquer, S., Potin, P., and Correa, J. A. (2016). Microbiota influences morphology and reproduction of the brown alga *Ectocarpus* sp. *Front. Microbiol* 7:197. doi: 10.3389/fmicb.2016.00197

Vallet, M., Strittmatter, M., Murúa, P., Lacoste, S., Dupont, J., Hubas, C., et al. (2018). Chemically-mediated interactions between macroalgae, their fungal endophytes, and protistan pathogens. *Front. Microbiol.* 9:3161. doi: 10.3389/fmicb.2018.03161

Wahl, M., Goecke, F., Labes, A., Dobretsov, S., and Weinberger, F. (2012). The second skin: ecological role of epibiotic biofilms on marine organisms. *Front. Microbiol.* 3:292. doi: 10.3389/fmicb.2012.00292

Wang, G., Shuai, L., Li, Y., Lin, W., Zhao, X., and Duan, D. (2007). Phylogenetic analysis of apiphytic marine bacteria on hole-rotten siseased sporophytes of *Laminaria japonica*. *J. Appl. Phycol.* 20, 403–409. doi: 10.1007/s10811-007-9274-4

Wang, T. N., Kaksonen, A. H., and Hong, P. Y. (2018). Evaluation of two autoinducer-2 quantification methods for application in marine environments. *J. Appl. Microbiol.* 124, 1469–1479. doi: 10.1111/jam.13725

Whiteley, M., Diggle, S. P., and Greenberg, E. P. (2017). Progress in and promise of bacterial quorum sensing research. *Nature* 551, 313–320. doi: 10.1038/nature24624

Wiese, J., Thiel, V., Nagel, K., Staufenberger, T., and Imhoff, J. F. (2009). Diversity of antibiotic-active bacteria associated with the brown alga *Laminaria saccharina* from the Baltic Sea. *Marine Biotechnol.* 11, 287–300. doi: 10.1007/s10126-008-9143-4

Wongsuk, T., Pumeesat, P., and Luplertlop, N. (2016). Fungal quorum sensing molecules: role in fungal morphogenesis and pathogenicity. *J. Basic Microbiol.* 56, 440–447. doi: 10.1002/jobm.201500759

Xu, F., Song, X., Cai, P., Sheng, G., and Yu, H. (2017). Quantitative determination of AI-2 quorum-sensing signal of bacteria using high performance liquid chromatography–tandem mass spectrometry. *J. Environ. Sci.* 52, 204–209. doi: 10.1016/j.jes.2016.04.018

Xu, X. Y., Shen, X. T., Yuan, X. J., Zhou, Y. M., Fan, H., Zhu, L. P., et al. (2018). Metabolomics investigation of an association of induced features and corresponding fungus during the Co-culture of *Trametes versicolor* and *Ganoderma applanatum*. *Front. Microbiol.* 8:2647. doi: 10.3389/fmicb.2017.02647

Zhang, W., and Li, C. (2016). Exploiting quorum sensing interfering strategies in Gram-negative bacteria for the enhancement of environmental applications. *Front. Microbiol.* 6:1535. doi: 10.3389/fmicb.2015.01535

Zhao, J., Chen, M., Quan, C. S., and Fan, S. D. (2015). Mechanisms of quorum sensing and strategies for quorum sensing disruption in aquaculture pathogens. *J. Fish Dis.* 38, 771–786. doi: 10.1111/jfd.12299

Zozaya-Valdes, E., Egan, S., and Thomas, T. (2015). A comprehensive analysis of the microbial communities of healthy and diseased marine macroalgae and the detection of known and potential bacterial pathogens. *Front. Microbiol* 6:146. doi: 10.3389/fmicb.2015.00146

Zuccaro, A., Schoch, C. L., Spatafora, J. W., Kohlmeyer, J., Draeger, S., and Mitchell, J. I. (2008). Detection and identification of fungi intimately associated with the brown seaweed *Fucus serratus*. *Appl. Env. Microbiol.* 74, 931–941. doi: 10.1128/AEM.01158-07

Zuccaro, A., Schulz, B., and Mitchell, J. I. (2003). Molecular detection of ascomycetes associated with *Fucus serratus*. *Mycol. Res.* 107, 1451–1466. doi: 10.1017/S0953756203008657

Conflict of Interest Statement: The authors declare that the research was conducted in the absence of any commercial or financial relationships that could be construed as a potential conflict of interest.

frontiers in Microbiology

ORIGINAL RESEARCH
published: 06 August 2019
doi: 10.3389/fmicb.2019.01758

In silico Analysis Reveals Distribution of Quorum Sensing Genes and Consistent Presence of LuxR Solos in the *Pandoraea* Species

*Kah-Ooi Chua[1], Wah-Seng See-Too[1], Robson Ee[1], Yan-Lue Lim[1], Wai-Fong Yin[1] and Kok-Gan Chan[1,2]**

[1]Division of Genetics and Molecular Biology, Institute of Biological Sciences, Faculty of Science, University of Malaya, Kuala Lumpur, Malaysia, [2]International Genome Centre, Jiangsu University, Zhenjiang, China

The most common quorum sensing (QS) system in Gram-negative bacteria consists of signaling molecules called *N*-acyl-homoserine lactones (AHLs), which are synthesized by an enzyme AHL synthase (LuxI) and detected by a transcriptional regulator (LuxR) that are usually located in close proximity. However, many recent studies have also evidenced the presence of LuxR solos that are LuxR-related proteins in Proteobacteria that are devoid of a cognate LuxI AHL synthase. *Pandoraea* species are opportunistic pathogens frequently isolated from sputum specimens of cystic fibrosis (CF) patients. We have previously shown that *P. pnomenusa* strains possess QS activity. In this study, we examined the presence of QS activity in all type strains of *Pandoraea* species and acquired their complete genome sequences for holistic bioinformatics analyses of QS-related genes. Only four out of nine type strains (*P. pnomenusa*, *P. sputorum*, *P. oxalativorans,* and *P. vervacti*) showed QS activity, and C8-HSL was the only AHL detected. A total of 10 canonical *luxI*s with adjacent *luxR*s were predicted by bioinformatics from the complete genomes of aforementioned species and publicly available *Pandoraea* genomes. No orphan *luxI* was identified in any of the genomes. However, genes for two LuxR solos (LuxR2 and LuxR3 solos) were identified in all *Pandoraea* genomes (except two draft genomes with one LuxR solo gene), and *P. thiooxydans* was the only species that harbored no QS-related activity and genes. Except the canonical LuxR genes, LuxIs and LuxR solos of *Pandoraea* species were distantly related to the other well-characterized QS genes based on phylogenetic clustering. LuxR2 and LuxR3 solos might represent two novel evolutionary branches of LuxR system as they were found exclusively only in the genus. As a few *luxR* solos were located in close proximity with prophage sequence regions in the genomes, we thus postulated that these *luxR* solos could be transmitted into genus *Pandoraea* by transduction process mediated by bacteriophage. The bioinformatics approach developed in this study forms the basis for further characterization of closely related species. Overall, our findings improve the current understanding of QS in *Pandoraea* species, which is a potential pharmacological target in battling *Pandoraea* infections in CF patients.

Keywords: cystic fibrosis, type strains, single molecule real-time sequencing, quorum sensing, LuxR solos

OPEN ACCESS

Edited by:
Ana Maria Otero, University of Santiago de Compostela, Spain

Reviewed by:
Navneet Rai, University of California, Davis, United States
Ralf Heermann, Johannes Gutenberg University Mainz, Germany

***Correspondence:**
Kok-Gan Chan
kokgan@um.edu.my

Specialty section:
This article was submitted to Infectious Diseases, a section of the journal Frontiers in Microbiology

Received: *26 February 2019*
Accepted: *16 July 2019*
Published: *06 August 2019*

Citation:
Chua K-O, See-Too W-S, Ee R, Lim Y-L, Yin W-F and Chan K-G (2019) In silico Analysis Reveals Distribution of Quorum Sensing Genes and Consistent Presence of LuxR Solos in the Pandoraea Species. Front. Microbiol. 10:1758. doi: 10.3389/fmicb.2019.01758

INTRODUCTION

Cystic fibrosis (CF) results from mutations in the cystic fibrosis transmembrane conductance regulator (CFTR) gene that functions in modulating chloride ion transport across epithelial cells (Trapnell et al., 1991; Pier et al., 1996). As a consequence to this gene abnormality, majority of CF patients suffer from secretion of thick and viscous mucus in their respiratory tracts. These copious respiratory secretions become the breeding ground for microorganisms, which lead to both chronic and transient pulmonary infections, inflammation, obstruction of airways, and ultimately life-threatening pulmonary dysfunction (Gibson et al., 2003). *Staphylococcus aureus*, *Pseudomonas aeruginosa*, *Burkholderia cepacia,* and a spectrum of other Gram-negative bacteria are frequently associated with bacterial lung infections in CF patients (Gibson et al., 2003; LiPuma, 2010). However, recent reports revealed unprecedented infections by a number of bacteria and *Pandoraea* species are among the novel bacteria associated with pulmonary infections in CF patients (Atkinson et al., 2006; Davies and Rubin, 2007).

The genus *Pandoraea* was proposed to accommodate a group of isolates cultured from sputum specimens of CF patients that were initially misidentified as *B. cepacia* and genus *Ralstonia*. In the process of taxonomical characterization, some members of genus *Burkholderia* are reclassified into *Pandoraea* based on genotypic characteristics as well (Coenye et al., 2000, 2001). Members of genus *Pandoraea* are commonly recovered from sputum specimens of patients with cystic fibrosis, but some species were isolated from various environmental sources too. These bacteria have been considered as emerging multi-drug resistant pathogens in the context of cystic fibrosis (Davies and Rubin, 2007), but our understanding about the epidemics of *Pandoraea* species remains scarce.

Bacterial cells are able to interact with one another *via* production and release of diffusible signaling molecules into their living environment. Detection of such molecules enables bacteria to coordinate gene expression in response to both high and low cell population densities. The process is termed as quorum sensing (QS) or bacterial cell-to-cell communication (Williams, 2007). The canonical LuxI/R QS system is one of the most studied QS systems in bacteria. In this system, the responsible signaling molecules are *N*-acyl homoserine lactones (AHLs) that are produced by an AHL synthase, LuxI activates a cognate transcriptional regulator, LuxR if the concentration of AHLs achieves a threshold. Upon activation, LuxR binds to the promoters or regulators of targeted genes in response to the cell density and causes coordinated gene expression in the bacterial population (Fuqua and Greenberg, 2002; Williams, 2007). *Via* this system, bacteria regulate a variety of activities including biofilm formation, production of extracellular enzymes, regulation of virulence genes, and so on.

With the advancement in DNA sequencing technologies, novel subgroups of *luxI* and *luxR* homologs have been identified in numerous bacterial species. While it led to reports that most typical *luxI*/*R* QS systems have both genes involved located almost adjacent to each other, additional *luxR* homologs that do not pair with a cognate *luxI* are frequently found. These unpaired *luxR* homologs that are termed as *luxR* solos possess modular homologies to the canonical LuxR with an AHL-binding domain at their N-terminus and a DNA-binding helix-turn-helix (HTH) domain at the C-terminus (Subramoni and Venturi, 2009). Bioinformatics prediction of QS genes in proteobacterial genomes had revealed the presence of numerous additional orphan *luxR* homologs with no *luxI* homologs in close proximity (Fuqua, 2006). In addition to their widespread distributions in proteobacteria, some of these LuxR solos are phylogenetically related and several surveys provided evidence on clustering of LuxR solos into different functionally relevant groups (Brameyer et al., 2014; Gan et al., 2015; Subramoni et al., 2015). It is believed that the presence of additional LuxR solos increases the range of gene regulatory activities by responding to self-produced AHLs or eavesdropping on exogenous AHLs and even other signaling molecules produced by other species (Hudaiberdiev et al., 2015; Subramoni et al., 2015). Interestingly, some LuxR solos harbored by non-QS bacteria are responding to non-AHL signaling molecules such as OryR of *Xanthomonas oryzae* pv. oryzae and XccR of *Xanthomonas campestris* pv. campestris that are capable of interacting with plant signaling molecules and play essential roles in their pathogenicity (Zhang et al., 2007; Ferluga and Venturi, 2009).

Members of genus *Pandoraea* have been reported with QS activity and are able to communicate *via* the production of AHLs (Ee et al., 2014). In this study, we investigated (1) if AHL-mediated QS is a common activity employed by all type strains of *Pandoraea* species and (2) the distribution of QS genes in *Pandoraea* genus. Our work was initiated by obtaining type strains of all species of the genus from culture collection to characterize their QS activity before we sequenced their complete genomes to provide molecular data on distributions and phylogenetic relationships of QS genes in the study species. A systematic bioinformatics prediction workflow was developed for the identification of LuxI and LuxR of *Pandoraea* species. Our findings indicated that AHL synthases of genus *Pandoraea* represent a novel evolutionary branch of QS system. We also identified the presence of two conserved LuxR solos in most members of *Pandoraea* genus, which prompted us to further discuss the acquisition mechanisms and possible roles of these LuxR solos in this study.

MATERIALS AND METHODS

Bacterial Strains and Culture Conditions

All type strains of species in *Pandoraea* genus were acquired from Leibniz Institute-Deutsche Sammlung von Mikroorganismen und Zellkulturen (DSMZ) culture collection. All bacteria strains were maintained in media and condition as listed in **Supplementary Table S1**.

Detection of Quorum Sensing Activity Using CVO26 Bioassay

Preliminary detection of QS activity was conducted by CVO26 bioassay in which the bacterial samples were streaked perpendicularly to CVO26 biosensor on Luria-Bertani (LB) agar and incubated in 28°C for 24 h. The CVO26 biosensor is

useful for the detection of short chain AHLs in the range of C4-HSL to C8-HSL (McClean et al., 1997). Positive result was observed with purple pigmentation of viocalein forming on the CVO26 biosensor. Positive and negative controls were set up with *E. carotovora* GS101 and *E. carotovora* PNP22, respectively.

Extraction of Acyl-Homoserine Lactone Signaling Molecules

All the strains were cultured in LB broth buffered with 50 mM 3-(N-morpholino) propanesulfonic acid (MOPS; pH 5.5) in their respective optimum culturing temperature for 24 h with 220 rpm agitation prior to AHL extraction. Spent culture supernatants were mixed thoroughly with an equal volume of 0.1% v/v glacial acetic acid-acidified ethyl acetate solvent until biphasic layers were formed, and the upper immiscible solvent layer was transferred out. Similar extraction was performed twice, and the organic solvent containing AHL extract was desiccated completely for mass spectrometry analysis.

Multiple Reaction Monitoring Mass Spectrometry Analysis

Desiccated AHL extracts were suspended with acetonitrile solvent prior to sample loading into an Agilent 1,290 Infinity LC system (Agilent Technologies Inc., Santa Clara, CA, USA). The liquid chromatography (LC) system was comprised of an Agilent ZORBAX Rapid Resolution High Definition SB-C18 Threaded Column (2.1 mm × 50 mm, 1.8 μm particle size) operated at 500 μl/min flow rate, 37°C with solvent A (0.1% formic acid buffered water) and solvent B (0.1% formic acid buffered acetonitrile) as the mobile phases. Three-step elution was performed with 7 min of linear gradient profile of 20–70% of solvent B, followed by 5 min of isocratic profile of 80% of solvent B, and 3 min of gradient profile of 80–20% of solvent B.

The LC-separated compounds were detected by electrospray ionization trap mass spectrometry (ESI-MS) using Agilent 6,490 Triple Quadrupole LC/MS system under positive-ion mode. The electrospray used nitrogen as nebulizing gas (pressure set to 20 p.s.i) and drying gas (flow set to 11 ml/h). The desolvation temperature was 200°C, and probe capillary voltage was set at 3 kV. AHL profiles were characterized using multiple reaction monitoring (MRM; Gould et al., 2006) by comparison of retention times and *m/z* transitions with those of the synthetic AHLs. A total of 10 synthetic AHLs varying in substitution oxo-group at C3 position (e.g., C6-HSL and 3-oxo-C6-HSL) and carbon length (ranging from C4-HSL to C12-HSL) were loaded in the MS analysis for reference as listed in **Supplementary Table S2**. The ions monitored in Q1 include the AHL precursor ion $[M+H]^+$, whereas both the lactone moiety at *m/z* 102 and the acyl moiety $[M+H-101]^+$ were monitored in Q3. Blanks (acetonitrile) were analyzed as control (data not shown). Data analysis was performed using Agilent MassHunter software.

Genome Sequencing

Genomic DNA (gDNA) was extracted using MasterPure DNA Purification Kit (EpiCenter, CA, USA) according to the manufacturer's instruction, and the quality of gDNA was assessed using gel electrophoresis, NanoDrop 2000 UV-Vis spectrophotometer (Thermo Scientific, MA, USA) and Qubit 2.0 fluorometer (Life Technologies, MA, USA), respectively. Whole genome sequencing was performed using PacBio (Pacific Biosciences, CA, USA) Single-Molecule Real Time (SMRT) sequencing technology.

Genome Assembly, Circularization, and Annotation

Raw data generated were assembled using hierarchical genome assembly process (HGAP) assembler. Circularity of genomes was assessed using Contiguity (Sullivan et al., 2015; Lim et al., 2015a), and the precise location of the overlapping region was determined using Gepard (Krumsiek et al., 2007; Lim et al., 2015b) prior to genome circularization using Minimus2 pipeline in the AMOS software package to generate the blunt-ended circular genomes with complete closure. The presence of plasmid was distinguished from the chromosomal genome, and functional annotation was performed using NCBI Prokaryotic Genome Annotation Pipeline (PGAP), Rapid Prokaryotic Genome Annotation (Prokka; Seemann, 2014), Rapid Annotation Search Tool (RAST; Aziz et al., 2008), KEGG database (Kanehisa et al., 2016), and IMG ER (Markowitz et al., 2009).

Systematic Bioinformatics Prediction of LuxI and LuxR

A systematic bioinformatics prediction and identification of LuxI and LuxR was employed in this study as presented in **Figure 1**. In short, translated proteomes were local blast against LuxI and LuxR databases downloaded from Uniprot and NCBI non-redundant protein database. Conserved domains of the putative LuxI (cl7182, N-acyltransferase superfamily) and LuxR (cd06170, C-terminal DNA-binding domain of LuxR-like proteins; PF03472, autoinducer-binding domain) were identified using conserved domain database (CDD) search tool in NCBI. All short-listed candidates were then scanned for signature protein family (Pfam) domain present in all LuxI (PF00765, autoinducer synthase), and LuxR (PF03472, autoinducer-binding domain). Lastly, a comprehensive InterProScan was conducted to provide high confidence authenticity of the identified LuxI and LuxR in which all LuxIs must contain three signature LuxI domains, IPR016181 (acyl-CoA N-acyltransferase), IPR001690 (autoinducer synthase), and IPR018311 (autoinducer synthesis, conserved site), while LuxR must contain four signature LuxR domains, IPR005143 (transcription factor LuxR-like, autoinducer-binding domain), IPR011991 (winged helix-turn-helix DNA-binding domain), IPR016032 (signal transduction response regulator, C-terminal effector), and IPR000792 (transcription regulator LuxR, C-terminal).

Multiple alignment of LuxI was performed with numbering relative to curated LuxI sequence of *Vibrio fischeri* (Entry: P12747) retrieved from Swiss-Prot database to determine the 10 conserved residues (R25, F29, W35, E44, D46, D49, R70, F84, E101, and E104) present in all LuxI (Fuqua and Greenberg, 2002). Multiple alignment of LuxR was performed with numbering relative to curated TraR sequence of *Agrobacterium tumefaciens* (Entry: P33905) retrieved from Swiss-Prot database to determine

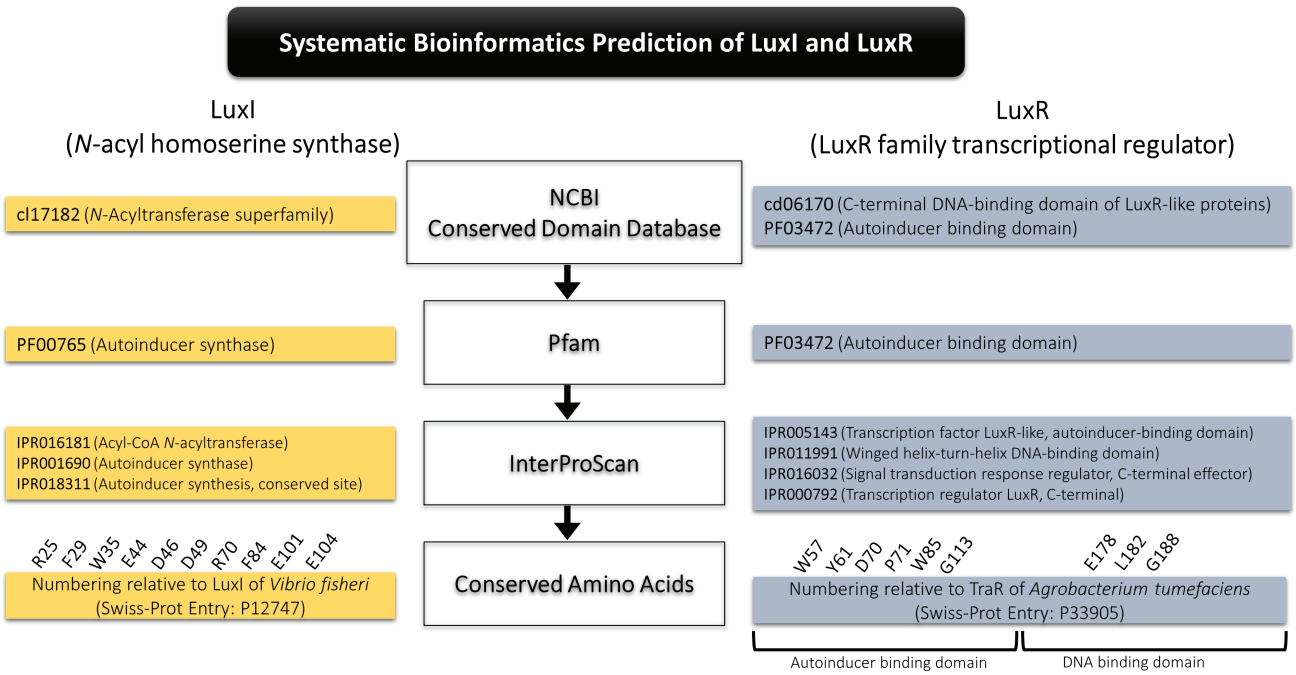

FIGURE 1 | Systematic bioinformatics prediction of LuxI and LuxR in this study.

the nine signature conserved residues (W57, Y61, D70, P71 W85, and G113, which are key amino acids in autoinducer-binding domain, and E178, L182, and G188, which are three key amino acids in DNA-binding domain) found in all LuxR (Subramoni et al., 2015).

Average Nucleotide Identity and Phylogenomics Analysis

Average nucleotide identity (ANI) analysis by Goris et al. (2007) was performed using ANI calculator[1]. Genome alignments were performed with a minimum length of 700 bp and a minimum identity of 70%. Genome fragments options were set with a window size of 1,000 bp and a step size of 200 bp. Phylogenomics tree was constructed using neighbor joining (NJ) method in MEGA 6.06 in which pairwise distances were acquired from ANI analysis (Saitou and Nei, 1987; Tamura et al., 2013).

Maximum Likelihood Phylogenetic and Pairwise Identity Matrix Analyses

Evolutionary analyses of QS genes were performed using MEGA 6.06 in which all *in silico* functionally validated amino acid sequences were aligned using MUSCLE algorithm (Edgar, 2004; Tamura et al., 2013). Phylogenetic analyses were performed using maximum likelihood (ML) method with Jones-Taylor-Thorton (JTT) model and 1,000 replications of bootstrap analysis (Jones et al., 1992). Initial tree was constructed automatically using NJ and BioNJ algorithms with nearest-neighbor-interchange (NNI) method. All gaps and missing data were not included in the analyses. Pairwise identity matrix analyses were performed using Sequence Demarcation Tool (SDT) version 1.2 (Muhire et al., 2014). Sequences alignment was performed using MUSCLE algorithm, and data were presented in three color modes.

[1]http://enve-omics.ce.gatech.edu/ani/

RESULTS AND DISCUSSION

Detection and Characterization of Quorum Sensing Activity in *Pandoraea* Genus

Following our previous discovery on QS activity in *P. pnomenusa* RB-38 and RB-44 (Han-Jen et al., 2013; Ee et al., 2014), we hypothesized that QS could be a common activity employed by all members in *Pandoraea* genus. To prove our hypothesis, all nine type strains of *Pandoraea* were first screened for their QS activity using CVO26 biosensor (McClean et al., 1997), and other possible AHLs were also extracted from spent culture prior to characterization of AHL signaling molecules using MRM MS analysis. Of nine strains, only four (*P. pnomenusa, P. sputorum, P. oxalativorans,* and *P. vervacti*) activated the CVO26 biosensor, and C8-HSL was the only AHL detected in MRM MS analysis (**Supplementary Figure S1**). Interestingly, not all clinically isolated strains were detected positive for AHL production as *P. apista* DSM 16535^T and *P. pulmonicola* DSM 16583^T have no QS activity detected.

Complete Genome Sequencing of Nine Type Strains of *Pandoraea* Species

As QS is not a common activity employed by all *Pandoraea* species, we questioned (1) if other non-AHL-producing

Pandoraea species (*P. apista, P. pulmonicola, P. norimbergensis, P. faecigallinarum,* and *P. thiooxydans*) are actually possessing mutated *luxI* and/or *luxR*, incapable of producing or detecting AHL (Sandoz et al., 2007) and (2) if they harbor *luxR* solo in their genomes? To prove these hypotheses, we sequenced the complete genomes of all nine type strains of *Pandoraea* using SMRT sequencing technology to facilitate the identification of the QS genes in the genomes. HGAP assembler was employed to assemble all genomes to complete closure, and circularization was performed to provide a high confidence genomic size of each *Pandoraea* strains. Plasmids were distinguished from the chromosomal DNA, and designation code was provided for each strain (**Table 1**). Besides, all *Pandoraea* genomes available in GenBank were also retrieved for investigation (**Supplementary Table S3**).

Genome sizes of species in *Pandoraea* genus range between 4.5 and 6.2 Mb with genomes of *P. thiooxydans* DSM 25325 T and *P. norimbergensis* DSM 11628^T representing the smallest and largest, respectively (**Table 1**). The G + C content of these genomes varies from 62.63 to 64.9%. The presence of plasmids was identified in four of nine type strains. Notably, *P. apista* DSM 16535^T is the only one harboring plasmid of five clinically isolated strains. The other three type strains harboring plasmid are *P. faecigallinarum* DSM 23572^T, *P. oxalativorans* DSM 23570^T, and *P. vervacti* DSM 23571^T that were isolated from oxalate-enriched cultures from different environments (**Table 1**; Sahin et al., 2011).

ANI analysis was subsequently performed to investigate the genetic and evolutionary distances of all *Pandoraea* species (**Supplementary Table S4**). Generally, 95% of ANI value is the accepted cut-off threshold for species-species delineation (Richter and Rosselló-Móra, 2009). The *Pandoraea* genomes in this study formed several clusters on a phylogenomic tree constructed using neighbor-joining algorithm (**Figure 2**). In Cluster 1 that included several *P. pnomenusa* and *P. pulmonicola* DSM 16583^T, we observed that the clinically isolated strains *P. pnomenusa* DSM 16536^T were distinguished from the other *P. pnomenusa* that were obtained from the environments by slightly further distances.

By contrast, *P. sputorum* DSM 21091^T was the only clinically isolated species that was clustered together with *P. oxalativorans* DSM 23570^T, *P. faecigallinarum* DSM 23572^T, and *P. vervacti* DSM 23571^T that were isolated from various environments despite being obtained from different origins. The strains *P. norimbergensis* DSM 11628^T and *P. thiooxydans* were found to be most distantly related to all other *Pandoraea* species (<85 and <79% ANI values, respectively; **Supplementary Table S4**) forming outgroups in the phylogenomic analysis of *Pandoraea* genus (**Figure 2**).

Results from the ANI analysis also suggested reclassification of several *Pandoraea* strains with uncertain taxonomic status. We deduce from the analysis that *Pandoraea* sp. E26 could be reclassified as *P. pnomenusa* E26 as it shares 99% ANI value with all *P. pnomenusa*. On the other hand, *P. pnomenusa* strains 6,399 and 7,641 that demonstrated ANI value <90% against all other *P. pnomenusa* suggested that reclassification might be necessary. This is supported by the observations that both the strains exhibited the highest ANI values with *P. apista* species (>88% ANI values; **Supplementary Table S4**) and were placed out of Cluster 1 (consisted of all other *P. pnomenusa* and *P. pulmonicola* DSM 16583^T) in phylogenomic tree (**Figure 2**). Unfortunately, the taxonomy of *Pandoraea* strains SD6-2 and B-6 remained questionable as both of them were having low ANI values (<88 and <86%, respectively; **Supplementary Table S4**) with all other *Pandoraea* in this study.

Identification of *luxI* and *luxR* Homologs in Genomes of Genus *Pandoraea*

To provide high confidence in authenticity of all LuxI and LuxR identified in this study, we created a stringent and effective systematic bioinformatics prediction of LuxI and LuxR as presented in **Figure 1**. A total of 10 *luxI*s were identified in genomes of *P. pnomenusa, P. sputorum, P. oxalativorans,* and *P. vervacti* (**Supplementary Table S5**). A typical authentic LuxI contains three signature InterPro domains (IPR016181, IPR001690, and IPR018311) and 10 signature conserved residues. Although all 10 LuxIs of *Pandoraea* species identified were found to contain only domains IPR016181 and IPR001690 (**Figure 3**), our previous gene cloning data of *PpnI* RB38 confirmed that LuxI of *Pandoraea* species could function properly despite the absence of domain IPR018311 (Lim et al., 2015a). Multiple alignment analysis of LuxI also revealed a consistent profile of signature conserved residues in all LuxIs of *Pandoraea* species, thus concordantly supported the evidence that these are authentic functional LuxI for the production of C8-HSL (**Supplementary Table S6**). No orphan *luxI* was identified in any of the *Pandoraea* genomes in this study.

Intriguingly, besides the expected canonical *luxR*, two additional *luxR* solos (named *luxR*2 solo and *luxR*3 solo) were identified in most *Pandoraea* genomes (**Supplementary Table S5**). *P. thiooxydans* DSM 25325^T is the only exception and does not harbor any canonical *luxI*/*R1* and *luxR* solo in its genome (**Supplementary Table S5**). *P. apista* TF81 and *Pandoraea* sp. E26 were also found to harbor only *luxR2* solo. However, we hypothesized that *luxR*3 solo could be missing in the gap of their draft genomes. All canonical LuxR and LuxR solos identified in this study contained all the four signature InterPro domains (IPR005143, IPR011991, IPR016032, and IPR000792), and all nine signature conserved residues (six key amino acids in autoinducer-binding domain and three key amino acids in DNA-binding domain) found in typical LuxR (**Supplementary Table S7**; Subramoni et al., 2015).

To date, there have been reports on LuxR solos responding to non-AHL signals. For examples, the PluR of *Photorhabdus luminescens* senses α-pyrone (Brachmann et al., 2013), while PauR of *P. asymbiotica* detects dialkylresorcinols and cyclohexanediones (Brameyer et al., 2015) signaling molecules instead of AHLs. These non-AHL-binding LuxRs, however, harbor substitutions in the conserved amino acid motif of autoinducer-binding domain compared to that in AHL sensors (Brameyer and Heermann, 2015). The autoinducer-binding domain of all LuxR solos in *Pandoraea* species contained

TABLE 1 | Designation code, sequencing information and general features of nine circularized genomes of *Pandoraea* type species.

Strains	Code	Assembler (coverage)	Chromosome				Plasmid			
			Accession no.	Genome size, bp	G + C content	Gene (protein)	Accession no.	Genome size, bp	G + C content	Protein (gene)
P. pnomenusa DSM 16536^T	Ppn DSM	HGAP3 (244.6×)	CP009553.2	5,389,285	64.90	4,811 (4,586)	–	–	–	–
P. pulmonicola DSM 16583^T	Ppu DSM	HGAP3 (110.5×)	CP010310.1	5,867,621	64.30	5,022 (4,820)	–	–	–	–
P. sputorum DSM 21091^T	Psp DSM	HGAP3 (215.16×)	CP010431.1	5,751,958	62.80	5,037 (4,859)	–	–	–	–
P. apista DSM 16535^T	Pap DSM	HGAP3 (243.8×)	CP013481.1	5,507,928	62.63	5,042 (4,864)	CP013482.1	77,293	62.63	5,042 (4,864)
P. norimbergensis DSM 11628^T	Pno DSM	HGAP3 (165.0×)	CP013480.1	6,167,399	63.10	5,417 (5,195)	–	–	–	–
P. faecigallinarum DSM 23572^T	Pfa DSM	HGAP3 (75×)	CP011807.1	5,261,138	63.70	4,619 (4,412)	CP011808.1	402,292	61.00	388 (334)
							CP011809.1	124,395	59.30	130 (103)
P. oxalativorans DSM 23570^T	Pox DSM	HGAP3 (215.2×)	CP011253.2	5,639,839	63.10	4,983 (4,711)	CP011518.1	640,227	63.80	516 (452)
							CP011519.1	135,985	60.60	136 (120)
							CP011520.1	85,789	59.80	94 (70)
							CP011521.1	46,278	59.20	52 (40)
P. thiooxydans DSM 25325^T	Pth DSM	HGAP3 (165.54×)	CP011568.1	4,464,186	63.20	4,117 (3984)	–	–	–	–
P. vervacti DSM 23571^T	Pve DSM	HGAP2 (185×)	CP010897.1	5,656,222	63.50	4,912 (4697)	CP010898.1	105,231	62.00	102 (95)

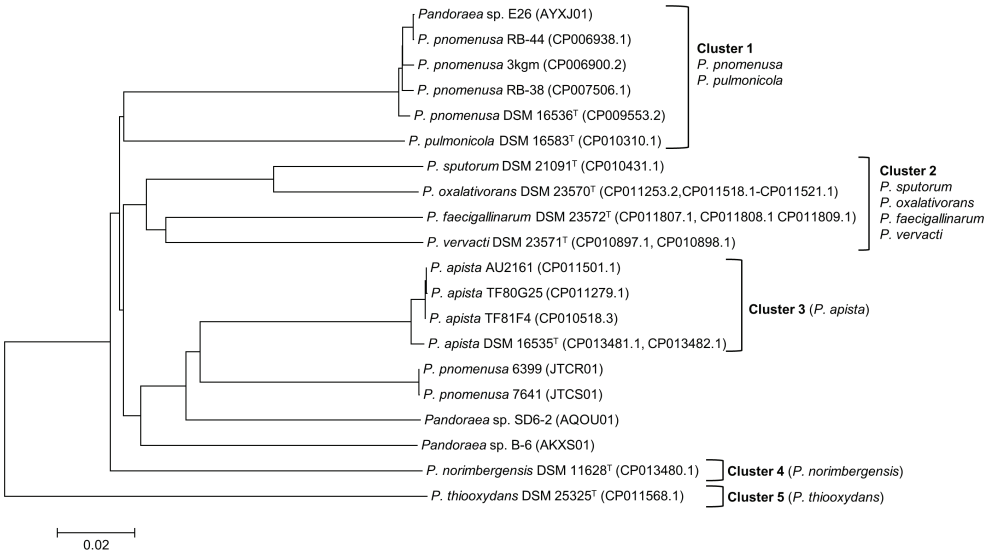

FIGURE 2 | Phylogenomic analysis depicting the genetic and evolutionary distances of all *Pandoraea* species. In general, *Pandoraea* genus was separated into five distinct clusters: Cluster 1 (*P. pnomenusa*, *P. pulmonicola*), Cluster 2 (*P. sputorum*, *P. oxalativorans*, *P. faecigallinarum*, *and P. vervacti*), Cluster 3 (*P. apista*), Cluster 4 (*P. norimbergensis*), and Cluster 5 (*P. thiooxydans*). Bar, 0.2 substitutions per nucleotide position.

FIGURE 3 | Signature InterPro domain of LuxI (top) and LuxR (bottom). LuxI of *Pandoraea* species contain two signature domains (IPR016181 and IPR001690), while LuxR of *Pandoraea* species contains four signature domains (IPR005143, IPR011991, IPR016032, and IPR000792).

the six conserved amino acids (W57, Y61, D70, P71, W85, and G113) with respect to TraR (**Supplementary Table S7**) and thus reflected a conserved motif for AHL-binding LuxR proteins.

From our analysis, we noticed that majority of the annotation pipelines often annotated *luxR*2 and *luxR*3 solo genes as hypothetical proteins making it a challenge in their identification process. Hence, we employed an *in silico* systematic bioinformatics prediction of these genes to aid in future identification of *luxR*2 and *luxR*3 solos. For nomenclature purpose, the gene products of canonical *luxI*/*R* identified in *Pandoraea* genomes were given designation with the first alphabet of the genus followed by the first two alphabet of species, for instances, PpnI, LuxI of *P. pnomenusa,* and PspR, LuxR of *P. sputorum* (**Supplementary Table S5**). Additionally, to differentiate between canonical LuxR and LuxR solos, canonical LuxR were given designation as LuxR1 (e.g., PpnI/R1 and PspI/R1), while LuxR solos were given designation

as LuxR2 and LuxR3 solos. Gene designations, accession numbers, amino acid length, GC content, and genetic orientation of all canonical LuxI/R1 and LuxR solos of *Pandoraea* species are presented in **Supplementary Table S5**. No QS gene was found on plasmid.

LuxI of *Pandoraea* Species Represents a Novel Evolutionary Branch of Quorum Sensing System

To determine the relatedness of LuxI in *Pandoraea* genus with the other well-characterized LuxI, phylogenetic and pairwise identity matric analyses were conducted. **Figure 4** shows the recent phylogenetic tree of LuxI from several groups that are most closely related to the LuxI in *Pandoraea* genus, together with pairwise identity matrix analysis. The analyses revealed that LuxI of *Pandoraea* species were highly conserved in *Pandoraea* genus forming a distinct cluster separated from the LuxI of *Burkholderia* species, SolI of *Ralstonia solanacearum*, and RhlI and LasI of *Pseudomonas aeruginosa*, representing a novel evolutionary branch of QS system (**Figure 4**). *Ralstonia* and *Burkholderia* are closely related genera to *Pandoraea*, and they shared highly similar phenotypic profiles that often resulted in the misidentification of *Pandoraea* species (Coenye et al., 2001; Henry et al., 2001). As *Pandoraea* were also predominantly recovered from CF patients, QS genes of *P. aeruginosa* (model organism for QS and CF patients) were also included in the analysis (Barr et al., 2015).

While analysis on the amino acid pairwise identity revealed that similarity of PpnI of different *P. pnomenusa* strains can be as high as 90%, pairwise identity shared between the LuxI of different *Pandoraea* species varied from about 50–90%, even though they were all placed in the same cluster in phylogenetic tree of LuxI (**Figure 4**). When compared to the LuxI of other genera, the LuxI of *Pandoraea* species are only 41–55% in pairwise identity with the well-characterized CepI of *Burkholderia cenocepacia* that catalyzes primarily the synthesis of C8-HSL and a minority of C6-HSL (Lewenza et al., 1999; Lewenza and Sokol, 2001); 48–55% in pairwise identity with SolI, which catalyzes the synthesis of C6-HSL and C10-HSL (Flavier et al., 1997); 26–41% in pairwise identity with CciI, which catalyzes primarily the synthesis of C6-HSL and a minority of C8-HSL (Malott et al., 2005); and lastly, about 26–33% pairwise identity with RhlI and LasI, which catalyzes primarily the synthesis of C4-HSL and 3-oxo-C12-HSL (Latifi et al., 1996). Besides, we also identified the 20 bp lux box located in the upstream region of the *luxI* of *Pandoraea* species

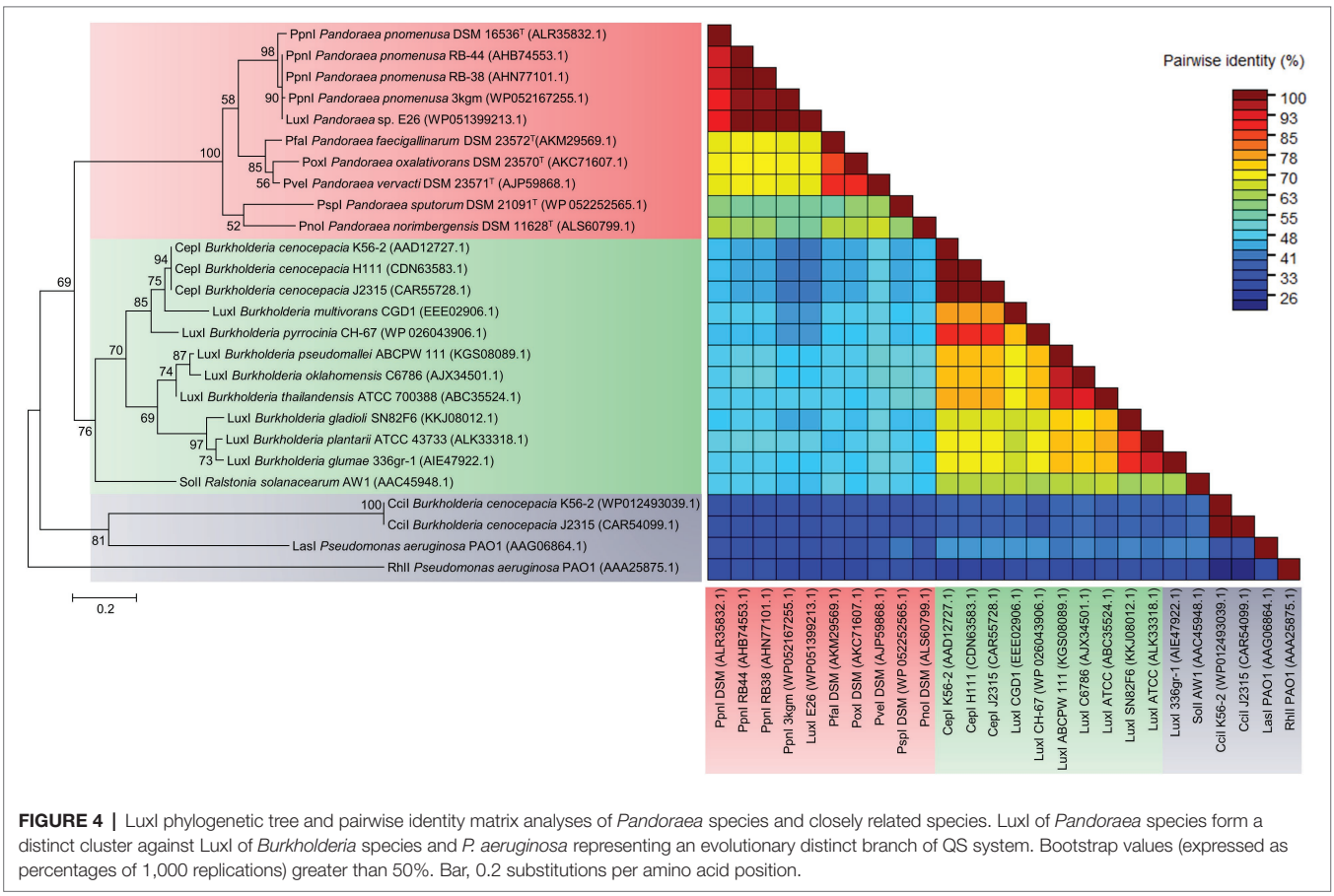

FIGURE 4 | LuxI phylogenetic tree and pairwise identity matrix analyses of *Pandoraea* species and closely related species. LuxI of *Pandoraea* species form a distinct cluster against LuxI of *Burkholderia* species and *P. aeruginosa* representing an evolutionary distinct branch of QS system. Bootstrap values (expressed as percentages of 1,000 replications) greater than 50%. Bar, 0.2 substitutions per amino acid position.

(**Supplementary Figure S2**). The lux box is a 20 bp palindromic sequence located upstream in the promoter region of *luxI,* which is required for the binding of AHL-activated LuxR (Lewenza et al., 1999). All *luxI* of *Pandoraea* species shared consensus in 14 of 20 lux box sequence (**Supplementary Figure S2**).

Canonical LuxR1 and LuxR Solos in *Pandoraea* Genus

Phylogenetic and pairwise identity matric analyses performed on all identified canonical LuxR1 of genus *Pandoraea* demonstrated close clustering with CepR from genus *Burkholderia* and SolR from genus *Ralstonia* with 96% bootstrap value (**Figure 5**). Similar to CepI of genus *Burkholderia*, the LuxI of *Pandoraea* produce C8-HSL, but SolI from *Ralstonia* produces two short-chain AHL signals (C6-HSL and C10-HSL). As all identified *luxR*1 of *Pandoraea* are located adjacent to *luxI*, it is believed that the primary function of LuxR1 is for the detection of C8-HSL produced by its canonical LuxI. A comparison on the amino acid sequences of multiple LuxR groups revealed the highest pairwise identity among canonical LuxR1 of *Pandoraea* (71–100%) but lower identity to all the LuxR of other groups (<41%), including the LuxR2 and LuxR3 solos in *Pandoraea*.

Intriguingly, LuxR2 and LuxR3 solos formed two separated clusters on phylogenetic tree with the canonical LuxR identified in *Pandoraea* genus. Both the LuxR solos were distinctive from each other and had CciR of *Burkholderia cenocepacia* and LasR of *P. aeruginosa* as outgroups of the clusters, respectively (**Figure 5**). The LuxR2 solos are highly conserved in the genus *Pandoraea* showing >85% in amino acid pairwise identity among different species, as compared to the canonical LuxR1 (>71% in pairwise identity) and LuxR3 solos (>56% in pairwise identity) (**Figure 5**). From the phylogenetic analysis, it might imply that these LuxR solos in *Pandoraea* represent two novel evolutionary branches of LuxR in QS system. This is supported by a comprehensive search in various databases, which did not return significant matches with any other species and thus indicated that LuxR2 and LuxR3 solos were found exclusively only in *Pandoraea* species.

The widespread distribution of LuxR solos in almost every *Pandoraea* species (except *P. thiooxydans* DSM 25325^{T})

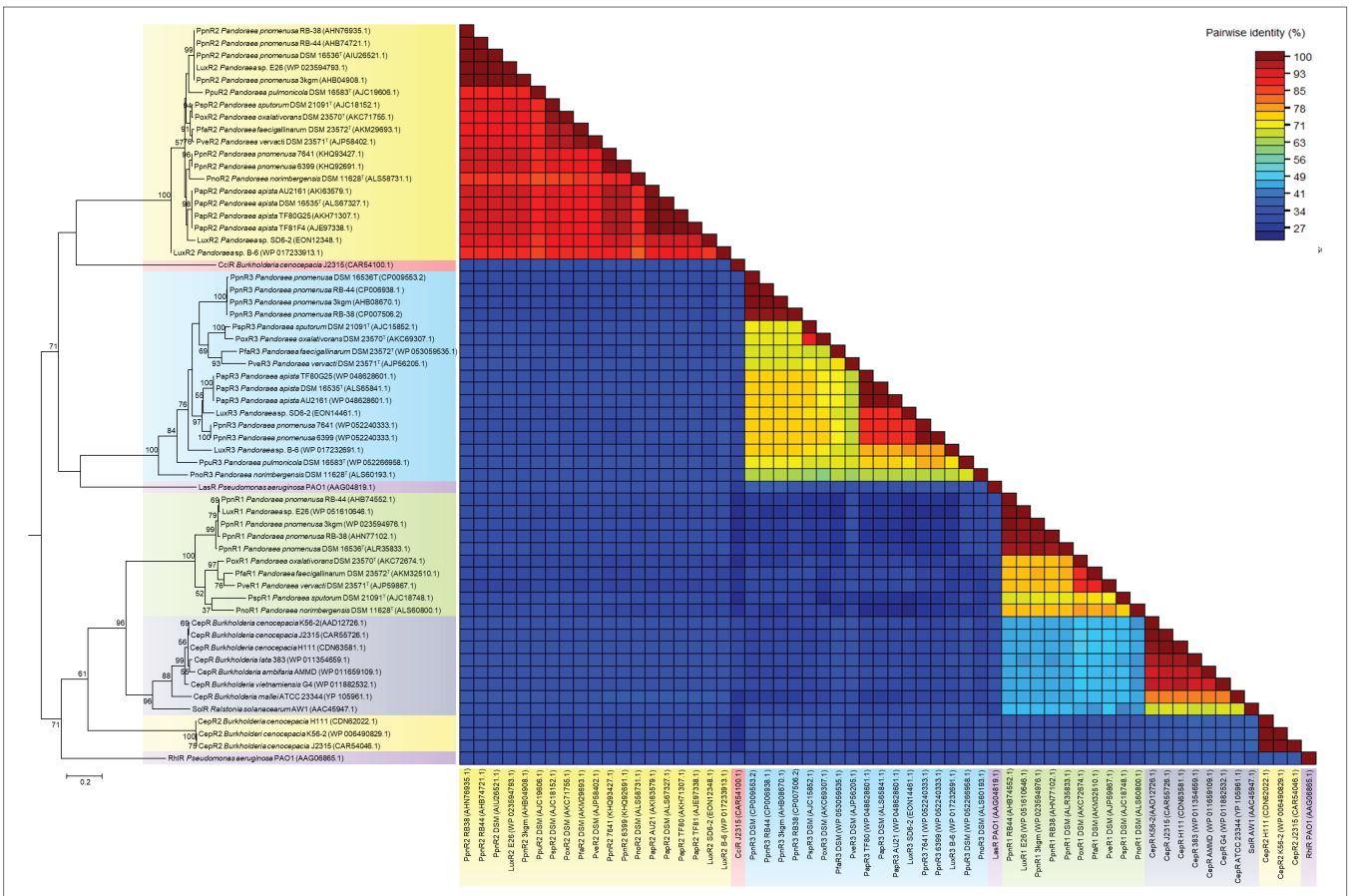

FIGURE 5 | LuxR phylogenetic tree and pairwise identity matrix analyses of *Pandoraea* species and closely related species. Canonical LuxR1 clustered closely with CepR and SolR. LuxR2 and LuxR3 solos formed a distinct cluster with CciR and LasR as the outgroup, respectively, representing evolutionary distinct branches of LuxR. Bootstrap values (expressed as percentages of 1,000 replications) greater than 50%. Bar, 0.2 substitutions per amino acid position.

indicated that they could be playing potential roles in survival and persistence of these species. For *Pandoraea* species that possess QS activity (*P. pnomenusa, P. sputorum, P. oxalativorans,* and *P. vervacti*), additional LuxR solos could function in detecting endogenous AHL signals produced by the AHL synthase to increase the regulatory targets of the complete canonical LuxI/R QS system. Notably, QS positive *P. pnomenusa* and *P. sputorum,* which are clinically isolated, might possess LuxR solos for their survival and persistence in respiratory tracts of CF patients as well as regulation of virulence factors. Similar phenomenon was observed in QscR solo of *Pseudomonas aeruginosa,* which is a LuxR solo that responds to endogenous 3-oxo-C12-HSL produced by LasI to control the timing of AHL production in the species for regulating expression of virulence factors. A study on *qscR* mutant demonstrated that it is hypervirulent in killing its host indicating that QscR solo is important for efficient regulation of QS-mediated virulence factors (Chugani et al., 2001).

In addition, the LuxR solos in *Pandoraea* species could be essential for detecting exogenous AHLs produced by neighboring species, especially for *Pandoraea* species that do not own a LuxI/R AHL system. In this study, AHL production was not observed in *P. apista* DSM 16535^{T} and *P. pulmonicola* DSM 21091^{T} that were isolated from sputa of CF patients. The presence of LuxR solos in these strains could be responsible for eavesdropping by detecting exogenous AHL molecules produced by *P. aeruginosa* that is chronically colonizing the respiratory tracts of CF patients. It is also noteworthy that many Gram-negative bacteria with QS activity such as *Burkholderia* and *Ralstonia* are common pathogens causing lung infections in CF patients. In fact, there are bacteria that possess LuxR solos even though they do not harbor any type of AHL synthase such as *Escherichia coli* and *Salmonella enterica* serovar Typhimurium. These bacteria carry a LuxR homolog, and SdiA was reported able to detect and respond to AHL signaling molecules produced by other bacterial species to activate their gene expression (Ahmer, 2004).

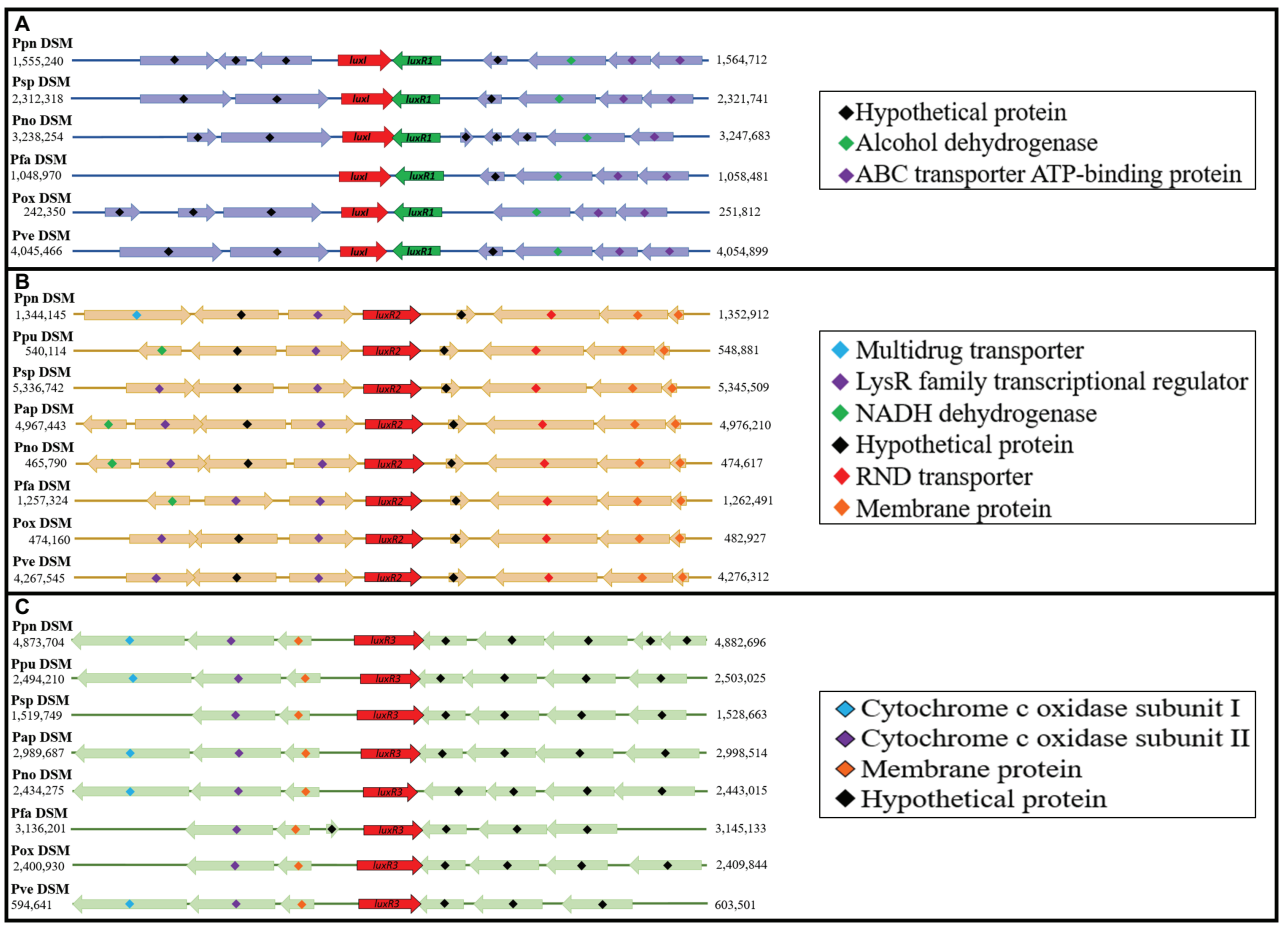

FIGURE 6 | Comparative gene mapping of all QS genes in type strains of *Pandoraea* species. All QS genes were highly conserved at syntenic genomic location. **(A)** Canonical *luxI* and *luxR*1 were found be convergently inverted and located upstream of alcohol dehydrogenase and ABC transporter ATP-binding protein. **(B)** *luxR*2 solos located between LysR transcriptional regulators and RND transporter. **(C)** *luxR*3 solo located downstream of cytochrome c oxidase subunits I and II and a membrane protein.

Comparative Gene Mapping of All Quorum Sensing Genes and Putative Acquisition Mechanism of LuxR Solos in Type Strains of *Pandoraea*

Since this is the first documentation of *luxR*2 and *luxR*3 solos in *Pandoraea* genus, we are determined to investigate the acquisition mechanism of these genes in *Pandoraea* genus. Hence, we performed comparative gene mapping to study the degree of conservation of all QS genes. All QS genes of *Pandoraea* were found to be highly conserved at syntenic genomic locations (**Figure 6**): all canonical *luxI*/*R*1 were found to be convergently inverted (only *luxI*/*R*1 of *P. sputorum* and *P. norimbergensis* overlapped with each other) and located upstream of an alcohol dehydrogenase and an ABC transporter ATP-binding protein (**Figure 6A**); *luxR*2 solos were consistently located between a LysR transcriptional regulators and a RND transporter (**Figure 6B**); and *luxR*3 solos were always found located downstream of cytochrome c oxidase subunits I and II and a membrane protein (**Figure 6C**). As there are hypothetical proteins located in the immediate upstream of *luxR*2 and *luxR*3, we questioned if these hypothetical proteins could be the canonical *luxI* that have mutated and lost its function or domain. However, after a comprehensive domain prediction was performed on these hypothetical proteins, there was no residue of *luxI* in these hypothetical proteins.

Subsequently, we also performed an extensive search for the presence of any QS genes in genomic island, prophages, and mobile genetic element regions to determine the possibility of horizontal gene transfer event. No QS gene was found on any genomic island, and no residue of transposase was found in close proximity of all QS genes. Although no QS gene was found within any intact prophage region, there are, however, few *luxR* solos that were found in close proximity with incomplete and intact prophage sequences, such as 53,482 bp between PpuR2 (63.0% GC content; 544,114–544,881 bp) with an incomplete prophage region 1 (63.7% GC content; 597,363–605,870 bp); 62,330 bp between PoxR2 (60.0% GC content; 478,160–478,927 bp) with an incomplete prophage region 1 (62.91% GC content; 533,510–541,257 bp); and 6,231 bp between PoxR3 (65.2% GC content; 2,404,930–2,405,844 bp) with an intact prophage region 8 (63.2% GC content; 2,391,675–2,398,699 bp). These observations suggested that *luxR*2 and *luxR*3 solos could be transmitted into *Pandoraea* genus by transduction event mediated by prophage. However, parts of these prophage sequences might be lost during evolution. Various QS-related genes had been reported in the genomes of bacteriophages including homologs of accessory gene regulator (*agr*) in the genome of *Clostridium difficile* phage phiCDHM1 (Hargreaves et al., 2014) and regulatory protein LuxR in the *Azospirillum brasilense* Cd bacteriophage's genome (Boyer et al., 2008).

QS activity in *Pandoraea* species has been related to the regulation of virulence factors, biofilm formation, extracellular enzymes production, antibiotic resistance, and various other lethal traits. Although not all *Pandoraea* species exhibit QS activity, findings in this study revealed that almost every *Pandoraea* species (except *P. thiooxydans* DSM 25325^T) possess LuxR solos genes in their genomes. The repertoire of LuxR solos in the genus increases the range of gene regulatory activities and is anticipated to play roles in QS-dependent regulation of phenotypic functions, which should be investigated further. The data presented are also useful in future application including quorum quenching (QQ) study that attempts to disrupt the bacterial cell-to-cell communication of *Pandoraea* species through QS (See-Too et al., 2018). QQ has been suggested as alternative antibacterial strategy to antibiotics, which might lead to emergence of multi-drug resistant bacteria (Tang and Zhang, 2014). Last but not least, we hope that findings from this study contribute to further research to elucidate the downstream roles of QS genes in *Pandoraea* species, including their LuxR solos.

CONCLUSIONS

Multiple species of the genus *Pandoraea* were frequently isolated from sputum samples of CF patients from all over the world, and *Pandoraea* species are identified as emerging pulmonary pathogen associated with CF. While some species were obtained from the environments, clinically isolated species such as *P. pnomenusa* has also been recovered from soils in the environment. This suggests the ubiquitous nature of this group of bacteria, and they are thus identified as opportunistic pathogens. The recent report on the QS activity in *P. pnomenusa* rapidly caught the attention of the scientific community as QS systems have been linked to the regulation of virulence factors, antibiotic resistance, and various traits that are dangerous to patients. Although this study revealed that only four type strains of nine species of genus *Pandoraea* possess AHL-based QS activity, we also reported the presence of two highly conserved *luxR* solos in most of their genomes. Our analyses had revealed that these LuxR solos belonged to different clusters of novel evolutionary branches in QS systems. We hypothesize that these LuxR solos in *Pandoraea* could potentially be responsive to AHLs or different signals produced by neighboring species and coordinate regulation of gene expression, thus playing important roles in the infection process and persistence of these pathogens in cystic fibrosis patients. In the process, we developed an *in silico* systematic bioinformatics prediction workflow, which is useful for LuxI and LuxR genes identification of other species. To summarize, this study lays the foundation for future study on QS systems of *Pandoraea* as a potential antimicrobial target in the treatment of *Pandoraea* infections.

DATA AVAILABILITY

Publicly available datasets were analyzed in this study. This data can be found here: https://www.ncbi.nlm.nih.gov/genome/.

AUTHOR CONTRIBUTIONS

KG-C and WF-Y conceived and designed the experiment. RE and YL-L conducted the experiments. KO-C, WS-ST, RE, and YL-L conducted the data analyses. KO-C, WS-ST, and RE wrote the manuscript. All authors read and approved the manuscript.

FUNDING

This work was supported by University of Malaya Research Grants (PG263-2016A and FP022-2018A), University of Malaya High Impact Research Grants (UM-MOHE HIR Grant UM.C/625/1/HIR/MOHE/ CHAN/14/1, Grant No. H-50001-A000027; UM-MOHE HIR Grant UM.C/625/1/HIR/MOHE/CHAN/01, Grant No. A-000001-50001) awarded to KG-C, Postgraduate Research (PPP) Grant (Grant No. PG084-2015B) awarded to RE and (PG089-2015B) to KO-C.

ACKNOWLEDGMENTS

KO-C thanks MyBrain15 Postgraduate Scholarship Programme for the scholarship (MyPhD, KPT(B)900909146137) awarded. WS-ST thanks the Bright Sparks Program of the University of Malaya for scholarship awarded.

SUPPLEMENTARY MATERIAL

The Supplementary Material for this article can be found online at: https://www.frontiersin.org/articles/10.3389/fmicb.2019.01758/full#supplementary-material

REFERENCES

Ahmer, B. M. M. (2004). Cell-to-cell signalling in *Escherichia coli* and *Salmonella enterica*. *Mol. Microbiol.* 52, 933–945. doi: 10.1111/j.1365-2958.2004.04054.x

Atkinson, R., Lipuma, J., Rosenbluth, D., and Dunne, W. M. (2006). Chronic colonization with *Pandoraea apista* in cystic fibrosis patients determined by repetitive-element-sequence PCR. *J. Clin. Microbiol.* 44, 833–836. doi: 10.1128/JCM.44.3.833-836.2006

Aziz, R. K., Bartels, D., Best, A. A., Dejongh, M., Disz, T., Edwards, R. A., et al. (2008). The RAST server: rapid annotations using subsystems technology. *BMC Genomics* 9:75. doi: 10.1186/1471-2164-9-75

Barr, H. L., Halliday, N., Cámara, M., Barrett, D. A., Williams, P., Forrester, D. L., et al. (2015). *Pseudomonas aeruginosa* quorum sensing molecules correlate with clinical status in cystic fibrosis. *Eur. Respir. J.* 46, 1046–1054. doi: 10.1183/09031936.00225214

Boyer, M., Haurat, J., Samain, S., Segurens, B., Gavory, F., González, V., et al. (2008). Bacteriophage prevalence in the genus *Azospirillum* and analysis of the first genome sequence of an *Azospirillum brasilense* integrative phage. *Appl. Environ. Microbiol.* 74, 861–874. doi: 10.1128/AEM.02099-07

Brachmann, A. O., Brameyer, S., Kresovic, D., Hitkova, I., Kopp, Y., Manske, C., et al. (2013). Pyrones as bacterial signaling molecules. *Nat. Chem. Biol.* 9, 573–578. doi: 10.1038/nchembio.1295

Brameyer, S., and Heermann, R. (2015). Specificity of signal-binding *via* non-AHL LuxR-type receptors. *PLoS One* 10:e0124093. doi: 10.1371/journal.pone.0124093

Brameyer, S., Kresovic, D., Bode, H. B., and Heermann, R. (2014). LuxR solos in *Photorhabdus* species. *Front. Cell. Infect. Microbiol.* 4:166. doi: 10.3389/fcimb.2014.00166

Brameyer, S., Kresovic, D., Bode, H. B., and Heermann, R. (2015). Dialkylresorcinols as bacterial signaling molecules. *Proc. Natl. Acad. Sci. USA* 112, 572–577. doi: 10.1073/pnas.1417685112

Chugani, S. A., Whiteley, M., Lee, K. M., D'argenio, D., Manoil, C., and Greenberg, E. P. (2001). QscR, a modulator of quorum-sensing signal synthesis and virulence in *Pseudomonas aeruginosa*. *Proc. Natl. Acad. Sci. USA* 98, 2752–2757. doi: 10.1073/pnas.051624298

Coenye, T., Falsen, E., Hoste, B., Ohlén, M., Goris, J., Govan, J., et al. (2000). Description of *Pandoraea* gen. nov. with *Pandoraea apista* sp. nov., *Pandoraea pulmonicola* sp. nov., *Pandoraea pnomenusa* sp. nov., *Pandoraea sputorum* sp. nov. and *Pandoraea norimbergensis* comb. nov. *Int. J. Syst. Evol. Microbiol.* 50, 887–899. doi: 10.1099/00207713-50-2-887

Coenye, T., Liu, L., Vandamme, P., and Lipuma, J. J. (2001). Identification of *Pandoraea* species by 16S ribosomal DNA-based PCR assays. *J. Clin. Microbiol.* 39, 4452–4455. doi: 10.1128/JCM.39.12.4452-4455.2001

Davies, J. C., and Rubin, B. K. (2007). Emerging and unusual gram-negative infections in cystic fibrosis. *Semin. Respir. Crit. Care Med.* 28, 312–321. doi: 10.1055/s-2007-981652

Edgar, R. C. (2004). MUSCLE: multiple sequence alignment with high accuracy and high throughput. *Nucleic Acids Res.* 32, 1792–1797. doi: 10.1093/nar/gkh340

Ee, R., Lim, Y.-L., Kin, L.-X., Yin, W.-F., and Chan, K.-G. (2014). Quorum sensing activity in *Pandoraea pnomenusa* RB38. *Sensors* 14, 10177–10186. doi: 10.3390/s140610177

Ferluga, S., and Venturi, V. (2009). OryR is a LuxR-family protein involved in interkingdom signaling between pathogenic *Xanthomonas oryzae* pv. *oryzae* and rice. *J. Bacteriol.* 191, 890–897. doi: 10.1128/JB.01507-08

Flavier, A. B., Ganova-Raeva, L. M., Schell, M. A., and Denny, T. P. (1997). Hierarchical autoinduction in *Ralstonia solanacearum*: control of acyl-homoserine lactone production by a novel autoregulatory system responsive to 3-hydroxypalmitic acid methyl ester. *J. Bacteriol.* 179, 7089–7097. doi: 10.1128/jb.179.22.7089-7097.1997

Fuqua, C. (2006). The QscR quorum-sensing regulon of *Pseudomonas aeruginosa*: an orphan claims its identity. *J. Bacteriol.* 188, 3169–3171. doi: 10.1128/JB.188.9.3169-3171.2006

Fuqua, C., and Greenberg, E. P. (2002). Signalling: listening in on bacteria: acyl-homoserine lactone signalling. *Nat. Rev. Mol. Cell Biol.* 3, 685–695. doi: 10.1038/nrm907

Gan, H. M., Gan, H. Y., Ahmad, N. H., Aziz, N. A., Hudson, A. O., and Savka, M. (2015). Whole genome sequencing and analysis reveal insights into the genetic structure, diversity and evolutionary relatedness of luxI and luxR homologs in bacteria belonging to the Sphingomonadaceae family. *Front. Cell. Infect. Microbiol.* 4:188. doi: 10.3389/fcimb.2014.00188

Gibson, R. L., Burns, J. L., and Ramsey, B. W. (2003). Pathophysiology and management of pulmonary infections in cystic fibrosis. *Am. J. Respir. Crit. Care Med.* 168, 918–951. doi: 10.1164/rccm.200304-505SO

Goris, J., Konstantinidis, K. T., Klappenbach, J. A., Coenye, T., Vandamme, P., and Tiedje, J. M. (2007). DNA–DNA hybridization values and their relationship to whole-genome sequence similarities. *Int. J. Syst. Evol. Microbiol.* 57, 81–91. doi: 10.1099/ijs.0.64483-0

Gould, T. A., Herman, J., Krank, J., Murphy, R. C., and Churchill, M. E. (2006). Specificity of acyl-homoserine lactone synthases examined by mass spectrometry. *J. Bacteriol.* 188, 773–783. doi: 10.1128/JB.188.2.773-783.2006

Han-Jen, R. E., Wai-Fong, Y., and Kok-Gan, C. J. S. (2013). *Pandoraea* sp. RB-44, a novel quorum sensing soil bacterium. *Sensors* 13, 14121–14132. doi: 10.3390/s131014121

Hargreaves, K. R., Kropinski, A. M., and Clokie, M. R. (2014). What does the talking?: quorum sensing signalling genes discovered in a bacteriophage genome. *PLoS One* 9:e85131. doi: 10.1371/journal.pone.0085131

Henry, D. A., Mahenthiralingam, E., Vandamme, P., Coenye, T., and Speert, D. P. (2001). Phenotypic methods for determining genomovar status of the *Burkholderia cepacia* complex. *J. Clin. Microbiol.* 39, 1073–1078. doi: 10.1128/JCM.39.3.1073-1078.2001

Hudaiberdiev, S., Choudhary, K. S., Vera Alvarez, R., Gelencsér, Z., Ligeti, B., Lamba, D., et al. (2015). Census of solo LuxR genes in prokaryotic genomes. *Front. Cell. Infect. Microbiol.* 5:20. doi: 10.3389/fcimb.2015.00020

Jones, D. T., Taylor, W. R., and Thornton, J. M. (1992). The rapid generation of mutation data matrices from protein sequences. *Bioinformatics* 8, 275–282. doi: 10.1093/bioinformatics/8.3.275

Kanehisa, M., Furumichi, M., Tanabe, M., Sato, Y., and Morishima, K. (2016). KEGG: new perspectives on genomes, pathways, diseases and drugs. *Nucleic Acids Res.* 45, D353–D361. doi: 10.1093/nar/gkw1092

Krumsiek, J., Arnold, R., and Rattei, T. (2007). Gepard: a rapid and sensitive tool for creating dotplots on genome scale. *Bioinformatics* 23, 1026–1028. doi: 10.1093/bioinformatics/btm039

Latifi, A., Foglino, M., Tanaka, K., Williams, P., and Lazdunski, A. (1996). A hierarchical quorum-sensing cascade in *Pseudomonas aeruginosa* links the transcriptional activators LasR and RhIR (VsmR) to expression of the stationary-phase sigma factor RpoS. *Mol. Microbiol.* 21, 1137–1146. doi: 10.1046/j.1365-2958.1996.00063.x

Lewenza, S., Conway, B., Greenberg, E., and Sokol, P. A. (1999). Quorum sensing in *Burkholderia cepacia*: identification of the LuxRI homologs CepRI. *J. Bacteriol.* 181, 748–756.

Lewenza, S., and Sokol, P. A. (2001). Regulation of ornibactin biosynthesis and N-acyl-l-homoserine lactone production by CepR in *Burkholderia cepacia*. *J. Bacteriol.* 183, 2212–2218. doi: 10.1128/JB.183.7.2212-2218.2001

Lim, Y.-L., Ee, R., How, K.-Y., Lee, S.-K., Yong, D., Tee, K. K., et al. (2015a). Complete genome sequencing of *Pandoraea pnomenusa* RB38 and molecular characterization of its N-acyl homoserine lactone synthase gene ppnI. *PeerJ* 3:e1225. doi: 10.7717/peerj.1225

Lim, Y.-L., Ee, R., Yong, D., Tee, K.-K., Yin, W.-F., and Chan, K.-G. (2015b). Complete genome of *Pandoraea pnomenusa* RB-38, an oxalotrophic bacterium isolated from municipal solid waste landfill site. *J. Biotechnol.* 214, 83–84. doi: 10.1016/j.jbiotec.2015.09.018

LiPuma, J. J. (2010). The changing microbial epidemiology in cystic fibrosis. *Clin. Microbiol. Rev.* 23, 299–323. doi: 10.1128/CMR.00068-09

Malott, R. J., Baldwin, A., Mahenthiralingam, E., and Sokol, P. A. (2005). Characterization of the cciIR quorum-sensing system in *Burkholderia cenocepacia*. *Infect. Immun.* 73, 4982–4992. doi: 10.1128/IAI.73.8.4982-4992.2005

Markowitz, V. M., Mavromatis, K., Ivanova, N. N., Chen, I.-M. A., Chu, K., and Kyrpides, N. C. (2009). IMG ER: a system for microbial genome annotation expert review and curation. *Bioinformatics* 25, 2271–2278. doi: 10.1093/bioinformatics/btp393

McClean, K. H., Winson, M. K., Fish, L., Taylor, A., Chhabra, S. R., Camara, M., et al. (1997). Quorum sensing and *Chromobacterium violaceum*: exploitation of violacein production and inhibition for the detection of N-acylhomoserine lactones. *Microbiologica* 143, 3703–3711. doi: 10.1099/00221287-143-12-3703

Muhire, B. M., Varsani, A., and Martin, D. P. (2014). SDT: a virus classification tool based on pairwise sequence alignment and identity calculation. *PLoS One* 9:e108277. doi: 10.1371/journal.pone.0108277

Pier, G. B., Grout, M., Zaidi, T. S., Olsen, J. C., Johnson, L. G., Yankaskas, J. R., et al. (1996). Role of mutant CFTR in hypersusceptibility of cystic fibrosis patients to lung infections. *Science* 271, 64–67. doi: 10.1126/science.271.5245.64

Richter, M., and Rosselló-Móra, R. (2009). Shifting the genomic gold standard for the prokaryotic species definition. *Proc. Natl. Acad. Sci. USA* 106, 19126–19131. doi: 10.1073/pnas.0906412106

Sahin, N., Tani, A., Kotan, R., Sedláček, I., Kimbara, K., and Tamer, A. U. (2011). *Pandoraea oxalativorans* sp. nov., *Pandoraea faecigallinarum* sp. nov. and *Pandoraea vervacti* sp. nov., isolated from oxalate-enriched culture. *Int. J. Syst. Evol. Microbiol.* 61, 2247–2253. doi: 10.1099/ijs.0.026138-0

Saitou, N., and Nei, M. (1987). The neighbor-joining method: a new method for reconstructing phylogenetic trees. *Mol. Biol. Evol.* 4, 406–425. doi: 10.1093/oxfordjournals.molbev.a040454

Sandoz, K. M., Mitzimberg, S. M., and Schuster, M. (2007). Social cheating in *Pseudomonas aeruginosa* quorum sensing. *Proc. Natl. Acad. Sci. USA* 104, 15876–15881. doi: 10.1073/pnas.0705653104

Seemann, T. (2014). Prokka: rapid prokaryotic genome annotation. *Bioinformatics* 30, 2068–2069. doi: 10.1093/bioinformatics/btu153

See-Too, W. S., Convey, P., Pearce, D. A., and Chan, K.-G. (2018). Characterization of a novel N-acylhomoserine lactonase, AidP, from Antarctic *Planococcus* sp. *Microb. Cell Factories* 17:179. doi: 10.1186/s12934-018-1024-6

Subramoni, S., Florez Salcedo, D. V., and Suarez-Moreno, Z. R. (2015). A bioinformatic survey of distribution, conservation, and probable functions of LuxR solo regulators in bacteria. *Front. Cell. Infect. Microbiol.* 5:16. doi: 10.3389/fcimb.2015.00016

Subramoni, S., and Venturi, V. (2009). LuxR-family 'solos': bachelor sensors/regulators of signalling molecules. *Microbiologica* 155, 1377–1385. doi: 10.1099/mic.0.026849-0

Sullivan, M. J., Zakour, N. L. B., Forde, B. M., Stanton-Cook, M., and Beatson, S. A. (2015). Contiguity: contig adjacency graph construction and visualisation. *PeerJ Prepr.* 3:e1273.

Tamura, K., Stecher, G., Peterson, D., Filipski, A., and Kumar, S. (2013). MEGA6: molecular evolutionary genetics analysis version 6.0. *Mol. Biol. Evol.* 30, 2725–2729. doi: 10.1093/molbev/mst197

Tang, K., and Zhang, X.-H. (2014). Quorum quenching agents: resources for antivirulence therapy. *Mar. Drugs* 12, 3245–3282. doi: 10.3390/md12063245

Trapnell, B. C., Chu, C.-S., Paakko, P. K., Banks, T. C., Yoshimura, K., Ferrans, V. J., et al. (1991). Expression of the cystic fibrosis transmembrane conductance regulator gene in the respiratory tract of normal individuals and individuals with cystic fibrosis. *Proc. Natl. Acad. Sci USA* 88, 6565–6569.

Williams, P. (2007). Quorum sensing, communication and cross-kingdom signalling in the bacterial world. *Microbiologica* 153, 3923–3938. doi: 10.1099/mic.0.2007/012856-0

Zhang, L., Jia, Y., Wang, L., and Fang, R. (2007). A proline iminopeptidase gene upregulated in planta by a LuxR homologue is essential for pathogenicity of *Xanthomonas campestris* pv. *campestris*. *Mol. Microbiol.* 65, 121–136. doi: 10.1111/j.1365-2958.2007.05775.x

Conflict of Interest Statement: The authors declare that the research was conducted in the absence of any commercial or financial relationships that could be construed as a potential conflict of interest.

frontiers in Microbiology

ORIGINAL RESEARCH
published: 03 September 2019
doi: 10.3389/fmicb.2019.02049

Quorum Quenching Lactonase Strengthens Bacteriophage and Antibiotic Arsenal Against *Pseudomonas aeruginosa* Clinical Isolates

Sonia Mion[1], Benjamin Rémy[1,2], Laure Plener[2], Fabienne Brégeon[1,3], Eric Chabrière[1] and David Daudé[2]**

[1] Aix-Marseille University, IRD, APHM, MEPHI, IHU-Méditerranée Infection, Marseille, France, [2] Gene&GreenTK, Marseille, France, [3] Service des Explorations Fonctionnelles Respiratoires Centre Hospitalo Universitaire Nord, Pôle Cardio-Vasculaire et Thoracique, Assistance Publique des Hôpitaux de Marseille, Marseille, France

OPEN ACCESS

Edited by:
Ana Maria Otero, University of Santiago de Compostela, Spain

Reviewed by:
Rodolfo García-Contreras, National Autonomous University of Mexico, Mexico
Jin Zhou, Graduate School at Shenzhen, Tsinghua University, China

***Correspondence:**
Eric Chabrière
eric.chabriere@univ-amu.fr
David Daudé
david.daude@gene-greentk.com

Specialty section:
This article was submitted to Antimicrobials, Resistance and Chemotherapy, a section of the journal Frontiers in Microbiology

Received: *23 May 2019*
Accepted: *20 August 2019*
Published: *03 September 2019*

Citation:
Mion S, Rémy B, Plener L, Brégeon F, Chabrière E and Daudé D (2019) Quorum Quenching Lactonase Strengthens Bacteriophage and Antibiotic Arsenal Against Pseudomonas aeruginosa Clinical Isolates. Front. Microbiol. 10:2049. doi: 10.3389/fmicb.2019.02049

Many bacteria use quorum sensing (QS), a bacterial communication system based on the diffusion and perception of small signaling molecules, to synchronize their behavior in a cell-density dependent manner. QS regulates the expression of many genes associated with virulence factor production and biofilm formation. This latter is known to be involved in antibiotic and phage resistance mechanisms. Therefore, disrupting QS, a strategy known as quorum quenching (QQ), appears to be an interesting way to reduce bacterial virulence and increase antibiotic and phage treatment efficiency. In this study, the ability of the QQ enzyme *Sso*Pox-W263I, a lactonase able to degrade acyl-homoserine lactones, was investigated for quenching both virulence and biofilm formation in clinical isolates of *Pseudomonas aeruginosa* from diabetic foot ulcers, as well as in the PA14 model strain. These strains were further evolved to resist to bacteriophage cocktails. Overall, 10 antibiotics or bacteriophage resistant strains were evaluated and *Sso*Pox-W263I was shown to decrease pyocyanin, protease and elastase production in all strains. Furthermore, a reduction of more than 70% of biofilm formation was achieved in six out of ten strains. This anti-virulence potential was confirmed *in vivo* using an amoeba infection model, showing enhanced susceptibility toward amoeba of nine out of ten *P. aeruginosa* isolates upon QQ. This amoeba model was further used to demonstrate the ability of *Sso*Pox-W263I to enhance the susceptibility of sensitive and phage resistant bacteria to bacteriophage and antibiotic.

Keywords: quorum quenching, quorum sensing, lactonase, AHL, *Pseudomonas aeruginosa*, multidrug resistant bacteria, antibiotics, bacteriophages

INTRODUCTION

Pseudomonas aeruginosa is an opportunistic human pathogen involved in numerous diseases from otitis to keratitis, wound and burn infections, pneumonia and urinary tract infections (Driscoll et al., 2007). *P. aeruginosa* isolates are among the most frequently found antibiotic-resistant pathogens involved in diabetic foot infections, their presence is usually associated with morbidity

(Ertugrul et al., 2012). Surveillance of *P. aeruginosa* infections has revealed trends of increasing resistance to antibiotic treatments (Breidenstein et al., 2011) and the priority to support research and development of effective drugs against antibiotic-resistant *P. aeruginosa* was recently defined as critical by the World Health Organization (WHO) (Tacconelli et al., 2018).

This last decade, bacteriophage (phage) therapy has regained interest as a new weapon to treat antibiotic-resistant infections (Rolain et al., 2015; Domingo-Calap et al., 2016) and is under consideration to treat *P. aeruginosa* infections. Phages are the most abundant predator of bacteria in nature (Suttle, 2005) and have been domesticated, especially in Eastern Europe, to treat enteric infections, such as cystic fibrosis (Rolain et al., 2015), dysentery (Salmond and Fineran, 2015), diabetic foot infection, chronic osteomyelitis and other surgical and wound infections (Kutter et al., 2010). Phages offer the advantage of specifically targeting their host bacteria by being harmless to the commensal flora (Loc-Carrillo and Abedon, 2011) and human cells (Domingo-Calap et al., 2016). In western countries, clinical trials have been conducted to assay the therapeutic potential of phages (Rhoads et al., 2009; Wright et al., 2009; Kakasis and Panitsa, 2018), for example to treat *P. aeruginosa* infected burns (Jault et al., 2018). However, as for antibiotics, phages suffer resistance phenomena that may hinder the development of bacteriophage-based therapy (Jault et al., 2018). Finding new therapeutic strategies to limit bacterial resistance is thus of great interest.

In this way, another alternative to treat *P. aeruginosa* infections aims to highjack its communication system referred to as quorum sensing (QS). In *P. aeruginosa*, QS mainly relies on the secretion and perception of *N*-acyl homoserine lactones (AHL) to orchestrate its behavior, including virulence and biofilm formation as well as the CRISPR-Cas defense system, in a cell-density dependent manner (Bassler and Losick, 2006; Høyland-Kroghsbo et al., 2017). Interconnections between bacterial QS and susceptibility to bacteriophage infections were also identified (Qin et al., 2017; Saucedo-Mora et al., 2017). Disrupting QS, a strategy referred to as quorum quenching (QQ), is highly attractive to counteract bacterial virulence by using QS inhibitors (QSI) or QQ enzymes (QQE). Among QQE, special attention has been paid to the robust lactonase *Sso*Pox-W263I (Hiblot et al., 2013) that was proved to efficiently inhibit virulence *in vitro* in model and clinical strains of *P. aeruginosa* (Guendouze et al., 2017) and to drastically decrease mortality in a rat pulmonary infection model (Hraiech et al., 2014). Furthermore, the impact of *Sso*Pox-W263I on CRISPR-Cas gene expression of *P. aeruginosa* was recently demonstrated in both model and clinical strains suggesting that enzymatic QQ may modulate bacterial susceptibility to bacteriophages (Mion et al., 2019).

Here, we consider the use of *Sso*Pox-W263I in clinical isolates of *P. aeruginosa* from diabetic foot ulcers together with the model strain PA14 and further evolved these strains to resist bacteriophages. Knowing that the evolutionary selection of phage resistance in bacteria can induce phenotypic shifts (Labrie et al., 2010), we focused our interest on determining the potential of QQ to control antibiotic and phage-resistant bacteria. Our results show that *Sso*Pox-W263I is efficient to decrease virulence or biofilm in these multi-resistant strains, both *in vitro* and *in vivo* using an amoeba model. In the last part, we investigate the QQE treatment to enhance the therapeutic effect of antibiotic and phage when used as a co-treatment in the amoeba infection model. This study shows that QQ is an interesting strategy to treat bacterial infections that can be used to strengthen the effect of antimicrobial treatments.

MATERIALS AND METHODS

Bacterial Strains and Growth Conditions

Experiments were conducted using model strain PA14 and three clinical isolates of *P. aeruginosa*, isolated from diabetic patients of the Nimes University Hospital presenting diabetic foot infections. All the patients received an oral information, were anonymized and gave a non-opposition statement to bacterial storage. This study was approved by the local ethics committee (South Mediterranean III) and was carried out in accordance with the Declaration of Helsinki as revised in 2008. Clinical isolates of *P. aeruginosa* and model strain PA14 (UCBPP-PA14) were inoculated from a single colony and pre-cultivated during 6 h at 37°C in Luria Bertani (LB) medium (10 g l^{-1} NaCl, 10 g l^{-1} Tryptone, 5 g l^{-1} yeast extract) with agitation at 650 rpm. Then, precultures were diluted by a 1,000 factor in MOPS minimal medium complemented with nitrogen (15 mM NH_4Cl), iron (5 μM Fe_2SO_4), phosphate (4 mM K_2HPO_4) and glutamate (25 mM) as carbon source (MOPS glutamate) (Welsh and Blackwell, 2016) and cultures were incubated at 37°C under agitation at 650 rpm. Enzymes were added, when indicated, at 0.5 mg ml^{-1}. For virulence factor and biofilm formation analysis cultures were incubated during 20 h.

Phage Production and Isolation

A bacteriophage cocktail (Intesti-bacteriophage, Microgen, Russia) was used for this study. Isolated phage ΦIntesti-PA14 corresponds to the isolation and concentration of plaque-forming unit (PFU) formed by the phage cocktail on *P. aeruginosa* PA14 according to the following protocol.

The double agar overlay plaque assay was used to determine the phage titer and isolate phages from phage cocktail (Kropinski et al., 2009). 500 μl of an overnight culture of bacteria was added to 4.5 ml of molten soft LB-agar (0.75%) and overlaid onto a hard LB-agar plate. Once dry, 10 μl drops of phage cocktail were spotted on the soft LB-agar layer. Plates were incubated overnight at 37°C. Lytic plaques were collected and suspended in 500 μl of $MgSO_4$ (10 mM). After chloroform treatment and 10 min of centrifugation at 4,500 *g*, the supernatant was filtered at 0.22 μm. The resulting phage suspension was again spotted on a double-layer plate, and the experiment was repeated until a 10^8 PFU ml^{-1} suspension was obtained. To estimate the phage titer, serial dilutions (from 10^0 to 10^{-10}) of phage suspension were performed in $MgSO_4$ (10 mM), then 10 μl of each dilution was spotted on the double-layer plate. The plate was incubated overnight at 37°C. The titer (PFU ml^{-1}) was determined by the calculation of lytic PFU for 1 ml of phage suspension.

Isolation of Phage Resistant *P. aeruginosa* Bacteria

Precultures were performed by inoculating one colony of the initial strains in LB medium during 6–8 h, then the precultures were diluted by a 10,000 factor in MOPS glutamate, 3 ml were transferred in each well of a 12-well plate. 10, 50, or 100 µl of bacteriophage containing cocktail (Intestibacteriophage, Ïicrogen, Russia) were added to each well. The plate was incubated at 37°C overnight under agitation at 650 rpm. The OD 600 nm was then measured using a plate reader (Synergy HT, BioTek). Cultures showing complete lysis were diluted in a solution of phosphate saline buffer (PBS) and 20% glycerol. The dilutions were then plated on LB agar. Plates were incubated at 37°C overnight.

After 16 h of incubation, the isolated colonies were picked, cultivated in LB medium and stocked in 20% glycerol at −150°C. The tolerance of the isolated bacteria to the phage cocktail was verified by exposing the strains to the same conditions as those used for their isolation and by verifying that the final OD 600 nm was indeed higher for the resistant strain than for the parental strain.

Protein Production and Purification

Two *Sso*Pox variants namely W263I and 5A8 were used as QQ and inactive enzymes, respectively. Productions were realized as previously described (Hiblot et al., 2012, 2013; Hraiech et al., 2014). Briefly, *Escherichia coli* BL21 (DE3)-pGro7/GroEL cells (TaKaRa), carrying plasmid pET22b-*Sso*Pox-W263I or pET22b-*Sso*Pox-5A8, were cultivated in ZYP-5052 medium complemented with 100 µg ml^{-1} ampicillin and 34 µg ml^{-1} chloramphenicol at 37°C until OD 600 nm reached 0.8–1. The expression of chaperone proteins was induced by adding L-arabinose at a final concentration of 0.2% (w/v). At the same time, the temperature was reduced to 23°C and 0.2 mM of $CoCl_2$ was added. After 20 h of incubation, the cells were harvested by centrifugation (4,400 *g*, 4°C, 20 min), the pellet was resuspended in lysis buffer [50 mM HEPES pH 8, 150 mM NaCl, 0.25 mg ml^{-1} lysozyme, 0.1 mM Phenylmethylsufonyl fluoride (PMSF) and 10 mg ml^{-1} DNaseI] and stored at −80°C during 16 h. Frozen cells were thawed at 37°C during 15 min and lysed by three steps of 30 s sonication (QSonica sonicator Q700, amplitude at 45). Cell debris were removed by centrifugation (21,000 *g*, 4°C, 15 min). Crude extract was incubated during 30 min at 80°C and then centrifuged to precipitate *E. coli* proteins (21,000 *g*, 4°C, 30 min). The enzyme was then concentrated by overnight incubation at 4°C in 75% ammonium sulfate. After resuspension in activity buffer (50 mM HEPES pH 8, 150 mM NaCl, 20.2 mM $CoCl_2$) ammonium sulfate was eliminated by desalting (HiPrep 26/10 desalting, GE Healthcare, ÄKTA Avant). The protein sample obtained was concentrated to 2 ml and then loaded on a size-exclusion chromatography column and purified to homogeneity (HiLoad 16/600 Superdex^{TM} 75pg, GE Healthcare, ÄKTA Avant). Protein purity was checked by migration on 10% SDS-PAGE and protein concentration was measured using a spectrophotometer NanoDrop 2000 (Thermo Scientific).

Antibiograms

Antibiotic sensitivity of the strains was determined on a Mueller Hinton agar (BioMerieux). The disk diffusion method was realized using the following antibiotics: amikacin (30 µg), cefepime (30 µg), ceftazidime (30 µg), ciprofloxacin (5 µg), doxycycline (30 µg), fosfomycin (50 µg), imipenem (10 µg), nitrofurantoin (300 µg), piperacillin/tazobactam (85 µg), ticarcillin (75 µg), ticarcillin/clavulanate (85 µg), trimethoprim/sulfamethoxazole (25 µg), tobramycin (10 µg), rifampicin (30 µg). The results were interpreted according to the EUCAST guidelines (European Society of Clinical Microbiology and Infectious Diseases, 2018[1]) using the Scan® 1200 (Interscience) (Diop et al., 2016).

Analysis of Virulence Factor Production

Virulence factor productions for the different strains were determined *in vitro* after a 20-h culture in presence of 0.5 mg ml^{-1} *Sso*Pox-W263I or inactive mutant *Sso*Pox-5A8 as control.

Pyocyanin Production

Cell-free culture supernatants were prepared by centrifugation for 5 min at 12,000 *g*. Pyocyanin was extracted by mixing 500 µl of cell-free supernatant with 250 µl of chloroform (Price-Whelan et al., 2007). After vortexing and 5 min of centrifugation at 12,000 *g*, 200 µl of the bottom chloroform phase were transferred into a quartz 96-well plate. The absorbance was measured at 690 nm using a plate reader (Synergy HT, BioTek).

Proteolytic Activity

The protease activity was measured using azocasein (Sigma) (Chessa et al., 2000). 675 µl of PBS solution pH 7 were mixed with 50 µl of azocasein (30 mg ml^{-1} in water) and 25 µl of cell-free supernatant. After 2 h of incubation at 37°C, 125 µl of 20% (w/v) trichloroacetic acid were added to stop the reaction. The solution was then centrifugated for 10 min at 10,000 *g* and the absorbance of 200 µl of the supernatant was measured at 366 nm using a plate reader (Synergy HT, BioTek).

Elastolytic Activity

Elastase B activity was measured using elastin-Congo red conjugate (Sigma) degradation assay (Smith et al., 2003). 50 µl of cell-free supernatant were added to 150 µl of elastin-Congo red solution (5 mg ml^{-1} in 10 mM Tris–HCl and 1 mM $CaCl_2$ buffer at pH 7.2) into a 96-well plate. The plate was then sealed with an aluminum membrane and incubated during 24 h at 37°C under agitation (300 rpm). After sedimentation of undigested elastin-Congo red conjugate 100 µl of the upper phase was transferred to an empty well and the absorbance was measured at 490 nm using a plate reader (Synergy HT, BioTek).

Biofilm Formation

The biofilm formed in each well was quantified using crystal violet (Sigma) staining as previously described (Stepanović et al., 2000). Briefly, planktonic cells (non-attached) were first removed

[1]http://www.eucast.org/clinical_breakpoints/

by washing the wells with 4 ml of PBS. The plates were then dried at 37°C and the biofilm was stained by adding 4 ml of crystal violet 0.05%, incubated for 3 min under agitation at 150 rpm. Then, the crystal violet was removed and each well was rinsed with 4 ml of PBS. Crystal violet was then resolubilized by adding 3 ml of ethanol 96%. 200 µl of the solution was transferred to a 96-well plate and the final concentration of crystal violet was measured at OD 595 nm using a plate reader (Synergy HT, BioTek).

Virulence Assay Toward Amoeba

In vivo virulence assay was adapted from a previously described procedure using *P. aeruginosa* and *Acanthamoeba polyphaga Linc AP1* (Fenner et al., 2006). Briefly, 3 ml of bacterial culture were pelleted down and resuspended in Page's amoeba saline (PAS) buffer (2 mM NaCl, 16 µM $MgSO_4$, 27 µM $CaCl_2$, 0.53 mM Na_2HPO_4, 1 mM KH_2PO_4, pH 6.9) after a culture in 6-well plates (Nunc^{TM}, Thermo Scientific). *A. polyphaga Linc AP1* was cultivated during 2–3 days into peptone yeast extract glucose (20 g l^{-1} proteose peptone, 2 g l^{-1} yeast extract, 0.1 M glucose, 4 mM $MgSO_4$, 0.53 mM $CaCl_2$, 3.4 mM sodium citrate, 50 µM $(NH_4)_2Fe(SO_4)_2$, 2.5 mM KH_2PO_4, 1.3 mM Na_2HPO_4, pH 6.8) medium at 28°C (Fenner et al., 2006). Amoeba cells were recovered after centrifugation at 750 *g* and resuspended into PAS buffer to 10^5 cells μl^{-1}. Then, 1 ml of bacterial suspension was spread on a PAS agar plate and was left to dry at room temperature. At the center of each plate, 5 µl of *A. polyphaga* were spotted and dried at room temperature. Then, plates were incubated at 30°C over 7 days and amoeba propagation was followed by directly measuring the central spot with a ruler.

To test the combinatory effect of enzymatic and antibiotic treatments, the MOPS bacterial culture was treated with 10 µg ml^{-1} of enzyme (either *Sso*Pox-W263I or inactive variant *Sso*Pox-5A8 as control) and 25 µg ml^{-1} ciprofloxacin was added to PAS buffer during the resuspension step.

To test the combinatory effect of enzymatic and phage treatments, the MOPS bacterial culture was treated with 10 µg ml^{-1} of enzyme (either *Sso*Pox-W263I or inactive variant *Sso*Pox-5A8 as control) and 10^7 PFU ml^{-1} of ΦIntesti-PA14 phage was added to PAS buffer during the resuspension step.

RESULTS

Evaluating Sensitivity of Clinical Isolates to Antibiotics and Bacteriophage Cocktail

PA14 is a model strain originally isolated from a burn wound (Soyza et al., 2013) and B10, C5, and C11 were isolated from diabetic foot ulcerations (Guendouze et al., 2017). Antibiotic susceptibility of the strains was evaluated using the disk diffusion method with 14 antibiotics and analyzed according the EUCAST recommendations (**Figure 1A**). The strains were non-susceptible (resistant or intermediate) to at least two different antibiotics tested belonging to rifamycin, sulfonamide or nitrofuran classes. All strains were found sensitive to the tested agents in β-lactam, aminoglycosides and fosfomycin antimicrobial classes which are commonly used to fight pseudomonal infections. In addition to antibiotic sensitivity, the impact of a commercial bacteriophage cocktail on the strains was evaluated. Interestingly, all the strains were sensitive to the cocktail resulting in drastic decreases in cell density (**Supplementary Figure 1**). These results confirm that bacteriophage-based therapy may constitute an alternative to antibiotherapies in case of resistant infections.

Isolation and Characterization of Phage-Resistant Variants

Although bacteriophages were virulent to all four strains, resistance phenomena were rapidly observed after exposure of PA14, B10, C5, and C11 to three different concentrations of phage cocktail for 16 h. For PA14, B10, and C11 one mutant was isolated from each strain: PA14R1, B10R1, and C11R1, respectively. Three different mutants, presenting different phenotypes, were isolated from C5: C5R1, C5R2, and C5R3. The newly isolated mutants were cultured in the presence of the same amount of phage cocktail as that used for their isolation to confirm their resistance (i.e., 100 µl for PA14 and PA14R1, 50 µl for B10 and B10R1 and 10 µl for C5, C5R1, C5R2, C5R3, C11, and C11R1). Cell density was compared to the initial strains in the presence of phages after a 16-h culture by measuring the OD 600 nm (**Figure 2**). In the presence of phages, growth was 4 to 7 times higher for all mutants than for parental strains (**Figure 2**). The resistance of the isolated mutants against the phage cocktail was thereby clearly highlighted (**Figure 2**). Antibiotic sensitivity patterns of the phage-resistant strains were further evaluated (**Figure 1B**). As for parental isolates, phage resistant strains were non-susceptible (resistant or intermediate) to at least two different antibiotics tested belonging to rifamycin, sulfonamide or nitrofuran classes. Phage-resistant strains were found to be sensitive to the tested agents in β-lactam, aminoglycosides, cephalosporins, carbapenems and fosfomycin antimicrobial classes. As noticed for B10, B10R1 showed intermediate resistance to rifampicin while all other strains were resistant to this antibiotic. Interestingly, the acquisition of bacteriophage resistance was detrimental to antibiotic resistance in the resistant clones isolated from C5. C5R1, C5R2, and C5R3 lost their resistance against doxycycline and ciprofloxacin, C5R1 being also sensitive to nitrofurantoin conversely to C5, C5R2, or C5R3. Similarly, C11R1 exhibited a lower tolerance to trimethoprim/sulfamethoxazole and doxycycline than C11.

Quenching Virulence Factors of Antibiotic or Phage Resistant Clones *in vitro*

The QQ effect of *Sso*Pox-W263I on *P. aeruginosa* isolates PA14, C5, C11, B10 and their bacteriophage resistant counterparts was investigated by measuring the production of three typical virulence factors *in vitro*: pyocyanin, protease, elastase as well as biofilm production. Under the tested conditions, the addition of *Sso*Pox-W263I significantly reduced the three virulence factors for all strains compared to controls (**Figures 3A–C**). All tested strains produced detectable levels of pyocyanin and elastolytic

A

Antibiotics	Clinical isolates PA14	B10	C5	C11
TIC (75 µg)	25.8	24.2	21.5	19.6
TCC (85 µg)	24.4	23.6	19.4	24
TZP (85 µg)	29.5	28.6	25.6	26
CAZ (30 µg)	28.6	26.9	25.5	24.6
FEP (30 µg)	30.4	28.4	26.6	25.6
IPM (10 µg)	32.7	26.1	31.7	26.5
RA (30 µg)	0	16.8	11.4	9.9
FF (50 µg)	25.3	19	21.1	18.6
SXT (25 µg)	12	10	13.5	0
F (300 µg)	0	11.2	7.6	0
TM (10 µg)	26.1	21.7	23.4	20.3
AN (30 µg)	28.7	21.8	23.7	20.3
DO (30 µg)	19.4	14.1	10.3	11.4
CIP (5 µg)	36.8	33.2	19.1	33.2

B

Antibiotics	Phage resistant isolates PA14R1	B10R1	C5R1	C5R2	C5R3	C11R1
TIC (75 µg)	25.2	24.2	23.2	24.1	25.6	24.5
TCC (85 µg)	22.8	23.9	25	25.3	26.2	25.3
TZP (85 µg)	31.1	26.5	31.6	30.8	34.4	29.2
CAZ (30 µg)	31.4	25.8	31.1	30.4	30.3	29.9
FEP (30 µg)	32.2	27	33.8	32.6	32.2	30.6
IPM (10 µg)	33.1	25.7	28.1	32.9	33.9	32.2
RA (30 µg)	8.9	12.6	9.7	9.9	12.3	10
FF (50 µg)	25.1	18	24.7	24.2	25.5	26.5
SXT (25 µg)	10.2	12.7	10.5	7.6	11.8	12.3
F (300 µg)	9	11.2	16.9	9.5	9.8	7.2
TM (10 µg)	27.2	21.3	26.1	26.2	26	25.4
AN (30 µg)	29.7	20.6	30	29.7	30	29.2
DO (30 µg)	19.6	11.9	19.8	20.3	19.2	17.3
CIP (5 µg)	43.2	33.6	35.2	36.3	36.4	36.1

Susceptibility expressed as: Resistant, red; Intermediate, orange; Sensitive, green. TIC: Ticarcillin, TCC: Ticarcillin/Clavulanate, TZP: Piperacillin/Tazobactam, CAZ: Ceftazidime, FEP: Cefepime, IPM: Imipenem, RA: Rifampicin, FF: Fosfomycin, SXT: Trimethoprim/Sulfamethoxazole, F: Nitrofurantoin, TM: Tobramycin, AN: Amikacin, DO: Doxycycline, CIP: Ciprofloxacin

FIGURE 1 | Interpretative zone diameters (mm) of 14 antibiotics used on clinical isolates of *Pseudomonas aeruginosa* **(A)** and their associated phage-resistant mutants **(B)**. Susceptibility is expressed as Resistant (red), Intermediate (orange), Sensitive (green).

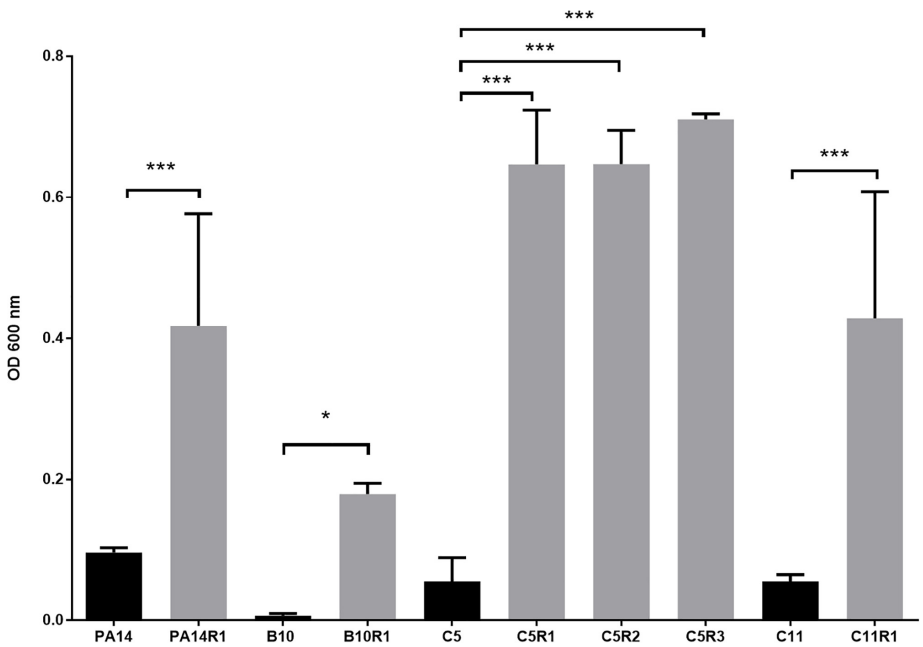

FIGURE 2 | Growth of phage resistant (gray) and the associated parental strains (black) in presence of phage cocktail. For each strain, bars represent the mean density (OD 600 nm) after 16 h of incubation in MOPS glutamate with phage cocktail. Error bars represent the standard deviations of three replicated experiments. *p-values < 0.05; ***p-values < 0.001 according to Student's t-test or ANOVA analysis.

activity. Pyocyanin levels were reduced by more than 75% in all strains upon enzymatic treatment, while elastase levels were reduced by at least 60% in nine out of ten strains with the addition of *Sso*Pox-W263I (C5 elastase level being reduced by only 25%). Proteolytic activity was detectable for all tested strains but one: the parental isolate C5 which did not produce sufficient levels of proteases with or without *Sso*Pox-W263I treatment to be detected. Conversely, the three phage-resistant derivatives obtained from C5 had each detectable protease activity in the absence of enzyme and this activity was completely extinguished by the addition of *Sso*Pox-W263I (**Figure 3A**). Biofilm production was significantly reduced by more than 70% in six strains when treated with *Sso*Pox-W263I (**Figure 3D**). Interestingly, the production of these four factors differed

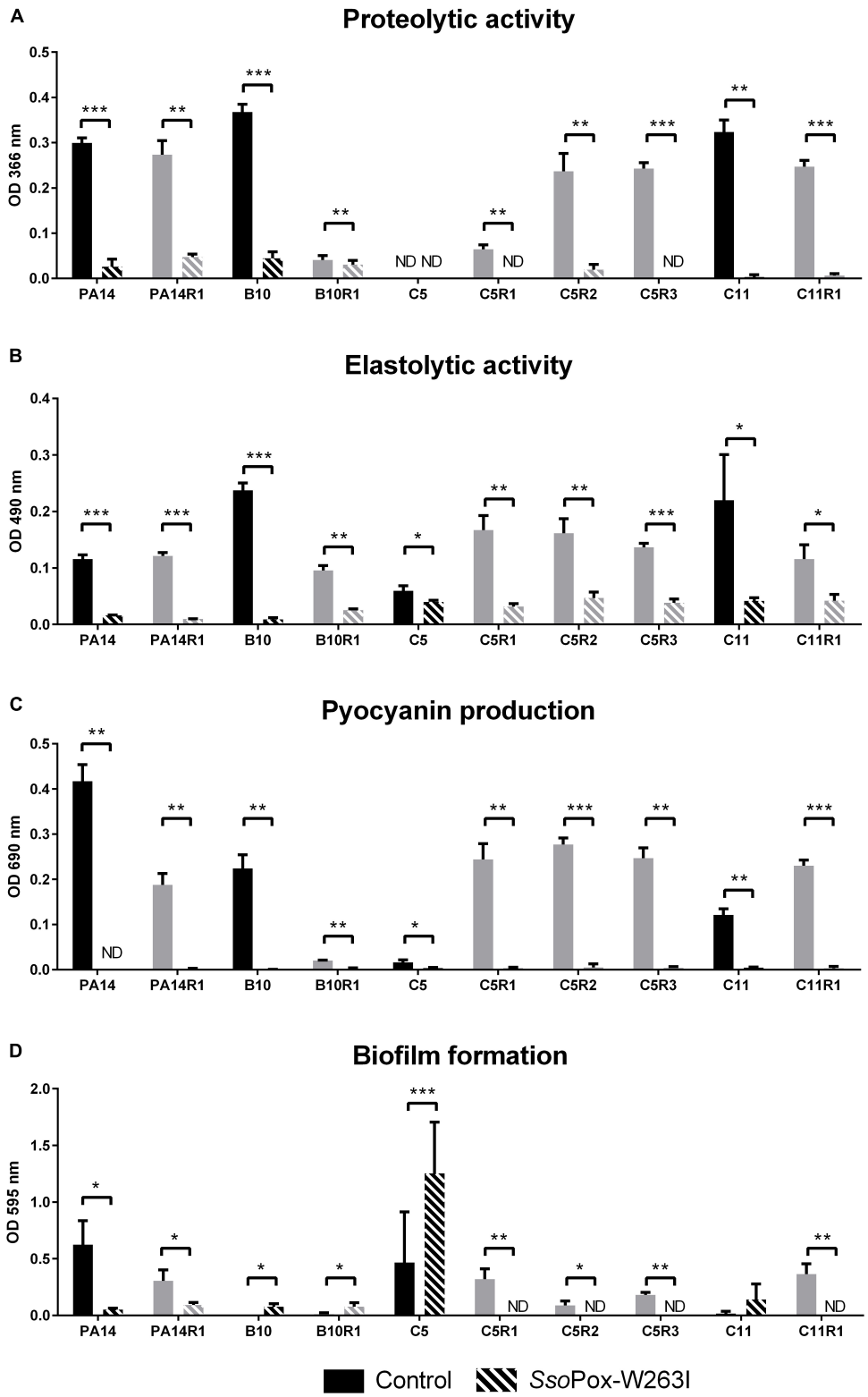

FIGURE 3 | Effect of *Sso*Pox-W263I on virulence factors of phage resistant mutants (gray) and the associated parental strains (black) *in vitro*. For each strain, bars represent the mean of protease **(A)**, elastase **(B)**, pyocyanin **(C)** and biofilm **(D)** levels of three experiments for treated culture with 0.5 mg ml^{-1} *Sso*Pox-W263I (striped bar) or inactive mutant 5A8 as negative control (empty bar). ND: not detected. Error bars represent the standard deviations of three experiments. **p*-values < 0.05; ***p*-values < 0.01; ****p*-values < 0.001 according to Student's *t*-test.

between the parental strains and their phage-resistant derivatives (**Figure 3**). It appears that the selection for phage-resistant clones did not result in the selection for mutants with only increased or only decreased biofilm formation. Similarly phage-resistant mutants did not all increase nor decrease virulence factor secretion as compared to their parental strains. Thereby no common trade-off due to the selection of phage resistant bacteria can be drawn at the level of these four phenotypic traits. Altogether, these results show the efficiency of *Sso*Pox-W263I in reducing the amount of three virulence factors characteristic of *P. aeruginosa* and modulating the production of biofilm *in vitro* in both antibiotic and phage-resistant isolates.

Evaluation of Quorum Quenching in Amoeba, Virulence Model

To further confirm the potential of *Sso*Pox-W263I to decrease the virulence of bacterial isolates, the *in vivo* protecting effect of the enzyme was assayed using the amoeba *A. polyphaga*. The virulence of treated and control bacteria toward amoeba was assayed by measuring the propagation of *A. polyphaga* on a plate flooded by a pretreated bacterial lawn (Fenner et al., 2006).

Overall, *Sso*Pox-W263I treatment decreased the virulence toward *A. polyphaga* of 9 out of 10 strains. No effect of QQ was observed for C11, for which virulence toward *A. polyphaga* remained unchanged with or without *Sso*Pox-W263I treatment, but its phage resisting mutant C11R1 recovered a high sensitivity to the amoeba upon treatment (**Figure 4**). C5, C5R1, and PA14R1 were initially not virulent enough to prevent the propagation of amoeba in the control condition; however, treatment by *Sso*Pox-W263I significantly enhanced its expansion (**Figure 4**). Consistently with *in vitro* observations on virulence factor production, the results obtained *in vivo* confirmed that parental and resistant strains behave differently, especially for PA14 and C5 (**Figure 4**). *Sso*Pox-W263I treatment showed a benefic effect in all but one case and no negative effects were observed, highlighting the efficiency of the QQ treatment in reducing the virulence of antibiotic and phage resistant isolates in an *in vivo* model.

Combined Effect of Enzymatic and Antimicrobial Treatment

Considering that PA14 displayed antibiogram comparable to most clinical isolates tested in this study, PA14 and its phage resistant mutant PA14R1 were further used as representative candidates to evaluate the combined effect of *Sso*Pox-W263I and antibiotic treatment using the amoeba infection model (**Figure 5**), then the combined effect of *Sso*Pox-W263I and phage treatment was also assayed (**Figure 6**). As observed in our first experiment, with an enzyme concentration of 500 $\mu g\ ml^{-1}$, QQ increases the sensitivity toward amoeba. Hence, to better assay the combined effect of enzymatic and antimicrobial treatments, lower doses of *Sso*Pox-W263I were considered. Thus, following a dose response experiment on PA14, 10 $\mu g\ ml^{-1}$ of *Sso*Pox-W263I was used with antimicrobial as it had a lower impact on the virulence (**Supplementary Figure 2**).

Synergistic effect was observed with a treatment of *Sso*Pox-W263I and 25 mg ml^{-1} ciprofloxacin on PA14, PA14R1 (**Figure 5**). At these concentrations, each treatment alone had no effect on the virulence of PA14 against the amoeba and the amoeba could not grow. However, with the combined treatment (ciprofloxacin + *Sso*Pox-W263I), the amoeba was able to completely colonize the Petri dish in 6 and 7 days, respectively, for PA14. PA14R1 virulence was slightly impacted by the antibiotic treatment alone or the QQE treatment alone, but the highest effect was observed with the combined treatment: the Petri dish limit (8.5 cm) was reached 1 day earlier than with the QQE treatment alone, and the growth of amoeba started after 1 day with the combined treatment against 4 days with ciprofloxacin alone.

As the composition of the commercial cocktail was toxic for amoeba, PA14 lytic phages were purified from the cocktail and concentrated to 10^8 PFU ml^{-1}. To test the combined effect of *Sso*Pox-W263I and phages, ΦIntesti-PA14 was used alone or in combination with the enzyme against PA14 and PA14R1. The isolated phages did not impact the growth of the amoeba. For both PA14 and PA14R1, amoeba growth was faster with *Sso*Pox-W263I alone, yet the combined treatment led to a further increase of amoeba growth (**Figure 6**).

DISCUSSION

In this study, four strains of *P. aeruginosa* were used, including three clinical isolates from diabetic foot infections. The antibiotic resistance profiles of the strains revealed that all the clinical isolates presented a significant tolerance to rifampicin, trimethoprim/sulfamethoxazole and nitrofurantoin, confirming previous observations regarding the increasing rate of multi-resistance in diabetic foot infections in the recent years (Lipsky, 2016).

To address antibioresistance issues, bacteriophages and QQ have emerged as promising therapeutic approaches. As with antibiotics, the use of bacteriophages suffers from rapid resistance phenomena such as the formation of a biofilm, the modification of phage receptor expression that can reduce phage entry (Chapman-McQuiston and Wu, 2008), or the cell adaptive inducible CRISPR-Cas (clustered regularly interspaced short palindromic repeat and CRISPR associated proteins) system that recognizes and degrades phage DNA (Barrangou et al., 2007). Interestingly, it has been extensively demonstrated that QQ reduces biofilm formation in *P. aeruginosa*, thereby increasing antimicrobial treatment efficacy, and a recent study has underlined that QS disruption can also decrease phage resistance by inhibiting QS stimulation of the CRISPR-Cas system (Høyland-Kroghsbo et al., 2017). The efficacy of *Sso*Pox-W263I to modulate CRISPR-Cas system regulation of proteobacteria, including *P. aeruginosa*, was recently demonstrated (Mion et al., 2019). In addition, recent studies have shown that even without involvement of CRISPR-Cas defense, the phage infection outcome could be different in QS-deficient mutant of *P. aeruginosa* than in wild type strains (Qin et al., 2017; Saucedo-Mora et al., 2017). As antibiotic or phage resistance can induce

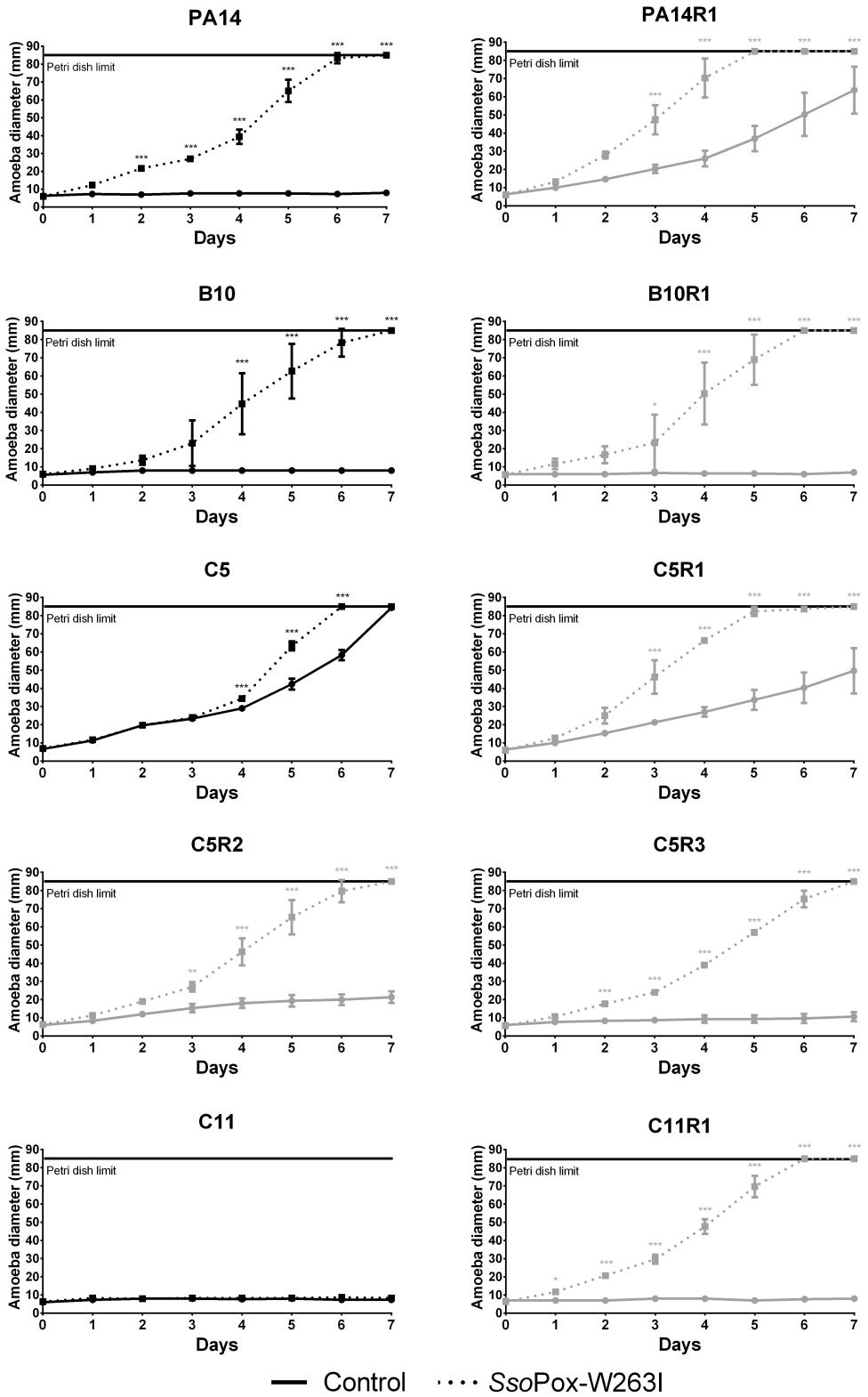

FIGURE 4 | Effect of *Sso*Pox-W263I on the virulence of clinical isolates (black) and phage resistant mutants (gray) against *A. polyphaga Linc AP1*. For each strain, curves represent the mean diameter of amoeba at different days of three experiments after incubation in presence of bacteria treated by 0.5 mg ml^{-1} of mutant *Sso*Pox-W263I (dotted line) or inactive mutant 5A8 (full line) as negative control. Error bars represent the standard deviations of three experiments. **p*-values < 0.05; ***p*-values < 0.01; ****p*-values < 0.001 according to ANOVA analysis.

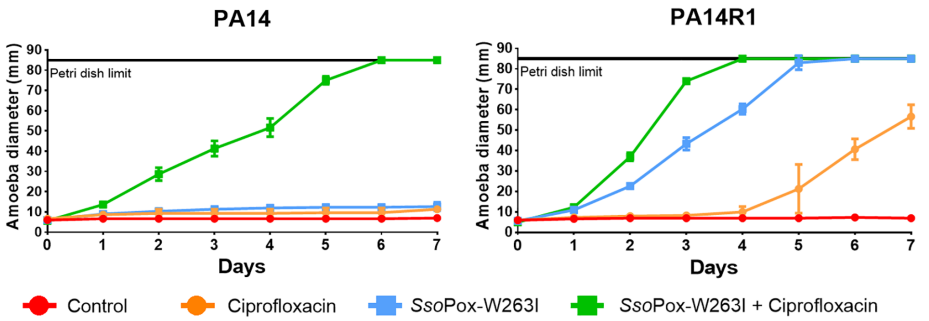

FIGURE 5 | Combinatory effect of *Sso*Pox-W263I and ciprofloxacin on the virulence of clinical isolates and phage resistant mutants against *A. polyphaga Linc AP1*. For each strain, curves represent the mean diameter of amoeba at different days after incubation in presence of bacteria without treatment (red) or treated with 25 mg ml^{-1} ciprofloxacin (orange), 10 μg ml^{-1} *Sso*Pox-W263I (blue), or 10 μg ml^{-1} *Sso*Pox-W263I and 25 mg ml^{-1} ciprofloxacin (green). Error bars represent the standard deviations of three experiments.

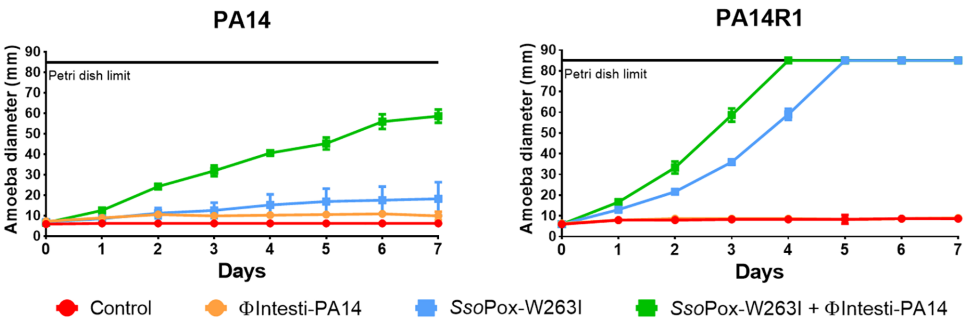

FIGURE 6 | Combinatory effect of *Sso*Pox-W263I and isolated phage on the virulence of PA14 and its phage resistant mutant against *A. polyphaga Linc AP1*. For each strain, curves represent the mean diameter of amoeba at different days after incubation in presence of bacteria without treatment (red) or treated with 10^7 PFU ml^{-1} ΦIntesti-PA14 (orange), 10 μg ml^{-1} *Sso*Pox-W263I (blue), or 10 μg ml^{-1} *Sso*Pox-W263I and 10^7 PFU ml^{-1} ΦIntesti-PA14 (green). Error bars represent the standard deviations of three experiments.

life-threatening complications, we evaluated the potential of QQ to act as an alternative therapeutic approach.

First, we selected six mutants derived from the four initial strains as phage resistant toward a commercial phage cocktail. The virulence profiles of each strain were then evaluated and the efficacy of three therapeutic approaches (antibiotics with ciprofloxacin, bacteriophages and QQ with *Sso*Pox-W263I) on the different strains was further assessed alone or in combinations.

In several cases bacteriophage resistance did not affect antibiotic resistance, although the selection pressure induced by the phage cocktail resulted in a loss of resistance to ciprofloxacin and doxycycline in the mutant strains isolated from C5. This evolutionary trade-off is coherent with a previous study, where the phage OMKO1 which targets OprM, the porin of a multi-drug efflux system of *P. aeruginosa* as receptor-binding site, selected resistant bacteria harboring a change in the efflux mechanism with increased sensitivity to different antibiotic classes, such as tetracycline and fluoroquinolone (Chan et al., 2016).

To determine the potential of QQ treatment on the different strains, four QS-regulated traits, biofilm formation and the production of three virulence factors (pyocyanin, protease and elastase) were measured *in vitro*. As reported in other studies, some phage resistant bacteria such as C5R1, C5R2, and C5R3 exhibited higher level of virulence factor production than the initial strain (Hosseinidoust et al., 2013). The ability of *Sso*Pox-W263I as QQ agent to decrease virulence in the different strains was also assayed. The QQ treatment significantly reduced the production of the virulence factors for the initial strains as well as their phage resistant mutants, showing that bacteria resistant to phage treatment conserved a functional QS system which can be inhibited by enzyme-mediated QQ. Strains harboring a higher virulence profile were also efficiently quenched using *Sso*Pox-W263I. In order to correlate *in vitro* production of virulence factors, biofilm formation and *in vivo* virulence, an amoeba-based assay was developed. Amoeba are eukaryotic organisms able to feed on bacteria. Their phagocytosis and digestion mechanisms are similar to those of macrophage bacterial elimination (Greub and Raoult, 2004), thus amoeba are frequently used to test *in vivo* virulence of bacteria (Rémy et al., 2018). The model of *A. polyphaga* feeding on *P. aeruginosa*, where the growth of the amoeba directly indicates the pathogenicity level of the bacteria, was chosen to assess the efficiency of QQ treatment with *Sso*Pox-W263I. The results showed that the inhibition of virulence by the QQ treatment was efficient for 9 out of 10 strains, allowing the

growth of the amoeba, independently from the resistance profiles to antibiotics or bacteriophages. Interestingly, *P. aeruginosa* was previously proved to use type III secretion system (T3SS) to kill biofilm-associated amoebae potentially suggesting that differences observed upon enzymatic treatment could be related in the modification of T3SS regulation (Matz et al., 2008). Although variable enzyme effects on virulence factor production or biofilm formation were observed *in vitro* depending on the strains, our results indicate that QQ is efficient *in vivo* on most of the antibiotic or phage resistant clinical isolates. This highlights the potential of enzymatic QQ treatment as an interesting alternative in case of therapeutic dead ends.

Furthermore, we evaluated the potential of *Sso*Pox-W263I to act as a complement of antibiotics or bacteriophages to counteract *P. aeruginosa* virulence toward *A. polyphaga*. Using lower concentrations of *Sso*Pox-W263I, the combination of QQ and ciprofloxacin enhanced the growth of the amoeba for ciprofloxacin-sensitive strains PA14 and PA14R1 as compared to the antibiotic or the enzymatic treatment alone. Consistently with previous reports using the lactonase from *Bacillus* sp. ZA12 with ciprofloxacin in a murine burn infection model (Gupta et al., 2015), our results show that enzymatic QQ works in synergy with fluoroquinolones in sensitive strains decreasing efficiently the amount of antibiotics required to fight bacterial infections.

In addition to antibiotics, the synergy of *Sso*Pox-W263I with bacteriophages was underlined. Synergistic effects were observed when *P. aeruginosa* PA14 was treated by the combined actions of isolated phage ΦIntesti-PA14 and *Sso*Pox-W263I. Interestingly, the synergy was also observed on PA14R1 strain, which was resistant to the phage cocktail. In concordance with these observations, recent reports showed close relationships between QS and phage tolerance mechanisms in *P. aeruginosa* (Mion et al., 2018).

Altogether, the results obtained *in vitro* and *in vivo* show that *Sso*Pox-W263I is efficient to decrease bacterial virulence in model and clinical isolates of *P. aeruginosa* and constitute a proof of concept suggesting that enzymatic QQ can strengthen the therapeutic arsenal available against *P. aeruginosa* infections by enhancing the efficiency of available treatments including bacteriophages or antibiotics. In addition, it has been shown that this enzyme, issued from an extremophilic organism, resists harsh industrial conditions (Rémy et al., 2016) confirming its tremendous potential for biopharmaceutical applications and should now be evaluated on mammalian models in order to reach clinical trials.

DATA AVAILABILITY

The datasets generated for this study are available on request to the corresponding author.

AUTHOR CONTRIBUTIONS

SM, BR, LP, FB, DD, and EC designed the study and wrote the manuscript. SM, BR, and LP performed the experiments. SM, BR, LP, and DD analyzed the data.

FUNDING

SM is a Ph.D. student granted by the Direction Générale de l'Armement (DGA). BR received a Ph.D grant from the "Emplois Jeunes Doctorants" program of Région Provence-Alpes-Côte d'Azur (PACA, France). This work was supported by Investissements d'avenir program (Méditerranée Infection 10-IAHU-03) of the French Agence Nationale de la Recherche (ANR). This work also received support from RAPID (LACTO-TEX) program from the Direction Générale de l'Armement (DGA).

ACKNOWLEDGMENTS

We thank Dr. M. Ansaldi and Dr. P. Masson for providing phages; Dr. G. Dubourg for the antibiogram experiment; Prof. B. La Scola for providing amoeba and Prof. J-P Lavigne for providing strains. We also thank Dr. Mikael Elias for fruitful discussions.

SUPPLEMENTARY MATERIAL

The Supplementary Material for this article can be found online at: https://www.frontiersin.org/articles/10.3389/fmicb.2019.02049/full#supplementary-material

REFERENCES

Barrangou, R., Fremaux, C., Deveau, H., Richards, M., Boyaval, P., Moineau, S., et al. (2007). CRISPR provides acquired resistance against viruses in prokaryotes. *Science* 315, 1709–1712. doi: 10.1126/science.1138140

Bassler, B. L., and Losick, R. (2006). Bacterially speaking. *Cell* 125, 237–246. doi: 10.1016/j.cell.2006.04.001

Breidenstein, E. B. M., de la Fuente-Núñez, C., and Hancock, R. E. W. (2011). *Pseudomonas aeruginosa*: all roads lead to resistance. *Trends Microbiol.* 19, 419–426. doi: 10.1016/j.tim.2011.04.005

Chan, B. K., Sistrom, M., Wertz, J. E., Kortright, K. E., Narayan, D., and Turner, P. E. (2016). Phage selection restores antibiotic sensitivity in MDR *Pseudomonas aeruginosa*. *Sci. Rep.* 6:26717. doi: 10.1038/srep26717

Chapman-McQuiston, E., and Wu, X. L. (2008). stochastic receptor expression allows sensitive bacteria to evade phage attack. part I: experiments. *Biophys. J.* 94, 4525–4536. doi: 10.1529/biophysj.107.120212

Chessa, J.-P., Petrescu, I., Bentahir, M., Van Beeumen, J., and Gerday, C. (2000). Purification, physico-chemical characterization and sequence of a heat labile alkaline metalloprotease isolated from a psychrophilic *Pseudomonas* species. *Biochim. Biophys.* 1479, 265–274. doi: 10.1016/S0167-4838(00)00018-2

Diop, A., Khelaifia, S., Armstrong, N., Labas, N., Fournier, P.-E., Raoult, D., et al. (2016). Microbial culturomics unravels the halophilic microbiota repertoire of table salt: description of *Gracilibacillus massiliensis* sp. nov. *Microb. Ecol. Health Dis.* 27:32049. doi: 10.3402/mehd.v27.32049

Domingo-Calap, P., Georgel, P., and Bahram, S. (2016). Back to the future: bacteriophages as promising therapeutic tools. *HLA* 87, 133–140. doi: 10.1111/tan.12742

Driscoll, J. A., Brody, S. L., and Kollef, M. H. (2007). The epidemiology, pathogenesis and treatment of *Pseudomonas aeruginosa* infections. *Drugs* 67, 351–368. doi: 10.2165/00003495-200767030-3

Ertugrul, B. M., Oncul, O., Tulek, N., Willke, A., Sacar, S., Tunccan, O. G., et al. (2012). A prospective, multi-center study: factors related to the management of diabetic foot infections. *Eur. J. Clin. Microbiol. Infect. Dis.* 31, 2345–2352. doi: 10.1007/s10096-012-1574-1

European Society of Clinical Microbiology and Infectious Diseases, (2018). Available at: http://www.eucast.org/clinical_breakpoints/ (accessed September 26, 2018).

Fenner, L., Richet, H., Raoult, D., Papazian, L., Martin, C., and La Scola, B. (2006). Are clinical isolates of *Pseudomonas aeruginosa* more virulent than hospital environmental isolates in amebal co-culture test? *Crit. Care Med.* 34, 823–828. doi: 10.1097/01.CCM.0000201878.51343.F1

Greub, G., and Raoult, D. (2004). Microorganisms resistant to free-living amoebae. *Clin. Microbiol. Rev.* 17, 413–433. doi: 10.1128/CMR.17.2.413-433.2004

Guendouze, A., Plener, L., Bzdrenga, J., Jacquet, P., Rémy, B., Elias, M., et al. (2017). Effect of quorum quenching lactonase in clinical isolates of *Pseudomonas aeruginosa* and comparison with quorum sensing inhibitors. *Front. Microbiol.* 8:277. doi: 10.3389/fmicb.2017.00227

Gupta, P., Chhibber, S., and Harjai, K. (2015). Efficacy of purified lactonase and ciprofloxacin in preventing systemic spread of *Pseudomonas aeruginosa* in murine burn wound model. *Burns* 41, 153–162. doi: 10.1016/j.burns.2014.06.009

Hiblot, J., Gotthard, G., Chabriere, E., and Elias, M. (2012). Characterisation of the organophosphate hydrolase catalytic activity of SsoPox. *Sci. Rep.* 2:779. doi: 10.1038/srep00779

Hiblot, J., Gotthard, G., Elias, M., and Chabriere, E. (2013). Differential active site loop conformations mediate promiscuous activities in the lactonase SsoPox. *PLoS One* 8:e75272. doi: 10.1371/journal.pone.0075272

Hosseinidoust, Z., van de Ven, T. G. M., and Tufenkji, N. (2013). Evolution of *Pseudomonas aeruginosa* virulence as a result of phage predation. *Appl. Environ. Microbiol.* 79, 6110–6116. doi: 10.1128/AEM.01421-3

Høyland-Kroghsbo, N. M., Paczkowski, J., Mukherjee, S., Broniewski, J., Westra, E., Bondy-Denomy, J., et al. (2017). Quorum sensing controls the *Pseudomonas aeruginosa* CRISPR-Cas adaptive immune system. *Proc. Natl. Acad. Sci. U.S.A.* 114, 131–135. doi: 10.1073/pnas.1617415113

Hraiech, S., Hiblot, J., Lafleur, J., Lepidi, H., Papazian, L., Rolain, J.-M., et al. (2014). Inhaled lactonase reduces *Pseudomonas aeruginosa* quorum sensing and mortality in rat pneumonia. *PLoS One* 9:e107125. doi: 10.1371/journal.pone.0107125

Jault, P., Leclerc, T., Jennes, S., Pirnay, J. P., Que, Y.-A., Resch, G., et al. (2018). Efficacy and tolerability of a cocktail of bacteriophages to treat burn wounds infected by *Pseudomonas aeruginosa* (PhagoBurn): a randomised, controlled, double-blind phase 1/2 trial. *Lancet Infect. Dis.* 19, 35–45. doi: 10.1016/S1473-3099(18)30482-1

Kakasis, A., and Panitsa, G. (2018). Bacteriophage therapy as an alternative treatment for human infections. A comprehensive review. *Int. J. Antimicrob. Agents* 53, 16–21. doi: 10.1016/j.ijantimicag.2018.09.004

Kropinski, A. M., Mazzocco, A., Waddell, T. E., Lingohr, E., and Johnson, R. P. (2009). Enumeration of bacteriophages by double agar overlay plaque assay. *Methods Mol. Biol.* 501, 69–76. doi: 10.1007/978-1-60327-164-6_7

Kutter, E., De Vos, D., Gvasalia, G., Alavidze, Z., Gogokhia, L., Kuhl, S., et al. (2010). Phage therapy in clinical practice: treatment of human infections. *Curr. Pharm. Biotechnol.* 11, 69–86. doi: 10.2174/138920110790725401

Labrie, S. J., Samson, J. E., and Moineau, S. (2010). Bacteriophage resistance mechanisms. *Nat. Rev. Microbiol.* 8, 317–327. doi: 10.1038/nrmicro2315

Lipsky, B. A. (2016). Diabetic foot infections: current treatment and delaying the 'post-antibiotic era.'. *Diabetes Metab. Res. Rev.* 32, 246–253. doi: 10.1002/dmrr.2739

Loc-Carrillo, C., and Abedon, S. T. (2011). Pros and cons of phage therapy. *Bacteriophage* 1, 111–114. doi: 10.4161/bact.1.2.14590

Matz, C., Moreno, A. M., Alhede, M., Manefield, M., Hauser, A. R., Givskov, M., et al. (2008). *Pseudomonas aeruginosa* uses type III secretion system to kill biofilm-associated amoebae. *ISME J.* 2, 843–852. doi: 10.1038/ismej.2008.47

Mion, S., Plener, L., Rémy, B., Daudé, D., and Chabrière, É. (2019). Lactonase SsoPox modulates CRISPR-Cas expression in gram-negative *proteobacteria* using AHL-based quorum sensing systems. *Res. Microbiol.* doi: 10.1016/j.resmic.2019.06.004 [Epub ahead of print].

Mion, S., Rémy, B., Plener, L., Chabrière, E., and Daudé, D. (2018). Empêcher les bactéries de communiquer: diviser pour mieux soigner. *Ann. Pharm. Fr.* 76, 249–264. doi: 10.1016/j.pharma.2018.02.004

Price-Whelan, A., Dietrich, L. E. P., and Newman, D. K. (2007). Pyocyanin alters redox homeostasis and carbon flux through central metabolic pathways in *Pseudomonas aeruginosa* PA14. *J. Bacteriol.* 189, 6372–6381. doi: 10.1128/JB.00505-7

Qin, X., Sun, Q., Yang, B., Pan, X., He, Y., and Yang, H. (2017). Quorum sensing influences phage infection efficiency via affecting cell population and physiological state. *J. Basic Microbiol.* 57, 162–170. doi: 10.1002/jobm.201600510

Rémy, B., Mion, S., Plener, L., Elias, M., Chabrière, E., and Daudé, D. (2018). Interference in bacterial quorum sensing: a biopharmaceutical perspective. *Front. Pharmacol.* 9:203. doi: 10.3389/fphar.2018.00203

Rémy, B., Plener, L., Poirier, L., Elias, M., Daudé, D., and Chabrière, E. (2016). Harnessing hyperthermostable lactonase from *Sulfolobus solfataricus* for biotechnological applications. *Sci. Rep.* 6:37780. doi: 10.1038/srep37780

Rhoads, D. D., Wolcott, R. D., Kuskowski, M. A., Wolcott, B. M., Ward, L. S., and Sulakvelidze, A. (2009). Bacteriophage therapy of venous leg ulcers in humans: results of a phase I safety trial. *J. Wound Care* 18, 237–243. doi: 10.12968/jowc.2009.18.6.42801

Rolain, J.-M., Hraiech, S., and Bregeon, F. (2015). Bacteriophage-based therapy in cystic fibrosis-associated *Pseudomonas aeruginosa* infections: rationale and current status. *Drug Des. Devel. Ther.* 9, 3653–3663. doi: 10.2147/DDDT.S53123

Salmond, G. P. C., and Fineran, P. C. (2015). A century of the phage: past, present and future. *Nat. Rev. Microbiol.* 13, 777–786. doi: 10.1038/nrmicro3564

Saucedo-Mora, M. A., Castañeda-Tamez, P., Cazares, A., Pérez-Velázquez, J., Hense, B. A., Cazares, D., et al. (2017). Selection of functional quorum sensing systems by lysogenic bacteriophages in *Pseudomonas aeruginosa*. *Front. Microbiol.* 8:1669. doi: 10.3389/fmicb.2017.01669

Smith, K. M., Bu, Y., and Suga, H. (2003). Induction and inhibition of *Pseudomonas aeruginosa* quorum sensing by synthetic autoinducer analogs. *Chem. Biol.* 10, 81–89. doi: 10.1016/S1074-5521(03)00002-4

Soyza, A. D., Hall, A. J., Mahenthiralingam, E., Drevinek, P., Kaca, W., Drulis-Kawa, Z., et al. (2013). Developing an international *Pseudomonas aeruginosa* reference panel. *MicrobiologyOpen* 2, 1010–1023. doi: 10.1002/mbo3.141

Stepanović, S., Vuković, D., Dakić, I., Savić, B., and Švabić-Vlahović, M. (2000). A modified microtiter-plate test for quantification of staphylococcal biofilm formation. *J. Microbiol. Methods* 40, 175–179. doi: 10.1016/S0167-7012(00)00122-6

Suttle, C. A. (2005). Viruses in the sea. *Nature* 437:356. doi: 10.1038/nature04160

Tacconelli, E., Carrara, E., Savoldi, A., Harbarth, S., Mendelson, M., Monnet, D. L., et al. (2018). Discovery, research, and development of new antibiotics: the WHO priority list of antibiotic-resistant bacteria and tuberculosis. *Lancet Infect. Dis.* 18, 318–327. doi: 10.1016/S1473-3099(17)30753-3

Welsh, M. A., and Blackwell, H. E. (2016). Chemical genetics reveals environment-specific roles for quorum sensing circuits in *Pseudomonas aeruginosa*. *Cell Chem. Biol.* 23, 361–369. doi: 10.1016/j.chembiol.2016.01.006

Wright, A., Hawkins, C. H., Änggård, E. E., and Harper, D. R. (2009). A controlled clinical trial of a therapeutic bacteriophage preparation in chronic otitis due to antibiotic-resistant *Pseudomonas aeruginosa*; a preliminary report of efficacy. *Clin. Otolaryngol.* 34, 349–357. doi: 10.1111/j.1749-4486.2009.01973.x

Conflict of Interest Statement: EC has a patent WO2014167140 A1 licensed to Gene&GreenTK. BR, LP, DD, and EC report personal fees from Gene&GreenTK during the conduct of the study.

The remaining authors declare that the research was conducted in the absence of any commercial or financial relationships that could be construed as a potential conflict of interest.

frontiers in Microbiology

ORIGINAL RESEARCH
published: 11 September 2019
doi: 10.3389/fmicb.2019.02131

Quorum Sensing Signaling Alters Virulence Potential and Population Dynamics in Complex Microbiome-Host Interactomes

*F. Jerry Reen[1,2], José A. Gutiérrez-Barranquero[1†], Ronan R. McCarthy[1†], David F. Woods[1], Sara Scarciglia[1], Claire Adams[1], Kristian Fog Nielsen[3], Lone Gram[3] and Fergal O'Gara[1,4,5]**

[1] BIOMERIT Research Centre, School of Microbiology, University College Cork, Cork, Ireland, [2] School of Microbiology, University College Cork, Cork, Ireland, [3] Department of Biotechnology and Biomedicine, Technical University of Denmark, Lyngby, Denmark, [4] Telethon Kids Institute, Perth Children's Hospital, Perth, WA, Australia, [5] School of Pharmacy and Biomedical Sciences, Curtin Health Innovation Research Institute, Curtin University, Perth, WA, Australia

Despite the discovery of the first *N*-acyl homoserine lactone (AHL) based quorum sensing (QS) in the marine environment, relatively little is known about the abundance, nature and diversity of AHL QS systems in this diverse ecosystem. Establishing the prevalence and diversity of AHL QS systems and how they may influence population dynamics within the marine ecosystem, may give a greater insight into the evolution of AHLs as signaling molecules in this important and largely unexplored niche. Microbiome profiling of *Stelletta normani* and BD1268 sponge samples identified several potential QS active genera. Subsequent biosensor-based screening of a library of 650 marine sponge bacterial isolates identified 10 isolates that could activate at least one of three AHL biosensor strains. Each was further validated and profiled by Ultra-High Performance Liquid Chromatography Mass Spectrometry, with AHLs being detected in 8 out of 10 isolate extracts. Co-culture of QS active isolates with *S. normani* marine sponge samples led to the isolation of genera such as *Pseudomonas* and *Paenibacillus*, both of which were low abundance in the *S. normani* microbiome. Surprisingly however, addition of AHLs to isolates harvested following co-culture did not measurably affect either growth or biofilm of these strains. Addition of supernatants from QS active strains did however impact significantly on biofilm formation of the marine *Bacillus* sp. CH8a sporeforming strain suggesting a role for QS systems in moderating the microbe-microbe interaction in marine sponges. Genome sequencing and phylogenetic analysis of a QS positive *Psychrobacter* isolate identified several QS associated systems, although no classical QS synthase gene was identified. The stark contrast between the biodiverse sponge microbiome and the relatively limited diversity that was observed on standard culture media, even in the presence of QS active compounds, serves to underscore the extent of diversity that remains to be brought into culture.

Keywords: quorum sensing (QS), microbiome, marine sponge-associated bacteria, cell–cell communication, acyl homoserine lactone (AHL)

OPEN ACCESS

Edited by:
Ana Maria Otero, University of Santiago de Compostela, Spain

Reviewed by:
Jürgen Tomasch, Helmholtz Center for Infection Research, Helmholtz Association of German Research Centers (HZ), Germany
Raphaël Lami, Sorbonne Universités, France

****Correspondence:***
Fergal O'Gara
f.ogara@ucc.ie

†Present address:
José A. Gutiérrez-Barranquero, Facultad de Ciencias, Departamento de Microbiología, Instituto de Hortofruticultura Subtropical y Mediterránea La Mayora (IHSM-UMA-CSIC), Universidad de Málaga, Málaga, Spain
Ronan R. McCarthy, Department of Life Sciences, Brunel University London, London, United Kingdom

Specialty section:
This article was submitted to Antimicrobials, Resistance and Chemotherapy, a section of the journal Frontiers in Microbiology

Received: *20 May 2019*
Accepted: *29 August 2019*
Published: *11 September 2019*

Citation:
Reen FJ, Gutiérrez-Barranquero JA, McCarthy RR, Woods DF, Scarciglia S, Adams C, Fog Nielsen K, Gram L and O'Gara F (2019) Quorum Sensing Signaling Alters Virulence Potential and Population Dynamics in Complex Microbiome-Host Interactomes. Front. Microbiol. 10:2131. doi: 10.3389/fmicb.2019.02131

INTRODUCTION

The marine ecosystem is considered to be an underexplored resource for the study of bacterial interactions within eukaryotic hosts. Despite a number of well-studied examples of bacterial interactions within marine hosts such as the density dependent production of luminescence by *Aliivibrio fischeri* within the light organ of *Euprymna scolopes*, relatively little is known about the interactions that occur within marine microbial communities (Hmelo, 2017). This is particularly true in the case of the ancient invertebrate, the marine sponge. Marine sponges are sessile filter feeders that consume bacteria and other marine matter (Taylor et al., 2007). Bacteria can inhabit the mesophyll matrix of these invertebrates with almost 60% of the biomass of a marine sponge being comprised of bacterial endosymbionts (Wang, 2006). This symbiotic relationship is mutually beneficial whereby bacteria are provided with a sheltered nutrient rich environment and the marine sponges acquire limiting nutrients from the microflora (Mohamed et al., 2008; Blunt et al., 2009; Mayer et al., 2010, 2011). Within the dense polymicrobial environment of a marine sponge, bacteria can engage in a form of chemical communication termed quorum sensing (QS) (Taylor et al., 2004a; Diggle et al., 2007; Hmelo, 2017). Several classes of QS signaling system are known, with autoinducer peptides favored by gram positive bacteria while *N*-acyl homoserine lactones (AHLs) predominate within gram negative bacteria (Whiteley et al., 2017). AHLs are capable of activating an autoinducing transcriptional regulator which controls the transcription of target genes involved in a wide variety of cellular processes including the production of virulence determinants (Diggle et al., 2007). There are relatively few studies on the prevalence of functional AHL based QS systems within microorganisms inhabiting marine sponges (Taylor et al., 2004b; Mohamed et al., 2008; Cuadrado-Silva et al., 2013; Britstein et al., 2018). A number of studies have focused on the identification of homologs of genes associated with QS pathways (Zan et al., 2011). However, sequence based approaches provide limited information on the functionality of these homologous systems, which for the most part remains to be determined. This homology-based approach is also limited by the lack of nucleotide sequence homology among AHL synthases and AHL responsive transcriptional regulators (Steindler and Venturi, 2007). More recently, screening of marine sponges for AHL signals has revealed a rich diversity likely encoded by the microbial communities residing in those sponges (Britstein et al., 2018). Given the difficulties faced in bringing marine sponge biodiversity into culture, it is intriguing to speculate that these signals may play a role in moderating the dynamics of the microbial communities within which they operate.

To gain more insight into the relevance of AHL based QS systems within the microbiota inhabiting marine sponges, bacterial sponge isolates were screened for the production of AHLs using classical AHL reporter strains. A total of 10 QS producing isolates were identified and characterized for AHL production. Co-culture of QS positive isolates with marine sponge samples resulted in increased culturable plate diversity from these communities, although no new genera were identified. While addition of AHLs alone did not influence growth or biofilm in the marine sponge isolates, supernatants from several QS positive isolates suppressed biofilm formation in the marine sponge *Bacillus* sp. CH8a sporeforming strain. This suggests that the anti-biofilm activity of the QS active supernatants may be mediated downstream of intact QS signaling systems in the producing isolates. Genome sequencing of a QS positive *Psychrobacter* sp. isolate identified in this study revealed the presence of LuxR DNA binding domains. However, there was no evidence of a LuxR autoinducer domain or an AHL synthase domain in this or any other sequenced *Psychrobacter* genome. Further establishing the prevalence, structure and diversity of AHL based QS systems will give a better understanding of the role of AHL signaling in the marine ecosystem, potentially unlocking some of the natural biodiversity encoded therein.

MATERIALS AND METHODS

Sponge Collection

Bacteria had previously been isolated from sponge genera including *Hexactinellida*, *Stelletta*, *Lissodendoryx*, *Poecillastra*, *Inflatella*. These sponges were collected using a remote operated vehicle on board the Celtic Explorer research vessel, 300 nautical miles off the west coast of Ireland as part of the marine biodiscovery cruise, May 2010. Sponge samples from the *Amphilectus* genus were collected in Gurraig Sound Kilkieran Bay, Galway (Kennedy et al., 2008). Whole sponge samples were rinsed with sterile artificial sea water (ASW, 3.33% (w/v) artificial sea salts, Instant Ocean) and immediately frozen at −80°C on board the ship until further processing. A sample of sponge tissue (1 g) was homogenized by grinding with a sterile porcelain pestle and mortar in 9 ml of sterile ASW. The sponge homogenate was subsequently serially diluted in ASW to 10^{-5} and 100 μl aliquots of the different dilutions were plated onto Marine agar (MA) (Difco, United Kingdom) and SYP-SW Agar (1% (w/v) starch, 0.4% (w/v) yeast extract, 0.2% (w/v) peptone and 3.33% (w/v) artificial sea salts, 1.5% (w/v) agar. Distinct morphologies were collected to form a library of approximately 650 isolates for subsequent screening and characterization.

Sponge Microbiome Profiling

As above, two independent samples of each sponge tissue (1 g) were homogenized by grinding with a sterile porcelain pestle and mortar in 10 ml of sterile PBS. DNA was extracted from 100 μl of these samples using the MoBio DNA extraction kit (MoBio) as per manufacturer's instructions. The extracted gDNA was used as a template to amplify the v3-v5 region of the 16S rRNA gene, these amplicons were sequenced to 2 × 300 bp on a Next Gen Illumina MiSeq (V3) platform. Prior to the microbiome analysis, raw reads were demultiplexed based on inline-barcode sequences. The reads were processed using Minimum Entropy Decomposition (Eren et al., 2015). To assign taxonomic information to each Operational Taxonomic Unit (OTU), BLAST alignments of representative sequences

to the NCBI database were performed. Further processing of OTUs was performed using the QIIME software package (version 1.8.0[1]). Microbiome data has been uploaded on the NCBI Sequence Read Archive (SRA) database (BioProject No. PRJNA555824).

Quorum Sensing Biosensor Assay

The following reporter strains were used to identify AHL production. Short chain AHLs were detected using the *Serratia marcescens* SP19 (Poulter et al., 2010). Upon production of short chain AHLs *S. marcescens* SP19 produces a red pigment, prodigiosin. *S. marcescens* SP19 is an AHL deficient mutant that only produces prodigiosin in response exogenous AHLs. Marine strains were cultured on Marine Broth (Difco, United Kingdom) supplemented with agar (1.5% w/v) for 72 h at 23°C. They were then overlaid with soft LB agar (0.1% agar) inoculated with *S. marcescens* SP19 at an $OD_{600\ nm}$ of 0.5. Overlaid plates were incubated at 30°C overnight. QS was identified by prodigiosin production. As a positive control, 20 μM C4-HSL (Sigma, United Kingdom) was used. C4-C8 chain AHLs were detected using *Chromobacterium violaceum* CV026. *C. violaceum* CV026 produces a purple compound called violacein in a QS dependent manner. *C. violaceum* CV026 contains a transposon in its indigenous AHL synthase gene thus it only produces violacein in response to exogenous AHLs (McClean et al., 1997). Marine strains were cultured on Marine Agar (Difco, United Kingdom) for 72 h at 30°C. They were then overlaid with soft LB agar (0.1% agar) inoculated with *C. violaceum* CV026 at an OD_{600nm} of 0.5. Overlaid plates were incubated at 30°C overnight. QS was identified by violacein production. 20 μM C8-HSL (Sigma, United Kingdom) was used as a positive control. The broad range *Agrobacterium tumefaciens* NTL4 biosensor was used for the detection of longer chain AHLs. It contains a plasmid pZLR4 carrying a *traG:lacZ* reporter fusion (Farrand et al., 1996; Yin et al., 2012). In response to exogenous AHLs the *lacZ* gene is transcribed resulting in the degradation of 5-bromo-4-chloro-3-indolyl-β-D-galactopyranoside in the media. The previously described plating protocol was observed except soft LB was supplemented with 50 μg/ml 5-bromo-4-chloro-3-indolyl-β-D-galactopyranoside. QS was identified by the breakdown of 5-bromo-4-chloro-3-indolyl-β-D-galactopyranoside resulting in a blue color. A concentration of 20 μM C10-HSL (Sigma, United Kingdom) was used as a positive control.

Strain Identification

Genomic DNA from bacterial isolates was extracted using the MoBio UltraClean DNA extraction kit (MoBio, United States) following manufacturers' guidelines. Strains were identified by PCR amplification of 16S rRNA genes which was carried out as described (Chan et al., 2010) using the universal primer pairs 27F (5′-AGAGTTTGATCMTGGCTCAG-3′) and 1525R (5′-AAGGAGGTGWTCCARCC-3′). PCR products were sequenced by MWG Eurofins, United Kingdom. Sequence identification was performed using BlastN and all sequences were submitted to the NCBI database (Accession numbers: MN209943-MN209952).

[1]http://qiime.org/

Extraction and TLC Analysis of Culture Supernatants

Extracts for thin layer chromatography (TLC) and ultra-high performance liquid chromatography-high resolution mass spectrometry (UHPLC-HRMS) were prepared from 200 ml cultures in Marine Broth (Difco, United Kingdom) that had been incubated for 72 h at 30°C and 180 rpm. Bacterial cells were pelleted by centrifugation at 4,000 rpm for 7 min and the supernatant was filter sterilized using a Nalgene® vacuum filtration system (0.2 μm, Sigma-Aldrich®, Germany). The supernatant was incubated with 1:1 volume of acidified ethyl acetate (1% formic acid) for 10 min at RT shaking at 180 rpm. The ethyl acetate phase was taken and dried using rotary evaporation. Residues were resuspended in 1 ml ethyl acetate and stored at −20°C. Ethyl acetate extracts were tested for QS activity by spotting 20 μL on C18 reverse phase TLC plates (20 cm × 20 cm TLC aluminum plates, Millipore, United Kingdom) with a methanol:water 7:3 (v/v) mobile phase. Once dried, TLC plates were overlaid with 25 ml of soft LB agar (0.1% agar) inoculated with the biosensor at an OD_{600nm} of 0.5. Following confirmation of extract activity, extracts were dried using nitrogen evaporation and analyzed by UHPLC-HRMS for identification.

UHPLC-HRMS Profiling of QS-Active Supernatant Extracts

Samples were resuspended in approx. 150 μl 50:50 (vol/vol) acetonitrile (ACN)-water 50:50 (vol/vol) and 2 μl subsamples analyzed by UHPLC-HRMS. This was done on an Agilent Infinity 1290 UHPLC system (Agilent Technologies, Santa Clara, CA, United States) coupled to an Agilent 6550 QTOF MS operated in positive electrospray (ESI) mode, scanning *m/z* 50-1700. A lock mass solution of 10 μM Hexakis(2,2,3,3-tetrafluoropropoxy)phosphazene (Apollo Scientific Ltd., Cheshire, United Kingdom) dissolved in 95% acetonitrile and infused in the secondary ESI sprayer using an extra LC pump at a flow of 20 μl/min, and the $[M + H]^+$ at m/z 922.0098 used as lock mass, resulting in a mass accuracy better than 3 ppm (deviation relative to theoretical m/z value).

An Agilent Poroshell 120 phenyl-hexyl column (2.1 × 150 mm, 2.7 μm), held at 60°C was used for separation. A linear gradient at 0.35 ml/min, consisting of water and ACN both buffered with 20 mM formic acid was started at 10% ACN and increased to 100% after 15 min, where it was held for 2 min. It was subsequently returned to 10% ACN in 0.1 min and maintained for 3 min (Kildgaard et al., 2014).

A reference standard mixture containing the following HSLs were included in the analytical sequence: C4, C6, C8, C10, C12, Oxo-C6, Oxo-C8, Oxo-C10, Oxo-C12, OH-C6, OH-C8, OH-C10, and OH-C12. Using the Agilent MassHunterQuant software, extracted ion chromatograms the $[M + H]^+$ and $[M + Na]^+$ ions ± 10 ppm were used for identification, along with the isotopic pattern (Kildgaard et al., 2014), and finally a retention time match ± 0.01 min.

Growth Analysis of Marine Isolates

Isolates with distinct morphologies that were cultured on QS-treated plates and identified by 16S rRNA sequencing were grown on marine agar for 72 h at 23°C. Cells were transferred into fresh marine broth, $OD_{600\ nm}$ 0.05, in the presence and absence of 50 nM–10 μM of 3-oxo-C12 HSL, with DMSO as carrier control. Growth was measured spectrophotometrically at $OD_{600\ nm}$ in honeycomb plates incubated at 23°C on a Bioscreen-C automated growth curves analysis system (Growth Curves USA).

Biofilm Assays

Bacillus sp. CH8a was grown in marine broth (MB) at 23°C overnight with shaking (Phelan et al., 2012). In order to monitor the impact on biofilm formation, 500 μl of cell-free supernatant (CFS) from the QS strain 3-day cultures was added to 500 μl of test cultures at $OD_{600\ nm}$ 0.1, grown in MB. As controls, 500 μl of fresh media was added to 500 μl of test cultures (media control) and 500 μl of the CFS of test cultures were added to 500 μl of corresponding test culture. In all cases, CFS was obtained by centrifugation at 8,000 rpm for 5 min followed by filtration through a 0.2 μm sterile filter. *Bacillus* sp. CH8a biofilms were incubated for 2 days at 23°C. Unattached cells were aspirated out of all wells which were washed once with 1 ml of sterile water. Attached cells were quantified using 0.1% (w/v) crystal violet. For marine isolate biofilm analysis, 3-oxo-C12-HSL was added at 10 μM to media and processed as described above.

Co-culture Sponge Enrichment Assays

A simple co-culture system was designed to expose marine sponge homogenate to signals and metabolites from actively growing QS active isolates. Costar Spin-X 0.22 μm cellulose acetate centrifuge tube filters (Corning) consisting of an upper chamber with a filter base and a lower receptacle chamber was used for this purpose. QS active isolates were grown in nutrient media in the top chamber, while marine sponge homogenate was incubated in the lower chamber. While the marine sponge homogenate was physically separate from the QS active isolate at all times, transfer of small molecular signals and metabolites between both chambers was possible. In order to establish the validity of the co-culture system for QS transfer between the upper and lower chambers, as well as the integrity of the filter system to prevent bacterial leakage, several test studies were performed. The upper chamber was removed, and 1 ml of LB broth was added to the lower chamber. The upper chamber was replaced and a known QS producing organism *P. aeruginosa* PA14 (500 μl) was added. The tubes were incubated at 37°C for 24 h after which time the top chamber was removed. Aliquots of the lower chamber were tested for (a) activation of AHL biosensor strains *C. violaceum* and *S. marcescens* and (b) contaminating bacterial growth.

Quorum sensing active isolates were grown in marine broth at 23°C for 72 h. *Stelletta normani* sponge sample (∼1 g) was homogenized in 10 ml of PBS. The upper chamber of the Costar Spin-X 0.22 μm cellulose acetate centrifuge tube filter (Corning) was removed, and 500 μl of sponge homogenate with 500 μl marine broth was added to the lower chamber of the filter tube. The filter was repositioned and 300 μl of QS active isolate in marine broth at $OD_{600\ nm}$ 0.2 was added. Several controls were included: (i) 300 μl of marine broth was added to the top chamber to provide a baseline profile of bacteria that could be cultured under the standard media conditions used, (ii) each QS active isolate was prepared as above with no sponge sample in the lower chamber to control for leakage through the membrane, and (iii) media controls were included to control for inadvertent contamination (**Figure 1**). The tubes were incubated at 23°C with gentle shaking at 50 rpm for 72 h at which time the upper chambers were carefully removed. The contents of the lower chamber were mixed gently and serially diluted. Dilutions were plated on marine agar and incubated at 23°C for at least 72 h. Colony numbers and morphologies were profiled and distinct isolates were identified by 16S rDNA sequencing.

Draft Genome Sequencing of QS Active *Psychrobacter* sp.

Total DNA of Psychrobacter sp. 230 strain was obtained using the UltraClean microbial DNA isolation kit (Mo Bio Laboratories, Inc., Carlsbad, CA, United States) and was used for DNA library preparation using a TruSeq exome library prep kit. The draft genome sequencing project of Psychrobacter sp. 230 strain was performed by the Beijing Genomics Institute (BGI, China) using the Illumina HiSeq 4000 sequencing platform involving paired-end reads with a read length of 150 bp. The superfast FASTA/Q file manipulation tool, readfq.v5 (BGI, unpublished software), was used for quality trimming. This software removes the paired-end reads with a certain proportion of low-quality bases (default, 40%; parameter setting, 6 bp), reads with a certain proportion of Ns (ambiguous bases; default, 10%; parameter setting, 10 bp), reads with adapter contamination (default, 15 bp overlapped between adapter and reads), and duplicate sequences. Thus, the high-quality-filtered reads were all 150 bp long. From a total of 5.417.936 raw paired-end reads of 150 bp length, 3.329.182 high-quality reads were generated after processing with readfq.v5. Assembly was performed using SOAPdenovo 2.04 with default parameters. The sequencing depth provided 47.5 coverage of the genome. The draft genome assembly comprised 69 contigs with an N50 value of 183,949 grouped into 69 scaffolds with a total size of 3,290,930 bp and an overall GC content of 42.8%. The whole-genome shotgun project was deposited at NCBI under the accession number: NZ_SNVH00000000.1. The raw reads obtained after processing with readfq.v5 have been submitted to NCBI SRA under the accession number SRP216019.

Phylogenetic Analysis

To infer the phylogenetic history, nucleotide sequences were retrieved and downloaded from NCBI: GenBank[2]. Sequences were aligned using Clustal Omega and were cut to consistent lengths (Sievers et al., 2011). The evolutionary analysis was conducted in MEGA X using the Neighbor-Joining method (Saitou and Nei, 1987; Kumar et al., 2018). The clustering was tested using Bootstrapping with 1,000 replicates (Felsenstein, 1985). The Tajima–Nei method was used to calculate the

[2]http://www.ncbi.nlm.nih.gov/

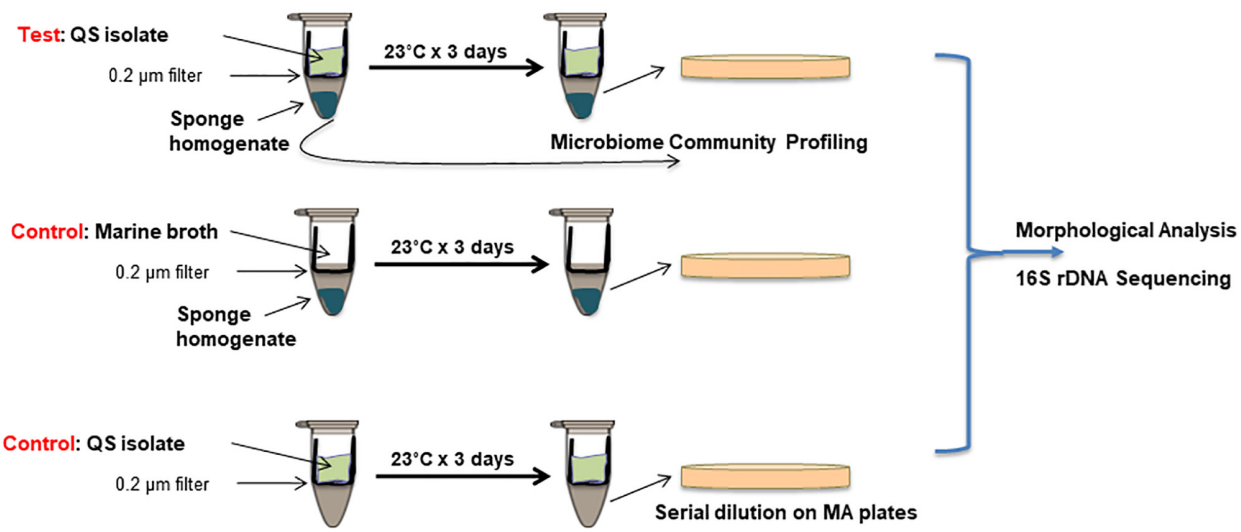

FIGURE 1 | Co-culture sponge enrichment assay protocol incorporating QS and QQ samples with appropriate controls. QS or QQ producing isolates are placed in the top chamber with marine both media to facilitate growth. These are separated from the lower chamber containing sponge material by a 0.2 µm filter. QS or QQ signals can transition from the top chamber into the lower chamber by diffusion. Controls are included to ensure no microbial transfer between chambers. Isolation of culturable organisms is achieved on marine agar plates following 3 day incubation. Distinct morphologies are scored and selected for 16S rRNA sequencing.

evolutionary distances (Tajima and Nei, 1984). There was a total of 1,459 positions in the final dataset.

RESULTS

QS Signaling Potential Within Marine Sponge Microbiomes

A range of QS active marine sponge microbial communities have been reported in recent years (Mohamed et al., 2008; Zan et al., 2012; Abbamondi et al., 2014; Britstein et al., 2018). The presence of QS systems in the sponge microbiota suggests a dynamic and ordered community that can respond to external cues and challenges. However, the extent to which QS producing bacteria colonize the marine sponge, and the role of QS within those microbial communities remains to be determined. Therefore, two distinct marine sponges were selected for microbial community profiling to establish the extent to which QS potential existed therein. Given the heterogeneity that exists in many clinical and ecological niches, with localized population profiles existing within relatively short distances of each other within a singular niche, two separate samples of each marine sponge species were selected. Homogenization and subsequent sequencing of two independently harvested triplicate samples revealed some interesting features of the respective microbiomes. Approximately 50% of the *S. normani* samples was identified only to the level of kingdom classification, suggesting a unique and unexplored bacterial diversity (**Supplementary Table S1**). The dominant phyla were Proteobacteria and Actinobacteria. At the genus level, *Iamia* [14.9% (±1.9)], *Pseudoalteromonas* [6.1% (±0.6)], *Moraxellaceae* [4.7% (±0.1)], and *Nitrospira* [2.5% (±0.6)] were the most abundant identifiable genera (**Figure 2A**). In contrast, the largest group identified for sponge BD1268 was the γ-Proteobacteria, representing between 85 and 94% of the OTUs in these samples. Sponge BD1268 was colonized by genera such as *Candidatus Pelagibacter* [12% (±4.5)], *Thioprofundum* [4.2% (±1.0)], and *Thiohalophilus* [2.4% (±0.4)]. Although the individual profiles remained relatively consistent from the perspective of the dominant phyla and families, there were differences in relative abundances between the microbiome profiles from the distinct sponge samples suggesting that heterogeneity of the population may exist within the sponge (**Figure 2A**). Diversity indexes (Shannon and Simpson) and OTU abundance was higher in the *S. normani* samples when compared with the respective samples from the BD1268 sponge (**Figure 2B**). As expected, independent samples clustered together based on sponge source (**Supplementary Figure S1**). Genera known to encode QS signaling systems (e.g., *Pseudomonas*, *Halomonas*, *Psychrobacter*) were present in the microbiomes of both sponges, although it was interesting to note that they were low in abundance when compared to the principal colonizers of the sponges. Therefore, notwithstanding the fact that genera previously shown to encode QS systems were present, the degree to which QS signaling pervades in these sponges remained to be determined.

Identification of AHL Activities in Bacteria Isolated From Marine Sponges

The collection of morphologically diverse bacterial isolates from the *S. normani* sponge described above had previously been

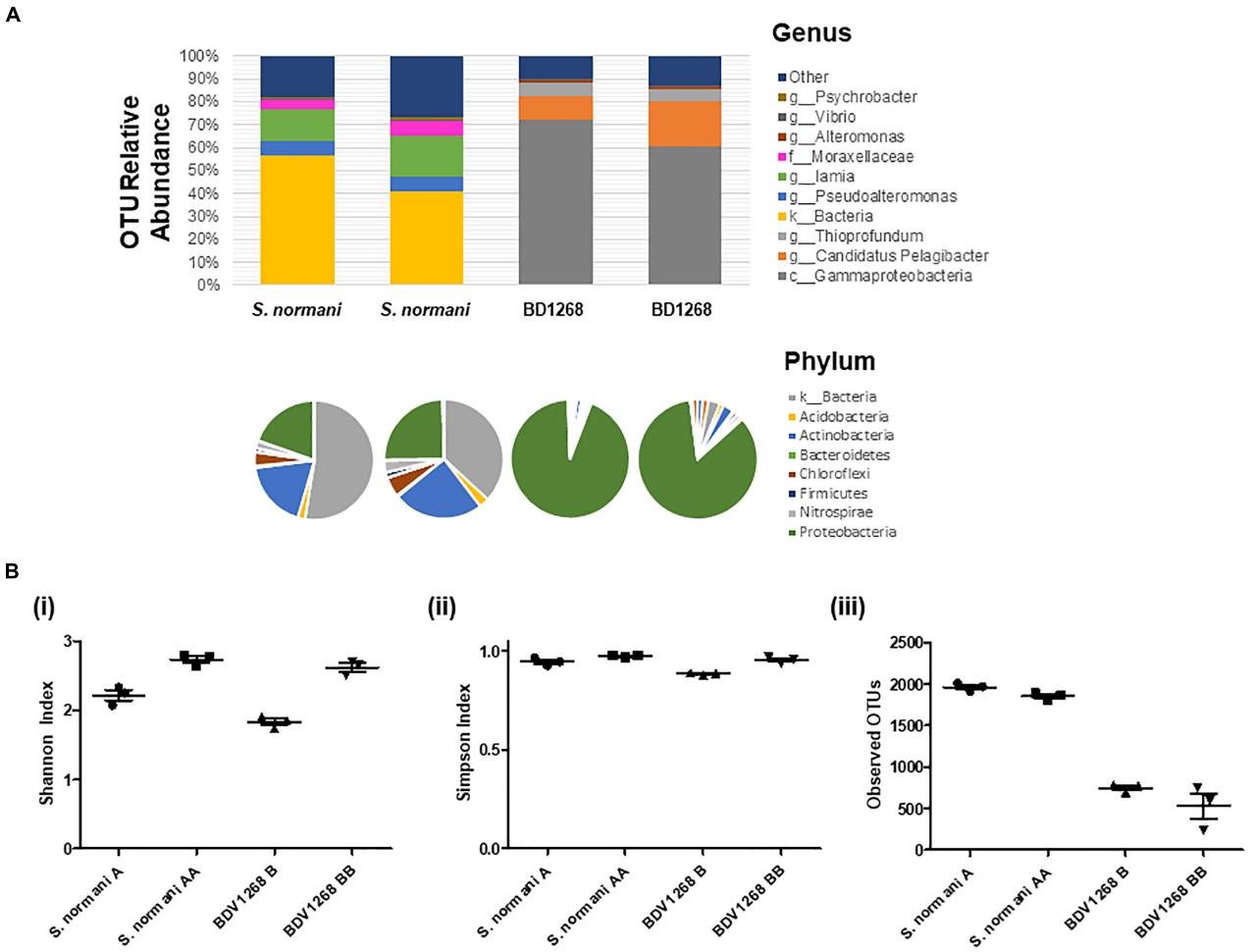

FIGURE 2 | (A) Microbiome 16S DNA bacterial community profiling of sponge DNA. Stacked charts show relative abundance at the genus level. Phylum community profiles are presented in pie-chart format above the corresponding genus-level stacked chart. Comparison with culturable microbiota reveals considerable challenge in activating the "silent" majority of genera present. Two independent samples were taken for each sponge and the average of three independent DNA extraction sequenced replicates is presented for each sample. **(B)** Diversity and OTU analysis on microbiome data (i) Shannon diversity index ($H = -\Sigma p_i \ln p_i$), (ii) Simpson diversity index, and (iii) OTU abundance.

reported (Gutierrez-Barranquero et al., 2017). Together with this, cultivation of bacteria from sponge tissue derived from other sponge families such as *Hexactinellida*, *Lissodendoryx*, *Poecillastra*, *Inflatella*, and *Amphilectus* had yielded a collection of bacteria from the Proteobacteria, Actinobacteria, Bacteroidetes and Firmicutes groups (Gutierrez-Barranquero et al., 2017). Within these groups a wide range of different families were represented. The most abundant families included Pseudoalteromonadaceae, Flavobacteriaceae, and Moraxellaceae. To establish the prevalence of AHL based QS within the sponge microbiome, over 650 sponge isolated bacteria were screened for AHL production. In total 10 AHL producing candidates were identified, representing approximately 0.015% of the culture collection (**Supplementary Figure S2** and **Table 1**). In order to identify the AHL positive isolates to a species level, the full length 16S rRNA (1,400 bp) sequence was determined. Among the isolates identified with AHL activity were a number of known AHL producers these included members of the *Halomonas*, *Psychrobacter*, *Vibrio*, *Pseudoaltermonas*, and *Pseudomonas* genera (Bruhn et al., 2005; Huang et al., 2009; Tahrioui et al., 2011; Ma et al., 2016). Despite the fact that the culture collection was populated by bacterial isolates harvested from six sponges, only four of these (*Stelletta*, *Hexactinellida*, *Inflatella*, and *Lissodendoryx*) yielded QS active isolates. The detection of QS active genera such as *Pseudomonas* and *Halomonas* from within the *S. normani* strains, despite the low abundance evident in the microbiome profile (**Supplementary Table S1**), is an important finding and suggests potentially a temporal role for QS active strains within communities. All QS active isolates were further validated by TLC analysis and soft agar biosensor overlay prior to selection for UHPLC-HRMS analysis and structural characterization (**Supplementary Figure S2**).

To identify the AHLs being produced by each of the QS positive candidates UHPLC-HRMS was performed

TABLE 1 | AHL profile of marine sponge QS active bacterial isolates.

Sample no	Sponge source	Biosensor activated-AHL	16S rRNA identification	UHPLC-HRMS verified QS profile
12	*Lissodendoryx*	*S. marcescens* SP19	*Pseudomonas* sp.	ND
142	*Inflatella*	*S. marcescens* SP19	*Pseudomonas* sp.	O-C12
163	*Lissodendoryx*	*A. tumefaciens* NTL4	*Vibrio* sp.	O-C10, O-C12
230	*Hexactinellida*	*A. tumefaciens* NTL4	*Psychrobacter* sp.	O-C12
211	*Hexactinellida*	*A. tumefaciens* NTL4	*Pseudoalteromonas* sp.	O-C12
214	*Hexactinellida*	*A. tumefaciens* NTL4	*Pseudoalteromonas* sp.	ND
335	*Stelletta*	*C. violaceum* CV026 *A. tumefaciens* NTL4	*Halomonas* sp.	O-C10
394	*Hexactinellida*	*A. tumefaciens* NTL4	*Pseudoalteromonas* sp.	O-C12
411	*Stelletta*	*S. marcescens* SP19	*Pseudomonas* sp.	C4, C6$^{\#}$
419	*Stelletta*	*A. tumefaciens* NTL4	*Pseudoalteromonas* sp.	OH-C6$^{\#}$, OH-C10, O-C10, O-C12

#Trace detected.

(**Supplementary Figure S2**). Ethyl acetate extracts were prepared for all isolates that had tested positive for AHL. All extracts were tested to ensure activation of respective AHL biosensors. Based on UHPLC-HRMS analysis, AHLs were identified in the majority of isolates (**Table 1**). The most abundant AHLs being produced by these isolates were 3-oxo-C10-HSL and 3-oxo-C12-HSL. Both AHLs, in addition to 3-OH-C10 HSL, were identified in extracts from *Psychrobacter* sp. and *Pseudoalteromonas* sp., the latter also producing trace amounts of 3-OH-C6 HSL. Only one isolate produced detectable amounts of C4-HSL, with the same *Pseudomonas* sp. isolate also producing trace amounts of C6-HSL. In some cases, no AHL traces were identified, notwithstanding the ability of the isolates to activate the respective biosensors.

Co-culture With QS Positive Isolates Influences Culturable Outputs From Marine Sponge

The marine sponges profiled in this study appear to sustain a significant network of QS systems which may be important in modulating the population in response to external cues. Previous studies have shown that the ratio of QS and QQ strains can change dramatically in response to environmental conditions (Tan et al., 2015). Therefore, we investigated whether the secretome of the QS active isolates could impact on the profile of culturable bacteria that could be obtained from marine sponges under the standard media conditions used. Filter based microtubes were used to establish a co-culture system whereby the QS active isolate was added to a well with a porous membrane through which secreted QS signals can be transferred to the chamber below containing *S. normani* sponge homogenate (**Figure 3A**). In three independent studies, distinct colony morphologies were observed on plates with QS treated samples when compared to untreated controls (**Figure 3B**). The fidelity of all controls was maintained throughout the experiments with no leakage or inadvertent contamination observed.

Pseudoalteromonas and *Vibrio* were both cultured from the *S. normani* sponge homogenate in the absence of any treatments. Upon co-culture with QS active isolates, *Pseudomonas*, *Paenibacillus* and *Psychrobacter* were isolated in independent experiments. This was in addition to *Pseudoalteromonas* and *Vibrio* as seen on the control plates. Co-culture with QS-active isolates 12 and 411 resulted in isolation of *Pseudomonas* while 214 and 211 led to isolation of *Paenibacillus*. *Psychrobacter* was isolated upon co-culture with all 211, 214, and 411. No representative from these genera was observed on the untreated control plates (**Figure 3**). All three genera were represented at a very low relative abundance within the microbiome from the untreated *S. normani* sponge samples (*Pseudomonas* [0.003% (±0.003), *Psychrobacter* [0.6% (±0.1)], and *Paenibacillus* only evident at Order level of *Bacillales* [0.02% (±0.05)]) suggesting a change in community structure (**Supplementary Table S1**). Together, these data suggest that cell-cell communication and QS can impact the dynamics of population growth within microbiomes and influence the culture-readiness of genera in response to external cues. It was notable that the impact of QS active supernatants was not restricted to gram negative organisms. However, the vast majority of microbiome constituents were not represented in the culturable diversity on the plates. Representatives of e.g., *Iamia*, *Nitrospira*, *Caldilinea*, or *Gaiella* were not observed on either control or test plates. Therefore, modification of the media to cater for additional supplemental requirements, or indeed to reduce nutritional richness, may be required to capture these unculturable components.

QS Phenotype Profiling

In order to understand how QS signaling might influence species dynamics within the marine sponge, we investigated whether marine isolates obtained following co-culture with QS positive marine sponge isolates responded to exogenous AHLs. As the most frequently identified AHL in this study, 3-oxo-C12 HSL was selected to assess its influence on two key QS associated phenotypes i.e., biofilm formation and growth. Somewhat surprisingly, neither was affected upon addition of 3-oxo-C12 HSL when compared to untreated samples (**Figure 4**). Addition of either 10 or 50 μM 3-oxo-C12 HSL did not impact on growth of test strains, either in exponential or stationary phase, as determined over 72 h (**Figure 4** and **Supplementary Figure S3**). Similarly, although the test isolates formed biofilms in multi-well plates, addition of either 10 or

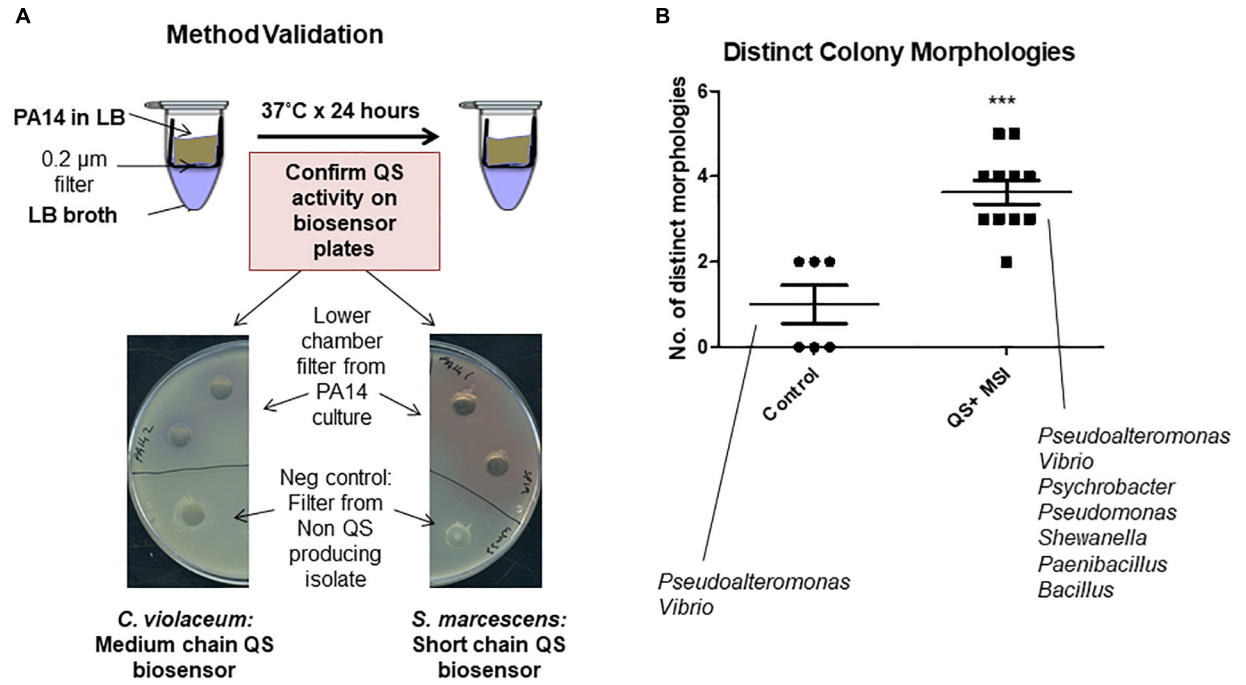

FIGURE 3 | Co-culture sponge enrichment analysis. **(A)** Proof of concept using QS producing strains. Transfer of the QS active compounds confirmed by validation on Biosensor seeded plates. **(B)** Outcome of QS-mediated sponge enrichment assays measuring recoverable morphologies which were subsequently 16S rRNA-typed. Each datapoint refers to the number of distinct species recovered after the designated treatment. The species listed represent recoverable isolates identified in the study. Data presented represents at least three independent assays encompassing distinct *S. normani* sponge preparations. Statistical analysis was performed by Student's *t*-test. ***$p \leq 0.001$.

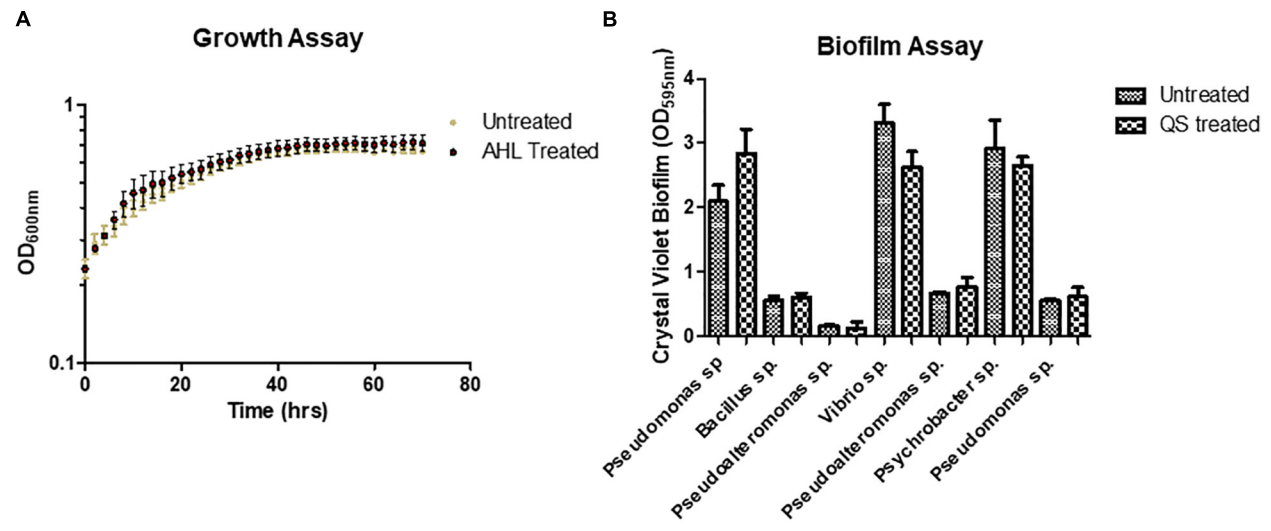

FIGURE 4 | Addition of purified 3-oxo-C12-HSL did not influence **(A)** growth of a *Pseudomonas* sp. isolate or **(B)** biofilm formation of marine sponge isolates recovered in this study following co-culture.

50 µM 3-oxo-C12 HSL did not significantly alter total attached biomass (**Figure 4**).

The ability of QS to control a range of virulence related phenotypes is well established. In addition to controlling biofilm formation and toxin secretion in important pathogens, QS is also known to elicit an antagonistic response toward co-colonizing organisms in producing strains. To test if this applied to the marine sponge QS active isolates, biofilm formation in the marine sponge sporefomer *Bacillus* sp. CH8a was investigated in the presence and absence of extracts from QS positive isolates.

Addition of extracts from several of the isolates led to a significant reduction in biofilm formation by CH8a when compared with the untreated control (**Figure 5**). This suggests that QS active strains would likely produce compound(s) that would moderate the behavior of co-existing microbes within the sponge microbiome.

Genome Sequencing and Identification of LuxR Domain Proteins Within the *Psychrobacter* Genus

Suppression of biofilm and activation of QS biosensors suggest that QS signaling is a highly networked and evolved system in the marine sponge niche. However, very little is known about the factors involved in newly emerging QS positive species. *Psychrobacter* sp. have only recently been shown to be QS positive, although the molecular mechanism underpinning this activity remains to be elucidated. To assess if any proteins encoded within *Psychrobacter* genomes could function as LuxR homologs the available *Psychrobacter* genomes were investigated via the Pfam Domain Search Tool to identify proteins with specific domains associated with LuxR type transcriptional regulators, i.e., the autoinducer binding domain (PFAM03472) or the LuxR DNA binding domain (PFAM00196). A total of 70 proteins were identified in 38 genomes that possessed a LuxR type DNA binding domain (**Supplementary Table S1**). However, neither an autoinducer binding domain nor a classical autoinducer synthase domain (PFAM00765) were identified in any of the available genome sequences. This raised two possibilities; (i) a potential novel AHL synthase with a low sequence homology to known AHL synthases may be functionally active within the *Psychrobacter* genus, or (ii) marine *Psychrobacter* sp. encode novel regions of DNA carrying the capacity for AHL production. Several reports exist in the literature of QS active strains where the corresponding genetic systems encoding that activity remain to be identified. The prevalence of horizontal gene transfer, and the phenotypic and genotypic heterogeneity that exists within communities is such that interrogating model genomes can be limited when searching for a particular functionality that may be strain specific. We considered it important to investigate the QS signaling potential that is encoded in the genome of the *Psychrobacter* species, particularly as we had a QS active strain with which to interrogate.

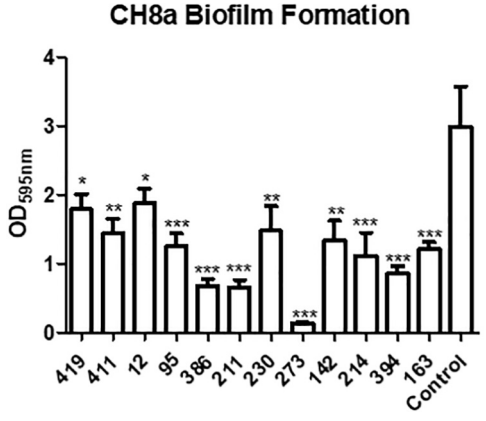

FIGURE 5 | Modulation of *Bacillus* sp. CH8a biofilm formation by extracts from QS active isolates. Data presented is the average of at least three independent biological replicates. Statistical analysis was performed by one-way ANOVA with *post hoc* Bonferroni corrective testing (*$p \leq 0.05$, **$p \leq 0.005$, ***$p \leq 0.001$).

Whole genome sequencing of the *Psychrobacter* sp. 230 isolate from this study revealed a genome encoding 2908 genes (**Supplementary Figure S4**). The draft genome assembly comprised 69 contigs with an N50 value of 183,949 grouped into 69 scaffolds with a total size of 3,290,930 bp and an overall GC content of 42.8% (**Table 2**). The *Psychrobacter* sp. 230 genome was searched for Lux domains and three putative LuxR domain proteins were identified. BLASTX sequence searches and SMART domain analysis suggested that these three proteins were transcriptional response regulator proteins, with no evidence of autoinducer domains. A LysE family homoserine(lactone) translocation protein was also encoded in the genome, as was a dienelactone hydrolase family protein. However, the absence of a LuxI-like synthase gene in the *Psychrobacter* genome indicates that the molecular mechanism through which AHL based QS is performed in this isolate remains to be ascertained. Cluster based analysis revealed that this *Pscyhrobacter* sp. grouped with three other *Psychrobacter* sp. isolates and distinct from other members of the genus suggesting it may be a genetic outlier within *Psychrobacter* (**Figure 6**). Previously, Ma et al. (2016) identified a *Psychrobacter* sp. isolate from mangrove with QS activity that clustered with *Psychrobacter* sp. isolates from deep sea sediments of the east Pacific Ocean. Therefore, a functional approach may be warranted to uncover the molecular basis of QS signaling in this species.

DISCUSSION

In this study, 650 marine sponge bacterial isolates were screened for the ability to produce AHLs. A total of 10 isolates were identified that were capable of activating AHL biosensor reporter strains. Mass spectrometry revealed that several of the isolates produced the same or similar AHLs (OC10–OC12 HSL). The capacity for AHL based signaling in the marine ecosystem has previously been reported. AHL signaling in marine snow was first described by Gram et al. (2002), with species of *Roseobacter* shown to be QS active. More recently, *Pantoea ananatis* has been reported to produce a spectrum of AHL signals in marine snow, governing extracellular enzyme production in

TABLE 2 | Genome data for *Psychrobacter* sp. 230 marine sponge isolate.

	***Psychrobacter* sp. 230**
Genome size	3,290,930
Contigs (*n*)	1
GC content (%)	42.8
Protein coding genes	2857
RNA genes	44

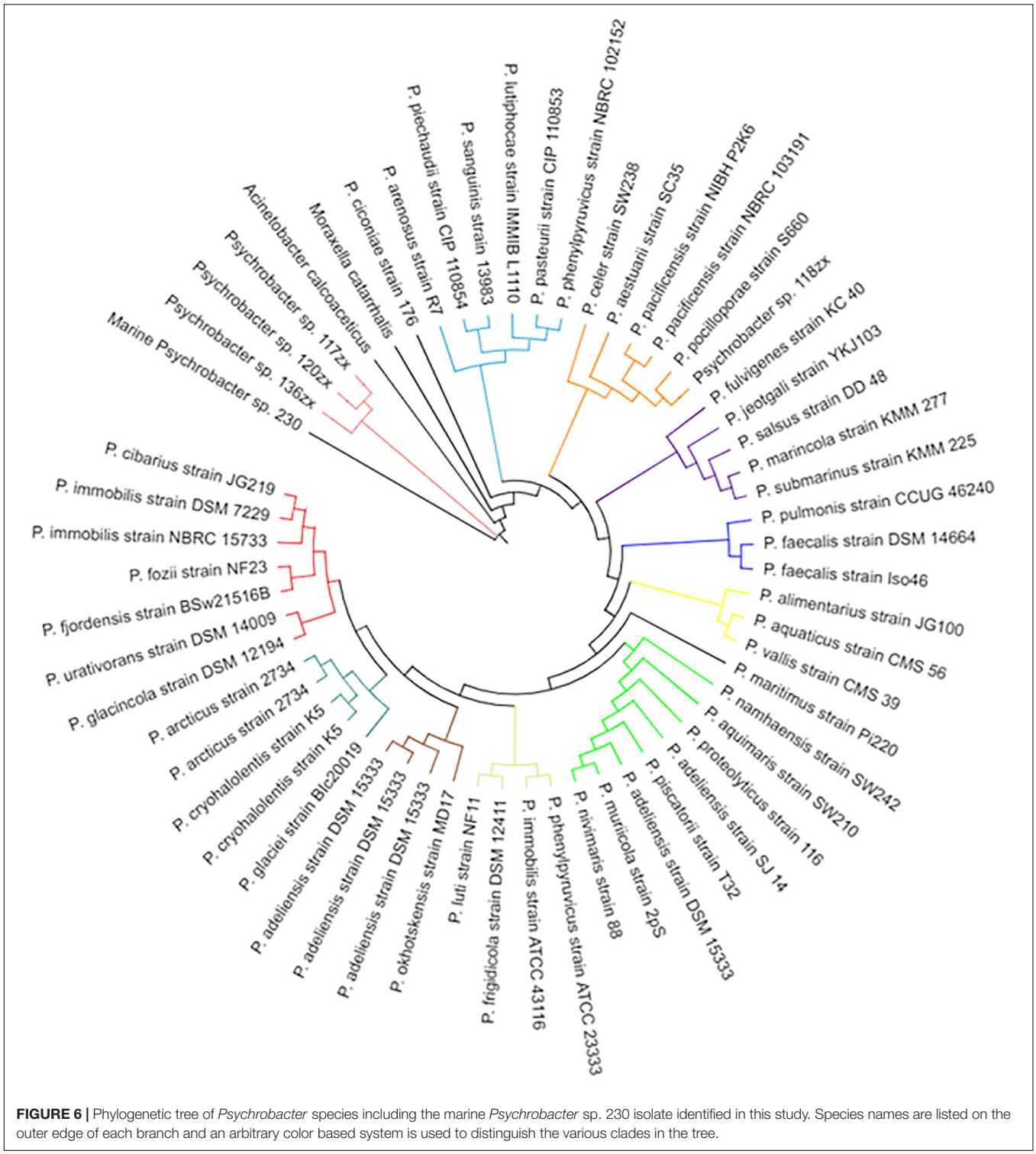

FIGURE 6 | Phylogenetic tree of *Psychrobacter* species including the marine *Psychrobacter* sp. 230 isolate identified in this study. Species names are listed on the outer edge of each branch and an arbitrary color based system is used to distinguish the various clades in the tree.

producing strains (Jatt et al., 2015). Since the first description of AHL based QS in *A. fischeri* species (Nealson and Hastings, 1979), where the LuxIR paradigm system was first identified, AHL signals have been found in a broad diversity of marine isolates (Hmelo, 2017). Rasch et al. (2007) described AHL production in *Aeromonas salmonicida* isolates, while a number of studies profiled members of the Vibrionaceae for AHL production (Yang et al., 2011; Purohit et al., 2013). The diversity of AHL signals that are encoded in the marine ecosystem has been highlighted by a recent study reporting AHLs with long (up to 19 carbons) and poly-hydroxylated acyl side chains (Doberva et al., 2017). At the same time, studies reporting

QS inhibition or quenching in the marine environment have also received considerable attention in recent years (Romero et al., 2012; Gutierrez-Barranquero et al., 2017; Ma et al., 2018). Primarily produced by microbial species, host derived quorum quenching (QQ) has also been described (Weiland-Brauer et al., 2019). Elucidating and profiling the extent of QS signaling within these environments is a key step in understanding the functional role played by QS in the host-microbe interaction.

Interspecies communication within the microbial communities of the marine sponge may offer a competitive advantage through cross-genus coordinated behavior. If several species all produce the same or similar AHLs, then they potentially could adopt community like behaviors more rapidly than species that are not part of this interspecies signaling network. This could arise from the activity threshold being reached more rapidly if several different species produce the same signaling molecule. Of course, conservation within receptor systems would also be an integral factor in moderating these responses. The prevalence of orphan LuxR receptor systems in sequenced microbial genomes highlights the complexity of signaling interactions that remain to be identified and understood (Patankar and Gonzalez, 2009). Adopting community-like behaviors through QS systems may offer a distinct competitive advantage as bacteria can attach to a form a biofilm like structure within the environment of the sponge. Community-based small molecular interactions may also be important with respect to intracellular sponge symbionts, such as the recently reported *Candidatus* Endohaliclona renieramycinifaciens intracellular interaction with *Haliclona* (Tianero et al., 2019).

The prevalence and diversity of AHLs being produced by the sponge bacterial isolates identified in this study suggests that mechanisms to inhibit these systems may also exist within the sponge microenvironment. The identification of novel compounds that are capable of inhibiting AHL based QS systems is one of the key areas of focus in the development of next generation antimicrobials. Previously, we have reported on the profiling of a subset of this collection of marine sponge isolates for quorum sensing inhibitory (QSI) or QQ activity. A total of 18/440 culturable isolates were found to encode QSI, being able to supress AHL signaling is an isolate dependent manner (Gutierrez-Barranquero et al., 2017). It was interesting to note in that study that several species possessed dual QS and QSI activities. In this current study the finding that *Psychrobacter* sp. isolates from the same sponge collection were also capable of QS activity suggests that community level moderation of group behavior is a highly evolved trait in the marine ecosystem. Tan et al. (2015) previously showed how the dynamics of QS and QSI/QQ producing organisms can fluctuate in response to changes in environmental conditions. It is noticeable in this regard that two species cultured from QS treated sponge homogenate, *Pseudomonas* and *Paenibacillus*, are themselves known to possess AHL signaling systems (Ma et al., 2016). Understanding the interplay between QS and QSI/QQ in the marine sponge ecosystem and the role of QQ in moderating community behavior will underpin advances in marine ecology and beyond.

The dynamics of AHL production in marine microbial communities is seen as a mechanism to enhance culturability of rare genera, many of which encode valuable biosynthetic gene clusters for natural products such as antibiotics and anti-cancer drugs (Reen et al., 2015). While co-culture with QS positive isolates did alter the profile of culturable bacteria isolated from marine sponge homogenates, they failed to introduce new genera into culture. This of course could be due to limitations in the culture conditions, including the general nature of the media used which is more conducive to the culture of fast-growing bacteria. Dilution based methods and modification of the growth conditions with regard to media, temperature, and time may provide the optimum conditions for culture of QS dependent organisms (Rygaard et al., 2017).

The absence of a LuxIR system in the QS positive *Pychrobacter* sp. 230 isolate would suggest that a hidden diversity to the molecular mechanisms underpinning QS signaling remains to be elucidated. This is consistent with previous reports of AinS and LuxM family autoinducer synthase enoding genes, quite distinct from their LuxI counterparts (Venturi and Subramoni, 2009). Recently, a new LuxIR based system termed TswIR has been identified in an uncultured symbiont from the Red Sea Sponge *Theonella swinhoei* (Britstein et al., 2016). The synthase protein TswI (COG3916) was annotated as both an autoinducer synthase and a GNAT acetyltransferase activity and while GNAT acetyltransferase proteins were identified in the *Psychrobacter* genomes, no members of the COG3916 family were found. Furthermore, the recent finding that LuxIR homologs can synthesize and respond to non-acyl HSL signals, serves to underscore the hidden complexity in these systems (Ahlgren et al., 2011). Two orphan Photorhabdus LuxR proteins, PluR and PauR, sense alpha-pyrones and dialkylresorcinols, respectively (Brameyer and Heermann, 2015). It is possible that other examples of non-AHL LuxR interactions may be uncovered in the future, something that would add greatly to the complexity of the signaling interactions as currently understood. The absence of homologs of these proteins in the *Psychrobacter* sp. 230 genome may necessitate a functional approach in order to elucidate the molecular mechanism through which AHL signaling is established in this and other marine genera.

DATA AVAILABILITY

The datasets generated for this study can be found in the NCBI Database accession nos: MN209943-MN209952, NZ_SNVH00000000.1, SRP216019 and PRJNA555824.

AUTHOR CONTRIBUTIONS

FR and FO'G conceived the study. FR, JG-B, CA, DW, RM, SS, and KN performed the experimental analysis. FR wrote the

manuscript with inputs from all the authors. FR and FO'G finalized the manuscript for submission.

FUNDING

FR and FO'G acknowledge support from Enterprise Ireland (CF-2017-0757-P) and the Health Research Board/Irish Thoracic Society (MRCG-2018-6). This research was also supported in part by grants awarded to FO'G by the European Commission (EU2020-634486-2015), Science Foundation Ireland (SSPC-2, 15/TIDA/2977), the Irish Research Council for Science, Engineering and Technology (GOIPG/2014/647), the Cystic Fibrosis Foundation, United States (OG1710), and the Health Research Board/Irish Thoracic Society (MRCG-2014-6). KN is grateful to Agilent technologies for the Thought Leader Donation of the UHPLC-QTOF system.

ACKNOWLEDGMENTS

The authors thank Iwona Kozak and Niall Dunphy for excellent technical assistance and Jamie Deery for generation of the PCA plots.

SUPPLEMENTARY MATERIAL

The Supplementary Material for this article can be found online at: https://www.frontiersin.org/articles/10.3389/fmicb.2019.02131/full#supplementary-material

FIGURE S1 | PCA bi-plot cluster analysis of microbiome samples performed using R (v. 3.5.2). Visualization was performed using the ggplot and ggfortify packages. Samples from both sponges form separate clusters reflecting their distinct microbial community profiles.

FIGURE S2 | (A) Screen of Marine Sponge Isolates using QS-Biosensor Strains. **(B)** QS positive isolates were grown in culture flasks to confirm biosensor activation. Species level identification was achieved by 16S rRNA sequencing and subsequent BLAST analysis. **(C)** Extracts were validated by TLC overlay and subsequently sent for UHPLC-HRMS analysis and classification.

FIGURE S3 | (A–F) Growth profiling of isolates harvested following co-culture with QS active strains in the presence of 10 μM 3-oxo-C12-HSL or DMSO carrier control. Data presented is the average (±SEM) of two independent biological replicates with five technical replicates in each experiment performed on the BioScreen-C.

FIGURE S4 | Genome representation of the newly sequenced *Psychrobacter* sp. 230 isolate identified as a 3-oxo-C12-HSL producer in this study. COG functional categories are presented on the outer ring, while forward and reverse strand gene annotations are presented in the inner rings in red and blue, respectively.

REFERENCES

Abbamondi, G. R., De Rosa, S., Iodice, C., and Tommonaro, G. (2014). Cyclic dipeptides produced by marine sponge-associated bacteria as quorum sensing signals. *Nat. Prod. Comm.* 9, 229–232.

Ahlgren, N. A., Harwood, C. S., Schaefer, A. L., Giraud, E., and Greenberg, E. P. (2011). Aryl-homoserine lactone quorum sensing in stem-nodulating photosynthetic bradyrhizobia. *Proc. Natl. Acad. Sci. U.S.A.* 108, 7183–7188. doi: 10.1073/pnas.1103821108

Blunt, J. W., Copp, B. R., Hu, W. P., Munro, M. H., Northcote, P. T., and Prinsep, M. R. (2009). Marine natural products. *Nat. Prod. Rep.* 26, 170–244. doi: 10.1039/b805113p

Brameyer, S., and Heermann, R. (2015). Specificity of signal-binding via Non-AHL LuxR-type receptors. *PLoS One* 10:e0124093. doi: 10.1371/journal.pone.0124093

Britstein, M., Devescovi, G., Handley, K. M., Malik, A., Haber, M., Saurav, K., et al. (2016). A new N-Acyl homoserine lactone synthase in an uncultured symbiont of the red sea sponge Theonella swinhoei. *Appl. Environ. Microbiol.* 82, 1274–1285. doi: 10.1128/AEM.03111-15

Britstein, M., Saurav, K., Teta, R., Sala, G. D., Bar-Shalom, R., Stoppelli, N., et al. (2018). Identification and chemical characterization of N-acyl-homoserine lactone quorum sensing signals across sponge species and time. *FEMS Microbiol. Ecol.* 94:fix182. doi: 10.1093/femsec/fix182

Bruhn, J. B., Dalsgaard, I., Nielsen, K. F., Buchholtz, C., Larsen, J. L., and Gram, L. (2005). Quorum sensing signal molecules (acylated homoserine lactones) in gram-negative fish pathogenic bacteria. *Dis. Aquat. Organ.* 65, 43–52. doi: 10.3354/dao065043

Chan, K. G., Wong, C. S., Yin, W. F., Sam, C. K., and Koh, C. L. (2010). Rapid degradation of N-3-oxo-acylhomoserine lactones by a *Bacillus cereus* isolate from Malaysian rainforest soil. *Antonie Van Leeuwenhoek* 98, 299–305. doi: 10.1007/s10482-010-9438-0

Cuadrado-Silva, C. T., Castellanos, L., Arevalo-Ferro, C., and Osorno, O. E. (2013). Detection of quorum sensing systems of bacteria isolated from fouled marine organisms. *Biochem. Syst. Ecol.* 46, 101–107. doi: 10.1016/j.bse.2012.09.010

Diggle, S. P., Crusz, S. A., and Camara, M. (2007). Quorum sensing. *Curr. Biol.* 17, R907–R910.

Doberva, M., Stien, D., Sorres, J., Hue, N., Sanchez-Ferandin, S., Eparvier, V., et al. (2017). Large diversity and original structures of acyl-homoserine lactones in strain MOLA 401, a marine rhodobacteraceae bacterium. *Front. Microbiol.* 8:1152. doi: 10.3389/fmicb.2017.01152

Eren, A. M., Morrison, H. G., Lescault, P. J., Reveillaud, J., Vineis, J. H., and Sogin, M. L. (2015). Minimum entropy decomposition: unsupervised oligotyping for sensitive partitioning of high-throughput marker gene sequences. *ISME J.* 9, 968–979. doi: 10.1038/ismej.2014.195

Farrand, S. K., Hwang, I., and Cook, D. M. (1996). The tra region of the nopaline-type Ti plasmid is a chimera with elements related to the transfer systems of RSF1010, RP4, and F. *J. Bacteriol.* 178, 4233–4247. doi: 10.1128/jb.178.14.4233-4247.1996

Felsenstein, J. (1985). Confidence-limits on phylogenies - an approach using the bootstrap. *Evolution* 39, 783–791. doi: 10.1111/j.1558-5646.1985.tb00420.x

Gram, L., Grossart, H. P., Schlingloff, A., and Kiorboe, T. (2002). Possible quorum sensing in marine snow bacteria: production of acylated homoserine lactones by Roseobacter strains isolated from marine snow. *Appl. Environ. Microbiol.* 68, 4111–4116. doi: 10.1128/aem.68.8.4111-4116.2002

Gutierrez-Barranquero, J. A., Reen, F. J., Parages, M. L., McCarthy, R., Dobson, A. D. W., and O'Gara, F. (2017). Disruption of N-acyl-homoserine lactone-specific signalling and virulence in clinical pathogens by marine sponge bacteria. *Microb. Biotechnol.* 12, 1049–1063. doi: 10.1111/1751-7915.12867

Hmelo, L. R. (2017). Quorum sensing in marine microbial environments. *Annu. Rev. Mar. Sci.* 9, 257–281. doi: 10.1146/annurev-marine-010816-060656

Huang, Y. L., Ki, J. S., Lee, O. O., and Qian, P. Y. (2009). Evidence for the dynamics of Acyl homoserine lactone and AHL-producing bacteria during subtidal biofilm formation. *ISME J.* 3, 296–304. doi: 10.1038/ismej.2008.105

Jatt, A. N., Tang, K., Liu, J., Zhang, Z., and Zhang, X. H. (2015). Quorum sensing in marine snow and its possible influence on production of extracellular hydrolytic enzymes in marine snow bacterium Pantoea ananatis B9. *FEMS Microbiol. Ecol.* 91, 1–13. doi: 10.1093/femsec/fiu030

Kennedy, J., Codling, C. E., Jones, B. V., Dobson, A. D. W., and Marchesi, J. R. (2008). Diversity of microbes associated with the marine sponge, Haliclona simulans, isolated from Irish waters and identification of polyketide synthase genes from the sponge metagenome. *Environ. Microbiol.* 10, 1888–1902. doi: 10.1111/j.1462-2920.2008.01614.x

Kildgaard, S., Mansson, M., Dosen, I., Klitgaard, A., Frisvad, J. C., Larsen, T. O., et al. (2014). Accurate dereplication of bioactive secondary metabolites from marine-derived fungi by UHPLC-DAD-QTOFMS and a MS/HRMS library. *Mar. Drugs* 12, 3681–3705. doi: 10.3390/md12063681

Kumar, S., Stecher, G., Li, M., Knyaz, C., and Tamura, K. (2018). MEGA X: molecular evolutionary genetics analysis across computing platforms. *Mol. Biol. Evol.* 35, 1547–1549. doi: 10.1093/molbev/msy096

Ma, Z. P., Lao, Y. M., Jin, H., Lin, G. H., Cai, Z. H., and Zhou, J. (2016). Diverse profiles of AI-1 type quorum sensing molecules in cultivable bacteria from the Mangrove (*Kandelia obovata*) rhizosphere environment. *Front. Microbiol.* 7:1957. doi: 10.3389/fmicb.2016.01957

Ma, Z. P., Song, Y., Cai, Z. H., Lin, Z. J., Lin, G. H., Wang, Y., et al. (2018). Anti-quorum sensing activities of selected coral symbiotic bacterial extracts from the South China Sea. *Front. Cell. Infect. Microbiol.* 8:144. doi: 10.3389/fcimb.2018.00144

Mayer, A. M. S., Glaser, K. B., Cuevas, C., Jacobs, R. S., Kem, W., Little, R. D., et al. (2010). The odyssey of marine pharmaceuticals: a current pipeline perspective. *Trends Pharmacol. Sci.* 31, 255–265. doi: 10.1016/j.tips.2010.02.005

Mayer, A. M. S., Rodriguez, A. D., Berlinck, R. G. S., and Fusetani, N. (2011). Marine pharmacology in 2007-8: marine compounds with antibacterial, anticoagulant, antifungal, anti-inflammatory, antimalarial, antiprotozoal, antituberculosis, and antiviral activities; affecting the immune and nervous system, and other miscellaneous mechanisms of action. *Compar. Biochem. Physiol. C-Toxicol. Pharmacol.* 153, 191–222. doi: 10.1016/j.cbpc.2010.08.008

McClean, K. H., Winson, M. K., Fish, L., Taylor, A., Chhabra, S. R., Camara, M., et al. (1997). Quorum sensing and *Chromobacterium violaceum*: exploitation of violacein production and inhibition for the detection of N-acylhomoserine lactones. *Microbiology* 143, 3703–3711. doi: 10.1099/00221287-143-12-3703

Mohamed, N. M., Cicirelli, E. M., Kan, J., Chen, F., Fuqua, C., and Hill, R. T. (2008). Diversity and quorum-sensing signal production of *Proteobacteria* associated with marine sponges. *Environ. Microbiol.* 10, 75–86. doi: 10.1111/j.1462-2920.2007.01431.x

Nealson, K. H., and Hastings, J. W. (1979). Bacterial bioluminescence: its control and ecological significance. *Microbiol. Rev.* 43, 496–518.

Patankar, A. V., and Gonzalez, J. E. (2009). Orphan LuxR regulators of quorum sensing. *FEMS Microbiol. Rev.* 33, 739–756. doi: 10.1111/j.1574-6976.2009.00163.x

Phelan, R. W., O'Halloran, J. A., Kennedy, J., Morrissey, J. P., Dobson, A. D., O'Gara, F., et al. (2012). Diversity and bioactive potential of endospore-forming bacteria cultured from the marine sponge Haliclona simulans. *J. Appl. Microbiol.* 112, 65–78. doi: 10.1111/j.1365-2672.2011.05173.x

Poulter, S., Carlton, T. M., Su, X. B., Spring, D. R., and Salmond, G. P. C. (2010). Engineering of new prodigiosin-based biosensors of Serratia for facile detection of short-chain N-acyl homoserine lactone quorum-sensing molecules. *Environ. Microbiol. Rep.* 2, 322–328. doi: 10.1111/j.1758-2229.2010.00140.x

Purohit, A. A., Johansen, J. A., Hansen, H., Leiros, H. K., Kashulin, A., Karlsen, C., et al. (2013). Presence of acyl-homoserine lactones in 57 members of the Vibrionaceae family. *J. Appl. Microbiol.* 115, 835–847. doi: 10.1111/jam.12264

Rasch, M., Kastbjerg, V. G., Bruhn, J. B., Dalsgaard, I., Givskov, M., and Gram, L. (2007). Quorum sensing signals are produced by *Aeromonas salmonicida* and quorum sensing inhibitors can reduce production of a potential virulence factor. *Dis. Aquat. Organ.* 78, 105–113. doi: 10.3354/dao01865

Reen, F. J., Romano, S., Dobson, A. D., and O'Gara, F. (2015). The sound of silence: activating silent biosynthetic gene clusters in marine microorganisms. *Mar. Drugs* 13, 4754–4783. doi: 10.3390/md13084754

Romero, M., Martin-Cuadrado, A. B., and Otero, A. (2012). Determination of whether quorum quenching is a common activity in marine bacteria by analysis of cultivable bacteria and metagenomic sequences. *Appl. Environ. Microbiol.* 78, 6345–6348. doi: 10.1128/AEM.01266-12

Rygaard, A. M., Thogersen, M. S., Nielsen, K. F., Gram, L., and Bentzon-Tilia, M. (2017). Effects of gelling agent and extracellular signaling molecules on the culturability of marine bacteria. *Appl. Environ. Microbiol.* 83:e00243-17. doi: 10.1128/AEM.00243-17

Saitou, N., and Nei, M. (1987). The neighbor-joining method - a new method for reconstructing phylogenetic trees. *Mol. Biol. Evol.* 4, 406–425.

Sievers, F., Wilm, A., Dineen, D., Gibson, T. J., Karplus, K., Li, W., et al. (2011). Fast, scalable generation of high-quality protein multiple sequence alignments using Clustal Omega. *Mol. Syst. Biol.* 7:539. doi: 10.1038/msb.2011.75

Steindler, L., and Venturi, V. (2007). Detection of quorum-sensing N-acyl homoserine lactone signal molecules by bacterial biosensors. *FEMS Microbiol. Lett.* 266, 1–9. doi: 10.1111/j.1574-6968.2006.00501.x

Tahrioui, A., Quesada, E., and Llamas, I. (2011). The hanR/hanI quorum-sensing system of Halomonas anticariensis, a moderately halophilic bacterium. *Microbiology* 157, 3378–3387. doi: 10.1099/mic.0.052167-0

Tajima, F., and Nei, M. (1984). Estimation of evolutionary distance between nucleotide-sequences. *Mol. Biol. Evol.* 1, 269–285.

Tan, C. H., Koh, K. S., Xie, C., Zhang, J., Tan, X. H., Lee, G. P., et al. (2015). Community quorum sensing signalling and quenching: microbial granular biofilm assembly. *NPJ Biofilms Microbiomes* 1:15006. doi: 10.1038/npjbiofilms.2015.6

Taylor, M. W., Radax, R., Steger, D., and Wagner, M. (2007). Sponge-associated microorganisms: evolution, ecology, and biotechnological potential. *Microbiol. Mol. Biol. Rev.* 71, 295–347. doi: 10.1128/mmbr.00040-06

Taylor, M. W., Schupp, P. J., Baillie, H. J., Charlton, T. S., de Nys, R., Kjelleberg, S., et al. (2004a). Evidence for acyl homoserine lactone signal production in bacteria associated with marine sponges. *Appl. Environ. Microbiol.* 70, 4387–4389. doi: 10.1128/aem.70.7.4387-4389.2004

Taylor, M. W., Schupp, P. J., Dahllof, I., Kjelleberg, S., and Steinberg, P. D. (2004b). Host specificity in marine sponge-associated bacteria, and potential implications for marine microbial diversity. *Environ. Microbiol.* 6, 121–130. doi: 10.1046/j.1462-2920.2003.00545.x

Tianero, M. D., Balaich, J. N., and Donia, M. S. (2019). Localized production of defence chemicals by intracellular symbionts of Haliclona sponges. *Nat. Microbiol.* 4, 1149–1159. doi: 10.1038/s41564-019-0415-8

Venturi, V., and Subramoni, S. (2009). Future research trends in the major chemical language of bacteria. *HFSP J.* 3, 105–116. doi: 10.2976/1.3065673

Wang, G. (2006). Diversity and biotechnological potential of the sponge-associated microbial consortia. *J. Ind. Microbiol. Biotechnol.* 33, 545–551. doi: 10.1007/s10295-006-0123-2

Weiland-Brauer, N., Fischer, M. A., Pinnow, N., and Schmitz, R. A. (2019). Potential role of host-derived quorum quenching in modulating bacterial colonization in the moon jellyfish *Aurelia aurita*. *Sci. Rep.* 9:34. doi: 10.1038/s41598-018-37321-z

Whiteley, M., Diggle, S. P., and Greenberg, E. P. (2017). Progress in and promise of bacterial quorum sensing research. *Nature* 551, 313–320. doi: 10.1038/nature24624

Yang, Q., Han, Y., and Zhang, X. H. (2011). Detection of quorum sensing signal molecules in the family Vibrionaceae. *J. Appl. Microbiol.* 110, 1438–1448. doi: 10.1111/j.1365-2672.2011.04998.x

Yin, W. F., Purmal, K., Chin, S., Chan, X. Y., and Chan, K. G. (2012). Long chain N-acyl homoserine lactone production by *Enterobacter* sp. isolated from human tongue surfaces. *Sensors* 12, 14307–14314. doi: 10.3390/s121114307

Zan, J., Cicirelli, E. M., Mohamed, N. M., Sibhatu, H., Kroll, S., Choi, O., et al. (2012). A complex LuxR-LuxI type quorum sensing network in a roseobacterial marine sponge symbiont activates flagellar motility and inhibits biofilm formation. *Mol. Microbiol.* 85, 916–933. doi: 10.1111/j.1365-2958.2012.08149.x

Zan, J., Fuqua, C., and Hill, R. T. (2011). Diversity and functional analysis of luxS genes in vibrios from marine sponges Mycale laxissima and Ircinia strobilina. *ISME J.* 5, 1505–1516. doi: 10.1038/ismej.2011.31

Conflict of Interest Statement: The authors declare that the research was conducted in the absence of any commercial or financial relationships that could be construed as a potential conflict of interest.

frontiers in Microbiology

ORIGINAL RESEARCH
published: 13 September 2019
doi: 10.3389/fmicb.2019.02140

Conserved Pheromone Production, Response and Degradation by *Streptococcus mutans*

Antonio Pedro Ricomini Filho[1†], *Rabia Khan*[2†], *Heidi Aarø Åmdal*[2] *and Fernanda C. Petersen*[2*]

[1] Department of Physiological Science, Piracicaba Dental School, University of Campinas, Piracicaba, Brazil, [2] Department of Oral Biology, Faculty of Dentistry, University of Oslo, Oslo, Norway

Streptococcus mutans, a bacterium with high cariogenic potential, coordinates competence for natural transformation and bacteriocin production via the XIP and CSP pheromones. CSP is effective in inducing bacteriocin responses but not competence in chemically defined media (CDM). This is in contrast to XIP, which is a strong inducer of competence in CDM but can also stimulate bacteriocin genes as a late response. Interconnections between the pathways activated by the two pheromones have been characterized in certain detail in *S. mutans* UA159, but it is mostly unknown whether such findings are representative for the species. In this study, we used bioassays based on luciferase reporters for the bacteriocin gene *cipB* and the alternative sigma factor *sigX* to investigate various *S. mutans* isolates for production and response to CSP and XIP pheromones in CDM. Similar to *S. mutans* UA159, endogenous CSP was undetectable in the culture supernatants of all tested strains. During optimization of the bioassay using the *cipB* reporter, we discovered that the activity of exogenous CSP used as a standard was reduced over time during *S. mutans* growth. Using a FRET-CSP reporter peptide, we found that *S. mutans* UA159 was able to degrade CSP, and that such activity was not significantly different in isogenic mutants with deletion of the protease gene *htrA* or the competence genes *sigX*, *oppD*, and *comR*. CSP cleavage was also detected in all the wild type strains, indicating that this is a conserved feature in *S. mutans*. For the XIP pheromone, endogenous production was observed in the supernatants of all 34 tested strains at peak concentrations in culture supernatants that varied between 200 and 26000 nM. Transformation in the presence of exogenous XIP was detected in all but one of the isolates. The efficiency of transformation varied, however, among the different strains, and for those with the highest transformation rates, endogenous XIP peak concentrations in the supernatants were above 2000 nM XIP. We conclude that XIP production and inducing effect on transformation, as well as the ability to degrade CSP, are conserved functions among different *S. mutans* isolates. Understanding the functionality and conservation of pheromone systems in *S. mutans* may lead to novel strategies to prevent or treat unbalances in oral microbiomes that may favor diseases.

Keywords: pheromone, streptococcus, competence, natural transformation, quorum-sensing, CSP, XIP, ComS

OPEN ACCESS

Edited by:
Cristina García-Aljaro, University of Barcelona, Spain

Reviewed by:
Indranil Biswas, The University of Kansas, United States
Jacqueline Abranches, University of Florida, United States
Stephen J. Hagen, University of Florida, United States

***Correspondence:**
Fernanda C. Petersen
f.c.petersen@odont.uio.no

[†]*These authors have contributed equally to this work*

Specialty section:
This article was submitted to Microbial Physiology and Metabolism, a section of the journal Frontiers in Microbiology

Received: *14 May 2019*
Accepted: *30 August 2019*
Published: *13 September 2019*

Citation:
Ricomini Filho AP, Khan R, Åmdal HA and Petersen FC (2019) Conserved Pheromone Production, Response and Degradation by Streptococcus mutans. Front. Microbiol. 10:2140. doi: 10.3389/fmicb.2019.02140

INTRODUCTION

Natural genetic transformation is widely distributed in bacteria. In streptococci it occurs during a genetically programmed differentiated state called competence. During this state the bacteria become capable of taking up DNA from the environment and incorporate it into their genomes. The capacity for natural transformation has been reported for more than 80 bacterial species (Johnsborg et al., 2007; Johnston et al., 2014). Among streptococci, competence for natural transformation includes most species of the mitis, salivarius, bovis, anginosus, and mutans groups (Johnsborg et al., 2007; Fontaine et al., 2010; Desai et al., 2012; Morrison et al., 2013). The core of the machinery necessary for streptococcal transformation relies on the transcription of the conserved alternative sigma factor SigX, also known as ComX. SigX orchestrates a core response in streptococcal species characterized by the induction of 27 to 30 genes (Khan et al., 2016). The functions of the core genes are predominantly related to transformation, most of them coding for competence effector proteins for DNA binding, uptake and recombination (Li et al., 2001; Mashburn-Warren et al., 2010; Khan et al., 2016).

Streptococcus mutans is a member of the mutans group and part of the human oral microbiota. Environmental factors disturbing the ecological balance in the oral cavity, such as increased sugar intake, may favor *S. mutans* growth. The *S. mutans* acidogenic and aciduric properties may then contribute to tooth demineralization and dental caries (Marsh et al., 2011). Natural transformation was first reported in *S. mutans* in 1981 (Perry and Kuramitsu, 1981). This and later studies showed that transformation in *S. mutans*, at least in the laboratory setting, is restricted to a limited range of strains and depends on environmental conditions not yet fully understood (Perry and Kuramitsu, 1981). Studies investigating the *S. mutans* pan-genome have recently revealed the ubiquity of *sigX* and competence effector genes in *S. mutans* (Cornejo et al., 2013; Palmer et al., 2013; Song et al., 2013), indicating that competence may be a conserved feature in *S. mutans*. Moreover, the extensive horizontal gene transfer observed in the genomes of *S. mutans* clinical isolates (Cornejo et al., 2013) indicates that transformation occurs in their natural habitat and may be a widespread feature in the species.

In *S. mutans* the competent state is triggered by two linear peptides, the CSP (competence stimulating peptide) (Li et al., 2001) and the XIP (*sigX*-inducing peptide) (**Figure 1**; Mashburn-Warren et al., 2010). CSP was the first described pheromone and, until recently, the only one known to activate the competence system for genetic transformation in *S. mutans*. The *comC* gene, which encodes CSP, is downstream of the *comDE* operon, encoding the ComD histidine kinase and the ComE response regulator. At least in the synthetic form, CSP is thought to bind to the ComD histidine kinase of the ComDE two-component system, leading to phosphorylation of the ComE response regulator (Peterson et al., 2004). Phosphorylated ComE directly up-regulates the transcription of clusters of bacteriocin-related genes (Petersen et al., 2006; Mashburn-Warren et al., 2010; Federle and Morrison, 2012; Khan et al., 2016). These include among others the SMU_1914 gene (also known as *nlmC* and *cipB*), encoding mutacin V, and the putative immunity protein SMU_1913, found in a *comE* downstream region. Mutacin V has been proposed to link the early CSP bacteriocin-inducing response to the competence response (Ween et al., 1999; van der Ploeg, 2005; Kreth et al., 2007; Dufour et al., 2011; Hung et al., 2011) by mechanisms that remain elusive. Essential for competence development is the activation of the XIP pheromone encoding gene, *comS*, followed by the upregulation of the alternative sigma factor SigX, the master core regulator of competence. In rich media, ComS seems to be processed to XIP inside the cells. Intracellular XIP and/or ComS then binds to ComR to activate the competence pathway (Underhill et al., 2018). The predicted CSP is in general conserved among *S. mutans* strains (Li et al., 2001; Petersen et al., 2006), and there are indications that *S. mutans* may form a single CSP pherotype (Petersen et al., 2006; Hossain and Biswas, 2012). The C-terminal of the CSP precursor (ComC) is exported outside of the cells, where it is further processed into the active 18 amino acid peptide (18-CSP) (Petersen et al., 2006; Hossain and Biswas, 2012).

The XIP pheromone system is found in several streptococci (Gardan et al., 2009; Fontaine et al., 2010; Mashburn-Warren et al., 2010; Fleuchot et al., 2011; Morrison et al., 2013). In *S. mutans* UA159 the XIP pheromone encoded by *comS* has been identified in culture supernatants grown in chemically defined medium (CDM) lacking peptides (Mashburn-Warren et al., 2010; Khan et al., 2012). XIP is produced as a pro-peptide (ComS) that is possibly exported and processed into the active XIP (N-GLDWWSL) (Mashburn-Warren et al., 2010; Desai et al., 2012; Khan et al., 2012). The presence of an exporter has, however, never been demonstrated, and recent studies indicate that release of XIP or ComS by autolysis is sufficient to promote intercellular communication in CDM (Kaspar et al., 2017). Under such conditions, response to the XIP depends on the Opp oligopeptide permease system, indicating that the peptide is internalized (Mashburn-Warren et al., 2010). Once inside the cells XIP is thought to bind to the Rgg-like regulator ComR to activate transcription of *sigX* and *comS*. In contrast with XIP, CSP shows no activity or low potency in triggering competence in CDM (Desai et al., 2012; Wenderska et al., 2012; Reck et al., 2015) but can still induce the expression of bacteriocin-related genes of the ComE regulon (Reck et al., 2015). When it comes to transformation, the use of synthetic CSP has led to higher levels of *S. mutans* transformation (Gaustad and Morrison, 1998; Petersen and Scheie, 2010) but has not extended the range of strains transformed in the absence of the synthetic pheromone. As for the synthetic XIP, evidence for competence induction and endogenous pheromone production has so far been restricted to the reference strain UA159, with few exceptions (Palmer et al., 2013).

In this study we investigated the functional conservation of the *S. mutans* CSP and XIP pheromone signaling systems in CDM. Extracellular CSP activity was not detected in any of the tested strains. Exposure to synthetic CSP revealed that *S. mutans* can indeed degrade CSP, a behavior that was conserved in the examined strains, and that at least in strain UA159 it was not abolished by deletion of *sigX*, *comR*, *oppD*, or the *htrA* protease gene. For the XIP pheromone, endogenous production

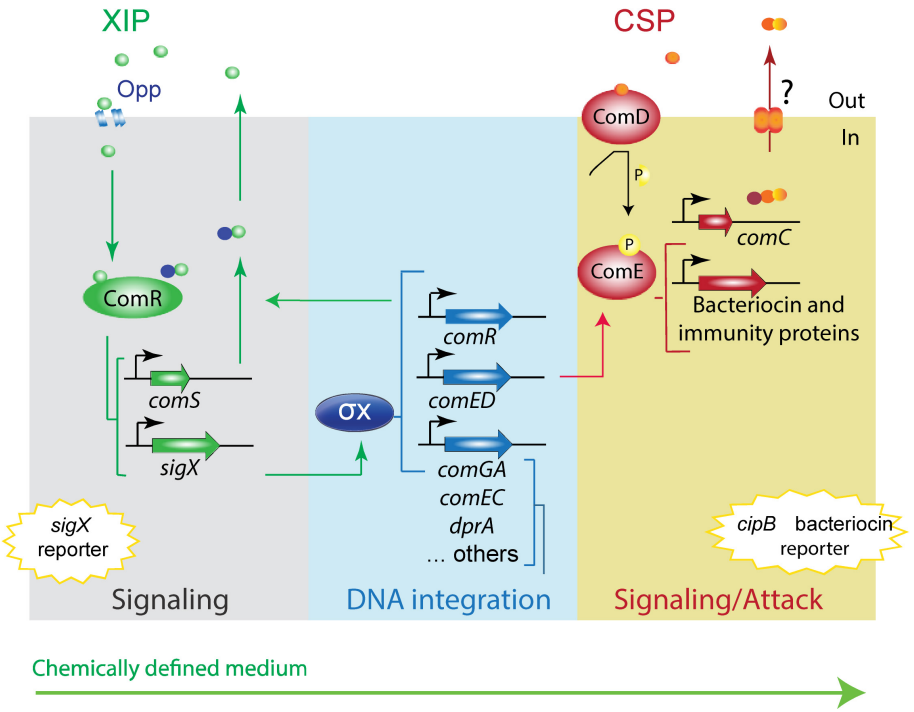

FIGURE 1 | Model of *S. mutans* XIP pheromone signaling pathway in peptide-free chemically defined medium. The model is based on the UA159 *S. mutans* strain. The *S. mutans* XIP pheromone is exported outside of the cells. Upon reaching a certain threshold, XIP is internalized via the Opp permease, and binds to the ComR regulator to activate *comS*, thus creating a positive feedback loop. ComS is the precursor of XIP but can also function in its unprocessed form as an internal signal to activate the ComR-pheromone signaling pathway. The ComR-pheromone complex activates *sigX*. This codes for the alternative sigma factor X (σX). σX is the master regulator of competence for natural transformation that regulates the expression of the streptococcal core set of genes involved in the competence response, most of them with functions that enable DNA acquisition and integration into its genome. σX induces also *comR* (Khan et al., 2017) and *comED* (Reck et al., 2015; Son et al., 2015; Khan et al., 2017). ComED is a two-component system comprising the histidine kinase ComD and the cognate response regulator ComE. ComD autophosphorylates upon CSP pheromone binding and transfers the phosphoryl group to ComE, which in turn induces the expression of bacteriocin and immunity proteins, including the gene for the non-lantibiotic bacteriocin *cipB*. In rich media, *cipB* expression is required for induction of *sigX* by an as yet unknown mechanism. In CDM, CSP induces the ComED pathway, but it is unknown whether the CSP pheromone system is endogenously activated. It is also unknown why in CDM *cipB* is stimulated by CSP, but not the competence response. The conservation of the CSP and XIP signaling pathways in CDM were examined in this study using *sigX* and *cipB* luciferase reporter bioassays.

was found in all tested strains, and transformation was found in all but one of the isolates grown in CDM. The results thus indicate the presence of a single *S. mutans* XIP pherogroup and suggest that *S. mutans* has a conserved ability to suppress CSP activity in CDM.

MATERIALS AND METHODS

Bacterial Strains and Media

The *Streptococcus mutans* strains used in this study and their relevant characteristics are listed in **Table 1**. The strains used in the study were selected from the collection of strains in our laboratory, representing strains known to be transformed (UA159, V403, OMZ175, LML-2, LML-4, GS5, NG8, BM71, LT11) and others in which genetic competence has not yet been characterized. Todd-Hewitt broth (THB; Becton Dickinson) was used to grow all the strains used for DNA extraction and DNA sequencing. Chemically Defined Medium (CDM) (Mashburn-Warren et al., 2010) was used to perform the genetic transformation assays and bioassay to measure the activity of exogenously added CSP in the supernatants of *S. mutans* and also to verify and quantify the concentration of extracellular native XIP in culture supernatants (Desai et al., 2012; Khan et al., 2012). The carbohydrate source was glucose at 1% final concentration, unless specified. The antibiotics erythromycin, kanamycin and spectinomycin were used at final concentrations of 10, 500, and 500 μg mL^{-1}, respectively. THB agar and THB agar supplemented with erythromycin were used to enumerate the total and transformed number of *S. mutans*.

Construction of Mutants

The deletion mutants were constructed using the PCR-ligation mutagenesis strategy (Lau et al., 2002). Sequence information was obtained from the *S. mutans* UA159 genome. Mutants with deletion of *sigX* and *htrA* were constructed. *Asc*I or *Fse*I sites were incorporated into the 5′-ends of the oligonucleotide primers and both ends of the resistance cassette. The kanamycin resistance cassette was amplified using primer pair FP001-FP068. The *comX* flanking regions were amplified with the primers pairs

TABLE 1 | Strains and plasmid used in this study.

Strain/plasmid	Relevant characteristics	References
***S. mutans* strains**		
UA159 [a]	Wild type, transformable strain, Erm^S	Murchison et al., 1986; Ajdic et al., 2002
LT 11	UA159 derivative, highly transformable	Tao et al., 1993; Petersen et al., 2005
BM71	Caries lesion isolate	Cvitkovitch et al., 1995
Ingbritt	Serotype c	Perch et al., 1974; Perry and Kuramitsu, 1981; Petersen and Scheie, 2000
OMZ 175[a]	Serotype f	Perch et al., 1974; Perry and Kuramitsu, 1981; Petersen and Scheie, 2000; Cornejo et al., 2013
UA130	Serotype c	Murchison et al., 1986; Petersen and Scheie, 2000
V403[a]	Serotype c; pVA403	Lindler and Macrina, 1986; Petersen and Scheie, 2000; Palmer et al., 2013
NG8	Serotype c	Knox et al., 1986
UAB90 (ATCC 31987)	Serotype c	
NCTC 10449[Ta]	Type strain	Coykendall, 1971; Perch et al., 1974; Song et al., 2013
KM1, 348, 357, 371, 388, 409, 415, 467, 503, 73A2, M1, M4, M6, GW2, GW37	Clinical isolates	Petersen and Scheie, 2000; Petersen et al., 2006
GS-5	serotype c	Perch et al., 1974; Waterhouse and Russell, 2006; Biswas and Biswas, 2012
LML-2, LML-4[a], LML-5[a], At10	Clinical isolates	Waterhouse and Russell, 2006; Cornejo et al., 2013
GUV-1	GS-5 derivative, fluoride resistant	van Loveren et al., 1993
CM7	Clinical isolate	
Serogroup C	Clinical isolate	
IB 78	Clinical isolate	
SM004	UA159:Δ*comC*:*kan*; Kan^R	Petersen et al., 2006
SM059	UA159:Φ(P_{cipB}-luc) Spc^R	Khan et al., 2012
SM066	UA159:Δ*comR*:*spc*; Spc^R; DNA source MW02 Mashburn-Warren et al., 2010	This study
SM067	UA159:Δ*oppD*:*spc*, Spc^R; DNA source MW04 Mashburn-Warren et al., 2010	This study
SM068	UA159: Φ(P_{sigX}-luc) Spc^R	Khan et al., 2012
SM091	UA159:Δ*comS*:*erm*; Φ(P_{sigX}-luc) Erm^R, Spc^R	Khan et al., 2012
SM121	UA159:Δ*sigX*:*kan*; Kan^R	This study
SM165	UA159: Δ*htrA*:*kan*; Kan^R	This study
Plasmid		
pVA838	Em^R; streptococcal replicative plasmid	Macrina et al., 1982
PCR amplicon		
aRJ02	Δ*dexA*:*kan*	Morrison et al., 2015

Erm, erythromycin; Spc, spectinomycin; Kan, kanamycin. [a]*Genome sequenced strains.* [T]*, type strain.*

FP462 (CTTGGTAGCAGGAGAGCAC), FP463 (AAAG CACAGCCTGCTTCAAT) and FP714 (TGCCGAACA CAGCAGTTAAG), FP715 (CATTCCCTCTTGTTGCCAAT). The *htrA* flanking regions were amplified with the primers pairs FP807 (TCCCTCCAATAACGAAGGTCA), FP808 (GGTAAGT GTTGA TATGACCCCT) and FP809 (GAAGGTAGCGTCTA TCAGCGA), FP810 (GCAGTCGAGGTTGATAGGGA). The resultant amplicons were digested with *Asc*I or *Fse*I whereas the kanamycin resistance cassette was digested with both enzymes. The upstream and downstream amplicons of target genes were ligated to the kanamycin cassette using T4 DNA ligase. The two ligated products were mixed and PCR amplified with distal primers. The resultant amplicons were used to transform *S. mutans*. Gene deletion was confirmed by PCR amplification and gel electrophoresis.

DNA Sequence Analysis

The chromosomal DNA of *S. mutans* strains were isolated as previously described (Petersen and Scheie, 2000). The primers FP678 (5′-ATGCGGAAGCTAAAAAGAGC-3′) and FP679 (5′-TCCAGTCTTCCTATCTGAGCAA-3′) were used to amplify a region of 431 bp, which contains the tRNA transcriptional terminator of *comR* (9 bp stem, a 4 nt loop and a T-rich region at the 3′ side of the stem-loop), the *comS* promoter and the *comS* sequence. First, a PCR was performed (20 μL reaction volume containing 2.5 mM $MgCl_2$, 2 pmol of each primer, 0.2 mM of each dNTP, 2 μL of 10× buffer, 50–100 ng of genomic DNA and 2 units of TaqDNA polymerase using a thermocycling profile of initial denaturing period of 3 min at 94°C; followed by 30 cycles of 30 s at 94°C, 30 s at 55°C and 2.5 min at 72°C; with a final extension period of 3 min at 72°C and the products were visualized on a 1% agarose gel to check the amplified fragments by the primers (Petersen and Scheie, 2000). The sequencing was performed bi-directionally in a single experiment for all the samples using BigDye® Terminator v1.1 Cycle Sequencing Kit (Applied Biosystems, Foster City, CA, United States) on an ABI 3730 DNA analyzer (Applied Biosystems, Foster City, CA, United States). All the sequence analysis was done using the Sequencher 5.0 software (Gene Codes, Ann Arbor, MI, United States). The electropherograms were checked and comparative analysis of the bidirectional sequences was performed using the *S. mutans* UA159 sequence as a reference.

Bioassay of CSP and XIP Activity in Culture Supernatants

The CSP bioassay was performed to measure the production of native CSP and activity of exogenously added CSP in the supernatants of *S. mutans* during growth, and the XIP bioassay was to verify and quantify the concentration of extracellular native XIP in culture supernatants. A P_{cipB}-luc reporter (SM059) was used in the CSP bioassay as previously described (Khan et al., 2012), and a P_{sigX}-luc reporter in a *comS* deletion background (SM091) was used to perform the XIP bioassay as described by Desai et al. (2012), with slight modifications (Khan et al., 2012).

To estimate CSP production and response, the supernatants were collected by 10× dilution of precultures at OD_{600} of 0.6 in CDM containing 10% bovine serum albumin (BSA). When added, 250 nM CSP concentration was used. Supernatants were collected for 6 h during growth. For XIP production and response, overnight cultures of *S. mutans* strains were diluted in fresh CDM to an optical density at 600 nm (OD_{600}) of 0.05 and incubated in air at 37°C. At each hour, from the second until the 10 h of bacterial growth, the OD_{600} was measured and 1 mL of the culture was centrifuged (10,000 *g* for 10 min at 4°C) to collect the supernatant. The indicator strains SM059 and SM091 were grown in CDM to an OD_{600} of 0.05 and stored in microcentrifuge tubes with 10% of glycerol at −80°C. The entire assay was performed with stock cultures from the same batch. The bioassay was performed adding 10 μL of each culture supernatant to 50 μL of the indicator strain, 40 μL fresh CDM and 20 μL of 1.0 mM D-luciferin (Synchem, Felsberg-Altenburg, Germany) in a flat-bottom 96-well plate (Nunc, Rochester, NY, United States). Luminescence was measured by reading the plates in a multidetection microplate reader (Synergy HT; BioTek Instruments, Winooski, VT, United States). To quantify the XIP concentrations in the culture supernatants, standard curves were performed at the same time, replacing the culture supernatant with 10 μL of CDM-standard solutions with different XIP concentrations. CDM without synthetic peptides was used to obtain background values that were subtracted from the sample values. For strains exhibiting no XIP activity in the supernatants, the experiment was repeated at least twice. The software SigmaPlot (version 12.0, Systat Software, Inc.) was used to calculate the XIP concentrations using the relative light unit (RLU) values.

Genetic Transformation

Overnight cultures of all *S. mutans* strains were diluted 1:10 in fresh CDM and incubated in 5% CO_2 at 37°C. The OD_{600} was followed until the cultures reached an absorbance value of 0.6, then 10% of glycerol was added and they were stored at −80°C. To perform the assay the stored cultures were diluted in fresh CDM 1:10 to an OD_{600} of 0.05 and incubated in air for 2 h at 37°C. The OD was measured and aliquots of 150 μL of the bacterial suspensions were transferred to 1.5 mL microcentrifuge tubes. The plasmid pVA838 (**Table 1**) was added to all tubes at a final concentration of 1 μg mL^{-1} and XIP was added in the experimental group at a final concentration of 1,000 nM. The samples were then incubated in air for an additional 4 h at 37°C, at which time the OD was measured again and the bacterial suspensions were serially diluted (up to 1 to 10^6) in PBS. The suspensions were plated in duplicate on THB agar and THB agar supplemented with erythromycin 10 μg mL^{-1}. The plates were incubated in 5% CO_2 for 48 h at 37°C before counting the colony-forming units (CFU). The number of genetically transformed cells was divided per total CFU to obtain the values for transformation frequency. Three independent experiments were performed to evaluate transformation in CDM.

In order to evaluate genetic transformation in the non-responsive strains, an independent experiment extending the incubation time to 10 h before plating was performed. In addition, at 6 h an extra load of pVA838 was added, which increased the final concentration to 2 μg mL^{-1}. For the remaining non-responsive strains, transformation was attempted using the 6.3 kb aRJ02 chromosomal PCR amplicon with a kanamycin marker, which is expected to have a higher sensitivity for detection of transformability (**Table 1**; Morrison et al., 2015; Salvadori et al., 2017).

Synthetic Pheromones

The synthetic XIP ($ComS_{11-17}$; GLDWWSL) (Mashburn-Warren et al., 2010; Khan et al., 2012) and the 18-CSP ($ComC_{26-43}$; SGSLSTFFRLFNRSFTQA) (Petersen et al., 2006) were synthesized by GenScript (GenScript Biotech Corporation, Piscataway, NJ, United States), both with an estimated purity of 98% (Khan et al., 2012). The stock solutions of both peptides were stored in small aliquots at −20°C. The final concentration used in the genetic transformation assays for XIP was 1,000 nM. For FRET-assays to investigate protease activity, the 18-CSP was synthesized using methoxycoumarin-acetic-acidyl (MCA) on the N-terminal and Lys-Dinitrophenyl on the C-terminal (Dnp) (MCA-SGSLSTFFRLFNRSFTQA-Dnp; GenScript). On cleavage of the peptide by potential proteases, the Dnp quencher separates from the MCA fluorophore. The fluorophore is then activated giving an increase in fluorescence.

FRET-18CSP Peptide Cleavage Reporter Assays

Growth in the Presence of FRET-18CSP

Pre-cultures of *S. mutans* were diluted in 2 mL CDM supplemented with 2% BSA to an OD_{600} of 0.04 to 0.05, and incubated at 37°C in air atmosphere to an OD_{600} of 0.06. The cultures were then distributed into the wells of a 96-well plate (115 μL in each well), and 5 μL of FRET-18CSP peptide was added (4 μM final concentration). The plate was incubated at 37°C in air, and fluorescence and optical density at 600 nm were measured at different time points during growth in a multi-detection microplate reader (Synergy, Cytation 3; excitation 325 nm, emission 392 nm).

Measurement of FRET-18CSP Cleavage in Culture Supernatants

Supernatants from *S. mutans* UA159 P_{cipB}-luc reporter (SM059) and Δ*htrA* (SM165) were collected by centrifugation (6000 *g* for 10 min at 4°C) at different time points during growth, corresponding to early, mid- and late exponential phases. The supernatants were then distributed into the wells of a 96-well plate (115 μL in each well), and 5 μL of FRET-18CSP peptide was added (4 μM final concentration). The plate was incubated at 37°C in air atmosphere for 1 h, and fluorescence was measured in a multi-detection microplate reader (Synergy, Cytation 3; excitation 325 nm, emission 392 nm). Supernatants without FRET-18CSP were used for detection of background fluorescence, which were then subtracted from the values in the tested samples exposed to FRET-18CSP.

RESULTS

Bioassay for CSP Detection in CDM

In this study we used a P_{cipB}luc reporter for detection of extracellular CSP activity, in CDM as previously described (Khan et al., 2012), except that high sensitivity was only achieved in the presence of BSA (**Figure 2A**). BSA was chosen because it is known to enhance competence of *S. mutans* in rich media (Ahn et al., 2006), and in *S. pneumoniae*, BSA prevents CSP proteolysis (Cassone et al., 2012).

The potency of CSP in inducing the activity of the *cipB* promoter was increased by approximately 33-fold in CDM supplemented with BSA compared with CDM alone (**Figure 2A**). BSA concentrations from 0.5 to 10% gave similar results (**Figure 2A**).

Failure of CSP to Induce *sigX* in CDM Was Independent of Carbohydrate Source

Since the induction of *cipB* was significantly enhanced in the presence of BSA, we decided to further examine the intriguing fact that CSP fails to stimulate *sigX* in CDM (Desai et al., 2012; Wenderska et al., 2012; Reck et al., 2015). Our hypothesis was that increased stimulation of the early response by CSP, as observed with BSA supplementation, would enable the activation of *sigX*, which is a late response in complex media. We used a similar bioassay as described above, but using the promoter of *sigX* linked to the luciferase gene instead. The results showed that CSP concentrations up to 1000 nM failed to induce the P_{sigX}luc reporter in CDM supplemented with BSA and glucose (**Figure 2B**).

Since the carbohydrate source, at least in complex media, has a large influence on the induction of *sigX* expression by CSP (Moye et al., 2016), we also investigated *sigX* expression in CDM supplemented with fructose and galactose (**Figures 2C,D**). CSP still failed in demonstrating *sigX* induction. Thus, although CSP induces strong expression of *cipB* in CDM supplemented with BSA and different sources of carbohydrate, it fails to induce the late response characterized by the induction of *sigX* expression at concentrations as high as 1000 nM.

Endogenous CSP Activity Was Not Detected in the Supernatants of *S. mutans*

Lack of endogenous CSP activity in the supernatants of *S. mutans* UA159 grown in CDM has been previously reported by our group (Khan et al., 2012). It is, however, unknown whether this is a conserved feature in the species. We investigated 6 other strains of *S. mutans*, and the *comC* deletion mutant SM004, for the CSP activity in their supernatants by growing them in CDM in the presence of BSA (**Figure 2E**). No *cipB*-inducing activity was detected in culture supernatants collected at early-, mid- or late- exponential phases of growth, thus indicating that the lack of extracellular CSP activity under such growth conditions may represent a conserved feature in *S. mutans*.

Suppression of CSP Activity During Growth in CDM

Supernatants of *S. mutans* cultures exposed to 250 nM synthetic CSP were collected at different time points during growth in CDM. CSP activity in the supernatants of *S. mutans* UA159 was measured by using the *cipB* luciferase reporter described above. Within the first 3 h, CSP had almost completely disappeared from the culture supernatants (**Figure 3A**).

Due to the recognizable role of CSP in the induction of competence, it was crucial to determine if the loss of CSP activity was dependent on the development of competence. For this, we investigated the CSP activity in the culture supernatants of UA159 deletion mutants for *sigX*, *oppD*, and *comR* (**Table 1**). In all of them, a dramatic reduction in activity of exogenously added CSP was observed (**Figure 3B**).

To determine whether such an inhibitory effect on CSP activity could be due to proteolytic cleavage, we supplemented the CDM medium with a FRET-18CSP reporter peptide (**Figure 3C**). We found that all three isogenic mutants (*sigX*, *oppD*, and *comR*) grown under such conditions promoted increase in fluorescence activity, as measured after 240 min incubation at 37°C (**Figure 3C**), thus suggesting that the ability of *S. mutans* to degrade CSP does not require expression of key elements of the competence regulon. We also examined the effect of inactivating the *htrA* gene coding for the *S. mutans* HtrA protease, which in *S. pneumoniae* inactivates the CSP and cleaves misfolded proteins. No reduction in CSP degradation was observed for the *htrA* mutant (**Figure 3C**). CSP activity was indeed slightly higher for the culture supernatants of the *htrA* mutant at mid- and late exponential phases of growth (**Figure 3D**).

Finally, we tested whether suppression of CSP activity is extended to other *S. mutans* strains. In all the strains tested, reduction in CSP activity was observed, though at different levels (**Figure 3E**). When grown in the presence of the FRET-18CSP reporter peptide, an increase in fluorescence was observed for all strains (**Figure 3F**). We conclude that *S. mutans* suppresses CSP activity during growth in CDM, and that the mechanisms involved are active in the absence of *htrA*, *sigX, comR* or *oppD*, indicating the involvement of competence-regulated independent factors. The potential proteolytic activity leading to CSP inactivation seems to be conserved in *S. mutans*.

XIP Activity Is Detected in the Culture Supernatants of Practically all *S. mutans* Strains Grown in CDM

S. mutans UA159 produces and responds to exogenous XIP in CDM (Mashburn-Warren et al., 2010; Desai et al., 2012). We investigated whether XIP production is conserved in *S. mutans*. We used the P_{sigX}luc Δ*comS* indicator (SM091) to estimate the XIP concentration in the supernatants of the different strains during growth. The minimum detection level was set at 10 nM, as determined by standard curve measurements using synthetic XIP. Our results showed the presence of extracellular XIP activity in all strains tested. The highest XIP concentrations in the supernatants of growing cultures ranged from approximately 200 to 26,000 nM (**Figure 4A**), with most showing XIP accumulation

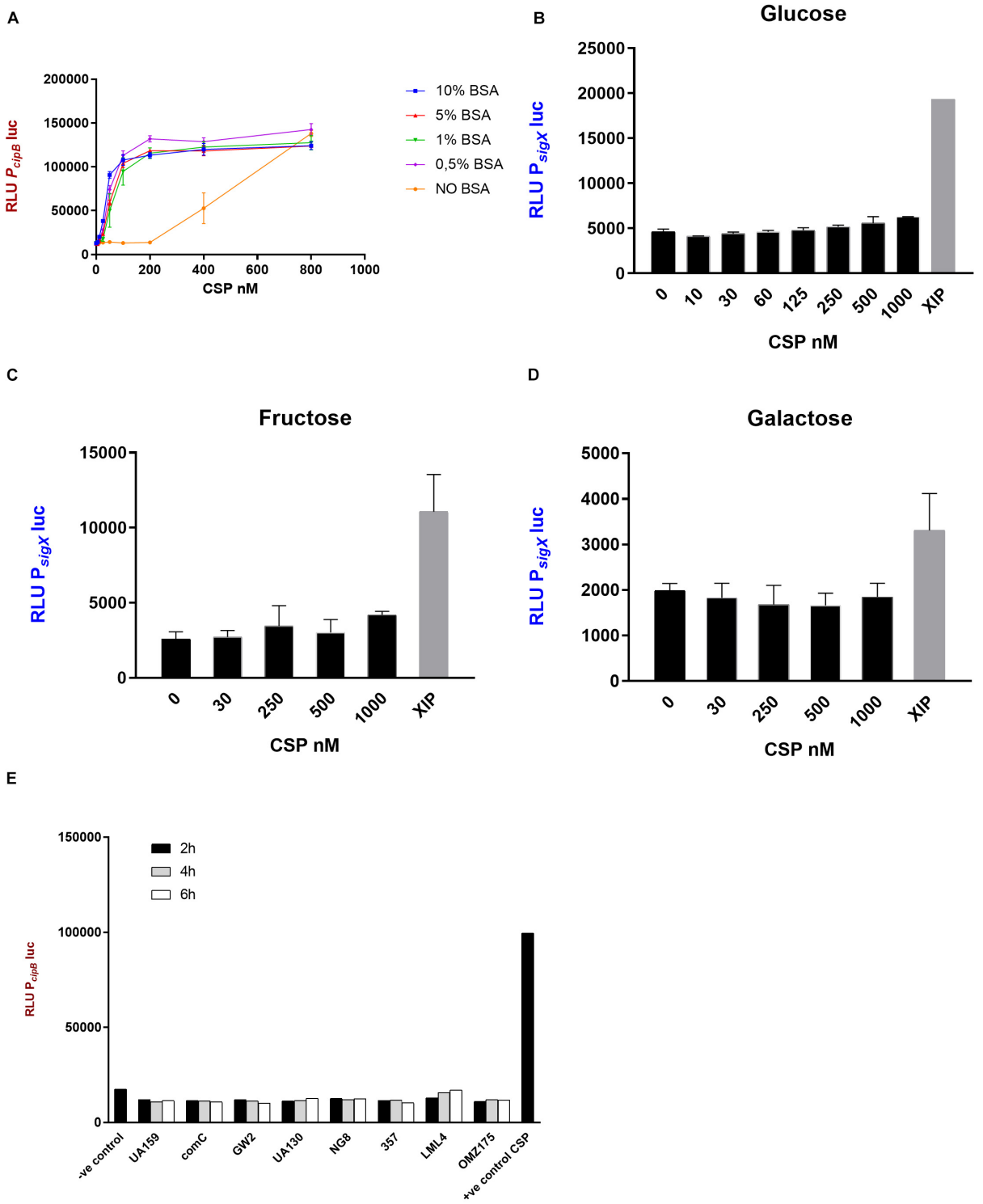

FIGURE 2 | CSP activity in CDM. **(A)** The indicator strain SM059 (P_{cipB}luc) was exposed to serial dilutions of synthetic CSP in the presence and absence of BSA. Different concentrations of BSA were tested. 10% BSA (blue), 5% BSA (red), 1% BSA (green), 0.5% BSA (pink), No BSA (orange). Bars correspond to standard errors of two to three independent experiments; RLU values were measured in a 96-well plate using a multi-detection microplate reader. **(B–D)** Activity of P_{sigX}luc was determined after addition of various concentrations of CSP and 1 μM XIP in CDM supplemented with **(B)** glucose, **(C)** fructose and **(D)** galactose. Mean and standard deviation for two independent experiments. **(E)** Supernatants were collected from different *S. mutans* strains at 2 h (black bars), 4 h (gray bars) and 6 h (white bars) growth in CDM and examined for CSP activity using SM059 (P_{cipB}luc) indicator strain. Medium alone was used as a negative control, and CSP (250 nM) was used as a positive control.

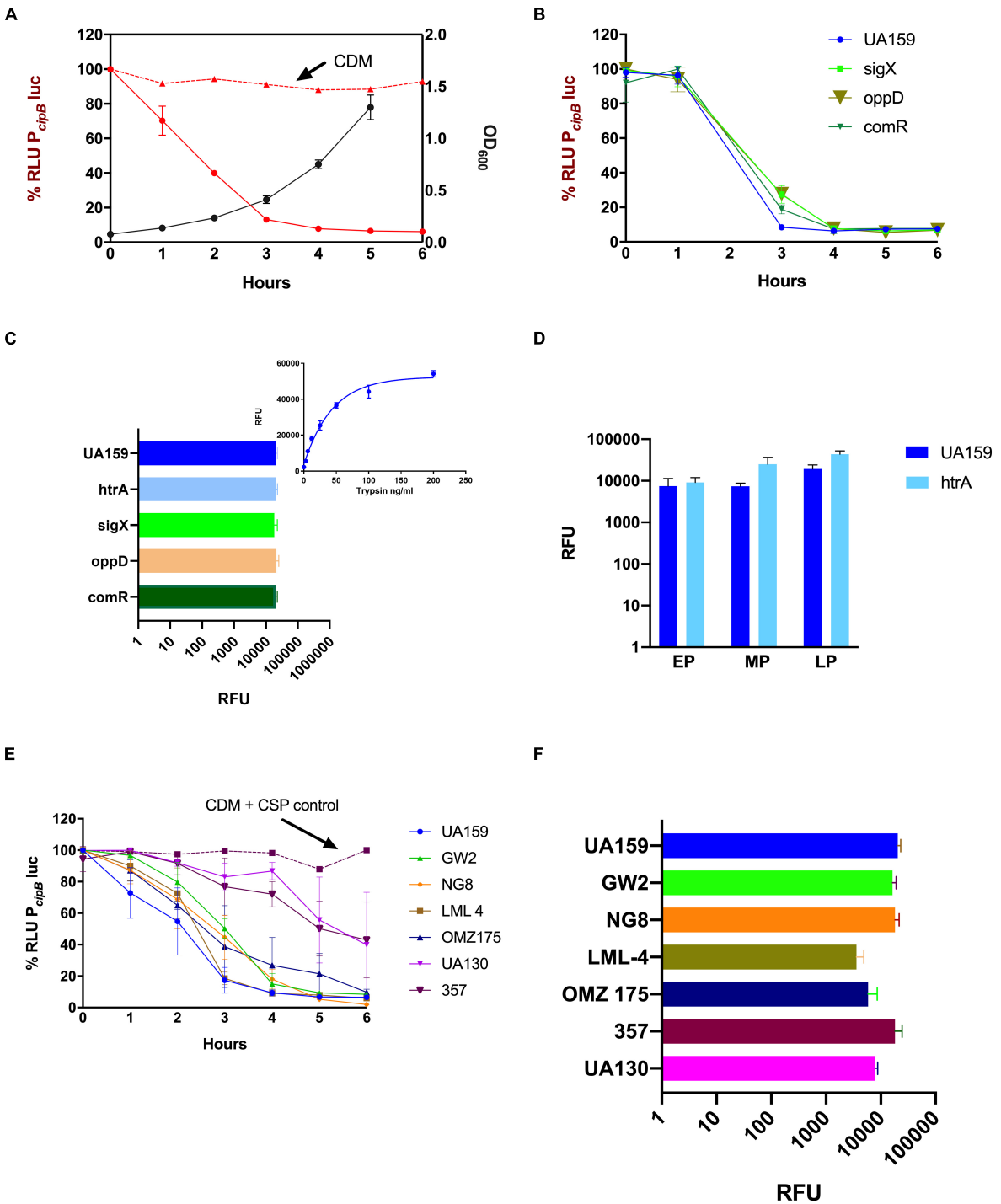

FIGURE 3 | Suppression of CSP activity during growth in CDM. Frozen stock cultures at OD_{600} 0.6 were diluted 10× in CDM containing 10% BSA, and 250 nM synthetic CSP **(A,B,E)** or 4 μM FRET-CSP **(C,D,F)**. **(A,B,E)** The P_{cipB}luc reporter was used to measure CSP concentration in the supernatants of different strains **(A)** *S. mutans* UA159 growth curve was measured at OD_{600} (black line) and indicates the time points when supernatants were collected. CSP activity in CDM alone (positive control) is represented by the red dashed line and in the supernatants of *S. mutans* UA159 by the red solid line. **(B)** Loss of CSP activity in the supernatants of UA159, Δ*sigX*, Δ*oppD* and Δ*comR*. **(C,F)** CSP cleavage measured at 240 min growth in the presence of the FRET-18CSP peptide, and recorded as relative fluorescence units (RFU) for panel **(C)** UA159, Δ*htrA*, Δ*sigX*, Δ*oppD*, and Δ*comR*, and **(F)** UA159, GW2, NG, LML-4, OMZ175, 357, and UA130. In panel **(C)**, right upper corner, a standard curve showing degradation of FRET-18CSP by trypsin is included as a reference. **(D)** FRET-18CSP proteolytic activity in supernatants of UA159 and the Δ*htrA* mutant collected at early (EP), mid- (MP) and late (LP) exponential phase of growth. RFU background values of the corresponding strains without FRET-CSP were subtracted. Error bars show standard error of mean from two to three independent experiments, with three parallels each.

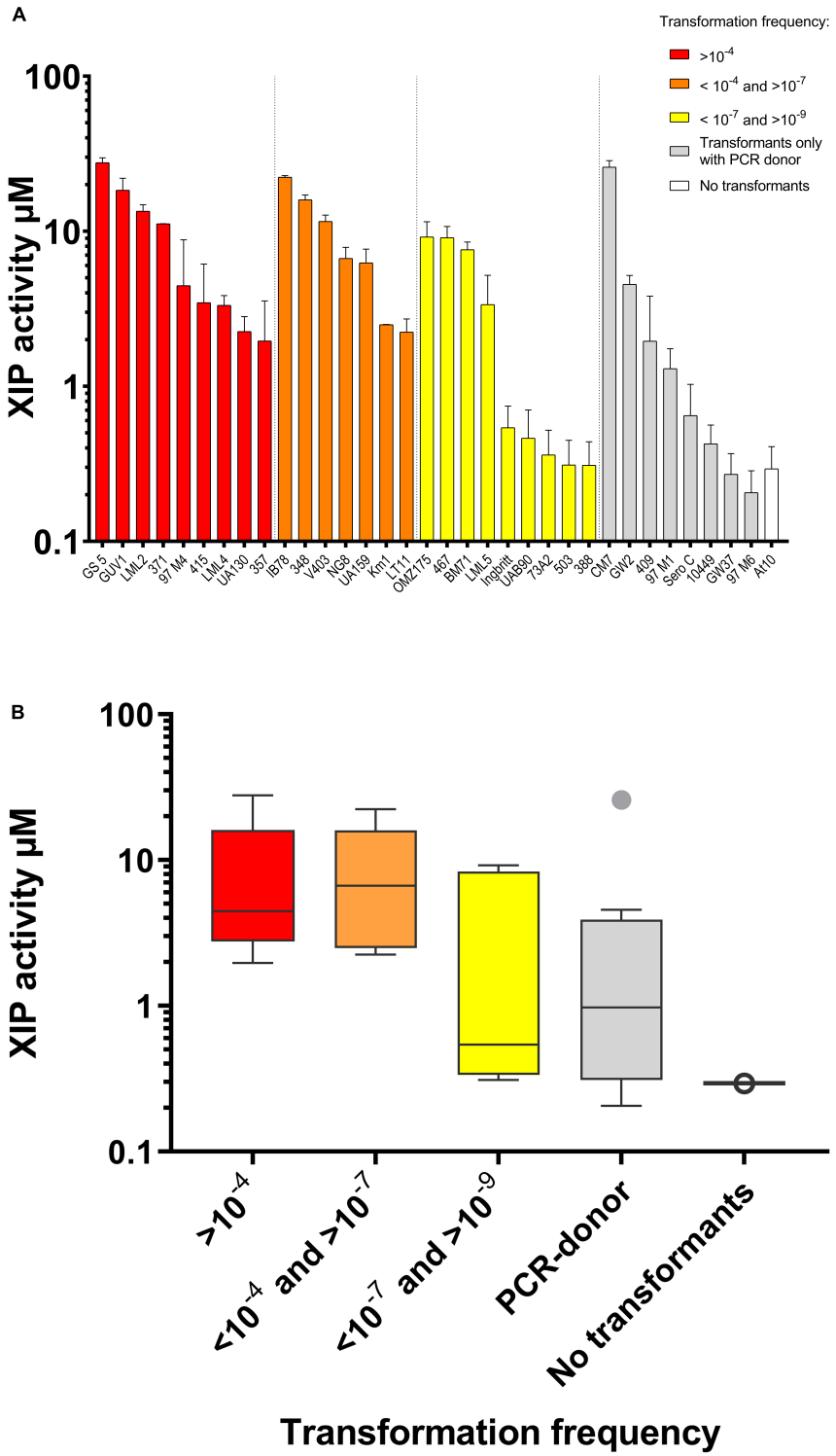

FIGURE 4 | Conservation of XIP production and transformation in CDM. Extracellular XIP concentration was measured in the supernatants collected from *S. mutans* strains grown overnight at 37°C in air. **(A)** Columns show average of XIP-equivalent concentration from three independent experiments. Bars correspond to standard error. The indicator strain used was a Δ*comS* P_{sigX}-luc reporter (SM091). Bars in different colors indicate transformation frequency in CDM supplemented with synthetic XIP by a plasmid donor (pVA838): (>10^{-4} in red, between 10^{-4} and 10^{-7} in orange, and between 10^{-7} and 10^{-8} in yellow). For those that were not transformed by the plasmid donor, transformation frequency with a 6.3 Kb PCR donor designed to be integrated into the chromosome by homologous recombination are shown (all frequencies below 10^{-7}; gray). Only At10 yielded no transformants (white). **(B)** Whisker plots showing the average of XIP activity of the strains shown in panel **(A)**, grouped according to transformation frequency.

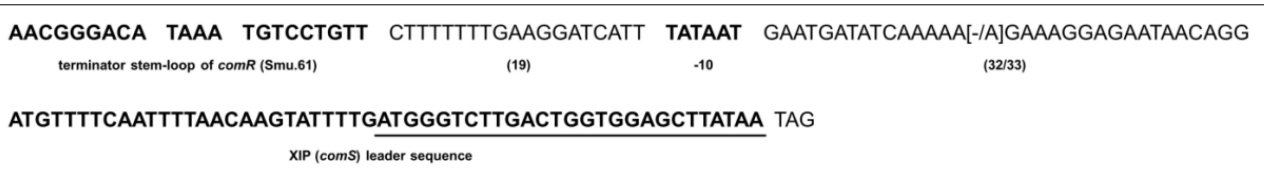

FIGURE 5 | Conservation of *comS* promoter and *comS* sequences in *S. mutans* strains. The first sequence in bold shows the terminator stem-loop of *comR* (Smu.61) thought to function as part of the *comS* promoter. Downstream the stem-loop is a 19 bp sequence, followed by the putative –10 element of the *comS* promoter distant 32 to 33 bases from the *comS* gene sequence shown in bold. Underlined is the sequence corresponding to the XIP functional heptapeptide ($ComS_{11-17}$ – GLDWWSL). Variable bases compared with *S. mutans* UA159 are in brackets.

starting at the mid-exponential growth phase and reaching maximal values at early stationary phase (data not shown). We conclude that the growth conditions that support extracellular XIP pheromone accumulation by UA159 may also sustain XIP production by a majority of the strains.

Thirty-Three Out of Thirty-Four Strains Were Naturally Transformable

Natural transformation without the addition of synthetic pheromone was detected in 23 of the 34 strains (data not shown). Because optimal levels of XIP may not be present at the time of competence under *in vitro* conditions, it was of interest to learn whether addition of synthetic XIP would result in higher transformation levels. Our results showed that synthetic XIP extended the range of transformed strains. Three of the strains with detectable XIP levels in the supernatants, including OMZ175, UAB90, and KM1 were transformed only upon addition of synthetic XIP. In the strains that were not transformed with the initial protocol, we increased the time during which they grew in the presence of synthetic XIP and donor DNA to 10 h, but even then no transformants were obtained (Murchison et al., 1986). We next used a more sensitive protocol based on the use of PCR large fragments as donor DNA (Morrison et al., 2015; Salvadori et al., 2017). With addition of the synthetic pheromone, 33 out of 34 strains were naturally transformable. Only strain At10 was not transformed, thus indicating that a majority of *S. mutans* are amenable to transformation. Overall, strains that exhibited lower transformation frequencies showed lower levels of XIP activity in their culture supernatants (**Figure 4B**).

The *comS* Gene Was Conserved in the 34 *S. mutans* Strains

The *S. mutans comS* gene encoding the XIP precursor is essential for competence development. Given the variability in transformation efficiency observed above, and that some strains were not amenable to transformation, we investigated whether the *comS* gene and its putative promoter sequences were conserved in the *S. mutans* strains included in the study. The results showed that *comS* was identical in all 34 strains (**Figure 5**). Highly conserved sequences were also found in the *comS* putative promoter. In this region the only difference in relation to UA159 was the presence or absence of an additional adenine between the −10 element and the *comS* translation initiation site. The additional adenine was present in 22 out of the 34 strains evaluated. In all the strains, *comS* was located 57–58 nt downstream of the tRNA transcriptional terminator of *comR* (SMU_61) and the putative −10 element was 32–33 nt upstream of the *comS* translation initiation site. While this study was being performed, new genomic sequences for 78 more strains of *S. mutans* were made available on public databases (Maruyama et al., 2009). In order to compare our results with the new genomic sequences we ran BLAST using the sequence shown in **Figure 5** against the CoGe database[1] (Lyons et al., 2011). The *comS* sequences in these strains were identical to the *S. mutans* UA159. In the *comS* promoter the sequences varied in only a single base pair at the same position as that observed in 22 of the strains sequenced in our study. Taken together the results indicate that the *comS* gene and promoter regions are highly conserved in the *S. mutans* strains analyzed, suggesting that variations in transformation levels and XIP production are not correlated with differences in this region.

DISCUSSION

In complex media, the CSP pheromone triggers the expression of bacteriocin-related genes, followed by a late response characterized by increased expression of the XIP-encoding gene *comS* and competence development (Kreth et al., 2005; Lemme et al., 2011; Khan et al., 2016). The mechanisms leading to activation of *comS* expression and competence remain unknown. It is also still unknown why CSP fails in stimulating competence in peptide-free defined medium. It has been suggested that *S. mutans* may perhaps produce a protease that, similar to the HtrA protease in *S. pneumoniae*, could inactivate the CSP (Desai et al., 2012). This possible explanation did not seem to match with the later finding that CSP is actually active in CDM, in that it can stimulate *cipB* and all other genes regulated by ComED (Reck et al., 2015). Our results show that *S. mutans* can indeed inactivate CSP by a mechanism that most probably involves proteolysis, given the results obtained with the FRET-18CSP reporter peptide. We confirmed previous results that CSP induces *cipB* (Reck et al., 2015) and found that a CSP concentration as low as 1 nM in the presence of BSA was sufficient to activate the early bacteriocin response. This is opposite to the CSP concentration to activate *sigX*, which

[1]http://genomevolution.org/CoGe/CoGeBlast.pl

requires values that exceed the maximum concentration used in this study (1000 nM) (data not shown). A higher threshold for *sigX* activation by CSP has also been observed in complex media (Son et al., 2012). A question that remains is why the threshold of CSP concentration to activate *sigX*, and therefore competence, is higher than for *cipB* activation, when CipB is thought to be the main link of CSP to *sigX* activation. One possibility is that at high concentrations CSP may activate or repress other two-component systems than ComED, which would then trigger a different link to competence. It is a well known phenomenon that although pheromones are usually highly specific to their cognate receptors, at high concentrations they may bind to other non-specific receptors (Hawver et al., 2016). However, several other mechanisms are possible, since the competence system is part of a signaling network of high complexity, affected by a variety of other systems not directly regulated by ComED, as recently reviewed (Kaspar and Walker, 2019). Irrespective of the mechanism, the higher threshold for CSP to induce competence indicates that CSP degradation may affect the competence response to this pheromone.

Inactivation of the *S. mutans* CSP by proteases produced by other streptococcal species has been known for more than 10 years (Wang and Kuramitsu, 2005). However, this is the first indication that *S. mutans* can also inhibit the activity of its own CSP, most probably via proteolytic activity. The genomes of *S. mutans* have more than 65 known or putative proteases, according to the MEROPS database[2], but only HtrA has shown a role in autologous CSP cleavage. However, unlike for *S. pneumoniae* (Cassone et al., 2012), the HtrA protease in *S. mutans* was not required for CSP inactivation.

In *S. pneumoniae*, luciferase and *gfp* reporter strains for CSP activity have been successfully used to identify pneumococcal CSP pheromones in culture supernatants (Moreno-Gamez et al., 2017). Also in the seminal study that identified the *S. pneumoniae* competence factor, the CSP was isolated and purified from the supernatant (Havarstein et al., 1995). In *S. mutans* UA159 grown in complex medium, endogenous CSP has been identified by mass spectrometry in the supernatant fraction (Hossain and Biswas, 2012). Based on these findings, we hypothesized that if *S. mutans* produces CSP in CDM, we would probably be able to detect it in its culture supernatant. However, despite the high sensitivity of the protocol used in the present study, we could not detect any CSP-inducing activity in the supernatants of the different strains tested. Thus, if CSP is produced, it is either rapidly degraded outside of the cells or it remains associated with the cells.

In contrast to CSP, endogenous XIP activity was present in the supernatants of most strains. Moreover, activation of the XIP system in CDM enabled transformation of all but one of the 34 strains tested. The *comS* gene encoding the pre-processed form of XIP was indeed found in all the strains, which is in line with the results of a recent study reporting *comS* as part of the *S. mutans* core genome (Cornejo et al., 2013). In general, higher levels of XIP detection in the supernatants correlated with increased transformability. Of note, some strains that produced high concentrations of endogenous XIP needed to be stimulated by synthetic XIP to transform. This was, however, not surprising, given the fact that maximum concentrations were in most cases observed only close to the stationary phase, which is a period during which competence under laboratory conditions is already shut off. For some of the strains that produced low levels of XIP, transformation was only detected by using a large PCR amplicon as DNA donor, which is known to result in increased recovery of transformants (Morrison et al., 2015; Junges et al., 2017).

Taken together, our results indicate that the XIP system is conserved in *S. mutans*, and that all *S. mutans* strains may belong to a single pherotype. Moreover, the conserved ability of *S. mutans* to cleave CSP under conditions that favor accumulation of XIP may provide an adaptive advantage to *S. mutans*, by allowing them to fine-tune competence and bacteriocin responses in response to environmental changes. While the knowledge on pheromone signaling for any species is mostly based on models derived from limited selected strains, understanding how the system works in different strains of a species is of high relevance for the development of strategies aiming at interfering with their communication systems.

DATA AVAILABILITY

All datasets generated for this study are included in the manuscript and or supplementary files.

AUTHOR CONTRIBUTIONS

All authors conceptualized the manuscript, drafted and critically revised the manuscript and approved the final version of the manuscript for publication.

FUNDING

This work was supported in part by the Coordenação de Aperfeiçoamento de Pessoal de Nível Superior - Brasil (CAPES) - Finance Code 001 (AR postdoctoral grant), and by the program International Partnership for Outstanding Education, Research, and Innovation (INTPART), RCN grant number 274867.

ACKNOWLEDGMENTS

We thank Andreas Podbielski for the kind gift of pFW5-luc and Roy Russel for providing the *S. mutans* strains LML-2, LML-4, LML-5, and At10. We are grateful to Anne Karin Kristoffersen for helpful assistance in DNA sequence analysis.

[2] https://www.ebi.ac.uk/merops/index.shtml

REFERENCES

Ahn, S. J., Wen, Z. T., and Burne, R. A. (2006). Multilevel control of competence development and stress tolerance in *Streptococcus mutans* UA159. *Infect. Immun.* 74, 1631–1642. doi: 10.1128/iai.74.3.1631-1642.2006

Ajdic, D., Mcshan, W. M., Mclaughlin, R. E., Savic, G., Chang, J., Carson, M. B., et al. (2002). Genome sequence of *Streptococcus mutans* UA159, a cariogenic dental pathogen. *Proc. Natl. Acad. Sci. U.S.A.* 99, 14434–14439. doi: 10.1073/pnas.172501299

Biswas, S., and Biswas, I. (2012). Complete genome sequence of *Streptococcus mutans* GS-5, a serotype c strain. *J. Bacteriol.* 194, 4787–4788. doi: 10.1128/JB.01106-12

Cassone, M., Gagne, A. L., Spruce, L. A., Seeholzer, S. H., and Sebert, M. E. (2012). The HtrA protease from *Streptococcus pneumoniae* digests both denatured proteins and the competence-stimulating peptide. *J. Biol. Chem.* 287, 38449–38459. doi: 10.1074/jbc.M112.391482

Cornejo, O. E., Lefebure, T., Bitar, P. D., Lang, P., Richards, V. P., Eilertson, K., et al. (2013). Evolutionary and population genomics of the cavity causing bacteria *Streptococcus mutans*. *Mol. Biol. Evol.* 30, 881–893. doi: 10.1093/molbev/mss278

Coykendall, A. L. (1971). Genetic heterogeneity in *Streptococcus mutans*. *J. Bacteriol.* 106, 192–196.

Cvitkovitch, D. G., Boyd, D. A., Thevenot, T., and Hamilton, I. R. (1995). Glucose transport by a mutant of *Streptococcus mutans* unable to accumulate sugars via the phosphoenolpyruvate phosphotransferase system. *J. Bacteriol.* 177, 2251–2258. doi: 10.1128/jb.177.9.2251-2258.1995

Desai, K., Mashburn-Warren, L., Federle, M. J., and Morrison, D. A. (2012). Development of competence for genetic transformation by *Streptococcus mutans* in a chemically defined medium. *J. Bacteriol.* 194, 3774–3780. doi: 10.1128/JB.00337-12

Dufour, D., Cordova, M., Cvitkovitch, D. G., and Levesque, C. M. (2011). Regulation of the competence pathway as a novel role associated with a streptococcal bacteriocin. *J. Bacteriol.* 193, 6552–6559. doi: 10.1128/JB.05968-11

Federle, M. J., and Morrison, D. A. (2012). One if by land, two if by sea: signalling to the ranks with CSP and XIP. *Mol. Microbiol.* 86, 241–245. doi: 10.1111/mmi.12029

Fleuchot, B., Gitton, C., Guillot, A., Vidic, J., Nicolas, P., Besset, C., et al. (2011). Rgg proteins associated with internalized small hydrophobic peptides: a new quorum-sensing mechanism in streptococci. *Mol. Microbiol.* 80, 1102–1119. doi: 10.1111/j.1365-2958.2011.07633.x

Fontaine, L., Boutry, C., De Frahan, M. H., Delplace, B., Fremaux, C., Horvath, P., et al. (2010). A novel pheromone quorum-sensing system controls the development of natural competence in *Streptococcus thermophilus* and *Streptococcus salivarius*. *J. Bacteriol.* 192, 1444–1454. doi: 10.1128/JB.01251-09

Gardan, R., Besset, C., Guillot, A., Gitton, C., and Monnet, V. (2009). The oligopeptide transport system is essential for the development of natural competence in *Streptococcus thermophilus* strain LMD-9. *J. Bacteriol.* 191, 4647–4655. doi: 10.1128/JB.00257-09

Gaustad, P., and Morrison, D. A. (1998). Induction of transformation in streptococci by synthetic competence stimulating peptides. *Methods Cell Sci.* 20, 65–70. doi: 10.1007/978-94-017-2258-2_7

Havarstein, L. S., Coomaraswamy, G., and Morrison, D. A. (1995). An unmodified heptadecapeptide pheromone induces competence for genetic transformation in *Streptococcus pneumoniae*. *Proc. Natl. Acad. Sci. U.S.A.* 92, 11140–11144. doi: 10.1073/pnas.92.24.11140

Hawver, L. A., Jung, S. A., and Ng, W. L. (2016). Specificity and complexity in bacterial quorum-sensing systems. *FEMS Microbiol. Rev.* 40, 738–752. doi: 10.1093/femsre/fuw014

Hossain, M. S., and Biswas, I. (2012). An extracelluar protease, sepm, generates functional competence-stimulating peptide in *Streptococcus mutans* UA159. *J. Bacteriol.* 194, 5886–5896. doi: 10.1128/JB.01381-12

Hung, D. C., Downey, J. S., Ayala, E. A., Kreth, J., Mair, R., Senadheera, D. B., et al. (2011). Characterization of DNA binding sites of the ComE response regulator from *Streptococcus mutans*. *J. Bacteriol.* 193, 3642–3652. doi: 10.1128/JB.00155-11

Johnsborg, O., Eldholm, V., and Havarstein, L. S. (2007). Natural genetic transformation: prevalence, mechanisms and function. *Res. Microbiol.* 158, 767–778. doi: 10.1016/j.resmic.2007.09.004

Johnston, C., Martin, B., Fichant, G., Polard, P., and Claverys, J. P. (2014). Bacterial transformation: distribution, shared mechanisms and divergent control. *Nat. Rev. Microbiol.* 12, 181–196. doi: 10.1038/nrmicro3199

Junges, R., Khan, R., Tovpeko, Y., Amdal, H. A., Petersen, F. C., and Morrison, D. A. (2017). Markerless genome editing in competent streptococci. *Methods Mol. Biol.* 1537, 233–247. doi: 10.1007/978-1-4939-6685-1_14

Kaspar, J., Underhill, S. A. M., Shields, R. C., Reyes, A., Rosenzweig, S., Hagen, S. J., et al. (2017). Intercellular communication via the comX-inducing peptide (XIP) of *Streptococcus mutans*. *J. Bacteriol.* 199:e00404-17. doi: 10.1128/JB.00404-17

Kaspar, J. R., and Walker, A. R. (2019). Expanding the vocabulary of peptide signals in *Streptococcus mutans*. *Front. Cell Infect. Microbiol.* 9:194. doi: 10.3389/fcimb.2019.00194

Khan, R., Junges, R., Amdal, H. A., Chen, T., Morrison, D. A., and Petersen, F. C. (2017). A positive feedback loop mediated by sigma X enhances expression of the streptococcal regulator ComR. *Sci. Rep.* 7:5984. doi: 10.1038/s41598-017-04768-5

Khan, R., Rukke, H. V., Hovik, H., Amdal, H. A., Chen, T., Morrison, D. A., et al. (2016). Comprehensive transcriptome profiles of *Streptococcus mutans* UA159 map core streptococcal competence genes. *mSystems* 1:e00038-15.

Khan, R., Rukke, H. V., Ricomini Filho, A. P., Fimland, G., Arntzen, M. O., Thiede, B., et al. (2012). Extracellular identification of a processed type II ComR/ComS pheromone of *Streptococcus mutans*. *J. Bacteriol.* 194, 3781–3788. doi: 10.1128/JB.00624-12

Knox, K. W., Hardy, L. N., and Wicken, A. J. (1986). Comparative studies on the protein profiles and hydrophobicity of strains of *Streptococcus mutans* serotype c. *J. Gen. Microbiol.* 132, 2541–2548. doi: 10.1099/00221287-132-9-2541

Kreth, J., Hung, D. C., Merritt, J., Perry, J., Zhu, L., Goodman, S. D., et al. (2007). The response regulator ComE in *Streptococcus mutans* functions both as a transcription activator of mutacin production and repressor of CSP biosynthesis. *Microbiology* 153, 1799–1807. doi: 10.1099/mic.0.2007/005975-0

Kreth, J., Merritt, J., Shi, W., and Qi, F. (2005). Co-ordinated bacteriocin production and competence development: a possible mechanism for taking up DNA from neighbouring species. *Mol. Microbiol.* 57, 392–404. doi: 10.1111/j.1365-2958.2005.04695.x

Lau, P. C., Sung, C. K., Lee, J. H., Morrison, D. A., and Cvitkovitch, D. G. (2002). PCR ligation mutagenesis in transformable streptococci: application and efficiency. *J. Microbiol. Methods* 49, 193–205. doi: 10.1016/s0167-7012(01)00369-4

Lemme, A., Grobe, L., Reck, M., Tomasch, J., and Wagner-Dobler, I. (2011). Subpopulation-specific transcriptome analysis of competence-stimulating-peptide-induced *Streptococcus mutans*. *J. Bacteriol.* 193, 1863–1877. doi: 10.1128/JB.01363-10

Li, Y. H., Lau, P. C., Lee, J. H., Ellen, R. P., and Cvitkovitch, D. G. (2001). Natural genetic transformation of *Streptococcus mutans* growing in biofilms. *J. Bacteriol.* 183, 897–908. doi: 10.1128/jb.183.3.897-908.2001

Lindler, L. E., and Macrina, F. L. (1986). Characterization of genetic transformation in *Streptococcus mutans* by using a novel high-efficiency plasmid marker rescue system. *J. Bacteriol.* 166, 658–665. doi: 10.1128/jb.166.2.658-665.1986

Lyons, E., Freeling, M., Kustu, S., and Inwood, W. (2011). Using genomic sequencing for classical genetics in *E. coli* K12. *PLoS One* 6:e16717. doi: 10.1371/journal.pone.0016717

Macrina, F. L., Tobian, J. A., Jones, K. R., Evans, R. P., and Clewell, D. B. (1982). A cloning vector able to replicate in *Escherichia coli* and *Streptococcus sanguis*. *Gene* 19, 345–353. doi: 10.1016/0378-1119(82)90025-7

Marsh, P. D., Moter, A., and Devine, D. A. (2011). Dental plaque biofilms: communities, conflict and control. *Periodontol* 2000, 16–35. doi: 10.1111/j.1600-0757.2009.00339.x

Maruyama, F., Kobata, M., Kurokawa, K., Nishida, K., Sakurai, A., Nakano, K., et al. (2009). Comparative genomic analyses of *Streptococcus mutans* provide insights into chromosomal shuffling and species-specific content. *BMC Genomics* 10:358. doi: 10.1186/1471-2164-10-358

Mashburn-Warren, L., Morrison, D. A., and Federle, M. J. (2010). A novel double-tryptophan peptide pheromone controls competence in *Streptococcus* spp. via an Rgg regulator. *Mol. Microbiol.* 78, 589–606. doi: 10.1111/j.1365-2958.2010.07361.x

Moreno-Gamez, S., Sorg, R. A., Domenech, A., Kjos, M., Weissing, F. J., Van Doorn, G. S., et al. (2017). Quorum sensing integrates environmental cues, cell density and cell history to control bacterial competence. *Nat. Commun.* 8:854. doi: 10.1038/s41467-017-00903-y

Morrison, D. A., Guedon, E., and Renault, P. (2013). Competence for natural genetic transformation in the *Streptococcus bovis* group streptococci *S. infantarius* and *S. macedonicus*. *J. Bacteriol.* 195, 2612–2620. doi: 10.1128/JB.00230-13

Morrison, D. A., Khan, R., Junges, R., Amdal, H. A., and Petersen, F. C. (2015). Genome editing by natural genetic transformation in *Streptococcus mutans*. *J. Microbiol. Methods* 119, 134–141. doi: 10.1016/j.mimet.2015.09.023

Moye, Z. D., Son, M., Rosa-Alberty, A. E., Zeng, L., Ahn, S. J., Hagen, S. J., et al. (2016). Effects of carbohydrate source on genetic competence in *Streptococcus mutans*. *Appl. Environ. Microbiol.* 82, 4821–4834. doi: 10.1128/AEM.01205-16

Murchison, H. H., Barrett, J. F., Cardineau, G. A., and Curtiss, R. III. (1986). Transformation of *Streptococcus mutans* with chromosomal and shuttle plasmid (pYA629) DNAs. *Infect. Immun.* 54, 273–282.

Palmer, S. R., Miller, J. H., Abranches, J., Zeng, L., Lefebure, T., Richards, V. P., et al. (2013). Phenotypic heterogeneity of genomically-diverse isolates of *Streptococcus mutans*. *PLoS One* 8:e61358. doi: 10.1371/journal.pone.0061358

Perch, B., Kjems, E., and Ravn, T. (1974). Biochemical and serological properties of *Streptococcus mutans* from various human and animal sources. *Acta Pathol. Microbiol. Scand. B Microbiol. Immunol.* 82, 357–370. doi: 10.1111/j.1699-0463.1974.tb02338.x

Perry, D., and Kuramitsu, H. K. (1981). Genetic transformation of *Streptococcus mutans*. *Infect. Immun.* 32, 1295–1297.

Petersen, F. C., Fimland, G., and Scheie, A. A. (2006). Purification and functional studies of a potent modified quorum-sensing peptide and a two-peptide bacteriocin in *Streptococcus mutans*. *Mol. Microbiol.* 61, 1322–1334. doi: 10.1111/j.1365-2958.2006.05312.x

Petersen, F. C., and Scheie, A. A. (2000). Genetic transformation in *Streptococcus mutans* requires a peptide secretion-like apparatus. *Oral. Microbiol. Immunol.* 15, 329–334. doi: 10.1034/j.1399-302x.2000.150511.x

Petersen, F. C., and Scheie, A. A. (2010). Natural transformation of oral streptococci. *Methods Mol. Biol.* 666, 167–180. doi: 10.1007/978-1-60761-820-1_12

Petersen, F. C., Tao, L., and Scheie, A. A. (2005). DNA binding-uptake system: a link between cell-to-cell communication and biofilm formation. *J. Bacteriol.* 187, 4392–4400. doi: 10.1128/jb.187.13.4392-4400.2005

Peterson, S. N., Sung, C. K., Cline, R., Desai, B. V., Snesrud, E. C., Luo, P., et al. (2004). Identification of competence pheromone responsive genes in *Streptococcus pneumoniae* by use of DNA microarrays. *Mol. Microbiol.* 51, 1051–1070. doi: 10.1046/j.1365-2958.2003.03907.x

Reck, M., Tomasch, J., and Wagner-Dobler, I. (2015). The alternative sigma factor sigX controls bacteriocin synthesis and competence, the two quorum sensing regulated traits in *Streptococcus mutans*. *PLoS Genet.* 11:e1005353. doi: 10.1371/journal.pgen.1005353

Salvadori, G., Junges, R., Khan, R., Amdal, H. A., Morrison, D. A., and Petersen, F. C. (2017). Natural transformation of oral streptococci by use of synthetic pheromones. *Methods Mol. Biol.* 1537, 219–232. doi: 10.1007/978-1-4939-6685-1_13

Son, M., Ahn, S. J., Guo, Q., Burne, R. A., and Hagen, S. J. (2012). Microfluidic study of competence regulation in *Streptococcus mutans*: environmental inputs modulate bimodal and unimodal expression of comX. *Mol. Microbiol.* 86, 258–272. doi: 10.1111/j.1365-2958.2012.08187.x

Son, M., Shields, R. C., Ahn, S. J., Burne, R. A., and Hagen, S. J. (2015). Bidirectional signaling in the competence regulatory pathway of *Streptococcus mutans*. *FEMS Microbiol. Lett.* 362:fnv159. doi: 10.1093/femsle/fnv159

Song, L., Wang, W., Conrads, G., Rheinberg, A., Sztajer, H., Reck, M., et al. (2013). Genetic variability of mutans streptococci revealed by wide whole-genome sequencing. *BMC Genomics* 14:430. doi: 10.1186/1471-2164-14-430

Tao, L., Macalister, T. J., and Tanzer, J. M. (1993). Transformation efficiency of EMS-induced mutants of *Streptococcus mutans* of altered cell shape. *J. Dent. Res.* 72, 1032–1039. doi: 10.1177/00220345930720060701

Underhill, S. A. M., Shields, R. C., Kaspar, J. R., Haider, M., Burne, R. A., and Hagen, S. J. (2018). Intracellular signaling by the comRS system in *Streptococcus mutans* genetic competence. *mSphere* 4:e00042-19.

van der Ploeg, J. R. (2005). Regulation of bacteriocin production in *Streptococcus mutans* by the quorum-sensing system required for development of genetic competence. *J. Bacteriol.* 187, 3980–3989. doi: 10.1128/jb.187.12.3980-3989.2005

van Loveren, C., Buijs, J. F., and Ten Cate, J. M. (1993). Protective effect of topically applied fluoride in relation to fluoride sensitivity of *mutans Streptococci*. *J Dent Res* 72, 1184–1190. doi: 10.1177/00220345930720080401

Wang, B. Y., and Kuramitsu, H. K. (2005). Interactions between oral bacteria: inhibition of *Streptococcus mutans* bacteriocin production by *Streptococcus gordonii*. *Appl. Environ. Microbiol.* 71, 354–362. doi: 10.1128/aem.71.1.354-362.2005

Waterhouse, J. C., and Russell, R. R. (2006). Dispensable genes and foreign DNA in *Streptococcus mutans*. *Microbiology* 152, 1777–1788. doi: 10.1099/mic.0.28647-0

Ween, O., Gaustad, P., and Havarstein, L. S. (1999). Identification of DNA binding sites for ComE, a key regulator of natural competence in *Streptococcus pneumoniae*. *Mol. Microbiol.* 33, 817–827. doi: 10.1046/j.1365-2958.1999.01528.x

Wenderska, I. B., Lukenda, N., Cordova, M., Magarvey, N., Cvitkovitch, D. G., and Senadheera, D. B. (2012). A novel function for the competence inducing peptide, XIP, as a cell death effector of *Streptococcus mutans*. *FEMS Microbiol. Lett.* 336, 104–112. doi: 10.1111/j.1574-6968.2012.02660.x

Conflict of Interest Statement: The authors declare that the research was conducted in the absence of any commercial or financial relationships that could be construed as a potential conflict of interest.

frontiers in Microbiology

ORIGINAL RESEARCH
published: 18 September 2019
doi: 10.3389/fmicb.2019.02108

Nitric Oxide Enters Quorum Sensing via the H-NOX Signaling Pathway in *Vibrio parahaemolyticus*

*Takahiro Ueno[1], Jonathan T. Fischer[1] and Elizabeth M. Boon[1,2]**

[1] Department of Chemistry, Stony Brook University, Stony Brook, NY, United States, [2] Institute of Chemical Biology & Drug Discovery, Stony Brook University, Stony Brook, NY, United States

Nitric oxide (NO) plays a major role in the regulation of mammalian biological functions. In recent years, NO has also been implicated in bacterial life cycles, including in the regulation of biofilm formation, and the metabolism of the bacterial second messenger signaling molecule cyclic-di-GMP. In a previous study, we reported the discovery of an NO-responsive quorum sensing (QS) circuit in *Vibrio harveyi*. Here, we characterize the homologous QS pathway in *Vibrio parahaemolyticus*. Spectroscopic analysis shows *V. parahaemolyticus* H-NOX is an NO sensory protein that binds NO in 5/6-coordinated mixed manner. Further, we demonstrate that through ligation to H-NOX, NO inhibits the autophosphorylation activity of an H-NOX-associated histidine kinase (HqsK; H-NOX-associated quorum sensing kinase) that transfers phosphate to the Hpt (histidine-containing phosphotransfer protein) protein LuxU. Indeed, among the three Hpt proteins encoded by *V. parahaemolyticus*, HqsK transfers phosphate only to the QS-associated phosphotransfer protein LuxU. Finally, we show that NO promotes transcription of the master quorum sensing regulatory gene *opaR* at low cell density.

Keywords: nitric oxide, quorum sensing, H-NOX, histidine kinase, *Vibrio*

OPEN ACCESS

Edited by:
Cristina García-Aljaro, University of Barcelona, Spain

Reviewed by:
Karen L. Visick, Loyola University Chicago, United States
Brett Mellbye, Oregon State University, United States

***Correspondence:**
Elizabeth M. Boon
elizabeth.boon@stonybrook.edu

Specialty section:
This article was submitted to Microbial Physiology and Metabolism, a section of the journal Frontiers in Microbiology

Received: *13 June 2019*
Accepted: *27 August 2019*
Published: *18 September 2019*

Citation:
Ueno T, Fischer JT and Boon EM (2019) Nitric Oxide Enters Quorum Sensing via the H-NOX Signaling Pathway in Vibrio parahaemolyticus. Front. Microbiol. 10:2108. doi: 10.3389/fmicb.2019.02108

INTRODUCTION

Quorum sensing (QS) is a cell-to-cell communication system utilized by bacteria to assess their population density and to coordinate population-wide changes in gene expression. Bacteria produce, secrete, and detect small signaling molecules called autoinducers (AI). Many types of autoinducers have been identified, some that are unique to a particular species, and some that are shared by multiple bacterial species (Eberhard et al., 1981; Engebrecht and Silverman, 1984; Henke and Bassler, 2004; Miller et al., 2004). Detection of AIs by a receptor protein in a QS pathway ultimately leads to changes in gene expression (Miller and Bassler, 2001). A classic example of a QS system is the well-studied LuxI-LuxR system found in several *Vibrio* species as well as other gram-negative bacteria (Miller and Bassler, 2001). In this system, LuxI synthesizes a homoserine lactone AI. This AI binds to the transcriptional regulator LuxR, which regulates the transcription of the *luxICDABE* operon. In addition to the LuxI-LuxR QS system, alternative QS circuits have also been characterized. Many QS systems in *Vibrio* species consist of an AI synthase, a corresponding AI-sensing histidine kinase (HK), and a cytoplasmic response regulator (RR). The QS-associated HKs in many bacteria are hybrid histidine kinases containing both kinase and receiver domains. These kinases typically have both kinase and phosphatase activities, allowing them to both phosphorylate

and remove phosphate from the cognate response regulator or, as an intermediary, the histidine-containing phosphotransfer protein (Hpt) (Aiba et al., 1989; Makino et al., 1989; Tanaka et al., 1991). Frequently, the response regulators are transcription factors whose activity is modulated by phosphorylation (Hoch, 2000; Galperin, 2006; Gao et al., 2007).

Quorum sensing controls gene expression patterns as a function of population density. At low cell density, AI concentrations are also low and therefore the HKs are not complexed with the AI. Under these conditions, kinase activity predominates, and phosphate is transferred to the RR. The phosphorylated RR then facilitates changes in gene expression patterns, resulting in an adaptive cellular response. At high cell density, elevated AI concentrations drives HK binding to the AI, which switches the function of the kinase to act predominantly as a phosphatase. This ultimately leads to the removal of phosphate from the RR and causes corresponding changes in gene expression (Waters and Bassler, 2005; Bassler and Losick, 2006; Boyer and Wisniewski-Dyé, 2009).

Vibrio parahaemolyticus is a marine bacterium widely distributed in sea water around the world (McCarter, 1999; FAO/WHO, 2011), and is the leading cause of seafood-borne illnesses (Yeung and Boor, 2004; McLaughlin et al., 2005). *V. parahaemolyticus* produces a number of virulence factors, including the type III secretion system 1 (T3SS1), that are regulated by QS (Gode-Potratz and McCarter, 2011). *V. parahaemolyticus* shares a QS architecture with *Vibrio harveyi*, which is composed of three AIs (AI-2, HAI-1, and CAI-1), their synthases, and cognate membrane-bound sensory histidine kinases (LuxM/N, LuxS/PQ, and cqsA/cqsS, respectively) (Henke and Bassler, 2004; Ng and Bassler, 2009). All three AI-sensing kinases engage in phosphotransfer with LuxU, a histidine-containing phosphotransfer protein (Hpt). LuxU transfers phosphate to the response regulator LuxO, a transcription factor that regulates the transcription of quorum regulatory RNAs (*qrrs*) (Ng and Bassler, 2009). Along with RNA-binding protein Hfq, these *qrrs* regulate the translation of two master QS regulatory proteins, AphA, and OpaR. AphA and OpaR are both transcription factors that regulate the expression of various genes, including many involved in motility, surface sensing, biofilm formation, and virulence (Gode-Potratz and McCarter, 2011; Zhang et al., 2012; van Kessel et al., 2013; Kalburge et al., 2017).

A recent study conducted in our laboratory identified a fourth arm in the *V. harveyi* QS circuit. In this pathway, the gaseous signaling molecule nitric oxide (NO) is integrated into QS via ligation to the hemoprotein H-NOX and its partner, an H-NOX-associated hybrid HK called HqsK (H-NOX-associated quorum sensing kinase) (Henares et al., 2012). Membrane-permeable NO is detected by H-NOX in the cytoplasm. The ligation state of H-NOX regulates the activity of HqsK. When NO is not present, HqsK functions as a kinase, transferring phosphate to LuxO via LuxU. Upon NO binding to H-NOX, HqsK switches its activity from a kinase to a phosphatase, causing a reverse in phosphate flow and contributing to dephosphorylation of LuxO (Henares et al., 2012). In this work, we further characterize the NO-responsive QS circuit in the pathogenic marine bacterium *V. parahaemolyticus*.

MATERIALS AND METHODS

Unless otherwise noted, all the reagents were purchased in their highest available qualities and used as received.

Bacterial Strains and Culture Method

Escherichia coli strain DH5α was used for cloning and *E. coli* BL21(DE3)pLysS was used for protein expression. DH5α was cultured in LB medium supplemented with 100 μg/mL ampicillin. BL21 (DE3) pLysS was cultured in 2XYT media (16 g/L Tryptone, 10 g/L yeast extract, and 5 g/L NaCl) supplemented with 100 μg/mL ampicillin and 34 μg/mL chloramphenicol. Both cultures were grown at 37°C with 250 rpm agitation. At A_{600nm} between 0.6 and 0.9, protein expression was induced with 100 μM isopropyl-β-D-thiogalactopyranoside (IPTG) for 15 h at 16°C, then cells were harvested. *V. parahaemolyticus* strain EB101 (ATCC17802) was purchased from American Type Culture Collection and was grown by following the supplier's culture method. In *V. parahaemolyticus* growth curve and qPCR experiment, an overnight culture of *V. parahaemolyticus* was diluted 1:500 into fresh media (BD234000 Nutrient broth with 3% NaCl), supplemented with 100 μg/mL ampicillin with various DETA NONO concentrations (Cayman Chemical). Cultures were grown at 37°C with agitation at 250 rpm. Bacterial growth was monitored by measuring A_{600nm} and harvested at designated ODs.

Molecular Cloning and Mutagenesis

The genome of *V. parahaemolyticus* strain EB101 has not been sequenced. Instead, we referred to the genome sequence of *V. parahaemolyticus* strain RIMD 2210633 for gene annotations and primer designing. *V. parahaemolyticus* genomic DNA was extracted using Zymo Research Quick-gDNA MiniPrep (D3006), by following the manufacturer's instructions. Extracted *V. parahaemolyticus* gDNA was used as a template to amplify *Vp* H-NOX (VP1877, gene ID: 1189384), HK (VP1876 gene ID: 1189383), LuxU (VP2098, gene ID: 1189609), and Hpt proteins (VP1472, gene ID: 1188978 and VP2127, gene ID: 1189639) by PCR. Primers for VP1877, VP1876 kinase domain only, VP1876 internal kinase domain only and VP2098 contained *Nde*I and *Xho*I up-stream/down-stream restriction sites, respectively. VP1472 and VP2127 primers contained *Nde*I and *Not*I restriction sites, respectively. For all PCR reactions, Phusion High-Fidelity DNA Polymerase (New England Biolabs, M0530S) was used. Amplified products were double digested then ligated into pET-20b(+) vector (Novagen) or pET-23aHis-TEV and sequenced (Stony Brook DNA sequencing facility). Site-directed mutagenesis to generate VP1876 HK H214A and D499A was carried out following the QuikChange Site-directed Mutagenesis kit protocol (Stratagene). The primer sequence used for cloning and site-directed mutagenesis will be provided upon request.

Protein Expression and Purification

All proteins contained a 6× His tag on either the N or C-terminus and were purified by immobilized metal ion affinity chromatography using Ni-NTA agarose. Protein concentrations

were determined by Bradford assay with bovine serum albumin as a standard (Bradford, 1976).

H-NOX Complex Preparation and Electronic Microscopy

In an anaerobic glove bag, purified *Vp* H-NOX protein was incubated with 10 mM potassium ferricyanide for 5 min to make Fe (III) H-NOX. Potassium ferricyanide was then removed using PD10 desalting column (GE Healthcare). Prepared *Vp* Fe (III) H-NOX was incubated with 20 mM sodium dithionite for 30 min then desalted to prepare Fe (II) H-NOX. Fe (II) H-NOX was further incubated with 3 mM DPTA NONOate (Cayman Chemicals) for 30 min then desalted to prepare Fe (II) NO·H-NOX. To make CO bound H-NOX, Fe (II) H-NOX was bubbled with CO for 10 min in a closed Reacti-Vial (Thermo Fisher Scientific). Electronic spectra of all samples were measured by a Cary 100 UV-Vis spectrophotometer (Agilent) equipped with Cary temperature controller set at 20○C. For temperature dependent 5, 6-coordinate NO·H-NOX distribution analysis, the sample's temperature was varied from 4 to 40°C utilizing the temperature controller.

NO Dissociation Rate Constant

This procedure has been described previously (Boon et al., 2006). Briefly, in an anaerobic glove bag, NO bound *Vp* Fe (II) H-NOX was diluted in 40 mM Tris-Cl, 150 mM KCl, 4 mM DTT, and 10% glycerol buffer at pH 8.0, then was rapidly mixed with an equal amount of the same buffer at 3, 30 or 300 mM of sodium dithionite saturated with CO. The absorption spectra were obtained by Cary 100 UV-Vis spectrophotometer (Agilent) equipped with a Cary temperature controller set at 20°C. NO dissociation was monitored by tracking increasing Fe (II) CO peak at 424 nm and decreasing Fe (II) NO peak at 399 nm. The resulting data was fitted to a two-phase exponential association equation, $y = y^0 + A_1*(1-e^{-x/t1}) + A_2*(1-e^{-x/t2})$ to determine the NO dissociation rate constant. The experiments were repeated a minimum of three times for each sodium dithionite concentration. The resulting average k_{off} (NO) rate constants were reported with standard error of the mean (SEM). The dissociation rate constants were independent of sodium dithionite concentrations.

HK Autophosphorylation Assay

[γ-^{32}P]-ATP (6000 Ci/mmol, 10 mCi/mL) was purchased from PerkinElmer Health Sciences Incorporated. All reactions were performed at room temperature. Reaction mixtures contained final concentrations of 40 mM Tris-Cl, 150 mM KCl, 4 mM DTT, 10% glycerol, 4 mM $MgCl_2$, 5 μM histidine kinase at pH 8.0. Histidine kinase in the reaction buffer was allowed to equilibrate at room temperature for a few minutes then reactions were initiated by the addition of ATP (2 mM) with trace amount of [γ-^{32}P]-ATP (10 μCi). For SDS-PAGE analysis, reactions were stopped by adding 5× SDS loading dye (0.25% bromophenol blue, 0.5 M dithiothreitol, 50% Glycerol, 10% sodium dodecyl sulfate, 0.25 M, pH 6.8 Tris-Cl) at indicated time points. Quenched reactions were separated by SDS-PAGE. After gel drying, the sample radioactivity was detected by a Typhoon scanner (Typhoon 9400, Amersham Biosciences) then quantified with image processing software ImageJ. For the dot blot assay, reactions were quenched with 25 mM H_3PO_4, and 30 μL aliquots were pipetted onto a nitrocellulose membrane in a dot blot apparatus as described previously (Fischer et al., 2017). The membrane was washed with 25 mM H_3PO_4 and dried before exposure to a storage phosphor screen. Radioactivity in each spot was detected by a Typhoon scanner and quantified with ImageJ.

HK Phosphatase Activity Assay

Purified *Vp* HK was mixed with the final concentration of 250 μM 3-O-methyl fluorescein phosphate (OMFP) in the reaction buffer (40 mM Tris–HCl, 150 mM KCl, and 10% glycerol at pH 8.0) at room temperature. HK's phosphatase activity was quantified by measuring the production of OMFP hydrolysis product, O-methylfluorescein (OMF) at 450 nm. All data acquisition was done by VICTOR X5 Multilabel Plate Reader (PerkinElmer).

HK/LuxU Phosphotransfer Assay

The components of the reaction mixture were the same as those used in the HK autophosphorylation assay. Reactions were performed at room temperature. The final concentration of 9.4 μM HK in the reaction buffer was incubated with ATP/[γ-^{32}P]-ATP mix solution for 40 min to autophosphorylate HK. The final concentration of 40.7 μM LuxU was then added to the reaction mixture to initiate phosphotransfer. Reactions were quenched by the addition of 5× SDS loading dye at various

TABLE 1 | Electronic absorption spectra Soret peaks and NO dissociation rate constants of various H-NOX proteins.

Protein	Soret peak (nm)			K_{off} (NO)	References
	Fe^{II}-unligated	Fe^{II}-CO	Fe^{II}-NO	× 10^{-4} s^{-1}	
sGC[a]	431	423	398	3.6 ± 0.8	Henares et al., 2012
Tt H-NOX[b]	431	424	420	5.6 ± 0.5	Bradford, 1976
Vp H-NOX	426	424	399/417	4.3 ± 0.5	This work
Vh H-NOX[c]	429	423	399	4.6 ± 0.9	Kalburge et al., 2017
Np H-NOX[d]	430	423	400/416	–	Boon et al., 2006

[a]*H-NOX domain from soluble guanylate cyclase from bovine lung.* [b]*H-NOX from Thermoanaerobacter tengcongensis.* [c]*H-NOX from Vibrio harveyi.* [d]*H-NOX from Nostoc punctiforme.*

time points followed by gel electrophoresis, gel drying and image scanning. Histidine kinase only with ATP mix solution, LuxU only with ATP mix solutions were run along with HK + LuxU as controls.

HK Autophosphorylation Activity Inhibition by H-NOX

All reactions were carried out at room temperature. The components of the reaction mixture were the same as those used in the HK autophosphorylation assay. In an anaerobic glove bag, different oxidation/ligation states of H-NOX [final concentration 69.4 μM or varying (NO·H-NOX) for the titration] were incubated with *Vp* HK (D499A, final concentration 5.3 μM) for 30 min. Reactions were initiated by the addition of ATP/[γ-^{32}P]-ATP mix solution. Thirty minutes after the initiation of the reaction, reactions were quenched by adding 5× SDS loading dye, followed by SDS-PAGE, gel drying and image scanning.

Phosphotransfer Profiling

The procedure followed what's been described by Laub (Laub et al., 2007). All reactions were performed at room temperature. The components of the reaction mixture were the same as those of the HK autophosphorylation assay. Final concentrations of 3.3 μM HK kinase domain and 3.3 μM internal kinase receiver (IKR) domain were incubated with ATP/[γ-^{32}P]-ATP mix solution for 60 min. Final concentrations of 33 μM histidine containing phosphotransfer proteins (VP1472, VP2098, or VP2127) were added to the reaction mixtures to initiate phosphotransfer. At various time points, reactions were quenched by adding 5× SDS loading dye. Proteins were separated by gel electrophoresis followed by gel drying and image scanning.

Phosphotransfer Specificity Test

All reactions were carried out at room temperature and the components of the reaction mixtures were the same as those used in phosphotransfer profiling. Reaction mixtures with various components, KD only, IKR only, VP1472 only, VP2098 (LuxU) only, VP2127 only, KD + IKR, KD + IKR + VP2098 (LuxU), KD + VP1472, KD + VP2098 (LuxU), and KD + VP2127, were incubated with ATP/[γ-^{32}P]-ATP mix solution for 60 min. Reactions were quenched by the addition of 5×

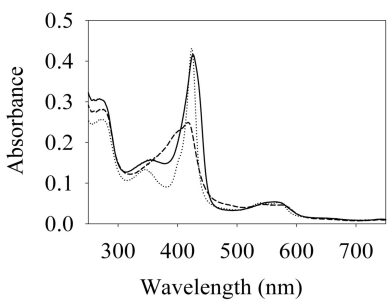

FIGURE 1 | Absorption spectra of *Vibrio parahaemolyticus*. Fe (II) (–), Fe (II)·CO (···) and Fe (II)·NO (– – –) H-NOX at 20°C. Their Soret peaks are 426, 424, and 399/417 nm, respectively.

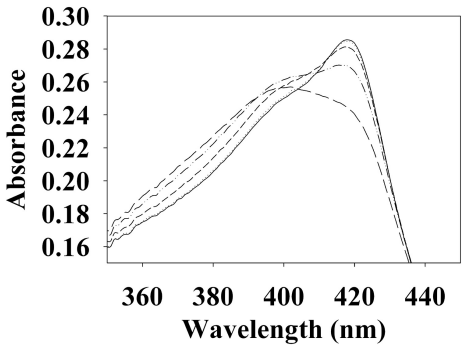

FIGURE 2 | Temperature dependent absorption spectra of *V. parahaemolyticus* Fe^{II}-NO H-NOX. The absorption spectrum shows the shift in the 5/6-coordinate Fe^{II}-NO H-NOX ratio by temperature, lower temperatures favoring 6-coordinate (417 nm) and higher temperatures favoring 5-coordinate (399 nm). Absorption spectra were taken at 4°C (–), 10°C (···), 20°C (- - -), 30°C (–·–·–), and 40°C (– – –).

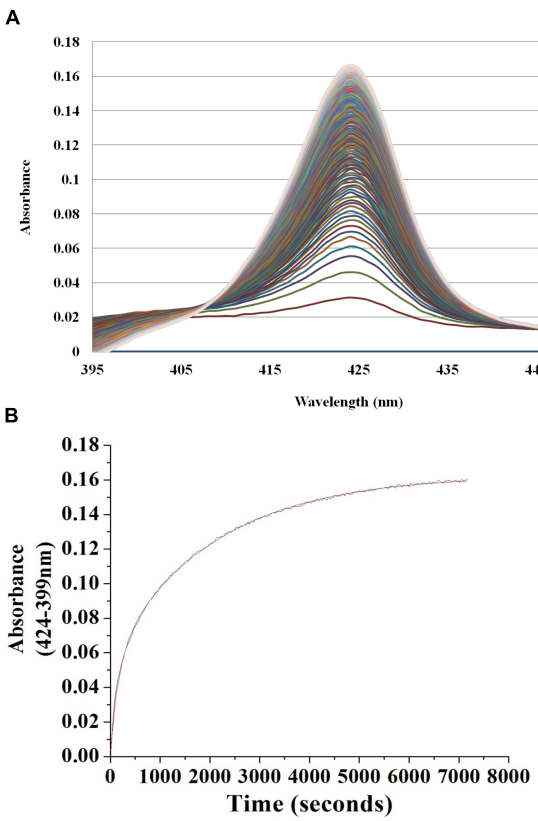

FIGURE 3 | Continuous absorbance spectra during *Vp* H-NOX Fe^{II}-NO dissociation rate constant determination. **(A)** Absorption spectra of *Vp* H-NOX Fe^{II}-NO over time in the presence of saturating CO and $Na_2S_2O_4$ as a released NO trap. **(B)** Absorbance difference spectrum shows the absorbance difference over time along with the exponential fit of the data.

SDS loading dye, followed by gel electrophoresis, gel drying and image scanning.

RNA Extraction, cDNA Synthesis, and qPCR

RNA was extracted from bacterial cultures using the PureLink RNA Mini Kit (Ambion). Extracted RNA was treated with dsDNase (Thermo Fisher Scientific). cDNA synthesis and qPCR were carried out using either DyNAmo SYBR Green 2-Step qRT-PCR Kit or Maxima First Strand cDNA Synthesis Kits for RT-qPCR and DyNAmo HS SYBR Green qPCR Kit (Thermo Fisher Scientific). qPCR was carried out using *secY* (VP0277) as a reference gene. Data was analyzed by ΔΔCT method (BIO-RAD). Sequences for primer sets used are as follows:

aphA forward: TCAGCGAAACTTATGGCTTG
aphA reverse: GTTGAAGGCGTTGCGTAGTA
opaR forward: GAAATTGCGCAAGTGTCTGT
opaR reverse: ACGGACAACATGGTTGAGAA
secY forward: CAGTGGTTTGGTCAGAATGG
secY reverse: GGGCTAAGAGCCAAAGACAC

RESULTS AND DISCUSSION

Vp H-NOX Is an NO-Binding Protein

To begin investigating the NO/H-NOX-mediated QS circuit in *V. parahaemolyticus*, we cloned, expressed, and purified *Vp* H-NOX (VP1877, gene ID: 1189384) and analyzed its spectroscopic and ligand-binding properties (**Figure 1** and **Table 1**). The absorption peaks of purified H-NOX from *V. parahaemolyticus* in various oxidation and ligation states are similar to those of the eukaryotic H-NOX homolog sGC, as well as *V. harveyi*, and other previously characterized H-NOX proteins (Stone and Marletta, 1994; Karow et al., 2004; Boon et al., 2006; Henares et al., 2012). The reduced-unligated (Fe^{II}-unligated) and CO-bound (Fe^{II}-CO) *Vp* H-NOX complexes have Soret band maxima at 426 nm and 424 nm, respectively (**Figure 1**). Interestingly, NO-bound (Fe^{II}-NO) *Vp* H-NOX has two Soret peaks, at 399 and 417 nm, which indicates the protein is a mixture of 5- and 6-coordinate heme at 20∘C. In previous work on the H-NOX from *Nostoc punctiforme*, it was shown that the distribution of the Fe^{II}-NO coordination state is temperature dependent, with lower temperatures favoring the 6-coordinate complex and higher temperature favoring the 5-coordinate state. We tested if this was also the case for *Vp* H-NOX by varying the temperature from 4 to 40∘C. Indeed,

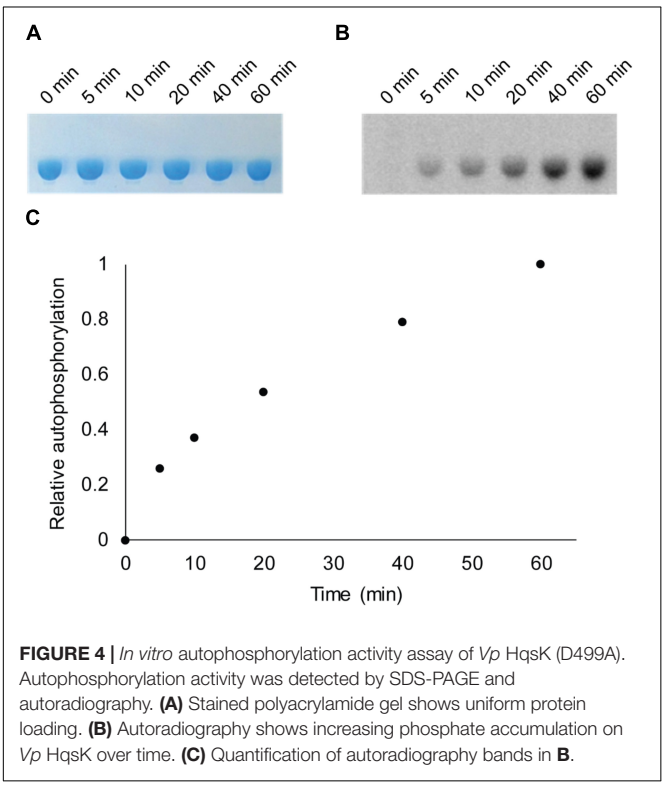

FIGURE 4 | *In vitro* autophosphorylation activity assay of *Vp* HqsK (D499A). Autophosphorylation activity was detected by SDS-PAGE and autoradiography. **(A)** Stained polyacrylamide gel shows uniform protein loading. **(B)** Autoradiography shows increasing phosphate accumulation on *Vp* HqsK over time. **(C)** Quantification of autoradiography bands in **B**.

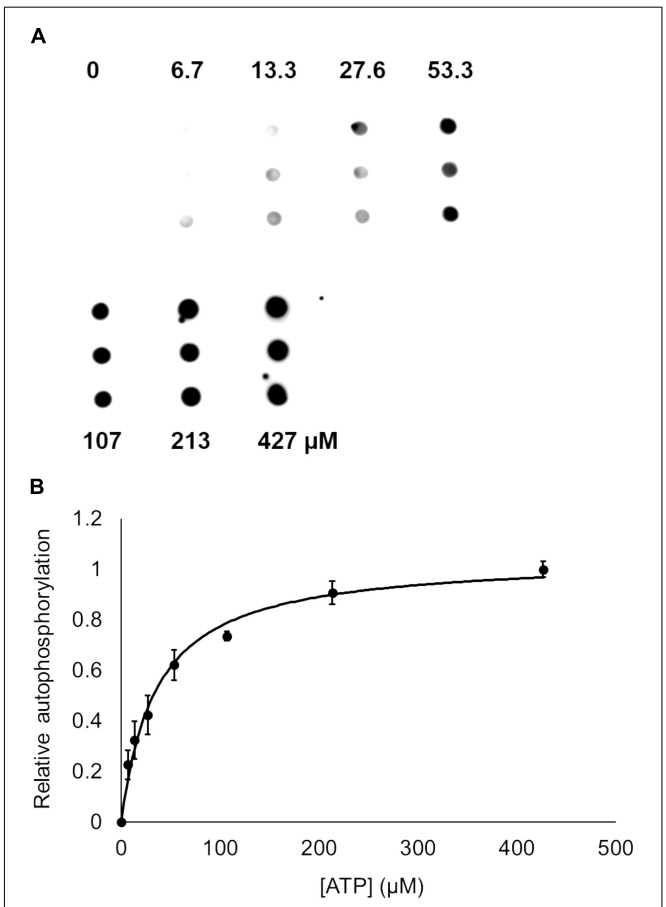

FIGURE 5 | Dependence of *Vp* HqsK D499A autophosphorylation on ATP concentration. **(A)** Dot blot assay showing radiolabeled *Vp* HqsK D499A bound to a nitrocellulose membrane shows HqsK autophosphorylation follows Michaelis-Menten kinetics. Each concentration of ATP was assayed in triplicate using biological replicates. **(B)** Quantification of *Vp* HqsK D499A autophosphorylation as a function of ATP concentration. The apparent K_m is 35 μM. Error bars indicate the standard deviation of three biological replicates.

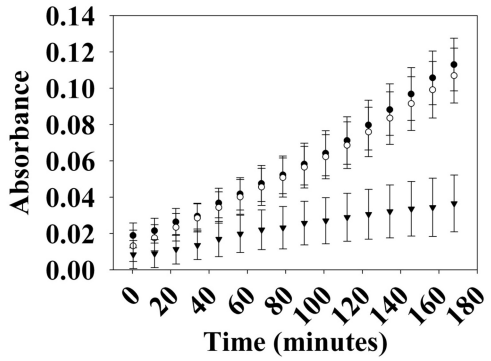

FIGURE 6 | Phosphatase activity of *Vp* HK. Phosphatase activity over time was monitored using OMFP as a substrate (open circles, WT; closed circles, H214A; inverted triangles, D499A). *Vp* HK has phosphatase activity, which was diminished upon the mutation of conserved aspartic acid (D499A) in the kinase receiver domain. The plot shows the average of three independent assays ± SEM.

we observed that the distribution of the 5- and 6-coordinate complexes was temperature dependent, being predominately 6-coordinate at 4°C with a shift toward 5-coordinate as the temperature was increased (**Figure 2**). This suggests that like *Np* H-NOX, a thermal equilibrium exists between 5- and 6- coordinate NO-bound *Vp* H-NOX, and cleavage of the Fe-His bond upon NO binding is temperature dependent. We also determined the NO dissociation rate constant for *Vp* H-NOX using a sodium dithionite/carbon monoxide trap (**Figure 3**; Kharitonov et al., 1997; Boon et al., 2005). We determined k_{off}(NO) to be (4.3 ± 0.5) × 10^{-4} s^{-1} at 20°C, indicating a slow NO dissociation rate constant, similar to those of other previously characterized H-NOX proteins (**Table 1**). All of these results support that *Vp* H-NOX is an NO-binding protein.

Vp HqsK Is an Active Hybrid Kinase With Kinase and Phosphatase Activities

Bacterial *hnoX* genes often neighbor genes that code for signaling proteins, such as HKs, cyclic-di-GMP metabolizing proteins, or methyl accepting chemotaxis proteins (Iyer et al., 2003). In all H-NOX homologs characterized to date, H-NOX has been demonstrated to regulate the activity of its associated signaling protein as a function of binding to NO. In *V. parahaemolyticus*, *hnoX* is encoded in the same operon as a hybrid HK predicted to be involved in QS. We named this kinase HqsK (H-NOX-associated QS kinase). To identify whether HqsK (VP1876, gene ID: 1189383) is a functional kinase, we cloned, expressed, and purified the protein, and then conducted autophosphorylation activity assays. When HqsK is incubated with ATP containing trace [γ-^{32}P]-ATP over time, the resulting autoradiography shows accumulating radiolabeled phosphate on the HK in a time-dependent manner, confirming kinase activity of *Vp* HqsK (**Figure 4**). We also tested the kinase activity as a function of ATP concentration (**Figure 5**). HqsK appears to follow Michaelis-Menten kinetics, with an apparent K_m of 35 μM.

Many hybrid HKs are dual-functioning enzymes that have phosphatase activity in addition to kinase activity, in order to regulate the phosphorylation state of a partner response regulator (Parkinson and Kofoid, 1992). To test whether *Vp* HqsK is such an enzyme, phosphatase activity was monitored using a generic phosphatase substrate 3-O-methyl-fluorescein phosphate (OMFP) that yields O-methylfluorescein (OMF) upon dephosphorylation. Wild-type HqsK displays increasing OMF fluorescence over time, indicating *Vp* HqsK has phosphatase activity (**Figure 6**).

The kinase and phosphatase activities of hybrid HKs are dependent on conserved His and Asp residues, respectively (Kwon et al., 2000; Albanesi et al., 2009; Goodman et al., 2009). To demonstrate the importance of these residues for phosphatase activity, we generated H214A and D499A mutant HqsKs and repeated the phosphatase assay. Wild-type and H214A HKs have

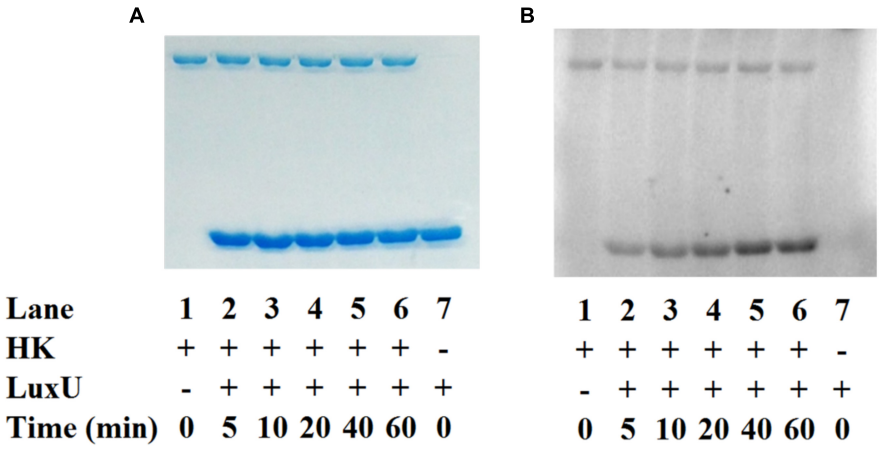

FIGURE 7 | *In vitro* phosphotransfer assay of *Vp* HqsK to LuxU. Phosphotransfer activity was detected by SDS-PAGE and autoradiography. Stained polyacrylamide is shown for uniform protein loading **(A)**. *Vp* HqsK transfers phosphate to LuxU over time in the presence of ATP **(B)**. Time indicates the length of incubation after the addition of LuxU to HK.

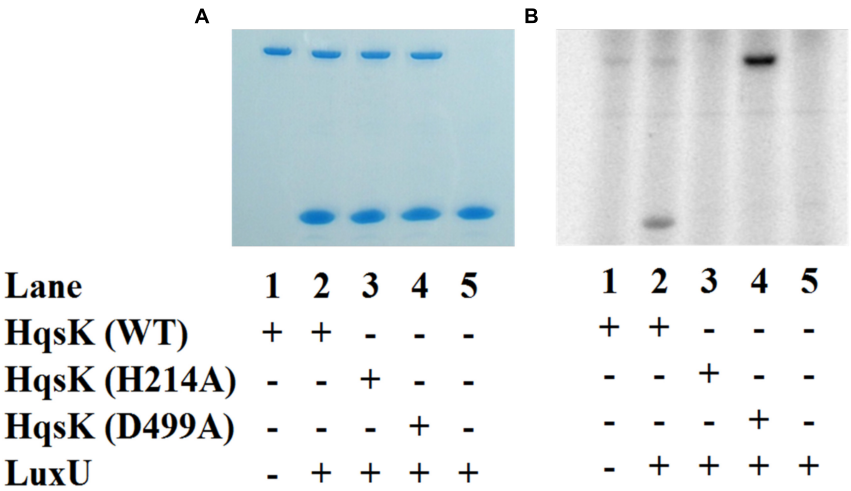

FIGURE 8 | Phosphotransfer specificity test. *In vitro* phosphotransfer assay from HqsK to LuxU with WT, H214A, and D499A HqsK. Stained polyacrylamide gel **(A)** and autoradiography **(B)** are shown. H214A HqsK has no autophosphorylation activity due to the phosphorylation site mutation. D499A, kinase receiver domain mutant autophosphorylates, but does not phosphotransfer to receiver domain nor LuxU.

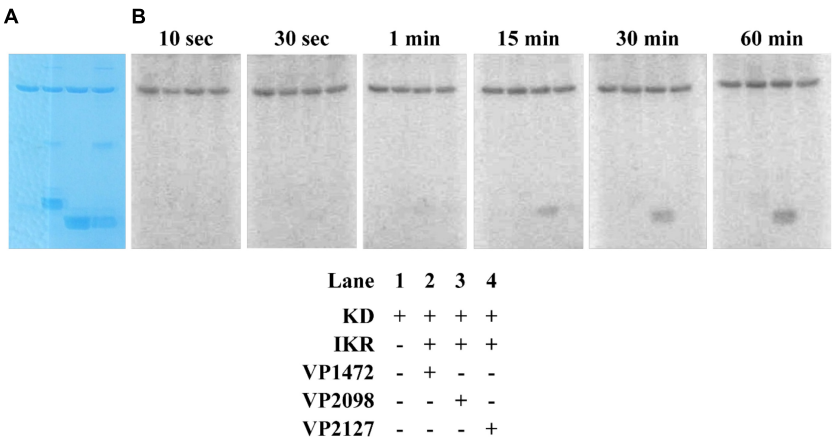

FIGURE 9 | Phosphotransfer profiling of *Vp* HqsK and three stand-alone *Vp* Hpt proteins (VP1472, VP2098, and VP2127). Stained polyacrylamide gel **(A)** and autoradiography **(B)** are shown. 1 μM each of KD and IKR were incubated with 10 μM each of Hpts. KD/IKR were loaded with phosphoryl group by preincubating with ATP for 90 min. Hpt proteins were then added to initiate the phosphotransfer. Phoshoryl group accumulation was observed only for VP2098 (LuxU) among three Hpts.

the same level of phosphatase activity as the wild-type enzyme, whereas D499A has significantly reduced phosphatase activity, indicating conserved D499 in the internal kinase receiver domain (IKR) is required for *Vp* HqsK phosphatase activity.

Vp HqsK Transfers Phosphate to the Quorum Sensing Phosphotransfer Protein LuxU

To establish the phosphotransfer circuit between *Vp* HqsK and the QS histidine-containing phosphotransfer protein LuxU, a phosphotransfer assay was conducted. Purified HqsK was incubated with ATP containing trace [γ-^{32}P]-ATP, followed by the addition of purified LuxU. The resulting autoradiography shows an accumulation of radiolabeled phosphate on LuxU over time, indicating *Vp* HqsK transfers phosphate to LuxU (**Figure 7**). We also tested HqsK/LuxU phosphotransfer using the H214A and D499A HqsK mutants to confirm the transfer is occurring, as predicted, via phosphotransfer from H214 to D499 in HqsK followed by transfer to H56 in LuxU. As expected, H214A HqsK showed neither autophosphorylation nor phosphotransfer activities, whereas D499A HqsK exhibited only autophosphorylation activity (**Figure 8**).

LuxU Is the Cognate Phosphotransfer Protein for *Vp* HqsK

Vibrio parahaemolyticus has three stand-alone Hpts. As described above, we have demonstrated that *Vp* HqsK transfers phosphate to LuxU, but since many HKs can transfer phosphate to

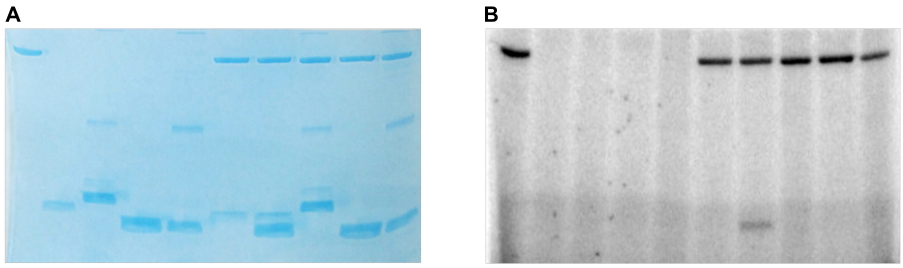

Lane	1	2	3	4	5	6	7	8	9	10
KD	+	-	-	-	-	+	+	+	+	+
IKR	-	+	-	-	-	+	+	-	-	-
VP1472	-	-	+	-	-	-	-	+	-	-
VP2098	-	-	-	+	-	-	+	-	+	-
VP2127	-	-	-	-	+	-	-	-	-	+

FIGURE 10 | *Vp* HK, Hpt phosphotransfer specificity test. Various combinations of KD, IKR, and Hpt proteins were mixed to observe phosphotransfer. Stained polyacrylamide gel **(A)** and autoradiography **(B)** are shown.

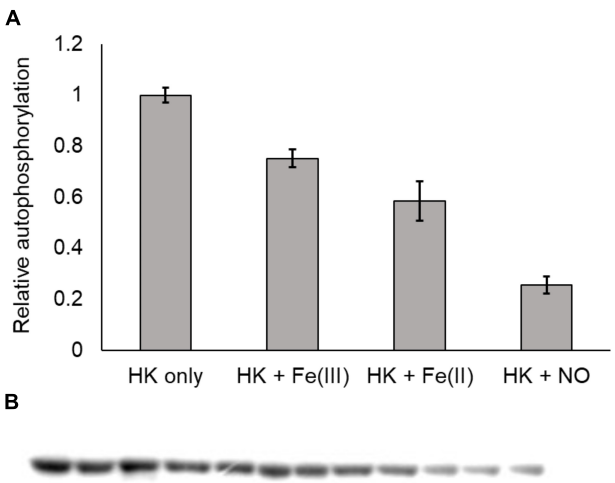

FIGURE 11 | *Vp* H-NOX inhibits kinase activity of HqsK. **(A)** Quantification of HqsK autophosphorylation in the presence of various H-NOX complexes. Fe (II)-NO H-NOX displays the strongest inhibition of HqsK activity. Band intensity was quantified with ImageJ. **(B)** Autoradiography results showing relative levels of phosphorylated HqsK in the presence of each H-NOX complex. Each condition was assayed in triplicate. Lanes 1–3, HqsK only; lanes 4–6, HqsK + Fe (III) H-NOX; lanes 7–9, HqsK + Fe (II) H-NOX; lanes 10–12, HqsK + Fe (II)-NO H-NOX. Error bars indicate the standard deviation of three biological replicates.

multiple partners, there remained a possibility that this HqsK/LuxU phosphotransfer was not exclusive and/or that LuxU is not a cognate phosphotransfer partner for HqsK. It has been demonstrated that *in vitro*, an HK will have a kinetic preference for its *in vivo* cognate response regulator, exhibiting a much faster rate of phosphotransfer with its cognate partner (Laub et al., 2007). This preference is determined in an experiment called phosphotransfer profiling, in which either loss of phosphate from the HK or the appearance of a preferentially phosphorylated Hpt is detected using PAGE followed by autoradiography (Laub et al., 2007).

The kinase domain and internal kinase receiver domain from *Vp* HqsK were separately cloned and expressed to isolate the kinase and receiver domains. We also purified all three stand-alone Hpt proteins from *V. parahaemolyticus*: LuxU (VP2098, gene ID: 1189609), VP1472 (gene ID: 1188978), and VP2127 (gene ID: 1189639). Then each Hpt was separately added to a mixture of *Vp* HqsK KD and IKR domains that had been preincubated with radiolabeled ATP. The resulting autoradiography showed no apparent band intensity loss from any of the kinase domains, nor band appearance for VP1472 or VP2098. However, a band corresponding to phosphorylated LuxU appears after 15 min and increases in intensity over time, indicating the accumulation of phosphate on LuxU (**Figure 9**). To verify this accumulation of phosphate on LuxU is not due to non-specific phosphorylation, but due to phosphotransfer through the HqsK KD/IKR domains, we conducted a phosphotransfer specificity test (**Figure 10**). The results indicate that LuxU does not phosphorylate itself, nor can it directly receive phosphate from the HqsK kinase domain, but it can only be phosphorylated via a His-Asp-His phosphotransfer through the HqsK kinase and IKR domains. Overall, these results show LuxU is the cognate phosphotransfer Hpt protein for HqsK.

H-NOX Suppresses *Vp* HqsK Autophosphorylation Upon NO Binding

In the NO-responsive QS circuit in *V. harveyi*, the basal kinase activity of *Vh* HqsK was repressed by H-NOX upon NO binding (Henares et al., 2012). To test whether *Vp* HqsK is regulated

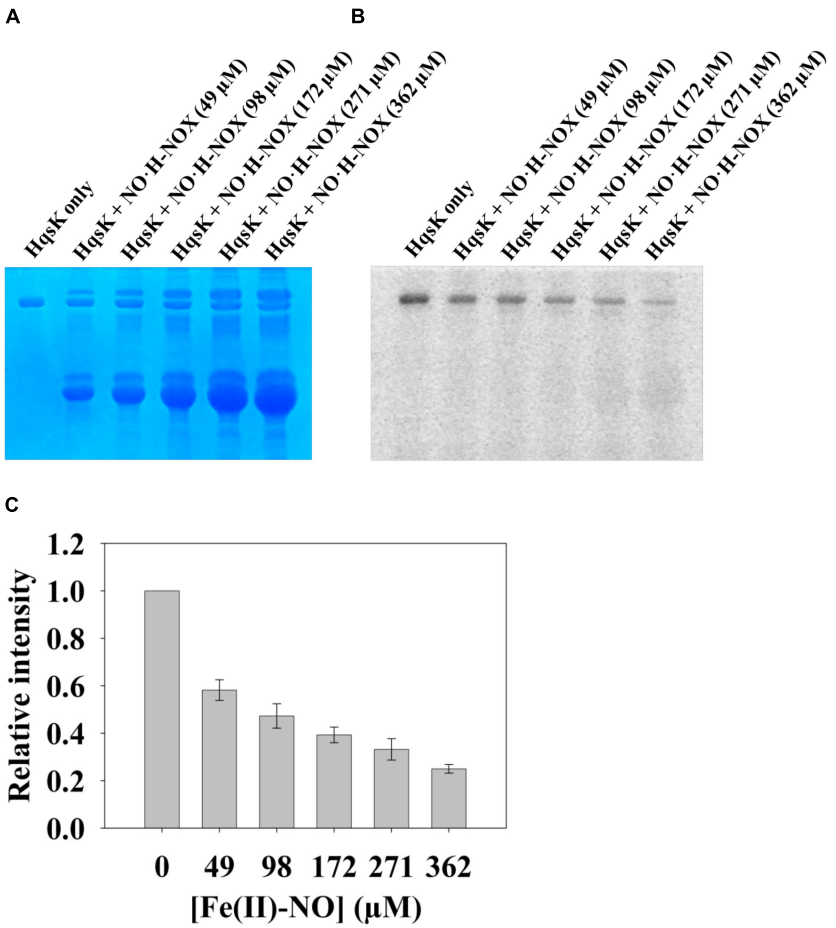

FIGURE 12 | NO bound H-NOX inhibits HqsK kinase activity in a dose-dependent manner. *Vp* HqsK (D499A) was incubated with varying concentrations of NO·H-NOX for 30 min then another 30 min after the addition of ATP. Stained polyacrylamide gel **(A)** and autoradiography **(B)** are shown. **(C)** Quantified band intensities of HqsK titration with Fe^{II}-NO H-NOX. Average of three independent assays ± SEM is plotted.

in a similar manner, various ligation states of *Vp* H-NOX were incubated with HqsK and the effects on autophosphorylation were observed. *Vp* HqsK and Fe^{II}-unligated, Fe^{II}-CO or Fe^{II}-NO *Vp* H-NOX were incubated in an anaerobic chamber, and then ATP with trace [γ-^{32}P]-ATP was added to initiate HqsK autophosphorylation. The resulting autoradiography showed significant kinase activity inhibition with all *Vp* H-NOX complexes, with the most inhibition (75%) by Fe^{II}-NO H-NOX (**Figure 11**). We also titrated HqsK with Fe^{II}-NO H-NOX and observed decreasing *Vp* HqsK autophosphorylation in an Fe^{II}-NO H-NOX concentration-dependent manner (**Figure 12**). Our data indicate that *Vp* H-NOX suppresses the kinase activity of the associated HqsK upon NO binding, similar to what has been observed in *V. harveyi*.

The Effect of NO on the Master Quorum Regulatory Genes opaR and aphA

In the *V. parahaemolyticus* QS circuit, LuxU and LuxO ultimately regulate the translation of two master quorum regulatory proteins, OpaR, and AphA (Rutherford et al., 2011). However, these master quorum regulatory proteins have also been shown to reciprocally regulate each other's gene transcription. AphA binds to the *luxR* promoter in *V. harveyi* and directly suppress transcription of *lux*R (Rutherford et al., 2011). In *V. parahaemolyticus*, OpaR binds to the *aphA* promoter and represses transcription of *aphA* (Zhang et al., 2012). These findings of transcriptional regulation of the master QS genes prompted us to investigate if NO has a role in regulating *aphA* and *opaR* transcription. Here, we analyze the effect of various concentrations of NO (delivered with the NO donor DETA NONOate) on the transcription of these master quorum regulatory proteins at low ($A_{600\,nm}$ = 0.2) cell density using qRT-PCR.

First, the growth of *V. parahaemolyticus* in the presence of various concentrations of DETA NONOate was monitored to determine the NO toxic threshold (**Figure 13**). The growth curve for cultures with 0, 50, 100, and 200 μM DETA NONOate [equivalent to 0, 190, 380, and 760 nM NO under these conditions (Bebok et al., 2002)] showed almost identical growth, but almost no cell growth was seen with 500 μM DETA NONOate (1900 nM NO). Accordingly, *V. parahaemolyticus* cultures grown with

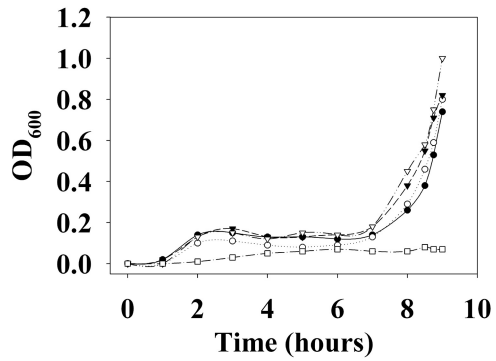

FIGURE 13 | Growth curve of *V. parahaemolyticus*. *V. parahaemolyticus* was grown with 0 (closed circles), 50 (open circles), 100 (closed triangles), 200 (open triangles), and 500 μM (open squares) DETA NONOate (equivalent to 0, 190, 380, 760, and 1900 nM NO, respectively). Almost no growth was observed with 500 μM NONOate. For the detailed growth condition, see section "Materials and Methods."

0–200 μM DETA NONOate were used to monitor *aphA* and *opaR* transcription (**Figure 14**). The gene expression levels of *opaR* and *aphA* were quantified using *secY* (VP0277, gene ID: 1187744) as a reference gene.

We observed a trend of increasing transcription of *opaR* as a function of NO (1.22-, 1.71-, and 2.04-fold change with 50, 100, and 200 μM DETA NONOate, respectively). The fold-change of 2.04 with 200 μM NONOate was significantly different ($p < 0.05$) with respect to no NONOate, but the other two were not ($p > 0.05$). Transcript levels of *aphA* remained almost constant with increasing NO, although at 200 μM NONOate, there was an increase of 1.56 with respect to no NONOate.

An NO-dependent increase in both *aphA* and *opaR* transcription is unexpected since *opaR* suppresses *aphA* transcription. The mechanism of this increased *aphA* transcription at higher NO concentration is unknown. It is possible that although 200 μM NONOate did not hinder the bacterial growth, it is causing stress to bacteria, and increased *aphA* transcription is a part of the stress response. Also, it is possible that NO may be activating an unidentified signaling cascade that is turned on only at higher NO concentrations.

DISCUSSION

Quorum sensing is a key signaling system bacteria use to orchestrate population-wide gene expression patterns appropriate for different stages of growth or environmental conditions. Bacteria employ various types of QS circuits, AIs, and AI receptors that are most suitable for their particular lifestyle or the environment in which they live. Not only do bacteria monitor the AI concentrations of their own and other bacterial species, many actively interfere with QS circuits of competing species through a process called quorum quenching (Leadbetter and Greenberg, 2000; Dong et al., 2001). Some pathogenic or symbiotic bacteria also integrate host-organism-originated signals into QS to manage effective colonization and pathogenicity (Beck von Bodman et al., 1992; Fuqua and Winans, 1994; Hwang et al., 1994). Similarly, eukaryotes monitor bacterial AIs to detect their presence and activate an immune response (Givskov et al., 1996; Chun et al., 2004). Autoinducer-mediated QS is a dynamic communication system that spans across different bacterial species and even across kingdoms. Recent studies have revealed increasing complexity in QS signaling, indicating the growing importance of QS not only in the regulation of the bacterial life cycle, but also in our eukaryotic immune response.

Nitric oxide has been shown to promote bacterial biofilm dispersal through the regulation of the bacterial second messenger signaling molecule c-di-GMP in *Shewanella woodyi* (Liu et al., 2012) and *Shewanella oneidensis*

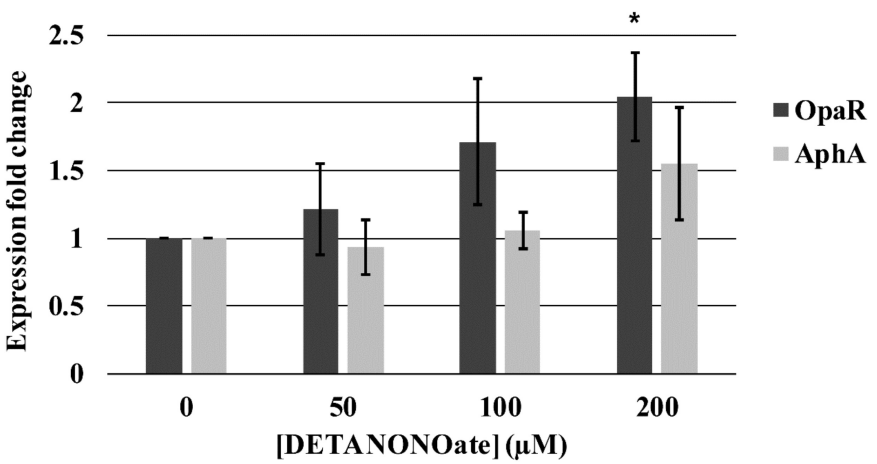

FIGURE 14 | *Vp* master quorum regulatory protein transcription analysis by qPCR. Transcription of two *Vp* master quorum regulatory proteins, *aphA* and *opaR*, in the presence of various concentrations of DETA NONOate was analyzed. 0, 50, 100, and 200 μM NONOate are equivalent to 0, 190, 380, and 760 nM NO, respectively. * denotes *p*-value < 0.05 compared to gene expression in 0 μM NONOate. Error bars represent SEM from four independent assays.

(Plate and Marletta, 2012). Although their mechanisms have not been identified, NO has also been shown to modulate biofilm formation in *Pseudomonas aeruginosa* (Barraud et al., 2006) and *Nitrosomonas europaea* (Schmidt et al., 2004). In *V. harveyi* QS circuits, the NO signal is integrated into a QS signaling cascade through H-NOX/HqsK (Henares et al., 2012). H-NOX shifts HqsK's activity from kinase to phosphatase upon NO binding. Together with other AI sensory HKs, it controls the phosphorylation state of the RR LuxO. LuxO ultimately regulates hundreds of gene expressions through two master quorum regulatory proteins LuxR (OpaR homolog) and AphA (Rutherford et al., 2011). Based on gene analysis, *V. harveyi* does not have an NO synthase. Thus, we hypothesize *V. harveyi* detects NO originated from its host organism or other NO-producing bacteria and integrates that information in its QS circuit. In this paper, we show that *V. parahaemolyticus* appears to also have an NO-responsive signaling pathway that feeds into the QS circuit.

The signaling cascade of *V. parahaemolyticus* NO-responsive QS circuit is similar to that of *V. harveyi*. NO is detected by a cytoplasmic H-NOX protein that switches the activity of HqsK between kinase and phosphatase. HqsK integrates the NO signal into a QS circuit to regulate the phosphorylation state of QS RR LuxO and ultimately control the transcription of two master quorum regulatory proteins OpaR and AphA. Studies on other *Vibrios* (*V. harveyi* and *V. cholerae*) show that low cell density promotes phosphorylation of LuxO and activation/suppression of *aphA*/*luxR* transcription. High cell density promotes dephosphorylation of LuxO and activation/suppression of *luxR*/*aphA* transcription. Our data suggest that NO functions as an AI and participates in the *V. parahaemolyticus* QS circuit. If OpaR and AphA's reciprocal regulatory circuit is conserved in *V. parahaemolyticus*, we expect increasing NO concentration would promote *opaR* transcription and suppress *aphA* transcription. Our qPCR result supported the former part of the hypothesis. Increasing NO concentration promoted *opaR* transcription in a concentration-dependent manner, supporting a role for NO in the QS circuit as an AI. However, *aphA* transcription also increased at high NO concentration (200 μM). This discrepancy may be due to NO toxicity or may mean the presence of an unidentified NO signaling cascade in *V. parahaemolyticus*. We are currently investigating the mechanism behind the increased *aphA* transcription caused by NO and the alternative NO signaling cascade in *V. parahaemolyticus*.

DATA AVAILABILITY

All datasets generated for this study are included in the manuscript and/or the supplementary files.

AUTHOR CONTRIBUTIONS

TU and JF performed the experiments. TU, JF, and EB wrote the manuscript.

FUNDING

This work was supported by the Stony Wold-Herbert Fund, the National Science Foundation (Grant CHE-1607532 to EB), and the National Institutes of Health (Grant GM118894-01A1 to EB).

ACKNOWLEDGMENTS

We thank Dr. Roger Johnson and the Boon Group for their helpful discussions.

REFERENCES

Aiba, H., Mizuno, T., and Mizushima, S. (1989). Transfer of phosphoryl group between two regulatory proteins involved in osmoregulatory expression of the ompF and ompC genes in *Escherichia coli*. *J. Biol. Chem.* 264, 8563–8567.

Albanesi, D., Martin, M., Trajtenberg, F., Mansilla, M. C., Haouz, A., Alzari, P. M., et al. (2009). Structural plasticity and catalysis regulation of a thermosensor histidine kinase. *Proc. Natl. Acad. Sci. U.S.A.* 106, 16185–16190. doi: 10.1073/pnas.0906699106

Barraud, N., Hassett, D. J., Hwang, S.-H., Rice, S. A., Kjelleberg, S., and Webb, J. S. (2006). Involvement of nitric oxide in biofilm dispersal of *Pseudomonas aeruginosa*. *J. Bacteriol.* 188, 7344–7353. doi: 10.1128/jb.00779-06

Bassler, B. L., and Losick, R. (2006). Bacterially speaking. *Cell* 125, 237–246. doi: 10.1016/j.cell.2006.04.001

Bebok, Z., Varga, K., Hicks, J. K., Venglarik, C. J., Kovacs, T., Chen, L., et al. (2002). Reactive oxygen nitrogen species decrease cystic fibrosis transmembrane conductance regulator expression and cAMP-mediated Cl- secretion in airway epithelia. *J. Biol. Chem.* 277, 43041–43049. doi: 10.1074/jbc.m203154200

Beck von Bodman, S., Hayman, G. T., and Farrand, S. K. (1992). Opine catabolism and conjugal transfer of the nopaline Ti plasmid pTiC58 are coordinately regulated by a single repressor. *Proc. Natl. Acad. Sci. U.S.A.* 89, 643–647. doi: 10.1073/pnas.89.2.643

Boon, E. M., Davis, J. H., Tran, R., Karow, D. S., Huang, S. H., Pan, D., et al. (2006). Nitric oxide binding to prokaryotic homologs of the soluble guanylate cyclase beta1 H-NOX domain. *J. Biol. Chem.* 281, 21892–21902. doi: 10.1074/jbc.m600557200

Boon, E. M., Huang, S. H., and Marletta, M. A. (2005). A molecular basis for NO selectivity in soluble guanylate cyclase. *Nat. Chem. Biol.* 1, 53–59. doi: 10.1038/nchembio704

Boyer, M., and Wisniewski-Dyé, F. (2009). Cell-cell signalling in bacteria: not simply a matter of quorum. *FEMS Microbiol. Ecol.* 70, 1–19. doi: 10.1111/j.1574-6941.2009.00745.x

Bradford, M. (1976). A rapid and sensitive method for the quantitation of microgram quantities of protein utilizing the principle of protein-dye binding. *Anal. Biochem.* 7, 248–254. doi: 10.1006/abio.1976.9999

Chun, C. K., Ozer, E. A., Welsh, M. J., Zabner, J., and Greenberg, E. P. (2004). From the cover: inactivation of a *Pseudomonas aeruginosa* quorum-sensing signal by human airway epithelia. *Proc. Natl. Acad. Sci. U.S.A.* 101, 3587–3590. doi: 10.1073/pnas.0308750101

Dong, Y. H., Wang, L. H., Xu, J. L., Zhang, H. B., Zhang, X. F., and Zhang, L. H. (2001). Quenching quorum-sensing-dependent bacterial infection by an N-acyl homoserine lactonase. *Nature* 411, 813–817. doi: 10.1038/35081101

Eberhard, A., Burlingame, A. L., Eberhard, C., Kenyon, G. L., Nealson, K. H., and Oppenheimer, N. J. (1981). Structural identification of autoinducer of *Photobacterium fischeri* luciferase. *Biochemistry* 20, 2444–2449. doi: 10.1021/bi00512a013

Engebrecht, J., and Silverman, M. (1984). Identification of genes and gene products necessary for bacterial bioluminescence. *Proc. Natl. Acad. Sci. U.S.A.* 81, 4154–4158. doi: 10.1073/pnas.81.13.4154

FAO/WHO (2011). *Risk Assessment of Vibrio parahaemolyticus in Seafood: Interpretative Summary and Technical report*. Geneva: World Health Organization.

Fischer, J., Johnson, R. A., and Boon, E. (2017). Quantification of bacterial histidine kinase autophosphorylation using a nitrocellulose binding assay. *J. Vis. Exp.* 119:e55129. doi: 10.3791/55129

Fuqua, W. C., and Winans, S. C. (1994). A LuxR-LuxI type regulatory system activates Agrobacterium Ti plasmid conjugal transfer in the presence of a plant tumor metabolite. *J. Bacteriol.* 176, 2796–2806. doi: 10.1128/jb.176.10.2796-2806.1994

Galperin, M. Y. (2006). Structural classification of bacterial response regulators: diversity of output domains and domain combinations. *J. Bacteriol.* 188, 4169–4182. doi: 10.1128/jb.01887-05

Gao, R., Mack, T. R., and Stock, A. M. (2007). Bacterial response regulators: versatile regulatory strategies from common domains. *Trends Biochem. Sci.* 32, 225–234. doi: 10.1016/j.tibs.2007.03.002

Givskov, M., de Nys, R., Manefield, M., Gram, L., Maximilien, R., Eberl, L., et al. (1996). Eukaryotic interference with homoserine lactone-mediated prokaryotic signalling. *J. Bacteriol.* 178, 6618–6622. doi: 10.1128/jb.178.22.6618-6622.1996

Gode-Potratz, C. J., and McCarter, L. L. (2011). Quorum sensing and silencing in *Vibrio parahaemolyticus*. *J. Bacteriol.* 193, 4224–4237. doi: 10.1128/JB.00432-11

Goodman, A. L., Merighi, M., Hyodo, M., Ventre, I., Filloux, A., and Lory, S. (2009). Direct interaction between sensor kinase proteins mediates acute and chronic disease phenotypes in a bacterial pathogen. *Genes Dev.* 23, 249–259. doi: 10.1101/gad.1739009

Henares, B. M., Higgins, K. E., and Boon, E. M. (2012). Discovery of a nitric oxide responsive quorum sensing circuit in *Vibrio harveyi*. *ACS Chem. Biol.* 7, 1331–1336. doi: 10.1021/cb300215t

Henke, J. M., and Bassler, B. L. (2004). Three parallel quorum-sensing systems regulate gene expression in *Vibrio harveyi*. *J. Bacteriol.* 186, 6902–6914. doi: 10.1128/jb.186.20.6902-6914.2004

Hoch, J. A. (2000). Two-component and phosphorelay signal transduction. *Curr. Opin. Microbiol.* 3, 165–170. doi: 10.1016/s1369-5274(00)00070-9

Hwang, I., Li, P. L., Zhang, L., Piper, K. R., Cook, D. M., Tate, M. E., et al. (1994). TraI, a LuxI homologue, is responsible for production of conjugation factor, the Ti plasmid N-acylhomoserine lactone autoinducer. *Proc. Natl. Acad. Sci. U.S.A.* 91, 4639–4643. doi: 10.1073/pnas.91.11.4639

Iyer, L. M., Anantharaman, V., and Aravind, L. (2003). Ancient conserved domains shared by animal soluble guanylyl cyclases and bacterial signaling proteins. *BMC Genomics* 4:5. doi: 10.1186/1471-2164-4-5

Kalburge, S. S., Carpenter, M. R., Rozovsky, S., and Boyd, E. F. (2017). Quorum sensing regulators are required for metabolic fitness in *Vibrio parahaemolyticus*. *Infect. Immun.* 85:e0930-16. doi: 10.1128/IAI.00930-16

Karow, D. S., Pan, D., Tran, R., Pellicena, P., Presley, A., Mathies, R. A., et al. (2004). Spectroscopic characterization of the soluble guanylate cyclase-like heme domains from *Vibrio cholerae* and *Thermoanaerobacter tengcongensis*. *Biochemistry* 43, 10203–10211. doi: 10.1021/bi049374l

Kharitonov, V. G., Sharma, V. S., Magde, D., and Koesling, D. (1997). Kinetics of nitric oxide dissociation from five- and six-coordinate nitrosyl hemes and heme proteins, including soluble guanylate cyclase. *Biochemistry* 36, 6814–6818. doi: 10.1021/bi970201o

Kwon, O., Georgellis, D., and Lin, E. C. C. (2000). Phosphorelay as the sole physiological route of signal transmission by the arc two-component system of *Escherichia coli*. *J. Bacteriol.* 182, 3858–3862. doi: 10.1128/jb.182.13.3858-3862.2000

Laub, M. T., Biondi, E. G., and Skerker, J. M. (2007). Phosphotransfer profiling: systematic mapping of two-component signal transduction pathways and phosphorelays. *Methods Enzymol.* 423, 531–548. doi: 10.1016/s0076-6879(07)23026-5

Leadbetter, J. R., and Greenberg, E. P. (2000). Metabolism of acyl-homoserine lactone quorum-sensing signals by *Variovorax paradoxus*. *J. Bacteriol.* 182, 6921–6926.

Liu, N., Xu, Y., Hossain, S., Huang, N., Coursolle, D., Gralnick, J. A., et al. (2012). Nitric oxide regulation of cyclic di-GMP synthesis and hydrolysis in *Shewanella woodyi*. *Biochemistry* 51, 2087–2099. doi: 10.1021/bi201753f

Makino, K., Shinagawa, H., Amemura, M., Kawamoto, T., Yamada, M., and Nakata, A. (1989). Signal transduction in the phosphate regulon of *Escherichia coli* involves phosphotransfer between PhoR and PhoB proteins. *J. Mol. Biol.* 210, 551–559. doi: 10.1016/0022-2836(89)90131-9

McCarter, L. (1999). The multiple identities of *Vibrio parahaemolyticus*. *J. Mol. Microbiol. Biotechnol.* 1, 51–57.

McLaughlin, J. B., DePaola, A., Bopp, C. A., Martinek, K. A., Napolilli, N. P., Allison, C. G., et al. (2005). Outbreak of *Vibrio parahaemolyticus* gastroenteritis associated with Alaskan oysters. *N. Engl. J. Med.* 353, 1463–1470.

Miller, M. B., and Bassler, B. L. (2001). Quorum sensing in bacteria. *Annu. Rev. Microbiol.* 55, 165–199.

Miller, S. T., Xavier, K. B., Campagna, S. R., Taga, M. E., Semmelhack, M. F., Bassler, B. L., et al. (2004). *Salmonella typhimurium* recognizes a chemically distinct form of the bacterial quorum-sensing signal AI-2. *Mol. Cell* 15, 677–687. doi: 10.1016/j.molcel.2004.07.020

Ng, W.-L., and Bassler, B. L. (2009). Bacterial quorum-sensing network architectures. *Annu. Rev. Genet.* 43, 197–222. doi: 10.1146/annurev-genet-102108-134304

Parkinson, J. S., and Kofoid, E. C. (1992). Communication modules in bacterial signaling proteins. *Annu. Rev. Genet.* 26, 71–112. doi: 10.1146/annurev.genet.26.1.71

Plate, L., and Marletta, M. A. (2012). Nitric oxide modulates bacterial biofilm formation through a multicomponent cyclic-di-GMP signaling network. *Mol. Cell* 46, 449–460. doi: 10.1016/j.molcel.2012.03.023

Rutherford, S. T., van Kessel, J. C., Shao, Y., and Bassler, B. L. (2011). AphA and LuxR/HapR reciprocally control quorum sensing in vibrios. *Genes Dev.* 25, 397–408. doi: 10.1101/gad.2015011

Schmidt, I., Steenbakkers, P. J. M., op den Camp, H. J. M., Schmidt, K., and Jetten, M. S. M. (2004). Physiologic and proteomic evidence for a role of nitric oxide in biofilm formation by *Nitrosomonas europaea* and other ammonia oxidizers. *J. Bacteriol.* 186, 2781–2788. doi: 10.1128/jb.186.9.2781-2788.2004

Stone, J. R., and Marletta, M. A. (1994). Soluble guanylate cyclase from bovine lung: activation with nitric oxide and carbon monoxide and spectral characterization of the ferrous and ferric states. *Biochemistry* 33, 5636–5640. doi: 10.1021/bi00184a036

Tanaka, T., Kawata, M., and Mukai, K. (1991). Altered phosphorylation of *Bacillus subtilis* DegU caused by single amino acid changes in DegS. *J. Bacteriol.* 173, 5507–5515. doi: 10.1128/jb.173.17.5507-5515.1991

van Kessel, J. C., Rutherford, S. T., Shao, Y., Utria, A. F., and Bassler, B. L. (2013). Individual and combined roles of the master regulators AphA and LuxR in control of the *Vibrio harveyi* quorum-sensing regulon. *J. Bacteriol.* 195, 436–443. doi: 10.1128/JB.01998-12

Waters, C. M., and Bassler, B. L. (2005). Quorum sensing: cell-to-cell communication in bacteria. *Annu. Rev. Cell Dev. Biol.* 21, 319–346. doi: 10.1146/annurev.cellbio.21.012704.131001

Yeung, P. S. M., and Boor, K. J. (2004). Epidemiology, pathogenesis, and prevention of foodborne *Vibrio parahaemolyticus* infections. *Foodborne Pathog. Dis.* 1, 74–88. doi: 10.1089/153531404323143594

Zhang, Y., Qiu, Y., Tan, Y., Guo, Z., Yang, R., and Zhou, D. (2012). Transcriptional regulation of *opaR*, *qrr2-4* and *aphA* by the master quorum-sensing regulator OpaR in Vibrio parahaemolyticus. *PLoS One* 7:e34622. doi: 10.1371/journal.pone.0034622

Conflict of Interest Statement: The authors declare that the research was conducted in the absence of any commercial or financial relationships that could be construed as a potential conflict of interest.

frontiers in Microbiology

MINI REVIEW
published: 24 September 2019
doi: 10.3389/fmicb.2019.02174

Insights Into Nitric Oxide Modulated Quorum Sensing Pathways

Ilana Heckler and Elizabeth M. Boon†*

Department of Chemistry, Institute of Chemical Biology & Drug Discovery, Stony Brook University, Stony Brook, NY, United States

The emerging threat of drug resistant bacteria has prompted the investigation into bacterial signaling pathways responsible for pathogenesis. One such mechanism by which bacteria regulate their physiology during infection of a host is through a process known as quorum sensing (QS). Bacteria use QS to regulate community-wide gene expression in response to changes in population density. In order to sense these changes in population density, bacteria produce, secrete and detect small molecules called autoinducers. The most common signals detected by Gram-negative and Gram-positive bacteria are acylated homoserine lactones and autoinducing peptides (AIPs), respectively. However, increasing evidence has supported a role for the small molecule nitric oxide (NO) in influencing QS-mediated group behaviors like bioluminescence, biofilm production, and virulence. In this review, we discuss three bacteria that have an established role for NO in influencing bacterial physiology through QS circuits. In two *Vibrio* species, NO has been shown to affect QS pathways upon coordination of hemoprotein sensors. Further, NO has been demonstrated to serve a protective role against staphylococcal pneumonia through S-nitrosylation of a QS regulator of virulence.

Keywords: nitric oxide, quorum sensing, gas sensing, hemoproteins, virulence, biofilm

OPEN ACCESS

Edited by:
Tom Defoirdt,
Ghent University, Belgium

Reviewed by:
Julia Van Kessel,
Indiana University Bloomington, United States
Gary J. Vora,
United States Naval Research Laboratory, United States

****Correspondence:***
Elizabeth M. Boon
elizabeth.boon@stonybrook.edu

†ORCID:
Elizabeth M. Boon
orcid.org/0000-0003-1891-839X

Specialty section:
This article was submitted to Microbial Physiology and Metabolism, a section of the journal Frontiers in Microbiology

Received: *12 June 2019*
Accepted: *05 September 2019*
Published: *24 September 2019*

Citation:
Heckler I and Boon EM (2019) Insights Into Nitric Oxide Modulated Quorum Sensing Pathways. Front. Microbiol. 10:2174. doi: 10.3389/fmicb.2019.02174

INTRODUCTION

Quorum sensing (QS) refers to the process by which bacteria regulate gene expression in response to small molecules called autoinducers. Autoinducers, typically acylated homoserine lactone molecules in Gram-negative bacteria or oligopeptides in Gram-positive bacteria, are synthesized inside the cell and freely diffuse across the membrane. As cell density rises, the concentration of autoinducers in the surrounding environment also increases. When a threshold level of autoinducers is reached, autoinducers bind to their respective receptors and initiate a signal transduction cascade downstream, ultimately resulting in the repression or expression of specific genes. QS has been shown to mediate several bacterial processes including bioluminescence, sporulation, competence, antibiotic production, biofilm formation, and virulence factor production (Miller and Bassler, 2001).

Bacterial receptors of autoinducers can be membrane bound hybrid histidine kinase proteins (Ng and Bassler, 2009). Hybrid histidine kinases contain a receiver domain, in addition to an input domain and kinase core. Upon binding ATP, the receptor will autophosphorylate on a conserved histidine residue in the kinase core. Phosphate is then transferred from the histidine residue to an aspartate residue on the same polypeptide. Hybrid histidine kinases rely on an intermediate histidine phosphotransferase (HPT) protein to then transfer the phosphate from the receiver domain of the kinase, to the receiver domain of a response regulator. The most

common autoinducers sensed by Gram-negative bacteria are acylated homoserine lactones, or an interfuranosyl borate diester interspecies signal named autoinducer-2 (Papenfort and Bassler, 2016). In Gram-positive bacteria, autoinducing peptides (AIPs) which are synthesized by ribosomes and secreted extracellularly by specific transporters, bind to receptor kinases at high cell density to initiate QS pathways.

Nitric oxide (NO) is a diatomic membrane-permeable gas molecule that has been implicated in a wide range of physiological processes in both eukaryotes and bacteria. Many of the interesting biological properties of NO can be attributed to its unique physical properties. Due to its size, neutral charge, and hydrophobic nature, NO is able to freely diffuse into the cytosol, where it may undergo a variety of reactions including protein S-nitrosylation and metal coordination. While at high (micromolar) concentrations, NO is cytotoxic, at low concentrations, NO has been shown to be a signaling molecule in both bacteria and eukaryotes (Murphy, 1999; Arora et al., 2015).

In mammals, NO is synthesized by nitric oxide synthases (NOS) from L-arginine, oxygen and NADPH. The first report of bacterial NOS activity came from studies of the *Nocardia* species (Chen and Rosazza, 1994). Although it does not appear that most bacteria synthesize NO enzymatically, bacteria can produce NO as a by-product of denitrification, through the anaerobic reduction of nitrite by nitrite reductase. NO is then subsequently reduced to nitrous oxide by NO reductase. Indeed, the expression of nitrite reductase and NO reductase in *Pseudomonas aeruginosa* biofilms were found to be QS-dependent, suggesting that QS is responsible for the maintenance of NO levels in this organism (Hentzer et al., 2005).

Bacteria could also respond to NO that is produced by a eukaryotic host during symbiotic or pathogenic engagement. The ability to respond to NO to mediate QS related behaviors may provide microbes with an evolutionary advantage when encountering NO during infection of a host. In addition to a role for NO as a QS signal, there may also be a connection between QS and the regulation of intracellular levels of NO.

NO AFFECTS QUORUM SENSING PATHWAYS THROUGH LIGATION TO CYTOSOLIC HEMOPROTEIN RECEPTORS

Evidence has suggested that bacteria can respond to low, physiologically relevant levels of NO for the regulation of cellular processes such as biofilm formation and dispersion (Arora et al., 2015). In mammals, NO sensing is essential to regulating vasodilation and is carried out by the soluble guanylyl cyclase (sGC) receptor, which coordinates NO at the ferrous center of a heme cofactor. Homologs of the heme binding domain of sGC have been discovered in bacteria, suggesting a role for NO in regulating bacterial physiology (Iyer et al., 2003). The most well characterized NO sensor in prokaryotes is a family of hemoproteins named heme-nitric oxide/oxygen (H-NOX) proteins (Karow et al., 2004; Plate and Marletta, 2017). H-NOX proteins bind NO selectively, and with picomolar affinity (Tsai et al., 2012). H-NOX domains are commonly encoded in putative operons with cyclic di-guanosine monophosphate (c-di-GMP) processing enzymes and/or histidine kinase proteins. c-di-GMP is a bacterial secondary messenger molecule that plays a role in controlling the switch between motile and sessile/biofilm lifestyles. For example, in *Shewanella oneidensis*, NO bound H-NOX was found to inhibit the activity of an associated histidine kinase, resulting in decreased phosphorylation of a response regulator protein involved with biofilm formation through modulation of c-di-GMP levels (Plate and Marletta, 2012). Recently, NO bound H-NOX was shown to also influence bacterial biofilm formation in the marine bacterium *Vibrio fischeri* through inhibition of its associated histidine kinase, HahK (Thompson et al., 2019).

However, not all bacteria that have been shown to respond to NO encode for an H-NOX protein in their genome. This discrepancy led to the discovery of another bacterial heme bound NO sensing protein named NosP. NosP was first characterized in *P. aeruginosa* where it was found to have a role in biofilm formation (Hossain and Boon, 2017). In the human pathogen *Vibrio cholerae*, and in the marine pathogen *Vibrio harveyi* (recently reclassified as *Vibrio campbellii*) (Lin et al., 2010), NO has been implicated in mediating QS through pathways involving either H-NOX or NosP, and will be discussed here. In addition, our lab has found evidence for a similar NO responsive QS circuit in the gastroenteritis causing bacterium *Vibrio parahaemolyticus* (Ueno et al., 2019).

Vibrio harveyi Biofilm, Bioluminescence, and Motility Are Regulated by a NO-Mediated QS Pathway

Vibrio harveyi is a bioluminescent opportunistic marine pathogen often found in tropical waters. *V. harveyi* bioluminescence, as well as biofilm, virulence and flagellar production, is controlled by QS. *V. harveyi* is thought to respond to at least three different autoinducers through the binding of three separate QS receptors (Bassler et al., 1993, 1994; Henke and Bassler, 2004). These receptors, LuxN, LuxQ, and CsqS are transmembrane hybrid histidine kinases. LuxQ also utilizes an accessory protein, LuxP, to sense its cognate autoinducer (Bassler et al., 1994; Neiditch et al., 2006). When cell density is low, the receptors LuxN, LuxQ, and CsqS autophosphorylate and subsequently transfer phosphate to a single histidine phosphotransfer protein LuxU (**Figure 1**). Phosphorylated LuxU then transfers phosphate downstream to a transcription factor LuxO which promotes the transcription of Quorum Regulatory RNAs (qrrs) (Freeman and Bassler, 1999a,b). Qrrs destabilize the mRNA encoding LuxR, the transcription regulator responsible for luciferase production and activator of biofilm related genes, consequently inhibiting bioluminescence as the light producing *lux* operon is not expressed (Lenz et al., 2004). However, when cell density increases, and autoinducer concentration is high, the receptors switch from kinases to phosphatases resulting in the dephosphorylation and inactivation of LuxO, and subsequent translation of LuxR leading to light production.

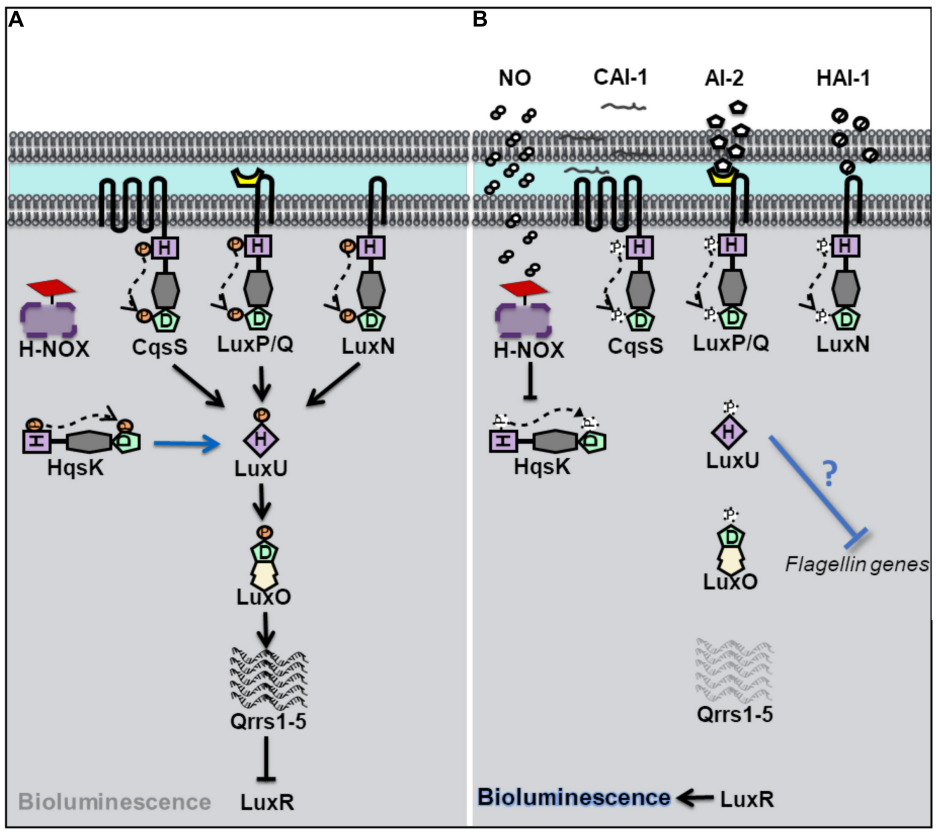

FIGURE 1 | Quorum sensing (QS) in *Vibrio harveyi* at high and low cell density. **(A)** At low cell density, when autoinducer concentration is small, *V. harveyi* hybrid histidine kinase receptors CqsS, LuxPQ, and LuxN transfer phosphate to a histidine phosphotransfer protein, LuxU. In the absence of NO, the cytosolyic hybrid histidine kinase HqsK, acts as a kinase, and participates in phosphotransfer with LuxU. Phosphorylated LuxU transfers phosphate to the transcription factor LuxU, resulting in the transcription of four small regulatory RNA molecules (Qrrs 1-5). Qrrs inhibit the expression of LuxR, the transcription regulator responsible for luciferase production and activator of biofilm related genes. **(B)** QS sensing signal transduction in *V. harveyi* at high cell density and in the presence of NO. When cell density is high, and autoinducer concentrations rise, CqsS, LuxPQ, and LuxN act as phosphatases, dephosphorylating LuxU. Qrrs are not expressed and LuxR is transcribed, resulting in bioluminescence, and the activation of biofilm related genes. In the presence of NO, NO bound H-NOX inhibits the autophosphorylation of HqsK resulting in decreased phosphate flow downstream, in addition to the repression of flagellin proteins by an unknown mechanism.

Vibrio harveyi has also been shown to contain a NO-mediated QS pathway (Henares et al., 2012). Low cell density cultures of *V. harveyi* exhibit increased bioluminescence in the presence of exogenous nanomolar NO, suggesting that NO can modulate QS pathways. The effect on NO on QS was attribute to a fourth hybrid histidine kinase, named Hqsk, that has both kinase and phosphatase activities and is able to transfer phosphate to LuxU. Unlike the other three previously characterized *V. harveyi* kinase receptors, HqsK is cytosolic, and does not contain a sensory domain in its primary sequence. Instead, HqsK activity was found to be regulated through interaction with an NO-sensitive H-NOX protein. NO-bound *Vh*H-NOX inhibits the kinase activity of HqsK which contributes to a loss of phosphorylated LuxU and a subsequent increase in light production through the LuxU/LuxO pathway described above. It should be reiterated here that *V. harveyi* contains three additional AI receptors, which together overwhelm the effect of NO at high cell density (when, presumably, the other three AIs are present at high concentration); the addition of NO to high cell density cultures of *V. harveyi* was not found to significantly increase bioluminescence (Henares et al., 2012). This suggests that NO may influence bioluminescence only at low cell density, or perhaps be only a minor contributor to the total QS output.

In addition to bioluminescence, NO was found to influence QS regulation of biofilm and flagellar production in *V. harveyi* (Henares et al., 2013). Many bacteria, including *V. harveyi*, rely on QS to initiate a switch between a motile and sessile (or biofilm) lifestyle. At high cell density, *V. harveyi* enters biofilm through the negative regulation of genes involved with motility (Waters and Bassler, 2006). Analogous to a high-density state, the addition of low nanomolar (50 nM) NO to cultures of *V. harveyi* resulted in thicker biofilms compared to cultures grown in the absence of NO. Further, the addition of NO to a Δ*hnoX* mutant strain lost the same biofilm enhancement phenotype as the wildtype strain, indicating that *Vh*H-NOX is involved in the NO-mediated biofilm pathway. As described previously, H-NOX plays a role in *V. harveyi* QS through an interaction with HqsK. Interestingly, the addition of autoinducers to cultures of *V. harveyi* did not

increase biofilm to the same degree that NO addition had (Henares et al., 2013). This finding suggests that the NO/H-NOX pathway is primary in the regulation of biofilm.

The initial stage of biofilm formation, when surface attachment occurs, is correlated with a decrease in motility and is dependent on functional flagella. While functional flagella are critical for colonization and initial attachment, late stage biofilms are often made up of bacteria that have lost their flagella. In the marine bacterium *V. fischeri*, flagellar proteins have been previously shown to be negatively regulated by QS (Lupp and Ruby, 2005). iTRAQ proteomics analysis was performed on *V. harveyi* in the presence of NO. Upon addition of 50 nM NO, the relative abundance of several *V. harveyi* flagellin genes, was shown to be decreased, consistent with the effect of NO on biofilm observed in the same study (Henares et al., 2013). Interestingly, however, the effect of NO on biofilm and flagellin concentration was NO concentration-dependent, however; as NO concentration increased, biofilm decreased and flagellin proteins increased (50–200 nM NO was studies). Nevertheless, since the loss of flagellin is associated with biofilm formation, these experiments provide a possible mechanism by which low nanomolar NO influences QS-mediated biofilm formation through the H-NOX/HqsK pathway.

> Key concept 1: NO mediates biofilm enhancement analogously to a high cell-density state in *Vibrio haveryi*.

Vibrio cholerae Contains a NO Sensing Hybrid Histidine Kinase Receptor

Vibrio cholerae relies on QS for the regulation of biofilm and virulence related genes (Kovacikova and Skorupski, 2002; Hammer and Bassler, 2003). Vibrio polysaccharide genes (*vps*), involved in the synthesis of the exopolymeric matrix of biofilms, and the master regulator of virulence factor production, AphA, are under QS control. Four separate QS pathways are believed to work in parallel in *V. cholerae* to allow for the detection of multiple signals (Jung et al., 2016). Four hybrid histidine kinase receptors have been identified. Three of these receptors, CqsS, LuxP/Q, and Vc1831 (CqsR), are membrane bound and the fourth, VpsS, is cytosolic (**Figure 2**; Miller et al., 2002; Shikuma et al., 2009). When autoinducer concentrations are high, CqsS, LuxP/Q and CqsR bind their cognate autoinducers and act as phosphatases, drawing phosphate away from the common phosphotransfer protein LuxU. At high cell density, HapR, the homolog of *V. harveyi*'s LuxR, is expressed, and represses genes responsible for biofilm and the master regulator of virulence factors, AphA (Rutherford et al., 2011). Therefore at high cell density, *V. cholerae* disperses from biofilm and is latent. However, when the concentration of autoinducers is small, typically at low cell density, the membrane bound receptors act as kinases and initiate phosphoryl transfer to LuxU and subsequently to the transcription factor LuxO. As in *V. harveyi*, phosphorylated LuxO in *V. cholerae*, initiates the expression of small regulatory RNA molecules qrrs (1-4) which inhibit HapR activity and also stabilize AphA (Svenningsen et al., 2008; Shao and Bassler, 2012). Repression of HapR activity derepresses expression of AphA and biofilm *vps* genes, resulting in increased virulence and biofilm at low cell density.

Until recently, the cognate autoinducer for the cytosolic kinase receptor VpsS was unknown, though VpsS was predicted to participate in QS based on studies demonstrating its purified receiver domain accepts phosphate from phosphorylated LuxU *in vitro* (Shikuma et al., 2009). Early studies of VpsS found that overexpression of *vpsS* in *V. cholerae* resulted in LuxO-mediated activation of *vps* genes and a hyperbiofilm phenotype. LuxO activation of *vps* genes was found to occur by activation of the positive regulator of *vps* gene expression, VpsR and is independent of HapR. Recently, our lab has shown that full-length VpsS participates in phosphotransfer with LuxU (Hossain et al., 2018). Like HqsK in *V. harveyi*, VpsS does not contain a sensory domain, which suggests that an accessory protein is used to regulate its activity. Our lab discovered that VpsS is co-cistronic with a novel NO sensing hemoprotein called NosP. Further, we showed that purified NO-bound NosP inhibits the autophosphorylation of VpsS, which subsequently results in decreased levels of phosphorylated LuxU *in vitro* (Hossain et al., 2018).

These experiments suggest that *V. cholerae* may sense NO to regulate gene expression through a QS pathway involving LuxU and LuxO. As in *V. harveyi*, NO appears to act analogously to an autoinducer to mimic a high cell density state where phosphate is transferred downstream through LuxU. Interestingly, *V. cholerae* has been shown to disperse from biofilm in the presence of nanomolar NO (Barraud et al., 2009). A decrease in phosphate flux downstream, as a result of NO-bound NosP inhibition of VpsS autophosphorylation, would explain the biofilm dispersal phenotype of *V. cholerae* in the presence of NO, as *vps* genes responsible for biofilm formation would be repressed. The relative effect of NO-contributed phosphate flux compared to that of the three other QS pathways in *V. cholerae* has not been quantified. It is possible, that like with *V. harveyi*, NO modulation of QS occurs predominantly at low cell density and/or is a minor overall contributor to phosphate flux through LuxU/LuxO. It is also possible that NO-modulated QS represents the broader possibility that exogenous environmental signals are able to modulate QS, a departure from QS outputs dependent on only true autoinducing (and thus cell density-dependent) molecules.

NO AND INNATE IMMUNITY

In response to a bacterial infection, the mammalian host produces high levels of NO through the upregulation of (iNOS). Nitrosative stress is an important component of the hosts innate immunity as it curbs microbial growth through the disruption of the fundamental physiological process including respiration, metabolism, and DNA replication (Murphy, 1999). However, bacteria have evolved to cope with nitrosative stress in order to circumvent host defenses during infection. In this section, we will discuss the discovery of a NO sensitive QS circuit in *Staphylococcus aureus* that may provide the bacterium with an evolutionary advantage when encountering high levels of NO during infection of a human host.

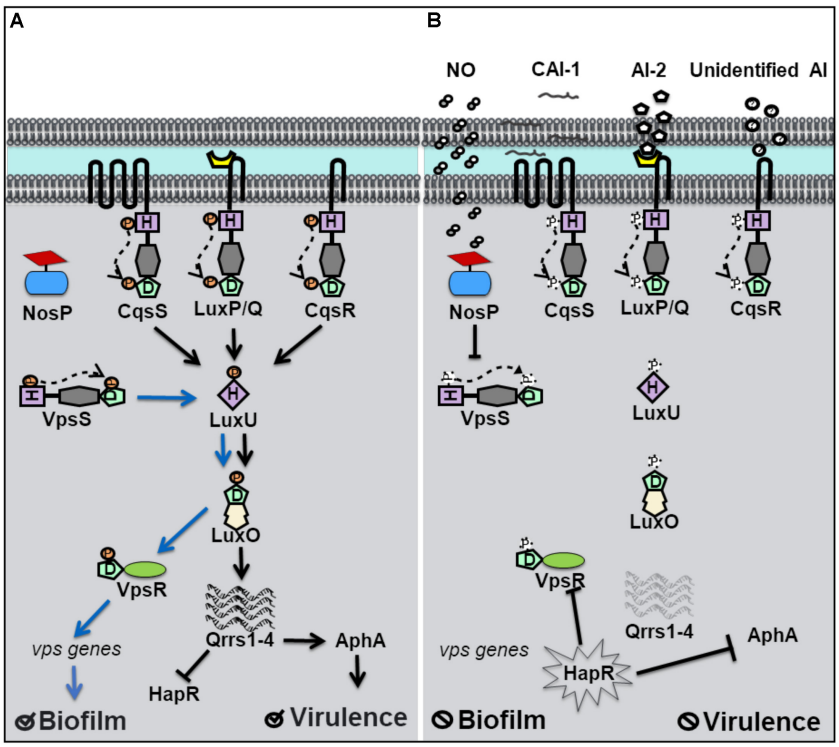

FIGURE 2 | Quorum sensing (QS) in *Vibrio cholerae* at high and low cell density. **(A)** At low cell density, when autoinducer concentration is small, *V. cholerae* hybrid histidine kinase receptors CqsS, LuxPQ, and CqsR transfer phosphate to a histidine phosphotransfer protein, LuxU. In the absence of NO, the cytosolyic hybrid histidine kinase VpsS, acts as a kinase, and participates in phosphotransfer with LuxU. Phosphorylated LuxU tranfers phosphate to the transcription factor LuxU, resulting in the transcription of four small regulatory RNA molecules (Qrrs 1-4). Qrrs activate the master regulator of virulence, AphA, and inhibit the expression of HapR, the master repressor of vibrio polysaccharide (*vps*) gene expression. Low cell density favors biofilm formation and virulence factor secretion. **(B)** QS signal transduction at high cell density and in the presence of NO. When cell density is high, and autoinducer concentrations rise, CqsS, LuxPQ, and CqsR act as phosphatases, dephosphorylating LuxU. Qrrs are not expressed and HapR is transcribed, resulting in the inhibition of AphA and genes involved in *vps* expression. Likewise, in the presence of NO, VcNosP FeII–NO inhibits the autophosphorylation activity of VpsS and results in decreased phosphate flux through LuxU.

Nitrosylation of a QS Regulator Inhibits Virulence of *S. aureus*

In addition to hemoprotein coordination, NO may exert its influence over bacterial QS pathways by protein S-nitrosylation (Kovacs and Lindermayr, 2013). NO modification of cystine residues is an important post translation modification governing protein function that has been observed in mammals, bacteria and plants. Free radical NO can react directly with thiyl radicals or may first react with an oxidant such as superoxide, oxygen or redox metals to form S-nitrosylating agents like peroxynitrite (Kovacs and Lindermayr, 2013). Not surprisingly, considering the inhibitory effect of NO on microbial survival, targets of S-nitrosylation within the genome of the commensal bacterium, *S. aureus*, include proteins involved in carbohydrate and lipid metabolism, tRNA and cell wall biosynthesis, DNA replication and repair, and amino acid metabolism (Urbano et al., 2018). Interestingly however, a small subset of S-nitrosylated proteins in S. *aureus* are responsible for antibiotic resistance and virulence. AgrA, a major transcriptional activator of virulence genes and a key component of staphylococcal QS, was found to be a target of S-nitrosylation at three separate cysteine residues C6, C123, and C199 (Urbano et al., 2018). In *S. aureus*, when cell density is high, AgrA is activated through phosphotransfer from the autophosphorylated AgrC receptor (**Figure 3**). When phosphosphylated, AgrA subsequently binds to several promotors responsible for the expression of virulence factors, including agrPIII, leading to positive autoregulation of the *agr* operon. Upon addition of a NO donor, the transcription of several AgrA targets was inhibited in a concentration dependent matter. Further, a NO insensitive mutant, in which C199 was replaced with serine residue, exhibited resistance to NO (Urbano et al., 2018). These findings suggest that NO inhibits QS-mediated virulence in *S. aureus* through the S-nitrosylation of AgrA cysteine residues, particularly C199. The authors also hypothesize that considering the conservation of cysteine residues across the LytTR family of regulators, NO might affect similar processes in other bacterial species through cysteine modification.

> Key concept 2: S-nitrosylation of AgrA cysteine residues impedes binding to target promoters.

α-toxin is a pore forming toxin that is the major contributor of *S. aureus* pathogenesis (Berube and Bubeck Wardenburg, 2013). In *S. aureus* pneumonia, α-toxin is responsible for lung

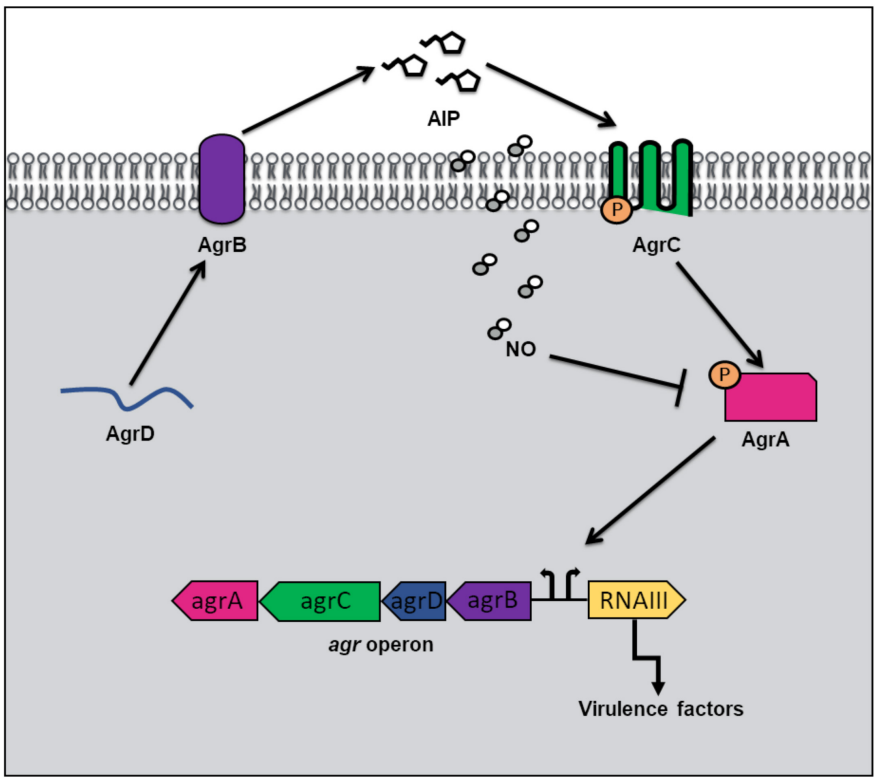

FIGURE 3 | Quorum sensing (QS) in *Staphylococcus aureus* at high cell density and in the presence of nitric oxide (NO). QS in *S. aureus* is mediated by an autoinducing peptide (AIP) that is formed from the cleavage of the propeptide AgrD. AgrD is exported across the membrane by the endopeptidase AgrB. At high cell density, the concentration of AIP rises until a threshold level is reached, and binding to AgrC receptor results. AgrC autophosphorylates upon binding AIP, and subsequently transfers its phosphate to the transcription factor AgrA. Phosphorylated AgrA induces the positive autoregulation of the *agr* operon, as well as the transcription of RNAIII, resulting in the expression of virulence factors. In the presence of NO, AgrA is inhibited, resulting in decreased transcription of the *agr* operon as well as toxin genes.

injury and inflammation (Bartlett et al., 2008). The production of α-toxin is regulated by AgrA, as activation of agrPIII induces RNAIII, a regulatory RNA molecule responsible for stimulation of α-toxin transcription (Morfeldt et al., 1995). The Fang laboratory discovered that the QS pathway used to regulate α-toxin production in *S. aureus* is affected by NO (Urbano et al., 2018). Congenic iNOS knockout mice were more susceptible to *S. aureus* infection than iNOS-competent mice suggesting that NO serves a protective role in the host during infection. While there were no significant differences in bacterial burden in the lungs of mice with and without iNOS, significantly higher levels of α-toxin were produced in iNOS-deficient mice compared with iNOS-competent mice (Urbano et al., 2018). Further, iNOS-deficient mice infected with a *S. aureus* mutant, in which C55 and C199 were replaced with NO insensitive residues, exhibited no differences in α-toxin levels compared to iNOS competent mice. Taken together, the *in vitro* and *in vivo* findings provide a mechanism by which NO serves a protective role during *S. aureus* infection by inhibiting AgrA activation of toxin expression through S-nitrosylation of AgrA cysteines required for promotor binding. The authors speculate that a potential advantage to *S. aureus*, of having a NO sensitive QS circuit to represses virulence, may be to maintain a balance between a pathogenic and commensal lifestyle during colonization of the human nose. Interestingly, asymptomatic nose carriers of *S. aureus* were found to contain bacteria with weak expression of Agr regulated toxins (Burian et al., 2010).

> Key concept 3: In a *S. aureus* model of infection, virulence, and not bacterial burden, is responsible for the differential disease severity between iNOS-deficient and iNOS-competent mice.

CONCLUDING REMARKS

In this review, the influence of NO on the QS-regulated behaviors of *V. harveyi*, *V. cholerae*, and *S. aureus* have been discussed. In *Vibrios*, NO ligation to hemoproteins has been found to influence the autophosphorylation of partner histidine kinases proteins that are integrated in QS pathways. NO appears to influence QS-mediated behaviors via a different mechanism in *S. aureus*, namely S-nitrosylation of a QS regulator protein. It has yet to be determined whether S-nitrosylation occurs in other bacterial species (including *V. harveyi* and *V. cholerae*) as a means to regulate cell-to-cell communication. Based on the currently

available data, it is likely that additional, as of yet undiscovered, NO-sensitive QS pathways exist in other bacterial species, both Gram-negative and Gram-positive strains. Like the examples first characterized and described here, these pathways are likely to detect NO concentrations through ligation to a hemoprotein or S-nitrosylation of cysteine residues.

Major questions concerning the role of NO in QS are outstanding and should be the subject of future study. There is no current evidence that NO is truly an autoinducer, as it may not be self-synthesized. Thus, one major question for future studies is what is the source of NO detected by QS circuits? Furthermore, if exogenous (either environmental or eukaryotic) NO is informing bacterial group decision making, another major open question is why? Finally, as molecules alternative to traditional AIs, including NO and lipids, have now been shown to modulate QS pathways, thus it may be appropriate to expand our understanding of QS from the traditionally understood role of monitoring cell density.

AUTHOR CONTRIBUTIONS

IH and EB wrote the manuscript.

FUNDING

This work was supported by the National Science Foundation (grant CHE-1607532 to EB) and the National Institutes of Health (grant GM118894-01A1 to EB).

REFERENCES

Arora, D. P., Hossain, S., Xu, Y., and Boon, E. M. (2015). Nitric oxide regulation of bacterial biofilms. *Biochemistry* 54, 3717–3728. doi: 10.1021/bi501476n

Barraud, N., Storey, M. V., Moore, Z. P., Webb, J. S., Rice, S. A., Kjelleberg, S., et al. (2009). Nitric oxide-mediated dispersal in single- and multi-species biofilms of clinically and industrially relevant microorganisms. *Microb. Biotechnol.* 2, 370–378. doi: 10.1111/j.1751-7915.2009.00098.x

Bartlett, A. H., Foster, T. J., Hayashida, A., and Park, P. W. (2008). α-Toxin facilitates the generation of CXC chemokine gradients and stimulates neutrophil homing in *Staphylococcus aureus* pneumonia. *J. Infect. Dis.* 198, 1529–1535. doi: 10.1086/592758

Bassler, B. L., Wright, M., Showalter, R. E., and Silverman, M. R. (1993). Intercellular signalling in *Vibrio harveyi*: sequence and function of genes regulating expression of luminescence. *Mol. Microbiol.* 9, 773–786. doi: 10.1111/j.1365-2958.1993.tb01737.x

Bassler, B. L., Wright, M., and Silverman, M. R. (1994). Multiple signalling systems controlling expression of luminescence in *Vibrio harveyi*: sequence and function of genes encoding a second sensory pathway. *Mol. Microbiol.* 13, 273–286. doi: 10.1111/j.1365-2958.1994.tb00422.x

Berube, B. J., and Bubeck Wardenburg, J. (2013). Staphylococcus aureus α-toxin: nearly a century of intrigue. *Toxins* 5, 1140–1166. doi: 10.3390/toxins5061140

Burian, M., Wolz, C., and Goerke, C. (2010). Regulatory adaptation of *Staphylococcus aureus* during nasal colonization of humans. *PLoS One* 5:e10040. doi: 10.1371/journal.pone.0010040

Chen, Y. J., and Rosazza, J. P. N. A. (1994). Bacterial, nitric oxide synthase from a *Nocardia species*. *Biochem. Biophys. Res. Commun.* 203, 1251–1258. doi: 10.1006/bbrc.1994.2317

Freeman, J. A., and Bassler, B. L. (1999a). Genetic analysis of the function of LuxO, a two-component response regulator involved in quorum sensing in *Vibrio harveyi*. *Mol. Microbiol.* 31, 665–677. doi: 10.1046/j.1365-2958.1999.01208.x

Freeman, J. A., and Bassler, B. L. (1999b). Sequence and function of LuxU: a two-component phosphorelay protein that regulates quorum sensing in *Vibrio harveyi*. *J. Bacteriol.* 181, 899–906.

Hammer, B. K., and Bassler, B. L. (2003). Quorum sensing controls biofilm formation in *Vibrio cholerae*. *Mol. Microbiol.* 50, 101–104. doi: 10.1046/j.1365-2958.2003.03688.x

Henares, B. M., Higgins, K. E., and Boon, E. M. (2012). Discovery of a nitric oxide responsive quorum sensing circuit in *Vibrio harveyi*. *ACS Chem. Biol.* 7, 1331–1336. doi: 10.1021/cb300215t

Henares, B. M., Xu, Y., and Boon, E. M. (2013). A nitric oxide-responsive quorum sensing circuit in *Vibrio harveyi* regulates flagella production and biofilm formation. *Int. J. Mol. Sci.* 14, 16473–16484. doi: 10.3390/ijms140816473

Henke, J. M., and Bassler, B. L. (2004). Three parallel quorum-sensing systems regulate gene expression in *Vibrio harveyi*. *J. Bacteriol.* 186, 6902–6914. doi: 10.1128/jb.186.20.6902-6914.2004

Hentzer, M., Eberl, L., and Givskov, M. (2005). Transcriptome analysis of *Pseudomonas aeruginosa* biofilm development: anaerobic respiration and iron limitation. *Biofilms* 2, 37–61. doi: 10.1017/s1479050505001699

Hossain, S., and Boon, E. M. (2017). Discovery of a novel nitric oxide binding protein and nitric oxide-responsive signaling pathway in *Pseudomonas aeruginosa*. *ACS Infect. Dis.* 3, 454–461. doi: 10.1021/acsinfecdis.7b00027

Hossain, S., Heckler, I., and Boon, E. M. (2018). Discovery of a nitric oxide responsive quorum sensing circuit in *Vibrio cholerae*. *ACS Chem. Biol.* 13, 1964–1969. doi: 10.1021/acschembio.8b00360

Iyer, L. M., Anantharaman, V., and Aravind, L. (2003). Ancient conserved domains shared by animal soluble guanylyl cyclases and bacterial signaling proteins. *BMC Genomics* 4:5.

Jung, S. A., Hawver, L. A., and Ng, W.-L. (2016). Parallel quorum sensing signaling pathways in *Vibrio cholerae*. *Curr. Genet.* 62, 255–260. doi: 10.1007/s00294-015-0532-8

Karow, D. S., Pan, D., Tran, R., Pellicena, P., Presley, A., Mathies, R. A., et al. (2004). Spectroscopic characterization of the soluble guanylate cyclase-like heme domains from *Vibrio cholerae* and *Thermoanaerobacter* tengcongensis. *Biochemistry* 43, 10203–10211. doi: 10.1021/bi049374l

Kovacikova, G., and Skorupski, K. (2002). Regulation of virulence gene expression in *Vibrio cholerae* by quorum sensing: HapR functions at the aphA promoter. *Mol. Microbiol.* 46, 1135–1147. doi: 10.1046/j.1365-2958.2002.03229.x

Kovacs, I., and Lindermayr, C. (2013). Nitric oxide-based protein modification: formation and site-specificity of protein S-nitrosylation. *Front. Plant Sci.* 4:137. doi: 10.3389/fpls.2013.00137

Lenz, D. H., Mok, K. C., Lilley, B. N., Kulkarni, R. V., Wingreen, N. S., Bassler, B. L., et al. (2004). The small RNA chaperone Hfq and multiple small RNAs control quorum sensing in *Vibrio harveyi* and *Vibrio cholerae*. *Cell* 118, 69–82. doi: 10.1016/j.cell.2004.06.009

Lin, B., Wang, Z., Malanoski, A. P., O'Grady, E. A., Wimpee, C. F., Vuddhakul, V., et al. (2010). Comparative genomic analyses identify the *Vibrio harveyi* genome sequenced strains BAA-1116 and HY01 as *Vibrio campbellii*. *Environ. Microbiol. Rep.* 2, 81–89. doi: 10.1111/j.1758-2229.2009.00100.x

Lupp, C., and Ruby, E. G. (2005). *Vibrio fischeri* uses two quorum-sensing systems for the regulation of early and late colonization factors. *J. Bacteriol.* 187, 3620–3629. doi: 10.1128/jb.187.11.3620-3629.2005

Miller, M. B., and Bassler, B. L. (2001). Quorum sensing in bacteria. *Annu. Rev. Microbiol.* 55, 165–199.

Miller, M. B., Skorupski, K., Lenz, D. H., Taylor, R. K., and Bassler, B. L. (2002). Parallel quorum sensing systems converge to regulate virulence in *Vibrio cholerae*. *Cell* 110, 303–314. doi: 10.1016/s0092-8674(02)00829-2

Morfeldt, E., Taylor, D., von Gabain, A., and Arvidson, S. (1995). Activation of alpha-toxin translation in *Staphylococcus aureus* by the trans-encoded antisense RNA, RNAIII. *EMBO J.* 14, 4569–4577. doi: 10.1002/j.1460-2075.1995.tb00136.x

Murphy, M. P. (1999). Nitric oxide and cell death. *Biochim. Biophys. Acta Bioenerg.* 1411, 401–414.

Neiditch, M. B., Federle, M. J., Pompeani, A. J., Kelly, R. C., Swem, D. L., Jeffrey, P. D., et al. (2006). Ligand-induced asymmetry in histidine sensor kinase complex regulates quorum sensing. *Cell* 126, 1095–1108. doi: 10.1016/j.cell.2006.07.032

Ng, W.-L., and Bassler, B. L. (2009). Bacterial quorum-sensing network architectures. *Annu. Rev. Genet.* 43, 197–222. doi: 10.1146/annurev-genet-102108-134304

Papenfort, K., and Bassler, B. L. (2016). Quorum sensing signal-response systems in Gram-negative bacteria. *Nat. Rev. Microbiol.* 14, 576–588. doi: 10.1038/nrmicro.2016.89

Plate, L., and Marletta, M. A. (2012). Nitric oxide modulates bacterial biofilm formation through a multicomponent Cyclic-di-GMP signaling network. *Mol. Cell* 46, 449–460. doi: 10.1016/j.molcel.2012.03.023

Plate, L., and Marletta, M. A. (2017). Nitric oxide-sensing H-NOX proteins govern bacterial communal behavior. *Trends Biochem. Sci.* 38, 566–575. doi: 10.1016/j.tibs.2013.08.008

Rutherford, S. T., van Kessel, J. C., Shao, Y., and Bassler, B. L. (2011). AphA and LuxR/HapR reciprocally control quorum sensing in *Vibrios*. *Genes Dev.* 25, 397–408. doi: 10.1101/gad.2015011

Shao, Y., and Bassler, B. L. (2012). Quorum-sensing non-coding small RNAs use unique pairing regions to differentially control mRNA targets. *Mol. Microbiol.* 83, 599–611. doi: 10.1111/j.1365-2958.2011.07959.x

Shikuma, N. J., Fong, J. C., Odell, L. S., Perchuk, B. S., Laub, M. T., Yildiz, F. H., et al. (2009). Overexpression of VpsS, a hybrid sensor kinase, enhances biofilm formation in *Vibrio cholerae*. *J. Bacteriol.* 191, 5147–5158. doi: 10.1128/JB.00401-09

Svenningsen, S. L., Waters, C. M., and Bassler, B. L. (2008). A negative feedback loop involving small RNAs accelerates *Vibrio cholerae*'s transition out of quorum-sensing mode. *Genes Dev.* 22, 226–238. doi: 10.1101/gad.1629908

Thompson, C. M., Tischler, A. H., Tarnowski, D. A., Mandel, M. J., and Visick, K. L. (2019). Nitric oxide inhibits biofilm formation by *Vibrio fischeri* via the nitric oxide sensor HnoX. *Mol. Microbiol.* 111, 187–203. doi: 10.1111/mmi.14147

Tsai, A.-L., Berka, V., Martin, E., and Olson, J. S. A. (2012). 'Sliding Scale Rule' for Selectivity among NO, CO, and O2 by heme protein sensors. *Biochemistry* 51, 172–186. doi: 10.1021/bi2015629

Ueno, T., Fischer, J. T., and Boon, E. M. (2019). Nitric oxide enters quorum sensing via the H-NOX signaling pathway in Vibrio parahaemolyticus. *Front. Microbiol.* 10:2108. doi: 10.3389/fmicb.2019.02108

Urbano, R., Karlinsey, J. E., Libby, S. J., Doulias, P. T., Ischiropoulos, H., Warheit-Niemi, H. I., et al. (2018). Host nitric oxide disrupts microbial cell-to-cell communication to inhibit staphylococcal virulence. *Cell Host Microbe* 23, 594–606.e7. doi: 10.1016/j.chom.2018.04.001

Waters, C. M., and Bassler, B. L. (2006). The *Vibrio harveyi* quorum-sensing system uses shared regulatory components to discriminate between multiple autoinducers. *Genes Dev.* 20, 2754–2767. doi: 10.1101/gad.1466506

Conflict of Interest: The authors declare that the research was conducted in the absence of any commercial or financial relationships that could be construed as a potential conflict of interest.

frontiers in Microbiology

ORIGINAL RESEARCH
published: 27 September 2019
doi: 10.3389/fmicb.2019.02212

Effect of Co-inhabiting Coagulase Negative Staphylococci on *S. aureus agr* Quorum Sensing, Host Factor Binding, and Biofilm Formation

*Pai Peng[1], Mara Baldry[1], Bengt H. Gless[2], Martin S. Bojer[1], Carmen Espinosa-Gongora[1], Sharmin J. Baig[3], Paal S. Andersen[1,3], Christian A. Olsen[2] and Hanne Ingmer[1]**

[1] Faculty of Health and Medical Sciences, Department of Veterinary and Animal Sciences, University of Copenhagen, Copenhagen, Denmark, [2] Faculty of Health and Medical Sciences, Department of Drug Design and Pharmacology, University of Copenhagen, Copenhagen, Denmark, [3] Department of Bacteria, Parasites and Fungi, Statens Serum Institut, Copenhagen, Denmark

OPEN ACCESS

Edited by:
Ana Maria Otero, University of Santiago de Compostela, Spain

Reviewed by:
Iñigo Lasa, Universidad Pública de Navarra, Spain
Joanna Nakonieczna, University of Gdańsk and Medical University of Gdańsk, Poland

***Correspondence:**
Hanne Ingmer
hi@sund.ku.dk

Specialty section:
This article was submitted to Antimicrobials, Resistance and Chemotherapy, a section of the journal Frontiers in Microbiology

Received: *28 February 2019*
Accepted: *10 September 2019*
Published: *27 September 2019*

Citation:
Peng P, Baldry M, Gless BH, Bojer MS, Espinosa-Gongora C, Baig SJ, Andersen PS, Olsen CA and Ingmer H (2019) Effect of Co-inhabiting Coagulase Negative Staphylococci on S. aureus agr Quorum Sensing, Host Factor Binding, and Biofilm Formation. Front. Microbiol. 10:2212. doi: 10.3389/fmicb.2019.02212

Staphylococcus aureus is a commensal colonizer of both humans and animals, but also an opportunistic pathogen responsible for a multitude of diseases. In recent years, colonization of pigs by methicillin resistant *S. aureus* has become a problem with increasing numbers of humans being infected by livestock strains. In *S. aureus* colonization and virulence factor expression is controlled by the *agr* quorum sensing system, which responds to and is activated by self-generated, autoinducing peptides (AIPs). AIPs are also produced by coagulase negative staphylococci (CoNS) commonly found as commensals in both humans and animals, and interestingly, some of these inhibit *S. aureus agr* activity. Here, we have addressed if cross-communication occurs between *S. aureus* and CoNS strains isolated from pig nares, and if so, how properties such as host factor binding and biofilm formation are affected. From 25 pig nasal swabs we obtained 54 staphylococcal CoNS isolates belonging to 8 different species. Of these, none were able to induce *S. aureus agr* as monitored by reporter gene fusions to *agr* regulated genes but a number of *agr*-inhibiting species were identified including *Staphylococcus hyicus*, *Staphylococcus simulans*, *Staphylococcus arlettae*, *Staphylococcus lentus*, and *Staphylococcus chromogenes*. After establishing that the inhibitory activity was mediated via AgrC, the receptor of AIPs, we synthesized selective AIPs to explore their effect on adhesion of *S. aureus* to fibronectin, a host factor involved in *S. aureus* colonization. Here, we found that the CoNS AIPs did not affect adhesion of *S. aureus* except for strain 8325-4. When individual CoNS strains were co-cultured together with *S. aureus* we observed variable degrees of biofilm formation which did not correlate with *agr* interactions. Our results show that multiple CoNS species can be isolated from pig nares and that the majority of these produce AIPs that inhibit *S. aureus agr*. Further they show that the consequences of the interactions between CoNS and *S. aureus* are complex and highly strain dependent.

Keywords: *Staphylococcus aureus*, coagulase-negative staphylococci, colonization, *agr*, quorum sensing interaction, cross-talk

INTRODUCTION

Staphylococcus aureus is a common colonizer and opportunistic pathogen of both animals and humans. The increasing spread of antibiotic resistance among *S. aureus* strains is of major concern in the treatment of staphylococcal infections, with methicillin-resistant *S. aureus* (MRSA) in particular being a proven health risk to humans, causing skin and soft tissue infections, food poisoning, and even fatal systemic disease (Fridkin et al., 2005; Kourbatova et al., 2005; King et al., 2006). MRSA strains are commonly divided into community, hospital or livestock associated and in recent years, the transmission of livestock-associated (LA)-MRSA from animals to humans has become a public health concern particularly in Europe, North America and Asia where pig farming is extensive. Within the EU alone nearly 46% of pigs are colonized by strains of the most predominant LA-MRSA type namely the clonal complex 398 (CC398) (Khanna et al., 2008; Lewis et al., 2008; Van Duijkeren et al., 2008; Authority, 2009; Smith et al., 2009; Golding et al., 2010; Köck et al., 2013; Chuang and Huang, 2015). Studies have revealed a high prevalence of nasal MRSA carriage in pig slaughterhouse workers and pig farmers, indicating that working with MRSA-colonized pigs is the predominant risk factor (Lewis et al., 2008; Van Cleef et al., 2010).

In general, *S. aureus* colonization is a multifactorial process involving a number of adhesins or host binding proteins that are expressed by, and located on, the surface of the bacterium (Josse et al., 2017). Particularly fibronectin binding proteins have been reported to be important for internalization and uptake of *S. aureus* by keratinocytes; to be key in the adhesion of *S. aureus* to keratinocytes of atopic skin and also to contribute to biofilm formation by MRSA strains (Cho et al., 2001; Kintarak et al., 2004; O'Neill et al., 2008; Josse et al., 2017). In addition to colonization factors, *S. aureus* also expresses a multitude of toxins and other factors necessary for virulence and biofilm formation (Archer et al., 2011; Kobayashi et al., 2015). Production of both adhesins and toxins are controlled by the accessory gene regulator (*agr*) quorum sensing system with the former being produced at low bacterial cell densities and the latter at high cell densities (Yarwood and Schlievert, 2003). *agr* is composed of a two component system which senses a self-generated autoinducing peptide (AIP) that, by binding to the sensor histidine kinase AgrC, leads to phosphorylation of the AgrA response-regulator and expression of the main *agr* effector molecule, RNAIII. As cells enter stationary phase, RNAIII is responsible for the down-regulation of host binding proteins such as Protein A encoded by *spa* and the concomitant upregulation of toxins such as α-hemolysin encoded by *hla* (Queck et al., 2008; Wang et al., 2014; Le and Otto, 2015). An RNAIII-independent *agr* gene regulation pathway also exists, involving AgrA-mediated expression of a family of toxins called the phenol soluble modulins (PSMs) (Periasamy et al., 2012). These PSMs are important players in biofilm formation and dispersal linking *agr* and biofilm formation (Boles and Horswill, 2008; Periasamy et al., 2012). Interestingly *agr* varies between *S. aureus* strains and can be divided into four groups (AgrC-I-IV) where AIPs from the corresponding group lead to self-activation whereas AIPs from other groups lead to cross-inhibition (Otto et al., 2001; Olson et al., 2014; Le and Otto, 2015). This group specificity has lead to an interest in studying the inhibitory activity of non-cognate AIPs as antivirulence sources targeting *agr* (Canovas et al., 2016; Tal-Gan et al., 2016).

Humans and animals are also colonized with a variety of other staphylococcal species. In contrast to *S. aureus* they do not produce coagulase and thus are termed the coagulase negative staphylococci (CoNS). Commonly, the CoNS are not pathogens and their presence has been suggested to influence *S. aureus* colonization. For example, in humans it has been proposed that *Staphylococcus epidermidis* may prevent colonization by *S. aureus* (Iwase et al., 2010), whereas in pigs, *S. aureus* colonization was not observed in the presence of *Staphylococcus sciuri*, *Staphylococcus cohnii*, or *Staphylococcus saprophyticus* (Verstappen et al., 2017). Interestingly, CoNS also encode AIP-like molecules and some of these are able to inhibit *S. aureus agr* (Otto et al., 1999; Canovas et al., 2016; Gless et al., 2017, 2019; Mahmmod et al., 2018). This cross-talk has been suggested to be involved in the competition between *S. aureus* and *S. epidermidis* on the skin (Otto et al., 2001) and in preventing MRSA colonization (Paharik et al., 2017).

The *agr*-mediated interactions between species isolated from the same host niche remains largely unexplored. In the present study we have examined which staphylococcal species co-colonize the pig nares and assessed the extent to which isolated CoNS strains are able to inhibit *S. aureus agr*. We have addressed if *agr* mediated cross-species communication affects *S. aureus* binding to fibronectin as well as biofilm formation, both elements that may be important for host colonization. Our results suggest extensive cross-communication between CoNS and *S. aureus* colonizing the same host niche. A better understanding of the role of *agr* cross-talk between colonizing staphylococci may provide insightful information that can be used for future exploitation in *S. aureus* colonization interference and anti-virulence therapy.

MATERIALS AND METHODS

Bacterial Strains and Growth Conditions

Strains used in this study are listed in **Table 1**. Unless otherwise stated, all bacterial strains were grown in Tryptone Soya Broth (TSB) from Oxoid, at a 1:10 volume/flask ratio, at 37°C with shaking at 200 rpm.

Sample Collection, Isolation, and Identification

Nasal swabs (E-Swab, Copan Diagnostics Inc., United States) were collected from the pig nasal cavity of randomly selected pigs (weighing 20–30 kg) at three organic farms in Denmark. It should be noted that no permission is required to sample the nostril of pigs according to the Danish Animal Experimentation Act § 1.2. Samples were sent within 24 h to the Department of Veterinary and Animal Sciences, University of Copenhagen, and analyzed on the day of arrival. In total, 25 samples from 25 pigs were analyzed. Swabs were suspended and diluted in saline solution and plated on SaSelect^{TM} plates (Bio-Rad)

TABLE 1 | Strains in this study and their source.

Strain	Description	References
8325-4	*S. aureus* producing AIP group I	Novick and Morse, 1967
PC203	*S. aureus* 8325-4, *spa:lacZ*	Chan and Foster, 1998
PC322	*S. aureus* 8325-4, *hla:lacZ*	Chan and Foster, 1998
SH101F7	*S. aureus* 8325-4, *rnaIII:lacZ*	Horsburgh et al., 2002
RN10829/p*agrC*-I	*S. aureus* AgrC-I P3*:blaZ*	Nielsen et al., 2014
RN10829/p*agrC*-II	*S. aureus* AgrC-II P3*:blaZ*	Gless et al., 2019
RN10829/p*agrC*-III	*S. aureus* AgrC-III P3*:blaZ*	Gless et al., 2019
RN10829/p*agrC*-IV	*S. aureus* AgrC-IV P3*:blaZ*	Gless et al., 2019
RN10829/p*agrC*-I-R23H (AgrC const.)	*S. aureus* AgrC-I-R23H P3*:blaZ*	Geisinger et al., 2009
RN6607	*S. aureus* producing AIP group II	(Lab stock)
MW2	*S. aureus* producing AIP group III	(Lab stock)
RN4850	*S. aureus* producing AIP group IV	(Lab stock)
61599	LA-MRSA CC398 strain	Tang et al., 2017b
8325-4Δ*agr*	Transduction from *S. aureus* RN6911	Canovas et al., 2016
HG001	*S. aureus* 8325-4, restored *rsbU*	Herbert et al., 2010
HG003	*S. aureus* 8325-4, restored *rsbU* and *tcaR*	Herbert et al., 2010

for staphylococcal species isolation. Species identification was carried out by matrix-assisted laser desorption ionization–time of flight mass spectrometry (MALDI-TOF MS) and *tuf* gene analysis by standard PCR-based methods (Hwang et al., 2011).

β-Galactosidase Plate Assay

This assay was performed as previously described (Nielsen et al., 2010; Bojer et al., 2017). Briefly, the fused reporter strains PC203 (*spa*:*lacZ*), PC322 (*hla*:*lacZ*), and SH101F7 (*rnaIII*:*lacZ*) all in the 8325-4 strain background, were grown in TSA agar supplemented with 150 μg/mL β-galactosidase substrate 5-bromo-4-chloro-3-indolyl-b-D-galactopyranoside (X-gal) and 5 μg/mL erythromycin. Sixty microliter supernatants of the identified staphylococcal strains or TSB medium were added to premade wells in the plates. The plates were incubated at 37°C for 10–24 h (the incubation time varies depending on the different reporter strains) until the plates appeared blue.

β-Lactamase Assay

This method was carried out as previously described with minor modifications (Nielsen et al., 2014; Bojer et al., 2017). Briefly, the reporter strains RN10829/p*agrC*-I-IV (WT) and RN10829/p*agrC*-I-R23H (AgrC const.) were treated with a 1/10 volume of CoNS supernatant at OD600 = 0.35, followed by the addition of a 1/10 volume of AIP-I-IV containing supernatant obtained separately from *S. aureus* strain 8325-4, RN6607, MW2 and RN4850. For the experiment investigating whether CoNS supernatants can induce *agr*, external AIP-I-IV supernatants were added as activation controls only. Samples were obtained after incubating at 37°C for 1 h, and optical density at 600 nm was recorded. Samples were stored at −80°C before thawing to test for β-lactamase activity as described (Bojer et al., 2017). Activity was calculated as arbitrary units based on nitrocefin conversion velocities (V_{max}, ΔOD486 nm/time) normalized to the sample cell densities.

Chemical Synthesis of AIPs

All AIPs were synthesized according to a previously reported protocol (Gless et al., 2017). Briefly, linear peptides were synthesized using automated 9-fluorenylmethyloxycarbonyl (Fmoc) solid-phase peptide synthesis (SPPS) on a Gly-ChemMatrix resin loaded with Fmoc-3-amino-4-(methylamino)-benzoic acid (Fmoc-MeDbz-OH). The last residue was incorporated as *N*-Boc protected amino acid. After SPPS, the MeDbz linker was converted to the *N*-acyl-benzimidazolinone (Nbz) species by treating the resin with 4-nitrophenyl-chloroformate in dichloromethane followed by a solution of *i*-Pr_2NEt in dimethylformamide. The activated Nbz-resin was then treated with a trifluoroacetic acid (TFA) solution to cleave protecting groups and after excessive washing, swelled in cyclization buffer (phosphate buffer, 0.2 M, pH 6.8 in 50% acetonitrile) and incubated at 50°C for 2 h. The AIP containing solution was separated from the resin and the desired AIP purified by preparative reverse-phase high performance liquid chromatography (RP-HPLC). Full characterization of all synthetic AIPs has been reported previously (Gless et al., 2019). The sequences and quality of the synthetic AIPs can be found in **Supplementary Table S1**.

Adhesion Assay

This assay was carried out as previously described (Baldry et al., 2016a). Ninety-six well plates were pre-coated with 100 μL/well of 10 μg/mL fibronectin (Fibronectin from human plasma, F2006, Sigma-Aldrich) and incubated for up to 24 h with mild shaking at 4°C. Respective overnight cultures of *S. aureus* strains 8325-4, 61599 (CC398 strain), HG001, HG003 and two *S. aureus* pig isolates (from this study) were diluted 1:100 and grown till OD_{600} = 0.5 in fresh TSB medium, after which the bacteria were treated with the synthesized AIPs belonging to *Staphylococcus hyicus* (10^{-4} mM), *Staphylococcus simulans* (10^{-4} mM), and *Staphylococcus chromogenes* (10^{-3} mM) separately, and grown at 37°C with shaking until OD_{600} = 1.7. The concentrations resulting in 100% inhibitory effect on the *agr* system were chosen according to their IC_{50} values. After removing and washing, untreated and treated *S. aureus* were added to fibronectin-coated wells and incubated statically at 37°C for 1 h. To avoid the toxic effect of DMSO on bacterial growth, the final solvent concentration of DMSO was maintained at 0.2% (v/v) for all experimental and control cultures. After removing the non-adhered bacteria and washing the wells, the attached bacteria were fixed with 2.5% glutaraldehyde in PBS statically for 1 h at 37°C. Binding activity of *S. aureus* was quantified by measuring the OD_{570} absorbance of resuspension in 96% ethanol after staining with 0.1% crystal violet at room temperature for 30 min. Arbitrary binding units were calculated by dividing the crystal violet absorption OD by the bacterial cell density of 1.7.

Static Biofilm Assay

As previously described (Nielsen et al., 2012; Goetz et al., 2017) and with minor modifications, overnight cultures were adjusted

to OD600 = 0.2 in TSB and then further diluted 1:100 in 66%TSB supplemented with 0.2% glucose. A total of 200 μL of the bacterial suspensions were added to wells where either *S. aureus* 8325-4 WT, 8325-4Δ*agr* (*agr*$^-$ strain), CoNS alone, or a 1:1 ratio of *S. aureus* + CoNS was added. After a 24–30 h incubation period, the medium was removed from each well; the plates were washed and allowed to air dry. Dried biofilms were stained with 125 μL of 0.1% crystal violet solution for 30 min, washed three times with PBS and allowed to dry. To quantify the biofilm formation, the stained biofilm was solubilized in 200 μL of 95% ethanol for 10–15 min and 100 μL were transferred to a new microtiter plate, after which the absorbance was measured at 590 nm. In this assay, three biological replicates were performed with eight technical replicates per experiment. Parallel samples were set for CFU quantification by subsequent plating on SaSelect^{TM} plates (Bio-Rad).

DNA Sequence Analysis

From purified DNA a sequencing library was generated using Nextera XT (Illumina) followed by (2 × 150 bp) paired-end sequencing on a NextSeq (Illumina) instrument. Genome sequences were *de novo* assembled using *skesa* with default settings (Souvorov et al., 2018). From assembled draft genomes the species were identified using the *tuf* gene, which has previously been described to discriminate between *Staphylococcus* species (McMurray et al., 2016; Strube et al., 2018).

Statistical Analysis

Where applied, we used a 1-way ANOVA analysis (GraphPad Prism version 7.04 software; GraphPad Software Inc., La Jolla, CA, United States). Differences were considered statistically significant at $P < 0.05$.

RESULTS

Nasal Colonization of *S. aureus* and Other Staphylococcal Species

To investigate CoNS strains colonizing pig nares we collected nasal swabs from 25 pigs originating from Danish organic pig farms and isolated staphylococcal species on Sa Select^{TM} plates. In total, 384 isolates were obtained of which 75 were identified by MALDI-TOF MS. *tuf* gene analysis and genome sequencing were performed to further verify some of the strains (Hwang et al., 2011; Loonen et al., 2012). Of the 75 isolates 21 were identified as *S. aureus*; corresponding to just over half of the swabs being positive for *S. aureus* (52%; 13/25 pigs). The remaining 54 isolates were identified and classified into 8 CoNS species originating from 20 of the 25 pigs (**Table 2**). *Staphylococcus sciuri* (40%) was the most dominant amongst the CoNS isolated, followed by *Staphylococcus lentus* (24%), *Staphylococcus xylosus* (24%), *S. simulans* (20%), *S. hyicus* (16%), *Staphylococcus arlettae* (16%), *S. chromogenes* (8%), and finally *Staphylococcus agnetis* (4%). These results show that there is substantial variation among pigs with respect to staphylococcal colonization and that they are commonly colonized by more than one species.

S. aureus Virulence Factor Expression Is Affected by CoNS Strains

Based on previous reports of cross-communication between *S. aureus* and CoNS strains we hypothesized that *S. aureus* interacts via *agr* with the surrounding microbial consortia including the resident CoNS. Therefore, the secreted products of the isolated CoNS strains were screened for their ability to modulate *S. aureus agr* using a previously established reporter assay. This assay is based on three reporter strains where the promoters of RNAIII, *hla* and *spa*, respectively, are fused to *lacZ* (Nielsen et al., 2010). Upon induction of *agr* such as is observed during entry into stationary growth phase, promoters of both RNAIII and *hla* will be induced while that of *spa* will be repressed. Therefore, after incorporation of the reporter strains together with the LacZ substrate into the agar plates they will become blue when containing the RNAIII and *hla* reporter strain fusions, but will remain colorless when containing the *spa* reporter strain after overnight incubation. Conversely, if an *agr* inhibiting compound has been added to a well in the agar plate reduced expression of *hla* and RNAIII but increased expression of *spa* will be observed. As seen in **Figure 1**, the extent to which CoNS supernatants affected the *S. aureus agr* (*agr*-I) system varied between species and in some cases even within species. Interestingly, while *S. sciuri* was the most prevalent species in the swabs, none of the supernatants from isolates of this species affected the *S. aureus agr* system. In contrast, isolates belonging to *S. hyicus*, *S. simulans*, and *S. lentus* species contained the most isolates with *S. aureus agr* modulation capabilities. These findings show that CoNS display varying ability to repress the *S. aureus agr* and that such repression is commonly observed.

Effect of CoNS Strains on *S. aureus agr* Groups I–IV

In the agar plate assay (**Figure 1**) we had determined the inhibitory activity of CoNS strains in a *S. aurues* strain belonging to AgrC group I. To determine if the CoNS AIPs are able to inhibit *agr* in *S. aureus* strains carrying the AgrC groups II to IV, and to obtain a quantative measure of the inhibitory effect we employed β-lactamase reporter strains that monitor expression of the RNAIII P3 promoter in cells expressing AgrC groups I to IV. As these strains have been engineered so that they do not produce intrinsic AIPs, induction of *agr* requires addition of supernatants from strains producing the corresponding AIP group (Nielsen et al., 2014). In this system, the activity of the reporter strains were measured in the presence or absence of cell-free, overnight culture supernatants of our CoNS isolates. Importantly, all the CoNS supernatants that displayed an *agr*-inhibitory activity in the plate assay also inhibited RNAIII expression in *S. aureus* strains carrying *agr* groups I, II, and III, whereas the inhibitory potential against group IV was only marginal (**Figures 2A1–D2**). Further we confirmed the notion that the CoNS AIPs affect *S. aureus agr* via competitive inhibition of AgrC as we saw little to no inhibition of the P3 promoter in a reporter strain encoding a constitutively active AgrC variant of *agr* group I that displays kinase activity in the absence of inducing AIP (Geisinger et al., 2009) (**Figures 2E1,E2**).

TABLE 2 | Frequency and presence of eight staphylococcal species isolated from 25 pigs.

Pig No.	% Isolation frequency – *species identity* – species isolated/pig								
	40% *S. sciuri*	24% *S. lentus*	24% *S. xylosus*	16% *S. hyicus*	16% *S. arlettae*	20% *S. simulans*	8% *S. chromogenes*	4% *S. agnetis*	52% *S. aureus*
1	X		X						X
2				X		X			X
3	X					X			X
4	X			X		X			X
5				X		X			X
6	X								X
7			X						X
8							X		X
9									X
10									X
11									X
12									X
13									X
14		X			X				
15	X					X			
16		X							
17		X	X						
18	X	X			X				
19		X			X				
20	X	X							
21				X			X	X	
22	X				X				
23	X		X						
24	X		X						
25			X						

Rows indicate the presence of staphylococci in the individual pigs. Columns contain the different staphylococcal species identified.

In addition to inhibition, we were also interested in exploring whether any of the staphylococcal supernatants could induce *S. aureus agr* activity. To this end we tested the ability of our CoNS isolates to induce *S. aureus agr* using the same β-lactamase reporters of the *S. aureus agr* groups, but in this case the staphylococcal supernatants were used as presumptive inducers omitting induction by the cognate AIP. Our results show that none of the CoNS supernatants were capable of activating any of the four *S. aureus agr* groups (**Supplementary Figure S1**). These results show that CoNS strains interfere with *agr* induction by competing with the *S. aureus* AIPs for AgrC binding and that they generally have inhibitory activity toward *S. aureus agr*.

Dual Species Biofilm Involving *S. aureus* and CoNS

As *S. aureus agr* is known to influence biofilm formation (Le and Otto, 2015), we asked if CoNS strains potentially producing *agr* repressing peptides affected biofilm formation. When grown individually, the CoNS strains were less robust at forming biofilm than *S. aureus* (**Figures 3**, **4** and **Supplementary Figure S2**). From these we selected 1-3 CoNS strains from each species to examine biofilm formation in the presence of *S. aureus.* While the biofilm biomass was quantified by crystal violet staining, bacterial composition of these dual-species biofilms was determined by inspection of CFU on SaSelect^{TM} plates. In all, we tested biofilm formation for eight combinations where the CoNS species had no inhibitory effect on *S. aureus agr* (**Figure 3**), eight combinations for those CoNS species with a strong *S. aureus agr* inhibitory effect (**Figure 4**), and another three combinations with CoNS strains with varying *agr* inhibitory effects (**Supplementary Figure S2**). When examining the composition of dual-species biofilm (**Figures 3B,D**, **4B,D** and **Supplementary Figure S2B**), both species were represented. For 8 out of the 19 dual-species combinations we observed increased biofilm biomass when compared to biofilm formation by individual strains. Importantly, these grouped almost evenly into the *agr* cross-inhibition group (5 out of 10) and the non-inhibitory group (3 out of 9). While this data already indicated that the increased biofilm in dual species biofilms was independent of *agr* cross-talk, we sought to consolidate this finding further. For this we chose one strain capable of *agr* cross-inhibition (*S. simulans* No. 17) and one strain from the non-inhibitory group (*S. sciuri* No. 52), and analyzed their effect on biofilm formation of a *S. aureus agr* mutant strain. These data indicate that the absence of a functional *agr* in *S. aureus* did not influence biofilm formation when mixed with CoNs strains (**Figure 5**). Collectively our data show that the

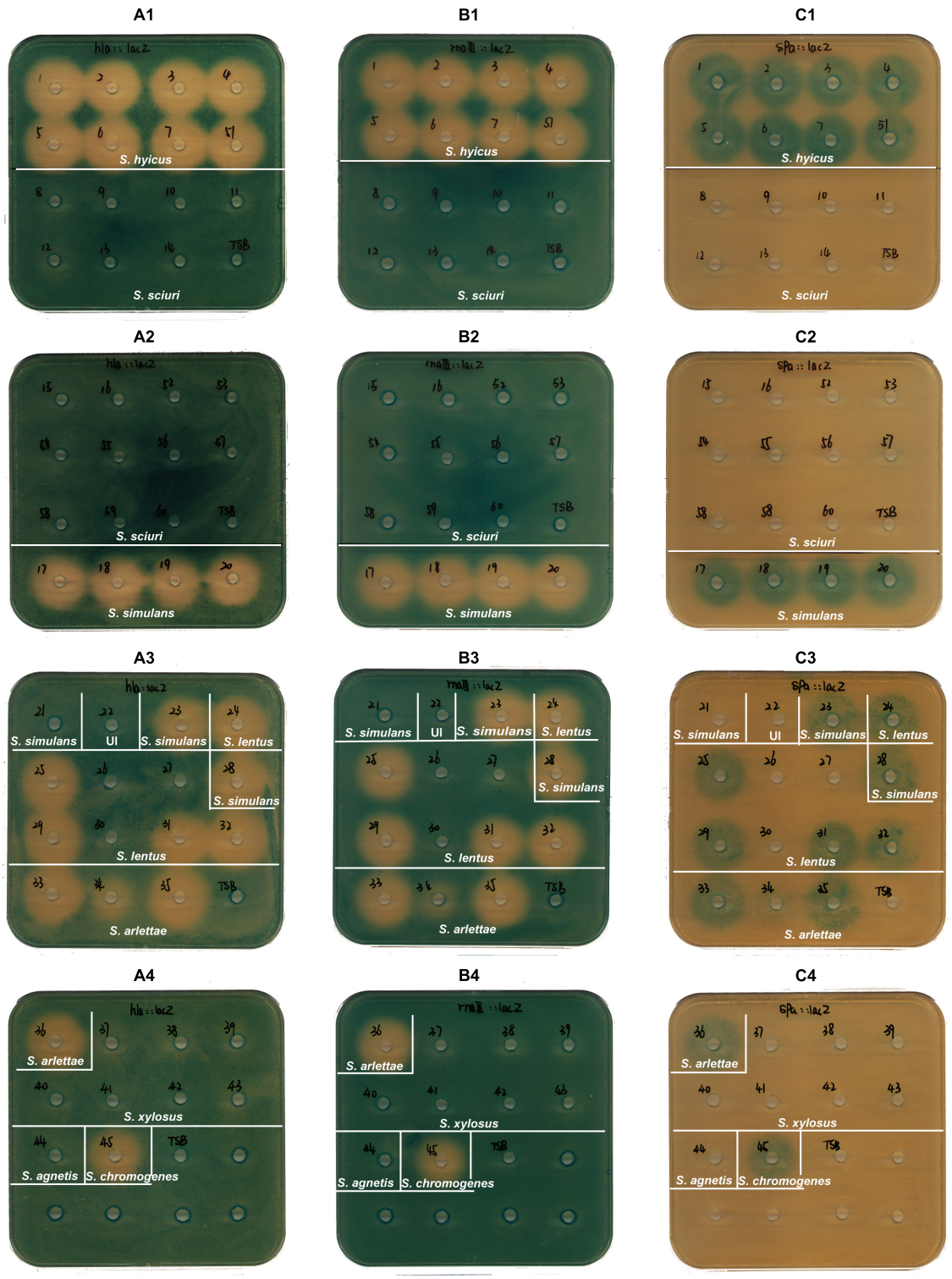

FIGURE 1 | Effect on virulence factor expression of *S. aureus* by CoNS culture supernatant. TSA agar plates (with erythromycin and X-gal) containing the *hla*:lacZ (PC322; Ery^r) (plates **A1–A4**), the *rnaIII*:*lacZ* (SH101F7; Ery^r) (plates **B1–B4**), or the *spa*:*lacZ* (PC203; Ery^r) (plates **C1–C4**) reporter strains of *S. aureus* were used to screen the cell-free overnight culture supernatants from 55 isolates. Sixty microliter of supernatant or TSB (as a negative control) were added to the wells in the plates. The supernatants in wells are from *S. hyicus* (wells 1–7 and 51); *S. sciuri* (wells 8–16 and 52–60); *S. simulans* (wells 17–21, 23 and 28); *S. lentus* (wells 24–27 and 29–32); *S. arlettae* (wells 33–36); *S. xylosus* (wells 37–43); *S. agnetis* (well 44); *S. chromogenes* (well 45); UI shown in well 22 stands for an unidentified isolate. The plates were incubated at 37°C for 10–24 h (until zones appeared). The assay was performed three times as biological replicates. This figure is representative of one set of screening plates.

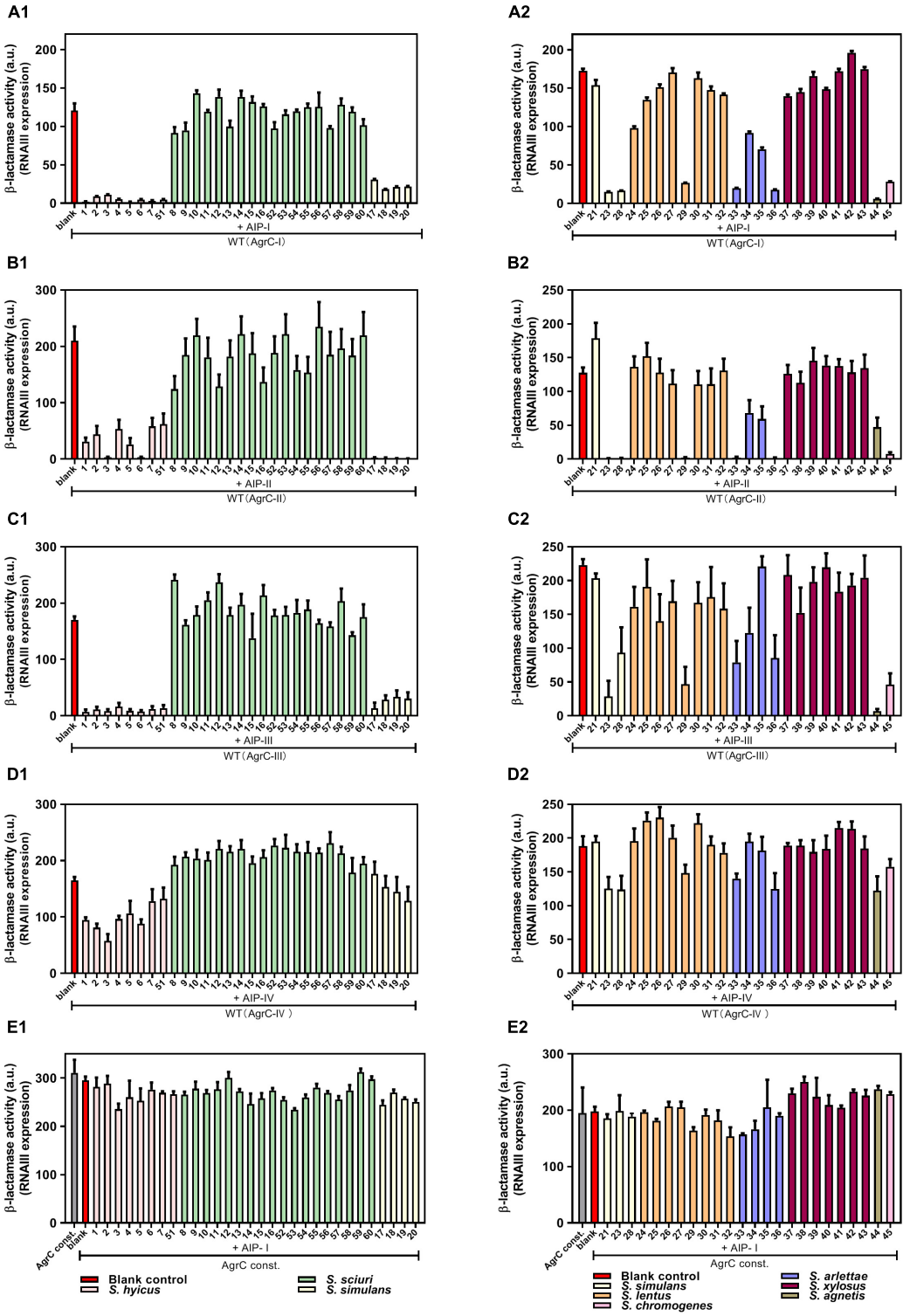

FIGURE 2 | AgrC-mediated interference of RNAIII expression by CoNS supernatants. Reporter strains RN10829 (P2-*agrA*: P3-*blaZ*)/p*agrC*-I-IV (WT) **(A1–D2)** and RN10829 (P2-*agrA*: P3-*blaZ*)/p*agrC*-I-R23H (AgrC const.) **(E1,E2)** were grown to OD600 = 0.35, and exposed to 1/10 volume supernatant of CoNS and 1/10 external inducing AIP-I-IV supernatant. After 45 min incubation, RNAIII expression was assessed using the nitrocefin hydrolysis method and analyzed for relative β-lactamase activity by nitrocefin conversion. The numbers displayed on the X-axis correspond to those in **Figure 1**: No. 1–7 and 51 (*S. hyicus*); No. 8–16 and 52–60 (*S. sciuri*); No. 17–21, 23 and 28 (*S. simulans*); No. 24–27 and 29–32 (*S. lentus*); No. 33–36 (*S. arlettae*); No. 37–43 (*S. xylosus*); No. 44 (*S. agnetis*); No. 45 (*S. chromogenes*). Each CoNS species is represented by a different color. Each column is representative of at least three biological replicates and the error bars represent the standard deviation.

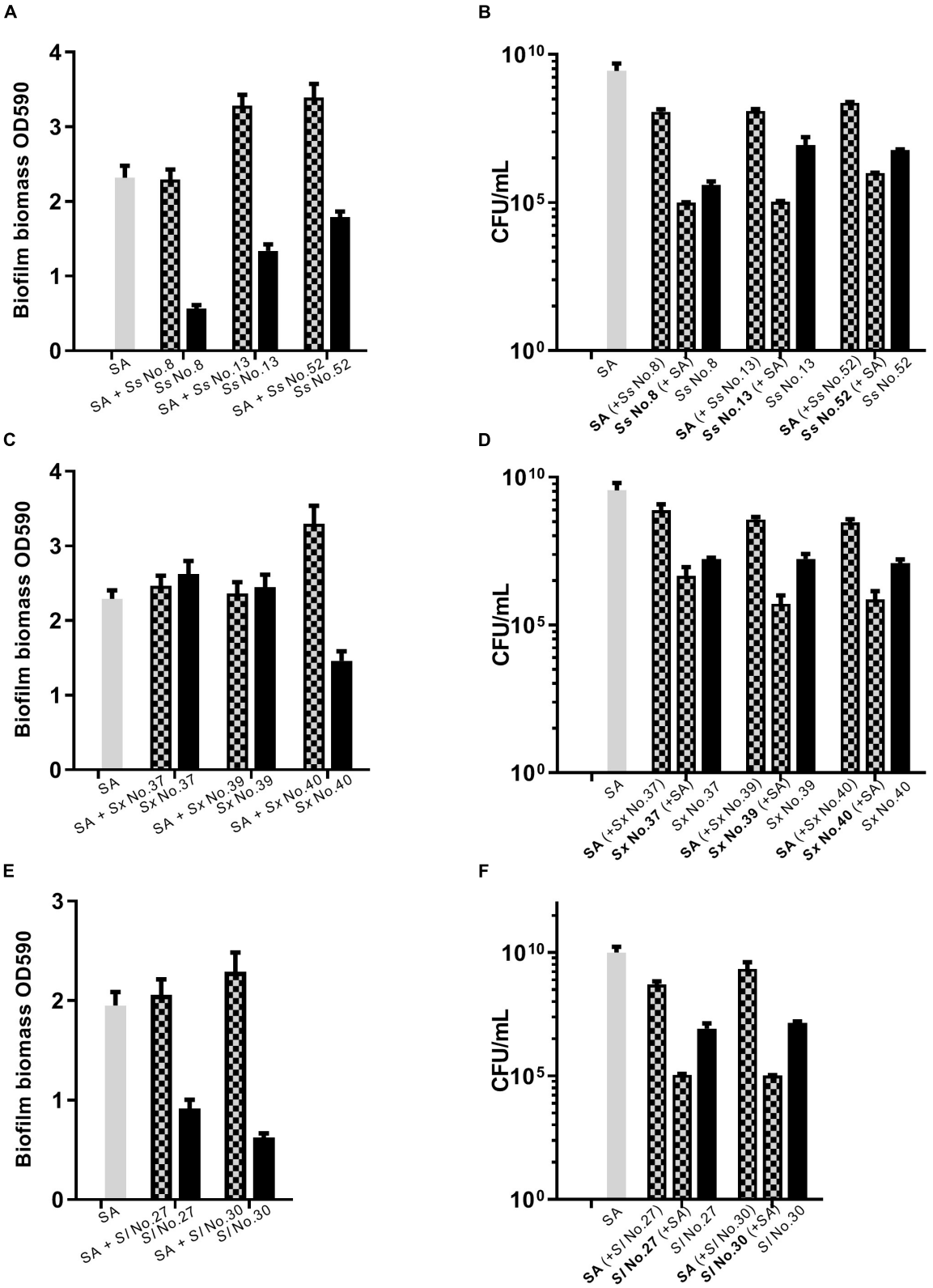

FIGURE 3 | Dual species biofilm formation between *S. aureus* and CoNS strains not displaying *agr* inhibitory activity. For dual-species biofilms, *S. aureus* 8325-4 (SA) was co-cultured together with one of *S. sciuri* (*Ss*, **A,B**), *S. xylosus* (*Sx*, **C,D**) and *S. lentus* (*Sl*, **E,F**) and biofilm biomass **(A,C,E)** or CFU **(B,D,F)** were determined as indicated by mix color bars and compared to biofilms formed by the individual species (SA indicated by gray bars and CoNS by black bars).

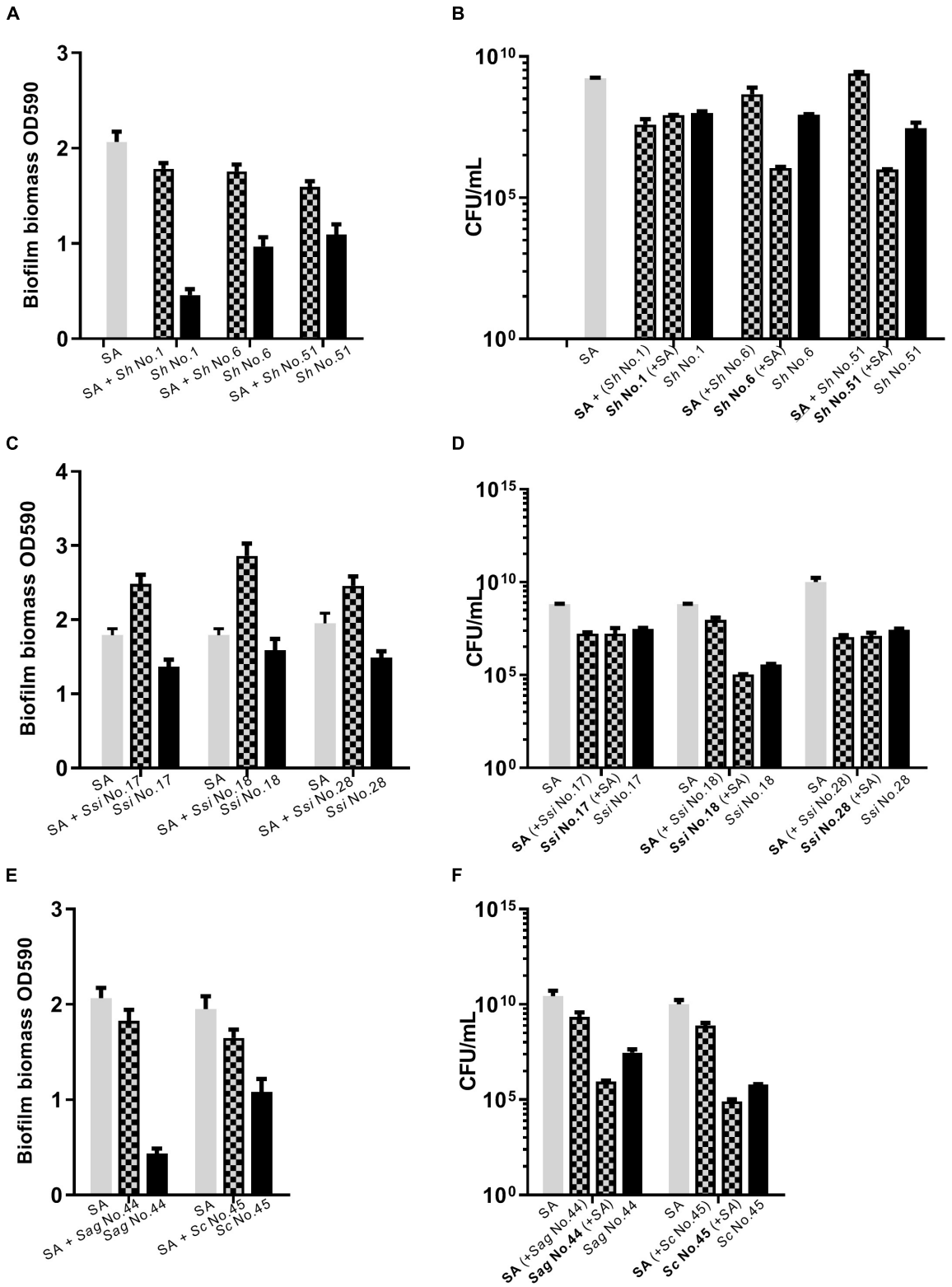

FIGURE 4 | Dual species biofilm formation between *S. aureus* and CoNS strains displaying *agr* cross-inhibition. For dual-species biofilms, *S. aureus* 8325-4 (SA) was co-cultured together with one of *S. hyicus* (*Sh*, **A,B**), *S. simulans* (*Ssi*, **C,D**), *S. agnetis* and *S. chromogenes* (*Sag*/*Sc*, **E,F**) and biofilm biomass **(A,C,E)** or CFU **(B,D,F)** were determined as indicated by mix color bars and compared to biofilms formed by the individual species (SA indicated by gray bars and CoNS by black bars).

presence of both *S. aureus* and CoNS may in some instances enhance biofilm formation when compared to that formed by the individual strains, but in those cases it is unrelated to *agr* mediated interactions.

Strain-Specific Enhancement of *S. aureus* Adherence to Fibronectin in the Presence of Synthesized CoNS AIPs

As inhibition of *S. aureus agr* leads to increased expression of surface adhesion proteins recognizing host factors, we were curious to see whether the addition of synthesized AIPs from CoNS would lead to increased binding of *S. aureus* to host factor. To address this, we studied the fibronectin binding capacity of different *S. aureus* strains namely the laboratory strain 8325-4 (CC8), the livestock associated CC398 strain 61599 (Tang et al., 2017b) as well as two *S. aureus* strains identified from the pig nares together with either *S. chromogenes* (A) or *S. hyicus* and *S. simulans* (B). *S. aureus* A was classified as CC8 and *S. aureus* B as CC45. Strains belonging to both CC8 and CC45 have previously been found associated with live stock (Tang et al., 2017a). When these strains were separately treated with synthesized AIPs of *S. hyicus*, *S. simulans*, and *S. chromogenes*, that have been detected in a previous study (Gless et al., 2019), we observed a significant increase in *S. aureus* 8325-4 binding to fibronectin in the presence of the CoNS AIPs, in comparison to the vehicle (DMSO)-treated control (**Figure 6**). However, neither strain 61599 nor the pig-derived *S. aureus* isolates obtained in this study and tested here were affected by the presence of CoNS AIPs over the vehicle control. In consideration of the known regulatory defects of *S. aureus* 8325-4, we also examined the adherence of repaired strains HG001 (restored *rsbU*, an activator of SigB) and HG003 (restored *rsbU* and *tcaR*, an activator of protein A transcription) under the same condition (Herbert et al., 2010) (**Supplementary Figure S3**). Both of these strains showed a low adhesion to fibronectin. Thus, exposure to CoNS AIPs does not lead to increased binding to fibronectin except for strain 8325-4.

DISCUSSION

Coagulase negative staphylococci comprise a diverse group of staphylococcal species that largely are harmless colonizers of both humans and animals. For a given host several CoNS are commonly present and the composition varies both within and between host species (Nagase et al., 2002). Likewise, pigs have been reported to be colonized by a variety of CoNS with one study describing 10 species including *S. hyicus*, *Staphylococcus haemolyticus*, *Staphylococcus warneri*, *S. simulans*, *S. xylosus*, and *S. sciuri* to be isolated at approximately equal frequency (Nagase et al., 2002). Others document higher CoNS species numbers (between 18 and 20 different CoNS) including the aforementioned, as well as *S. saprophyticus* and *S. cohnii* (Schoenfelder et al., 2017; Verstappen et al., 2017). However, both the latter studies report a marked increase in *S. sciuri* prevalence over the other species amounting to between 30 and 46% of the total colonizing CoNS species (Schoenfelder et al., 2017; Verstappen et al., 2017). In our investigation we also found *S. sciuri* to be the most prevalent CoNS being isolated from 40% of the pigs followed by *S. lentus* and *S. xylosus.* Unlike the Verstappen study though, we did not isolate *S. saprophyticus* or *S. cohnii* which were the other most prominent species identified along with *S. sciuri* (Verstappen et al., 2017).

Interestingly CoNS strains appear to be common producers of AIP molecules that resemble the AIPs of the *S. aureus agr* quorum sensing system. Analogous to the cross-inhibition of *agr* that occurs between *S. aureus* strains belonging to different AgrC subgroups, the CoNS AIPs also tend to inhibit expression of *agr* controlled genes. Previously we showed that out of 52 staphylococcal isolates obtained from a common

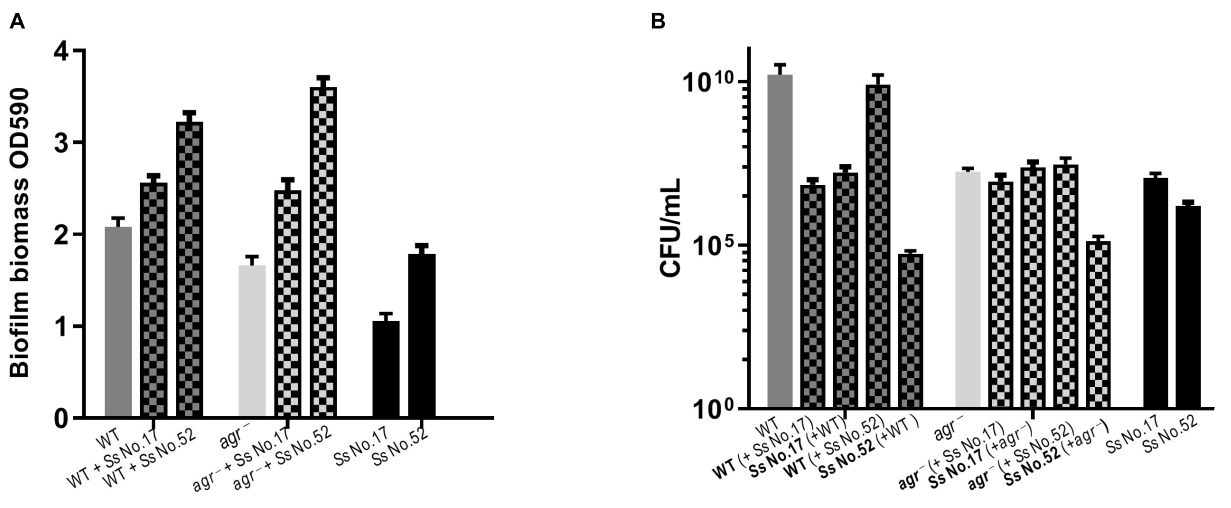

FIGURE 5 | Biofilm formation does not correlate with *agr* inhibition. For dual-species biofilms, *S. aureus* 8325-4 WT or *agr*⁻ (Δ*agr*) mutant strains were co-cultured together with either *S. simulans* (Ss No. 17) or *S. sciuri* (Ss No. 52) and biofilm biomass **(A)** or CFU **(B)** were determined as indicated by mix color bars and compared to biofilms formed by the individual species (SA indicated by gray bars and CoNS by black bars).

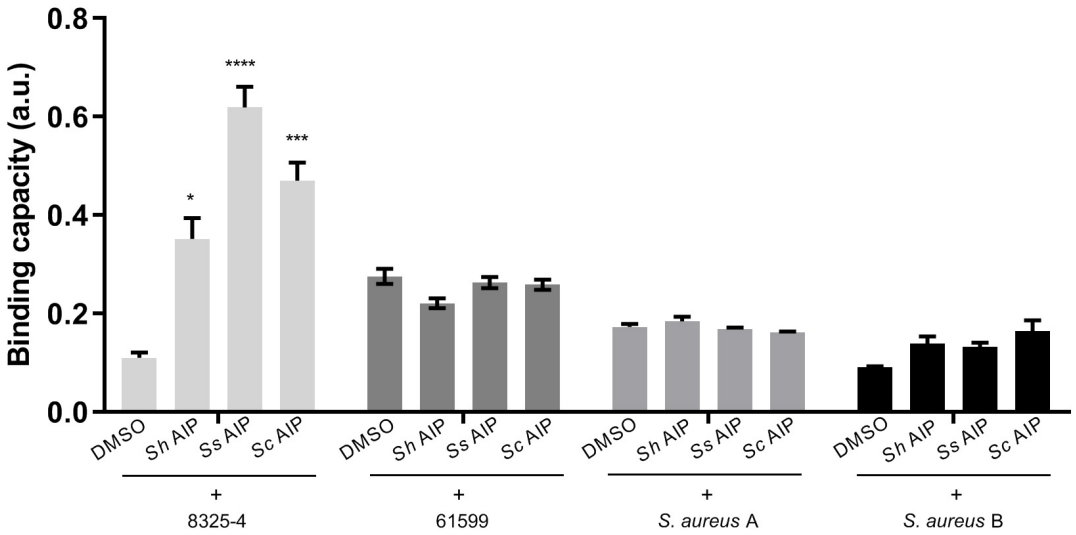

FIGURE 6 | Synthesized AIPs from *S. hyicus* (*Sh* AIP), *S. simulans* (*Ss* AIP), and *S. chromogenes* (*Sc* AIP) enhance *S. aureus* adherence to host factors fibronectin *in vitro*. *S. aureus* strains were separately treated with AIPs (10^{-4} mM *S. hyicus*, 10^{-4} mM *S. simulans* AIPs and 10^{-3} mM *S. chromogenes*), incubated and fixed in human fibronectin pre-coated 96-well plates. Crystal violet staining was performed to quantify the amount of *S. aureus* adhering to host factors via measurement of OD_{590}. Results shown are representative of 3 independent experiments. Each bar represents the average of 8 biological replicates and the error bars represent the standard deviation. $^{*}P < 0.05$; $^{***}P < 0.001$; $^{****}P < 0.0001$.

strain collection, 37 were capable of inhibiting *agr* of *S. aureus* representing 17 different CoNS species (Canovas et al., 2016). Here, we aimed to investigate the extent to which CoNS strains isolated form the same niche environment (i.e., from individual pigs) were able to repress *S. aureus agr*. Our results show that out of 25 pigs we isolated 8 different CoNS species of which 24 out of 54 strains had quorum quenching properties. Interestingly out of 18 tested *S. sciuri* strains none were able to repress *agr*. Similar was observed for *S. xylosus* whereas for *S. lentus*, which was present in 24% of the pigs, *agr* was repressed by some strains but unaffected by others. In contrast, all isolates of both *S. hyicus* and *S. simulans* displayed strong *agr* repressing activity. Using a constitutively active AgrC variant we were able to show that the CoNS strains likely repress *agr* through production of AIP-like molecules that are secreted to the culture supernatant and compete with *S. aureus* AIPs for binding to *S. aureus* AgrC, as opposed to other *agr* quorum quenching mechanisms such as via AgrA binding (Baldry et al., 2016b). This notion was confirmed by synthesis of selective CoNS AIP molecules. Furthermore, we observed correlation between the inhibitory potential of individual CoNS strains against *S. aureus agr* group I and the inhibition exerted on groups II and III, while the inhibition pattern was not clearly reflected on group IV. Low inhibitory activity against *agr* group IV for entities that are highly active against other groups have been described before (Gless et al., 2019). We also examined if any of the CoNS strains were able to induce the *S. aureus agr* system; however, none of the strains demonstrated such activity. For *P. aeruginosa*, analogs of quorum sensing molecules have been reported to induce quorum sensing (Smith et al., 2003) and we have observed that synthesized AIPs of *S. schleiferi* and *Staphylococcus hominis* are capable of inducing *S. aureus* AgrC group IV (Gless et al., 2019). However, cross-species induction of *agr* appears to be a rare phenomenon and the vast majority of *agr* modulating compounds interfere with quorum sensing induction (Hansen et al., 2018).

Previously it has been suggested that presence or absence of CoNS strains may correlate with *S. aureus* colonization. For example, Verstappen et al. observed a lower frequency of *S. aureus* colonization in the presence of *S. sciuri*, *S. cohnii*, or *S. saprophyticus*. We did not identify any *S. cohnii* or *S. saprophyticus* in our sampled pigs, and out of the 10 pigs positive for *S. sciuri*, 4 were co-isolated with *S. aureus* while 6 were not. However, we did observe that all *S. arlettae* and *S. lentus* isolates were colonizing pig nares where *S. aureus* was not found to be present. To investigate competitive behavior between CoNS strains and *S. aureus* we performed a series of dual-species biofilm studies based on the notion that *agr* has been reported to influence both biofilm formation and dispersal (Boles and Horswill, 2008; Periasamy et al., 2012). This rational was also made interesting by the recent observations by Gonzalez et al. that *S. epidermidis* secreted soluble products (when added to *S. aureus* cultures) inhibit *S. aureus* biofilm formation, but when the two species are co-inoculated and grow in physical contact they are capable of forming a robust dual-species biofilm (Gonzalez et al., 2018). Our data corroborate Gonzalez's observations in that we also show robust biofilm formation in the dual-species setting with no evident out-competition of one over the other species. Such dual-species interactions can benefit both species in that they can persist in a colonizing state more robustly, as biofilms are extremely hard to eradicate by both the host and by antimicrobial therapies, and thus also providing a constant reservoir for possible *S. aureus* chronic infections (Archer et al., 2011). Moreover, even though we have observed the effect of interaction between *S. aureus* and CoNS on biofilm formation,

no correlation to *agr*-inhibition was seen. Further studies are needed to better understand the complexity of these interactions.

In context of antibacterial therapy, cross-talk between staphylococci and *S. aureus* via *agr* has become a topic of interest. We recently showed that *agr* inhibition by AIP-like molecules reduces *S. aureus* induced lesions in an atopic dermatitis model (Baldry et al., 2018) and this was supported by the finding that CoNS strains reduce skin barrier damage by inhibiting production of proteases and phenol-soluble modulins secreted by *S. aureus* (Williams et al., 2019). Another study reports a synthetic AIP from *Staphylococcus caprae* that dramatically reduced dermonecrotic injury caused by *S. aureus* and reduced cutaneous bacterial burden relative to controls (Paharik et al., 2017). However, as inhibition of *agr* is associated with increased expression of surface adhesion proteins favoring host adhesion and immune evasion (Novick et al., 1993), one could speculate that CoNS strains may increase the ability of *S. aureus* to colonize. For only one strain of *S. aureus*, namely 8325-4, we observed a significant increase in adhesion to human fibroncetin in the presence of CoNS AIPs. This was not seen for the livestock associated MRSA strain 61599 belonging to CC398, the two *S. aureus* isolates obtained from pigs in the present study, nor for the strains HG001 or HG003 that are derivatives of 8325-4 and restored by *rsbU* or *rsbU*/*tcaR* regulatory genes. Thus, we could not consistently demonstrate an effect of CoNS AIPs on *S. aureus* binding to fibronectin. In conclusion, the interactions between coagulase-negative staphylococci and *S. aureus* are complex and involve both *agr* dependent and independent factors, which future studies will be required to elucidate.

CONCLUSION

We have conducted an investigation of the possible role of the *agr* cross-talk between *S. aureus* and CoNS strains isolated from the same colonizing location. We show that there are substantial variations with respect to species colonization amongst the pig hosts tested, as well as in *S. aureus agr*-modulation capacity of isolated CoNS species. Importantly, our results document multiple interactions between *S. aureus* and CoNS and they suggest that *S. aureus* adhesion and dual-species biofilm formation can indeed be influenced by CoNS in both *agr*-dependent and *agr*-independent manners.

DATA AVAILABILITY STATEMENT

All datasets analyzed for this study are included in the manuscript/**Supplementary Files**.

ETHICS STATEMENT

No permission is required to sample the nostril of pigs according to the Danish Animal Experimentation Act § 1.2.

AUTHOR CONTRIBUTIONS

PP, MB, MSB, and HI designed the study. PP, BG, SB, and CE-G conducted the experimental work. PP, MB, MSB, HI, CO, BG, PA, CE-G, and SB analyzed the data. PP, MB, MSB, BG, CO, and HI wrote the manuscript.

SUPPLEMENTARY MATERIAL

The Supplementary Material for this article can be found online at: https://www.frontiersin.org/articles/10.3389/fmicb.2019.02212/full#supplementary-material

REFERENCES

Archer, N. K., Mazaitis, M. J., Costerton, J. W., Leid, J. G., Powers, M. E., and Shirtliff, M. E. (2011). Staphylococcus aureus biofilms: properties, regulation, and roles in human disease. *Virulence* 2, 445–459. doi: 10.4161/viru.2.5.17724

Authority, E. F. S. (2009). Analysis of the baseline survey on the prevalence of methicillin-resistant *Staphylococcus aureus* (MRSA) in holdings with breeding pigs, in the EU, 2008-Part A: MRSA prevalence estimates. *EFSA J.* 7:1376. doi: 10.2903/j.efsa.2009.1376

Baldry, M., Kitir, B., Frøkiær, H., Christensen, S. B., Taverne, N., Meijerink, M., et al. (2016a). The agr inhibitors solonamide B and analogues alter immune responses to *Staphylococccus aureus* but do not exhibit adverse effects on immune cell functions. *PLoS One* 11:e0145618. doi: 10.1371/journal.pone.0145618

Baldry, M., Nielsen, A., Bojer, M. S., Zhao, Y., Friberg, C., Ifrah, D., et al. (2016b). Norlichexanthone reduces virulence gene expression and biofilm formation in *Staphylococcus aureus*. *PLoS One* 11:e0168305. doi: 10.1371/journal.pone.0168305

Baldry, M., Nakamura, Y., Nakagawa, S., Frees, D., Matsue, H., Núñez, G., et al. (2018). Application of an agr-specific antivirulence compound as therapy for *Staphylococcus aureus*-induced inflammatory skin disease. *J. Infect. Dis.* 218, 1009–1013. doi: 10.1093/infdis/jiy259

Bojer, M. S., Baldry, M., and Ingmer, H. (2017). "Protocols for screening antimicrobial peptides that influence virulence gene expression in *Staphylococcus aureus*," in *Antimicrobial Peptides. Methods in Molecular Biology*, ed. P. Hansen, (New York, NY: Humana Press), 387–394. doi: 10.1007/978-1-4939-6737-7_28

Boles, B. R., and Horswill, A. R. (2008). Agr-mediated dispersal of *Staphylococcus aureus* biofilms. *PLoS Pathog.* 4:e1000052. doi: 10.1371/journal.ppat.1000052

Canovas, J., Baldry, M., Bojer, M. S., Andersen, P. S., Grzeskowiak, P. K., Stegger, M., et al. (2016). Cross-talk between *Staphylococcus aureus* and other staphylococcal species via the agr quorum sensing system. *Front. Microbiol.* 7:1733. doi: 10.3389/fmicb.2016.01733

Chan, P. F., and Foster, S. J. (1998). The role of environmental factors in the regulation of virulence-determinant expression in *Staphylococcus aureus* 8325-4. *Microbiology* 144, 2469–2479. doi: 10.1099/00221287-144-9-2469

Cho, S.-H., Strickland, I., Boguniewicz, M., and Leung, D. Y. (2001). Fibronectin and fibrinogen contribute to the enhanced binding of *Staphylococcus aureus* to atopic skin. *J. Allergy Clin. Immunol.* 108, 269–274. doi: 10.1067/mai.2001.117455

Chuang, Y.-Y., and Huang, Y.-C. (2015). Livestock-associated meticillin-resistant *Staphylococcus aureus* in Asia: an emerging issue? *Int. J. Antimicrob. Agents* 45, 334–340. doi: 10.1016/j.ijantimicag.2014.12.007

Fridkin, S. K., Hageman, J. C., Morrison, M., Sanza, L. T., Como-Sabetti, K., Jernigan, J. A., et al. (2005). Methicillin-resistant *Staphylococcus aureus* disease in three communities. *New Engl. J. Med.* 352, 1436–1444.

Geisinger, E., Muir, T. W., and Novick, R. P. (2009). "Agr receptor mutants reveal distinct modes of inhibition by staphylococcal autoinducing

peptides," in *Proceedings of the National Academy of Sciences*, PNAS.

Gless, B. H., Bojer, M. S., Peng, P., Baldry, M., Ingmer, H., and Olsen, C. A. (2019). Identification of autoinducing thiodepsipeptides from staphylococci enabled by native chemical ligation. *Nat. Chem.* 11, 1–7. doi: 10.1038/s41557-019-0256-3

Gless, B. H., Peng, P., Pedersen, K. D., Gotfredsen, C. H., Ingmer, H., and Olsen, C. A. (2017). Structure–activity relationship study based on autoinducing peptide (aip) from dog pathogen S. schleiferi. *Organ. Lett.* 19, 5276–5279. doi: 10.1021/acs.orglett.7b02550

Goetz, C., Tremblay, Y. D., Lamarche, D., Blondeau, A., Gaudreau, A. M., Labrie, J., et al. (2017). Coagulase-negative staphylococci species affect biofilm formation of other coagulase-negative and coagulase-positive staphylococci. *J. Dairy Sci.* 100, 6454–6464. doi: 10.3168/jds.2017-12629

Golding, G. R., Bryden, L., Levett, P. N., McDonald, R. R., Wong, A., Wylie, J., et al. (2010). Livestock-associated methicillin-resistant *Staphylococcus aureus* sequence type 398 in humans, Canada. *Emerg. Infect. Dis.* 16:587. doi: 10.3201/eid1604.091435

Gonzalez, T., Baatyrbek-kyzy, A., Andersen, H., Haslam, D. B., Myers, J. M. B., Hershey, G. K. K., et al. (2018). Investigating the role of staphylococcal biofilms in the pathogenesis of pediatric atopic dermatitis. *J. Allergy Clin. Immunol.* 141:AB93.

Hansen, A. M., Peng, P., Baldry, M., Perez-Gassol, I., Christensen, S. B., Vinther, J. M. O., et al. (2018). Lactam hybrid analogues of solonamide B and autoinducing peptides as potent S. aureus AgrC antagonists. *Eur. J. Med. Chem.* 152, 370–376. doi: 10.1016/j.ejmech.2018.04.053

Herbert, S., Ziebandt, A.-K., Ohlsen, K., Schäfer, T., Hecker, M., Albrecht, D., et al. (2010). Repair of global regulators in *Staphylococcus aureus* 8325 and comparative analysis with other clinical isolates. *Infect. Immun.* 78, 2877–2889. doi: 10.1128/IAI.00088-10

Horsburgh, M. J., Aish, J. L., White, I. J., Shaw, L., Lithgow, J. K., and Foster, S. J. (2002). σB modulates virulence determinant expression and stress resistance: characterization of a functional rsbU strain derived from *Staphylococcus aureus* 8325-4. *J. Bacteriol.* 184, 5457–5467. doi: 10.1128/jb.184.19.5457-5467.2002

Hwang, S. M., Kim, M. S., Park, K. U., Song, J., and Kim, E.-C. (2011). Tuf gene sequence analysis has greater discriminatory power than 16S rRNA sequence analysis in identification of clinical isolates of coagulase-negative staphylococci. *J. Clin. Microbiol.* 49, 4142–4149. doi: 10.1128/JCM.05213-11

Iwase, T., Uehara, Y., Shinji, H., Tajima, A., Seo, H., Takada, K., et al. (2010). *Staphylococcus epidermidis* Esp inhibits *Staphylococcus aureus* biofilm formation and nasal colonization. *Nature* 465:346. doi: 10.1038/nature09074

Josse, J., Laurent, F., and Diot, A. (2017). Staphylococcal adhesion and host cell invasion: fibronectin-binding and other mechanisms. *Front. Microbiol.* 8:2433. doi: 10.3389/fmicb.2017.02433

Khanna, T., Friendship, R., Dewey, C., and Weese, J. (2008). Methicillin resistant *Staphylococcus aureus* colonization in pigs and pig farmers. *Vet. Microbiol.* 128, 298–303. doi: 10.1016/j.vetmic.2007.10.006

King, M. D., Humphrey, B. J., Wang, Y. F., Kourbatova, E. V., Ray, S. M., and Blumberg, H. M. (2006). Emergence of community-acquired methicillin-resistant *Staphylococcus aureus* USA 300 clone as the predominant cause of skin and soft-tissue infections. *Ann. Int. Med.* 144, 309–317.

Kintarak, S., Whawell, S. A., Speight, P. M., Packer, S., and Nair, S. P. (2004). Internalization of *Staphylococcus aureus* by human keratinocytes. *Infect. Immun.* 72, 5668–5675. doi: 10.1128/iai.72.10.5668-5675.2004

Kobayashi, S. D., Malachowa, N., and DeLeo, F. R. (2015). Pathogenesis of *Staphylococcus aureus* abscesses. *Am. J. Pathol.* 185, 1518–1527. doi: 10.1016/j.ajpath.2014.11.030

Köck, R., Schaumburg, F., Mellmann, A., Köksal, M., Jurke, A., Becker, K., et al. (2013). Livestock-associated methicillin-resistant *Staphylococcus aureus* (MRSA) as causes of human infection and colonization in Germany. *PLoS One* 8:e55040. doi: 10.1371/journal.pone.0055040

Kourbatova, E. V., Halvosa, J. S., King, M. D., Ray, S. M., White, N., and Blumberg, H. M. (2005). Emergence of community-associated methicillin-resistant *Staphylococcus aureus* USA 300 clone as a cause of health care-associated infections among patients with prosthetic joint infections. *Am. J. Infect. Control* 33, 385–391. doi: 10.1016/j.ajic.2005.06.006

Le, K. Y., and Otto, M. (2015). Quorum-sensing regulation in staphylococci–an overview. *Front. Microbiol.* 6:1174. doi: 10.3389/fmicb.2015.01174

Lewis, H. C., Mølbak, K., Reese, C., Aarestrup, F. M., Selchau, M., Sørum, M., et al. (2008). Pigs as source of methicillin-resistant *Staphylococcus aureus* CC398 infections in humans, Denmark. *Emerg. Infect. Dis.* 14:1383. doi: 10.3201/eid1409.071576

Loonen, A. J., Jansz, A. R., Bergland, J. N., Valkenburg, M., Wolffs, P. F., and van den Brule, A. J. (2012). Comparative study using phenotypic, genotypic and proteomics methods for identification of coagulase-negative staphylococci. *J. Clin. Microbiol.* 50, 1437–1439. doi: 10.1128/JCM.06746-11

Mahmmod, Y. S., Klaas, I. C., Svennesen, L., Pedersen, K., and Ingmer, H. (2018). Communications of *Staphylococcus aureus* and non-aureus *Staphylococcus* species from bovine intramammary infections and teat apex colonization. *J. Dairy Sci.* 101, 7322–7333. doi: 10.3168/jds.2017-14311

McMurray, C. L., Hardy, K. J., Calus, S. T., Loman, N. J., and Hawkey, P. M. (2016). Staphylococcal species heterogeneity in the nasal microbiome following antibiotic prophylaxis revealed by tuf gene deep sequencing. *Microbiome* 4:63.

Nagase, N., Sasaki, A., Yamashita, K., Shimizu, A., Wakita, Y., Kitai, S., et al. (2002). Isolation and species distribution of staphylococci from animal and human skin. *J. Vet. Med. Sci.* 64, 245–250. doi: 10.1292/jvms.64.245

Nielsen, A., Mansson, M., Bojer, M. S., Gram, L., Larsen, T. O., Novick, R. P., et al. (2014). Solonamide B inhibits quorum sensing and reduces *Staphylococcus aureus* mediated killing of human neutrophils. *PLoS One* 9:e84992. doi: 10.1371/journal.pone.0084992

Nielsen, A., Nielsen, K. F., Frees, D., Larsen, T. O., and Ingmer, H. (2010). Method for screening compounds that influence virulence gene expression in *Staphylococcus aureus*. *Antimicrob. Agents Chemother.* 54, 509–512. doi: 10.1128/AAC.00940-09

Nielsen, L. N., Roggenbuck, M., Haaber, J., Ifrah, D., and Ingmer, H. (2012). Diverse modulation of spa transcription by cell wall active antibiotics in *Staphylococcus aureus*. *BMC Res. Notes* 5:457. doi: 10.1186/1756-0500-5-457

Novick, R. P., and Morse, S. I. (1967). In vivo transmission of drug resistance factors between strains of *Staphylococcus aureus*. *J. Exper. Med.* 125:45. doi: 10.1084/jem.125.1.45

Novick, R. P., Ross, H., Projan, S., Kornblum, J., Kreiswirth, B., and Moghazeh, S. (1993). Synthesis of staphylococcal virulence factors is controlled by a regulatory RNA molecule. *EMBO J.* 12, 3967–3975. doi: 10.1002/j.1460-2075.1993.tb06074.x

Olson, M. E., Todd, D. A., Schaeffer, C. R., Paharik, A. E., Van Dyke, M. J., Büttner, H., et al. (2014). The *Staphylococcus* epidermidis agr quorum-sensing system: signal identification, cross-talk, and importance in colonization. *J. Bacteriol.* 196, 3482–3493. doi: 10.1128/JB.01882-14

O'Neill, E., Pozzi, C., Houston, P., Humphreys, H., Robinson, D. A., Loughman, A., et al. (2008). A novel *Staphylococcus aureus* biofilm phenotype mediated by the fibronectin-binding proteins, FnBPA and FnBPB. *J. Bacteriol.* 190, 3835–3850. doi: 10.1128/JB.00167-08

Otto, M., Echner, H., Voelter, W., and Götz, F. (2001). Pheromone cross-inhibition between *Staphylococcus aureus* and *Staphylococcus* epidermidis. *Infect. Immun.* 69, 1957–1960. doi: 10.1128/iai.69.3.1957-1960.2001

Otto, M., Süßmuth, R., Vuong, C., Jung, G., and Götz, F. (1999). Inhibition of virulence factor expression in *Staphylococcus aureus* by the *Staphylococcus* epidermidis agr pheromone and derivatives. *FEBS Lett.* 450, 257–262. doi: 10.1016/s0014-5793(99)00514-1

Paharik, A. E., Parlet, C. P., Chung, N., Todd, D. A., Rodriguez, E. I., Van Dyke, M. J., et al. (2017). Coagulase-negative staphylococcal strain prevents *Staphylococcus aureus* colonization and skin infection by blocking quorum sensing. *Cell Host Microbe* 22, 746–756. doi: 10.1016/j.chom.2017.11.001

Periasamy, S., Joo, H.-S., Duong, A. C., Bach, T.-H. L., Tan, V. Y., Chatterjee, S. S., et al. (2012). How *Staphylococcus aureus* biofilms develop their characteristic structure. *Proc. Natl. Acad. Sci. U.S.A.* 109, 1281–1286. doi: 10.1073/pnas.1115006109

Queck, S. Y., Jameson-Lee, M., Villaruz, A. E., Bach, T.-H. L., Khan, B. A., Sturdevant, D. E., et al. (2008). RNAIII-independent target gene control by the agr quorum-sensing system: insight into the evolution of virulence regulation in *Staphylococcus aureus*. *Mol. Cell* 32, 150–158. doi: 10.1016/j.molcel.2008.08.005

Schoenfelder, S. M., Dong, Y., Feßler, A. T., Schwarz, S., Schoen, C., Köck, R., et al. (2017). Antibiotic resistance profiles of coagulase-negative staphylococci in livestock environments. *Vet. Microbiol.* 200, 79–87. doi: 10.1016/j.vetmic.2016.04.019

Smith, K. M., Bu, Y., and Suga, H. (2003). Induction and inhibition of *Pseudomonas aeruginosa* quorum sensing by synthetic autoinducer analogs. *Chem. Biol.* 10, 81–89. doi: 10.1016/s1074-5521(03)00002-4

Smith, T. C., Male, M. J., Harper, A. L., Kroeger, J. S., Tinkler, G. P., Moritz, E. D., et al. (2009). Methicillin-resistant *Staphylococcus aureus* (MRSA) strain ST398 is present in midwestern US swine and swine workers. *PLoS One* 4:e4258. doi: 10.1371/journal.pone.0004258

Souvorov, A., Agarwala, R., and Lipman, D. J. (2018). SKESA: strategic k-mer extension for scrupulous assemblies. *Genome Biol.* 19:153. doi: 10.1186/s13059-018-1540-z

Strube, M. L., Hansen, J. E., Rasmussen, S., and Pedersen, K. (2018). A detailed investigation of the porcine skin and nose microbiome using universal and Staphylococcus specific primers. *Sci. Rep.* 8:12751. doi: 10.1038/s41598-018-30689-y

Tal-Gan, Y., Ivancic, M., Cornilescu, G., and Blackwell, H. E. (2016). Characterization of structural elements in native autoinducing peptides and non-native analogues that permit the differential modulation of AgrC-type quorum sensing receptors in *Staphylococcus aureus*. *Organ. Biomol. Chem.* 14, 113–121. doi: 10.1039/c5ob01735a

Tang, Y., Larsen, J., Kjeldgaard, J., Andersen, P. S., Skov, R., and Ingmer, H. (2017a). Methicillin-resistant and-susceptible *Staphylococcus aureus* from retail meat in Denmark. *Int. J. Food Microbiol.* 249, 72–76. doi: 10.1016/j.ijfoodmicro.2017.03.001

Tang, Y., Nielsen, L. N., Hvitved, A., Haaber, J. K., Wirtz, C., Andersen, P. S., et al. (2017b). Commercial biocides induce transfer of prophage Φ13 from human strains of Staphylococcus aureus to livestock CC398. *Front. Microbiol.* 8:2418. doi: 10.3389/fmicb.2017.02418

Van Cleef, B., Broens, E., Voss, A., Huijsdens, X., Züchner, L., Van Benthem, B., et al. (2010). High prevalence of nasal MRSA carriage in slaughterhouse workers in contact with live pigs in The Netherlands. *Epidemiol. Infect.* 138, 756–763. doi: 10.1017/S0950268810000245

Van Duijkeren, E., Ikawaty, R., Broekhuizen-Stins, M., Jansen, M., Spalburg, E., De Neeling, A., et al. (2008). Transmission of methicillin-resistant *Staphylococcus aureus* strains between different kinds of pig farms. *Vet. Microbiol.* 126, 383–389. doi: 10.1016/j.vetmic.2007.07.021

Verstappen, K. M., Willems, E., Fluit, A. C., Duim, B., Martens, M., and Wagenaar, J. A. (2017). *Staphylococcus aureus* nasal colonization differs among pig lineages and is associated with the presence of other staphylococcal species. *Front. Vet. Sci.* 4:97. doi: 10.3389/fvets.2017.00097

Wang, B., Zhao, A., Novick, R. P., and Muir, T. W. (2014). Activation and inhibition of the receptor histidine kinase AgrC occurs through opposite helical transduction motions. *Mol. Cell* 53, 929–940. doi: 10.1016/j.molcel.2014.02.029

Williams, M. R., Costa, S. K., Zaramela, L. S., Khalil, S., Todd, D. A., Winter, H. L., et al. (2019). Quorum sensing between bacterial species on the skin protects against epidermal injury in atopic dermatitis. *Sci. Transl. Med.* 11:eaat8329. doi: 10.1126/scitranslmed.aat8329

Yarwood, J. M., and Schlievert, P. M. (2003). Quorum sensing in *Staphylococcus* infections. *J. Clin. Invest.* 112, 1620–1625. doi: 10.1172/jci20442

Conflict of Interest: The authors declare that the research was conducted in the absence of any commercial or financial relationships that could be construed as a potential conflict of interest.

frontiers in Microbiology

REVIEW
published: 04 October 2019
doi: 10.3389/fmicb.2019.02073

Profile of the Intervention Potential of the Phylum Actinobacteria Toward Quorum Sensing and Other Microbial Virulence Strategies

*Hema Bhagavathi Sarveswari and Adline Princy Solomon**

Quorum Sensing Laboratory, Centre for Research in Infectious Diseases (CRID), School of Chemical and Biotechnology, SASTRA Deemed to be University, Thanjavur, India

The rapid dissemination of antimicrobial resistance amongst microorganisms and their deleterious effect on public health has propelled the exploration of alternative interventions that target microbial virulence rather than viability. In several microorganisms, the expression of virulence factors is controlled by quorum sensing systems. A comprehensive understanding into microbial quorum sensing systems, virulence strategies and pathogenesis has exposed potential targets whose attenuation may alleviate infectious diseases. Such virulence attenuating natural products sourced from the different phyla of bacteria from diverse ecosystems have been identified. In this review, we discuss chemical entities derived from the phylum Actinobacteria that have demonstrated the potential to inhibit microbial biofilms, enzymes, and other virulence factors both *in vivo* and *in vitro*. We also review Actinobacteria-derived compounds that can degrade quorum sensing signal molecules, and the genes encoding such molecules. As many Actinobacteria-derived compounds have been translated into pharmaceutically important agents including antibiotics, the identification of virulence attenuating compounds from this phylum exemplifies their significance as a prospective source for anti-virulent drugs.

Keywords: anti-biofilm, anti-virulence, microbial natural product, Actinobacteria, anti-pathogenic agents

OPEN ACCESS

Edited by:
Cristina García-Aljaro, University of Barcelona, Spain

Reviewed by:
Gloria Soberón-Chávez, National Autonomous University of Mexico, Mexico
Christopher Milton Mathew Franco, Flinders University, Australia

***Correspondence:**
Adline Princy Solomon
adlineprinzy@biotech.sastra.edu; adlineprincy@gmail.com

Specialty section:
This article was submitted to Antimicrobials, Resistance and Chemotherapy, a section of the journal Frontiers in Microbiology

Received: *16 April 2019*
Accepted: *22 August 2019*
Published: *04 October 2019*

Citation:
Sarveswari HB and Solomon AP (2019) Profile of the Intervention Potential of the Phylum Actinobacteria Toward Quorum Sensing and Other Microbial Virulence Strategies. Front. Microbiol. 10:2073. doi: 10.3389/fmicb.2019.02073

INTRODUCTION

Antimicrobials have remained the only mode of prophylaxis and therapeutics for microbial infections since its discovery. In the past century, antimicrobials have undeniably revolutionized clinical practices, laying the foundation for breakthroughs in surgeries, organs transplantations, cancer therapy, treatment of burns and trauma wounds, subsequently improving human health. However, the current antimicrobial resistance (AMR) era threatens the reversal of all breakthroughs achieved thus far (Brown and Wright, 2016; Marston et al., 2016). In the United States alone, AMR contributes to 2 million infections and 23,000 deaths per year, substantially increasing the medical expenses by up to 20 billion US dollars each year (Gelband et al., 2015; Centers for Disease Control, and Prevention, 2017). Healthcare agencies across the world have prioritized AMR, and the scientific community has proposed and developed many innovative strategies including the discovery of novel drug targets and other alternative therapeutic interventions to minimize the development of antimicrobial resistance amongst pathogens (Marston et al., 2016).

Virulence factors produced by pathogens are constructive in deteriorating host fitness during infection. A virulence factor could be a structure, or a product, or a strategy that enables the

pathogen to gain access and survive within the non-colonized region or cellular compartment of the host. Adhesins, enzymes (invasins and internalins), toxins (hemolytic, cytolytic and neurotoxins), and superantigens are some crucial virulence factors expressed by a pathogen to damage the host's physiological condition (Hill, 2012). In several pathogens, the expression of these virulence factors are regulated by a cell density-dependent signaling system called quorum sensing (QS) system (Miller and Bassler, 2001; Fetzner, 2015). QS system enables microorganisms across inter and intraspecies within a community to initiate controlled and co-ordinated behavior (Greenberg, 2003; Kaufmann et al., 2008). Although many facets of the intricate prokaryotic QS system remain undeciphered, the available knowledge on the domain's diverse QS systems provides many targets for the development of drugs that could inhibit the expression of virulence. Given the unrelatedness of virulence to the viability of a pathogen, the cultivation of resistance toward the anti-virulence agent through selective pressure is presumed to be non-existential (Clatworthy et al., 2007).

What is so paramount in the evolution of bacteria is the co-development of secondary metabolites that can disrupt the QS signal molecules and attenuate the virulence of other microorganisms. The competency to disrupt the QS signal molecules [quorum quenching (QQ)] could have been evolved in quorum sensing bacteria to remove or repurpose its own QS signal molecules, or the signal molecules of microorganisms that co-inhabit a competitive environment (Grandclément et al., 2016). Bacteria could have also evolved molecules for degrading N-acyl homoserine lactone (AHL) to utilize AHL as a sole source of carbon and nitrogen, or as armor against antibiotic-producing bacteria (Gonzalez and Keshavan, 2006).

Since the discovery of the AHL degrading enzyme AhlD (acyl homoserine lactone degradation enzyme) from *Arthrobacter* sp. IBN 110 (Park et al., 2003), and the demonstration of the attenuation of *Erwinia carotovora* pathogenesis in transgenic plants expressing autoinducer inactivating aiiA gene from *Bacillus* sp. (Dong et al., 2001), an array of bacterial natural components with quorum quenching properties have been reported. These include secondary metabolites produced by bacteria from various phyla including Actinobacteria, Bacteroidetes, Firmicutes, Proteobacteria, and Cyanobacteria. In this article, we review the natural compounds from the phylum Actinobacteria that have been reported to produce AHL degrading enzymes, the corresponding genes, and other Actinobacteria derived compounds that inhibits or attenuates microbial virulence both *in vitro* and *in vivo* (**Tables 1**, **2**).

FAMILY: *Micrococcaceae*; GENUS: *Arthrobacter*

Arthrobacter was one of the first genera in the phylum Actinobacteria reported to possess a gene dedicated to the degradation of AHL. *Arthrobacter* sp. IBN110 demonstrated the potential to degrade AHLs of different lengths and acyl side chains including N-3-oxohexanoyl-L-homoserine lactone (OHHL), N-octanoyl-L-homoserine lactone (OHL), and N-3-oxododecanoyl-L-homoserine lactone (OdDHL) (Park et al., 2003). When OHHL producing *Erwinia carotovora N98* was co-cultured with strain IBN110, the concentration of OHHL and OHHL mediated pectate lyase activity significantly reduced, indicating the potential of IBN110 to disrupt AHL. Indeed, the strain IBN110 possessed acyl homoserine lactone degradation gene (ahlD) that encoded AhlD protein with characteristic zinc-binding motif HXDH≈H≈D crucial for N-acyl homoserine lactonase (AHLase) activity (Dong et al., 2002). HPLC and mass spectrometry analysis revealed that AhlD hydrolyzed the ester bond in N-acyl homoserine lactone molecules and released the homoserine lactone ring. Multiple sequence alignment of AhlD with the other known AHLases, including AttM and AiiA revealed < 26% overall sequence similarity (Park et al., 2003).

Arthrobacter sp. PGVB1 derived arthroamide and turnagainolide A (cyclic depsipeptides) demonstrated the ability to inhibit agr signaling in a *Staphylococcus aureus* agr reporter strain. At 5–10 μM concentrations, the compounds suppressed the expression of the agr-dependent gene without cytotoxicity. The inhibitory concentration value (IC_{50}) of arthroamide and turnagainolide A against *Staphylococcus aureus* agr reporter strain was 0.3 and 0.8 μM, respectively (Igarashi et al., 2015). The *Arthrobacter* B4-EPS1 exopolysaccharide abolished *Pseudomonas aeruginosa* biofilms at a lower concentration (about 86.1% at 50 μg/mL) than the exopolysaccharides reported from other genera (Li et al., 2015) including EPS (exopolysaccharide) from *Streptococcus phocae* PI80 (about 20% inhibition at 1 mg/mL) (Kanmani et al., 2011), r-EPS (released-exopolysaccharide) from *Lactobacillus acidophilus* A4 (about 80% inhibition at 1 mg/mL) (Kim et al., 2009), and A101 from *Vibrio* sp. QY101 (about 75% inhibition at 100 μg/mL) (Jiang et al., 2011). The B4-EPS1 exopolysaccharide also expressed broad-spectrum inhibitory activity against the *Staphylococcus epidermidis, Enterococcus faecium, Klebsiella pneumonia, Escherichia coli, and Morganella morganii* biofilms (Li et al., 2015). Dex410, a dextranase from marine *Arthrobacter* sp. strain (Arth410) inhibited biofilms of *Streptococcus mutans* with minimum biofilm inhibitory concentration ($MBIC_{50}$) ranging between 1.27 and 6.35 μM/ml. Dex410 also reduced the 24 h biofilms of *Streptococcus mutans* with minimum biofilm reduction value ($MBRC_{50}$) of 3.81–8.89 μM/ml. This concentration was significantly lesser than the antibacterial chlorhexidine ($MBRC_{50}$ > 20 μM) present in the commercially available oral care products. The animal experiment showed that long term usage of Dex410 effectively prevented dental caries (Jiao et al., 2014). *Arthrobacter oxydans* KQ11-1 derived dextranase displayed $MBIC_{50}$ and $MBIC_{90}$ values of 2 U/m1 and 6 U/ml, respectively toward *Streptococcus mutans* biofilm. The $MBRC_{50}$ against preformed *Streptococcus mutans* biofilm was 5 U/ml and the dextranase decreased the thickness of the biofilm up to 36.67 μm (Wang et al., 2016).

FAMILY: *Brevibacteriaceae*; GENUS: *Brevibacterium*

In 1959, when Grecz and his team reported the inhibitory activity of culture filtrates of *Brevibacterium linens* ATCC 9174 and

TABLE 1 | Compounds identified from Actinobacteria displaying anti-virulence properties.

Serial No.	Organism	Source	Protein/Compound/ Enzyme	Target/Reporter Organism	Anti-virulence activity	References
Family: *Micrococcaceae*; Genus: *Arthrobacter*						
1	*Arthrobacter* sp. Arth410	Beach mud and the homogenates from fishes and seaweeds	Dextranase (Dex410)	*Streptococcus mutans* ATCC 25175	Inhibition of biofilm formation	Jiao et al., 2014
2	*Arthrobacter* sp. B4	Soil	B4-EPS1	*Pseudomonas aeruginosa* PAO1	Inhibition of biofilm formation	Li et al., 2015
3	*Arthrobacter* sp. PGVB1	Sandstone	Arthroamide Turnagainolide A	*Staphylococcus aureus* agr reporter strain 8325-4	Reduces the luminescent level of the agr-dependent gene expression	Igarashi et al., 2015
4	*Arthrobacter oxydans* KQ11-1	Marine	Dextranase	*Streptococcus mutans*	Inhibition of adhesion and biofilm formation	Wang et al., 2016
Family: *Brevibacteriaceae*; Genus: *Brevibacterium*						
5	*Brevibacterium casei MSA19*	*Dendrilla nigra*	Glycolipid surfactant	Clinical isolates of human and fish pathogens and marine biofilm forming bacteria	Inhibit biofilm formation	Kiran et al., 2010
6	*Brevibacterium casei* MS104	*Dendrilla nigra*	Poly-hydroxy butyrate (PHB) polymer	*V. vulnificus V. fischeri V. parahaemolyticus V. alginolyticus V. harveyi*	Inhibition of adhesion	Kiran et al., 2014
7	*Brevibacterium casei* MS104	*Dendrilla nigra*	Poly-hydroxy butyrate (PHB) polymer	*Vibrio campbelli* strain PUGSK8	Inhibition of motility, hemolysis activity and biofilm formation	Kiran et al., 2016
Family: *Nocardioidaceae*; Genus: *Kribbella*						
8	*Kribbella* sp. BFI 1562	Soil	Protease	*Staphylococcus aureus* ATCC 25923 *Staphylococcus aureus* ATCC 6538	Inhibition of Biofilm formation Dispersion of preformed biofilms	Park et al., 2012
Family: *Nocardiopsaceae*; Genus: *Nocardiopsis*						
9	*Nocardiopsis dassonvillei subsp. dassonvillei* XG-8-1	Marine sediments collected from the seashore	Nocapyrone H Nocapyrone I Nocapyrone M	QS reporter strains; *P. aeruginosa* QSIS-lasI25 and *Chromobacterium violaceum* CV026	Inhibition of QS controlled gene expression	Fu et al., 2013
10	*Nocardiopsis* sp. GRG1 (KT23540)	Brown algae	Zinc oxide nanosheets	Multi Drug Resistant *Proteus mirabilis* BDUMS1 and *Escherichia coli* BDUMS3	Inhibition of biofilm and attenuate biofilm architecture	Rajivgandhi et al., 2018
Family: *Streptomycetaceae*; Genus: *Streptomyces*						
11	*Streptomyces* sp. TOHO-Y209 *Streptomyces* sp. TOHO-O348	Soil	Piericidin A1, 3′-rhamnopiericidin A1, Piericidin E	*Chromobacterium violaceum* CV026	Inhibition of violacein production	Ooka et al., 2013
12	*Streptomyces* sp. NIO 10068	Marine Invertebrate	Cinnamic acid Linear dipeptide (Pro-Gly and N-amido- α- proline)	*Pseudomonas aeruginosa* ATCC 27853	Reduction of motility, formation of biofilm, production of pyocyanin, production of rhamnolipid, production of Las A protease, swimming and twitching	Naik et al., 2013
13	*Streptomyces* sp. *BFI 250*	Soil	Protease	*Staphylococcus aureus* ATCC 25923 *Staphylococcus aureus* ATCC 6538	Inhibition of Biofilm formation Dispersion of preformed biofilms	Park et al., 2012

(Continued)

TABLE 1 | Continued

Serial No.	Organism	Source	Protein/Compound/ Enzyme	Target/Reporter Organism	Anti-virulence activity	References
14	*Streptomyces parvulus*	*Codonopsis lanceolata*	Actinomycin D	MSSA ATCC 25923 MSSA ATCC 6538 MRSA ATCC 33591	Reduce formation of biofilm, hemolysis, slime production and hydrophobicity of bacterial cell.	Lee et al., 2016
15	*Streptomyces parvulus HY026*	Sea water	Actinomycin D	*Pseudomonas aeruginosa* PAO1 *Staphylococcus aureus* 95005	Reduction in biofilm formation	Miao et al., 2017
16	*Streptomyces fradiae* PE7	Estuarine sediment	Quercetin	*Anabaena* species and *Nostoc* species	Reduction of germination of spores	Gopikrishnan et al., 2016
17	*Streptomyces coelicoflavus* S17	Soil	1H-pyrrole-2-carboxylic acid Docosanoic acid	*Pseudomonas aeruginosa* PAO1 *Pseudomonas aeruginosa* PAO1	Reduction in the production of elastase, protease and pyocyanin. Elimination of expression of las genes and rhl/pqs cascade. Reduction in the production of elastase, protease and pyocyanin.	Hassan et al., 2016
18	*Streptomyces* sp. CCB-PSK207	Marine sediment	Fatty acid methyl esters	*C. elegans* infected with *Pseudomonas aeruginosa* PA14	Induction of host immunity	Fatin et al., 2017
19	*Streptomyces* sp. OUCMDZ-3436	*Enteromorpha prolifera*	4-Hydroxy-3-methyl-6-propylpyridin-2(1H)-one 3-Ethyl-4-hydroxy-6-isopropylpyridin-2(1H)-one 4-Hydroxy-6-isobutyl-3-methylpyridin-2(1H)-one (S)-6-(sec-Butyl)-4-hydroxy-3-methylpyridin-2(1H)-one	*Pseudomonas aeruginosa* ATCC10145	Inhibition of gene expression controlled by quorum sensing in *Pseudomonas aeruginosa* QSIS-lasI.	Du et al., 2018
20	*Streptomyces albus*/pAlnuori Δ*aln6*	Recombinant Strain	Alnumycin D	*Staphylococcus aureus* ATCC 25923	Inhibition of biofilm	Oja et al., 2015
21	*Streptomyces violaceoruber* Tü22	Microbial culture collection	Granaticin B	*Staphylococcus aureus* ATCC 25923	Inhibition of biofilm	Oja et al., 2015
22	*Streptomyces minutiscleroticus* M10A62	Mangesite mine soil	Selenium nanoparticle (SeNP)	Antibiotic resistant *Acinetobacter* species	Inhibition of biofilm	Ramya et al., 2015
23	*Streptomyces* sp. *SCSGAA 0027*	*Subergorgia suberosa*	Hygrocin C	*Bacillus amyloliquefaciens* SCSGAB0082	Inhibition of biofilm, adhesion, EPS production, cell motility, and surface hydrophobicity	Wang et al., 2018
24	*Streptomyces* sp. *CNQ343*	Seafloor sediment sample	Bahamaolide A	*C. albicans* ATCC 10231	Inhibition of Isocitrate lyase (ICL) in glyoxylate cycle	Lee et al., 2014
25	*Streptomyces xanthocidicus KPP01532*	Natural product library	Piericidin A and Glucopiericidin A	*Erwinia carotovora subsp. atroseptica* (Eca) *C. violaceum* CV026	Reduction of soft rot disease symptoms in potato Inhibition of violacein production	Kang et al., 2016
26	*Streptomyces* sp. strain MC11024	Library of culture extracts of actinomycetes	Streptorubin B	MRSA N315	Inhibition of biofilm formation	Suzuki et al., 2015
27	*Streptomyces* sp. ZL-24	Wet soil	Melanin	*P. aeruginosa* ATCC 9027 and *S. aureus* ATCC 6538	Inhibition of biofilm formation	Wang et al., 2019

(Continued)

TABLE 1 | Continued

Serial No.	Organism	Source	Protein/Compound/ Enzyme	Target/Reporter Organism	Anti-virulence activity	References
28	*Streptomyces* sp. AT37	Desert soil	5-[(5E,7E,11E)-2,10-dihydroxy-9,11-dimethyl-5,7,11-tridecatrien-1-yl]-2-hydroxy-2-(1-hydroxyethyl)-4-methyl-3(2H)-furanone	Methicillin sensitive *Staphylococcus aureus* and methicillin resistant *Staphylococcus aureus*	Inhibition of biofilm	Driche et al., 2017
29	*Streptomyces griseoincarnatus* HK12	*Callyspongia* sp.	9Z-Octadecenal, arachidic acid, erucic acid, 13Z-Octadecenal and tetracosanoic acid.	*Pseudomonas aeruginosa* and *Staphylococcus aureus*	Inhibition of biofilm	Kamarudheen and Rao, 2019
30	*Streptomyces* Strain K01-0509	Soil	Guadinomines A and Guadinomines B	Enteropathogenic *E. coli*	Inhibition of type III secretion system	Iwatsuki et al., 2008
31	*Streptomyces* sp. *ANK313*	soil	Khatmiamycin Aloesaponarin II	Zoospores of *Plasmopara viticola*	Inhibition of motility	Abdalla et al., 2011
32	*Streptomyces* TOHO-M025	Soil	Maniwamycins	*C. violaceum* CV026	Inhibition of violacein production	Fukumoto et al., 2016
33	*Streptomyces* sp. *MC025*	Unidentified red alga	Collismycin C	Methicillin sensitive *Staphylococcus aureus* and methicillin resistant *Staphylococcus aureus*	Inhibition of biofilm	Lee et al., 2017
34	*Streptomyces* sp. *strain FA-70*	Soil	FA-70C1 (Phenylalanyl-ureido-citrullinyl-valinyl-cycloarginal)	*Porphyromonas gingivalis* ATCC33277 and *Porphyromonas gingivalis* KDP129	Inhibition of Arg-gingipain (Rgp)	Kadowaki et al., 2003
35	*Streptomyces griseorubens* AU2	Soil	Silver nano particles	*Pseudomonas aeruginosa* ATCC 27853 and *Staphylococcus aureus* ATCC 25923	Inhibition of biofilm	Baygar and Ugur, 2017
36	*Streptomyces* sp. OUCMDZ-3436	*Enteromorpha prolifera*	1. 4-hydroxy- 3-methyl-6-propylpyridin-2(1H)-one 2. 3-ethyl-4-hydroxy- 6-isopropylpyridin-2(1H)-one 3. 4-hydroxy-6-isobutyl-3-meth- ylpyridin-2(1H)-one 4. (S)-6-(sec-butyl)-4-hydroxy-3-methylpyridin-2(1H)-one	*Pseudomonas aeruginosa* QSIS-lasI biosensors	Inhibition of QS controlled gene expression	Du et al., 2018
Others						
37	*Actinomycete* strain DSW812	Soil, Marine sediment, Sea water and Plants	WS9326A and WS9326B	VirSR system of *Clostridium perfringens S. aureus 8325–4 (type-I AIP), K12 (type-II AIP) and K9 (type-IV AIP) S. aureus Newman and S. aureus K3*	Suppression of expression of pfoA (Perfringolysin O) Inhibition of the production of hemolysin Reduction of S. aureus cytotoxicity in human corneal epithelial cells	Desouky et al., 2015

Brevibacterium linens ATCC 9175 toward the germination of *Clostridium botulinum* type A spores, little did they know that it was one of the earliest reports of anti-infective property ever reported from the Genus *Brevibacterium* (Grecz et al., 1959). In fact, it was only during the mid 2000s that the evidence of quorum sensing in *Clostridium botulinum* and its role in regulating the germination of botulinum spores was established (Zhao et al., 2006). Today, out of the 51 known species of *Brevibacterium*[1] only two strains from *Brevibacterium casei* (*Brevibacterium casei* MSA19 and MS104), both interestingly isolated from the marine sponge *Dendrilla nigra,* have been reported to produce compounds with anti-virulence property against bacterial pathogens (Kiran et al., 2010, 2016; **Table 1**).

At a concentration of 30 μg/ml, *Brevibacterium casei* MSA19 glycolipid affected the formation of biofilm by inhibiting the initial attachment of the bacteria mediated by pili and flagella. At a very low concentration, the *Brevibacterium* glycolipid significantly reduced the formation of both individual and mixed bacterial biofilms (Kiran et al., 2010; **Table 1**). Microtiter plate assay and CLSM images revealed that polyhydroxy butyrate (PHB) derived from *Brevibacterium casei* MSI04 suppressed the adhesion of pathogenic *Vibrio* species on both polystyrene

[1]http://www.bacterio.net

TABLE 2 | Extract from Actinobacteria displaying anti-virulence activity.

Serial No.	Organism	Origin	Medium	Target Organism	Activity	Concentration	References
1	*Actinomycetes* C5-5Y	Library collection	Partially purified yellow pigment	*Staphylococcus aureus and Streptococcus mutans*	Inhibition of biofilm formation, inhibition of protease and lipase activity, reduction in cell surface hydrophobicity	10 μg/ml	Soundari et al., 2014
2	*Kribbella* sp. BFI 1562	Library collection	Spent medium	*Pseudomonas aeruginosa*	Inhibition of biofilm formation	1% (v/v)	Kim et al., 2012
3	*Streptomyces albus* A66	Marine Sediment	Extract	*Vibrio harveyi*	Inhibition of biofilm formation and dispersal of mature biofilms.	2.5% (v/v)	You et al., 2007
4	*Streptomyces akiyoshiensis* CAA-3	Coral reef	Methanolic extracts	*S. aureus* ATCC 11632, methicillin resistant *S. aureus* ATCC 33591	Biofilm inhibition Inhibition of intestinal colonization in *C. elegans*	0.1 mg/ml	Bakkiyaraj and Pandian, 2010
5	*Streptomyces akiyoshinensis A3 Actinobacterium* sp. A10	*Acropora digitifera*	Ethyl acetate extract	*Streptococcus pyogenes*	Inhibition of Biofilms	10–200 μg/ml	Nithyanand et al., 2010
6	*Streptomyces* sp. A745	Arctic Sediment	Diethyl ether fraction	*Vibrio cholerae* (MCV09)	Inhibition of Biofilm	200 μg/ml	Augustine et al., 2012
7	*Streptomyces* sp. BFI 230	Actinomycetes culture library	Spent medium	*Pseudomonas aeruginosa*	Inhibition of biofilm formation and Interference in iron uptake	1% (v/v)	Kim et al., 2012
8	*Streptomyces* sdLi	Marine sediment	Ethyl acetate extract	*Proteus mirabilis* UCB4	Suppression of urease production and swarming motility Inhibition of biofilm	10 mg/ml 15 mg/ml	Younis et al., 2016
9	*Streptomyces* sp. SBT343	*Petrosia ficiformis*	Ethyl acetate extract	*Staphylococcus epidermidis,* methicillin resistant *Staphylococcus aureus* and methicillin sensitive *Staphylococcus aureus*	Inhibition of biofilm	62.5–250 μg/ml	Balasubramanian et al., 2017
10	*Streptomyces albogriseolus* GIS39Ama	Soil	Ethyl acetate extract	(1) *Klebsiella pneumoniae* MTCC 3384, (2) *Vibrio cholerae* MTCC 3906, (3) *Escherichia coli* MTCC 687 and (4) *Pseudomonas aeruginosa* MTCC 2453	Inhibition of biofilm Reduction in EPS production, biofilm density and viability	1. 625 ppm 2. 625 ppm 3. 312 ppm 4. 1250 ppm	Lokegaonkar and Nabar, 2017
11	*Nocardiopsis* sp. ZoA1	*Zingiber Officinale_*	Spent medium	Multidrug-resistant *Staphylococci capitis* 267 and *Staphylococci haemolyticus* 41	Inhibition of biofilm	200 μg/ml	Sabu et al., 2017
12	*Nocardiopsis* sp. A731	Arctic Sediment	Culture supernatant	*Vibrio cholerae* (MCV09)	Inhibition of Biofilm	20% (v/v)	Augustine et al., 2012

and glass surfaces at a concentration of 0.6 mg (200 μl). In fact, the PHB was most effective in inhibiting the formation of biofilm than dislodging pre-formed biofilm (Kiran et al., 2014). At 50 μg/ml concentration, PHB inhibited bioluminescence, and at 150 μg/ml reduced the formation of *Vibrio campbellii* PUGSK8 biofilm. Infection of *Vibrio* species in brine shrimp (*Artemia* sp.) is typically fatal, and, treatment of ≥ 50 μg/ml of PHB resulted in the elicitation of protection to shrimps up to 48 h. This research revealed that the ß-hydroxy butyric acid, an intermediate released during the PHB degradation indeed regulates the expression of the virulence factors in PUGSK8 (Kiran et al., 2016).

FAMILY: *Mycobacteriaceae*; GENUS: *Mycobacterium*

The discovery of AHL lactonases in *Mycobacterium* was an outcome of exploration for the establishment of promiscuity of the divergence of bacterial phosphotriesterase (PTE), an

enzyme first discovered in *Pseudomonas diminuta* with efficient paraoxonase activity (Raushel and Holden, 2000; Roodveldt and Tawfik, 2005). The absence of naturally occurring specific substrate and the evolutionary elusiveness of PTE led to a BLAST search for genes homologs to *Pseudomonas diminuta* PTE. Three genes including two from the phylum Actinobacteria; PPH (putative parathion hydrolase) in *Mycobacterium tuberculosis* and AhlA (N-acyl-homoserine lactone acylase) in *Rhodococcus erythropolis* sharing a 34 and 28% identity and SsoPox (phosphotriesterase with natural lactonase activity) from an archeon *Sulfolobus solfataricus* with 31% identity were identified (Afriat et al., 2006). The PPH and AhlA have been classified as phosphotriesterase-like lactonase (PLL) from the amidohydrolase superfamily that hydrolysis substrates with either ester or amide functional groups at phosphorus and carbon centers (Seibert and Raushel, 2005). A subsequent exploration into the enzymology of PPH and AhlA revealed that the paraoxonases activity was rather a promiscuous function that could have emerged in PLLs from its progenitor lactonase activity (Afriat et al., 2006).

Expression of PPH gene in *Escherichia coli* in the presence of three metal ions (Zn^{2+}, Co^{2+} and Mn^{2+}) prompted a 2000-fold increase in PPH's lactonase activity than the paraoxonase activity. Further research revealed that these metal ions were vital for PPH's enzymatic activity and that metal chelation inactivated PPH. The K_M and k_{cat}/K_M values of PPH during the hydrolyzes of lactones ranged between e20 and 230 μM, and from 1.4×10^4 to 5×10^5 s^{-1} M^{-1}, respectively. The k_{cat}/K_M values generally increased with six membered lactone ring and lactones with longer and more hydrophobic side chains. However, no visible lactonase activity against N-acyl thiolactone analog derived from homocysteine was observed (Afriat et al., 2006). Another orthologous of PLL, MCP (AHL lactonase from *Mycobacterium avium* subsp. *paratuberculosis* K-10), also degraded a wide range of AHLs and displayed up to 92% sequence similarity with PPH. MCP also demonstrated low paraoxonase activity indicating that the naturally occurring substrate for MCP does not contain phosphate esters. Introduction of a single point mutation in ßα loop at the carboxyl-terminal end of eighth β-strand of the MCP resulted in a mutant (N266Y) with enhanced AHL lactonase activity than the wild type MCP. The N266Y mutant (substitution of TAC for AAC at 266 codon) increased the k_{cat}/K_M values up to 4 to 32-fold for C12-HSL and C6-HSL than the wild type. Further research with the mutants including the N266 showed that a suitable amino acid substitution at the 266 residue, and its proximity to the lactone ring of AHL provide the possibility to enhance AHL lactonase activity by introducing an AHL binding geometry (Chow et al., 2009).

FAMILY: *Microbacteriaceae*; GENUS: *Microbacterium*

Several strains of *Microbacterium* species isolated from potato tuber plant (*Solanum tuberosum*) have been reported to degrade AHLs with both short and long acyl side chains (Morohoshi et al., 2009; Wang et al., 2010, 2012). An infestation of *Pectobacterium carotovorum* subsp. *carotovorum* in potato crop results in soft rot disease, a consequence of coordinated expression of virulence factors mediated by QS signal molecule N-(3-oxohexanoyl)-L-homoserine lactone (Chatterjee et al., 1995). Two endophytic strains: *Microbacterium testaceum* StLB018 and *Microbacterium testaceum* StLB037 attenuated virulence in *Pectobacterium carotovorum* subsp. *carotovorum* NBRC 3830 without bactericidal activity (Morohoshi et al., 2009). Nucleotide sequence analysis of StLB037 revealed a complete open reading frame encoding a protein of 295 amino acids that belonged to α/ßhydrolase fold family encompassing the characteristic catalytic active site Gly-X-Ser-X-Gly (Holmquist, 2000). Named as autoinducer inactivation gene from *Microbacterium testaceum* (aiiM), the expression of StLB037 AiiM protein in the NBRC 3830, drastically reduced the pectinase production and also attenuated tissue maceration non-bactericidally (Morohoshi et al., 2009). HPLC analysis with fraction containing maltose binding protein-AiiM (MBP-AiiM) fusion protein and C10-HSL produced two peaks that coordinated with the standards of C10-HSL, and the opened lactone ring of C10-HSL. As this established the role of AiiM in degrading AHL, further study revealed that AiiM was not influenced by the length or the substitution of the acyl side chains. The partially purified MBP-AiiM protein exhibited relatively better activity against C12-HSL and 3-oxo-substituted AHLs than C6-HSL, C8-HSL, C10-HSL and other unsubstituted AHLs (Wang et al., 2010).

Investigation into the distribution and diversity of AiiM among the Genus *Microbacterium* with various strains isolated from different sources including potato plant, scarlet runner bean, rapeseed, Chinese paddy, milk, cheese, air, soil, activated sludge, imperial moth and many more, exposed that the superior level of AHL degradation exhibited by the *Microbacterium* strains was due to the presence of aiiM gene encoded in the chromosome of bacterium. Out of 26 *Microbacterium* strains included in the study, only 9 strains exhibited high degrading ability against C6-HSL, 3OC6-HSL, C10-HSL, and 3OC10-HSL. Remarkably, these strains were of potato plant origin and were positive for aiiM gene in their genetic material. The remaining 17 strains lacked the ability to degrade C6-HSL and exhibited low to relatively intermediate degrading ability against 3OC6-HSL, C10-HSL, and 3OC10-HSL. These strains were of non-potato origin and were negative for aiiM gene in their DNA (Wang et al., 2012). Comparison of the nine aiiM positive strains with phylogenetically related *Microbacterium* strains (*Microbacterium* sp. *PcRB024* and *M. testaceum ATCC 15829*) revealed the absence of significant AHL degrading activity or the aiiM gene in the chromosome. The aforementioned evidence led to a conclusion that the aiiM was not conserved among the Genus *Microbacterium* and could have spread amongst the *Microbacterium* strains inhabiting potato tuber ecosystem through the non-horizontal mode of transmission supposedly due to the absence of transposons flaking the aiiM (Wang et al., 2012). Although *Microbacterium testaceum* aiiM homologous gene with high sequence similarities have been identified in other actinobacterial strains including *Rhodococcus erythropolis* PR4 and *Rhodococcus opacus* B-4, their expression as MBP-AiiM protein lacked AHL lactonase activity. The *Microbacterium*

StLB037 encoded AiiM bears < 15% similarity with other known AHL lactonases including AidP, AiiA, AttM, AhlD, QsdA, QlcA, BpiB01, BpiB04 and BpiB07. The absence of conserved zinc-binding domains found in AHL lactonases from metallo-ß-lactamase super family and PTE family proteins affirmed the novelty and ingenuity of AiiM (Wang et al., 2010).

FAMILY: *Nocardiopsaceae*; GENUS: *Nocardiopsis*

The culture supernatant of cold temperature adapted *Nocardiopsis* sp. A731, at a concentration of 20% (v/v) inhibited about 80% of *V. cholerae* biofilm (Augustine et al., 2012). Three novel α-pyrones; nocapyrone H **(1)**, nocapyrone I **(2)**, and nocapyrone M **(3)** (**Tables 1**, **3**), were extracted from *Nocardiopsis dassonvillei* subsp. dassonvillei XG-8-1 inhibited QS controlled virulence in *P. aeruginosa* QSIS-lasI biosensor and *Chromobacterium violaceum* CV026 at a concentration of 100 μg/mL (Fu et al., 2013). At 200 μg/ml concentration, the crude extract of *Nocardiopsis* sp. ZoA1 inhibited the formation of *Staphylococcus haemolyticus* 41 and *Staphylococcus capitis* 267 biofilms by ≥ 90% (**Table 2**). Dose-dependent biofilm inhibition assay with ZoA1extract supported the assumption that inhibition of multidrug-resistant coagulase negative staphylococci (CONS) was due to the inhibition of production of proteinaceous factors and exopolysaccharide. However, ZoA1 strain also possessed broad-spectrum antibacterial activity against *Staphylococcus aureus, Bacillus subtilis, Salmonella typhi*, and *Vibrio cholerae* (Sabu et al., 2017). The spent medium of soil *Nocardiopsis* sp. TRM 46200 showed ≥ 90% inhibition against the *Staphylococcus epidermidis* biofilms for over 24 h. The major metabolite in the culture supernatant was proteinous in nature and exhibited both antibiofilm and protease activity. The crude protein derived from TRM 46200 reduced the cell surface hydrophobicity, and also degrade DNA and the extracellular polymeric substance (EPS) of *Staphylococcus epidermidis* strains (ATCC 35984 and 5-121-2) (Xie et al., 2018). The culture supernatant of *Nocardiopsis* sp. GKU 213 inhibited biofilm formation of *Staphylococcus aureus* ATCC 25923 by 60% without anti-bacterial activity (Leetanasaksakul and Thamchaipenet, 2018). Zinc oxide nano-sheets (ZnO NSs) produced by *Nocardiopsis* sp. GRG1 (KT23540) effectively inhibited the biofilms of multi-drug resistant *Proteus mirabilis* BDUMS1 and *Escherichia coli* BDUMS3 by 92 and 90%, at 20 μg/ml concentration, respectively. CLSM images and fluorescent light microscopic analysis showed that ZnO NSs disintegrated the biofilm architecture of uropathogens, by dispersing the bacterial cells leaving only fewer adherent cells and cell aggregates (Rajivgandhi et al., 2018).

FAMILY: *Nocardiceae*; GENUS: *Rhodococcus*

While the possible presence of γ-butyrolactone dependent quorum sensing system in *Rhodococcus* species could be understood only by *in silico* genomic analysis of *Rhodococcus*

TABLE 3 | Metabolites derived from Actinobacteria exhibiting virulence inhibitory activity.

S. No.	Compound Name	Structure
1.	Nocapyrone H	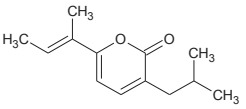
2.	Nocapyrone I	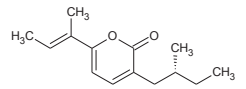
3.	Nocapyrone M	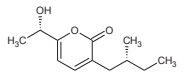
4.	FA-70C1 (Phenylalanyl-ureido-citrullinyl-valinyl-cycloarginal)	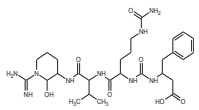
5.	Guadinomine A	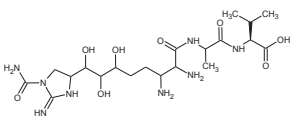
6.	Guadinomine B	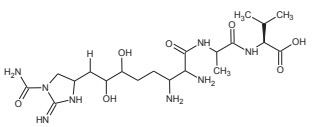
7.	Piercidin A1	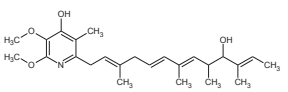
8.	Rhamnopiericidin A1	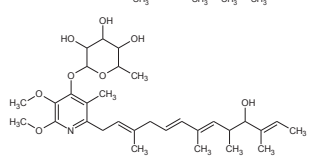
9.	Piercidin E	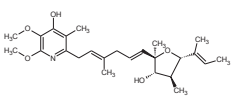
10.	Alnumycin D	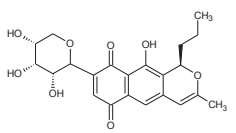
11.	1H-pyrrole-2-carboxylic acid	
12.	Behenic acid (Docosanoic acid)	
13.	Maniwamycins D	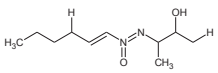
14.	Maniwamycins E	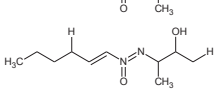
15.	Maniwamycins C	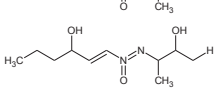

(Continued)

TABLE 3 | Continued

S. No.	Compound Name	Structure
16.	Quercetin	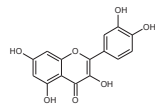
17.	Piericidin A	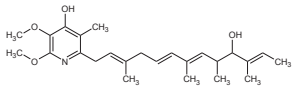
18.	Glucopiericidin A	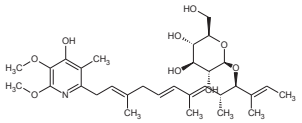
19.	Antibiotic AT37-1	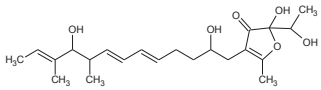
20.	Collismycin C	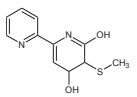
21.	Pyrisulfoxin A	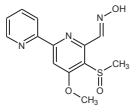
22.	13Z-Octadecenal	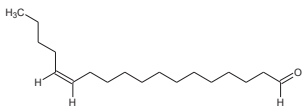
23.	α- pyridone Compound 16	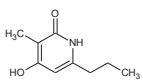
24.	α- pyridone Compound 17	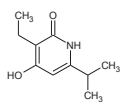
25.	α- pyridone Compound 19	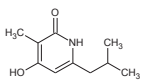
26.	α- pyridone Compound 20	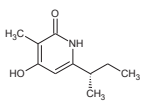
27.	Bahamaolide A	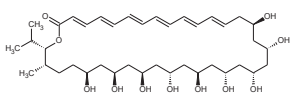
28.	Khatmiamycin	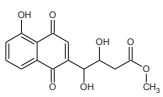
29.	Aloesaponarin II	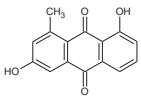

erythropolis PR4 and *Rhodococcus* strain RHA1, the quorum quenching mechanism of this genera is one of the well-established among bacteria (Wuster and Babu, 2007; Latour et al., 2013). Indeed, *Rhodococcus* sp. is a unique organism possessing three different mechanisms for N-acyl homoserine lactone degradation; an AHL lactonase, an oxidoreductase and an amidase (Uroz et al., 2003, 2005, 2008, 2009; Park et al., 2006), unraveling the unprecedented evolution of multiple QQ strategies within a bacterium.

In 2003, Uroz and his team demonstrated that a 'wild type' *Rhodococcus erythropolis* W2 can degrade C6-HSL, and attenuate the QS-regulated pathogenesis in *Pectobacterium carotovorum subsp. carotovorum*, a pathogen of potato tubers, without limiting or inhibiting its growth (Uroz et al., 2003). Although primarily identified on the basis of its ability to utilize 3-oxo-C6 HSL, the *Rhodococcus erythropolis* W2 interestingly degraded the 3-oxo derivative of acyl homoserine lactone less efficiently than the other known AHL degrading bacteria (Leadbetter and Greenberg, 2000). The broad substrate specificity, rapid AHL inactivation and interference with QS regulated pathogenesis exhibited by *Rhodococcus erythropolis* W2, instigated a series of studies to understand the underlying catabolic mechanism involved in AHL degradation (Uroz et al., 2003, 2005, 2009). Incubation of N-(3-oxooctanoyl)-L-homoserine lactone (3O,C8-HSL), N-(3-oxodecanoyl)-L-homoserine lactone (3O,C10-HSL), N-(3-oxododecanoyl)-L-homoserine lactone (3O,C12-HSL), N-(3-oxotetradecanoyl)-L-homoserine lactone (3O,C14-HSL) with whole cells of W2 in phosphate buffer saline resulted in the production of 3-hydroxy derivatives: 3OH,C8-HSL, 3OH,C10-HSL, 3OH,C12-HSL and 3OH,C14-HSL, respectively. This reaction was mediated by oxidoreductase activity (Uroz et al., 2005). The broad substrate specificity of oxidoreductase also catalyzed the reduction of AHL derivatives substituent with aromatic acyl side chains or without lactone ring including N-(3-oxo-6-phenylhexanoyl) homoserine lactone and 3-oxododecanamide, respectively (Uroz et al., 2005).

Interestingly, the oxidoreductase activity observed in the whole cell of *Rhodococcus erythropolis* W2 was absent in the culture extract. The complete elimination of unsubstituted and substituted (3-oxo or 3-hydroxy) AHLs from the incubation medium containing the culture extract of W2, suggested the presence of another mechanism to degrade AHL. This was later validated to be an acylase that catalyzed AHL degradation by releasing dansylated homoserine lactone from the incubated reaction mixture of N-(3-oxodecanoyl)-L-homoserine lactone and cell culture extract of W2 strain. The AHL acylase cleaved the amide bond of both short and long chain AHLs yielding homoserine lactone through amidolytic activity (Uroz et al., 2005).

Identification of a soil bacterium that displayed the potential to utilize AHL led to the discovery of AHL lactonase, the third mechanism for the catabolism of AHL in *Rhodococcus* species (Park et al., 2006). Two strains of *Rhodococcus* sp. LS31 and PI33 displayed different substrate specificity for N-3-oxo-hexanoyl-L-homoserine lactone (OHHL), and mass spectrometric analysis revealed that both the strains hydrolyzed the lactone ring of AHL (Park et al., 2006). *Rhodococcus* sp. strain LS31 degraded AHL of different lengths with different acyl side chain substitutions, contradicting the higher degrading activity exhibited by *Rhodococcus erythropolis* W2 against

3-oxo-substituent AHLs than unsubstituted AHLs (Uroz et al., 2003, 2005). The AHL lactonase from both the strains LS31 and PI33 destroyed AHL, while the *R. erythropolis* W2 attenuated the signal molecules (Park et al., 2006). Although much of the enzymology underlying *Rhodococcus* AHL acylase and AHL oxidoreductase has been unraveled, the genetic determinant of these enzymes still remains unknown.

QsdA, a product of the gene qsdA (quorum sensing signal degradation), was reported as the another AHL lactonase utilized by *Rhodococcus erythropolis* strain W2 to degrade AHL. This novel class of AHL lactonase did not show homology to any previously reported AHL degrading enzymes that were characterized from the two protein super families: Zinc-dependent glyoxylase and N-AHSL amidohydrolases of the β lactam acylases (Uroz et al., 2008). In fact, the QsdA belonged to the group of phosphotriesterase (PTE) like lactonase (PLL) within the amidohydrolase superfamily (Hawwa et al., 2009) that possessed the characteristic binuclear metal center inside a TIM- barrel $(\beta/\alpha)_{\delta}$ - barrel-shaped scaffold). Though initially this enzyme was described as paraoxonases due to their activity against organophosphate pesticide paraoxon (Afriat et al., 2006), later experiments showed that the enzymes also hydrolyzed lactones including the N-acyl homoserine lactones with 6 to 14 carbon in acyl side chains, irrespective of carbon 3 substitution (Uroz et al., 2008). The qsdA operon can also be utilized for the assimilation of various lactone in the milieu including the γ-lactone, and also for the disruption of QS signals of competitive bacteria (Latour et al., 2013). The qsdA homologue is conserved in reference strains including, *Rhodococcus erythropolis* DCL14 (de Carvalho and da Fonseca, 2005) and it was suggested that the detection of AHL signals or the γ- capro lactones in the environment can lead to the transcription of qsdA within qsd operon (Barbey et al., 2012, 2013). A putative transcriptional regulator homologous to TetR (QsdR) had been reported upstream of *qsd* operon (Latour et al., 2013), which, in the absence of AHL could bind to the promoter inhibiting the expression of qsdA. In the presence of AHL or γ-butyro lactones, the QsdR might undergo conformational change leading to the transcription of the gene qsdA (Cuthbertson and Nodwell, 2013; Barbey et al., 2018).

Attenuation of QS-regulated pathogenesis in *Pectobacterium carotovorum subsp. carotovorum*, a pathogen of *Solanum tuberosum* (potato tubers), by rhizosphere soil *Rhodococcus erythropolis* W2 illustrates the interaction between a QS producer, a QQ producer, and their plant host. The treatment of rhizosphere soil of potato plant with growth stimulator such as gamma- caprolactone (GCL), provoked the growth of native AHL degrading strains especially *Rhodococcus erythropolis* (Cirou et al., 2007, 2011). Another study with *Rhodococcus* sp. R138 isolated from GCL treated potato rhizosphere soil exhibited strong biocontrol activity in potato tuber assay by degrading AHL and through assimilating GCL (Cirou et al., 2011). *Rhodococcus erythropolis* not only increased its population in response to GCL (a natural plant molecule) but also assimilated GCL, a reaction proposed to have been catalyzed by QsdA and other rhodococcal enzymes (Cirou et al., 2012). Drastic reduction in AHL mediated virulence of *Pectobacterium atrospeticum by Rhodococcus erythropolis* was identified by transcriptome analysis (Kwasiborski et al., 2015). *Rhodococcus* sp. BH4 encapsulated within free moving alginate cell trapping beads (CEBs) quenched AHL and reduced the synthesis of extracellular matrix of biofilm-forming microbial cells in membrane bioreactors. This property of quenching AHL by strain BH4, in combination with the physical friction exerted by alginate beads, has been proposed as prospective model for controlling biofouling (Kim et al., 2013).

FAMILY: *Streptomycetaceae*; GENUS: *Streptomyces*

An AHL acylase termed as AhlM (N-acyl homoserine lactone acylase) derived from *Streptomyces* sp. strain M664 was the first AHL degrading enzyme characterized from the genera *Streptomyces* (Park et al., 2005). Discovered based on its potential to obstruct N-acyl homoserine lactone facilitated violacein production, the AHL acylase catalyzed the hydrolysis of an amide bond between homoserine lactone and acyl side chain in AHL. The active enzyme was composed of 804 amino acids that were arranged in a pattern characteristic of a penicillin acylase class of proteins belonging to Ntn hydrolase superfamily. Amino acid sequence analysis of AhlM with known AHL acylases: AiiD from *Ralstonia* strain XJ12B (Lin et al., 2003) and PvdQ from *Pseudomonas aeruginosa* (Huang et al., 2003) displayed < 35% sequence identity. Apart from the acylase activity, the AhlM also displayed deacylation activity against long acyl chain AHLs and was suggested of possessing the ability to degrade cyclic lipopeptides. At a concentration of 20 μg/ml, AhlM significantly reduced the production of elastase, total protease, and Las A protease in *P. aeruginosa* PAO1 (Park et al., 2005).

A metabolite phenylalanyl-ureido-citrullinyl-valinyl-cycloarginal termed as FA-70C1 **(4)** (**Tables 1**, **3**) isolated from *Streptomyces* species FA-70, strongly inhibited arg-gingipain (Rgp), an enzyme crucial for survival and proliferation of *Porphyromonas gingivalis* both *in vitro and in vivo* (Kadowaki et al., 1998, 2003).

Guadinomines A **(5)** and B **(6)** (**Table 3**) derived from *Streptomyces* K01-0509 showed dose-dependent inhibitory activity against hemolysis caused by enteropathogenic *Escherichia coli* (EPEC), potentially through the inhibition of type III secretion system. The inhibitory concentration (IC_{50}) value of guadinomine B and guadinomine A was 0.007 mg/ml and 0.02 mg/ml, respectively (Iwatsuki et al., 2008). Piericidin A1 **(7)**, a major metabolite of *Streptomyces* sp. TOHO-Y209 and TOHO-O348, displayed an IC_{50} value of 10 μg/ml against violacein production by *C. violaceum* CV026. 3′-rhamnopiericidin A1 **(8)**, and piericidin E **(9)** also expressed QSI activity but much lesser than piericidin A1 (Ooka et al., 2013). Alnumycin D **(10)**, a C-ribosylated pathway shunt product isolated from recombinant strain *Streptomyces albus*, effectively inhibited the biofilm and planktonic cells of *Staphylococcus aureus* ATCC 25923 by 12 to 22-fold higher than alnumycin A. Similarly, granaticin B, a polyketide metabolite from *Streptomyces violaceoruber,* could disrupt pre-formed staphylococcal biofilms. The structural similarities observed between the two compounds, including

glycosylation at the C-8 position with ribopyranosyl unit in alnumycin D and the aglycone unit through C–C bond at C-7 and C-8 positions in granaticin B, were suggested to have contributed to the biofilm inhibitory activity. In addition to this, the oxygenation pattern within the naphthoquinone ring, carbonyl oxygen atom in alnumycin D and hydroxyl group in granaticin B, were also suggested to have contributed to the anti-biofilm activity (Oja et al., 2015).

Well studied for its role in suppressing (Tzaridis et al., 2016) and treating tumors (Walsh et al., 2016; Das et al., 2017; Schmidt et al., 2017; Lamture et al., 2018), actinomycin D from *Streptomyces parvulus* also possessed biofilm inhibitory activity *in vitro*. At 0.1 μg/ml concentration, actinomycin D reduced the formation of biofilm of methicillin sensitive *Staphylococcus aureus* strains (ATCC 25923 and ATCC 6538) and methicillin resistant *Staphylococcus aureus* strain (ATCC 33591) by ≥ 70%, ≥ 80%, and ≥ 80%, respectively (Lee et al., 2016). At the same concentration, actinomycin D reduced the biomass and mean thickness of *Staphylococcus aureus* biofilm by 98%, and the hemolytic activity by ≥ 85%. This led to the suggestion that the inhibitory activity of actinomycin D toward *Staphylococcus aureus* was partly concatenated with its ability to inhibit hemolysis. Besides, *Streptomyces parvulus* derived actinomycin D also reduced the hydrophobicity of the staphylococcal cells, a property crucial for the bacterial adherence to the substrata (Krasowska and Sigler, 2014). The failure of the actinomycin D to disperse preformed staphylococcal biofilms highlighted the non-association of actinomycin D with protease or the staphylococcal agr QS system (Lee et al., 2016). Conversely, actinomycin D derived from *Streptomyces parvulus* HY026 significantly reduced the production of violacein by *C. violaceum* up to 90.7% at 50 μg/ml concentration. Although the potential of actinomycin D from endophytic *Streptomyces parvulus* (1% (v/v) concentration) to inhibit staphylococcal biofilms does seem to be more superior than the actinomycin D from *Streptomyces parvulus* HY026 (10% v/v concentration), the non-agr QS mediated mode of biofilm inhibition by the former strain and anti-QS activity of actinomycin D from HY026 exemplifies the outstanding functional adaptation of actinomycin D at molecular level (Miao et al., 2017; **Table 1**).

Streptomyces coelicoflavus S17 derived 1H-pyrrole-2-carboxylic acid **(11)** and docosanoic acid **(12)** (**Table 3**) significantly attenuated the virulence of *P. aeruginosa* PAO1 at 1 mg/ml concentration. While 1H-pyrrole-2-carboxylic acid decreased the production of elastase, protease, and pyocyanin by 96, 74, and 44%, respectively, the docosanoic acid reduced their production by 91.8, 46.1, and 64.45%, respectively. The compound 1H-pyrrole-2-carboxylic acid eliminated the expression of las genes; lasA, lasB, lasI and lasR by 88, 92, 80, and 87%, respectively. The compound also inhibited rhl/pqs cascade including pqsA, pqsR, rhlI and rhlR by 97, 78, 69, and 89%, respectively (Hassan et al., 2016). All maniwamycins from *Streptomyces* TOHO-M025 reduced the production of violacein by *C. violaceum* CV026 in a dose-dependent manner at a concentration ranging from 0.01 to 1 mg/ml. Maniwamycins D **(13)** and E **(14)** displayed higher QS inhibitory activity than C **(15)** and F. Maniwamycin E showed IC_{50} value of 0.12 mg/ml (Fukumoto et al., 2016).

Quercetin **(16)** from marine *Streptomyces fradiae* PE7 reduced the germination of *Anabaena* and *Nostoc* sp. spores by 70% at 100 μg/ml concentration (Gopikrishnan et al., 2016). The addition of culture extract from *Streptomyces xanthocidicus* KPP01532 (≥ 2.5 μL), reduced the violacein production by CV026 considerably. Transcriptomic analysis on the effect of purified piericidin A **(17)** and glucopiericidin A **(18)** from the KPP01532 media extract on *E. carotovora subsp. atroseptica* revealed that the reduction in the expression of genes encoding hydrolytic enzymes including pectate lyase (*PelC*), cellulase *(CelV*), polygalacturonase (*PehA*) and QS controlled virulence-associated gene (*nip*). Treatment of potato tubers with 50 and 100 μM of piericidin A also reduced the development of soft rot disease symptoms. Similar results were also obtained *in vitro* with KPP01532 glucopiericidin A (Kang et al., 2016).

Hygrocin C (an ansamycin) derived from *Streptomyces* sp. SCSGAA0027 displayed a biofilm inhibitory concentration (BIC_{80}) value of 12.5 μg/ml, 25.0 μg/ml and 200 μg/ml against *Bacillus amyloliquefaciens, Staphylococcus aureus* and *P. aeruginosa,* respectively. At a dosage of 12.5 to 100 μg/ml, hygrocin C reduced pre-formed biofilms of *Bacillus amyloliquefaciens* by 11.73 to 54.76%. Transcriptomic analysis showed that in the presence of hygrocin C, 107 genes were upregulated, and 102 genes were downregulated. While the downregulated genes were crucial for motility including FliC and FliA (Flagellar genes), MotB (Flagellar motor protein) and two-component systems including ResE (Sensor histidine kinase ResE) and CydB (Cytochrome-bd-ubiquinol oxidase), the upregulated genes led to the mass synthesis of arginine and histidine. The unbalanced level of histidine and arginine, and the downregulation of genes essential for motility were suggested to have contributed to the repression of biofilm formation. It was also suggested that the suppression of bacteria's survival was due to the downregulation of nitric oxide dioxygenase (HmpA) (Wang et al., 2018).

Metal nanoparticles including selenium and silver nanoparticles synthesized from *Streptomyces* species have also been effective in attenuating virulence of microbial pathogens. Selenium nanoparticles synthesized by *Streptomyces minutiscleroticus* M10A62 inhibited biofilm of antibiotic-resistant strains of *Acinetobacter* species at a concentration of 3.2 μg/ml (Ramya et al., 2015). Silver nanoparticles from *Streptomyces griseorubens* AU2 suppressed the biofilm of *Staphylococcus aureus* ATCC 25923 and *P. aeruginosa* ATCC 27853 at a concentration 20 μg/ml and 10 μg/ml, respectively (Baygar and Ugur, 2017). A furonone derivative from *Streptomyces* sp. AT37 5-[(5E,7E,11E)-2,10-dihydroxy-9,11-dimethyl-5,7,11-tridecatrien-1-yl]-2-hydroxy-2-(1-hydro-xyethyl)-4-methyl-3(2H)-furanone or antibiotic AT37-1 **(19)** exhibited minimum biofilm inhibition concentration ($MBIC_{50}$) of 10–15 μg/mL against methicillin ensitive *Staphylococcus aureus* (MSSA) ATCC 29523 and methicillin resistant *Staphylococcus aureus* (MRSA) ATCC 43300 (Driche et al., 2017). Streptorubin

B from *Streptomyces* sp. strain MC11024 displayed IC_{50} value of 0.56 μM against the biofilms of m MRSA N315. Although streptorubin B inhibited the growth of MRSA N315 at 2–4 μg/mL, the compound also exhibited anti-biofilm activity (Bauermeister et al., 2019).

At a dosage of 2.5% (v/v), the metabolites from marine *Streptomyces albus* A66 repressed the formation of *V. harveyi* biofilms by 99.3% and dispersed the mature biofilms of *V. harveyi* by 75.6%. The A66 metabolite was suggested to affect the development of *Vibrio* biofilms by attenuating the initiation and maturation stage (You et al., 2007; **Table 2**). Methanolic extract from the spent medium of *Streptomyces akiyoshiensis* CAA-3 inhibited staphylococcal biofilms at a concentration of 0.1 mg/ml. The extract also possessed the ability to inhibit the colonization of *Staphylococcus aureus* in the intestine of *Caenorhabditis elegans* up to 70% (**Table 2**; Bakkiyaraj and Pandian, 2010). Culture extracts of *Streptomyces* sp. BFI 250 at 0.01% (v/v) inhibited the biofilm formation and detachment of preformed biofilms of *Staphylococcus aureus* ATCC 25923 by ≥ 80% for more than 17 h. The ability to subdue both the formation and detachment of biofilms by *Streptomyces* sp. BFI 250 was due to the extracellular protease in the extract that was equivalent to approximately 0.1 μg of proteinase K/ml (Park et al., 2012). Extracts from *Streptomyces* sp. NIO 10068 spent medium reduced motility, formation of biofilm, production of pyocyanin, rhamnolipid and Las A protease, swimming and twitching by 90, 67, 45, 45, 43, 20, and 15%, respectively in *P. aeruginosa* ATCC 27853. Among the several active compounds including cinnamic acid, linear dipeptides N-amido-a-proline, pro-line–glycine and aromatic acids characterized from the extract of strain NIO 10068, only linear dipeptide and cinnamic acid expressed quorum sensing inhibitory (QSI) activity (Naik et al., 2013). DNA microarray analysis revealed that the spent medium of the strain BFI 230 repressed 42 genes and induced 78 genes in *P. aeruginosa* cells embedded within the biofilm. The 78 genes that were induced were essential for utilization of iron, biosynthesis of phenazine (phz operon), pyoverdine (pvd operon) and pyochelin (pch). At 1% (v/v) concentration, spent medium of BFI 230 repressed 90% of the *P. aeruginosa* biofilm. However, at this concentration other virulence factors including swarming and the production of pyoverdine and pyocyanin increased. As the transcriptomic analysis showed that the BFI 230 spent medium induced the genes for iron uptake, external addition of ferrous compounds ($FeCl_3$ and $FeSO_4$) in the presence of the BFI 230 spent medium resulted in the restoration *P. aeruginosa* biofilms. The study revealed that proteins or peptides native to the *Streptomyces* sp. BFI 230 spent medium suppressed the formation of *P. aeruginosa* biofilms either indirectly interfering with the bacterium's iron utilization or through linking iron with quorum sensing system (Kim et al., 2012).

Characterization of quorum quenching activity in 63 *Streptomyces* soil isolates showed that 3 strains St11, St61 and St62 degraded synthetic hexanoyl homoserine lactone (HHL). The acylase was stable in the presence of heavy metals and chelating agents, and maintained a maximum catalytic activity between 20 to 50°C up to pH 8 (Sakr et al., 2015). The extracts of *Streptomyces akiyoshinensis* (A3) inhibited *Streptococcus pyogenes* biofilms at a concentration of 10 to 50 μg/ml. The extract from *Streptomyces akiyoshinensis* affected the cell hydrophobicity, and the initial colonization of *Streptococcus pyogenes* (Nithyanand et al., 2010). About 200 μg/ml of diethyl ether extracts of *Streptomycetes* species A745 culture subdued the formation of *V. cholerae* biofilm by 60% (Augustine et al., 2012). Crude fatty acid extract from three *Streptomyces* isolates (*Streptomyces sps* isolates S8, S9, and S15) inhibited formation of *Streptococcus pyogenes* ATCC 19615 biofilm at a concentration of 10 μg/ml. Remarkably, the lipids found in the crude extract of these *Streptomyces* species influenced the secretion of extracellular proteins especially streptolysin S (Rajalakshmi et al., 2014). The extract of *Streptomyces* sp. SBT343 displayed BIC_{50} value of 62.5 μg/ml toward *Staphylococcus epidermidis* RP62A biofilm. At 125 μg/ml, the extract subdued the formation of biofilms of MRSA, MSSA and *Staphylococcus epidermidis*. Physiochemical characterization of the extract revealed that the bioactive molecule(s) mediating the inhibitory activity toward staphylococcal biofilm were thermostable and non-proteinaceous in nature (Balasubramanian et al., 2017). Hexane partition of *Streptomyces* sp. CCB-PSK207 spent medium gradually increased the survival of *P. aeruginosa* PA14 infected *C. elegans* from 45.33 to 72.71% at the concentration ranging from 50 to 400 μg/ml. Phenotypical analysis on the expression of virulence factors of PA14 showed that the metabolites (fatty acid methyl esters) in the extract were indifferent on the formation of biofilm or on the production of protease and pyocyanin. However, restoration of the green fluorescent protein (GFP) expression in transgenic lys-7:GFP *C. elegans* strain SAL105 revealed that the hexane partition of CCB-PSK207 did not repress the killing of *C. elegans* by subduing the virulence of PA14, but rather through boosting the immunity in the nematode by inducing the expression of lysozyme 7 (*lys*-7) (Fatin et al., 2017). The minimum biofilm inhibitory concentration of metabolites from *Streptomyces albogriseolus* GIS39Ama were 312 ppm against *Escherichia coli* MTCC 687, 625ppm against *Klebsiella pneumoniae* MTCC 3384 and *Vibrio cholerae* MTCC 3906, and 1250 ppm against *Pseudomonas aeruginosa* MTCC 2453. *Streptomyces albogriseolus* GIS39Ama reduced the production of violacein by *C. violaceum* MTCC 2656 by 87.67% (Lokegaonkar and Nabar, 2017). The extract from *Streptomyces* sp. MC025 isolated from an unidentified red alga suppressed the formation of *Staphylococcus aureus* biofilm by ≥ 90% with minimal bactericidal effect on planktonic cells. Bioactivity-guided fractionation of the crude extract *Streptomyces* sp. MC025 led to the identification of 6 bipyridines molecules, of which, collismycins C **(20)** and pyrisulfoxin A **(21)** showed inhibitory activity against MSSA ATCC 6538 at 50 μg/mL. Further studies revealed that Collismycin C was the major component initiating anti-biofilm activity by chelating Fe ions, and that the location of the OH group on bipyridines were vital for anti-biofilm activity against *Staphylococcus aureus* (Lee et al., 2017).

Screening of 101 marine *Actinomycetes* led to the discovery of *Streptomyces* strains that could suppress biofilms of *Escherichia coli* (by 61 – 80%) and *Staphylococcus aureus* (by 60%) (Leetanasaksakul and Thamchaipenet, 2018). Extracts from the spent medium of *Streptomyces* sp. TRM 41337 suppressed the

formation of *Staphylococcus epidermidis* (ATCC 35984 and 5-121-2) biofilms by ≥ 90% in a dose-dependent manner for over 24 h. While the culture extracts of *Streptomyces* sp. TRM 41337 effectively degraded DNA of *S. epidermidis*, the protein metabolite from the extract reduced the cell surface hydrophobicity and degraded EPS of *Staphylococcus epidermidis*. Thus, it was suggested that through these properties, the crude protein was able to prevent the formation of *S. epidermidis* biofilm (Xie et al., 2018).

Melanin pigment (soluble and insoluble forms) purified from *Streptomyces* sp. ZL-24 suppressed the formation of *P. aeruginosa* ATCC 9027 and *Staphylococcus aureus* ATCC 6538 biofilms up to 67.5 and 74.6% and 79.2 and 71.7%, respectively (Wang et al., 2019). Similarly, the extract from *Streptomyces griseoincarnatus*

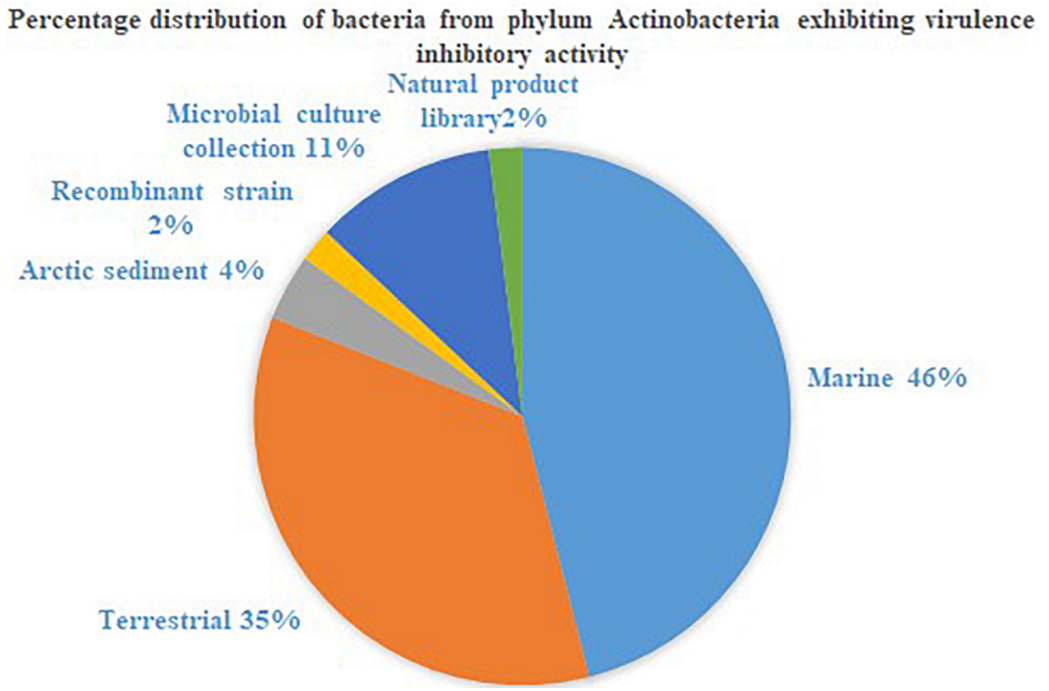

FIGURE 1 | Percentage distribution of bacteria from phylum Actinobacteria exhibiting virulence inhibitory activity.

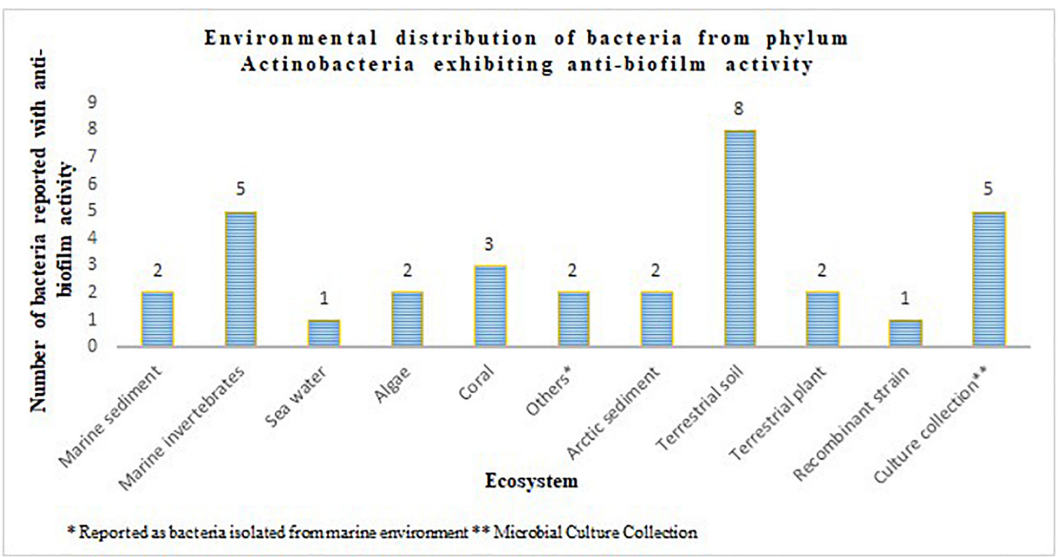

FIGURE 2 | Environmental distribution of bacteria from phylum Actinobacteria exhibiting anti-biofilm activity.

HK12 suppressed *P. aeruginosa* and *Staphylococcus aureus* biofilms by 82.657 and 78.973%, respectively. GC-MS analysis of the extract showed the presence of five active compounds including arachidic acid, erucic acid, 13Z-octadecenal **(22)**, 9Z-octadecenal and tetracosanoic acid. *In silico* docking of all the five active compounds with LasI of *P. aeruginosa* showed that the 13Z-octadecenal interacted with LasI and formed pi-alkyl bond with the conserved residues Trp33 and Phe2 in LasI. It was suggested that the downregulation of QS-regulated virulence gene was due to the small molecule mediated inhibition of LasI binding to its native ligand LasR. This study also suggested that the presence of fatty acyl molecule in HK12 spent medium could have exerted both synergistic or independent anti-biofilm activity (Kamarudheen and Rao, 2019). Four new α- pyridones (compound 16 **(23)**,17 **(24)**,19 **(25)** & 20 **(26)**) generated through chemical transformation of the compounds derived from culture extract of *Streptomyces* sp., inhibited the expression of *P. aeruginosa* QSIS-lasI biosensors at a concentration of 6.35 μg/well (Du et al., 2018).

Dimorphic fungi *Candida albicans* can potentiate clinically significant systemic infections due to its complex and multifactorial virulence factors including isocitrate lyase (ICL), a glyoxylate cycle enzyme (Lorenz and Fink, 2001; Ramírez and Lorenz, 2007; Mayer et al., 2013). Bahamaolide A **(27)** purified from *Streptomyces* sp. *CNQ343* strongly inhibited the mRNA expression of ICL with an IC_{50} value of 11.82 μM. Due to the absence of ICL in mammals, Bahamaolide A has been suggested as a promising anti-virulent agent for *C. albicans* (Lee et al., 2014).

Pre-exposure of *C. albicans* to the *Streptomyces toxytricini* Fz94 culture extract at a concentration of 5 g/L prevented the formation of biofilm up to 92%. At 7 g/L, the extract destroyed up to 82% of biofilms after 120 min (Sheir et al., 2017). Partially purified fractions of *Streptomyces chrestomyceticus* strain ADP4 strongly inhibited the secretory aspartic proteases (Saps) in *C. albicans* which has been shown to be vital for the formation of hyphae, phenotypic switching, adhesion, digestion of host cell membrane, and also for the evasion of host immune system by the yeast (Srivastava et al., 2017). A metabolite from *Streptomyces* sp. ADR1 displayed MBIC $\leq$ 15.625 μg/ml and $<$ 500 μg/ml against preformed biofilm of pathogenic *Staphylococcus aureus* (Singh and Dubey, 2018). Khatmiamycin **(28)** and aloesaponarin II **(29)** derived from *Streptomyces* sp. ANK313 inhibited the motility of zoospores of *Plasmopara viticola* with a MIC value of 10 μg/ml and 25 10 μg/ml, respectively (Abdalla et al., 2011).

OTHERS

Partially purified pigment from *Actinomycetes* C5-5Y inhibited the cell surface hydrophobicity, proteolytic and lipase activity of *Streptococcus mutans* and *Staphylococcus aureus* (**Table 2**). When treated with the pigment, cell surface hydrophobicity of these nosocomial pathogens reduced by 23 and 24% compared to the 91 and 89% hydrophobicity observed in the control cells. Furthermore, at 10 μg/ml concentration, the pigment also significantly reduced the formation of *Streptococcus mutans* and *Staphylococcus aureus* biofilms, leading to the suggestion that *Actinomycetes* C5-5Y derived pigment were capable of quenching quorum sensing signals (Soundari et al., 2014). Transcriptomic

TABLE 4 | List of compounds characterized from Actinobacteria and their specific virulence inhibitory function.

Target Organisms	Virulence determinants evaluated	Actinobacterial compound exhibiting anti-virulence property
P. aeruginosa (ATCC 27853, ATCC 10145, ATCC 9027, *PA01*)	Motility (Swimming and Twitching)	Cinnamic acid linear dipeptide (Pro-Gly and N-amido-α-proline)
	Biofilm	B4-EPS1 Actinomycin D Cinnamic acid linear dipeptide (Pro-Gly and N-amido-α-proline) Melanin 9Z-Octadecenal Arachidic acid, Erucic acid 13Z-Octadecenal and tetracosanoic acid, Silver nano particles
	Pyocyanin	Cinnamic acid linear dipeptide (Pro-Gly and N-amido-α-proline) 1H-pyrrole-2-carboxylic acid Docosanoic acid
	Rhamnolipid	Cinnamic acid linear dipeptide (Pro-Gly and N-amido-α-proline)
	Production of elastase	1H-pyrrole-2-carboxylic acid Docosanoic acid
	Production of protease	1H-pyrrole-2-carboxylic acid Docosanoic acid
	Expression of las genes	1H-pyrrole-2-carboxylic acid 4-Hydroxy-3-methyl-6-propylpyridin-2(1H)-one 3-Ethyl-4-hydroxy-6-isopropylpyridin-2(1H)-one 4-Hydroxy-6-isobutyl-3-methylpyridin-2(1H)-one (S)-6-(sec-Butyl)-4-hydroxy-3-methylpyridin-2(1H)-one Nocapyrone H Nocapyrone I Nocapyrone M
	Expression of rhl/pqs cascade	1H-pyrrole-2-carboxylic acid
Staphylococcus aureus (ATCC 25923, ATCC 6538, ATCC 33591, ATCC 95005, N315)	Biofilm	Protease Actinomycin D Alnumycin D Granaticin B Streptorubin B Melanin 5-[(5E,7E,11E)-2,10-dihydroxy-9,11-dimethyl-5,7,11-tridecatrien-1-yl]-2-hydroxy-2-(1-hydro-xyethyl)-4-methyl-3(2H)-furanone Collismycin C Silver nano particles
	Hemolysis	Actinomycin D WS9326A WS9326B
	Slime	Actinomycin D
	Cell hydrophobicity	Actinomycin D
Staphylococcus aureus agr reporter strain 8325-4	Agr-dependent gene expression	Arthroamide Turnagainolide A

analysis on the effect of cyclodepsipeptides (WS9326A and WS92326B) from *Actinomycetes* strain DSW812 on the VirSR system of *C. perfringens,* revealed that the WS9326A suppressed the expression of pfoA encoding perfringolysin O in dose-dependent manner at sub-micromolar IC_{50} concentration. As WS9326B lacked this activity, the absence of double bonds in the dehydrotyrosine of WS92326B was concluded to be crucial for the cyclodepsipeptide binding to VirS system. However, the study also showed that WS9326B effectively decreased the cytotoxicity of *Staphylococcus aureus* on human corneal epithelial cells significantly. WS9326A and WS9326B also repressed hemolysin production by *S. aureus* 8325–4 (type-I AIP), *S. aureus* K12 (type-II AIP) and *S. aureus* K9 (type-IV AIP), indicating the specificity of *Actinomycetes* cyclodepsipeptides toward the different auto inducing peptides (AIP). Cochinmicins II and III from *Actinomycetes* strains GMKU369, have also been suggested to function as an antagonist like cyclodepsipeptides due to their similarities in structure, molecular size, and hydrophobicity (Desouky et al., 2015).

OPINION AND FUTURE PERSPECTIVE

The phylum Actinobacteria encompasses a group of organisms well known for its prodigious production of secondary metabolites with complex scaffolding and chemical entities. This actinic uniqueness has been beneficial in terms of its pharmaceutical adaptability, as clinically significant antimicrobials, anti-tumor agents, immunosuppressants, anti-proliferative agents, anti-parasitic agents and herbicides than any other bacterial origin natural product. In this regard, identification of secondary metabolites from the phylum Actinobacteria with potential to attenuate virulence in other microorganisms, and the broad-spectrum specificity toward different AHLs, could be advantages for engineering the much anticipated anti-virulence drugs. Actinobacteria strains that suppressed microbial virulence have been reported majorly from marine and terrestrial environment (**Figures 1**, **2**). Over the past decade, several marine natural products (MNP) derived from various phyla of bacteria, alga, seaweeds and invertebrates exhibiting anti-virulence property including anti-biofilm property have been reported. This could be the reflection of the recent trend in exploring the metabolite profile of microbiome from uninhabited areas including arctic regions, to prevent the re-isolation of known active metabolites. While the active metabolites from the Actinobacteria have been demonstrated with virulence suppressing potential against a wide range of bacteria and yeast cells, the assays employed to evaluate the virulence inhibiting potential are very limited (**Table 4**). The Actinobacteria derived products were mainly evaluated for their potential to inhibit biofilm formation or the production of enzymes, pigments, cell hydrophobicity, and motility. Yet, many crucial virulence factors including iron uptake, immune cell evasion and suppression of host immune system should have been considered as promotion of pathogenesis by bacteria like *Staphylococcus aureus* is site-specific. Similarly, evaluation of the majority of actinobacterial origin anti-virulence agents has been against very limited bacterial reference strains and reporter strains particularly *Staphylococcus aureus* and *Pseudomonas aeruginosa*. Although, undeniably, these organisms are highly virulent with or without AMR, researches with a wide range of organisms especially variant cell populations such as persister cells that have been demonstrated to be the etiological agents of chronic infections would help to establish the potency of metabolites as anti-virulences. To conclude, in the evolutionary struggle for co-existence between microorganism and humans, the single-sided supremacy observed during the prodromal antibiotic era convincingly advocates requirement of multifactor approach to target pathogenesis of microorganism in the host body.

AUTHOR CONTRIBUTIONS

Both authors contributed equally to the preparation and completion of the manuscript.

FUNDING

The authors would like to thank the support of DST-SERB (EMR/2016/002296) and SASTRA Deemed to be University, Thanjavur, India.

REFERENCES

Abdalla, M. A., Win, H. Y., Islam, M. T., von Tiedemann, A., Schüffler, A., and Laatsch, H. (2011). Khatmiamycin, a motility inhibitor and zoosporicide against the grapevine downy mildew pathogen *Plasmopara viticola* from *Streptomyces* sp. ANK313. *J. Antibiot.* 64, 655–659. doi: 10.1038/ja.2011.68

Afriat, L., Roodveldt, C., Manco, G., and Tawfik, D. S. (2006). The latent promiscuity of newly identified microbial lactonases is linked to a recently diverged phosphotriesterase. *Biochemistry* 45, 13677–13686. doi: 10.1021/bi061268r

Augustine, N., Wilson, P. A., Kerkar, S., and Thomas, S. (2012). Arctic actinomycetes as potential inhibitors of *Vibrio cholerae* biofilm. *Curr. Microbiol.* 64, 338–342. doi: 10.1007/s00284-011-0073-4

Bakkiyaraj, D., and Pandian, S. K. (2010). In vitro and in vivo antibiofilm activity of a coral associated actinomycete against drug resistant *Staphylococcus aureus* biofilms. *Biofouling* 26, 711–717. doi: 10.1080/08927014.2010.511200

Balasubramanian, S., Othman, E. M., Kampik, D., Stopper, H., Hentschel, U., Ziebuhr, W., et al. (2017). Marine sponge-derived *Streptomyces* sp. *SBT*343 extract inhibits staphylococcal biofilm formation. *Front. Microbiol.* 8:236. doi: 10.3389/fmicb.2017.00236

Barbey, C., Chane, A., Burini, J.-F., Maillot, O., Merieau, A., Gallique, M., et al. (2018). A rhodococcal transcriptional regulatory mechanism detects the common lactone ring of AHL quorum-sensing signals and triggers the quorum-quenching response. *Front. Microbiol.* 9:2800. doi: 10.3389/fmicb.2018.02800

Barbey, C., Crépin, A., Bergeau, D., Ouchiha, A., Mijouin, L., Orange, N., et al. (2013). *In planta* biocontrol of *Pectobacterium atrospeticum* by *Rhodococcus erythropolis* involves silencing of pathogen communication by the Rhodococcal gamma-lactone catabolic pathway. *PLoS One* 8:e66642. doi: 10.1371/journal.pone.0066642

Barbey, C., Crépin, A., Cirou, A., Budin-Verneuil, A., Orange, N., Feuilloley, M., et al. (2012). Catabolic pathway of gamma-caprolactone in the biocontrol agent *Rhodococcus erythropolis*. *J. Proteome Res.* 11, 206–216. doi: 10.1021/pr200936q

Bauermeister, A., Pereira, F., Grilo, I. R., Godinho, C. C., Paulino, M., Almeida, V., et al. (2019). Intra-clade metabolomic profiling of MAR4 *Streptomyces* from the Macaronesia Atlantic region reveals a source of anti-biofilm metabolites. *Environ. Microbiol.* 21, 1099–1112. doi: 10.1111/1462-2920.14529

Baygar, T., and Ugur, A. (2017). In vitro evaluation of antimicrobial and antibiofilm potentials of silver nanoparticles biosynthesised by *Streptomyces griseorubens*. *IET Nanobiotechnol.* 11, 677–681. doi: 10.1049/iet-nbt.2016.0199

Brown, E. D., and Wright, G. D. (2016). Antibacterial drug discovery in the resistance era. *Nature* 529, 336–343. doi: 10.1038/nature17042

Centers for Disease Control, and Prevention, (2017). *Antibiotic Use in the United States, 2017: Progress and Opportunities*. Atlanta, GA: Centers for Disease Control, and Prevention. Available at: https://www.cdc.gov/antibiotic-use/stewardship-report/pdf/stewardship-report.pdf (accessed March 02, 2019).

Chatterjee, A., Cui, Y., Liu, Y., Dumenyo, C. K., and Chatterjee, A. K. (1995). Inactivation of rsmA leads to overproduction of extracellular pectinases, cellulases, and proteases in *Erwinia carotovora* subsp. *carotovora* in the absence of the starvation/cell density-sensing signal, N - (3-Oxohexanoyl) - L - homoserine lactone. *Appl. Environ. Microbiol.* 61, 1959–1967.

Chow, J. Y., Wu, L., and Yew, W. S. (2009). Directed evolution of a quorum-quenching lactonase from *Mycobacterium avium* subsp. *paratuberculosis* K-10 in the amidohydrolase superfamily. *Biochemistry* 48, 4344–4353. doi: 10.1021/bi9004045

Cirou, A., Diallo, S., Kurt, C., Latour, X., and Faure, D. (2007). Growth promotion of quorum-quenching bacteria in the rhizosphere of *Solanum tuberosum*. *Environ. Microbiol.* 9, 1511–1522. doi: 10.1111/j.1462-2920.2007.01270.x

Cirou, A., Mondy, S., An, S., Charrier, A., Sarrazin, A., Thoison, O., et al. (2012). Efficient biostimulation of native and introduced quorum-quenching *Rhodococcus erythropolis* populations is revealed by a combination of analytical chemistry, microbiology, and pyrosequencing. *Appl. Environ. Microbiol.* 78, 481–492. doi: 10.1128/AEM.06159-11

Cirou, A., Raffoux, A., Diallo, S., Latour, X., Dessaux, Y., and Faure, D. (2011). Gamma-caprolactone stimulates growth of quorum-quenching *Rhodococcus* populations in a large-scale hydroponic system for culturing *Solanum tuberosum*. *Res. Microbiol.* 162, 945–950. doi: 10.1016/j.resmic.2011.01.010

Clatworthy, A. E., Pierson, E., and Hung, D. T. (2007). Targeting virulence: a new paradigm for antimicrobial therapy. *Nat. Chem. Biol.* 3, 541–548. doi: 10.1038/nchembio.2007.24

Cuthbertson, L., and Nodwell, J. R. (2013). The TetR family of regulators. *Microbiol. Mol. Biol. Rev.* 77, 440–475. doi: 10.1128/MMBR.00018-13

Das, T., Nair, R. R., Green, R., Padhee, S., Howell, M., Banerjee, J., et al. (2017). Actinomycin D down-regulates SOX2 expression and induces death in breast cancer stem cells. *Anticancer Res.* 37, 1655–1663. doi: 10.21873/anticanres.11496

de Carvalho, C. C. R., and da Fonseca, M. M. R. (2005). The remarkable *Rhodococcus erythropolis*. *Appl. Microbiol. Biotechnol.* 67, 715–726. doi: 10.1007/s00253-005-1932-3

Desouky, S. E., Shojima, A., Singh, R. P., Matsufuji, T., Igarashi, Y., Suzuki, T., et al. (2015). Cyclodepsipeptides produced by actinomycetes inhibit cyclic-peptide-mediated quorum sensing in Gram-positive bacteria. *FEMS Microbiol. Lett.* 362, 1–9. doi: 10.1093/femsle/fnv109

Dong, Y.-H., Gusti, A. R., Zhang, Q., Xu, J.-L., and Zhang, L.-H. (2002). Identification of quorum-quenching *N*-acyl homoserine lactonases from *Bacillus* Species. *Appl. Environ. Microbiol.* 68, 1754–1759. doi: 10.1128/AEM.68.4.1754-1759.2002

Dong, Y. H., Wang, L. H., Xu, J. L., Zhang, H. B., Zhang, X. F., and Zhang, L. H. (2001). Quenching quorum-sensing-dependent bacterial infection by an N-acyl homoserine lactonase. *Nature* 411, 813–817. doi: 10.1038/35081101

Driche, E. H., Sabaou, N., Bijani, C., Zitouni, A., Pont, F., Mathieu, F., et al. (2017). *Streptomyces* sp. *AT37* isolated from a Saharan soil produces a furanone derivative active against multidrug-resistant *Staphylococcus aureus*. *World J. Microbiol. Biotechnol.* 33:105. doi: 10.1007/s11274-017-2265-y

Du, Y., Sun, J., Gong, Q., Wang, Y., Fu, P., and Zhu, W. (2018). New α-Pyridones with quorum-sensing inhibitory activity from diversity-enhanced extracts of a *Streptomyces* sp. derived from marine algae. *J. Agric. Food Chem.* 66, 1807–1812. doi: 10.1021/acs.jafc.7b05330

Fatin, S. N., Boon-Khai, T., Shu-Chien, A. C., Khairuddean, M., and Al-Ashraf Abdullah, A. (2017). A marine actinomycete rescues *Caenorhabditis elegans* from *Pseudomonas aeruginosa* infection through restitution of Lysozyme 7. *Front. Microbiol.* 8:2267. doi: 10.3389/fmicb.2017.02267

Fetzner, S. (2015). Quorum quenching enzymes. *J. Biotechnol.* 201, 2–14. doi: 10.1016/j.jbiotec.2014.09.001

Fu, P., Liu, P., Gong, Q., Wang, Y., Wang, P., and Zhu, W. (2013). α -Pyrones from the marine-derived actinomycete *Nocardiopsis dassapnvillei* subsp. *dassonvillei* XG-8-1. *RSC Adv.* 3, 20726–20731. doi: 10.1039/c3ra43656j

Fukumoto, A., Murakami, C., Anzai, Y., and Kato, F. (2016). Maniwamycins: new quorum-sensing inhibitors against *Chromobacterium violaceum* CV026 were isolated from *Streptomyces* sp. TOHO-M025. *J. Antibiot. (Tokyo)* 69, 395–399. doi: 10.1038/ja.2015.126

Gelband, H., Miller-Petrie, M., Pant, S., Gandra, S., Levinson, J., Barter, D., et al. (2015). *The State of the World's Antibiotics*. Washington DC: The Center for Disease Dynamics, Economics & Policy. Available at: https://cddep.org/wp-content/uploads/2017/06/swa_edits_9.16.pdf (accessed March 02, 2019).

Gonzalez, J. E., and Keshavan, N. D. (2006). Messing with bacterial quorum sensing. *Microbiol. Mol. Biol. Rev.* 70, 859–875. doi: 10.1128/MMBR.00002-6

Gopikrishnan, V., Radhakrishnan, M., Shanmugasundaram, T., Pazhanimurugan, R., and Balagurunathan, R. (2016). Antibiofouling potential of quercetin compound from marine-derived actinobacterium, *Streptomyces fradiae* PE7 and its characterization. *Environ. Sci. Pollut. Res.* 23, 13832–13842. doi: 10.1007/s11356-016-6532-5

Grandclément, C., Tannières, M., Moréra, S., Dessaux, Y., and Faure, D. (2016). Quorum quenching: role in nature and applied developments. *FEMS Microbiol. Rev.* 40, 86–116. doi: 10.1093/femsre/fuv038

Grecz, N., Wagenaar, R. O., and Dack, G. M. (1959). Inhibition of *Clostridium botulinum* by culture filtrates of *Breibacterium linens*. *J. Bacteriol.* 78, 506–510.

Greenberg, E. P. (2003). Bacterial communication and group behavior. *J. Clin. Invest.* 112, 1288–1290. doi: 10.1172/JCI20099

Hassan, R., Shaaban, M. I., Abdel Bar, F. M., El-Mahdy, A. M., and Shokralla, S. (2016). Quorum sensing inhibiting activity of *Streptomyces coelicoflavus* isolated from soil. *Front. Microbiol.* 7:659. doi: 10.3389/fmicb.2016.00659

Hawwa, R., Aikens, J., Turner, R. J., Santarsiero, B. D., and Mesecar, A. D. (2009). Structural basis for thermostability revealed through the identification and characterization of a highly thermostable phosphotriesterase-like lactonase from *Geobacillus stearothermophilus*. *Arch. Biochem. Biophys.* 488, 109–120. doi: 10.1016/j.abb.2009.06.005

Hill, C. (2012). Virulence or niche factors: what ' s in a name? *J. Bacteriol.* 194, 5725–5727. doi: 10.1128/JB.00980-12

Holmquist, M. (2000). Alpha/Beta-hydrolase mechanisms fold enzymes: structures, functions and mechanisms. *Curr. Protein Pept. Sci.* 1, 209–235. doi: 10.2174/1389203003381405

Huang, J. J., Han, J.-I., Zhang, L.-H., and Leadbetter, J. R. (2003). Utilization of acyl-homoserine lactone quorum signals for growth by a soil pseudomonad and *Pseudomonas aeruginosa* PAO1. *Appl. Environ. Microbiol.* 69, 5941–5949. doi: 10.1128/aem.69.10.5941-5949.2003

Igarashi, Y., Yamamoto, K., Fukuda, T., Shojima, A., Nakayama, J., Carro, L., et al. (2015). Arthroamide, a cyclic depsipeptide with quorum sensing inhibitory activity from *Arthrobacter* sp. *J. Nat. Prod.* 78, 2827–2831. doi: 10.1021/acs.jnatprod.5b00540

Iwatsuki, M., Uchida, R., Yoshijima, H., Ui, H., Shiomi, K., Matsumoto, A., et al. (2008). Guadinomines, type III secretion system inhibitors, produced by *Streptomyces* sp. *K*01-0509. I. Taxonomy, fermentation, isolation and biological properties. *J. Antibiot. (Tokyo)* 61, 222–229. doi: 10.1038/ja.2008.32

Jiang, P., Li, J., Han, F., Duan, G., Lu, X., Gu, Y., et al. (2011). Antibiofilm activity of an exopolysaccharide from marine bacterium *Vibrio* sp. *QY*101. *PLoS One* 6:e18514. doi: 10.1371/journal.pone.0018514

Jiao, Y. L., Wang, S. J., Lv, M. S., Jiao, B. H., Li, W. J., Fang, Y. W., et al. (2014). Characterization of a marine - derived dextranase and its application to the prevention of dental caries. *J. Ind. Microbiol. Biotechnol.* 41, 17–26. doi: 10.1007/s10295-013-1369-0

Kadowaki, T., Kitano, S., Baba, A., Takii, R., Hashimoto, M., Katunuma, N., et al. (2003). Isolation and characterization of a novel and potent inhibitor of Arg-gingipain from *Streptomyces* sp. strain FA-70. *Biol. Chem.* 384, 911–920.

Kadowaki, T., Nakayama, K., Yoshimura, F., Okamoto, K., Abe, N., and Yamamoto, K. (1998). Arg-gingipain acts as a major processing enzyme for various cell surface proteins in *Porphyromonas gingivalis*. *J. Biol. Chem.* 273, 29072–29076. doi: 10.1074/jbc.273.44.29072

Kamarudheen, N., and Rao, K. V. B. (2019). Fatty acyl compounds from marine *Streptomyces griseoincarnatus* strain HK12 against two major bio-film forming nosocomial pathogens; an in vitro and in silico approach. *Microb. Pathog.* 127, 121–130. doi: 10.1016/j.micpath.2018.11.050

Kang, J. E., Han, J. W., Jeon, B. J., and Kim, B. S. (2016). Efficacies of quorum sensing inhibitors, piericidin A and glucopiericidin A, produced by *Streptomyces xanthocidicus* KPP01532 for the control of potato soft rot caused by *Erwinia carotovora* subsp. *atroseptica*. *Microbiol. Res.* 184, 32–41. doi: 10.1016/j.micres.2015.12.005

Kanmani, P., Satish, R., Yuvaraj, N., Paari, K. A., Pattukumar, V., and Arul, V. (2011). Production and purification of a novel exopolysaccharide from lactic acid bacterium *Streptococcus phocae* PI80 and its functional characteristics activity in vitro. *Bioresour. Technol.* 102, 4827–4833. doi: 10.1016/j.biortech.2010.12.118

Kaufmann, G. F., Park, J., and Janda, K. D. (2008). Bacterial quorum sensing: a new target for anti-infective immunotherapy. *Expert Opin. Biol. Ther.* 8, 719–724. doi: 10.1517/14712598.8.6.719

Kim, S. R., Oh, H. S., Jo, S. J., Yeon, K. M., Lee, C. H., Lim, D. J., et al. (2013). Biofouling control with bead-entrapped quorum quenching bacteria in membrane bioreactors: physical and biological effects. *Environ. Sci. Technol.* 47, 836–842. doi: 10.1021/es303995s

Kim, Y., Oh, S., and Kim, S. H. (2009). Released exopolysaccharide (r-EPS) produced from probiotic bacteria reduce biofilm formation of enterohemorrhagic *Escherichia coli* O157:H7. *Biochem. Biophys. Res. Commun.* 379, 324–329. doi: 10.1016/j.bbrc.2008.12.053

Kim, Y. G., Lee, J. H., Kim, C. J., Lee, J. C., Ju, Y. J., Cho, M. H., et al. (2012). Antibiofilm activity of *Streptomyces* sp. *BFI* 230 and *Kribbella* sp. BFI 1562 against *Pseudomonas aeruginosa*. *Appl. Microbiol. Biotechnol.* 96, 1607–1617. doi: 10.1007/s00253-012-4225-7

Kiran, G. S., Lipton, A. N., Priyadharshini, S., Anitha, K., Suárez, L. E., Arasu, M. V., et al. (2014). Antiadhesive activity of poly-hydroxy butyrate biopolymer from a marine *Brevibacterium casei* MS104 against shrimp pathogenic vibrios. *Microb. Cell Fact.* 13:114. doi: 10.1186/s12934-014-0114-3

Kiran, G. S., Priyadharshini, S., Dobson, A. D. W., Gnanamani, E., and Selvin, J. (2016). Degradation intermediates of polyhydroxy butyrate inhibits phenotypic expression of virulence factors and biofilm formation in luminescent Vibrio sp. *PUGSK*8. *NPJ Biofilms Microbiomes* 2:16002. doi: 10.1038/npjbiofilms.2016.2

Kiran, G. S., Sabarathnam, B., and Selvin, J. (2010). Biofilm disruption potential of a glycolipid biosurfactant from marine *Brevibacterium casei*. *FEMS Immunol. Med. Microbiol.* 59, 432–438. doi: 10.1111/j.1574-695X.2010.00698.x

Krasowska, A., and Sigler, K. (2014). How microorganisms use hydrophobicity and what does this mean for human needs? *Front. Cell Infect. Microbiol.* 4:112. doi: 10.3389/fcimb.2014.00112

Kwasiborski, A., Mondy, S., Chong, T. M., Barbey, C., Chan, K. G., Beury-Cirou, A., et al. (2015). Transcriptome of the quorum-sensing signal-degrading *Rhodococcus erythropolis* responds differentially to virulent and avirulent *Pectobacterium atrosepticum*. *Heredity* 114, 476–484. doi: 10.1038/hdy.2014.121

Lamture, G., Crooks, P. A., and Borrelli, M. J. (2018). Actinomycin-D and dimethylamino-parthenolide synergism in treating human pancreatic cancer cells. *Drug Dev. Res.* 79, 287–294. doi: 10.1002/ddr.21441

Latour, X., Barbey, C., Chane, A., Groboillot, A., and Burini, J.-F. (2013). *Rhodococcus erythropolis* and its γ-lactone catabolic pathway: an unusual biocontrol system that disrupts pathogen quorum sensing communication. *Agronomy* 3, 816–838. doi: 10.3390/agronomy3040816

Leadbetter, J. R., and Greenberg, E. P. (2000). Metabolism of acyl-homoserine lactone quorum-sensing signals by *Variovorax paradoxus*. *J. Bacteriol.* 182, 6921–6926. doi: 10.1128/jb.182.24.6921-6926.2000

Lee, J. H., Kim, E., Choi, H., and Lee, J. (2017). Collismycin C from the micronesian marine bacterium *Streptomyces* sp. *MC*025 inhibits *Staphylococcus aureus* biofilm formation. *Mar. Drugs* 15:E387. doi: 10.3390/md15120387

Lee, J. H., Kim, Y. G., Lee, K., Kim, C. J., Park, D. J., Ju, Y., et al. (2016). Streptomyces-derived actinomycin D inhibits biofilm formation by *Staphylococcus aureus* and its hemolytic activity. *Biofouling* 32, 45–56. doi: 10.1080/08927014.2015.1125888

Lee, S.-H., Moon, K., Kim, H., Shin, J., Oh, D.-C., and Oh, K.-B. (2014). Bahamaolide A from the marine-derived *Streptomyces* sp. *CNQ*343 inhibits isocitrate lyase in *Candida albicans*. *Bioorg. Med. Chem. Lett.* 24, 4291–4293. doi: 10.1016/j.bmcl.2014.07.021

Leetanasaksakul, K., and Thamchaipenet, A. (2018). Potential anti-biofilm producing marine actinomycetes isolated from sea sediments in Thailand. *Agricult. Nat. Resour.* 52, 228–233. doi: 10.1016/j.anres.2018.09.003

Li, Y., Li, Q., Hao, D., Jiang, D., Luo, Y., Liu, Y., et al. (2015). Production, purification, and antibiofilm activity of a novel exopolysaccharide from *Arthrobacter* sp. *B*4. *Prep. Biochem. Biotechnol.* 45, 192–204. doi: 10.1080/10826068.2014.907180

Lin, Y.-H., Xu, J.-L., Hu, J., Wang, L.-H., Ong, S. L., Leadbetter, J. R., et al. (2003). Acyl-homoserine lactone acylase from *Ralstonia* strain XJ12B represents a novel and potent class of quorum-quenching enzymes. *Mol. Microbiol.* 47, 849–860. doi: 10.1046/j.1365-2958.2003.03351.x

Lokegaonkar, S., and Nabar, B. (2017). In vitro antibiofilm, antiquroum sensing activity of gamma tolerant *Streptomyces* against gram negative pathogens. *Int. J. Pharmaceut. Sci. Clin. Res.* 9, 665–670.

Lorenz, M. C., and Fink, G. R. (2001). The glyoxylate cycle is required for fungal virulence. *Nature* 412, 83–86. doi: 10.1038/35083594

Marston, H. D., Dixon, D. M., Knisely, J. M., Palmore, T. N., and Fauci, A. S. (2016). Antimicrobial resistance. *JAMA*. 316, 1193–1204. doi: 10.1001/jama.2016.11764

Mayer, F. L., Wilson, D., and Hube, B. (2013). *Candida albicans* pathogenicity mechanisms. *Virulence* 4, 119–128. doi: 10.4161/viru.22913

Miao, L., Xu, J., Yao, Z., Jiang, Y., Zhou, H., Jiang, W., et al. (2017). The anti-quorum sensing activity and bioactive substance of a marine derived *Streptomyces*. *Biotechnol. Biotechnol. Equip.* 31, 1007–1015. doi: 10.1080/13102818.2017.1348253

Miller, M. B., and Bassler, B. L. (2001). Quorum sensing in bacteria. *Annu. Rev. Microbiol.* 55, 165–199. doi: 10.1146/annurev.micro.55.1.165

Morohoshi, T., Someya, N., and Ikeda, T. (2009). Novel N -acylhomoserine lactone-degrading bacteria isolated from the leaf surface of *Solanum tuberosum* and their quorum-quenching properties. *Biosci. Biotechnol. Biochem.* 73, 2124–2127. doi: 10.1271/bbb.90283

Naik, D. N., Wahidullah, S., and Meena, R. M. (2013). Attenuation of *Pseudomonas aeruginosa* virulence by marine invertebrate-derived *Streptomyces* sp. *Lett. Appl. Microbiol.* 56, 197–207. doi: 10.1111/lam.12034

Nithyanand, P., Thenmozhi, R., Rathna, J., and Pandian, S. K. (2010). Inhibition of streptococcus pyogenes biofilm formation by coral-associated actinomycetes. *Curr. Microbiol.* 60, 454–460. doi: 10.1007/s00284-009-9564-y

Oja, T., San Martin Galindo, P., Taguchi, T., Manner, S., Vuorela, P. M., Ichinose, K., et al. (2015). Effective antibiofilm polyketides against *Staphylococcus aureus* from the pyranonaphthoquinone biosynthetic pathways of *Streptomyces* species. *Antimicrob. Agents Chemother.* 59, 6046–6052. doi: 10.1128/AAC.00991-15

Ooka, K., Fukumoto, A., Yamanaka, T., Shimada, K., Ryo, I., Anzai, Y., et al. (2013). Piericidins, Novel quorum-sensing inhibitors against chromobacterium violaceum CV026, from *Streptomyces* sp. TOHO-Y209 and TOHO-O348. *Open J. Med. Chem.* 3, 93–99. doi: 10.4236/ojmc.2013.34012

Park, J. H., Lee, J. H., Kim, C. J., Lee, J. C., Cho, M. H., and Lee, J. (2012). Extracellular protease in Actinomycetes culture supernatants inhibits and detaches *Staphylococcus aureus* biofilm formation. *Biotechnol. Lett.* 34, 655–661. doi: 10.1007/s10529-011-0825-z

Park, S.-Y, Kang, H.-O., Jang, H.-S., Lee, J.-K., Koo, B.-T., and Yum, D.-Y. (2005). Identification of extracellular *N*-acylhomoserine lactone acylase from a *Streptomyces* sp. and its application to quorum quenching. *Appl. Environ. Microbiol.* 71, 2632–2641. doi: 10.1128/aem.71.5.2632-2641.2005

Park, S. Y., Hwang, B. J., Shin, M. H., Kim, J. A., Kim, H. K., and Lee, J. K. (2006). N-acylhomoserine lactonase-producing *Rhodococcus* spp. with different AHL-degrading activities. *FEMS Microbiol. Lett.* 261, 102–108. doi: 10.1111/j.1574-6968.2006.00336.x

Park, S. Y., Lee, S. J., Oh, T. K., Oh, J. W., Koo, B. T., Yum, D. Y., et al. (2003). AhlD, an N-acylhomoserine lactonase in *Arthrobacter* sp., and predicted homologues in other bacteria. *Microbiology* 149, 1541–1550. doi: 10.1099/mic.0.26269-0

Rajalakshmi, M., Srinivasan, P., Poffe, M. F., Suresh, R., and Priyadarisini, V. B. (2014). Crude fatty acid extracts of *Streptomyces* sps inhibits the biofilm forming *Streptococcus pyogenes* ATCC 19615. *J. Biochem. Technol.* 5, 679–684.

Rajivgandhi, G., Maruthupandy, M., Muneeswaran, T., Anand, M., and Manoharan, N. (2018). Antibiofilm activity of zinc oxide nanosheets (ZnO NSs) from *Nocardiopsis* sp. *GRG*1 (KT23540) against MDR strains of gram negative *Proteus mirabilis* and *Escherichia coli*. *Process Biochem.* 67, 8–18. doi: 10.1016/j.procbio.2018.01.015

Ramírez, M. A., and Lorenz, M. C. (2007). Mutations in alternative carbon utilization pathways in *Candida albicans* attenuate virulence and confer pleiotropic phenotypes. *Eukaryot. Cell* 6, 280–290. doi: 10.1128/EC.00372-06

Ramya, S., Shanmugasundaram, T., and Balagurunathan, R. (2015). Biomedical potential of actinobacterially synthesized selenium nanoparticles with special reference to anti-biofilm, anti-oxidant, wound healing, cytotoxic and anti-viral activities. *J. Trace Elem. Med. Biol.* 32, 30–39. doi: 10.1016/j.jtemb.2015.05.005

Raushel, F. M., and Holden, H. M. (2000). Phosphotriesterase: an enzyme in search for its natural substrate. *Adv. Enzymol. Relat. Areas Mol. Biol.* 74, 51–93. doi: 10.1002/9780470123201.ch2

Roodveldt, C., and Tawfik, D. S. (2005). Directed evolution of phosphotriesterase from *Pseudomonas* diminuta for heterologous expression in *Escherichia coli* results in stabilization of the metal-free state. *Protein Eng. Des. Sel.* 18, 51–58. doi: 10.1093/protein/gzi005

Sabu, R., Soumya, K. R., and Radhakrishnan, E. K. (2017). Endophytic *Nocardiopsis* sp. from Zingiber officinale with both antiphytopathogenic mechanisms and antibiofilm activity against clinical isolates. *3 Biotech.* 7:115. doi: 10.1007/s13205-017-0735-4

Sakr, M., Aboshanab, K., and Aboulwafa, M. (2015). Characterization of the quorum quenching activity of *Streptomyces minutiscleroticus*: a new ap proach for infection control. *Afr. J. Microbiol. Res.* 9, 492–502. doi: 10.5897/AJMR2014.7316

Schmidt, C., Schubert, N. A., Brabetz, S., Mack, N., Schwalm, B., Chan, J. A., et al. (2017). Preclinical drug screen reveals topotecan, actinomycin D, and volasertib as potential new therapeutic candidates for ETMR brain tumor patients. *Neuro Oncol.* 19, 1607–1617. doi: 10.1093/neuonc/nox093

Seibert, C. M., and Raushel, F. M. (2005). Structural and catalytic diversity within the amidohydrolase superfamily. *Biochemistry* 44, 6383–6391. doi: 10.1021/bi047326v

Sheir, D. H., Ma, H., and Hafez, M. (2017). Antibiofilm activity of *Streptomyces toxytricini* Fz94 against *Candida albicans* ATCC 10231. *Microb. BioSyst. J.* 2, 26–39. doi: 10.21608/mb.2017.5255

Singh, R., and Dubey, A. (2018). "Inhibition of *Staphylococcus aureus* and its biofilm by the metabolites of endophytic *Streptomyces* sp. ADR1," in *Proceedings of the Conference on MOL2NET* (Basel: MDPI sciforum), 4.

Soundari, A. P. G., Nagarajan, C., Mani, V. M., and Priyadarisini, V. B. (2014). Quorum quenching activity of pigments produced by actinomycetes. *IJSR* 358, 2252–2257.

Srivastava, V., Singla, R., and Dubey, A. (2017). "Inhibition of secretory aspartyl protease of *Candida albicans* by metabolites of *Streptomyces chrestomyceticus* strain ADP4," in *Proceedings of the Conference on MOL2NET* (Basel: MDPI sciforum), 3.

Suzuki, N., Ohtaguro, N., Yoshida, Y., Hirai, M., Matsuo, H., Yamada, Y., et al. (2015). A compound inhibits biofilm formation of *Staphylococcus aureus* from *Streptomyces*. *Biol. Pharm. Bull.* 38, 889–892. doi: 10.1248/bpb.b15-00053

Tzaridis, T., Milde, T., Pajtler, K. W., Bender, S., Jones, D. T. W., Müller, S., et al. (2016). Low-dose actinomycin-D treatment re-establishes the tumour suppressive function of P53 in RELA-positive ependymoma. *Oncotarget* 7, 61860–61873. doi: 10.18632/oncotarget.11452

Uroz, S., Chhabra, S. R., Cámara, M., Williams, P., Oger, P., and Dessaux, Y. (2005). N-acylhomoserine lactone quorum-sensing molecules are modified and degraded by *Rhodococcus erythropolis* W2 by both amidolytic and novel oxidoreductase activities. *Microbiology* 151, 3313–3322. doi: 10.1099/mic.0.27961-0

Uroz, S., D'Angelo-Picard, C., Carlier, A., Elasri, M., Sicot, C., Petit, A., et al. (2003). Novel bacteria degrading N-acylhomoserine lactones and their use as quenchers of quorum-sensing-regulated functions of plant-pathogenic bacteria. *Microbiology* 149, 1981–1989. doi: 10.1099/mic.0.26375-0

Uroz, S., Dessaux, Y., and Oger, P. (2009). Quorum sensing and quorum quenching: the Yin and Yang of bacterial communication. *Chembiochem* 10, 205–216. doi: 10.1002/cbic.200800521

Uroz, S., Oger, P. M., Chapelle, E., Adeline, M. T., Faure, D., and Dessaux, Y. (2008). A *Rhodococcus* qsdA-encoded enzyme defines a novel class of large-spectrum quorum-quenching lactonases. *Appl. Environ. Microbiol.* 74, 1357–1366. doi: 10.1128/AEM.02014-7

Walsh, C., Bonner, J. J., Johnson, T. N., Neuhoff, S., Ghazaly, E. A., Gribben, J. G., et al. (2016). Development of a physiologically based pharmacokinetic model of actinomycin D in children with cancer. *Br. J. Clin. Pharmacol.* 81, 989–998. doi: 10.1111/bcp.12878

Wang, J., Nong, X. H., Amin, M., and Qi, S. H. (2018). Hygrocin C from marine-derived *Streptomyces* sp. SCSGAA 0027 inhibits biofilm formation in *Bacillus amyloliquefaciens* SCSGAB0082 isolated from South China Sea gorgonian. *Appl. Microbiol. Biotechnol.* 102, 1417–1427. doi: 10.1007/s00253-017-8672-z

Wang, L., Li, Y., and Li, Y. (2019). Metal ions driven production, characterization and bioactivity of extracellular melanin from *Streptomyces* sp. ZL-24. *Int. J. Biol. Macromol.* 123, 521–530. doi: 10.1016/j.ijbiomac.2018.11.061

Wang, W. Z., Morohishi, T., Someya, N., and Ikeda, T. (2012). Diversity and distribution of N -acylhomoserine lactone (AHL) -degrading activity and AHL-lactonase (AiiM) in genus *Microbacterium*. *Microbes Environ.* 27, 330–333. doi: 10.1264/jsme2.me11341

Wang, W. Z., Morohoshi, T., Ikenoya, M., Someya, N., and Ikeda, T. (2010). AiiM, a novel class ot N-acylhomoserine lactonase from the leaf-associated bacterium *Microbacterium testaceum*. *Appl. Environ. Microbiol.* 76, 2524–2530. doi: 10.1128/AEM.02738-9

Wang, X., Cheng, H., Lu, M., Fang, Y., Jiao, Y., Li, W., et al. (2016). Dextranase from *Arthrobacter oxydans* KQ11-1 inhibits biofilm formation by polysaccharide hydrolysis. *Biofouling* 32, 1223–1233. doi: 10.1080/08927014.2016.1239722

Wuster, A., and Babu, M. M. (2007). "Chemical molecules that regulate transcription and facilitate cell-to-cell communication," in *Wiley Encyclopedia of Chemical Biology*, ed. T. P. Begley (New Jersey, NJ: John Wiley & Sons), 1–8.

Xie, T. T., Zeng, H., Ren, X. P., Wang, N., Chen, Z. J., Zhang, Y., et al. (2018). Antibiofilm activity of 3 Actinomycete strains against *Staphylococcus epidermidis*. *Lett. Appl. Microbiol.* 68, 73–80. doi: 10.1111/lam.13087

You, J., Xue, X., Cao, L., Lu, X., Wang, J., Zhang, L., et al. (2007). Inhibition of *Vibrio* biofilm formation by a marine actinomycete strain A66. *Appl. Microbiol. Biotechnol.* 76, 1137–1144. doi: 10.1007/s00253-007-1074-x

Younis, K. M., Usup, G., and Ahmad, A. (2016). Secondary metabolites produced by marine streptomyces as antibiofilm and quorum-sensing inhibitor of uropathogen *Proteus mirabilis*. *Environ. Sci. Pollut. Res. Int.* 23, 4756–4767. doi: 10.1007/s11356-015-5687-9

Zhao, L., Montville, T. J., and Schaffner, D. W. (2006). Evidence for quorum sensing in *Clostridium botulinum* 56A. *Lett. Appl. Microbiol.* 42, 54–58. doi: 10.1111/j.1472-765X.2005.01807.x doi: 10.1111/j.1472-765x.2005.01807.x

Conflict of Interest Statement: The authors declare that the research was conducted in the absence of any commercial or financial relationships that could be construed as a potential conflict of interest.

frontiers in Microbiology

ORIGINAL RESEARCH
published: 14 November 2019
doi: 10.3389/fmicb.2019.02657

AiiM Lactonase Strongly Reduces Quorum Sensing Controlled Virulence Factors in Clinical Strains of *Pseudomonas aeruginosa* Isolated From Burned Patients

*Luis Esaú López-Jácome[1,2], Georgina Garza-Ramos[3], Melissa Hernández-Durán[2], Rafael Franco-Cendejas[2], Daniel Loarca[1], Daniel Romero-Martínez[3], Phuong Thi Dong Nguyen[4], Toshinari Maeda[4], Bertha González-Pedrajo[5], Miguel Díaz-Guerrero[5], Jorge Luis Sánchez-Reyes[1], Dánae Díaz-Ramírez[1] and Rodolfo García-Contreras[1]**

[1] Laboratorio de Bacteriología, Departamento de Microbiología y Parasitología, Facultad de Medicina, Universidad Nacional Autónoma de México, Mexico City, Mexico, [2] Laboratorio de Infectología, Centro Nacional de Investigación y Atención de Quemados, Instituto Nacional de Rehabilitación, Mexico City, Mexico, [3] Laboratorio de Fisicoquímica e Ingeniería de Proteínas, Departamento de Bioquímica, Universidad Nacional Autónoma de México, Mexico City, Mexico, [4] Department of Biological Functions Engineering, Gradute School of Life Sciences and System Engineering, Kyushu Institute of Technology, Kitakyushu, Japan, [5] Departamento de Genética Molecular, Instituto de Fisiología Celular, Universidad Nacional Autónoma de México, Mexico City, Mexico

OPEN ACCESS

Edited by:
Ana Maria Otero, University of Santiago de Compostela, Spain

Reviewed by:
Giordano Rampioni, Roma Tre University, Italy
Wim J. Quax, University of Groningen, Netherlands

***Correspondence:**
Rodolfo García-Contreras
rgarc@bq.unam.mx

Specialty section:
This article was submitted to Microbial Physiology and Metabolism, a section of the journal Frontiers in Microbiology

Received: *15 May 2019*
Accepted: *31 October 2019*
Published: *14 November 2019*

Citation:
López-Jácome LE, Garza-Ramos G, Hernández-Durán M, Franco-Cendejas R, Loarca D, Romero-Martínez D, Nguyen PTD, Maeda T, González-Pedrajo B, Díaz-Guerrero M, Sánchez-Reyes JL, Díaz-Ramírez D and García-Contreras R (2019) AiiM Lactonase Strongly Reduces Quorum Sensing Controlled Virulence Factors in Clinical Strains of Pseudomonas aeruginosa Isolated From Burned Patients. Front. Microbiol. 10:2657. doi: 10.3389/fmicb.2019.02657

Pseudomonas aeruginosa is an opportunistic bacterium associated with healthcare infections in intensive care units (ICUs), ventilator-associated pneumonia (VAP), surgical site infections, and burns. This bacterium causes 75% of death in burned patients, since it can develop a persistent biofilm associated with infections, express several virulence factors, and antibiotic-resistance mechanisms. Some of these virulence factors are proteases such as elastase and alkaline protease, or toxic metabolites such as pyocyanin and is one of the few microorganisms able to produce cyanide, which inhibits the cytochrome oxidase of host cells. These virulence factors are controlled by quorum sensing (QS). In this work, 30 *P. aeruginosa* clinical strains isolated from burned patients from a tertiary hospital in Mexico City were studied. Antibiotic susceptibility tests were done, and virulence factors (elastase, alkaline protease, HCN, and pyocyanin) were determined in presence of an N-acylhomoserine lactonase, AiiM able to hydrolyze a wide range of acyl homoserine lactones. The treatment reduced significantly the activities of elastase and alkaline protease, and the production of pyocyanin and HCN in all producer strains but not the secretion of toxins through the type III secretion system. Our work suggests that AiiM treatment may be an effective therapy to combat *P. aeruginosa* infection in burn patients.

Keywords: AiiM lactonase, virulence factors, *Pseudomonas aeruginosa*, quorum quenching, burned patients, anti-virulence therapy

INTRODUCTION

Pseudomonas aeruginosa is an opportunistic bacteria associated with healthcare infections in intensive care units (ICUs), ventilator-associated pneumonia (VAP), central line-associated blood stream infections, surgical site infections (Cohen et al., 2017), burnt wounds (Fournier et al., 2016), and urinary tract infections, otitis media, and keratitis (Chatterjee et al., 2016; Olivares et al., 2016). In the United States, according to the Centers for Disease Control and Prevention, in 2013 it was estimated that every year around 51,000 health-care infections are associated to *P. aeruginosa,* of which 6,700 are multidrug resistant, causing 440 deaths per year (Centers for Disease Control and Prevention, 2018)[1]. Both *P. aeruginosa* and *Acinetobacter baumannii* complex are the most important, resistant and dangerous microorganisms infecting burnt patients (Tredget et al., 1992; Estahbanati et al., 2002; Turner et al., 2014; Centers for Disease Control and Prevention, 2019). Despite medicine advances, these sorts of complications are still a huge problem to solve, and as a consequence, around 75% of burned infected patients die. Burn infections related to *P. aeruginosa* often promote a faster deterioration allowing the spread of bacteria causing death in weeks and even in days (Mcmanus et al., 1985; Turner et al., 2014). *P. aeruginosa* has a wide arsenal of virulence factors that enable it to colonize and cause infections in the host, the relevance of these virulence factors has been demonstrated using *P. aeruginosa* strains with deficiencies in their production, leading to a reduced ability of colonizing and a lower dissemination in the host (Pavlovskis and Wretlind, 1979; Rumbaugh et al., 2009; Jimenez et al., 2012; Castillo-Juarez et al., 2015). Elastase is a metalloprotease that disrupts several proteins such as: collagen, elastin, immunoglobulins (IgA and IgG), complement components, and cytokines like interferon gamma and tumor necrosis factor alpha (Pavlovskis and Wretlind, 1979; Lyczak et al., 2000; Ben Haj Khalifa et al., 2011). Alkaline protease is also a zinc metalloprotease that inhibits phagocytosis, killing through neutrophils, opsonization, the action of the complement cascade by degrading C3b and is as well related to corneal damage (Howe and Iglewski, 1984; Ben Haj Khalifa et al., 2011; Laarman et al., 2012; Lee and Zhang, 2015). *P. aeruginosa* is one of the few microorganisms that can synthesize cyanide through the oxidative decarboxylation of glycine by hydrogen cyanide synthase enzyme, under micro-aerobic conditions (O_2 < 5%). HCN is a poison that inhibits respiration by inactivating cytochrome oxidase C (Huber et al., 2016). Another important virulence factor is pyocyanin, a blue phenazine, that promotes oxidative stress, which inhibits ciliary movement and delays inflammatory response due to the damage of neutrophils and apoptosis induction (Ben Haj Khalifa et al., 2011; Lee and Zhang, 2015). In burn injuries, pyocyanin plays an important role because it stimulates colonization, damage of surrounding tissue and promotes dissemination. Furthermore, *P. aeruginosa* strains are often multi-drug resistant, limiting treatment options in healthcare settings around the globe, owing this the World Health Organization classified *P. aeruginosa* as the second more threatening bacterium. Moreover, although new antibiotics are available, each time, resistance against those new drugs quickly appears (Fournier et al., 2016; Shortridge et al., 2017; Karampatakis et al., 2018; Shields et al., 2018). In many pathogenic bacteria, virulence factors are controlled by cell to cell communication known as quorum sensing (QS). *P. aeruginosa* has two QS systems mediated by N-acyl homoserine lactones, Las and Rhl, each one is constituted by three elements, a synthase, a signal receptor and an autoinducer signal. The Las system is formed by LasI which is the synthase, the receptor is LasR and the autoinducer is N-3-oxo-dodecanoyl-L-homoserine lactone, meanwhile the Rhl system is formed by the synthase RhlI, RhlR as receptor and the auto-inducer is N-butyryl-homoserine lactone. These two systems are hierarchically organized and each one of them controls several virulence factors. The Las system regulates the Rhl system and virulence factors such as elastase, protease, exotoxin A, alkaline protease and type II secretion system; while the Rhl system enhances the production of rhamnolipids, hydrogen cyanide, and pyocyanin (Van Delden and Iglewski, 1998; Douzi et al., 2011; Lee and Zhang, 2015). Due to the fast increase in bacterial resistance, alternative strategies such as quorum quenching (QQ) have been proposed. QQ consists of blocking or inhibiting cell to cell communication by obstructing the autoinducer synthases, the signal receptors or by degrading the autoinducers via two enzymatic strategies: disrupting the lactone ring through a lactonase or through the cleavage of the acylic tail by acylases (Defoirdt et al., 2013; Defoirdt, 2018). The aim of this work is to evaluate the activity of AiiM, a lactonase enzyme, in *P. aeruginosa* clinical bacterial strains isolated from burnt patients in a third level center of Mexico City, in order to find out if its utilization could eventually be proposed to treat infected burnt patients.

MATERIALS AND METHODS

Clinical Strains

Randomly 200 strains were selected[2] from the collection belonging to Infectious Diseases Laboratory at Centro Nacional de Investigación y Atención de Quemados at Instituto Nacional de Rehabilitación Luis Guillermo Ibarra, to avoid genomic redundancy pulsed field, gel electrophoresis was performed and only one strain per clonal group was selected for further experiments. Clinical strains were identified with Vitek 2 Compact® (Biomerieux, France) with Gram negative card identification, some biochemical tests included were oxidase, indole production, growth at 42°C, arginine dihydrolase and glucose oxidation/fermentation. The origin of each clinical isolate is shown in **Supplementary Table S1**.

Minimal Inhibitory Concentrations

Minimal inhibitory concentrations were determined according to Clinical and Laboratory Standards Institute® (CLSI) M07-A10 (CLSI, 2015) in 96-well plates. Breakpoints interpretation were made according to the M100 Performance Standards for

[1] https://www.cdc.gov/hai/organisms/pseudomonas.html

[2] www.randomization.com

Antimicrobial susceptibility testing 28th edition (CLSI, 2019). Antibiotics included were amikacin (Sigma Aldrich A1774), gentamicin (Sigma Aldrich G3632), aztreonam (Sigma Aldrich PZ0038), ceftazidime (Sigma Aldrich C3809), cefepime (Sigma Aldrich PHR1763), ciprofloxacin (Sigma Aldrich 17850), levofloxacin (Sigma Aldrich 28266), doripenem (Sigma Aldrich 32138), imipenem (Sigma Aldrich I0160), meropenem (Sigma Aldrich M2574), colistin (Sigma Aldrich C4461), and piperacillin/tazobactam (Sigma Aldrich P8396/T2820). *P. aeruginosa* ATCC® 27853 was used as control as according to CLSI (**Supplementary Table S1**).

las/*rhl* Genes Detection

DNA Extraction

Pseudomonas aeruginosa strains were cultured in 5% sheep blood agar during 18 h at 37°C, and then one single colony was taken and lysed in an Eppendorf tube with 500 μL of TE buffer (10 mM Tris–HCl, 1 mM EDTA, pH 7.5) and were set into a heat block at 95°C for 5 min. Tubes were centrifuged, and the supernatant was added into a new tube.

Genes related to Las and Rhl systems were amplified (**Table 1**) in a final volume of 25 μL of buffer 1X, 3 mM $MgCl_2$, 200 μM dNTP′s, 0.2 μM primer forward and reverse, 0.026 U/μL Taq polymerase (Amplitaq Gold® DNA Polymerase, Applied Biosystems N808-0241, United States). The amplification conditions used were: 95°C 10 min, 95°C 30 s, 58°C 45 s and 72°C 50 s during 35 cycles, 72°C 5 min and finally 4°C (Veriti 96 Well thermal cycler, Applied Biosystems, United States). Amplification products were loaded into a 1% agarose gel stained with SYBR® green I (S7567, Life Technologies, United States) and visualized with Gel DOC™ XR + with Image Lab™ software (Bio-Rad, United States). *P. aeruginosa* PAO1 was used as positive control in each one of the systems and Δ *lasR/rhlR* PAO1 as negative control of transcriptional regulators.

AiiM Purification

AiiM construction was provided by Dr. Toshinari Maeda (Nguyen et al., 2019). Briefly 50 mL *Escherichia coli* M15/pQE30 AiiM was grown overnight (ON) in Luria Bertani broth with 100 μg/mL of carbenicillin (Sigma Aldrich C1389) and 50 μg/mL of kanamycin (Sigma Aldrich K1876), afterward, 10 mL of the ON cultures were taken and inoculated into 1 L of terrific broth with carbenicillin and kanamycin as above described, cultures were incubated at 37°C 220 rpm, optical density (OD) at 600 nm was measured until the culture reached an OD of 0.5 and immediately after, it was induced with 500 μM IPTG. The cultures were incubated at 37°C 220 rpm for 6 h and centrifuged at 10,000 rpm for 40 min. Pellets were resuspended in 40 mL of purification buffer (50 mM NaH_2PO_4, 300 mM NaCl and 10% glycerol, pH adjusted to 8.0) and 500 μM PMSF (Sigma Aldrich P7626), sonicated (45% amplitude for 45 s and 2 min of rest, all this 10 times; Ultrasonic processor, Cole Parmer) and centrifuged at 10,000 rpm during 40 min. The supernatants were passed through a 0.2 nm filter and loaded onto Protino® Ni-TED resin (Macherey-Nagel, 745200.600) for purification of His-tagged proteins previously equilibrated with 3 column volumes (CV) of 20 mL of purification buffer, then filtered protein extracts were passed through the column, after that, 2 additional CV of purification buffer were passed. Protein was eluted with 150 mM imidazole (Sigma Aldrich I5513) in 2 CV of purification buffer. AiiM fractions with higher purity were selected, concentrated with polyethylene glycol 35 KDa (Sigma Aldrich 946-46) into dialysis tubing cellulose membrane (Sigma Aldrich D9777). Afterward, dialysis was done to remove imidazole using dialysis buffer (50 mM Tris, 300 mM NaCl adjusted at pH 7.5). SDS-PAGE was done to estimate the amount and purity of AiiM. Protein was quantified by its absorbance at 280 nm with NanoDrop 2000 (Thermo Fisher Scientific, United States), using an extinction coefficient (Abs 0.1%) of 1.08. Aliquots of protein were made and stored at −20°C until they were used.

TABLE 1 | Primers used in this study.

Primer	Tm (°C)	Size (bp)
lasI-F 5′-CGCGAAGAGTTCGATAAA-3′	59.7	531
lasI-R 5′-GGTCTTGGCATTGAGTTC-3′	58.7	
lasR-F 5′-ATGGCCTTGGTTGACGGT-3′	65.9	706
lasR-R 5′-GACCCAAATTAACGGCCA-3′	63.7	
rhlI-F 5′-TTGCTCTCTGAATCGCTG-3′	61	590
rhlI-R 5′-GCCATCGACAGCGGTACG-3′	68.3	
rhlR-F 5′-ATGAGGAATGACGGAGGC-3′	63.2	675
rhlR-R 5′-CGCGTCGAACTTCTTCTG-3′	62.9	

AiiM Activity Against N-acyl Homoserine Lactones

To evaluate the HSL lytic activity of the purified AiiM, an analytical assay was developed in an Alliance HPLC system (Waters, United States) with a Symmetry (Waters, United States) C18 Column (75 mm, 3.5 mm). Both short and long acylated chains were included, 1 mM *N*-butyryl-DL-homoserine lactone (C4-HSL; Sigma Aldrich 09945), 1 mM *N*-(3-oxooctanoyl)-L-homoserine lactone (3OC8-HSL;Sigma Aldrich O1764), 1 mM *N*-decanoyl-DL-homoserine lactone (C10-HSL; Sigma Aldrich 17248), 1 mM *N*-(3-oxodecanoyl)-L-homoserine lactone (3OC10-HSL; Sigma Aldrich O9014), and *N*-(3-oxododecanoyl) homoserine lactone (3OC12-HSL; Sigma Aldrich O9139). 60 mM NaOH was used as positive control since it can hydrolyze HSL molecules and the reaction was stopped with the addition of 2N HCl. Several concentrations, from 250, 100, 50, 25, 10, and 5 μg/mL of purified AiiM were tested. Time exposition was also varied; 24 h, 2 h, 1 h, 30 min, 20 min, 10 min, and 5 min. All experiments were performed in triplicate. Chromatographic conditions were: column temperature 25°C, sample temperature 25°C, injection volume 10 μL, flow rate 1 mL/min, detection 205 nm. Elution mixture was made with 50 mM phosphates buffer pH 2.9:acetonitrile. For C4-HSL the relation was 90:10, 3OC8-HSL 60:40, C10-HSL 60:40, 3OC10-HSL 60:40, and 3OC12-HSL 50:50.

Bacterial Growth With and Without AiiM

Grow curves were analyzed to test the effect of AiiM on *P. aeruginosa* PAO1 and Δ *lasR/rhlR* PAO1 growth kinetics.

A 50 mL flask with 5 mL of LB was inoculated with each one of the strains at an initial OD_{600nm} of 0.05 with and without 5 μg/mL of AiiM, samples were taken each hour for 12 h.

Virulence Factors Determination

Elastase was determined for clinical strains and *P. aeruginosa* PAO1 Δ*lasR/rhlR* and Δ*lasI/rhlI* PAO1 mutants according to methods previously described (Ohman et al., 1980), with some modifications. ON of each clinical strain and control strains were cultured in LB at 37°C 220 rpm and were inoculated at an initial OD_{600nm} of 0.05 in 5 mL of LB with and without AiiM (5 μg/mL), samples were incubated for 18 h at 37°C and 220 rpm, and centrifuged at 14,000 rpm for 2 min. 50 μL of the supernatant were taken and set into 950 μL of elastase buffer (100 mM Tris–HCl, 1 mM $CaCl_2$, pH 7.5) with 2.5 mg of elastin-congo red (Sigma Aldrich reference E0502) as substrate. Tubes were incubated at 37°C, 220 rpm for 2 h, centrifuged at 14,000 rpm for 5 min and the released die in the supernatant was measured at 495 nm with a spectrophotometer SmartSpec Plus (Bio-Rad, United States). All determinations were performed by triplicate.

Alkaline Protease

Alkaline protease was determined according to methods previously described (Howe and Iglewski, 1984), with some modifications. ON of each strains were cultured into LB at 37°C 220 rpm and were inoculated in 5 mL of LB at an initial OD_{600nm} of 0.05 with and without AiiM (5 μg/mL). AiiM protein was added at the beginning of the cultures, samples were incubated for 18 h at 37°C and 220 rpm, and centrifuged at 14,000 rpm for 2 min. 50 μL of supernatant were taken and added into 950 μL of protease buffer with 2.5 mg of Hide-Remazol brilliant blue R (Sigma Aldrich reference H6268) as substrate. Tubes were incubated at 37°C, 220 rpm for 20 min centrifuged at 14,000 rpm 5 min and the supernatant was measured at 595 nm with a spectrophotometer SmartSpec Plus (Bio-Rad, United States).

Pyocyanin

For pyocyanin production ON of each clinical and control strains were cultured in LB at 37°C at 220 rpm and inoculated into 5 mL of LB at an initial OD_{600nm} 0.05 with and without AiiM (5 μg/mL). AiiM protein was added at the beginning, samples were incubated 18 h at 37°C and 220 rpm. One milliliter of supernatant was taken, centrifuged at 14,000 rpm for 5 min, and then 800 μL of supernatant were set into new 1.5 mL conic tube and 400 μL of chloroform was added, each tube was mixed in vortex for 2 min. Tubes were centrifuged for 5 min at 14,000 rpm, 300 μL of the organic phase were taken and deposited into a new tube, 800 μL of 0.2 N HCl were added and mixed for 2 min in vortex then samples were read at 520 nm (Maeda et al., 2012). *P. aeruginosa* PAO1, Δ*lasR/rhlR* PAO1 and Δ*lasI/rhlI* PAO1 were used as positive and negative controls, respectively.

HCN Determination

For HCN determination, bacteria were cultured in 3 mL of LB medium in flasks with rubber stoppers at 37°C and 200 rpm for 18 h, after the incubation two needles were inserted in the rubber stopper, one of them was used for pumping air for 1 h and the other to collect the outflow in 5 mL of 4 M NaOH. HCN concentrations were determined as described by Gallagher and Manoil (2001), briefly, samples were mixed with a 1:1 fresh mixture of 0.1 M *o*-dinitrobenzene and 0.2 M *p*-nitrobenzaldehyde both dissolved in 2-methoxyethanol, and following 20 min of incubation at room temperature, the absorbance at 578 nm was determined and compared with a calibration curve made with KCN standards.

AiiM Dose Response Curve and Suppression of Its Activity by Exogenous Addition of 3OC12-HSL

For these control experiments, the PAO1 reference strain and the clinical isolate P809 were used. Three independent cultures per strain were inoculated in LB medium at an initial OD_{600nm} of 0.05 without and with AiiM at 0.5, 1, 2.5, and 5 μg/mL, and incubated 37°C at 220 rpm, supernatants were then obtained and used for the determination of pyocyanin concentration and elastase activity (as described before). In addition another 3 cultures per strain with AiiM 0.5 μg/mL were grown to an OD_{600nm} of $\sim$ 1.0, supplemented with a final concentration of 30 μM of 3OC12-HSL, and incubated until 18 h of incubation were completed, supernatants were collected and pyocyanin concentration and elastase activity determined.

Long Chain HSL Autoinducer Detection and Its Inactivation by AiiM

To identify autoinducer production and its inactivation by AiiM, each one of the 30 clinical strains were grew up onto MacConkey agar plates, then one colony was taken and inoculated into 5 mL of LB for ON growth. After that, new cultures were inoculated at an initial OD_{600nm} 0.05 in 5 mL of LB and grown at 37°C, with 220 rpm shaking during 18 h, with AiiM 5 μg/mL and without AiiM enzyme. LB cultures then were centrifuged 14,000 rpm for 5 min. Supernatants were separated in new tubes. For long chain HSL detection *Agrobacterium tumefaciens* NT1 pZLR4 (Shaw et al., 1997) was used as a biosensor strain. Previously the biosensor strain was grown in one liter of M9 medium and incubated at 37°C and 220 rpm for 18 h. Bacteria were concentrated by centrifugation at 12,000 rpm during 5 min to a final volume of 15 mL, then aliquots of 1 mL of concentrated bacteria were separated. M9 agar plates were prepared and before solidification 1 mL of the concentrated biosensor plus Xgal at a final concentration of 40 μg/mL (5-bromo-4-chloro-3-indolyl- ß-D-galactopyranoside, USB corporation, Cleveland, OH, United States) were added for 100 mL of M9 agar. 15 μL of each supernatant (with and without AiiM) were then added onto 6 mm filter paper sterile disk on the M9 agar. All experiments were done by triplicate. 1 mM *N*-decanoyl-DL-homoserine lactone (C10-HSL; Sigma Aldrich 17248), 1 mM *N*-(3-oxodecanoyl)-L-homoserine lactone (3OC10-HSL; Sigma Aldrich O9014) and *N*-(3-oxododecanoyl) homoserine lactone (3OC12-HSL; Sigma Aldrich O9139) were used as positive controls and the molecules treated with AiiM 5 μg/mL as negative controls. Plates were incubated at 28°C and results were observed, a positive reaction associated to the production of long chain HSL was observed as a green halo and inactivation of the signals when the halo was absent.

Type III Protein Secretion Profiles

For type III secretion assays *P. aeruginosa* strains (PAO1, PA14, and the clinical isolates H015 and P729) were grown overnight in LB medium. Bacteria were diluted 1:200 into 4 mL of a modified LB medium supplemented with 10 mM $MgCl_2$, 0.5 mM $CaCl_2$ and 5 mM EGTA (pH 7.4) in the presence or absence of 5 μg/mL of AiiM, and grown at 37°C to an OD_{600nm} of 0.8 to 1.0. 1 mL of each culture was collected into a microcentrifuge tube and bacteria were pelleted by centrifugation. The resulting pellet was resuspended in 200 μl of 1× Laemmli SDS sample buffer normalized for OD_{600nm}. The supernatant was centrifuged once again and the resulting supernatant was transferred into a clean tube. Supernatant proteins were precipitated overnight at 4°C by adding trichloroacetic acid to a final concentration of 10%, pelleted by centrifugation and resuspended in 20 μL of 1x Laemmli SDS sample buffer containing 10% saturated Tris base normalized for OD_{600nm}. Samples were separated by 15% SDS-PAGE, transferred onto a nitrocellulose membrane and probed for the presence of the effectors ExoS and ExoU by immunoblotting. Detection was performed using the Immobilon Western chemiluminescent HRP substrate (Millipore), and bands were visualized on X-ray films (Carestream MXB Film).

ß-Lactams Inactivation

As ß-lactams have a lactone ring, we performed the inactivation disk method to determine whether AiiM would be able to inactivate this kind of antibiotics. Briefly, 2 mL of 0.8% isotonic saline solution (ISS) was added into sterile 12 mm × 75 mm tube, disks of 30 μg ceftazidime (Becton Dickinson, United States), 30 μg cefepime (Becton Dickinson, United States), 10 μg imipenem (Becton Dickinson, United States), and 10 μg meropenem (Becton Dickinson, United States). One set of disks containing ISS was used as negative control, another set of all antibiotics above mentioned with 5 μg/mL of AiiM, and finally, since NaOH can break the lactone ring another set of all antibiotics was used as positive control with 60 mM NaOH. *Escherichia coli* ATCC® 25922 was used as a pansusceptible strain. Disks were incubated for 1 and 10 min, 2 and 24 h. A suspension of 0.5 McFarland was made with *E. coli* ATCC® 25922 and was plated onto Müller Hinton agar (Becton Dickinson, United States), tubes were incubated at 37°C until their use. All experiments were made by triplicate; the inhibition diameter was measured using a Vernier device.

RESULTS

All clinical isolates were obtained from burned patients infected with *P. aeruginosa*. The most common burn etiology was fire (66.7%) followed by scalds (23.3%) and electrical burns (10%). Medians of hospital length of stay were 53 days (8-303), the mean total body surface area was 40% (10-85%) with a mortality rate of 26.6% ($n = 8$). *P. aeruginosa* strains were isolated from urine ($n = 8$), quantitative biopsies ($n = 8$), blood ($n = 6$), endotracheal aspirates ($n = 3$), bronchoalveolar lavage fluid ($n = 2$), catheter tips ($n = 2$), and qualitative biopsy ($n = 1$).

Pseudomonas aeruginosa Antibiotic Susceptibility Patterns

Susceptibility tests were carried out for all clinical isolates with different antibiotic families including aminoglycosides, monobactams, cephalosporins, fluoroquinolones, carbapenems, lipopeptides, and ß-lactam combination agents. The strains were resistant to almost all antibiotics except colistin (**Figure 1**), resistance rates against all antibiotics families were over 50%. The highest resistance rates were for carbapenems which, until recent decades, were the most potent antibiotics against *P. aeruginosa* and other non-fermentative Gram negative rods; therefore colistin represents the last treatment option for these types of infections (**Supplementary Table S1**).

Gene Amplification

In order to determine if Las/Rhl systems were present in *P. aeruginosa* isolated from burned patients, PCR was performed using the primers described in **Table 1**. Results showed that the genes encoding the Las system (*lasI* and *lasR*) and Rhl system (*rhlI* and *rhlR*) were found in all the clinical strains. *P. aeruginosa* PAO1 was used as positive control and Δ*lasR/rhlR* PAO1 was used as negative control (data not shown).

AiiM Purification

AiiM protein was obtained at a purity of >90% as judged by SDS-PAGE. After elution with 150 mM imidazole, fractions were collected, and those in which AiiM was present were concentrated into dialysis tubing cellulose membrane with polyethylene glycol, then protein concentration was determined and kept at −20°C until used. The purified protein consists of a single band of ≈ 27 kDa, compared with a theoretical molecular mass of 27.2 kDa (**Supplementary Figure S1**).

AiiM Activity Against Homoserine Lactones

In order to prove AiiM activity against acylated chains of diverse HSL, cleavage was determined by HPLC. Five HSL autoinducers with both short and long chains were tested (C4-HSL, 3OC8-HSL, C10-HSL, 3OC10-HSL, and 3OC12-HSL). First HSL alone was run to identify retention times (**Supplementary Table S2**), later the same HSL were treated with 60 mM NaOH to disrupt the lactone ring and finally HSL molecules were treated with AiiM and HPLC experiments were performed under the same conditions. Several AiiM concentrations (250 μg/mL, 100 μg/mL, 50 μg/mL, 25 μg/mL, 10 μg/mL, and 5 μg/mL) were used, in order to identify the lowest one suitable for inhibiting the expression of virulence factors. Each HSL was used at 1 mM. The lowest concentration of AiiM tested (5 μg/mL) was enough to cleave all the HSLs in 5 min (**Figure 2** and **Supplementary Figure S2**) and therefore, this concentration was used for all subsequent experiments.

AiiM Does Not Affect *Pseudomonas aeruginosa* Growth

Growth curves of *P. aeruginosa* with and without AiiM were done to determine if its addition had any effect in the growth rates.

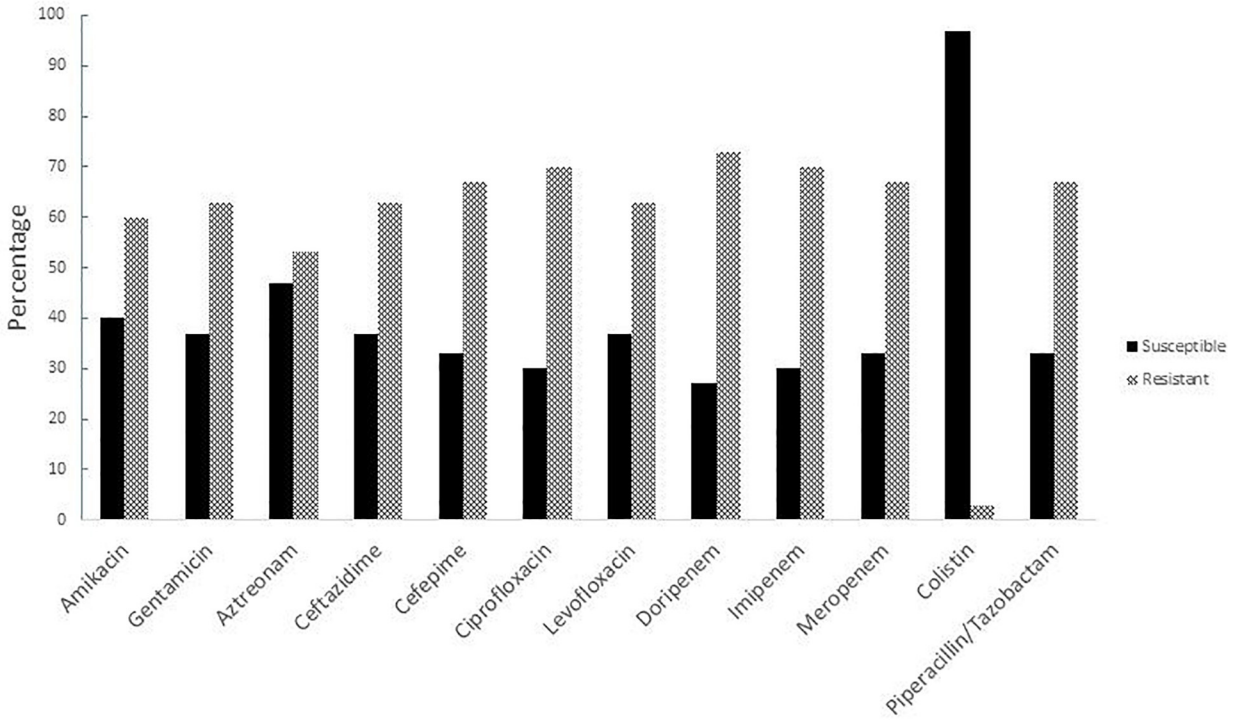

FIGURE 1 | Susceptibility patterns of clinical *P. aeruginosa* strains isolated from burned patients.

As expected, there was no difference in the growing dynamics between these cultures (**Supplementary Figure S3**). PAO1 and Δ *lasR/rhlR* strains were used as controls.

QS-Controlled Virulence Factors Inhibition

Once it was confirmed that AiiM did not affect *P. aeruginosa* growth, its effect over the expression of the QS-controlled virulence factors was determined. Experiments were classified in two groups, one without AiiM addition, and the other with 5 μg/mL addition of AiiM. For elastolytic activity (**Figure 3A**), activity was found in 29 clinical samples, while for alkaline protease activity (**Figure 3B**) there were 27 producing strains; only 12 strains produced pyocyanin (**Figure 3C**), and seven strains were HCN producers (**Figure 3D**). At the same time, experiments with AiiM addition were carried out and the same virulence factors were measured. A significant decrease in the production of each virulence factor was found (elastase $p = 0.000002$, protease $p = 0.000004$, pyocyanin $p = 0.001$ and $p = 0.008$ for HCN).

In addition, AiiM dose response experiments using it at 0.5, 1, 2.5 and 5 μg/mL were performed with the reference strain PAO1 and the clinical isolate P809 measuring pyocyanin production and elastase activity, as expected the degree of inhibition of both phenotypes was dependent in the concentration of AiiM for both virulence factors (**Supplementary Figure S4**). Moreover the effect of 0.5 μg/mL was partially reversed by the addition of 30 μM of 3OC12-HSL (**Supplementary Figure S4**). In order to verify that the clinical strains had active QS systems and that the inhibitory effect in the expression of QS-dependent virulence factors exerted by AiiM was mediated by the degradation of QS signals. Identification of long chain HSL for each strain was done using the biosensor strain *Agrobacterium tumefaciens* NT1 pZLR4 (Shaw et al., 1997), as expected all strains were long chain HSL producers, moreover also for all strains AiiM at 5 μg/mL was enough to degrade the long chain HSL of all strains as determined with the biosensor strain (**Supplementary Figure S5**).

AiiM Does Not Inhibit the Type III Secretion System

Despite its strong inhibitory activity against QS-controlled virulence factors, AiiM had no effect on the secretion of T3SS effectors in both PA14 and PAO1 type strains as well as in the clinical strains P729 and H015 at 5 μg/mL (**Supplementary Figure S6**) and even using 20 μg/mL (data not shown). These two clinical strains were selected as representative examples of a secretion profile similar to strains PAO1 or PA14, respectively.

AiiM Does Not Inactivate ß-Lactam Antibiotics

Wang et al. (2010) defined AiiM as a member of the superfamily of alpha/beta hydrolases, this may represent a problem if it has the ability to inactivate the broad spectrum of ß-lactam antibiotics

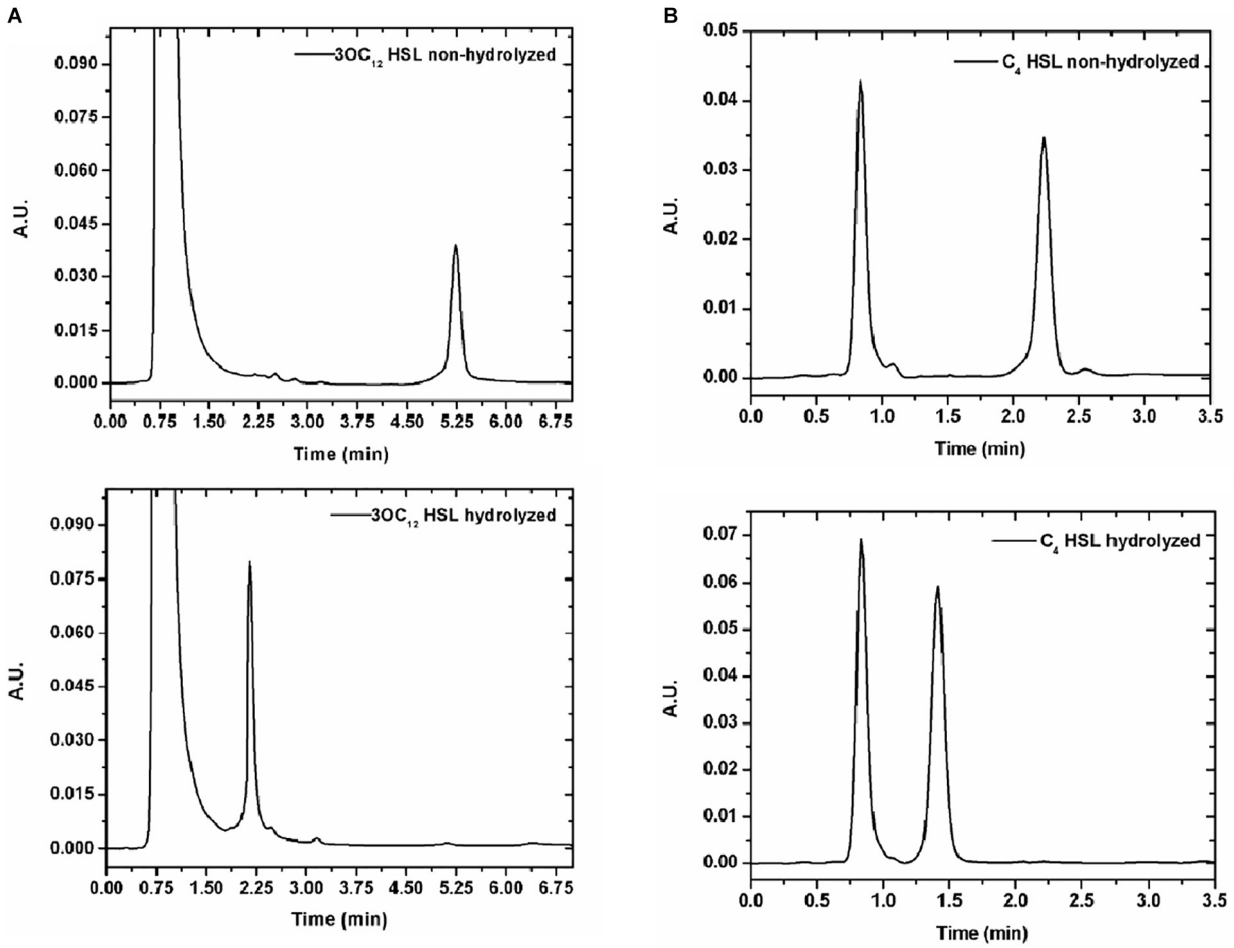

FIGURE 2 | (A) HPLC of HSL without (above) and with 5 μg/mL of AiiM (below) after 5 min of exposition. 2A *N*-(3-oxododecanoyl) homoserine lactone. Retention time for non-hydrolyzed HSL is 5.3 min whereas for hydrolyzed is 2.24 min. **(B)** 2B *N*-butyryl-DL-homoserine lactone. Retention time for non-hydrolyzed is 2.29 min whereas for hydrolyzed is 1.42 min.

as other carbapenem enzymes do, such as NDM, IMP or VIM. In order to test this, we exposed anti *Pseudomonas* ß-lactam antibiotics to 5 μg/mL of AiiM (**Supplementary Figures S7, S8**). Nevertheless, AiiM did not degrade any anti *Pseudomonas* ß-lactam antibiotics.

DISCUSSION

Pseudomonas aeruginosa is one of the main bacteria that causes hospital acquired infections in immunocompromised patients and vulnerable ones (Azam and Khan, 2018). *P. aeruginosa* is one of the 12 priority multi-drug resistant bacteria according to the WHO list published in 2017 (WHO, 2017) and belongs to the ESKAPE group, together with *Enterococcus faecium, Staphylococcus aureus, Klebsiella pneumoniae, A. baumannii,* and *Enterobacter* species (Chen et al., 2018). In addition to acquired resistance mechanisms such as carbapenemases (Carmeli et al., 2016), *P. aeruginosa* has many intrinsic antibiotic tolerance mechanisms, for instance low permeability in its external membrane, and expression of several efflux pumps (Malhotra et al., 2018; Ferrer-Espada et al., 2019).

Burn injuries are one of the most common and devastating forms of trauma and patients with serious thermal injury require immediate specialized care in order to minimize morbidity and mortality (Church et al., 2006). *P. aeruginosa* is one of the most frequent bacteria associated to infection in burn patients together with *A. baumannii* (Li et al., 2018). In a recent Mexican study (Garza-Gonzalez et al., 2019), *P. aeruginosa* had around 27% of resistance to carbapenems, in a global context it was one of the main bacteria in 47 Mexican health centers in 20 states, 175/1995 strains were multi-drug-resistant, 165/1995 were possible extreme drug resistant and 87/1995 possible pandrug resistant. In our 30 isolates we had more than 60% of resistance to cephalosporins (ceftazidime and cefepime), carbapenems (dorypenem, imipenem, and meropenem), aminoglycosides (amikacin and gentamicin), fluoroquinolones (ciprofloxacin and levofloxacin), and piperacillin/tazobactam. Moreover, one strain was resistant to colistin, which is the last antibiotic resource.

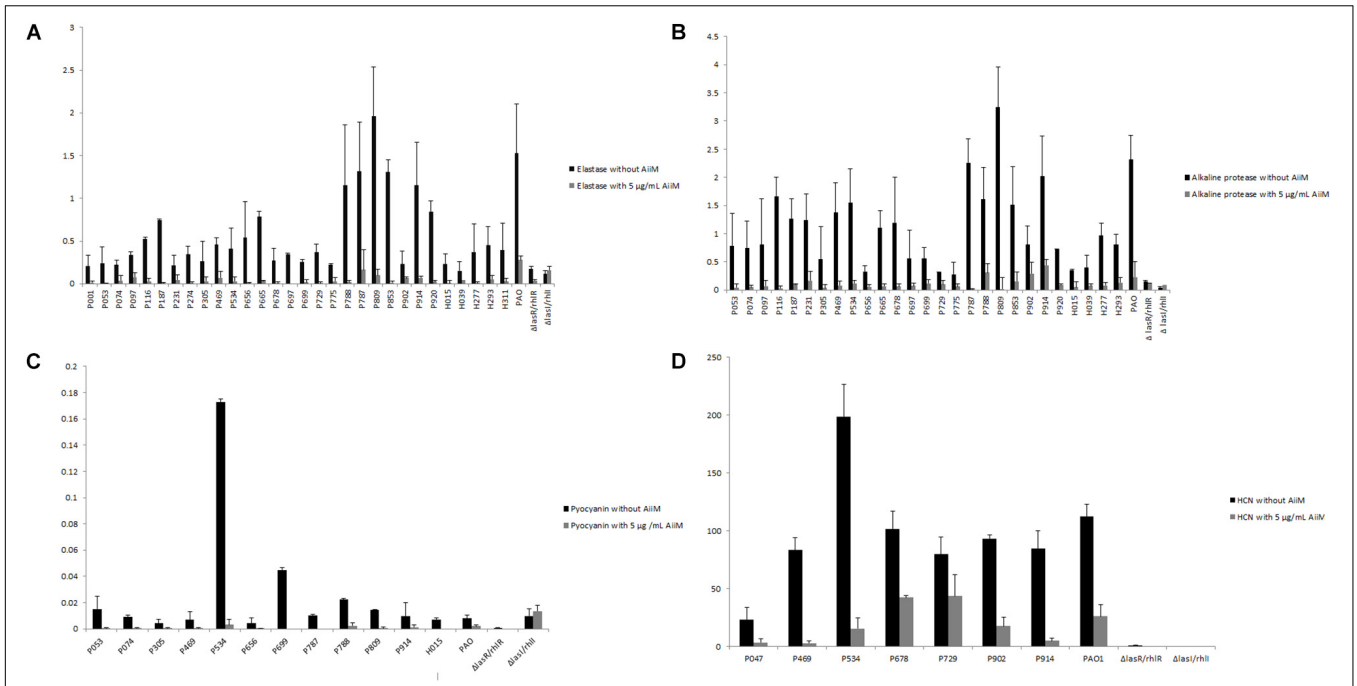

FIGURE 3 | (A) Elastase activity, black bars correspond to clinical strains determination without addition of AiiM, gray bars correspond to clinical strains with 5 µg/mL of AiiM with $p = 0.000002$. **(B)** Alkaline protease activity, black bars correspond to clinical strains without AiiM addition while gray bars correspond to strains with the addition of 5 µg/mL of AiiM with $p = 0.000004$. **(C)** Pyocyanin production, black bars correspond to clinical strains without AiiM addition, whereas gray bars correspond to clinical strains with AiiM 5 µg/mL with $p = 0.001$. **(D)** HCN production, black bars correspond to clinical strains without AiiM addition while gray bars correspond to clinical strains with AiiM 5 µg/mL having a $p = 0.008$.

AiiM showed a wide activity and was able to cut all HSL molecules tested, consistent with a previous report by Wang et al. (2010). Even though we did not analyze it in a quantitative form, we infer a strong activity of AiiM due to its ability to degrade all HSL tested within 5 min of exposition, moreover in our study 5 µg/mL were enough to break down these molecules. One of the main characteristics that a quorum quencher must fulfill is that it should not inhibit bacterial growth (Defoirdt et al., 2013; Defoirdt, 2018) and as expected, AiiM treatment did not affect *P. aeruginosa* growth kinetic.

In contrast, AiiM significantly reduced the four QS-dependent virulence factors tested in our study following a dose response pattern; moreover, others have demonstrated that AiiM had very good activity in a mouse model of acute pneumonia (Migiyama et al., 2013) and reduces methane production in waste sewage sludge (Nguyen et al., 2018). Although to date, the majority of studies with QQ enzymes have been performed only in type strains like PAO1, PA14 (Fetzner, 2015), recently, Guendouze et al. (2017) did the first investigation with *P. aeruginosa* clinical strains isolated from diabetic foot using the lactonase *Sso*Pox with a substitution in the amino acid 263 changing a tryptophan to isoleucine, in order to increase the enzymatic activity, using 0.5 mg/mL of protein, they found some strains with certain tolerance to the *Sso*Pox addition. In our study, AiiM reduced elastase and alkaline protease activities, pyocyanin and HCN concentrations, and we did not find any strain with tolerance against AiiM treatment, in spite that AiiM was used at a 100 times lower concentration than SsoPox. Moreover, AiiM effectivity is much higher than the effectivity of small molecule QS inhibitors such as brominated furanones and 5-fluorouracil, that cannot inhibit QS-virulence factor production of several of the clinical strains tested, and that are very toxic to some of them (García-Contreras et al., 2013, 2015; García-Contreras, 2016; García-Contreras et al., 2016; Guendouze et al., 2017).

Nevertheless, for type III secretion, no inhibition by AiiM was found, which is consistent with recent findings showing that in a Δ*lasR/rhlR* mutant of *P. aeruginosa* PAO1, T3SS effector toxins are secreted at the same levels than in the wild-type strain, demonstrating that this virulence factor is not positively regulated by QS (Soto-Aceves et al., 2019), instead it may be used at low cell densities to establish infections in the host (Hauser, 2009). These highlights the importance of targeting both QS and T3SS to develop robust anti-virulence therapies (García-Contreras, 2016). Moreover, other results indicate that the inhibition of QS systems and T3SS by molecules such as coumarin (Zhang et al., 2018) must be due to independent effects over the QS systems and T3SS.

One possible limitation of the utilization of AiiM and other QQ enzymes for treating *P. aeruginosa* infections is the fact that *lasR* defective mutants are often found in infections and although in principle these mutants will produce low levels of QS-dependent virulence factors, this is not always the case due to a rewiring of the virulence factor regulation

(Morales et al., 2017). And these strains could be tolerant against the effect of QQ enzymes.

Since AiiM is a member of the alpha/beta hydrolases superfamily and several antibiotics are inactivated by metallo ß-lactamases, reducing clinical options to treat infections (Hong et al., 2015), we tested if AiiM could cleave these ß-lactamase antibiotics, however, AiiM did not inactivate those tested, and hence it could be safely used in combination with them.

Although *in vivo* tests in burn infection models are lacking, our work suggests that AiiM treatment may be an effective addition for the treatment of *P. aeruginosa* infections, and since research by other groups had shown also the utility of the lactonase *Sso*Pox against clinical isolates from diabetic foot patients *in vitro* (Guendouze et al., 2017) and *in vivo* using an amoeba model (Mion et al., 2019), and in rat pneumonia against the PAO1 strain (Hraiech et al., 2014) lactonase utilization became an strong candidate for its eventual application in the clinical practice, moreover although *in vivo* studies using acylases are scarce, recently it was shown the PvdQ in addition to their inhibitory properties *in vitro* (Sio et al., 2006) and in *Caenorhabditis elegans* model was also able to increase survival, reduce damage and decrease bacterial loads in a pulmonary infection mice model (Papaioannou et al., 2009; Utari et al., 2018). Hence QQ enzymes may be beneficial for the treatment of burn and lung infections as well.

CONCLUSION

AiiM showed a strong activity against C4-HSL, 3OC8-HSL, C10-HSL, 3OC10-HSL, and 3OC12-HSL. It reduced elastase and alkaline protease activities as well as pyocyanin and HCN concentrations in all tested clinical strains of *P. aeruginosa* isolated from burned patients and no AiiM tolerant strain was found. However, it had no inhibitory effect against the T3SS.

DATA AVAILABILITY STATEMENT

All datasets generated for this study are included in the article/**Supplementary Material**.

ETHICS STATEMENT

Pseudomonas aeruginosa clinical strains used in this study were isolated as part of routine clinical hospital procedures to diagnose infection and hence ethical approval was not required, according to the National Institute of Rehabilitation ethical committee. All bacterial isolates were stored as part of laboratory and epidemiology necessities.

AUTHOR CONTRIBUTIONS

LL-J, GG-R, MH-D, DR-M, PN, MD-G, DL, JS-R, and DD-R performed the experiments. RF-C, TM, BG-P, GG-R, LL-J, and RG-C designed the study, supervised the project and discussed the results. LL-J wrote the manuscript with input from all authors.

FUNDING

This work was supported by Grants from the Programa de Apoyo a Proyectos de Investigación e Innovación Tecnológica (PAPIIT), the Universidad Nacional Autónoma de México number IN214218, the Consejo Nacional de Ciencia y Tecnología number SEP-CONACYT CB-A1-S-8530, and the CONACYT INFR-2015-252140 grant.

ACKNOWLEDGMENTS

RG-C is grateful to Beatriz Meráz Rios for her assistance with some experiments. We acknowledge Dr. Norma Espinosa Sánchez and Eugenia Flores Robles for technical assistance. LL-J is a doctoral student from the Programa de Doctorado en Ciencias Biomédicas, Universidad Nacional Autónoma de México.

SUPPLEMENTARY MATERIAL

The Supplementary Material for this article can be found online at: https://www.frontiersin.org/articles/10.3389/fmicb.2019.02657/full#supplementary-material

REFERENCES

Azam, M. W., and Khan, A. U. (2018). Updates on the pathogenicity status of *Pseudomonas aeruginosa*. *Drug. Discov. Today* 24, 350–359. doi: 10.1016/j.drudis.2018.07.003

Ben Haj Khalifa, A., Moissenet, D., Vu Thien, H., and Khedher, M. (2011). Virulence factors in *Pseudomonas aeruginosa*: mechanisms and modes of regulation. *Ann. Biol. Clin.* 69, 393–403. doi: 10.1684/abc.2011.0589

Carmeli, Y., Armstrong, J., Laud, P. J., Newell, P., Stone, G., Wardman, A., et al. (2016). Ceftazidime-avibactam or best available therapy in patients with ceftazidime-resistant *Enterobacteriaceae* and *Pseudomonas aeruginosa* complicated urinary tract infections or complicated intra-abdominal infections (REPRISE): a randomised, pathogen-directed, phase 3 study. *Lancet Infect. Dis.* 16, 661–673. doi: 10.1016/S1473-3099(16)30004-4

Castillo-Juarez, I., Maeda, T., Mandujano-Tinoco, E. A., Tomas, M., Perez-Eretza, B., Garcia-Contreras, S. J., et al. (2015). Role of quorum sensing in bacterial infections. *World J Clin Cases* 3, 575–598. doi: 10.12998/wjcc.v3.i7.575

Centers for Disease Control and Prevention, (2018). *Pseudomonas* aeruginosa in Healthcare Settings. Available at: https://www.cdc.gov/hai/organisms/pseudomonas.html (accessed March 9, 2018).

Centers for Disease Control and Prevention, (2019). *Diseases and Organisms in Healthcare Settings*. Atlanta GA: Centers for Disease Control and Prevention.

Chatterjee, M., Anju, C. P., Biswas, L., Anil Kumar, V., Gopi Mohan, C., and Biswas, R. (2016). Antibiotic resistance in *Pseudomonas aeruginosa* and alternative therapeutic options. *Int. J. Med. Microbiol.* 306, 48–58. doi: 10.1016/j.ijmm.2015.11.004

Chen, J. W., Lau, Y. Y., Krishnan, T., Chan, K. G., and Chang, C. Y. (2018). Recent advances in molecular diagnosis of *Pseudomonas aeruginosa* infection

by state-of-the-art genotyping techniques. *Front. Microbiol* 9:1104. doi: 10.3389/fmicb.2018.01104

Church, D., Elsayed, S., Reid, O., Winston, B., and Lindsay, R. (2006). Burn wound infections. *Clin. Microbiol. Rev* 19, 403–434.

CLSI, (2015). *M07-A10 Methods for Dilution Antimicrobial Susceptibility Test for Bacteria that Grow Aerobically; Approved Standard*, 10th Edn. Wayne, PA: Clinical and Laboratory Standards Institute.

CLSI, (2019). *M100 Performance Standards for Antimicrobial Susceptibility Testing*, 29th Edn. Wayne, PA: Clinical and Laboratory Standards Institute.

Cohen, R., Babushkin, F., Cohen, S., Afraimov, M., Shapiro, M., Uda, M., et al. (2017). A prospective survey of *Pseudomonas aeruginosa* colonization and infection in the intensive care unit. *Antimicrob. Resist. Infect. Control* 6:7.

Defoirdt, T. (2018). Quorum-sensing systems as targets for antivirulence therapy. *Trends Microbiol.* 26, 313–328. doi: 10.1016/j.tim.2017.10.005

Defoirdt, T., Brackman, G., and Coenye, T. (2013). Quorum sensing inhibitors: how strong is the evidence? *Trends Microbiol* 21, 619–624. doi: 10.1016/j.tim.2013.09.006

Douzi, B., Ball, G., Cambillau, C., Tegoni, M., and Voulhoux, R. (2011). Deciphering the Xcp *Pseudomonas aeruginosa* type II secretion machinery through multiple interactions with substrates. *J. Biol. Chem.* 286, 40792–40801. doi: 10.1074/jbc.M111.294843

Estahbanati, H. K., Kashani, P. P., and Ghanaatpisheh, F. (2002). Frequency of *Pseudomonas aeruginosa* serotypes in burn wound infections and their resistance to antibiotics. *Burns* 28, 340–348. doi: 10.1016/s0305-4179(02)00024-4

Ferrer-Espada, R., Shahrour, H., Pitts, B., Stewart, P. S., Sanchez-Gomez, S., and Martinez-De-Tejada, G. (2019). A permeability-increasing drug synergizes with bacterial efflux pump inhibitors and restores susceptibility to antibiotics in multi-drug resistant *Pseudomonas aeruginosa* strains. *Sci. Rep.* 9:3452. doi: 10.1038/s41598-019-39659-4

Fetzner, S. (2015). Quorum quenching enzymes. *J. Biotechnol.* 201, 2–14. doi: 10.1016/j.jbiotec.2014.09.001

Fournier, A., Voirol, P., Krahenbuhl, M., Bonnemain, C. L., Fournier, C., Pantet, O., et al. (2016). Antibiotic consumption to detect epidemics of *Pseudomonas aeruginosa* in a burn centre: a paradigm shift in the epidemiological surveillance of *Pseudomonas aeruginosa* nosocomial infections. *Burns* 42, 564–570. doi: 10.1016/j.burns.2015.10.030

Gallagher, L. A., and Manoil, C. (2001). *Pseudomonas aeruginosa* PAO1 kills *Caenorhabditis elegans* by cyanide poisoning. *J. Bacteriol.* 183, 6207–6214. doi: 10.1128/jb.183.21.6207-6214.2001

García-Contreras, R. (2016). Is quorum sensing interference a viable alternative to treat *Pseudomonas aeruginosa* infections? *Front. Microbiol.* 7:1454. doi: 10.3389/fmicb.2016.01454

García-Contreras, R., Maeda, T., and Wood, T. K. (2016). Can resistance against quorum-sensing interference be selected? *ISME J.* 10, 4–10. doi: 10.1038/ismej.2015.84

García-Contreras, R., Martinez-Vazquez, M., Velazquez Guadarrama, N., Villegas Paneda, A. G., Hashimoto, T., Maeda, T., et al. (2013). Resistance to the quorum-quenching compounds brominated furanone C-30 and 5-fluorouracil in *Pseudomonas aeruginosa* clinical isolates. *Pathog. Dis.* 68, 8–11. doi: 10.1111/2049-632X.12039

García-Contreras, R., Perez-Eretza, B., Jasso-Chavez, R., Lira-Silva, E., Roldan-Sanchez, J. A., Gonzalez-Valdez, A., et al. (2015). High variability in quorum quenching and growth inhibition by furanone C-30 in *Pseudomonas aeruginosa* clinical isolates from cystic fibrosis patients. *Pathog. Dis.* 73:ftv040. doi: 10.1093/femspd/ftv040

Garza-Gonzalez, E., Morfin-Otero, R., Mendoza-Olazaran, S., Bocanegra-Ibarias, P., Flores-Trevino, S., Rodriguez-Noriega, E., et al. (2019). A snapshot of antimicrobial resistance in Mexico. Results from 47 centers from 20 states during a six-month period. *PLoS One* 14:e0209865. doi: 10.1371/journal.pone.0209865

Guendouze, A., Plener, L., Bzdrenga, J., Jacquet, P., Remy, B., Elias, M., et al. (2017). Effect of quorum quenching lactonase in clinical isolates of *Pseudomonas aeruginosa* and comparison with quorum sensing inhibitors. *Front. Microbiol.* 8:227. doi: 10.3389/fmicb.2017.00227

Hauser, A. R. (2009). The type III secretion system of *Pseudomonas aeruginosa*: infection by injection. *Nat. Rev. Microbiol.* 7, 654–665. doi: 10.1038/nrmicro2199

Hong, D. J., Bae, I. K., Jang, I. H., Jeong, S. H., Kang, H. K., and Lee, K. (2015). Epidemiology and characteristics of metallo-beta-lactamase-producing *Pseudomonas aeruginosa*. *Infect. Chemother.* 47, 81–97. doi: 10.3947/ic.2015.47.2.81

Howe, T. R., and Iglewski, B. H. (1984). Isolation and characterization of alkaline protease-deficient mutants of *Pseudomonas aeruginosa* in vitro and in a mouse eye model. *Infect. Immun.* 43, 1058–1063.

Hraiech, S., Hiblot, J., Lafleur, J., Lepidi, H., Papazian, L., Rolain, J. M., et al. (2014). Inhaled lactonase reduces *Pseudomonas aeruginosa* quorum sensing and mortality in rat pneumonia. *PLoS One* 9:e107125. doi: 10.1371/journal.pone.0107125

Huber, P., Basso, P., Reboud, E., and Attree, I. (2016). *Pseudomonas aeruginosa* renews its virulence factors. *Environ. Microbiol. Rep.* 8, 564–571. doi: 10.1111/1758-2229.12443

Jimenez, P. N., Koch, G., Thompson, J. A., Xavier, K. B., Cool, R. H., and Quax, W. J. (2012). The multiple signaling systems regulating virulence in *Pseudomonas aeruginosa*. *Microbiol. Mol. Biol. Rev.* 76, 46–65. doi: 10.1128/MMBR.05007-11

Karampatakis, T., Antachopoulos, C., Tsakris, A., and Roilides, E. (2018). Molecular epidemiology of carbapenem-resistant *Pseudomonas aeruginosa* in an endemic area: comparison with global data. *Eur. J. Clin. Microbiol. Infect. Dis.* 37, 1211–1220. doi: 10.1007/s10096-018-3244-4

Laarman, A. J., Bardoel, B. W., Ruyken, M., Fernie, J., Milder, F. J., Van Strijp, J. A., et al. (2012). *Pseudomonas aeruginosa* alkaline protease blocks complement activation via the classical and lectin pathways. *J. Immunol.* 188, 386–393. doi: 10.4049/jimmunol.1102162

Lee, J., and Zhang, L. (2015). The hierarchy quorum sensing network in *Pseudomonas aeruginosa*. *Protein Cell* 6, 26–41. doi: 10.1007/s13238-014-0100-x

Li, L., Dai, J. X., Xu, L., Chen, Z. H., Li, X. Y., Liu, M., et al. (2018). Antimicrobial resistance and pathogen distribution in hospitalized burn patients: a multicenter study in Southeast China. *Medicine* 97:e11977. doi: 10.1097/MD.0000000000011977

Lyczak, J. B., Cannon, C. L., and Pier, G. B. (2000). Establishment of *Pseudomonas aeruginosa* infection: lessons from a versatile opportunist. *Microbes Infect.* 2, 1051–1060. doi: 10.1016/s1286-4579(00)01259-4

Maeda, T., Garcia-Contreras, R., Pu, M., Sheng, L., Garcia, L. R., Tomas, M., et al. (2012). Quorum quenching quandary: resistance to antivirulence compounds. *ISME J.* 6, 493–501. doi: 10.1038/ismej.2011.122

Malhotra, S., Limoli, D. H., English, A. E., Parsek, M. R., and Wozniak, D. J. (2018). Mixed communities of mucoid and nonmucoid *Pseudomonas aeruginosa* exhibit enhanced resistance to host antimicrobials. *mBio* 9:e275-18. doi: 10.1128/mBio.00275-18

Mcmanus, A. T., Mason, A. D., Mcmanus, W. F., and Pruitt, B. A. (1985). Twenty-five year review of *Pseudomonas aeruginosa* bacteremia in a burn center. *Eur. J. Clin. Microbiol.* 4, 219–223. doi: 10.1007/bf02013601

Migiyama, Y., Kaneko, Y., Yanagihara, K., Morohoshi, T., Morinaga, Y., Nakamura, S., et al. (2013). Efficacy of AiiM, an N-acylhomoserine lactonase, against *Pseudomonas aeruginosa* in a mouse model of acute pneumonia. *Antimicrob. Agents Chemother.* 57, 3653–3658. doi: 10.1128/AAC.00456-13

Mion, S., Remy, B., Plener, L., Bregeon, F., Chabriere, E., and Daude, D. (2019). Quorum quenching lactonase strengthens bacteriophage and antibiotic arsenal against *Pseudomonas aeruginosa* clinical isolates. *Front. Microbiol.* 10:2049. doi: 10.3389/fmicb.2019.02049

Morales, E., Gonzalez-Valdez, A., Servin-Gonzalez, L., and Soberon-Chavez, G. (2017). *Pseudomonas aeruginosa* quorum-sensing response in the absence of functional LasR and LasI proteins: the case of strain 148, a virulent dolphin isolate. *FEMS Microbiol. Lett.* 364:fnx119. doi: 10.1093/femsle/fnx119

Nguyen, P. D. T., Mustapha, N. A., Kadokami, K., Garcia-Contreras, R., Wood, T. K., and Maeda, T. (2018). Quorum sensing between Gram-negative bacteria responsible for methane production in a complex waste sewage sludge consortium. *Appl. Microbiol. Biotechnol.* 103, 1485–1495. doi: 10.1007/s00253-018-9553-9

Nguyen, P. D. T., Mustapha, N. A., Kadokami, K., Garcia-Contreras, R., Wood, T. K., and Maeda, T. (2019). Quorum sensing between Gram-negative bacteria responsible for methane production in a complex waste sewage sludge consortium. *Appl. Microbiol. Biotechnol.* 103, 1485–1495. doi: 10.1007/s00253-018-9553-9

Ohman, D. E., Cryz, S. J., and Iglewski, B. H. (1980). Isolation and characterization of *Pseudomonas aeruginosa* PAO mutant that produces altered elastase. *J. Bacteriol.* 142, 836–842.

Olivares, E., Badel-Berchoux, S., Provot, C., Jaulhac, B., Prevost, G., Bernardi, T., et al. (2016). The biofilm ring test: a rapid method for routine analysis of *Pseudomonas aeruginosa* biofilm formation kinetics. *J. Clin. Microbiol.* 54, 657–661. doi: 10.1128/JCM.02938-15

Papaioannou, E., Wahjudi, M., Nadal-Jimenez, P., Koch, G., Setroikromo, R., and Quax, W. J. (2009). Quorum-quenching acylase reduces the virulence of *Pseudomonas aeruginosa* in a *Caenorhabditis elegans* infection model. *Antimicrob. Agents Chemother.* 53, 4891–4897. doi: 10.1128/AAC.00380-09

Pavlovskis, O. R., and Wretlind, B. (1979). Assessment of protease (elastase) as a *Pseudomonas aeruginosa* virulence factor in experimental mouse burn infection. *Infect. Immun.* 24, 181–187.

Rumbaugh, K. P., Diggle, S. P., Watters, C. M., Ross-Gillespie, A., Griffin, A. S., and West, S. A. (2009). Quorum sensing and the social evolution of bacterial virulence. *Curr. Biol.* 19, 341–345. doi: 10.1016/j.cub.2009.01.050

Shaw, P. D., Ping, G., Daly, S. L., Cha, C., Cronan, J. E. Jr., Rinehart, K. L., et al. (1997). Detecting and characterizing N-acyl-homoserine lactone signal molecules by thin-layer chromatography. *Proc. Natl. Acad. Sci. U.S.A.* 94, 6036–6041. doi: 10.1073/pnas.94.12.6036

Shields, R. K., Clancy, C. J., Pasculle, A. W., Press, E. G., Haidar, G., Hao, B., et al. (2018). Verification of ceftazidime-avibactam and ceftolozane-tazobactam susceptibility testing methods against carbapenem-resistant *Enterobacteriaceae* and *Pseudomonas aeruginosa*. *J. Clin. Microbiol.* 56:e1093-17. doi: 10.1128/JCM.01093-17

Shortridge, D., Castanheira, M., Pfaller, M. A., and Flamm, R. K. (2017). Ceftolozane-tazobactam activity against *Pseudomonas aeruginosa* clinical isolates from U.S. Hospitals: report from the PACTS antimicrobial surveillance program, 2012 to 2015. *Antimicrob. Agents Chemother.* 61:e465-17. doi: 10.1128/AAC.00465-17

Sio, C. F., Otten, L. G., Cool, R. H., Diggle, S. P., Braun, P. G., Bos, R., et al. (2006). Quorum quenching by an N-acyl-homoserine lactone acylase from *Pseudomonas aeruginosa* PAO1. *Infect. Immun.* 74, 1673–1682. doi: 10.1128/iai.74.3.1673-1682.2006

Soto-Aceves, M. P., Cocotl-Yanez, M., Merino, E., Castillo-Juarez, I., Cortes-Lopez, H., Gonzalez-Pedrajo, B., et al. (2019). Inactivation of the quorum-sensing transcriptional regulators LasR or RhlR does not suppress the expression of virulence factors and the virulence of *Pseudomonas aeruginosa* PAO1. *Microbiology* 165, 425–432. doi: 10.1099/mic.0.000778

Tredget, E. E., Shankowsky, H. A., Joffe, A. M., Inkson, T. I., Volpel, K., Paranchych, W., et al. (1992). Epidemiology of infections with *Pseudomonas aeruginosa* in burn patients: the role of hydrotherapy. *Clin. Infect. Dis* 15, 941–949. doi: 10.1093/clind/15.6.941

Turner, K. H., Everett, J., Trivedi, U., Rumbaugh, K. P., and Whiteley, M. (2014). Requirements for *Pseudomonas aeruginosa* acute burn and chronic surgical wound infection. *PLoS Genet.* 10:e1004518. doi: 10.1371/journal.pgen.1004518

Utari, P. D., Setroikromo, R., Melgert, B. N., and Quax, W. J. (2018). PvdQ quorum quenching acylase attenuates *Pseudomonas aeruginosa* virulence in a mouse model of pulmonary infection. *Front. Cell Infect. Microbiol.* 8:119. doi: 10.3389/fcimb.2018.00119

Van Delden, C., and Iglewski, B. H. (1998). Cell-to-cell signaling and *Pseudomonas aeruginosa* infections. *Emerg. Infect. Dis* 4, 551–560.

Wang, W. Z., Morohoshi, T., Ikenoya, M., Someya, N., and Ikeda, T. (2010). AiiM, a novel class of N-acylhomoserine lactonase from the leaf-associated bacterium *Microbacterium testaceum*. *Appl. Environ. Microbiol.* 76, 2524–2530. doi: 10.1128/AEM.02738-09

WHO, (2017). *WHO Publishes List of Bacteria for Which New Antibiotics are Urgently Needed*. Available at: https://www.who.int/en/news-room/detail/27-02-2017-who-publishes-list-of-bacteria-for-which-new-antibiotics-are-urgently-needed (accessed February 2, 2018).

Zhang, Y., Sass, A., Van Acker, H., Wille, J., Verhasselt, B., Van Nieuwerburgh, F., et al. (2018). Coumarin reduces virulence and biofilm formation in *Pseudomonas aeruginosa* by affecting quorum sensing, type III secretion and C-di-GMP levels. *Front. Microbiol.* 9:1952. doi: 10.3389/fmicb.2018.01952

Conflict of Interest: The authors declare that the research was conducted in the absence of any commercial or financial relationships that could be construed as a potential conflict of interest.

Advantages of publishing in Frontiers

OPEN ACCESS
Articles are free to read for greatest visibility and readership

FAST PUBLICATION
Around 90 days from submission to decision

HIGH QUALITY PEER-REVIEW
Rigorous, collaborative, and constructive peer-review

TRANSPARENT PEER-REVIEW
Editors and reviewers acknowledged by name on published articles

Frontiers
Avenue du Tribunal-Fédéral 34
1005 Lausanne | Switzerland

Visit us: www.frontiersin.org
Contact us: info@frontiersin.org | +41 21 510 17 00

REPRODUCIBILITY OF RESEARCH
Support open data and methods to enhance research reproducibility

DIGITAL PUBLISHING
Articles designed for optimal readership across devices

FOLLOW US
@frontiersin

IMPACT METRICS
Advanced article metrics track visibility across digital media

EXTENSIVE PROMOTION
Marketing and promotion of impactful research

LOOP RESEARCH NETWORK
Our network increases your article's readership